Disordered, ultracold quantum gases: Theoretical studies and experimental perspectives

Laurent Sanchez-Palencia

Laboratoire Charles Fabry
Institut d'Optique
Centre National de la Recherche Scientifique
Université Paris-Sud
2, avenue Augustin Fresnel
F-91127 Palaiseau cedex, France
http://www.atomoptic.fr/∼theory
http://www.atomoptic.fr/∼lsp

HABILITATION A DIRIGER DES RECHERCHES DE L'UNIVERSITE PARIS-SUD

présentée par

LAURENT SANCHEZ-PALENCIA

Sujet du mémoire :

DISORDERED, ULTRACOLD QUANTUM GASES: THEORETICAL STUDIES AND EXPERIMENTAL PERSPECTIVES

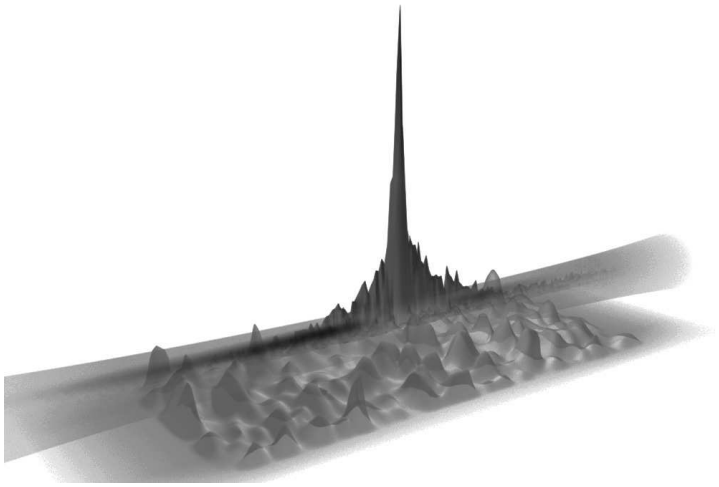

Soutenue le 3 février 2011 devant le jury composé de :

Alain ASPECT	Examinateur
Jean DALIBARD	Président
Thierry GIAMARCHI	Rapporteur
Massimo INGUSCIO	Rapporteur
Maciej LEWENSTEIN	Examinateur
Peter ZOLLER	Rapporteur

Ce mémoire est la version finale du 4 avril 2010 avec quelques mises à jour de références.

In the memory of Professor Gilbert Grynberg

ACKNOWLEDGEMENTS

”Ce commerce que tant de motifs puissants nous engagent à former avec les autres hommes, augmente bientôt l'étendue de nos idées, et nous en fait naître de très nouvelles pour nous, et de très éloignées, selon toute apparence, de celles que nous aurions eues par nous-mêmes sans un tel secours.” [1]

Jean Le Rond d'Alembert,
Encyclopédie, ou Dictionnaire raisonné des sciences, des arts et des métiers – Discours préliminaire (1751)

This manuscript reports the work realized after my Ph-D thesis, first at the Institute for Theoretische Physik of the University of Hannover (Germany) and then at Laboratoire Charles Fabry at Institut d'Optique. I am indebted to Alain Aspect, Jean Dalibard, Thierry Giamarchi, Massimo Inguscio, Maciej Lewenstein and Peter Zoller for having accepted to form part of my Habilitation committee. Finding a date for the defense that fitted all their busy diaries turned out to be a hard puzzle. I thank them all for not having given up and the strong interest they showed for this work. I am particularly grateful to Thierry Giamarchi, Massimo Inguscio and Peter Zoller who kindly took on the demanding charge of referees.

My first thoughts go to Gilbert Grynberg, who has been my PhD advisor for about three years. Gilbert guided my first steps in research at Laboratoire Kastler Brossel of Ecole Normale Supérieure. He offered me a wonderful subject on dissipative optical lattices but even more important, he taught me how to approach a subject from naive ideas to deeper understanding. I cannot number the occasions where we reconsidered a subject we though was almost clear and came up with a more satisfying description. After a long and incapacitating disease, Gilbert died in January 2003, a couple of months before the end of my thesis. I keep from him the memory of a cultured man, a rigorous and imaginative scientist and a kind and patient advisor. In writing

[1] ”This interchange which so many powerful motives cause us to form with other men soon increases the scope of our ideas and gives birth to entirely new ones in us, by all appearances far removed from those we would have had by ourselves without such aid.” [Translation due to Richard N. Schwab]

these lines, I miss him more than ever.

Together with Gilbert Grynberg, Jean Dalibard and Alain Aspect have played a major role in my choice to enter the field of ultracold atoms by their wonderful and inspiring lectures at Ecole Polytechnique. I am very indebted to Jean for his insightful guidance at the end of my thesis and for his invaluable support at a difficult time. In the occasion of several discussions we had at that time, I have been very impressed by his acute sense of physics and his ability to catch immediately the most important points and give them a deeper and more general meaning. Jean was also the first to suggest I contact Maciej Lewenstein for a post-doc position, and Alain strongly supported it. I am very indebted to them for promoting the right choice.

I then joined the group of Maciej Lewenstein as a post-doc fellow in October 2003 with a stimulating project on disordered quantum gases. This was the starting point of a long-standing collaboration I enjoy every day and I am indebted to Maciej for offering me this opportunity. I am very impressed by his broad scientific culture and his deep understanding of physics, as well as by the number of original ideas that come to his mind every second. During the (too short) time I spent in his group, I discovered the beautiful physics of degenerate quantum gases, Bose-Einstein condensates, Fermi seas and disordered systems, as well as many other things. When I left Hannover late 2004, the kind words of Maciej let me with the certainty that I can always count on him.

I am very indebted to Alain Aspect for offering me the opportunity of joining his group in November 2004. Being initially the only theoretician in the group was an adventure for me, and presumably a gamble for him. It is an invaluable chance to work with Alain who combines an acute sense of pedagogy, a remarkable flurry of ideas, the experimental touch and an impressive theoretical understanding. Our frequent discussions are a source of knowledge and inspiration. They have triggered most of the recent works of the theory team. I also admire his remarkable sense of management, which makes his group not only a nice and active place but also a very stimulating environment. Alain is a very demanding physicist who never feels satisfied with fuzzy ideas or answers. His sense of kindly but strongly pushing people as well as projects to their best is an invaluable help for a young researcher and I very much appreciate his mentorship and support in good as well as bad times. Alain has strongly supported the emergence of an independent theory team, and I am very indebted to him for his active help. In brief, it is hard to summarize all I owe him in a couple of words. I may simply say that I thank Alain for teaching me the most beautiful and fascinating side of my job.

Hence I joined Laboratoire Charles Fabry at Institut d'Optique. It is a wonderful place, which offers fantastic opportunities for young researchers. In many respects, I am very indebted to his former director, Pierre Chavel, and his successor, Christian Chardonnet, for their attentive and strong support since I joined the laboratory in 2004. I am grateful to Annie Montagnac, Philippe Lalanne, Philippe Grangier and Antoine Browaeys for their valuable help in certain (and distinct) occasions. I also thank the administrative staff at Institut d'Optique for their kindness, availability and efficient work.

It is a great chance to be a member of the Atom Optics group, where so many beautiful and landmark experiments are performed. Far from being an isolated theoretician, I have been immediately integrated in the group, thanks to the active efforts of Alain Aspect, but also thanks to the team leaders, Philippe Bouyer and Chris Westbrook. I am particularly grateful to Philippe for his valuable help and enthusiasm in connecting my work to the first experiments on disordered condensates realized in his team. I very much appreciate our collaboration and I hope we will

keep on working together for a long time. More generally, I thank all members of the group and in particular the permanent members, Denis Boiron, Isabelle Bouchoule, Thomas Bourdel, Vincent Josse, Karen Perronet and Nathalie Westbrook as well as André Villing and Frédéric Moron, for so many interesting discussions we have on various aspects of ultracold atoms and beyond.

I am particularly indebted to my most direct collaborators. It should be stressed that none of the works that are reported in this manuscript would have been possible without the remarkable work of all present or past members of the theory team, Tung-Lam Dao, Ben Hambrecht, Pierre Lugan, Luca Pezzé, and Marie Piraud. I particularly thank them all for joining what was a virtual team at that time. Their work has certainly much contributed to the emergence of a theoretical activity on its own in the group. I would also like to associate David Clément who was a PhD student in the team of Philippe Bouyer. I very much enjoyed our frequent discussions, both about theory and experiments, which turned out be fruitful in many occasions. He will soon join us back as a permanent researcher, which I foresee as a promising perspective. Our work also much benefits from strong interactions with the members of the experimental teams of the group, in particular with Vincent Josse and Thomas Bourdel.

Almost all works reported in the manuscript result from many fruitful and stimulating collaborative works. In particular, they owe very much to Luis Santos and Anna Sanpera when I was in Hannover, to collaborations with Georgy Shlyapnikov and Dominique Delande, and, as already mentioned, to illuminating collaborative work with Alain Aspect, Philippe Bouyer and Maciej Lewenstein. I also acknowledge fruitful discussions with all authors of the papers I contributed to: Veronica Ahufinger, Baptiste Allard, Alain Bernard, Juliette Billy, Jean-Philippe Brantut, Dimitri Gangardt, Jean-Claude Garreau, Benoît Grémaud, Ben Hambrecht, Mathilde Hugbart, Robin Kaiser, Adrian Kantian, Anders Kastberg, Christian Miniatura, Cord Müller, Armand Niederberger, Thomas Plisson, Martin Robert-de-Saint-Vincent, Jocelyn Retter, Krzysztof Sacha, Thomas Schulte, Bart van Tiggelen, Andrès Varòn, Jan Wehr, Jakub Zakrzewski, and Zhanchun Zuo.

Another aspect of my activity is teaching. I thank Jean-Francois Roch and François Treussart for giving me the opportunity to join the 'Phytem' programme and the 'Préparation à l'Agrégation de Physique' at Ecole Normale Supérieure de Cachan, and Nathalie Westbrook for offering me to create a course of Statistical Quantum Physics at Institut d'Optique. Teaching with Antoine Browaeys, Alice Sinatra and Thomas Bourdel is a great chance, and I thank them all for many interesting discussions.

It is rather hard to thank on their own merit all those who influenced my work through discussions, elusive remarks or even books, articles and talks. All these aspects of scientific communication are sometimes reduced to evaluation process or competition. Their main purpose is however to exchange ideas and results, which primarily aims at forging a joint piece. In this senses also, the work presented in the manuscript should not be reduced to my sole contribution.

In addition to many other things, my parents, Jacqueline and Henri, played an invaluable role, which goes much beyond an education. Their taste for Science, their sense of ethics and their rigorous mind are examples I will always try to follow. Needless to say how much I owe Aurélie and our sons Paul and Arthur for beyond-physics life. The culture and open mind of Aurélie are an invaluable source of joy and broadening of my scope.

TABLE OF CONTENTS

INTRODUCTORY SUMMARY

In this manuscript, I report my scientific work on disordered ultracold gases, performed after my Ph-D thesis in the group of Gilbert Grynberg at Laboratoire Kastler-Brossel (Ecole Normale Supérieure, France). My Ph-D thesis work was devoted to another subject, namely the theoretical study of the dynamics of cold atoms in dissipative optical lattices, and is reported elsewhere (Sanchez-Palencia, 2003). I started working on disordered systems when I joined the theory group of Maciej Lewenstein in Hannover (Germany) as a Post-Doc researcher in 2003. I then pursued in this stimulating field when I joined the group of Alain Aspect at Institut d'Optique (Orsay and then Palaiseau, France) in 2004. During the first two years, I worked in strong collaboration with the team of Philippe Bouyer, which, together with the group of Massimo Inguscio at LENS, pioneered experiments on disordered Bose-Einstein condensates in 2005. I then participated to the theoretical analysis of the experiments performed in the group. Then, in 2006, I created, in agreement with Alain Aspect, a theory team at Institut d'Optique, which keeps on developing. Besides strong involvement in the analysis of experiments, more advanced theoretical works were then developed, mainly on (i) single-particle Anderson localization in speckle potentials, (ii) interplay of disorder and interactions in Bose gases, and (iii) effects of disorder in spin-like systems simulated with ultracold atoms. These works result from collaborations with many valuable people, and should not regarded as my sole contribution.

Our approach: A theoretical work at the interface with experiments

Before summarizing the contributions reported in the manuscript (see next section), let me comment about the general approach we have developed. It has been strongly favored by the original status of our theory team, which is independent but strongly connected to the experiments performed at Institut d'Optique. This lead us to have a twofold activity, namely direct collaborations with state-of-the-art experimental work, and development of prospective theoretical work.

Joining theoretical efforts to experimental advances - Milestone advances in physics usually result from parallel development of theoretical ideas and experimental discoveries. Confronting theory with experiments is particularly stimulating and fruitful in the field of ultracold atoms because, on one hand, experiments can be designed to precisely explore situations that have been shown to be interesting theoretically, and on the other hand, theory can perform tractable calculations in situations that are directly relevant to experiments. Therefore advances on one side can have immediate impact on the other side. Landmark examples of successful interplay

of theory and experiments in the field of ultracold atoms include works on the Mott transition (Jaksch *et al.*, 1998; Greiner *et al.*, 2002), phase fluctuations in elongated Bose-Einstein condensates (Petrov *et al.*, 2001; Dettmer *et al.*, 2001), Tonks-Girardeau gases (Paredes *et al.*, 2004), and last but not least Anderson localization (Sanchez-Palencia *et al.*, 2007; Billy *et al.*, 2008).

An independent theoretical work - In view of the rapid development of the field of disordered quantum gases (Sanchez-Palencia and Lewenstein, 2010), independent theoretical activities are however necessary for several reasons. First, frontier research demands long-lasting development of ideas, which are not limited to a single experiment. For instance, our papers (Lugan *et al.*, 2007a; Clément *et al.*, 2008) have impacted experiments by the groups at LENS (Deissler *et al.*, 2010) and Rice University (Chen *et al.*, 2008). Second, valuable theoretical work requires sophisticated techniques (*e.g.* beyond meanfield and simple perturbation theory), so that full-time theoretical effort is necessary to master the most powerful ones. Third, experimentalists and theoreticians can have complementary viewpoints. Developing both activities in parallel and confronting the outcomes and ideas can prove very fruitful. For instance, our theoretical proposal to observe Anderson localization (Sanchez-Palencia *et al.*, 2007) paved the way to breakthrough experiments (Billy *et al.*, 2008). In turn, the experimental use of speckle patterns for realizing disordered potentials triggered our interest and lead us to identify unexpected effective mobility edges (Sanchez-Palencia *et al.*, 2007; Lugan *et al.*, 2009).

These two aspects have guided the works that are reported in the present manuscript and will definitely keep on doing so in the future.

Main results reported in the manuscript

The manuscript reports the contributions of our theory team to the field of disordered quantum gases performed during the last six years (2003-2009), which are outlined below.

Chapter 1 reviews recent advances in the field of quantum gases and open issues in the field of disordered systems. It serves to set our work, not only in the emerging field of disordered quantum gases, which bridges the gap between the two communities, but also in the general context of current efforts heading at realizing ultracold-atom quantum simulators, relevant to condensed-matter physics.

Chapter 2 is devoted to Anderson localization in quasi-periodic and disordered potentials. We study non-interacting particles, which is the case considered by Anderson in his seminal work. We first review basic knowledge of Anderson localization in condensed-matter physics. We then present a scheme to observe single-particle localization using interacting Bose-Einstein condensates, which consists in inducing transport via release of the condensate from a harmonic trap. For strong disorder and strong meanfield interactions, localization shows up. We however show that it is not related to Anderson localization, but rather to the so-called disorder-induced trapping effect. Conversely, for weak disorder and weak interactions, this scheme leads to Anderson localization of the condensate and allows for a direct probe of the localization length of a non-interacting particle with a controlled energy. Finally, we discuss the consequences of the original features of speckle potentials, as used in the experiments. They are non-standard models of non-Gaussian disorder, with a power spectrum of finite support. This has important consequences, in particular, the existence of unusual effective mobility edges in one-dimensional systems.

In Chapter 3, we report investigations of the interplay of disorder and repulsive interactions. We study Bose gases at equilibrium and in the meanfield regime towards various directions.

We first develop a perturbative approach for the Gross-Pitaevskii equation, valid for disordered potentials of amplitude smaller than the chemical potential of the condensate and arbitrary correlation length. We show that repulsive interactions induce complete delocalization of the condensate, and we calculate analytically the condensate wavefunction. A direct application allowed us to explain the development of strong density modulations during time-of-flight imaging of a disordered Bose-Einstein condensate released from a harmonic trap.

We then study the quantum-state diagram of a Bose gas in a disordered potential and in the presence of weak repulsive interactions. We identify three regimes: Anderson-Lifshits glass, fragmented condensate and connected condensate. Our analysis allows us to derive analytical formulas for the typical crossovers between the various states, as well as for the corresponding equations of state.

We finally investigate many-body Anderson localization in interacting Bose-Einstein condensates. Although repulsive interactions destroy localization of single particles, we show that Anderson localization survives strong meanfield interactions in the form of localization of collective eigenstates, *i.e.* localization of the Bogolyubov quasi-particles. Our approach enlightens the role of screening, and allows us to derive an analytical formula for the localization length of the Bogolyubov quasi-particles, in excellent agreement with exact numerical calculations in one dimension.

In Chapter 4, we report studies of two-component ultracold atomic gases, *i.e.* Fermi-Bose and Bose-Bose mixtures. For optical lattices in the strongly-correlated regime, composite particles made of bare particles or the corresponding holes of both species are formed. The dynamics of the composites is governed by extended Hubbard models, the parameters of which can be calculated analytically from those of the two-component bare-particle Hamiltonian. We show that disorder in these systems leads to a very rich physics.

For instance, in Fermi-Bose mixtures, weak disorder leads to composite fermions with random interactions between nearest-neighbor sites, which can be all attractive, all repulsive, or randomly attractive and repulsive. It is then possible to form a non-interacting Fermi gas, a weakly-interacting Fermi liquid, a checker-board insulator and a domain insulator. For strong on-site inhomogeneities, it is possible to map the effective Hamiltonian onto a disordered Ising-like model, which realizes an analogue to the very debated spin glasses.

The case of Bose-Bose mixtures is equally interesting. It is possible to map the two-component Hamiltonian onto spin Hamiltonians (Ising or Heisenberg). Then, weak disorder allows simulation of random magnetic fields, which have interesting properties, in particular the so-called random-field induced order (RFIO) phenomenon. It corresponds to counter-intuitive situations where introduction of disorder favors spin ordering. RFIO is however very weak in optical lattice systems, owing to strong finite-size effects. Interestingly, ultracold atoms offer an original way to overcome this difficulty. We show that two-component Bose-Einstein condensates in the absence of a lattice can realize the continuous counterpart of the same effect and that in this case RFIO is strong and robust. It is signaled by a fixed relative phase between the two components.

In the Conclusion, we discuss future challenges posed to disordered quantum gases. We argue that ultracold atomic gases offer unprecedented possibilities to shed new and original light on many debated questions in the field of disordered systems. These include Anderson localization in dimensions higher than one, the interplay of disorder and interactions, in both weakly-interacting and strongly-interacting regimes, and effects of disorder in spin-like systems.

Chapter 1

QUANTUM GASES GO DISORDERED

In brief – *Ultracold atoms have been developing rapidly during the past three decades, opening successive new horizons. Development of laser cooling in the 1980's and evaporative cooling in the 1990's paved the way to the realization of quantum degenerate gases, i.e. Bose-Einstein condensates and degenerate Fermi seas. Ultracold atoms have reached a new frontier with the advent of controlled quantum systems in the 2000's. Realizing quantum simulators for complex systems of direct relevance to condensed-matter physics is now more than ever within our grasp. Landmark results in this direction have been reported recently, for instance Bose and Fermi Mott insulators, Tonks-Girardeau gases, the BCS-BEC crossover, quantized vortices in Fermi gases, the Berezinskii-Kosterlitz-Thouless transition, and quantum spin-like exchange to name of few.*

A particular field where ultracold-atom quantum simulators are very promising is that of disordered systems. Disorder is ubiquitous in physical systems and affects many phenomena in mesoscopic physics, such as electronic conductivity, magnetism, superfluidity and superconductivity, and the propagation of light and sound waves in inhomogeneous media. Recent progress on disordered quantum gases offer promising perspectives to shed new light on many long-standing debated questions. These include Anderson localization in dimensions higher than one, interplay of disorder and particle-particle interactions, and effects of disorder on spin-exchange couplings. In addition, ultracold atomic gases realize new systems with their own features (e.g. specific correlation functions or harmonic trapping). This poses new questions and new challenges which remain to be understood.

Research on ultracold atomic gases in disordered potentials is currently attracting a growing interest triggered by theoretical studies and recent experimental success in observing fundamental effects of disorder in quantum systems, in particular Anderson localization of matter-waves (Aspect and Inguscio, 2009; Sanchez-Palencia and Lewenstein, 2010). The field of disordered quantum gases bridges the gap between atomic physics and disordered systems. On one hand, ultracold atoms are very well controlled and versatile systems in which a variety of precise studies combining theoretical and experimental work can be performed. On the other hand, quantum disordered systems raise a number of challenging questions. They require new paradigms and new approaches compared to the usual ones that prove powerful for ordered systems but inefficient for disordered systems, *e.g.* Bloch waves and standard perturbation theory. Combining the two fields is thus very promising with a view towards precise understanding of the effects of disorder

in precisely-defined quantum systems. The field of disordered quantum gases is one aspect of a more general trend in frontier research on ultracold atoms, which aims at realizing quantum simulators with ultracold atoms to address a variety of open questions in complex systems, in particular those that are relevant to condensed-matter physics. This possibility, which is now within our grasp, is the direct result of about thirty years of impressive successful achievements in the field of ultracold atomic gases.

Hereafter, we first review past achievements and current challenges to ultracold atoms, from early times to present. We then introduce disordered systems, pointing out the most important challenges that are relevant to this field. We finally present current works that combine the two domains and we argue that ultracold atoms not only can shed new light on long-standing questions on disordered systems, but also show original features, which poses new questions and new challenges to research on disordered systems.

1.1 A brief history of ultracold atoms

Research on ultracold atomic gases has been developing dramatically during the last three decades, opening successive exciting perspectives. It is hardly possible to review all successful advances in a couple of pages, so we restrict ourselves to those that, in our view, are the most important achievements. This is a quite subjective exercise and at no rate we believe it can be exhaustive. Somehow arbitrarily, one can divide the history of ultracold atoms into three periods.

From 1980 to 1990: Towards ultralow temperatures - The history of ultracold atoms starts with first works devoted to theoretical proposals and experimental realizations of efficient schemes to cool down –*i.e.* decrease the thermal agitation – and to trap neutral atoms. The pioneering idea of using the interaction of two-level (alkaline) atoms with almost-resonant laser light was proposed in the 1970's (Wineland and Dehmelt, 1975; Hänsch and Schawlow, 1975). The so-called Doppler cooling scheme exploits imbalanced Doopler shifts on counter-propagating laser beams to produce a friction-like force. Then, competition with photon-scattering-induced fluctuating forces results in a limit temperature proportional to the linewidth of the excited state, $T_{\rm D} = \hbar\Gamma/2k_{\rm B}$. The first experiments where performed at Bell labs, showing possibility of cooling a gas of sodium atoms down to a couple of hundreds of μK (Chu *et al.*, 1985). Since then, a race towards lower temperatures started, which lasted for about ten years. Using a slightly different experimental setup, the group of William D. Phillips at NIST succeeded in reaching temperatures of a couple of tens of μK, below the theoretical Doppler limit (Lett *et al.*, 1988). This surprising result was rapidly explained by an elegant theory developed independently at Ecole Normale Supérieure (Dalibard and Cohen-Tannoudji, 1989) and at Bell labs (Ungar *et al.*, 1989) –so-called Sisyphus cooling– which accounts for different light shifts and subtle optical pumping cycles between the various atomic Zeeman sub-levels. In Doppler and Sisyphus cooling, the temperature is limited by diffusion in momentum space due to random recoils of atoms scattering photons. This yields a fundamental minimum temperature of the order of $T_{\rm R} = \hbar^2 k_{\rm L}^2/2m$ where $k_{\rm L} = 2\pi/\lambda_{\rm L}$ is the laser wavevector and m is the atomic mass (Cohen-Tannoudji, 1992). To decrease the temperature below the recoil limit, more elaborated techniques have been developed during the same period. For instance, Velocity-Selective Coherent Population Trapping (Aspect *et al.*, 1988; 1989) combines the existence of a non-absorbing (dark) state at zero momentum ($p = 0$) in a three-internal level Λ system with random walk in momentum space due to photon scattering from states at

$p \neq 0$ towards states at $p \simeq 0$. Then, the atom recoil is no longer a limit and temperatures of the order of $T_R/800$ have been achieved in metastable helium gases (Saubaméa *et al.*, 1997). Another scheme, called Raman cooling, is based on a sequence of velocity-dependent stimulated Raman pulses and optical pumping in a three-internal level system and also allows to confine atoms in near-zero momentum states (Kasevich and Chu, 1992a). Temperatures of the order of $T_R/70$ were achieved for instance in cesium atomic gases using sub-recoil Raman cooling (Reichel *et al.*, 1995).

The second challenge that was to face at that time was trapping. In Doppler and Sisyphus cooling schemes, the dynamics of the atoms can be described as a Brownian motion of classical particles, where friction results from imbalanced velocity-dependent Doppler shifts (Doppler cooling) or from delayed transfer downwards the Zeeman state of minimum energy (Sisyphus cooling), and fluctuations result from photon scattering and/or random transfer between the Zeeman sub-levels. As a result, the atoms diffuse away and escape from the experiment. There are basically two ways to trap the atoms. The first was proposed by Jean Dalibard (1987) and then demonstrated in the groups of David E. Pritchard and Carl E. Wieman (Raab *et al.*, 1987; Sesko *et al.*, 1989). It consists in using position-dependent Zeeman shifts in inhomogeneous magnetic fields to create a force towards the center of the experiment, thus realizing so-called magneto-optical traps, which are now widely used in most experiments with ultracold atoms. The second option is to use the dipole interaction of the atoms with some laser light. It creates a conservative force which points towards the regions of high laser intensity (for 'red-detuned' laser light) or towards the regions of low laser intensity (for 'blue-detuned' laser light). An important advantage of the dipole potential is its very simple dependence on the laser intensity and the detuning, $V_D \propto I_L/\Delta$. Hence, control of optical fields allows easy design of atomic traps in a variety of geometrical configurations, including one-dimensional waveguides, two-dimensional films and –most often– three-dimensional traps. In addition, optical dipole traps allow for time-dependent control of confining potentials with negligible delay, in contrast to magnetic traps.

From 1990 to 2000: Optical lattices and the advent of quantum gases - This early successful story was recognized by the award of the Nobel prize in physics to Steven Chu, Claude Cohen-Tannoudji and William D. Phillips in 1997 (Chu, 1998; Cohen-Tannoudji, 1998; Phillips, 1998), and stimulated enormous interest. The field then separated into roughly two lines of research, which remained almost independent for about ten years.

Optical lattices - The first line of research explored a new avenue offered by accurate control of parameters in cold atomic gases: the simulation of systems of interest for various branches of physics, beyond atomic physics. The most direct method is provided by laser cooling schemes themselves. For instance, Doppler cooling produces atomic gases which can be described by classical Brownian motion (Gordon and Ashkin, 1980), thus offering a first connection to statistical physics. Sisyphus cooling is even more interesting because the interference pattern of counter-propagating laser beams creates a periodic modulation of the laser intensity. Matter-light interaction then forms a periodic potential for the atoms, the so-called *dissipative optical lattices*[1] (Westbrook *et al.*, 1990; Verkerk *et al.*, 1992; Jessen *et al.*, 1992). For sufficiently low density and temperature, laser cooled atoms thus form the prototype model at the basis of the Bloch theory of electrons in solids (Ashcroft and Mermin, 1976): non-interacting particles evolving in a

[1]Dissipative optical lattices refer to schemes in which the lasers are close to the resonance of the atomic frequency, thus allowing dissipative processes such as optical pumping at the origin of Sisyphus cooling.

periodic potential made of connected trapping sites. This offers a relation to solid-state physics. A major interest of optical lattices is that the periodic potential can be controlled via the geometrical arrangement of the lasers (Jessen and Deutsch, 1996; Grynberg and Robilliard, 2001). The first experimental realization of two-dimensional (Hemmerich and Hänsch, 1993; Grynberg *et al.*, 1993) and three-dimensional (Grynberg *et al.*, 1993; Hemmerich *et al.*, 1993; Gerz *et al.*, 1993; Hemmerich *et al.*, 1994; Verkerk *et al.*, 1994) optical lattices in the early 1990's then stimulated many experimental and theoretical studies, devoted to localization in the lattice sites (Grison *et al.*, 1991; Marte *et al.*, 1993; Taïeb *et al.*, 1993; Raithel *et al.*, 1997; Gatzke *et al.*, 1997; Castin and Mølmer, 1995), the behavior of the kinetic temperature (Castin *et al.*, 1991; Berg-Sørensen *et al.*, 1993; Castin *et al.*, 1994; Raithel *et al.*, 1997; Gatzke *et al.*, 1997; Sanchez-Palencia *et al.*, 2002; Jersblad *et al.*, 2003), and spatial diffusion in extended Brownian motion models (Hodapp *et al.*, 1995; Sanchez-Palencia *et al.*, 2002). Later on, dissipative optical lattices were used to demonstrate a number of interesting phenomena, relevant to Brownian motion or more generally to statistical physics: laser cooling in disordered (Horak *et al.*, 1998; Boiron *et al.*, 1999; Grynberg *et al.*, 2000a) and quasi-periodic lattices (Guidoni *et al.*, 1997; Guidoni *et al.*, 1999), mechanical bistability (Grynberg *et al.*, 2000b), stochastic resonance (Sanchez-Palencia *et al.*, 2002; Schiavoni *et al.*, 2002; Sanchez-Palencia and Grynberg, 2003), as well as atomic ratchets in the spatial domain (Mennerat-Robilliard *et al.*, 1999), in the temporal domain (Schiavoni *et al.*, 2003; Gommers *et al.*, 2008), and ratchets in double periodic lattices (Sanchez-Palencia, 2004; Sjölund *et al.*, 2006).

It is worth stressing that, in spite of these successful achievements, there are important differences between realistic models of solids and optical lattices. First, the cohesion of solids is ensured by the interplay of Coulomb repulsion and exchange coupling between the crystal atoms, resulting in a lattice spacing of the order of a couple of $\AA$. In contrast, optical lattices are formed in the interference pattern of lasers, providing a lattice spacing of the order of 1μm, *i.e.* four orders of magnitude larger. Second, true solids host phonons, which play a major role in thermal and electronic conductivity (Ashcroft and Mermin, 1976). In contrast, optical lattices are created with very well stabilized lasers, thus suppressing phonon-like modes. Third, densities and temperatures are very different: In solids, the density of conduction electrons is $n \sim 10^{29}\mathrm{m}^{-3}$ and the temperature $T \sim 300$K. Such high densities and low temperatures bring electrons deep in the quantum regime (here, the phase-space density is $n\lambda_{\mathrm{T}}^3 \sim 10^4 \gg 1$, where $\lambda_{\mathrm{T}} = \sqrt{2\pi\hbar^2/mk_{\mathrm{B}}T}$ is the thermal de Broglie wavelength), as it is well known[2]. In contrast, Sisyphus cooling in dissipative optical lattices leads to much lower temperatures, $T \sim 10\mu$K, but also much lower atomic densities, $n \sim 10^{18}\mathrm{m}^{-3}$, corresponding to a phase-space density of $n\lambda_{\mathrm{T}}^3 \sim 10^{-4} \ll 1$. This strongly distinguishes the two systems and constitutes the major drawback of dissipative optical lattices to simulate solid-state physics (see Fig. 1.1). Finally, although classical Brownian motion is a good qualitative and reasonable quantitative model to describe atomic gases produced by laser cooling, the relevant parameters (*i.e.* friction force and dissipation) are complicated functionals of the natural parameters of the matter-light interaction (*i.e.* atom-laser detuning, laser intensity, and atomic linewidth), and it is very difficult to adjust the former values on demand via control of the latter ones.

[2]The condition for quantum degeneracy in solid-state physics –and more generally in Fermi systems– is more often written as $T \ll T_{\mathrm{F}}$ where T_{F} is the Fermi temperature. It is actually equivalent to the condition $n\lambda_{\mathrm{T}}^d \gg 1$, since $\frac{T}{T_{\mathrm{F}}} \propto \frac{1}{n_{d\mathrm{D}}^{2/d}\lambda_{\mathrm{T}}^2}$ in a homogeneous d-dimensional system. Here, we rather use the condition $n\lambda_{\mathrm{T}}^d \gg 1$, which is applicable irrespective to the quantum statistics, *i.e.* for fermions as well as for bosons.

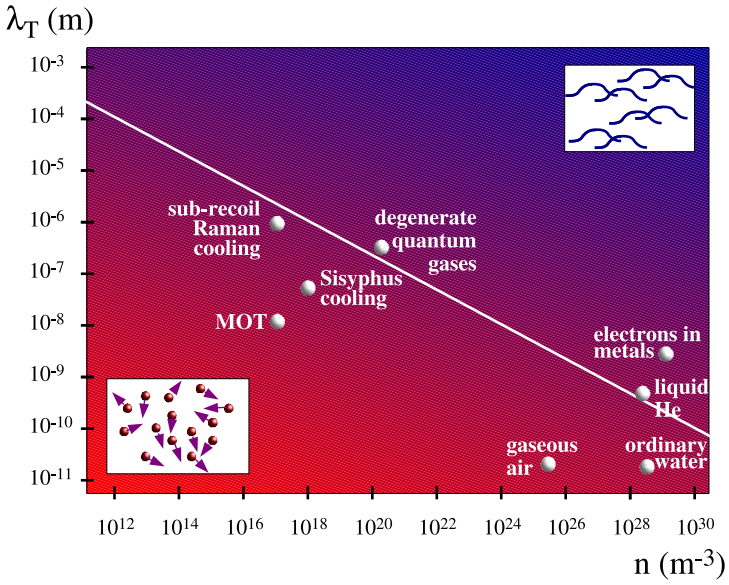

Figure 1.1 | Density-temperature diagram of condensed-matter and ultracold atom systems. The density is shown in the x-axis (in m^{-3}) and the temperature appears in the form of the thermal de Broglie wavelength, $\lambda_T = \sqrt{2\pi\hbar^2/mk_BT}$ (in m), both in log scale. The bottom-left part corresponds to classical systems ($n\lambda_T^3 \ll 1$, red), and the top-right part to quantum systems ($n\lambda_T^3 \gg 1$, blue). The white line represents the transition or crossover between the two regimes ($n\lambda_T^3 \sim 1$). The positions of the various systems correspond to typical values.

Quantum degenerate gases - The second line of research aimed at getting rid of the main drawback of Doppler and Sisyphus cooling schemes, *i.e.* limitation of achievable temperatures to the micro-Kelvin range due to dissipative processes. As discussed above, the motional degrees of freedom of the atoms behave classically, although quantum mechanics plays a major role in the dynamics of internal states. In order to reach quantum degeneracy, stronger cooling schemes needed to be developed. Strong efforts were devoted to this challenge, and finally resulted in the *evaporative cooling* method. The basic idea of which is to eliminate the highest-energy atoms from magnetic or optical traps and let it re-thermalize thanks to atom-atom interactions, so as to lower the average energy. Technically, this is achieved by reducing slowly the depth of the trap, so that high-energy atoms can escape from it. This method is in a sense very crude, since, although the temperature decreases, most of the atoms are lost during the evaporation. In the process however cooling is in a sense more efficient than atom losses, and one can cool down the atoms downwards the nano-Kelvin range, with a final density of the order of 10^{19}-$10^{20}\mathrm{m}^{-3}$ (Ketterle and van Druten, 1996). This is enough to reach quantum degeneracy (see Fig. 1.1), which appears when the de Broglie wavelength of the atoms exceeds the average distance between the atoms, *i.e.* for $n\lambda_T^3 \gtrsim 1$.

These achievements paved the way to the realization of degenerate quantum gases, which bridges the gap now from atomic physics to quantum statistical physics. For bosons, quantum degeneracy manifests itself as Bose-Einstein condensation, as predicted by Albert Einstein in 1924 (Einstein, 1924). In three-dimensional gases, this is a phase transition, which occurs at the critical temperature T_c such that $n\lambda_{T_c}^3 \simeq 2.612$. Progress in evaporative cooling allowed for the first time, the direct observation of Bose-Einstein condensation, using dilute ultracold gases in 1995 (Anderson *et al.*, 1995; Davis *et al.*, 1995). This achievement was a revolution, recognized by the award of the Nobel prize in physics to Eric A. Cornell, Wolfgang Ketterle and Carl E. Wieman in 2001 (Cornell and Wieman, 2002; Ketterle, 2002). Bose-Einstein condensation plays a major role in condensed-matter physics: It is strongly related (but not equivalent) to superfluidity, as conjectured by Fritz London (1938) and superconductivity –via condensation of Cooper pairs– (Bardeen, Cooper and Schrieffer, 1957). In these systems however, interactions are so strong that

Bose-Einstein condensation is difficult to observe without ambiguity. In contrast, ultracold atomic gases are very dilute systems, so that interactions are much weaker[3]. It allowed observation of dilute gas Bose-Einstein condensates of most of the alkaline atoms: lithium (Bradley *et al.*, 1997), sodium (Davis *et al.*,1995), potassium (Modugno *et al.*, 2001), rubidium (Anderson *et al.*, 1995; Cornish *et al.*, 2000), cesium (Weber *et al.*, 2003), as well as hydrogen (Fried *et al.*, 1998), helium (Robert *et al.*, 2001; Pereira Dos Santos *et al.*, 2001), ytterbium (Takasu *et al.*, 2003) chromium (Griesmaier *et al.*, 2005), calcium (Kraft *et al.*, 2009) and strontium (Stellmer *et al.*, 2009; Martinez de Escobar *et al.*, 2009). Summarizing all achievements and discoveries which have followed these works in a couple of lines is doomed to failure, given the amount and interest of each. More modestly, we leave the interested reader with very complete and comprehensive reviews on the subject (Dalfovo *et al.*, 1999; Ketterle *et al.*, 1999; Pitaevskii and Stringari, 2003).

For (non-interacting) fermions, quantum degeneracy corresponds to the crossover from Boltzmann (classical) statistics to Fermi-Dirac (quantum) statistics when the temperature decreases down to the Fermi temperature T_F ($n\lambda_{T_F} \simeq 0.75$ in a single-component homogeneous three-dimensional gas). This is associated to the onset of Fermi pressure –which plays a key role in the stability of matter– and the concept of Fermi surfaces –relevant in many areas of condensed-matter physics, for instance in electronic conductivity of metals. First ultracold-atom Fermi degenerate gases were produced in the early 2000, in the groups of Deborah Jin, Randall Hulet, Massimo Inguscio, and Christophe Salomon with ^{40}K atoms (DeMarco and Jin, 1999; Modugno *et al.*, 2002) and ^{6}Li atoms (Truscott *et al.*, 2001; Schreck *et al.*, 2001). Technically, Fermi gases where obtained using the so-called *sympathetic cooling* technique, which is an extension of evaporative cooling to mixtures of different atoms. At low energies (*i.e.* low temperatures) identical fermions only interact very weakly because of the Pauli exclusion principle, which prevents s-wave scattering, thus making evaporative cooling of single-component Fermi gases very inefficient. The solution is thus to cool down the Fermi gas simultaneously with another atomic species (boson, fermion or even the same fermion species but in a different internal state), so that s-wave interspecies interactions induce the re-thermalization necessary for evaporative cooling. From then on, the field of ultracold, degenerate Fermi gases has developed rapidly and, again, it is just impossible to summarize all achievements. We thus leave the interested reader with more complete reviews (Giorgini *et al.*, 2008; Ketterle and Zwerlein, 2008).

Ultracold atoms in the 21th century: Where are we now ? - The fantastic development of the field has open a new frontier to the physics of ultracold atoms towards realizing systems of direct relevance to other fields of physics. Atomic gases produced by laser cooling in the early 1990's offered a first approach to condensed-matter physics but suffered from the impossibility to reach quantum degeneracy, and from lack of full control of the parameters due to the complicated physics behind laser cooling. Conversely, degenerate quantum gases produced in the 2000's no longer suffer these drawbacks, in particular because they get rid of laser cooling (in the last cooling stage) and can be considered at thermodynamical equilibrium (although not at chemical equilibrium[4]). Ultracold atoms are now very well mastered in a number of experimental teams all over the world. On one hand, almost all parameters are accurately known, and most importantly

[3]Notable exception is cesium which has naturally strong interactions (Guéry-Odelin *et al.*, 1998). Condensation of cesium was possible only by controlling interactions via Feshbach resonance techniques (Weber *et al.*, 2003).

[4]The typical duration of an experiment on ultracold atoms is much lower than the typical time to form alkali solids, which are the true chemical equilibrium state of these systems. However, as gases, they are in thermodynamical metastable equilibrium.

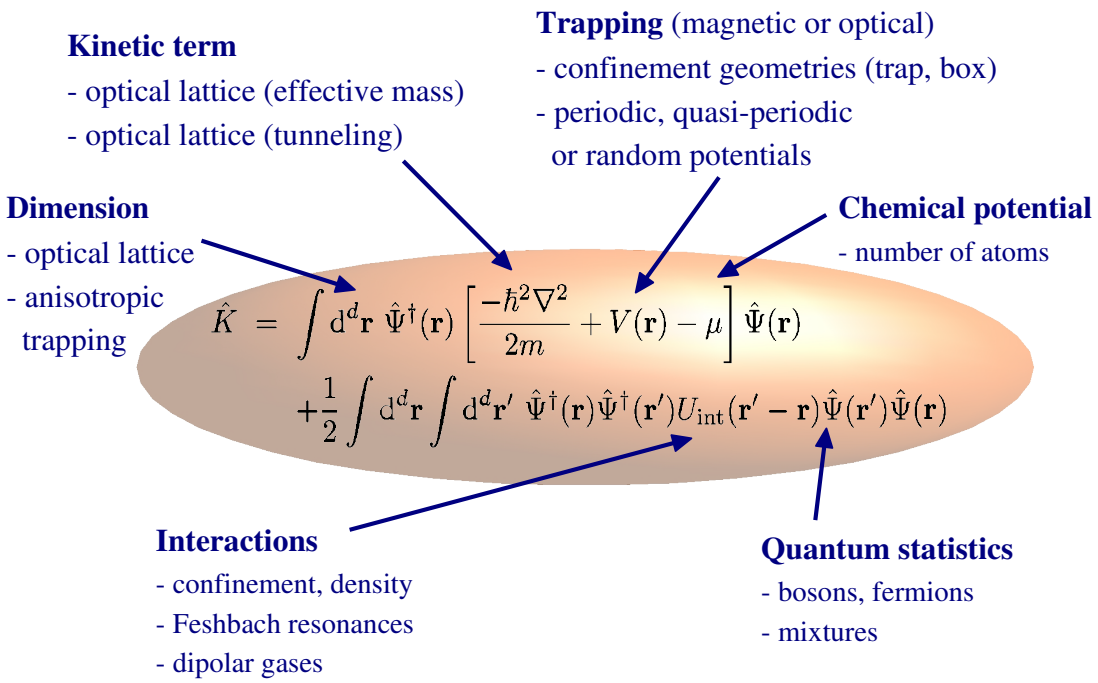

Figure 1.2 | Control toolbox for ultracold atomic gases. The figure represents an ultracold atomic gas governed by the single-species version of Hamiltonian (1.1) in the grand-canonical ensemble, $\hat{K} = \hat{H} - \mu \int d\mathbf{r}\, \hat{\Psi}^\dagger(\mathbf{r})\hat{\Psi}(\mathbf{r})$, and the tools that can be used to control the various parameters.

can be precisely controlled via a number of magnetic and/or optical field techniques (see Fig. 1.2). This offers unprecedented possibilities to

- realize quantum gases of bosons, fermions or even mixtures of the two;
- produce quantum gases in $d = 1$, 2 or 3 dimensions using anisotropic confining traps or $(3-d)$-dimensional optical lattices;
- control interactions via Feshbach resonance techniques;
- produce harmonic or box-shaped traps;
- control magnetic and/or light potentials in various geometries.

On the other hand, ultracold atoms offer a number of powerful measurement techniques, *e.g.* time-of-flight (Greiner *et al.*, 2002), spectroscopy based on interaction shifts (Jördens *et al.*, 2008), time-dependent potential modulations (Schneider *et al.*, 2008; Delande and Zakrzewski, 2009) direct imaging (Billy *et al.*, 2008; Roati *et al.*, 2008), noise interferometry (Altman *et al.*, 2004; Fölling *et al.*, 2005; Rom *et al.*, 2006), or Angle-Resolved Photo-Emission Spectroscopy-like method (Dao *et al.*, 2007; Stewart *et al.*, 2008). Precise measurement of original quantities –which are not all accessible to usual systems in condensed-matter physics– offers original perspectives.

Another important aspect is that progress in the field has very much benefited from joint experimental and theoretical work. The main reason why interactions between experiments and theory is so fruitful in ultracold atomic systems is that true experiments can be described by exact Hamiltonians, without referring to toy models, as it is usually the case in traditional condensed-matter physics. Moreover, these Hamiltonians are usually not very complicated owing to the

strong dilution of ultracold atomic gases, so that the prominent inter-particle interactions are usually two-body interactions while many-body interactions can often be ignored[5]. This leads to tractable equations for cases directly relevant to true experiments and makes the life of theoreticians easier. In the general case of mixtures of different species (labelled by σ), and possibly beyond meanfield, the physics of ultracold atoms is governed by the Hamiltonian

$$\begin{aligned}\hat{H} &= \sum_{\sigma}\int d\mathbf{r}\,\hat{\Psi}^{\dagger}_{\sigma}(\mathbf{r})\left[-\frac{\hbar^2\nabla^2}{2m_{\sigma}}+V_{\sigma}(\mathbf{r})\right]\hat{\Psi}_{\sigma}(\mathbf{r}) \\ &\quad+\frac{1}{2}\sum_{\sigma,\sigma'}\int d\mathbf{r}\int d\mathbf{r}'\,\hat{\Psi}^{\dagger}_{\sigma}(\mathbf{r})\hat{\Psi}^{\dagger}_{\sigma'}(\mathbf{r}')U_{\sigma,\sigma'}(\mathbf{r}'-\mathbf{r})\hat{\Psi}_{\sigma'}(\mathbf{r}')\hat{\Psi}_{\sigma}(\mathbf{r})\end{aligned} \tag{1.1}$$

where $\hat{\Psi}_{\sigma}$ and m_{σ} are the field operator and the mass of an atom of species σ. The first integral in Eq. (1.1) represents the Hamiltonian of a single particle in the potential $V_{\sigma}(\mathbf{r})$. The latter is controlled by the configuration of the magnetic and/or optic fields. The second integral in Eq. (1.1) represents the interaction operator, which can often be substituted to a contact effective potential[6,7], $U_{\sigma,\sigma'}(\mathbf{r}'-\mathbf{r}) = g_{\sigma,\sigma'}\delta(\mathbf{r}'-\mathbf{r})$ where $g_{\sigma,\sigma'}$ is the coupling constant for interacting atoms of same or different species. Repulsive and attractive interactions correspond to $g_{\sigma,\sigma'}>0$ and $g_{\sigma,\sigma'}<0$, respectively. The value and the sign of $g_{\sigma,\sigma'}$ can be controlled in quantum gases using Feshbach resonances. There are several limiting cases that we briefly outline below.

Meanfield regime - The most usual limit is the weak-interaction regime where quantum correlations are weak. One can then use a meanfield approximation, which amounts to replace the field operator $\hat{\Psi}(\mathbf{r})$, by a complex classical field $\psi(\mathbf{r})$. Minimization of the corresponding energy functional in the grand-canonical form then leads to the Gross-Pitaevskii (non-linear Schrödinger) equation (Pitaevskii and Stringari, 2003):

$$\mu\psi(\mathbf{r}) = \left[-\frac{\hbar^2\nabla^2}{2m}+V(\mathbf{r})+g|\psi(\mathbf{r})|^2\right]\psi(\mathbf{r}) \tag{1.2}$$

where μ is the chemical potential. Equation (1.2) or its time-dependent counterpart (obtained by replacing the left-hand-side term by $i\hbar\partial_t\psi$) is relevant to very many experiments on Bose-Einstein condensates (Ketterle *et al.*, 1999).

Optical lattices - An other important case is that of optical lattices. In strong contrast with the Sisyphus cooling scheme where both are intimately related, here cooling and trapping in a periodic lattice can now be separated from each other. Optical lattices can thus be produced in dissipationless systems and reach the quantum degenerate regime. Ultracold atomic lattice gases and solid-state systems are then governed by similar Hamiltonians[8]. Hence, ultracold atomic systems have become of direct relevance to condensed-matter physics (Bloch, 2005; Lewenstein *et al.*, 2007).

[5]Exceptions include the physics of three-body (Petrov, 2004; Kraemer *et al.*, 2006; Levinsen *et al.*, 2009) and four-body (Ferlaino *et al.*, 2009) Efimov states.

[6]Important exceptions however concern chromium gases or heteronuclear molecules which interactions are long-range dipole-dipole interactions (Lahaye *et al.*, 2009).

[7]For simplicity, we omit here the regularization term in the expression of $U_{\sigma,\sigma'}$ (Castin, 2001).

[8]It is worth stressing that the characteristic parameters of ultracold atomic systems and usual condensed-matter systems differ by orders of magnitude (see Fig. 1.1). Nevertheless, what is relevant is the ratio of the various parameters, which can be similar for the two systems.

For instance, it was possible to observe Bloch oscillations (Ben Dahan *et al.*, 1996; Peik *et al.*, 1997), and to directly image Bloch bands (Greiner *et al.*, 2001) with bosons, and Fermi surfaces of non-interacting lattice fermions (Köhl *et al.*, 2005). A major advance in the physics of optical lattices was then realized in 1998 by the group of Peter Zoller, which paved the way to strongly-correlated lattice systems (Jaksch *et al.*, 1998). In deep lattices, atoms in the quantum regime are trapped in lattice wells. They can jump from site to site via quantum tunnelling (with a rate τ), and two atoms interact mainly in the same site (with an energy U). This physics can thus be modeled by the so-called Hubbard Hamiltonian (Hubbard, 1963), *i.e.* the discrete version of Hamiltonian (1.1):

$$\hat{H} = -\sum_{\sigma,\langle j,l\rangle} \tau_\sigma \left(\hat{a}^\dagger_{\sigma,j}\hat{a}_{\sigma,l} + \text{h.c.}\right) + \sum_{\sigma,j} V_{\sigma,j}\, \hat{a}^\dagger_{\sigma,j}\hat{a}_{\sigma,j} + \frac{U_{\sigma,\sigma'}}{2} \sum_{\sigma,\sigma',j} \hat{a}^\dagger_{\sigma,j}\hat{a}^\dagger_{\sigma',j}\hat{a}_{\sigma',j}\hat{a}_{\sigma,j} \qquad (1.3)$$

where the sum over $\langle j,l\rangle$ covers all pairs of nearest-neighbor lattice sites and, $\hat{a}_{\sigma,j}$ is the annihilation operator of an atom of species σ in site j. Hence, ultracold atoms (bosons or fermions) in optical lattices mimic the Hubbard model, which is widely considered in condensed-matter physics (Auerbach, 1994; Sachdev, 1999), for instance to capture the essential physics of electrons in solids. In contrast to condensed-matter systems however, Hamiltonian (1.3) can be shown to be exact in the limit of deep lattices, low temperatures and low interactions. The parameters τ_σ, $V_{\sigma,j}$ and $U_{\sigma,\sigma'}$ in Eq. (1.3) can indeed be calculated *ab initio* from the potential $V_\sigma(\mathbf{r}) \rightarrow V_\sigma(\mathbf{r}) + V_\sigma^{\text{latt}}(\mathbf{r})$ and the coupling constant $g_{\sigma,\sigma'}$ in Eq. (1.1) and are thus controllable in experiments (Jaksch *et al.*, 1998; Werner *et al.*, 2005).

Strongly-correlated, continuous systems - Hamiltonian (1.1) is a generic model in many areas of condensed-matter physics, which is not restricted to lattice systems. In systems with contact interactions, strong correlations generically appear when the meanfield interaction energy, gn, becomes larger than the kinetic energy, $\hbar^2/mn^{-2/d}$, needed to localize the particles in distinct (non-overlapping) regions, *i.e.* when $\gamma \equiv mgn^{1-2/d}/\hbar^2 \gtrsim 1$. Interestingly, this regime can be achieved also in continuous systems in two ways, without optical lattices. First, one can directly tune the strength of interactions taking advantage of the strong dependence of the coupling parameter g on magnetic fields in the vicinity of Feshbach resonances (Inouye *et al.*, 1998; Cornish *et al.*, 2000). Second, one may change the atomic density but this method strongly depends on the dimension of the system. In three dimensions, one should increase the density but it is hardly possible to do it enough so as to reach the strongly-correlated regime without an optical lattice. In two dimensions, the condition of strong correlations actually does depend on the density, so this method does not work. In one dimension, quite paradoxically, one should decrease the density in order to reach the strongly-correlated regime, which corresponds here to the so-called Tonks-Girardeau gas (Tonks, 1936; Girardeau, 1960; Olshanii, 1998; Petrov *et al.*, 2000b).

Present perspectives - As shown above, the past decades have witnessed impressive progress in the field of ultracold atomic systems. Many challenging bottlenecks have been remarkably passed through but they just opened new promising horizons. Unprecedented control in these systems as well as development of original measurement techniques now change the research perspectives in the field. On one hand, development of robust advanced systems with ultracold atoms is just starting. This includes for instance atom lasers (Mewes *et al.*, 1997; Anderson and Kasevich, 1998; Hagley *et al.*, 1999; Bloch, 1999; Guerin *et al.*, 2006), atomic clocks (Kasevich *et al.*, 1989; Clairon *et al.*, 1991; Sortais *et al.*, 2001), as well as inertial sensors, such

as accelerometers (Kasevich and Chu, 1992b; Snadden *et al.*, 1998; Peters *et al.*, 1999; Peters *et al.*2001; McGuirk *et al.*, 2002) and gyroscopes (Riehle *et al.*, 1991; Gustavson *et al.*, 1997; Gustavson *et al.*, 2000). On the other hand, ultracold atoms are more and more considered to realize quantum simulators, *i.e.* clean, versatile and controlled physical systems that can be used to solve exactly complicated problems (Feynman, 1982; Lloyd, 1996; Cirac and Zoller, 2004). An important application domain is condensed-matter physics, the most generic models of which are governed by Hamiltonians which are almost exact for degenerate quantum gases. Several experiments have already succeeded in demonstrating the ability of ultracold atoms to address complex problems by mimicking model-systems of condensed-matter physics[8]. Landmark results –depicted in Fig. 1.3– include observation of Bose (Greiner *et al.*, 2002) and Fermi (Jördens *et al.*, 2008; Schneider *et al.*, 2008) Mott insulators, Tonks-Girardeau physics (Kinoshita *et al.*, 2004; Paredes *et al.*, 2004), the BCS-BEC crossover (Greiner *et al.*, 2003; Jochim *et al.*, 2003; Zwerlein *et al.*, 2003; Bourdel *et al.*, 2004), quantized vortices in Fermi gases (Zwierlein *et al.*, 2005), Berezinskii-Kosterlitz-Thouless physics (Hadzibabic *et al.*, 2006), quantum spin-like exchange (Anderlini *et al.*, 2007; Trotzky *et al.*, 2008) and Anderson localization (Billy *et al.*, 2008; Roati *et al.*, 2008). Hence, realizing quantum simulators is now within our grasp. Quantum simulators could then replace (hypothetic) ultra-powerful and dedicated computers and address a number of issues in various complex systems where many questions are open or even controversial. Examples include fermionic superfluidity, high-T_c superconductivity or frustrated systems. Another important class of systems where ultracold atoms are extremely promising to pursue a number of outstanding challenges is that of disordered systems.

1.2 Disordered systems: An active research field with many open questions

Disordered systems form a central field of condensed-matter physics, which encompasses basically all systems that cannot be described by the clean models we are used to, for instance homogeneous media or perfectly-periodic crystal solids. An immediate example concerns is the propagation of waves in fully a random medium, which can be seen as a potential or a refractive-index field with no long-range order. It also concerns almost any system with very small imperfections. Hence, the physics of disordered systems roots back to early studies of electrons in solids, and particularly to efforts to understand why some materials are metals are some others are insulators. Besides band and Mott insulators (see Sec. 2.1.1), it was indeed proposed by Philip W. Anderson that disorder (*i.e.* small imperfections in solids) can lead to metal-insulator transitions by localizing quantum particles (Anderson, 1958).

Disorder is actually ubiquitous in Nature and thus plays a central role in many areas of physics, beyond condensed-matter physics itself, for instance in Optics, Acoustics, Microfluidics and Seismology. In a sense, disordered systems are more generic than ordered systems. Beside practical interest for designing high-precision devices (*e.g.* interferometers, accelerometers, gyroscopes, ...), or for analyzing wave signals propagating in imperfect media, understanding the effects of disorder is a major issue from a fundamental point of view. Hence, when attempting to understand the effects of disorder in condensed-matter systems, one faces severe difficulties. First, standard theoretical concepts developed in the context of clean systems (*e.g.* Bloch waves or ferromagnetism) break down in the presence of disorder. New paradigms and sophisticated techniques, such as diagrams (Lee and Ramakrishnan, 1985), the scaling theory (Abrahams *et al.*, 1979), ultrametric-

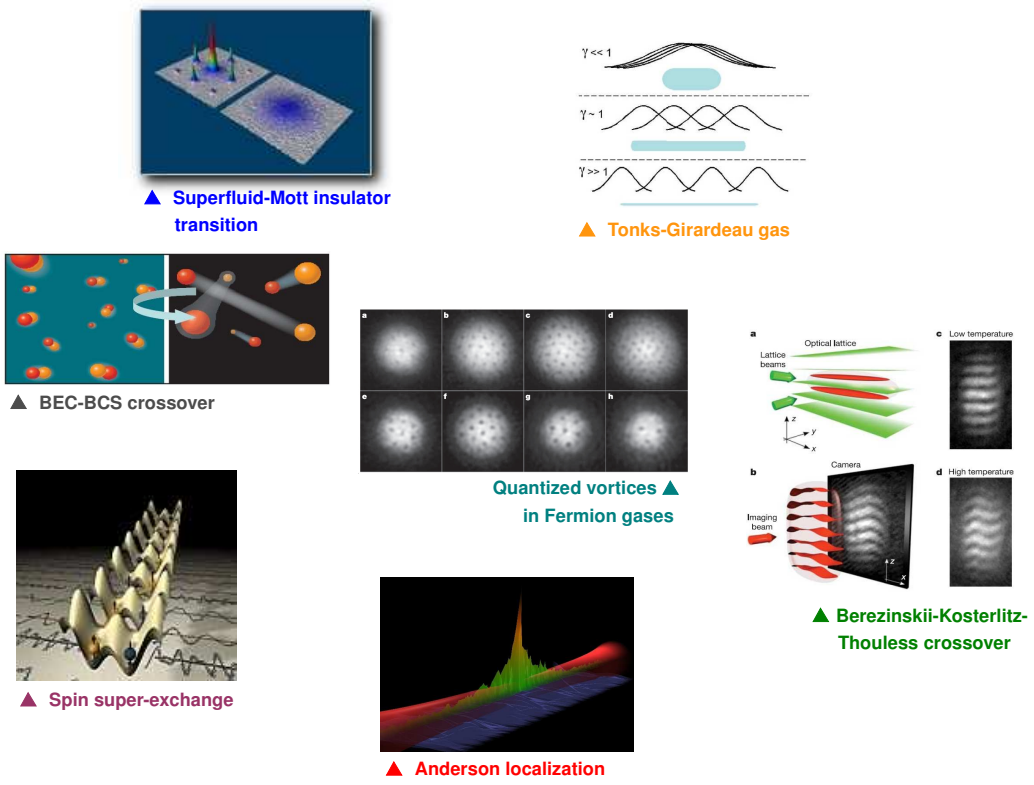

Figure 1.3 | Towards quantum simulators with ultracold atoms. From top to bottom and from left to right: Mott insulators (Munich, Zurich and Mainz groups), Tonks-Girardeau gases (Penn State and Mainz groups), BEC-BCS crossover (JILA, Innsbrück, MIT and ENS groups), quantized vortices in Fermi gases (MIT group), Berezinskii-Kosterlitz-Thouless physics (ENS group), quantum spin-like exchange (NIST and Mainz groups), Anderson localization (Institut d'Optique and Florence groups).

ity (Mézard *et al.*, 1986), supersymmetry (Efetov, 1983) or the replica method (Mézard *et al.*, 1986; Giamarchi *et al.*, 2004) are thus required. Second, the phase or Hilbert space is often too large to perform exact numerical calculations in systems of relevant size, and restriction to relevant sub-spaces is difficult owing to the system complexity. Finally, it is often difficult to control experimentally the amount and nature of impurities, so as to isolate effects which are purely due to disorder. Hence, rather than studying the complete Hamiltonians of real systems, our understanding of disorder in physical systems is mainly based on the simplest models one can construct to represent reasonably a given physical situation.

Strikingly enough, even a small amount of impurities can strongly affect physical systems, in particular in mesoscopic physics where interference effects govern a variety of phenomena (Akkermans and Montambaux, 2006). The most celebrated example is Anderson localization of waves. It results from destructive interference between the diffusive paths associated to multiple scattering from random impurities, yielding wavefunctions with exponentially decaying tails and absence of diffusion (Lee and Ramakrishnan, 1985). In condensed-matter physics where the concept of localization was introduced for the first time fifty years ago, the Anderson transition (Anderson, 1958) is now considered, together with electronic band gaps (Ashcroft and Mermin, 1976) and the Mott transition (Mott, 1949; 1968), as one of the central paradigms of metal-insulator transitions.

However, full description of disordered solids is very demanding because disorder, interactions, kinetic energy and possibly spin couplings usually play entangled roles.

Research on disordered systems is now an interdisciplinary field, which, after fifty years of Anderson localization, is more active than ever, as witnessed by several landmark results reported in the last few years on various systems such as light waves, sound waves, and matter waves (Lagendijk *et al.*, 2009; Aspect and Inguscio, 2009). However many questions are still open or even controversial. This concerns for instance

- Anderson transition of non-interacting quantum particles in dimensions one, two and three;
- The role of inter-particle interactions on localization;
- Strongly-correlated disordered systems (and the associated Bose or Fermi glasses);
- Spin systems with random exchange coupling terms (and the associated spin glasses).

All these challenging issues lie at the forefront of modern research on disordered systems. In the past decades, Optics has been one of the leading areas in the field, where Anderson localization has been first reported (Wiersma *et al.*, 1997). However, several of the above challenging issues on disordered systems lie beyond the scope of Optics. This concerns for instance the effect of particle-particle interactions or the effect of disorder on quantum magnetism. It is thus worth developing alternative fields where these long-standing challenges can be pursued with novel viewpoints. In this respect, ultracold atoms offer a novel perspective because model systems can be designed at will, for instance in fully controlled disordered potentials (Sanchez-Palencia and Lewenstein, 2010).

1.3 Disordered quantum gases: Controlled disorder in controlled systems

It may appear strange to investigate disorder with ultracold atoms, which are very clean and naturally free of random impurities (Dalfovo *et al.*, 1999; Ketterle *et al.*, 1999; Giorgini *et al.*, 2008; Ketterle and Zwerlein, 2008). The key is that one can subject ultracold atoms to *controlled disordered potentials*, a rather rare opportunity in usual systems. The most promising technique to produce disorder in ultracold atomic systems is to use optical potentials (either truly disordered speckle fields or quasi-periodic bichromatic lattices) because their statistical properties (*e.g.* the average intensity and the correlation length) can be precisely controlled (Clément *et al.*, 2006; Fallani *et al.*, 2008). In the last few years, research on disordered quantum gases has emerged fast and one can now consider that it is at the early stage of maturity since –as we will see– on one hand, landmark results have been already reported, and, on the other hand, many challenging issues are still open (Sanchez-Palencia and Lewenstein, 2010).

Investigation of disorder with cold atoms dates back to 1994 with first studies of one-dimensional dynamical localization in kicked-rotors (Graham *et al.*, 1992; Moore *et al.*, 1994), and of three-dimensional cooling and classical diffusion in speckle potentials (Horak *et al.*, 1998; Boiron *et al.*, 1999; Grynberg *et al.*, 2000a). In 2003, Maciej Lewenstein, Peter Zoller and coworkers (Damski *et al.*, 2003), and Robert Roth and Keith Burnett (2003) proposed to realize quantum degenerate bosons in truly disordered potentials and investigate two of the most outstanding issues in the field of disordered systems, namely Anderson localization and Bose glasses. These works have triggered enormous interest, and experimental investigations, pioneered by the groups of Massimo Inguscio (Lye *et al.*, 2005; Fort *et al.*, 2005), Alain Aspect (Clément *et al.*,

2005) and Wolfgang Ertmer (Schulte *et al.*, 2005), started immediately. The field is still growing with several groups in Europe [LENS (Lye *et al.*, 2005; Fort *et al.*, 2005; Fallani *et al.*, 2007; Roati *et al.*, 2008; Deissler *et al.*, 2010), Institut d'Optique (Clément *et al.*, 2005; Clément *et al.*, 2006; Clément *et al.*, 2008; Billy *et al.*, 2008), Hannover (Schulte *et al.*, 2005; Drenkelforth *et al.*, 2008.), Lille (Chabé *et al.*, 2008)], and in the United-States [Rice University (Chen *et al.*, 2008), Urbana Champain (White *et al.*, 2008; Pasienski *et al.*, 2009), NIST (Edwards *et al.*, 2008)] working on disordered quantum gases. In parallel, many theoretical works have been performed, for instance in Hannover/Barcelona (Damski *et al.*, 2003; Schulte *et al.*, 2005; Sanpera *et al.*, 2004; Wehr *et al.*, 2006; Neiderberger *et al.*, 2008; Neiderberger *et al.*, 2009), in Bayreuth/Nice/Paris (Kuhn *et al.*, 2005; Kuhn *et al.*, 2007; Zakrzewski and Delande, 2009), in Orsay (Bilas and Pavloff, 2006; Paul *et al.*, 2007; Albert *et al.*, 2008; Albert and Leboeuf, 2010), in Regensburg (Paul *et al.*, 2007; Hartung *et al.*, 2008), in Israel (Shapiro, 2007; Akkermans *et al.*, 2008; Gurevich and Kenneth, 2009), in Grenoble (Skipetrov *et al.*, 2008), in Francfort (Bissbort and Hofstetter, 2009; Byczuk *et al.*, 2009) and in our team at Institut d'Optique (Sanchez-Palencia, 2006; Sanchez-Palencia *et al.*, 2007; Lugan *et al.*, 2007a; Lugan *et al.*, 2007b; Clément *et al.*, 2008; Sanchez-Palencia *et al.*, 2008; Lugan *et al.*, 2009; Pezzé *et al.*, 2009; Piraud *et al.*, 2011; Pezzé and Sanchez-Palencia, 2011).

In the first years, the main motivation of these works was a quest for the 'Holy Grail', *i.e.* direct signatures of Anderson localization of matter-waves using Bose-Einstein condensates. Reaching the goal was extremely challenging and indeed, the first attempts showed a localization effect which was not related to Anderson localization (Clément *et al.*, 2005; Fort *et al.*, 2005) but rather to the so-called disorder-induced trapping effect (Sanchez-Palencia *et al.*, 2008). Then, new theoretical works (Schulte *et al.*, 2005; Sanchez-Palencia *et al.*, 2007) showed new routes and both groups at Institut d'Optique and LENS succeeded in observing Anderson localization with Bose-Einstein condensates (Billy *et al.*, 2008; Roati *et al.*, 2008). These results are the first direct signatures of Anderson localization of a matter-wave of any kind. The main ingredients of the success are i) accurate control of the disorder, ii) negligible inter-atomic interactions, iii) strong isolation from the environment, iv) direct imaging of density profiles and last but not least v) joint theoretical and experimental efforts. The combination of all these features is a unique possibility offered by ultracold quantum gases.

Beyond a dramatic success in the fifty-year-old quest to observe Anderson localization of (quantum) matter-waves, it is worth realizing that these experiments (Billy *et al.*, 2008; Roati *et al.*, 2008) now open the path towards many profound studies and fundamental discoveries in the field of disordered systems, beyond ultracold atoms and beyond Anderson localization. In particular, the good agreement between experiments and theory reported in these works shows that we can trust the potential of such experiments to realize quantum simulators for more complicated situations, in particular the challenges pointed out above (see list on page 26). In spite of many landmark results, numerous related issues are still open or even controversial. We argue below that ultracold atoms offer extremely promising perspectives to shed new light on these questions. In addition, we show that they pose new questions and new challenges that have not been addressed before.

The reason why ultracold atoms are so promising to shed new light on disordered systems is twofold. First, they are highly controlled and versatile systems, so that theories can be tested directly in experiments. The main aim of theoretical works is thus to propose feasible experiments to address relevant questions. Second, ultracold atoms offer a number of original measurement

techniques (*e.g.* time-of-flight, spectroscopy based on interaction shifts, ...), which are complementary to those of condensed-matter physics (*e.g.* conductivity and transport measurements). This triggers many advanced works in the field of ultracold atoms, and, for instance, many theoretical studies aim at identifying new observables and new approaches. It is however worth going beyond this approach. Indeed, it is important to keep in mind that, although ultracold atoms are very well controlled systems, they do not always reproduce exactly standard toy-models of condensed-matter physics, but introduce new ingredients. This is a fundamental point of both experimental and theoretical importance, which is sometimes disregarded. On one hand, new ingredients turn out to be crucial to realize certain systems. For instance, harmonic traps, which are always present in experiments with ultracold atoms, can paradoxically help by avoiding delicate control of atom number to ensure integer filling of potential wells in Mott insulators (Jaksch *et al.*, 1998; Greiner *et al.*, 2002; Jördens *et al.*, 2008; Schneider *et al.*, 2008). On the other hand, it can significantly change usual pictures. For instance, true Bose-Einstein condensates do exist in one- and two-dimensional trapped gases (Petrov *et al.*, 2000a; Petrov *et al.*, 2000b; Petrov *et al.*, 2004) while they don't in homogeneous systems in the thermodynamical limit. Another example, which is directly relevant to Anderson localization of matterwaves (Billy *et al.*, 2008), is provided by speckle potentials. They indeed form an original class of disorder, where effective mobility edges exist in one dimension (Sanchez-Palencia *et al.*, 2007). This is a very unusual case, which is a direct consequence of long-range correlations of speckle potentials (Gurevich and Kenneth, 2009; Lugan *et al.*, 2009). Yet another example is the effect of harmonic trapping, which significantly affects localization properties, showing unusual coexistence of localized and extended states (Pezzé and Sanchez-Palencia, 2011).

Hence, the original features of ultracold atoms provide new tools and new viewpoints to the field of disordered systems. These features are of great promise to shed new light on challenging issues in the field of disordered systems in general, by providing new results, new questions, and maybe new ideas. Let us finally stress that the case of Anderson localization in speckle potentials exemplifies the fact that current efforts devoted to realize quantum simulators call for joint experimental and theoretical work, to

- Propose new experiments;
- Identify relevant observables;
- Explore novel situations that have not been yet addressed;
- Develop new theories applicable to ultracold atoms.

Chapter 2

ANDERSON LOCALIZATION IN DISORDERED QUANTUM GASES

In brief – *Anderson localization is a paradigm effect in disordered systems. It is an ubiquitous phenomenon in wave physics, which in particular plays a central role in metal-insulator transitions. It results from interference of multiply-scattered paths from defects of the medium, yielding absence of diffusion and wavefunctions with exponential tails. First evidence of Anderson localization was reported for classical waves from the late 1990's, but it remained elusive for matterwaves. In this respect, ultracold atoms offer new perspectives. Here, we first introduce Anderson localization, i.e. basic theoretical knowledge and experimental evidence of localization of classical waves. We then present our theoretical contributions to the study of localization of matterwaves in quasi-periodic and disordered potentials.*

Quasi-periodic potentials can simulate disorder in finite-size systems. We show that a condensate at equilibrium in a two-dimensional quasi-periodic lattice acquires quasi-periodic long-range order, which can be evidenced with time-of-flight techniques. When released from a trap in such a potential, the condensate gets localized, i.e. diffusion is completely suppressed.

True disorder can be realized using optical speckle. We show that an initially interacting Bose-Einstein condensate released from a harmonic trap in a speckle potential offers an ideal probe of Anderson localization of non-interacting particles. For strong disorder, localization occurs. It is however not related to Anderson localization, but rather to fragmentation of the condensate. For weak disorder, Anderson localization shows up in the form of exponential tails. We show that speckle potentials are non-standard models of disorder, which are non-symmetric and non-Gaussian but inherit some properties of Gaussian disorder. This induces unusual features, such as effective mobility edges in one dimension. Our prediction were confirmed by recent experiments.

2.1 Introduction to Anderson localization

Condensed-matter physics is devoted to the investigation of dense systems, the main characteristics of which are strong interactions and relevance of quantum mechanics. Both usually play non-trivial combined roles. As a result, even simple questions have generally complex answers

and very often require long developments of ideas, concepts, theoretical calculations and experimental investigation. For instance, in electronic conductivity, which lies at the very heart of condensed-matter physics, such a question is: Why are some materials insulators, while other ones are metals ? Of course, the well-known Bloch theory of solids provides an immediate answer directly related to the band structure of the single-electron spectrum. It was however rapidly understood that this is just a small part of the story, as both electron-electron interactions (Mott and Peierls, 1937) and crystal imperfections (Anderson, 1958) should play a non-negligible role, which is still debated.

2.1.1 Metal-insulator transitions in condensed-matter physics

Metal-insulator transitions in condensed-matter physics are conveniently described by the Hubbard model on a d-dimensional hypercubic lattice [see Introduction, Eq. (1.3)]:

$$\hat{H} = -\tau \sum_{\langle j,l\rangle,\sigma} \left(\hat{c}^{\dagger}_{\sigma,j} \hat{c}_{\sigma,l} + \text{h.c.} \right) + \sum_{\sigma,j} V_j \, \hat{c}^{\dagger}_{\sigma,j} \hat{c}_{\sigma,j} + \frac{U}{2} \sum_{j} \hat{c}^{\dagger}_{\uparrow,j} \hat{c}^{\dagger}_{\downarrow,j} \hat{c}_{\downarrow,j} \hat{c}_{\uparrow,j}, \tag{2.1}$$

where the sum over $\langle j,l\rangle$ covers all pairs of nearest-neighbor lattice sites. In Hamiltonian (2.1), τ is the nearest-neighbor tunneling rate, $\hat{c}_{\sigma,j}$ is the annihilation operator of an electron of spin σ in site j, V_j is the energy attached to site j, and U represents the interaction energy, which is assumed to be restricted to two electrons with opposite spins in a single site. One then distinguishes three types of insulators:

Band insulators - For $V_j \equiv 0$ and $U = 0$, we are left with non-interacting electrons in a periodic homogeneous lattice. This is the situation described by the quantum theory of solids of Felix Bloch (Ashcroft and Mermin, 1976). All single-electron states are periodic and thus extend over the full system. Hence, they can in principle support electronic transport. Splitting of the energy spectrum into a succession of bands should however be taken into account. If the Fermi energy lies inside a band, the electrons can indeed move under the effect of an infinitesimal force, and the material is a metal. If instead, the Fermi energy lies in between two bands, electronic transitions between different states are strongly suppressed due to the band gap, and the material is an insulator (see Fig. 2.1a).

Mott insulators - In the presence of weak repulsive interactions ($U > 0$, but still $V_j \equiv 0$), the Fermi liquid theory shows that the above picture is not strongly modified, provided that one considers quasi-particles rather than bare particles. Quasi-particles incorporate the effect of interactions in their dispersion relation. As shown by Nevill Mott however, strong repulsive interactions induce a metal-insulator transition at half-filling of a band (Mott, 1949; Mott, 1968). For strong-enough interactions, $U \gg \tau$, and low-enough temperature, $k_{\rm B}T \lesssim U$, the many-body states of the Fermi system are formed of particles, each localized in a different lattice site[1]: $|\Psi\rangle \propto \Pi_j \, \hat{c}^{\dagger}_{j,\sigma_j} |0\rangle$. Here, electronic transport is strongly suppressed because the electrons are localized in the lattice sites and mutually hamper their motion, owing to either Pauli blocking or repulsive interactions. Indeed, moving an electron, say with spin $\uparrow$, from site j to a neighboring site l is forbidden if the electron in l has spin $\uparrow$, and requires at least the finite amount of energy U if the electron localized in l has spin $\downarrow$ (see Fig. 2.1b).

[1] Below the Néel temperature, $T_{\rm N} \sim 4\tau^2/k_{\rm B}U$, the Fermi-Mott insulator displays anti-ferromagnetic order, *i.e.* the σ_j's are opposite in adjacent sites (Georges, 2008).

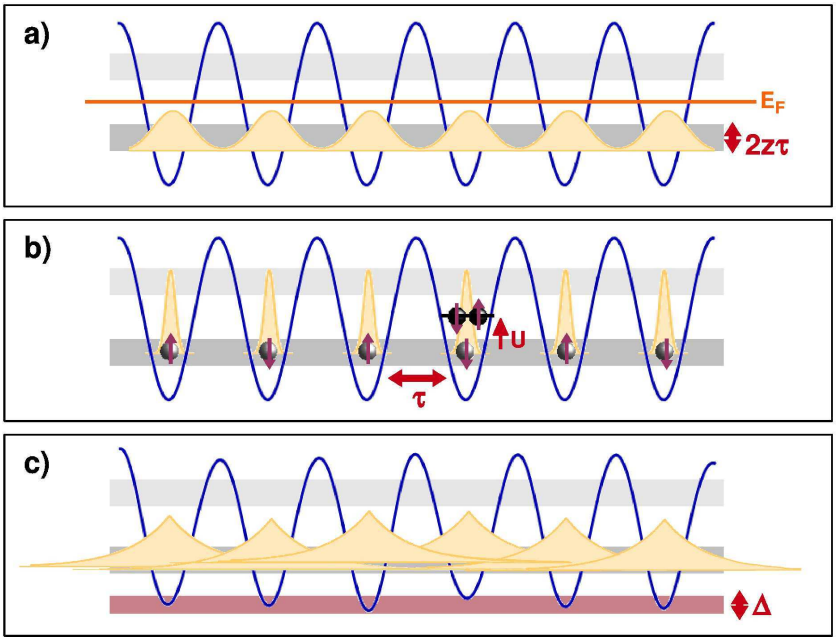

Figure 2.1 | **Insulators in condensed-matter physics. a)** Band insulator: The electronic states are Bloch waves, which are all extended and may support transport. When the Fermi energy $E_{\rm F}$ lies in a band gap, transport is however suppressed due to full filling of the conduction band. **b)** Mott insulator: The electrons populate localized Wannier states. Transport is governed by the competition between tunneling and interactions. At half filling ($N_\uparrow = N_\downarrow = N_{\rm sites}/2$), when the interaction energy U gained by the system when an electron jumps from one site to the other exceeds the tunneling energy $z\tau$, transport vanishes. **c)** Anderson insulator: In a disordered lattice, non-interacting electrons populate localized states, which do not support transport even for partial filling of the Bloch bands.

Anderson insulators - There is yet another way to form an insulator from the Hubbard model, as shown by Philip W. Anderson (1958). Let us consider non-interacting fermions ($U = 0$) but now in an inhomogeneous lattice (the V_j's are not all equal). The translation invariance by integer numbers of a lattice period –which is at the origin of the Bloch theorem– is now broken, and the question arises as to know whether the single-particle electron states are extended –thus supporting transport– or not. Anderson considered the case of a disordered lattice, *i.e.* with random valued V_j, hence mimicking lattice imperfections in real solids. In the simplest model, one considers independent random V_j, uniformally distributed in the interval $[-\Delta/2, +\Delta/2]$ (see Fig. 2.1c). The dynamics of Hamiltonian (2.1) is then governed by the sole parameter[2] Δ/τ. For $\Delta = 0$, the spectrum is continuous but limited to the lowest band of the lattice, *i.e.* $-z\tau < E < z\tau$, where the coordination number, z equals $2d$ in a d-dimensional hypercubic lattice. Now, do electrons diffuse away in such a model for $\Delta \neq 0$?

Inspired by experimental data showing long-lived electronic spins in doped semi-conductors,

[2]Note that in a bi-partite lattice –*i.e.* a lattice made of two sub-lattices A and B with twice the period each and displaced by one lattice period, *e.g.* a cubic lattice– the localization properties do not depend on the sign of τ. Indeed, any single-particle state can be written as $|\psi\rangle = \left(\sum_{j\in A} \alpha_j \hat{c}_j^\dagger + \sum_{l\in B} \alpha_l \hat{c}_l^\dagger\right)|0\rangle$. Now, if $|\psi\rangle$ is an eigenstate of $\hat{H}(+\tau)$, then the associated staggered state, $|\widetilde{\psi}\rangle = \left(\sum_{j\in A} \alpha_j \hat{c}_j^\dagger - \sum_{l\in B} \alpha_l \hat{c}_l^\dagger\right)|0\rangle$, is an eigenstate of $\hat{H}(-\tau)$ with same energy. Since, the localization properties are determined by the behavior of the $|\alpha_j|$'s only (with $j \in \{A, B\}$), they are the same for $|\psi\rangle$ and $|\widetilde{\psi}\rangle$.

thus compatible with electron localization, Anderson considered an initially single electron (spin) located in a given site and then estimated the probability to diffuse away. The calculation is quite tedious and may be summarized by the following now quite consensual picture. In each site, a part of the wave packet is transmitted and the other one is scattered. This yields many Feynman paths which have to be summed up coherently. In a perfect –*i.e.* non-disordered– lattice, the scattering processes work in phase from site to site, giving rise to the band structure. In a disordered lattice, the wave packets acquire a random phase and interfere destructively. It leads to the following conclusion applicable to a three-dimensional cubic lattice (Anderson, 1958): For strong-enough disorder, diffusion is completely suppressed and the electronic wavefunctions decay rapidly at large distances (exponential localization; see Fig. 2.1c). Conversely, for low disorder, the electronic wavefunctions are extended. Hence, in the disordered case, there exists a critical value of the disorder, $\Delta_c \propto |\tau|$, which separates a metallic region –where almost all states are extended– from an insulating region –where almost all states are localized.

This prediction is confirmed by numerical calculations in the three-dimensional Anderson model (Kroha *et al.*, 1990). More precisely, for $\Delta < \Delta_c \simeq 16.5|\tau|$, most of the states are extended and hopping –*i.e.* transport– dominates for all energies (see Fig. 2.2). Only electronic states in the vicinity of the band edges $E \simeq \pm 2d\Delta$ are localized. In contrast, for $\Delta > \Delta_c$, almost all states are localized, and the system is an insulator. This physics features a metal-insulator transition –so-called Anderson transition– in non-interacting three-dimensional electronic systems [for reviews, see for instance (Mott, 1967; 1968; Lee and Ramakrishnan, 1985; van Tiggelen, 1999)]. The Anderson transition is characterized by two critical exponents ν and s. In the localized phase, the localization length diverges as $L_{\rm loc} \propto |\Delta - \Delta_c|^{-\nu}$ at the critical point, which has been numerically shown to be $\nu = 1.57 \pm 0.02$ (Schreiber and Grussbach, 1996; Slevin *et al.*, 2001). In the extended regime, the diffusion coefficient vanishes as $D_* \propto |\Delta_c - \Delta|^s$ at the critical point. The scaling theory of localization (see Sec. 2.1.2) predicts that the two exponents are related by the relation $s = (d-2)\nu$ (Abrahams *et al.*, 1979).

Each type of insulator has its own interest, and in particular, a huge amount of work has been devoted independently to Mott insulators and Anderson insulators. Interestingly, analogues of all types of insulators have been convincingly observed with ultracold atoms: band structures (Greiner *et al.*, 2001; Köhl *et al.*, 2005), bosonic (Greiner *et al.*, 2002) and fermionic Mott insulators (Jördens *et al.*, 2008; Schneider *et al.*, 2008), and Anderson localization (Billy *et al.*, 2008; Roati *et al.*, 2008). In the following, we focus on Anderson localization.

2.1.2 Anderson localization: one, two, three (dimensions)

The work of Anderson has triggered much interest, although after a latency period of more than a decade. It is now understood that Anderson localization is an ubiquitous phenomenon, relevant not only to electrons but also to any quantum or classical wave diffusing in a disordered medium. Many variants of the Anderson model have been studied so far. For instance, more complicated statistical distributions of on-site energies V_j, or random tunnel coupling, fluctuating from site to site have been considered. More generally, it appears that the mechanism that sparks Anderson localization is quite universal in the sense that it does not depend on the microscopic details of the considered model. Indeed, Anderson localization results from interference of the many paths associated to coherent multiple scattering from random impurities. A central aspect of Anderson localization is however that it strongly depends on the dimension of the system.

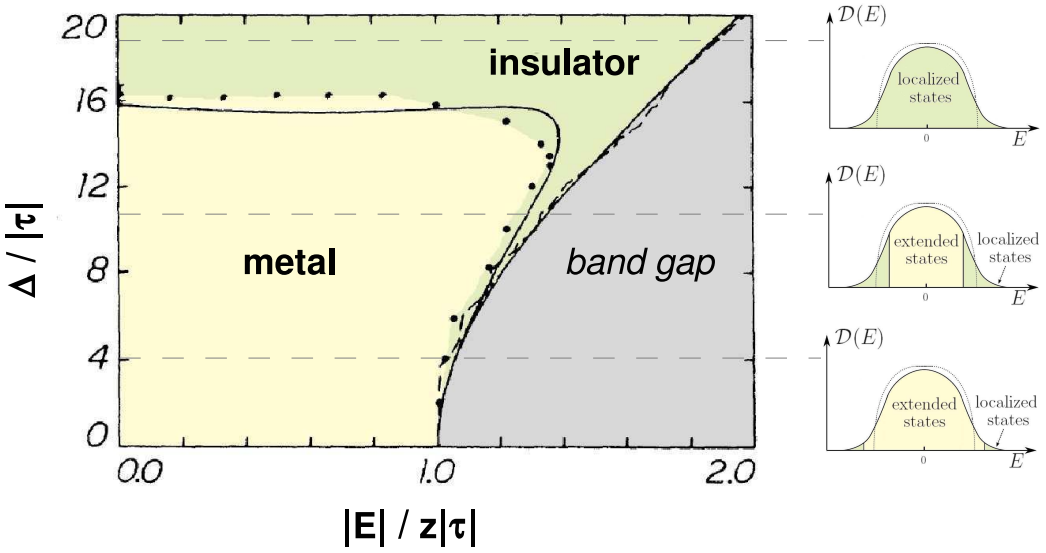

Figure 2.2 | **Phase diagram of the 3D Anderson model.** The diagram exhibits two phases (metal and insulator), separated by a transition found numerically (points) and from the self-consistent theory (solid line) [adapted from (Kroha *et al.*, 1990)]. The left-hand-side panels show the density of states and the location of localized and extended states. The localized states first appear near the band edge, and progressively fill up the band as disorder increases.

Scaling theory of localization - The strong dependence of Anderson localization on the spatial dimension can be understood on the basis of the scaling theory, the starting point of which is the description of localization as a universal phenomenon. The first step is the identification of a minimal number of relevant parameters, ultimately one. In a series of works, Thouless and his coworkers proposed the following approach (Thouless, 1974). Let us construct a piece of material by piling up d-dimensional blocks of linear size L, and try to identify a physically-relevant quantity governing the nature of the eigenstates associated to two blocks. Two energy scales appear. First, in each block, the energy levels are discrete, which provides us with a first energy scale, *i.e.* the level spacing or *Heisenberg energy*, $\Delta E = 1/\mathcal{D}(E)L^d$, where $\mathcal{D}(E)$ is the density of state per unit volume. Second, scattering from the impurities may induce diffusion, which we assume to be normal. This defines the *Thouless time*, $t_{\rm T} \sim L^2/D_{\rm B}$ where $D_{\rm B}$ is the Boltzmann diffusion constant, which corresponds to the necessary time for an electron to diffuse over the whole volume of the block. The Thouless time can be viewed as a broadening of the levels, which provides us with a second energy scale, $\delta E = \hbar/t_{\rm T} \sim \hbar D_{\rm B}/L^2$. Then, when piling up two blocks, one expects that the states in two different blocks are connected only when δE exceeds ΔE, *i.e.* when the level broadening exceeds the level spacing. Hence, one expects that the eigenstates of the full material are extended for $\delta E \gg \Delta E$, and localized for $\delta E \ll \Delta E$. Intuitively, the dimensionless conductance, $g(L) = \frac{G(L)}{e^2/\hbar}$, should thus be an increasing function of the ratio $\delta E/\Delta E$, which was proposed as the most relevant parameter for Anderson localization (Edwards and Thouless, 1972).

Landmark development of these ideas, now known as the *scaling theory of localization* came from the combination of single-parameter scaling with perturbative calculations (Abrahams *et al.*, 1979). Here, we refer to $g = \delta E/\Delta E$ as the dimensionless conductance[3]. Let us have a look at

[3]The exact conductance may have a different form, for instance in one dimension (Anderson and Lee, 1981;

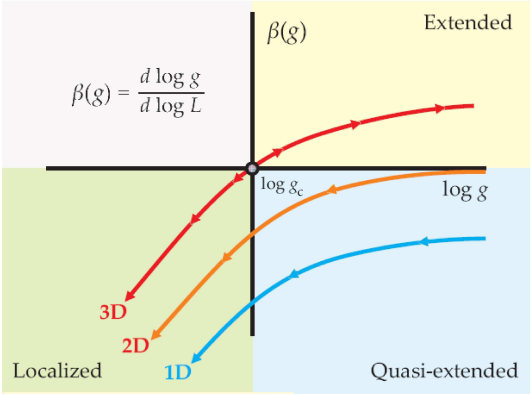

Figure 2.3 | Scaling flow for Anderson localization. The plot shows the scaling parameter $\beta(g) = \frac{d\ln(g)}{d\ln(L)}$ as a function of the logarithm of the dimensionless conductance g in one-, two- and three-dimensional spaces. The position of the y-axis corresponds to the three-dimensional critical dimensionless conductance g_c, such that $\beta(g_c) = 0$. The arrows show the flow followed by the dimensionless conductance when the linear size of the system, L, increases [adapted from (Lagendijk *et al.*, 2009)].

the behavior of g as a function of the linear size of the system, and define the scaling parameter $\beta = \frac{d\ln(g)}{d\ln(L)}$, which was argued to only depend on g itself [for details, see for instance (Lee and Ramakrishnan, 1985)]. For large g, we are in the diffusive regime and the arguments of the preceding paragraph hold, so that $g \sim L^{d-2}$ and thus $\beta(g) \sim (d-2)$. Single-scattering corrections to the Boltzmann transport theory lead more precisely to $\beta(g) \simeq (d-2) - a/g$. Conversely, for small g, we are in the localized regime, and since tunneling from different blocks is exponentially suppressed, we expect $g \propto \exp(-L/L^*)$, where L^* scales as the localization length, so that $\beta(g) \simeq \beta_0 + \ln(g)$. The behavior of g versus L is finally inferred from interpolation of these formulas, assuming continuity, which is justified by the fact that we are dealing with finite-size systems. The result is depicted in Fig. 2.3, showing drastically different behaviors in one-, two- and three-dimensional infinite systems (Abrahams *et al.*, 1979):

– In one dimension, one finds $\beta(g) < 0$ for any value of g. Let us start from a certain (finite) size L, which corresponds to a certain point on the lower (blue) curve in Fig. 2.3. Since $\beta(g) < 0$, the conductance g decreases when L increases, thus following the curve towards the right-hand side, and ultimately ending in the localized region where $g \sim \exp(-L/L^*)$. One thus concludes that all states are localized in infinite one-dimensional systems, which confirms more direct treatments (Gertsenshtein and Vasil'ev, 1959; Mott and Twose, 1961; Borland, 1963). Hence, counter-intuitively, one finds that even states with energy much higher than the amplitude of the disorder are exponentially localized.

– The behavior in two dimensions, associated to the intermediate (orange) curve in Fig. 2.3, is similar, leading to the conclusion that all states in infinite two-dimensional systems are localized. There is however a fundamental difference compared to the one-dimensional case. Here, $\lim_\infty \beta(g) = 0$, which leads to qualify dimension two as the marginal dimension of Anderson localization. The localization behavior can thus be expected to be very sensitive to any perturbation, possibly leading for instance to a small but positive value of $\beta(g = +\infty)$ as in the three-dimensional case (see below). For instance, it is believed that particle-particle interactions might lead to such a scenario (Kravchenko *et al.*, 1994; Kravchenko, 1995; Abrahams, 2001).

– In three dimensions, the behavior is significantly richer because $\beta(g)$ crosses zero for a critical value g_c as shown in the upper (red) curve of Fig. 2.3. Let us start with a sample

Singha Deo, 1997), but it does not change the discussion.

of small conductance, $g < g_c$. Then, $\beta(g) < 0$ so that g decreases when L increases, and ultimately ends up in the localized regime for infinite three-dimensional systems. In contrast, if one starts from a sample of large conductance, $g > g_c$, the scaling flow is opposed and g increases with L. In the limit of an infinite system, the sample thus ends up in the extended (diffusive) regime. Since the value of g_c depends on both disorder and energy, one concludes in favor of the existence of a metal-insulator transitions (Anderson, 1958) as a function of the strength of disorder and the particle energy in agreement with the results reported on Fig. 2.2.

Microscopic approaches - Further knowledge of Anderson localization requires more detailed treatments. Several microscopic approaches have been developed. One may consider several starting points, *e.g.* hyper-cubic lattice systems, Cayley trees, continuous systems (van Tiggelen, 1999), but since localization is a universal phenomenon, they are more or less all equivalent. Let us consider here a free particle of mass m and energy E, in a d-dimensional disordered potential $V(\mathbf{r})$ in continuous space, the wavefunction $\psi(\mathbf{r})$ of which is governed by the Schrödinger equation

$$E\psi(\mathbf{r}) = -\frac{\hbar^2\nabla^2}{2m}\psi(\mathbf{r}) + V(\mathbf{r})\psi(\mathbf{r}). \tag{2.2}$$

In one dimension, there exists a number of methods to solve Eq. (2.2) [for a review, see for instance (Lifshits *et al.*, 1988)]. Let us focus on a very general and efficient one, the so-called *phase formalism approach*, which is valid for any weak disorder with finite-range correlations. Let us write the wave-function (which we choose to be real-valued) in amplitude-phase-like representation, such that $\psi(z) = r(z)\sin[\theta(z)]$ and $\partial_z\psi(z) = kr(z)\cos[\theta(z)]$, where $r(z)$ represents the amplitude, $\theta(z)$ is the phase[4], and $k = \sqrt{2mE}/\hbar$ would be the particle wavevector in free space. Substituting this form into Eq. (2.2) leads to two coupled equations: The first one is a closed, nonlinear differential equation of first order on $\theta(z)$, while the second one couples $\theta(z)$ to $r(z)$, proving an explicit formula for $r(z)$ as a function of an integral of $\theta(z)$ [for details, see for instance (Sanchez-Palencia *et al.*, 2008; Lugan *et al.*, 2009)]. The power of the method lies in the separation of these quantities, which react very differently to disorder. For weak-enough disorder and large-enough particle energy, the phase is only weakly affected by the local modulations of the disordered potential, so that one can write $\theta(z) \simeq \theta_0 + kz + \delta\theta(z)$, and develop a perturbation theory in powers of $\delta\theta(z)$. In contrast, the amplitude $r(z)$ is strongly affected even in arbitrary weak disorder[5], and one should integrate the second one directly (*i.e.* without perturbation technique). Since, the most interesting case is when disorder is weak, lowest-order calculations are often sufficient[6], which yields the Lyapunov exponent (inverse localization length)

$$\gamma(k) \propto \frac{\langle \hat{V}(+2k)\hat{V}(-2k)\rangle}{k^2} = \frac{\hat{C}(2k)}{k^2}, \tag{2.3}$$

where $\hat{V}$ is the Fourier transform of the disordered potential, and $C(z) = \langle V(z_0)V(z_0+z)\rangle - \langle V\rangle^2$ is the autocorrelation function for homogeneous disorder (Lifshits *et al.*, 1988). Equation (2.3)

[4]Note that this is possible whatever the behavior of the real-valued function $\psi(z)$.

[5]In the absence of disorder, we have $r(z) = 1$, corresponding to an extended plane wave. In contrast, $r(z)$ decays exponentially as soon as disorder is not zero, so that at large distances, $r(z) \ll 1$.

[6]Higher-order terms usually lead to small corrections to the Lyapunov exponent, which serve for quantitative studies only. We will however show in Sec. 2.3.3 that it is not always so, and higher-order terms can be crucial to understand the qualitative behavior of $\gamma(k)$ [see also (Gurevich and Kenneth, 2009; Lugan *et al.*, 2009)].

enlightens in particular the primary role of coherent second-order back-scattering, $+k \to -k \to +k$, in the localization process.

Higher dimensions are much more demanding as the above method cannot be straightforwardly extended. Landmark advance has been the so-called *self-consistent theory* of localization (Vollhardt and Wölfle, 1980a; 1980b; 1982; 1992). It takes root to works on weak localization, which is now seen as a precursor of Anderson localization (Akkermans and Montambaux, 2006). The idea is the following. One first uses perturbation theory to calculate quantities associated to incoherent scattering, *i.e.* those that do not take into account the phases accumulated along the various scattering paths (see Fig. 2.4). This allows one to estimate the scattering mean free path, l^* –which measures the typical length over which a wave propagating in the disordered medium looses memory of its initial phase– and the transport (Boltzmann) mean free path, l_{B} –which measures the typical length over which the wave looses memory of its initial direction– as a function of the particle energy. This approach thus only accounts for classical terms, which leads to classical diffusion, so that the average squared size of the particle cloud scales as the time, $\langle \mathbf{r}^2 \rangle = 2D_{\text{B}}t$, with $D_{\text{B}}(E) = vl_{\text{B}}/d$ the diffusion constant and $v = \hbar k/m$ the particle velocity.

In quantum physics of course, the contributions of the various multiple-scattering paths should be added coherently, thus taking into account the various phases accumulated along all paths. For most contributions, it is actually not necessary. Consider the scattering paths (for instance paths 1 and $1'$ in Fig. 2.4) from a certain point $\mathbf{r}_0$ to another one $\mathbf{r}_1$. They all follow different routes and thus accumulate independent phases, so that cross-terms which depend on the relative phase of two paths vanish when averaging over the disorder. There are however important cross-term contributions that do not vanish (Langer and Neal, 1966). This concerns the various loop processes for which a particle starts from point $\mathbf{r}_0$, suffers a couple of scattering processes and then comes back to $\mathbf{r}_0$ (see for instance paths 2 and 3 in Fig. 2.4). The key is that the reverse process –corresponding to follow the same scattering path but the other way round (paths $2'$ and $3'$)– has to be summed up coherently with the former because the phase accumulation, although random, is exactly the same in both processes. This leads to constructive interference and enhancement of the return probability by a factor two, compared to classical calculations. The quantum corrections to the Boltzmann diffusion constant can be calculated from lowest-order perturbation theory, yielding the modified diffusion constant

$$D^{(\text{w.l.})}(E) = D_{\text{B}} - \delta D(E). \tag{2.4}$$

As expected, one thus finds that, although non zero, the diffusion constant is reduced, a phenomenon known as weak localization (Akkermans and Montambaux, 2006).

Going beyond using perturbation theory is very difficult. Rather, one then resorts on a self-consistent argument. The point is that the weak-localization correction δD to the Boltzmann diffusion constant D_{B} can be expressed as a function of D_{B} itself. In order to account for all loop processes at all orders, Vollhardt and Wölfle (1980a) proposed to replace both $D^{(\text{w.l.})}$ and D_{B} in the expression of δD by the actual diffusion constant $D(E)$. One is thus left with an implicit self-consistent equation on $D(E)$, which remains to be solved. The self-consistent theory of localization is now widely used and yields the following results:

– In one dimension, one finds that all states are localized, and $L_{\text{loc}} \propto l_{\text{B}}$. This agrees with prediction of the scaling theory, as well as with exact results and approaches more specialized to one-dimensional systems (Lifshits *et al.*, 1988).

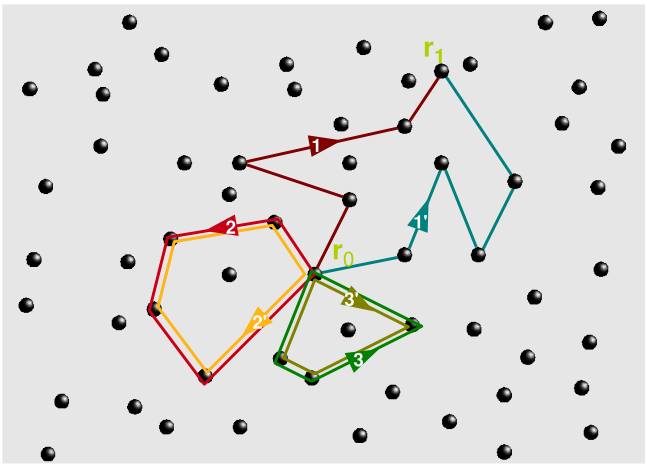

Figure 2.4 | Scattering paths in a disordered medium. Consider a particle diffusing in the time interval $[t_0, t_1]$ from point $\mathbf{r}_0$. The density at point $\mathbf{r}_1$ and time t_1 is determined by the squared sum of all contributions of the scattering paths from $\mathbf{r}_0$ to $\mathbf{r}_1$. For open paths (*i.e.* $\mathbf{r}_1 \neq \mathbf{r}_0$, as for paths 1 and 1′), cross terms vanish because the accumulated relative phases are random and independent. Conversely, for loop paths returning to the initial point (*i.e.* $\mathbf{r}_1 = \mathbf{r}_0$, as for paths 2 and 2′ or 3 and 3′), the accumulated phases are equal, and the corresponding contributions have to be summed up coherently.

– In two dimensions, one also finds that all states are localized, but the localization length behaves very differently, namely $L_{\rm loc} \propto l_{\rm B} \exp(\pi k l_{\rm B}/2)$ where $k = \sqrt{2mE}/\hbar$. Hence, the two-dimensional localization length, $L_{\rm loc}$, explodes exponentially for $k > 1/l_{\rm B}$, inducing a crossover from extended (diffusion regime) to localized (localization regime) states in finite-size systems.

– The situation differs dramatically in three dimensions, where a proper phase transition (the Anderson transition) shows up, in agreement with the scaling theory. The Anderson transition is found to occur at the so-called mobility edge, $E_{\rm mob} = \hbar^2 k_{\rm mob}^2/2m$. Hence, while low-energy states with $k < k_{\rm mob}$ are exponentially localized, those with $k > k_{\rm mob}$ are extended. The position of the mobility edge is approximately captured by the Ioffe-Regel criterion (Ioffe and Regel, 1960; Mott, 1967), which basically states that localization requires that the phase accumulated between two successive deflecting scattering processes does not exceed 1, thus yielding $k_{\rm mob} \sim 1/l_{\rm B}$. In other words, the de Broglie wavelength must exceed the distance travelled by the particle during the memory time of its initial particle direction. The exact features of the mobility edge are however not correctly described by the self-consistent theory of localization. When applied to the disordered cubic lattice model (Anderson, 1958), the predictions of the self-consistent theory actually differ from exact numerical calculations. For instance, the predicted critical exponent ν, such that $L_{\rm loc} \sim (E_{\rm mob} - E)^{-\nu}$ for $E \lesssim E_{\rm mob}$, is $\nu_{\rm sc} = 1$ (Vollhardt and Wölfle, 1980b), while numerical calculations provide $\nu_{\rm num} \simeq 1.6$ (MacKinnon and Kramer, 1983; Kroha *et al.*, 1990).

2.1.3 Localization: An ubiquitous phenomenon in disordered media

As discussed above, Anderson localization was introduced in the context of electronic transport in disordered materials. It is now recognized as a fundamental effect, which may account for certain metal-insulator transitions. A major drawback of electronic systems is however that in its initial form, the Anderson model emanates from an oversimplified model of disordered solids, as it does not incorporate important ingredients, such as the Coulomb interaction, the interaction with phonons, and spin-coupling effects. All these effects play combined roles, and it is hardly possible to clearly isolate effects that are purely due to disorder. Fortunately, Anderson localization turns

out to be an ubiquitous phenomenon in wave physics. It thus occurs for any wave in any disordered medium, at least a sufficiently strong one in three dimensions. It was first pointed out in the context of electromagnetic waves in disordered media (John, 1984), and later extended to nearly any kind of waves, quantum or classical (Anderson, 1985; Souillard, 1987; van Tiggelen, 1999).

The advantages of classical waves, in particular photons, is that (i) they do not interact, (ii) strongly-scattering media can be synthesized in the laboratory, (iii) one can work at room temperature, and (iv) many observables that are sensitive to Anderson localization (*e.g.* intensity, complex amplitude, statistical distributions of these quantities) can be measured. A drawback however is that absorption is difficult to avoid (Scheffold *et al.*, 1999). This is particularly unenviable for light as the Beer-Lambert absorption law leads to exponential extenuation of the intensity, which is qualitatively similar to Anderson localization. The possibility of observing Anderson localization with classical waves has prompted much experimental work in a variety of systems [see recent reviews by Lagendijk *et al.* (2009) and Aspect and Inguscio (2009)]. So far, evidence of Anderson localization has been reported for light in diffusive media (Wiersma *et al.*, 1997; Storzer *et al.*, 2006; Aegerter *et al.*, 2006), in one-dimensional (Lahini *et al.*, 2008) and two-dimensional (Schwartz *et al.*, 2007) photonic crystals, for microwaves (Chabanov *et al.*, 2000) and for sound waves in two (Weaver, 1990) and three (Hu *et al.*, 2008) dimensions.

For matter-waves, Anderson localization remained elusive for a longer time. First experiments were conducted in doped semiconductors, and conductivity was measured close to the metal-insulator transition. However critical exponents were difficult to extract due to strong temperature dependence (Paalanen, 1983; Rosenbaum *et al.*, 1983). Recent advances in the field of ultracold atoms have open new opportunities to study localization in disordered media in various directions. In particular, coherent back-scattering of light in a disorder created with cold atoms in a magneto-optical trap (Labeyrie *et al.*, 1999; 2000), and dynamical localization of cold atoms in kicked-rotor systems (Moore *et al.*, 1994; Chabé *et al.*, 2008) were reported. In the very recent years, ultracold atoms have been proposed to investigate the effects of disorder on quantum matter (Damski *et al.*, 2003; Roth *et al.*2008). This has triggered much interest (see Introduction), and in particular, theoretical works proposed routes to directly observe Anderson localization in controlled disordered potentials (Schulte *et al.*, 2005; Sanchez-Palencia *et al.*, 2007). In 2008, the groups of Philippe Bouyer and Alain Aspect at Institut d'Optique and of Massimo Inguscio at LENS reported the first direct observation of Anderson localization using Bose-Einstein condensates (Billy *et al.*, 2008; Roati *et al.*, 2008). This is the first direct evidence of Anderson localization of a matter-wave.

2.2 Transport of matterwaves in quasi-periodic and disordered potentials

In this section, we present our first works on localization of a Bose-Einstein condensate. A scheme based on release of initially interacting condensates from harmonic traps is proposed to probe localization. Localization is found for a two-dimensional quasi-periodic lattice, and for a one-dimensional speckle potential. In the regime considered here, localization cannot be clearly related to Anderson localization, but rather to strong suppression of tunneling in the quasi-periodic potential and to disorder-induced trapping in the case of a speckle potential.

2.2.1 Bose-Einstein condensates in quasi-periodic lattices

▷ *see paper reprinted on page 57*

In collaboration with Luis Santos (University of Hannover, Germany), we have investigated the physics of Bose-Einstein condensates in *quasi-periodic lattices* in two spatial dimensions. Such a lattice can be produced optically in ultracold atomic gases from a simple arrangement of laser beams, as first demonstrated in the group of Gilbert Grynberg in the context of laser (Sisyphus) cooling (Guidoni, 1997; Guidoni, 1999). The idea consists in using five-laser beams arranged in a fivefold rotational symmetry[7] (see Fig. 2.5a). Such a configuration is known to be incompatible with crystallographic order (Ashcroft and Mermin, 1976), *i.e.* it cannot exhibit long-range periodic order. The dipole potential $V(\mathbf{r})$ associated to this laser configuration is thus neither periodic, nor disordered, as can be seen in Fig. 2.5b: It is actually made of clearly identified wells, which are not arranged periodically, but however exhibit long-range orientational order. Indeed, one can see that elementary patterns (for instance a circular arrangement of ten wells, which appears in the center) repeat almost exactly and almost regularly in space. This is a first hint in *quasi-periodic order*, which is somehow intermediate between full order and disorder. This kind of potentials is particularly interesting from a fundamental perspective, but also with a view towards simulating quasi-periodic crystals, which have been discovered in artificial Al-Mn alloys (Shechtman *et al.*, 1984; Levine and Steinhardt, 1984), and very recently in natural aluminum-copper-iron alloys (Bindi *et al.*, 2009).

Equilibrium properties - Quasi-periodicity is more rigorously defined in reciprocal space[8]: The (spatial) Fourier spectrum should be discrete, periodic order is a peculiar case of which. This is indeed the case of the considered configuration, since, by geometrical construction, the light field contains $N_\mathrm{b} = 5$ components. The dipole potential –which is proportional to the square modulus of the light field– thus contains *a priori* $5^2 = 25$ Fourier components. Actually only 21 are different: corresponding to

- $\mathbf{k} = \mathbf{0}$,
- the 5 vectors $\mathbf{k} = \kappa_j$ where $\kappa_0 = \mathbf{k}_1 - \mathbf{k}_0$ and $\kappa_j = \mathcal{R}[2\pi j/5]\kappa_0$ with $\mathcal{R}[\theta]$ the rotation of angle θ, and the opposite vectors,
- the 5 vectors $\kappa_{j+2} - \kappa_j$ and the opposite vectors.

This property offers an immediate method to demonstrate quasi-periodic order in ultracold atomic gases (Sanchez-Palencia and Santos, 2005). Let us consider a Bose-Einstein condensate, the wavefunction of which is accurately described by the Gross-Pitaevskii equation (1.2). In the Thomas-Fermi regime, the solution reads $\psi(\mathbf{r}) = \sqrt{[\mu - V(\mathbf{r})]/g}$. Expanding the square root and turning to Fourier space, we find[9]

$$\widehat{\psi}(\mathbf{p}) = \sqrt{\frac{\mu}{g}} \sum_{n\geq 0} \binom{1/2}{n} \frac{(-1)^n}{\mu^n} \widehat{V^n}(\mathbf{p}), \tag{2.5}$$

[7] In d-dimensional space, the relative phases of up to $d+1$ laser beams do not modify the topology of the corresponding potential, but just affect its origin (Grynberg and Robilliard, 2000). For more than $d+1$ laser beams, the topology does depend on the relative phases, which should thus be locked. It is so for the two-dimensional five beam configuration considered here.

[8] Quasi-crystals were actually identified form anomalous Bragg diffraction experiments (Shechtman *et al.*, 1984).

[9] Here, $\widehat{f}(\mathbf{p}) = (2\pi\hbar)^{-d/2} \int d^d\mathbf{r}\, f(\mathbf{r}) \mathrm{e}^{-i\mathbf{p}.\mathbf{r}/\hbar}$ is the Fourier transform of function f.

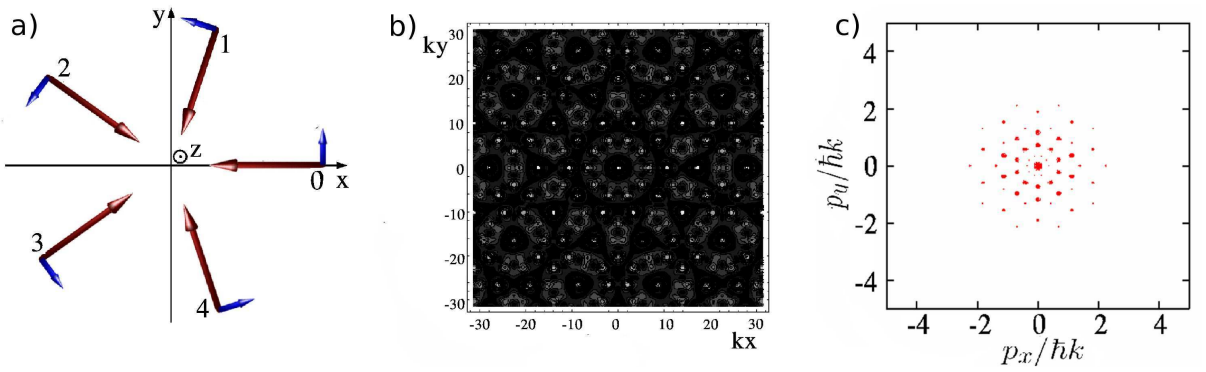

Figure 2.5 | **Quasi-periodic optical lattices. a)** Five-laser configuration. **b)** Quasi-periodic potential. **c)** Momentum distribution of a trapped Bose-Einstein condensate in the Thomas-Fermi regime in a quasi-periodic lattice [adapted from (Sanchez-Palencia and Santos, 2005)].

and

$$\widehat{V^n}(\mathbf{p}) \propto \int d\mathbf{k}_1 \dots d\mathbf{k}_n \, \widehat{V}(\mathbf{k}_1) \dots \widehat{V}(\mathbf{k}_n) \, \delta^{(d)}(\mathbf{k}_1 + \dots + \mathbf{k}_n - \mathbf{k}). \tag{2.6}$$

The condensate wavefunction in Fourier space –which can be observed experimentally from time-of-flight experiments (Ketterle *et al.*, 1999)– thus contains a numerable ensemble of components, corresponding to all combinations of the 5 vectors κ_j with integer coefficients: $\sum_{j\in\{0\dots4\}} n_j\kappa_j$ with $n_j \in \mathbb{Z}$. The results of numerical calculations performed within the Gross-Pitaevskii approach confirm this prediction (see Fig. 2.5c). These results exhibit discrete sharp peaks, pretty similarly as what is now routinely observed in time-of-flight experiments of Bose-Einstein condensates (in the superfluid phase) released from periodic optical lattices (Greiner *et al.*, 2001). However, here, the peaks are not periodically arranged, but rather form a fivefold rotationnaly symmetric pattern, thus demonstrating quasi-periodic order.

Transport properties - Although the system shows long-range order as in the periodic case, its transport properties are completely different. In order to study transport, we have proposed a scheme (Sanchez-Palencia and Santos, 2005) which is now used in most experiments on transport of ultracold atoms in disordered or quasi-disordered potentials (Clément *et al.*, 2005; Fort *et al.*, 2005; Billy *et al.*, 2008; Roati *et al.*, 2008):

- One creates a Bose-Einstein condensate in a harmonic trap and in the presence of the quasi-periodic potential.
- At time $t = 0$, one releases the trap, keeping the quasi-periodic potential on, which induces the expansion (transport) of the condensate.

We thus demonstrated localization of the condensate in the quasi-periodic potential, *i.e.* the condensate expansion rapidly stops. This behavior strongly contrasts with the periodic case, which shows ballistic expansion at large times with a reduced effective mass (see Inset of Fig. 2.6). It also contrasts with the case of classical particles in quasi-periodic potentials, which shows diffusive transport as demonstrated with cold atoms for the first time in the group of Gilbert Grynberg (Guidoni, 1997; Guidoni, 1999).

Localization can be investigated more precisely by adjusting the laser intensity of two beams, say lasers 1 and 4 on Fig. 2.5a, thus interpolating from periodic (for zero intensity of lasers 1 and 4) to fully quasi-periodic (for full intensity of lasers 1 and 4) potential. This is a wonderful

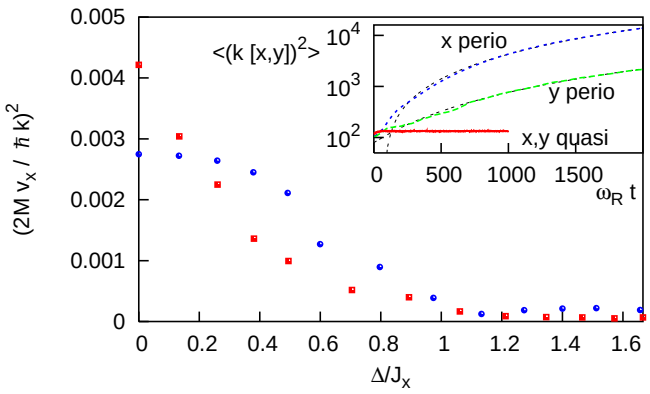

Figure 2.6 | Crossover from ballistic expansion to localization of a Bose-Einstein condensate in a quasi-periodic optical lattice. The figure shows numerical results for the expansion velocity along direction x (see Fig. 2.5a) as a function of quasi-disorder (Δ), with (red squares) and without (blue circles) repulsive interactions. The inset shows the expansion as a function of time in periodic and quasi-periodic lattices [from (Sanchez-Palencia and Santos, 2005)].

possibility of ultracold atoms, without a counterpart in condensed-matter physics. Numerical integration of the time-dependent Gross-Pitaevskii equation (Pitaevskii and Stringari, 2003):

$$i\hbar\frac{\partial\psi(\mathbf{r})}{\partial t} = \left[-\frac{\hbar^2\nabla^2}{2m} + V(\mathbf{r}) + g|\psi(\mathbf{r})|^2\right]\psi(\mathbf{r}), \tag{2.7}$$

shows a crossover from ballistic expansion ($\langle x^2\rangle \simeq v_x^2 t^2$) to localization when turning from periodic to quasi-periodic potentials (see Fig. 2.6). It should be noted that the crossover occurs when the *quasi-periodic parameter* Δ –defined as the variance of the differences of energies in adjacent sites– equals the tunneling rate J (Sanchez-Palencia and Santos, 2005). This result generalizes to two dimensions the work of Aubry and André (1980), which demonstrates the existence of a metal-insulator transition in one-dimensional quasi-periodic lattices. It opens the route to the extension of the work reported by the group of Massimo Inguscio in one-dimensional quasi-periodic lattices (Roati *et al.*, 2008) to higher dimensions[10].

These results also show a non-trivial effect of interactions. For a weak quasi-periodic component, repulsive interactions tend to increase the velocity of the ballistic expansion, as could be intuited. For a larger quasi-periodic component however, they decrease the expansion velocity. This is due to non-linear self-trapping, which has been identified in the context of periodic lattices (Trombettoni and Smerzi, 2001; Anker *et al.*, 2005). Stated in simple words, the initial trapping potential induces inhomogeneous on-site energy shifts which results in inhomogeneous density and thus inhomogeneous interaction energy in the different lattice sites. When the trap is released abruptly, the interaction energy shifts make tunneling to be off resonance, thus impeding transport.

[10]Note that for the parameters used in our work, the tunneling rate J is much smaller than the lattice amplitude. Hence, the crossover to localization ($\Delta \simeq J$) occurs in a regime where the potential can be described as a periodic potential, slightly perturbed with quasi-periodic on-site energy shifts, pretty much like in the experiments at LENS (Roati *et al.*, 2008). In contrast, with equal intensity of all five lasers, the potential is completely different from a periodic potential (see Fig. 2.5b).

2.2.2 Suppression of transport of a Bose-Einstein condensate in a one-dimensional disordered potential

▷ *see paper reprinted on page 63*

In collaboration with Georgy V. Shlyapnikov and with the experiments performed in the group of Philippe Bouyer and Alain Aspect at Institut d'Optique, we have theoretically investigated the transport of a Bose-Einstein condensate in a disordered potential (Clément *et al.*, 2005), pretty much like in the previous section[11]. The idea here is the same as before: We create an interacting condensate with strong meanfield interactions (Thomas-Fermi regime) in a harmonic trap and in the presence of disorder. Then, at time $t = 0$, we release the trap and let the condensate expand in the disordered potential[12]. There are however two crucial differences. First, we now work with one-dimensional systems, since localization effects are expected to be at their strongest. Second, we use a truly disordered potential, created from laser speckle (see Box 1).

Using numerical integration of the one-dimensional Gross-Pitaevskii equation (2.7), we have demonstrated localization (*i.e.* suppression of transport) of the condensate in a regime where the amplitude of the disordered potential is smaller than the expansion energy per particle of the condensate, *i.e.* typically its chemical potential (see Fig. 2.7a). These results are in good qualitative and quantitative agreement with experimental observations (Clément *et al.*, 2005; Fort *et al.*, 2005). They clearly demonstrate localization, in strong contrast with ballistic expansion (with a reduced effective mass) obtained for periodic potentials with similar amplitude and period (Sanchez-Palencia *et al.*, 2008).

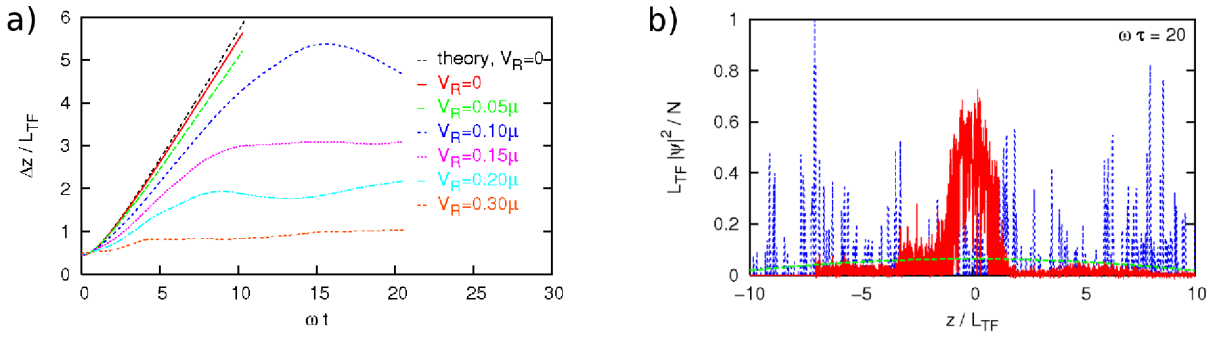

Figure 2.7 | Localization of an interacting Bose-Einstein condensate in one-dimensional disorder. **a)** Time-evolution of the rms-size of the condensate for several values of the amplitude V_R. The (black) dashed line is the theoretical prediction of the scaling theory with a vanishing disordered potential (Kagan *et al.*, 1996; Castin and Dum, 1996). Here, we have used $\sigma_R = 0.012 L_{TF}$ and $\xi_{in} = 5.7 \times 10^{-4} L_{TF}$. **b)** Density profile of the localized condensate after an expansion time of $\tau = 10/\omega$ for $V_R = 0.2\mu$ (solid red line). The corresponding non-disordered Thomas-Fermi profile (dashed green lines) and the disordered potential normalized so as to be homogeneous to a density (V/g; dotted blue line) are also shown [from (Sanchez-Palencia *et al.*, 2008)].

[11] Similar experiments were performed at the same time in the group of Massimo Insgucio at LENS, showing similar results (Fort *et al.*, 2005).

[12] In the experiment, the configuration is not exactly one-dimensional because the condensate radial size slightly exceeds the length of the radial harmonic oscillator. However, the disordered potential is really one-dimensional as the speckle grains are strongly anisotropic with a radial size much larger than the condensate width.

Box 1 | Creating controlled disordered potentials.

In atomic gases, disorder can be created in a controlled way. For instance, the so-called speckle potentials are formed as follows (Goodman, 2007). A coherent laser beam is diffracted through a ground-glass plate and focused by a converging lens (Box 1 Fig. 1a). The ground-glass plate transmits the laser light without altering the intensity, but imprinting a random phase profile on the emerging light. Then, the complex electric field $\mathcal{E}(\mathbf{r})$ on the focal plane results from the coherent superposition of many independent waves with equally-distributed random phases, and is thus a Gaussian random process. In such a light field, atoms with a resonance slightly detuned with respect to the laser light experience a disordered potential $V(\mathbf{r})$ which, up to a shift introduced to ensure that the statistical average $\langle V\rangle$ of $V(\mathbf{r})$ vanishes, is proportional to the light intensity, $V(\mathbf{r}) \propto \pm(|\mathcal{E}(\mathbf{r})|^2 - \langle|\mathcal{E}|^2\rangle)$, an example of which in shown in Box 1 Fig. 1b. Hence, the laws of optics allows us to precisely determine all statistical properties of speckle potentials. First, although the electric field $\mathcal{E}(\mathbf{r})$ is a complex Gaussian random process, the disordered potential $V(\mathbf{r})$ is not Gaussian itself, and its single-point probability distribution is a truncated, exponential decaying function, $P(V(\mathbf{r})) = \mathrm{e}^{-1}|V_\mathrm{R}|^{-1}\exp(-V(\mathbf{r})/V_\mathrm{R})\Theta(V(\mathbf{r})/V_\mathrm{R}+1)$, where $\sqrt{\langle V^2\rangle} = |V_\mathrm{R}|$ is the disorder amplitude and Θ is the Heaviside function. Both modulus and sign of V_R can be controlled experimentally (Clément *et al.*, 2006): The modulus is proportional to the incident laser intensity while the sign is determined by the detuning of the laser relative to the atomic resonance (V_R is positive for 'blue-detuned' laser light (Clément *et al.*, 2005; Clément *et al.*, 2006; Clément *et al.*, 2008; Billy *et al.*, 2008), and negative for 'red-detuned' laser light (Lye *et al.*, 2005; Fort *et al.*, 2005; Chen *et al.*, 2008)). Second, the two-point correlation function of the disordered potential, $C_2(\mathbf{r}) = \langle V(\mathbf{r})V(0)\rangle$, is determined by the overall shape of the ground-glass plate but not by the details of its asperities (Goodman, 2007). It is thus also controllable experimentally (Clément *et al.*, 2006). There is however a fundamental constraint: Since speckle potentials result from interference between light waves of wavelength λ_L coming from a finite-size aperture of angular width 2α (Box 1 Fig. 1a) they do not contain Fourier components beyond a value $2k_\mathrm{c}$, where $k_\mathrm{c} = (2\pi/\lambda_\mathrm{L})\sin(\alpha)$. In other words, $C_2(2\mathbf{k}) = 0$ for $|\mathbf{k}| > k_\mathrm{c}$.

Speckle potentials can be used directly to investigate the transport of matter-waves in disordered potentials (Lye *et al.*, 2005; Clément *et al.*, 2005; Fort *et al.*, 2005; Schulte *et al.*, 2005). They can also be superimposed to deep optical lattices (White *et al.*, 2009).

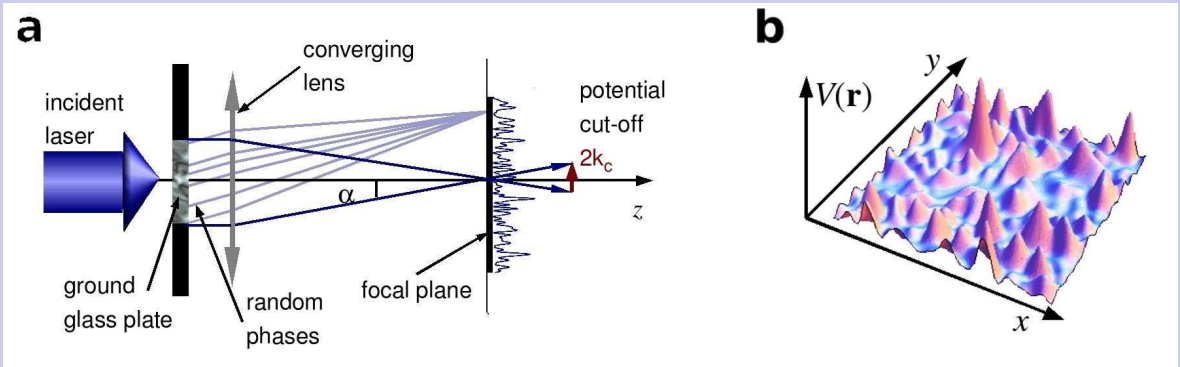

Box 1 Figure 1 | Optical speckle potentials. a) Optical configuration. **b)** Two-dimensional representation of a speckle potential [from (Sanchez-Palencia and Lewenstein, 2010)].

We have however shown that, in the considered regime, the presence of repulsive atom-atom interactions in the expanding condensate strongly changes the scenario envisioned by Anderson, in which interference of many quantum paths plays a major role. A first indication of this is that our numerically-calculated density profiles do not show exponentially decaying tails, characteristic of Anderson localization (see Fig. 2.7b). We have elaborated a completely different scenario of *disordered-induced localization* (Sanchez-Palencia *et al.*, 2008) in which strong disorder and interactions play a central role. In this, the subtle interference of quantum paths that spark Anderson localization (see Sec. 2.1) is completely destroyed. In brief, one must distinguish two spatial regions in the (first expanding and then localized) condensate. The two have very different densities, and thus behave drastically differently in the presence of meanfield interactions:

– In the central region, the initial density and thus the meanfield interaction are large[13]. In the Thomas-Fermi regime, relevant to the experiments of 2005 (Clément *et al.*, 2005; Fort *et al.*, 2005), the initial density profile follows the modulations of the disordered potential: $n(z) = [\mu - V(z)]/g_{1D}$. Due to the initial expansion of the condensate, the density slowly lowers and the dynamics can be regarded as quasi-static, so that the density profile still follows the modulations of the disordered potential but with a (slowly decreasing) effective chemical potential: $n(z) \simeq [\mu_{\rm eff} - V(z)]/g_{1D}$. Then, the condensate fragments when the effective chemical potential $\mu_{\rm eff}$ becomes smaller than the amplitude of two peaks in the speckle potential. This has two consequences. First, it results in the halt of the expansion of the central part of the condensate. Second, the central part of the condensate becomes stationary. From this idea, one can extract an analytical estimate of the averaged density of the central part of the fragmented condensate, yielding:

$$n_{\rm c} \simeq \frac{1}{0.75}\left(\frac{V_{\rm R}}{g_{1D}}\right)\ln\left[\frac{0.30 L_{\rm TF}}{2\sigma_{\rm R}}\right] \tag{2.8}$$

for $n_{\rm c} < 11\mu/12 g_{1D}$ corresponding to the initial average density. This approximate formula is characteristic of the above scenario. It is confirmed by the analysis of our numerical calculations as shown in Fig. 2.8 (Sanchez-Palencia *et al.*, 2008) and experimental data (Clément *et al.*, 2006).

– In the tails of condensate, the situation is completely different, because interactions are negligible owing to a much lower density. Hence the density profile in the tails of the condensate does not follow the modulations of the disordered potential and is not stationary, *i.e.* it shows strong temporal fluctuations (Sanchez-Palencia *et al.*, 2008). Then, the halt of the expansion in the tails of the condensate results from quasi-total reflections from large peaks of the disordered potential. This is signaled by the density profiles plotted in Fig. 2.7b, which shows sharp drops of the density (*e.g.* at positions $z \simeq -7L_{\rm TF}$ and $z \simeq -3.5L_{\rm TF}$). Note that significant drops correspond either (i) to modulations of the disordered potential larger than the initial chemical potential μ (classical reflections; *e.g.* at $z \simeq -7L_{\rm TF}$) or (ii) to concentrations of weaker barriers (quantum reflections; *e.g.* at $z \simeq -3.5L_{\rm TF}$).

It results that the localization process relevant to the experiments of 2005 (Clément *et al.*, 2005; Fort *et al.*, 2005) does not involve interference of many multiply-scattered wavepackets

[13]The experiments of 2005 at Institut d'Optique and LENS are performed in the same regime. Interactions are initially strong, so that the condensate is in the Thomas-Fermi regime, *i.e.* $V_{\rm R} < \mu$ and $\xi_{\rm in} \ll \sigma_{\rm R}$ [$V_{\rm R}/\mu \lesssim 0.7$, $\xi_{\rm in} \simeq 0.11\mu$m and $\sigma_{\rm R} \simeq 1.7\mu$m in the experiment at Institut d'Optique (Clément *et al.*, 2005)].

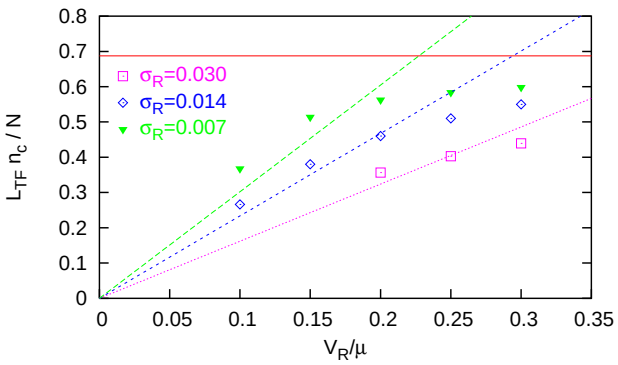

Figure 2.8 | Disorder-induced localization. Average density in the core of the localized condensate versus the amplitude of the disordered potential V_R for different values of the correlation length σ_R. The points correspond to numerical calculations and the lines to the analytic estimate (2.8). The horizontal (red online) line corresponds to the saturation limit $n_c = 11\mu/12g_{1D}$ [from (Sanchez-Palencia *et al.*, 2008)].

from the disorder, neither in the center nor in the tails of the condensate. Whether this effect should be called "Anderson localization" or not is a matter of taste as it depends on the definition adopted for Anderson localization[14]. Our point of view is that Anderson localization in its most appealing form results from interference of waves, for which single-scattering from the disordered potential is weak. In particular, it requires a smooth (exponential) decay in the tails of the wavefunction, which is not the case here. We thus do not call this effect Anderson localization, but rather disorder-induced localization.

2.3 Single-particle Anderson localization in disordered potentials created from speckle patterns

The experiments performed in 2005 at Institut d'Optique and LENS on the expansion of interacting Bose-Einstein condensates in speckle potentials were quite disappointing and at that time, most people in the community were very pessimistic about the possibility of observing Anderson localization with ultracold atoms, at least in speckle potentials. An important difficulty is that speckle potentials support large peaks (in blue-detuned speckles) or large wells (in red-detuned speckles), which can induce strong single-scattering as in the disorder-induced localization effect observed in 2005 (Sanchez-Palencia *et al.*, 2008). Important efforts were then devoted to design other kinds of potentials, in particular ones that are bounded in order to avoid strong single-scattering, and which may be better suited to observe Anderson localization. Particularly interesting routes that were put forward are (i) use of polychromatic quasi-periodic potentials, which mimic disorder in finite-size samples (Schulte *et al.*, 2005), and (ii) use of impurity atoms realized with a second atomic species trapped at random positions of a deep optical lattice, thus realizing very short-range correlated potentials (Gavish and Castin, 2005; Paredes *et al.*, 2005).

In spite of these difficulties, we decided to go ahead with speckle potentials. This was motivated by a couple of ideas. First, clear observation of Anderson localization in the form of exponential tails requires very weak disordered potentials in any model of disorder. Large peaks in speckle potentials will thus be suppressed anyway in interesting regimes. Second, a major feature of Anderson localization is that it is a universal phenomenon. Therefore, what might be observed with peculiar models of disorder should be observable with speckle potentials. Last but

[14] We had discussions with many specialists of disorder at that time. Although there were not so much debates about our interpretation, the relevance of the term "Anderson localization" in this context has been discussed, without reaching consensual agreement.

not least, speckle potentials are truly disordered potentials and they are very accurately controlled in ultracold atomic systems [see (Clément *et al.*, 2006) and Box 1, page 43]. Hence, should Anderson localization be observed in speckle potentials, it would open unprecedented routes to investigate many effects with full control of the disordered potential, for instance, effects of statistical correlations in the disorder, of atom-atom interactions, or even magnetism in disordered systems (Sanchez-Palencia and Lewenstein, 2010).

In collaboration with Georgy V. Shlyapnikov, we pursued this challenge and eventually came up with a proposal to observe Anderson localization with Bose-Einstein condensates expanding in one-dimensional speckle potentials (Sanchez-Palencia *et al.*, 2007). As we will see in the next paragraphs, our proposal not only paved the way to the first experimental observation of Anderson localization of a matterwave[15] (Billy *et al.*, 2008), but also raised interesting questions and opened new perspectives.

2.3.1 Single-particle localization emerges from the expansion of interacting Bose-Einstein condensates

▷ *see paper reprinted on page 67*

The starting point of our work is a very simple idea: In order to avoid strong reflections by the grains of the speckle potential, on should (i) lower the amplitude of the disordered potential (mainly to avoid classical reflections), and (ii) decrease the width of the speckle grains, *i.e.* decrease the correlation length (mainly to avoid quantum reflections). In order to understand what should then be expected from an expansion experiment as that of 2005, we have developed the model depicted in Fig. 2.9 (Sanchez-Palencia *et al.*, 2007):

– The condensate is first prepared in a harmonic trap (at $t<0$). Then, it is abruptly released from the trap at $t=0$ in the presence of the disordered potential[16]. In a first stage and for weak-enough disorder, interactions dominate the initial expansion and the disorder plays a marginal role. Then, the interaction energy is rapidly converted into kinetic (expansion) energy. For long-enough times ($t \gtrsim 1/\omega$, where ω is the frequency of the initial trap), the momentum distribution $\mathcal{D}(k)$ becomes stationary. The latter can be calculated explicitly from the scaling theory of expansion (Kagan *et al.*, 1996; Castin and Dum, 1996), which is valid for a condensate initially in the Thomas-Fermi regime as considered here. One finds $\mathcal{D}(k) \propto 1-(k\xi_{\rm in})^2$, where $\xi_{\rm in}=\hbar/\sqrt{4m\mu}$ is the healing length of the initially trapped condensate[17]. A feature which turns out to be crucial in the following is that $\mathcal{D}(k)$ drops to zero at the finite momentum, $k_{\rm max}=\xi_{\rm in}^{-1}$. The condensate can be described as a coherent superposition of plane waves e^{ikz}, which are almost non-interacting when the density has significantly dropped (*i.e.* for $t \gg 1/\omega$):

$$\psi(z,t)=\int \frac{dk}{\sqrt{2\pi}}\,\widehat{\psi}(k,t)\,e^{ikz}, \tag{2.9}$$

[15] Localization of a non-interacting Bose-Einstein condensate in a bi-chromatic lattice was observed at the same time in the group of Massimo Inguscio at LENS (Roati *et al.*, 2008).

[16] The condensate can be prepared either in the presence or in the absence of disorder. We have checked numerically that, for weak-enough amplitudes of the disordered potential, switching on the disorder on when the condensate is released from the trap, or already in the preparation stage does not affect significantly the subsequent dynamics.

[17] In this work, we use a definition of the healing length that differs by a factor of $\sqrt{2}$ from the usual definition. It allows us to significantly simplify the formulas below.

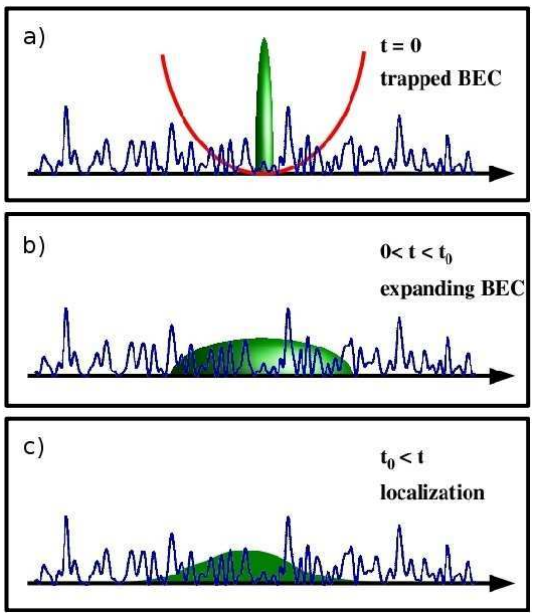

Figure 2.9 | Scheme used to evidence single-particle localization from expanding condensates. **a)** The condensate is initially prepared at equilibrium in a harmonic trap (possibly in the presence of weak disorder). We assume that, initially the meanfield interactions are strong, *i.e.* $\mu \gg V_{\mathrm{R}}, \hbar\omega$. **b)** The trap is then abruptly switched off at time $t = 0$ and the condensate starts to expand. The initial interaction energy is converted into kinetic (*i.e.* expanding) energy in the typical time $t_0 \sim 1/\omega$. **c)** When the density has sufficiently dropped that the interaction energy become negligible, the condensate can be described as a superposition of independent (non-interacting) waves. Each of these waves interacts with the disordered potential and eventually localizes. The condensate wavefunction is thus the superposition of all the corresponding localized waves.

where $|\widehat{\psi}(k,t)|^2 = \mathcal{D}(k)$.

– In the second stage, the disorder starts to play a significant role as it now dominates over the interactions. As a result, each plane wave localizes in the sense of Anderson, so that

$$\mathrm{e}^{ikz} \to \phi_k(z), \tag{2.10}$$

where $\phi_k(z)$ is a localized wave of energy[18] $E_k = \hbar^2 k^2/2m$, characterized by exponential localization. At short distance ($|z| < L_{\mathrm{loc}}$), the exponential localization is characterized by $\ln(|\phi_k(z)|) \sim -|z|/L_{\mathrm{loc}}(k)$, while at larger distance (not considered in the following) the exponential decay rate is a factor of 4 smaller (Piraud *et al.*, 2011). The localization behavior of a wave is actually more complicated Once all waves are localized, the expansion of the condensate stops and the density profile of the localized condensate is determined by the superposition of all localized states, each with its own localization length, and weighted by $\sqrt{\mathcal{D}(k)}$. Most importantly, we recall that the localization length $L_{\mathrm{loc}}(k)$ depends on the energy (or equivalently on the k-parameter) of the considered wave. Since we are working with weak disorder, the localization length can be calculated using the phase-formalism approach (see Sec. 2.1.2), which provides an analytical formula for the Lyapunov exponent (*i.e.* the inverse localization length). To lowest order and for a speckle potential created with a square aperture (see Box 1, page 43), we find:

$$\gamma(k) \equiv L_{\mathrm{loc}}(k) = \frac{\pi m^2 V_{\mathrm{R}}^2 \sigma_{\mathrm{R}}(1-k\sigma_{\mathrm{R}})}{2\hbar^4 k^2}\,\Theta(1-k\sigma_{\mathrm{R}}) \tag{2.11}$$

where Θ is the Heaviside step function. This formula is particularly interesting because it evidences a very peculiar property of one-dimensional speckle potentials: the existence of

[18] Localized states are solely defined by their energy E. It is however worth referring to the parameter $k = \sqrt{2mE}/\hbar$ –which corresponds to the wave vector in the absence of disorder– as it naturally appears in the expansion stage [Eq. (2.9)] as well as in the microscopic approaches of Anderson localization (see Sec. 2.1.2).

an *effective mobility edge* at $k_c \equiv 1/\sigma_R$ (Sanchez-Palencia *et al.*, 2007). In speckle potentials, long-range correlations induce a sharp crossover at $k = k_c \equiv 1/\sigma_R$ where the localization length jumps to very high values[19]. Then, the behavior of Anderson localization is very different below and above the effective mobility edge. In practice, while the waves with $k < k_c$ are Anderson localized with a localization length reasonably small, those with $k > k_c$ have much longer localization lengths and thus escape to distances much larger than the system size.

What are then the features of localization of the condensate ? The halt of the expansion is a first evidence of Anderson localization but it is not a sufficient proof since, for instance, it is not qualitatively different from the experiments of 2005 (Clément *et al.*, 2005; Fort *et al.*, 2005). It is thus crucial to determine the profile of the localized condensate. To do so, we just need to use the model outlined above: The initial expansion of the condensate driven by the interactions has populated momenta with a weight $\mathcal{D}(k)$, and the subsequent interaction with the disorder has localized each k-wave as $\phi_k(z)$. The condensate wavefunction is thus $\psi(z,t) = \int dk\, \sqrt{\mathcal{D}(k)}\, e^{-i\theta_k}\, e^{-iE_k t/\hbar}\, \phi_k(z)$, where θ_k is determined by the initial expansion of the condensate and microscopic details of the disordered potential. Since the phase of all waves evolve at very different frequencies and considering that the θ_k are random, all coherence terms vanish when averaging over time and disorder. The condensate density, $n_0(z) = |\psi(z,t)|^2$, thus reduces to

$$n_0(z) \simeq \int dk\, \mathcal{D}(k) \langle |\phi_k(z)|^2 \rangle. \tag{2.12}$$

In order to evaluate this integral, we have to remember that both $\mathcal{D}(k)$ and $\langle |\phi_k(z)|^2 \rangle$ have high-momentum cut-offs. Indeed, $\mathcal{D}(k) = 0$ for $k > k_{max}$, and, according to the theory of localization to lowest order [see Eq. (2.11)], $\gamma(k) = 0$ so that $\langle |\phi_k(z)|^2 \rangle = 0$ for $k > k_c$. It turns out that the localization of the condensate is very different depending on whether $k_{max} < k_c$ or $k_{max} > k_c$ (Sanchez-Palencia *et al.*, 2007):

– For $k_{max} < k_c$ (*i.e.* for $\xi_{in} > \sigma_R$), all k-waves created by the initial expansion process are strongly localized with a Lyapunov exponent larger than $\gamma(k_{max})$, since $\gamma(k)$ decreases with k [see Eq. (2.11)]. Then, the localization of the condensate is dominated at large distances by the longest localization lengths (*i.e.* the smallest Lyapunov exponents), and performing the integral in Eq. (2.12), we find exponential localization of the condensate density profile, with localization length

$$L_{BEC} = L_{loc}(1/\xi_{in}). \tag{2.13}$$

In other words, the localization length of the condensate is that of a *non-interacting* particle of momentum $k = 1/\xi_{in}$.

– For $k_{max} > k_c$ (*i.e.* for $\xi_{in} < \sigma_R$), a part of the k-waves (those with $k_c < k < k_{max}$) do not significantly localize and extend over distances much larger than the system size. In turn, the k-waves that localize (those with $k < k_c$) are exponentially localized, but with no lower

[19] General theorems state that all states are localized in one-dimensional disorder (see Sec. 2.1.2), irrespective to the particle energy. We have checked numerically that the Lyapunov exponent drops by one or two orders of magnitude in one-dimensional speckle potentials at the effective mobility edge (Sanchez-Palencia *et al.*, 2007). More detailed studies of effective mobility edges in one-dimensional speckle potentials are reported in (Gurevich and Kenneth, 2009; Lugan *et al.*, 2009) and in Sec. 2.3.3.

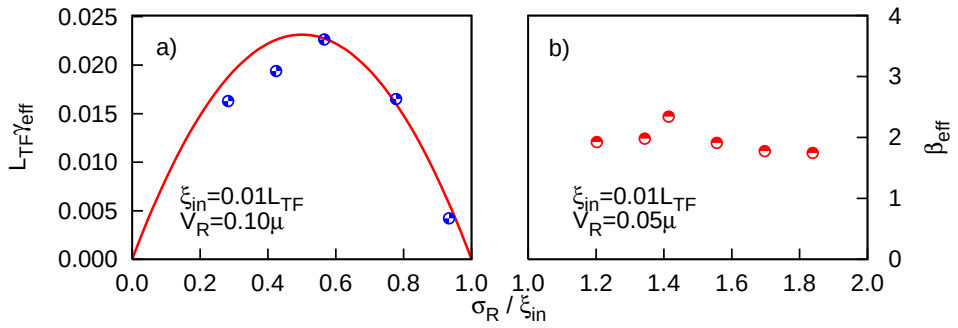

Figure 2.10 | Anderson localization of expanding Bose-Einstein condensates in one-dimensional speckle potentials. a) Exponential localization regime: Lyapunov exponent of the condensate as a function of the ratio σ_R/ξ_{in} for a fixed ratio $V_R/\mu = 0.10$, where $\mu = \hbar^2/4m\xi_{in}^2$ is the chemical potential of the initially trapped condensate. The red solid line corresponds to the analytical prediction [Eqs. (2.11) and (2.13)] and the blue points to fits of exponential functions to the tails of localized profiles calculated numerically **b) Algebraic localization regime:** Exponent of the algebraic decay obtained from numerical calculations as a function of the ratio σ_R/ξ_{in} for $V_R/\mu = 0.05$ [from (Sanchez-Palencia *et al.*, 2007)].

bound on the Lyapunov exponents [$\min_k(\gamma(k)) = \gamma(k_c) = 0$]. As a result, when integrating Eq. (2.12), we do not find exponential but *algebraic* localization:

$$n(z) \propto 1/|z|^2. \tag{2.14}$$

The exponent $\beta = 2$ is characteristic of the linear drop of $\gamma(k)$ when k approaches k_c from below. This result was quite unexpected. It shows that Anderson localization of expanding Bose-Einstein condensates should not be searched for only in the form of exponential decay of the tails.

In order to validate our analytical calculations, we have performed numerical calculations within the meanfield Gross-Pitaevskii approach. They confirm our predictions, not only qualitatively but also quantitatively, in both exponential ($k_{max} < k_c$) and algebraic ($k_{max} > k_c$) localization regimes, as shown in Fig. 2.10. Further analytical work and numerical calculations including the initial density profile and the spectral broadening induced by the disorder show a more complicated behavior, which we do not discuss here (Piraud *et al.*, 2011).

At this point, it is worth commenting a couple of points:

- *What does exponential localization of the expanding condensate reveal ?*
  Here, the key equation is Eq. (2.13), which shows that the localization length of the initially interacting condensate equals that of a non-interacting particle with the momentum k equal to the typical momentum of the expanding condensate, $k_{max} = \xi_{in}^{-1}$. Thus, this schemes allows for a direct measurement of localization length of non-interacting particles.

- *A central conclusion of the pioneer works of 2005 (Clément et al., 2005; Fort et al., 2005) is that one should get rid of interactions to observe Anderson localization with expanding condensates. In the present scheme, interactions play an important role, as they determine the momentum distribution $\mathcal{D}(k)$, in particular the value of k_{max}. Should one really get rid of interactions ?*

Paradoxically, it turns out that interactions strong enough that the condensate is initially in the Thomas-Fermi regime help observation of Anderson localization ! Indeed, the shape of the localized density profile is related to the momentum distribution, as Eq. (2.12) shows. Exponential localization crucially depends on the fact that the momentum distribution has a finite support. If one completely cancels the interactions (for instance using Feshbach resonance techniques), the momentum distribution of the expanding condensate would be a Gaussian (Basdevant and Dalibard, 2002), and the localized condensate can deviate from exponential localization[20]. In our scheme, the initial interactions actually control the value of the momentum at which we probe single-particle localization: $k = \xi_{\rm in}^{-1}$. Hence control of the initial chemical potential $\mu = \hbar^2/4m\xi_{\rm in}^2$ –via the coupling constant g or the density– allows to probe single-particle localization as a function of k, *i.e.* as a function of the energy.

- *What does algebraic localization reveal ?*
  It is worth stressing that algebraic localization of the condensate is not in contradiction with the theorems that non-interacting particles are all exponentially localized (Gertsenshtein and Vasil'ev, 1959; Mott and Twose, 1961; Borland, 1963; Beresinskii, 1974; Efetov, 1983). First, algebraic decay is expected at *intermediate* distances, that is at distances such that $L_{\rm loc}(k < k_{\rm c}) \ll |z| \ll L_{\rm loc}(k > k_{\rm c})$. In usual disordered potentials, such a region does not exist because the localization behaves smoothly as a function of k. Conversely, it does exist for speckle potentials because of the existence of an effective mobility edge at $k = k_{\rm c}$ (see above). Second, algebraic decay results from the sum of functions which are all exponentially localized, although with no lower bound for the Lyapunov exponent.

2.3.2 Experimental observation of Anderson localization in a one-dimensional speckle potential

▷ *see paper reprinted on page 73*

These results paved the way to a world-première: the first direct experimental observation of Anderson localization of matterwaves in the group of Philippe Bouyer and Alain Aspect at Institut d'Optique[15] (Billy *et al.*, 2008). The experiment is performed pretty much like in our proposal. An interacting Bose-Einstein condensate of 1.7×10^4 to 1.7×10^5 ^{87}Rb atoms is prepared in an elongated trap of frequencies $\omega_\perp = 2\pi \times 70$Hz and $\omega_z = 2\pi \times 5.4$Hz and in the presence of a speckle potential. The speckle potential is effectively one-dimensional: It is made of very anisotropic light grains, which are ellipsoids of radial sizes 97μm and 10μm much larger than the condensate radial size of about 3μm. In turn, the longitudinal size of the grains is very small, about $\pi\sigma_{\rm R} = 0.82\mu$m. At time $t = 0$, the speckle potential and the radial trap are maintained while the longitudinal trap is switched off. This produces a disordered one-dimensional guide along which the condensate expands, and eventually localizes (see Fig. 2.11).

Before turning to the discussion of the experimental results, it is worth stressing that there is an important difference compared to our model. With the above experimental values, the initial condensate is not one-dimensional, *i.e.* the radial profile does not coincide with the ground state of the radial trap. Indeed, the three-dimensional Thomas-Fermi chemical potential[21] ranges from

[20] For instance, with uncorrelated potentials, one can expect $n(z) \sim \exp\left(-\sqrt{|z|}\right)$.

[21] In the Thomas-Fermi regime, the chemical potential reads $\mu_{\rm TF}^{\rm (3D)} = \frac{\hbar\overline{\omega}}{2}\left(\frac{15Na_{\rm sc}}{\overline{\sigma}}\right)^{2/5}$, where N is the number of

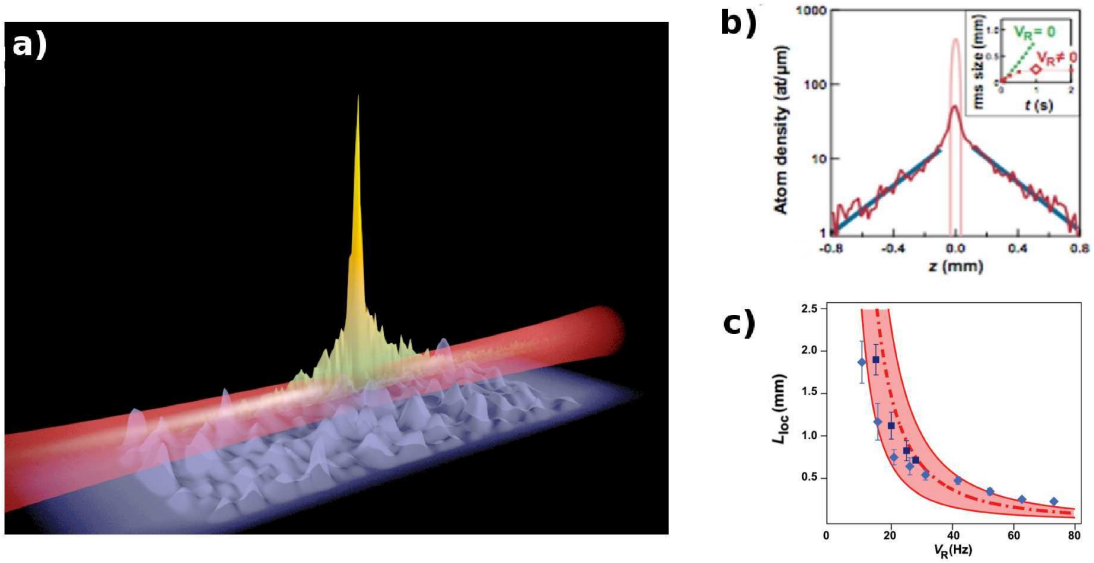

Figure 2.11 | Experimental observation of Anderson localization of matterwaves. a) An interacting condensate expands in a one-dimensional guide (red) in the presence of a speckle potential (blue). The expansion stops in less than 500ms and the density profile of the condensate is directly imaged [orange-green; from the data of (Billy *et al.*, 2008)]. **b)** The column density, plotted in semi-logarithmic scale, shows a clear exponential decay –characteristic of Anderson localization– for $k_{\max}\sigma_R < 1$. **c)** The localization length $L_{\rm loc}$, extracted by fitting a linear function $-2|z|/L_{\rm loc}$ to the tails of the logarithm of the density, shows a good agreement with theoretical calculations (Sanchez-Palencia *et al.*, 2007) [from (Bouyer *et al.*, 2008)].

$2\pi\hbar \times 200$Hz for 1.7×10^4 atoms and $2\pi\hbar \times 500$Hz for 1.7×10^5 atoms which exceeds $\hbar\omega_\perp$. Therefore, the proposed scenario must be adapted –but actually not much– in the initial expansion stage, where the disorder can be ignored. When the longitudinal trap is switched off, the condensate expands along the guide. Since the radial trap is maintained, the radial profile only changes due to the decrease of the density. The longitudinal expansion thus slaves the radial dynamics, with a typical time $1/\omega_z$. Hence, when the density decreases, the radial profile in a slice of length dz centered at position z adiabatically follows that of a two-dimensional condensate of $n_{\rm 1D}dz$ atoms[22] at equilibrium in a harmonic trap of frequency $\omega_\perp$, thus turning from inverted parabola (for $n_{\rm 1D}a_{\rm sc} \gg 1$) to Gaussian (for $n_{\rm 1D}a_{\rm sc} \ll 1$) when the one-dimensional density lowers. In other words, the condensate turns from a three-dimensional Thomas-Fermi profile to a one-dimensional expanding gas with a radial wavefunction frozen in the radial ground state, once the one-dimensional density has dropped below $a_{\rm sc}^{-1}$. With Ben Hambrecht, we have checked numerically the validity of this scenario for experimentally-relevant parameters, confirming in particular that the guided expansion does not significantly excite radial modes. We have also found that for weak-enough interactions (as in the experiment), the one-dimensional momentum distribution is still compatible with an inverted parabola with $k_{\max} \simeq \sqrt{4m\mu_{\rm TF}^{\rm (3D)}}/\hbar$. This has also been checked in the experiment by measuring directly the momentum distribution of the expanding condensate in the absence of disorder. We can thus safely rely to the initial one-dimensional model, using the correct value for $k_{\max}$.

atoms, $a_{\rm sc} = mg/4\pi\hbar^2$ is the scattering length ($a_{\rm sc} \simeq 5.1 \times 10^{-9}$m for ^{87}Rb atoms), $\overline{\omega} = (\omega_x\omega_y\omega_z)^{1/3}$ is the geometrical average of the trap frequencies, and $\overline{\sigma} = \sqrt{\hbar/m\overline{\omega}}$ (Pitaevskii and Stringari, 2003).

[22]Here, $n_{\rm 1D} = \int d\rho_\perp\, n(\rho_\perp, z)$ is the one-dimensional density.

What is then the experimental verdict ? The experiment performed at Institut d'Optique is described in details in the Ph-D thesis of Juliette Billy (Billy, 2010). Here, we only report and comment the main results.

– For $k_{\max}\sigma_R \simeq 0.65 < 1$, the condensate stops expanding in a fraction of a second. Direct imaging of the localized density profile shows clear exponentially decaying tails (see Fig. 2.11b), $\ln[n(z)] \sim -2|z|/L_{\rm loc}$, which have been shown to be stationary over more than 2 seconds (Billy *et al.*, 2008). This is the direct signature of Anderson localization. Even more interesting, the density profiles are good-enough to directly extract the localization lengths from simple linear fits to the tails of the profiles plotted in semi-logarithmic scale. The localization length $L_{\rm loc}$ plotted as a function of the amplitude of disorder, V_R (see Fig. 2.11c) shows quite a good agreement with our prediction (Sanchez-Palencia *et al.*, 2007):

$$L_{\rm loc} = \frac{2\hbar^4 k_{\max}^2}{\pi m^2 V_R^2 \sigma_R (1 - k_{\max}\sigma_R)}. \tag{2.15}$$

In the first experiment (Billy *et al.*, 2008) [light blue diamonds in Fig. 2.11c], there is however a non-negligible discrepancy. For the smallest values of V_R, the discrepancy was due to a limited width of the speckle potential, thus making the largest measured values of $L_{\rm loc}$ questionable. Using a wider speckle potential, the agreement with the analytical predictions is much better (Bouyer *et al.*, 2008) [dark blue squares in Fig. 2.11c]. For the largest values of V_R ($V_R/h > 40$Hz), a discrepancy still remains. In this case, the localization lengths are the smallest and the hypothesis on small-distance behavior is questionable. As detailed in (Piraud *et al.*, 2011), localization lengths measured to be larger that $L_{\rm loc}(1/\xi_{\rm in})$ may be a signature of the cross-over from short-distance to long-distance behavior.

– For $k_{\max}\sigma_R \simeq 1.15 > 1$, the condensate also stops expanding, but it turns out that the tails of the localized profile no longer decay exponentially, but rather as a power-low, $n(z) \sim 1/|z|^\beta$. The precision of the experimental data is good enough to indeed clearly distinguish between exponential decay and algebraic decay (see Fig. 2.12). Again, the exponent β can be extracted from linear fits to the tails of the profile, but now in log-log scale. This confirms our prediction of algebraic localization in this regime (Sanchez-Palencia *et al.*, 2007). The experimental fits provide $\beta \simeq 1.95 \pm 0.10$, in excellent quantitative agreement with our prediction, $\beta = 2$.

These results have attracted much attention. First, they are the first experimental direct observation of Anderson localization of a matter-wave, fifty years after the work of Anderson. Second, the observation of algebraic localization in the regime $k_{\max}\sigma_R > 1$ constitutes the first evidence of effective mobility edges in one-dimensional speckle potentials. In our view, even more important is the fairly good agreement that was found between theoretical predictions and experimental data. It proves that we can now trust the potential of experiments with ultracold atoms to realize *quantum simulators* for more complicated situations. It thus paves the way to address many outstanding challenges in the field of disordered systems, for instance (i) Anderson localization of non-interacting particles in dimensions larger than one; (ii) interplay of interactions and localization; (iii) effects of disorder on spin-exchange coupling in spin systems (see Conclusions and perspectives).

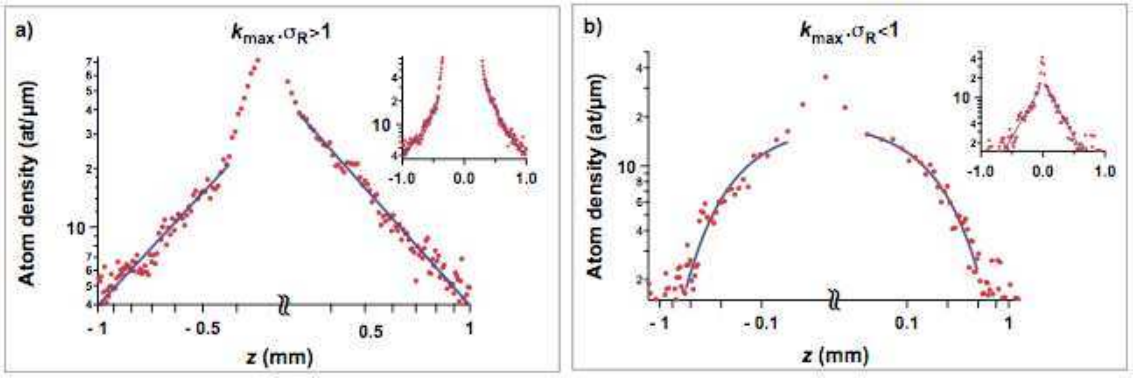

Figure 2.12 | **Algebraic versus exponential regimes in a one-dimensional speckle potential.** Log-log (main figures) and semi-log (insets) plots of the density profiles showing the difference between the algebraic ($k_{max}\sigma_R > 1$) and the exponential ($k_{max}\sigma_R < 1$) regimes. **a)** Density profile for $V_R/\mu = 0.15$ and $k_{max}\sigma_R = 1.16 \pm 0.14$. The fit to the tails with a power law decay $1/|z|^\beta$ yields $\beta \simeq 1.95 \pm 0.10$. The same data, plotted in semi-log scale in the inset, confirm the non-exponential decay. **b)** For comparison, similar set of plots in the exponential regime with the same V_R/μ but with $k_{max}\sigma_R = 0.65 \pm 0.09$. It confirms that a non-algebraic but exponential decay in the tails [from (Billy *et al.*, 2008)].

2.3.3 Effective mobility edges in one-dimensional speckle potentials

▷ *see paper reprinted on page 77*

As shown above, Bose-Einstein condensates released from a harmonic trap into quasi-periodic or fully disordered potentials offer a fantastic tool to investigate the physics of localization (Sanchez-Palencia and Santos, 2005; Sanchez-Palencia *et al.*, 2007). It allows one to demonstrate fundamental phenomena. So far, the most important of which is the direct observation of one-dimensional Anderson localization for the first time with a matter-wave (Billy *et al.*, 2008). It may be naively believed that Anderson localization in one dimension is fairly well understood and that there is little point in reappraising them. It is not so in the field of ultracold atoms for two reasons. First, quantitative investigations are possible thanks to the good control of parameters, and details that are ignored in universal approaches to Anderson localization, such as the scaling theory for instance, turn out to play crucial roles. Second, ultracold atom systems have their own features, which are usually not accounted for in toy models of condensed-matter physics. As discussed above, speckle potentials show particular localization properties, which fundamentally differ from the mostly-considered uncorrelated disordered potentials. Such a property is the existence of effective mobility edges, which are direct consequences of the finite support of the power spectrum of speckle potentials. First evidence of effective mobility edges is the crossover from exponential localization (for $\xi_{in} > \sigma_R$) to algebraic localization (for $\xi_{in} < \sigma_R$) in expanding condensates (Sanchez-Palencia *et al.*, 2007; Billy *et al.*, 2008).

On the basis of the usual second-order perturbative expansion, one may conclude that particles with $k > \sigma_R^{-1}$ do not localize (*i.e.* the Lyapunov exponent $\gamma(k) = L_{loc}^{-1}$ vanishes), and the question to know whether one-dimensional speckle potentials have true mobility edges was raised. In view of general theorems, based on fairly general assumptions (Molchanov, 1978; Carmona, 1982; Leschke *et al.*, 2003; Leschke *et al.*, 2005; Figotin *et al.*, 2007) and also of numerical evidence that L_{loc} does not vanish but however shows a sharp step at $k > k_c = \sigma_R^{-1}$ (Sanchez-Palencia *et al.*, 2007), it is definitely not the case. In contrast, the relevant question is to precisely understand

how does the Lyapunov exponent $\gamma(k)$ behave across the effective mobility edge.

Together with Pierre Lugan, we have addressed this question by calculating the Lyapunov exponent up to fourth perturbation order, in the framework of the phase-formalism, which is valid for any kind of weak correlated one-dimensional disordered potentials (Lifshits *et al.*, 1988). The calculations are quite tedious but analytical expressions can be found (Lugan *et al.*, 2009). Earlier studies were restricted to disorder with symmetric probability distribution (Tessieri, 2002), which do not apply to speckle potentials. Examples were exhibited, for which exponential localization does occur even for $k > k_c$. It was also concluded that for Gaussian disorder, there is a second effective mobility edge at $2k_c$, while for non-Gaussian disorder, it is generally not so. However, these results do not apply to speckle potentials whose probability distribution is asymmetric (see Box 1, page 43). Moreover, although speckle potentials are not Gaussian, they derive from the squared modulus of a Gaussian field, and the above conclusions must be re-examined (Gurevich and Kenneth, 2009; Lugan *et al.*, 2009). Hence, speckle potentials are not usual disordered potentials. They actually form an original class of non-Gaussian disorder which nevertheless inherits properties of an underlying Gaussian process.

Let us discuss the main features of Anderson localization in one-dimensional speckle potentials[23]. We find that there exist several effective mobility edges at $k_c^{(p)} = pk_c$ with $p \in \mathbb{N}$, such that Anderson localization in the successive intervals $k_c^{(p-1)} < k < k_c^{(p)}$ results from scattering processes of increasing order. Effective mobility edges are thus characterized by sharp crossovers in the k-dependence of the Lyapunov exponent γ. This is illustrated in Fig. 2.13a, which shows the Lyapunov exponent $\gamma(k)$ as calculated up to order four for a usual speckle potential, as a function of k and of the strength of disorder $\varepsilon_R = 2m\sigma_R^2 V_R/\hbar^2$. For a fixed value of ε_R, we see that $\gamma(k)$ decreases smoothly, except in the vicinity of $k \simeq \sigma_R^{-1}$, where $\gamma(k)$ suffers a sharp step[24]. Moreover, we find that the step increases when the strength of the disorder ε_R decreases. These perturbative calculations are in excellent agreement with exact numerical calculations, which have been performed by Dominique Delande with an impressive precision (Lugan *et al.*, 2009).

The fact that Anderson localization results from scattering processes of increasing order as k increases can be understood from the property that the n-th order Lyapunov exponent is a function of the n-th order correlation function of the disordered potential. In a speckle potential, it contributes up to $k = \lfloor n/2 \rfloor k_c$, where $\lfloor\ .\ \rfloor$ represents the integer part. More precisely, we find that $\gamma(k) \sim \sigma_R^{-1}(\varepsilon_R/k\sigma_R)^{2n}$ for $(n-1)k_c < k < nk_c$. Note that since speckle potentials are asymmetric, odd terms do not vanish and they can actually have significant contributions (Lugan *et al.*, 2009). However, only the even terms affect the positions of the effective mobility edges, which can be easily understood by *reductio ad absurdum*: If the odd term $\gamma^{(2n+1)}(k)$ would not vanish for $k > nk_c$, it would be the dominant term (since all lower-order terms do vanish for $k > nk_c$). This is not possible because $\gamma^{(2n+1)}(k)$ changes sign when V_R changes sign, so that it would be negative (and thus non physical) for either blue- or red-detuned speckles.

Let us finally re-examine more precisely the experimental results obtained with a Bose-Einstein condensate expanding in a speckle potential. Due to limited spatial extension of the speckle potential and finite resolution of the imaging system, the effective system half size was $L_{max} = 4$mm, which defines the maximum localization that can be measured. The behavior of the Lyapunov exponent obtained from fourth-order calculations for ε_R close to the experimental values of Fig 2.12

[23] More detailed calculations and discussions are reported in (Lugan *et al.*, 2009) reprinted on page 77.

[24] One can also see a sharp step at $k = 2\sigma_R^{-1}$ but full description of it requires calculations up to sixth order, which are not included in the figure.

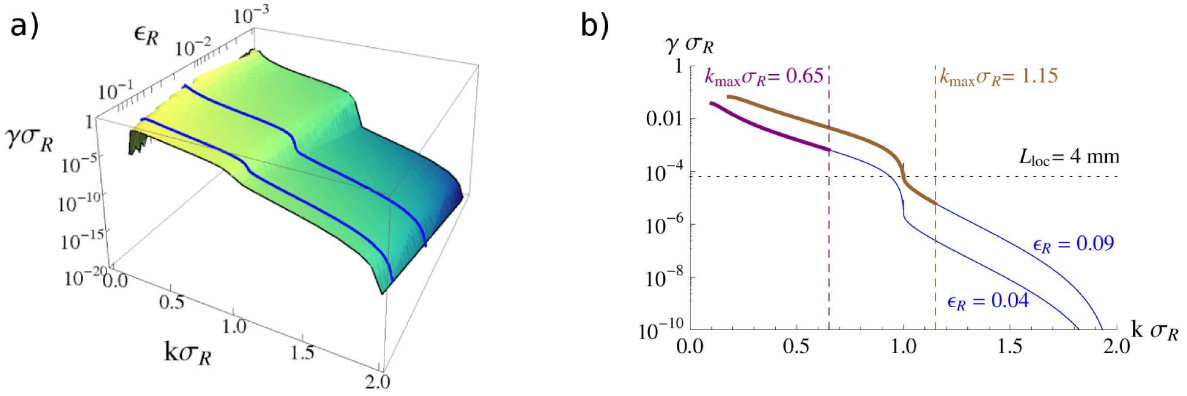

Figure 2.13 | Effective mobility edges in one-dimensional speckle potentials. a) Lyapunov exponent calculated up to fourth order in the perturbation series for particles in one-dimensional speckle potentials created with a square diffusive plate, versus the particle momentum $\hbar k$ and the strength of disorder ε_R. The solid blue lines correspond approximately to the extreme values used in the experiment at Institut d'Optique ($\varepsilon_R = 0.1$ and $\varepsilon_R = 0.02$) [from (Lugan *et al.*, 2009)]. **b)** Lyapunov exponent versus the particle momentum for two fixed values of the strength of disorder ($\varepsilon_R = 0.09$ corresponding approximately to Fig. 2.12a, and $\varepsilon_R = 0.04$ corresponding approximately to Fig. 2.12b). The vertical dashed lines correspond to the edge of the momentum distributions of the expanding condensate and the horizontal dotted line to the maximum visible localization length in the experiment of Institut d'Optique [from (Lugan, 2010)].

is plotted in Fig. 2.13b.

– For $k_{max}\sigma_R < 1$ (Fig. 2.12b), we have $\varepsilon_R \simeq 0.04$ and $k_{max}\sigma_R = 0.65$. We see in Fig. 2.13b that the maximum localization length of the k-components in the expanding condensate is less than L_{max}. We thus expect to observe exponential localization of the condensate with a localization length equal to $L_{loc}(1/\xi_{in})$, *i.e.* the longest localization length of the populated states. This is indeed what is observed in Fig. 2.12b.

– For $k_{max}\sigma_R > 1$ (Fig. 2.12a), we have $\varepsilon_R \simeq 0.09$ and $k_{max}\sigma_R = 1.15$. In this case, we see in Fig. 2.13b that L_{max} lies in the sharp step associated to the effective mobility edge, which is about one order of magnitude. This confirms that the contributions of all k-components with $k > k_{max}$ can be ignored, leading to algebraic localization as predicted by us Sanchez-Palencia *et al.*, 2007 and demonstrated experimentally (Billy *et al.*, 2008). This is a first evidence of the existence of effective mobility edges in speckle potentials. Direct proof would however require to measure localization lengths across the effective mobility edge. With the parameters of the experiment by Billy *et al.* (2008), this means increasing the effective size of the system, L_{max}, by at least one order of magnitude.

2.4 Reprints of papers associated with the chapter

1. SANCHEZ-PALENCIA L. and SANTOS L., *Bose-Einstein condensates in optical quasicrystal lattices*, Phys. Rev. A **72**, 053607 (2005); ▷ *page 57*.

2. CLÉMENT D., VARON A.F., RETTER J.A., BOUYER P., SANCHEZ-PALENCIA L., GANGARDT D.M., SHLYAPNIKOV G.V., and ASPECT A., *Suppression of transport of*

an interacting elongated Bose-Einstein condensate in a random potential, Phys. Rev. Lett. **95**, 170409 (2005); ▷ ***page 63***.

3. SANCHEZ-PALENCIA L., CLÉMENT D., LUGAN P., BOUYER P., SHLYAPNIKOV G.V., and ASPECT A., *Anderson localization of expanding Bose-Einstein condensates in random potentials*, Phys. Rev. Lett. **98**, 210401 (2007); ▷ ***page 67***.

4. BILLY J., JOSSE V., ZUO Z., BERNARD A., HAMBRECHT B., LUGAN P., CLÉMENT D., SANCHEZ-PALENCIA L., BOUYER P., and ASPECT A., *Direct observation of Anderson localization of matter-waves in a controlled disorder*, Nature **453**, 891 (2008); ▷ ***page 73***.

5. LUGAN P., ASPECT A., SANCHEZ-PALENCIA L., DELANDE D., GRÉMAUD B., MÜLLER C.A., and MINIATURA C., *One-dimensional Anderson localization in certain correlated random potentials*, Phys. Rev. A **80**, 023605 (2009); ▷ ***page 77***.

Bose-Einstein condensates in optical quasicrystal lattices

L. Sanchez-Palencia[1,2] and L. Santos[3]
[1]*Laboratoire Charles Fabry, Institut d'Optique, Université Paris-Sud XI, F-91403 Orsay, France*
[2]*Institut für Theoretische Physik, Universität Hannover, D-30167 Hannover, Germany*
[3]*Institut für Theoretische Physik III, Universität Stuttgart, D-70569 Stuttgart, Germany*
(Received 24 February 2005; published 8 November 2005)

We analyze the physics of Bose-Einstein condensates confined in two dimensional (2D) quasiperiodic optical lattices, which offer an intermediate situation between ordered and disordered systems. First, we analyze the time-of-flight interference pattern that reveals quasiperiodic long-range order. Second, we demonstrate localization effects associated with quasidisorder as well as quasiperiodic Bloch oscillations associated with the extended nature of the wave function of a Bose-Einstein condensate in an optical quasicrystal. In addition, we discuss in detail the crossover between diffusive and localized regimes when the quasiperiodic potential is switched on, as well as the effects of interactions.

DOI: 10.1103/PhysRevA.72.053607 PACS number(s): 03.75.Lm, 32.80.Pj, 71.30.+h

The last few years have witnessed a fastly growing interest on ultracold atomic gases in laser-generated periodic potentials [optical lattices (OLs)]. These present neither defects nor phonons, offering a powerful tool for investigating the quantum behavior of periodic systems under unique control possibilities. Thus, ultracold atoms trapped in OLs show fascinating resemblances with solid-state physics, which range from Bloch oscillations [1,2] and Wannier-Stark ladders [3], to Josephson arrays of Bose-Einstein condensates (BECs) [4], or to the superfluid to a Mott-insulator transition [5].

These remarkable experiments have been performed in regular cubic OLs. However, these lattices do not exhaust the rich possibilities offered by optical potentials. More sophisticated lattice geometries have been proposed, as honeycomb [6] or Kagomé and triangular [7] lattices. Beyond, controlled defects may be introduced to generate random or pseudorandom potentials [8], allowing for the realization of Kondo-like physics [9], Anderson localization, and Bose-Glass phases [10]. Exploiting this possibility, laser speckle fields have been employed very recently to produce BECs in random potentials [11–13] opening very exciting experimental possibilities.

Bridging between ordered and disordered structures, quasicrystals (QC) have attracted a wide interest since their discovery in 1984 [14]. QCs are long-range ordered materials but without translational invariance, and consequently they share properties with both ordered crystals and amorphous solids [15]. In particular, QCs show intriguing structure [16] as well as electronic conduction properties [17] at the border between ordered and disordered systems.

Surprisingly, up to now, few works have been devoted to optical analogues of QCs, despite of the fact that OLs offer dramatic possibilities for designing a wide range of geometries [18]. Optical QCs have been first studied in laser cooling experiments [19], in which the atomic gas, far from quantum degeneracy, was confined in a dissipative OL where quantum coherence was lost due to spontaneous emission. In these systems, the temperature and spatial diffusion were found to behave similarly as in periodic OLs. The physics of one-dimensional (1D) quasiperiodic OLs has also been subject of recent research in the context of cold atomic gases, including a proposal for the atom-optical realization of the Harper model [20], and the analysis of Fibonacci potentials [21].

In this paper, we study the dynamics of a BEC in a two-dimensional (2D) optical QC. First, we show that the BEC wave function displays quasiperiodic long-range order, a property that may be easily probed via matter-wave interferometry. Second, we show that macroscopic quantum coherence dramatically modifies the transport on the lattice compared with the dissipative case. On the one hand, due to quasidisorder in optical QC, spatial localization occurs, in contrast to ballistic expansion in periodic lattices. The crossover between ballistic expansion and localization is analyzed when the quasiperiodicity of the lattices is continuously increased. On the other hand, we show that due to the extended character of the BEC wave function, Bloch oscillations take place. These oscillations are however quasiperiodic rather than periodic. Additionally, we briefly discuss the effects of the interatomic interactions in the BEC diffusion.

In the following we consider a dilute Bose gas trapped in the combination of a smooth harmonic potential $V_{\rm ho}(\vec{r})=(M/2)(\omega_\perp^2\vec{r}_\perp^2+\omega_z^2 z^2)$ plus an OL $V_{\rm latt}(\vec{r}_\perp)$. In the previous expression, M is the atomic mass, ω_j are the harmonic trap frequencies, and $\vec{r}_\perp=(x,y)$ is the position vector on the lattice plane. We assume ω_z to be large enough to keep a 2D physics on the xy plane. We consider a laser configuration [19] consisting on $N_{\rm b}$ laser beams arranged on the xy plane with $N_{\rm b}$-fold symmetry rotation (Fig. 1). The polarization $\vec{\epsilon}_j$ of laser j with wave vector $\vec{k}_j$ is linear and makes an angle α_j with the xy plane. The optical potential is thus [22]

$$V_{\rm latt}(\vec{r}_\perp)=\frac{V_0}{\left|\sum_j \varepsilon_j\right|^2}\left|\sum_{j=0}^{N_{\rm b}}\varepsilon_j\vec{\epsilon}_j e^{-i(\vec{k}_j\cdot\vec{r}_\perp+\varphi_j)}\right|^2, \qquad (1)$$

where $0\leqslant\varepsilon_j\leqslant 1$ stand for eventually different laser intensities and φ_j are the corresponding phases. In the following, we are mostly interested in the fivefold symmetric configuration ($N_{\rm b}=5$, $\varepsilon_j=1$), similar to the Penrose tiling [23], which supports no translational invariance (see Fig. 1). The

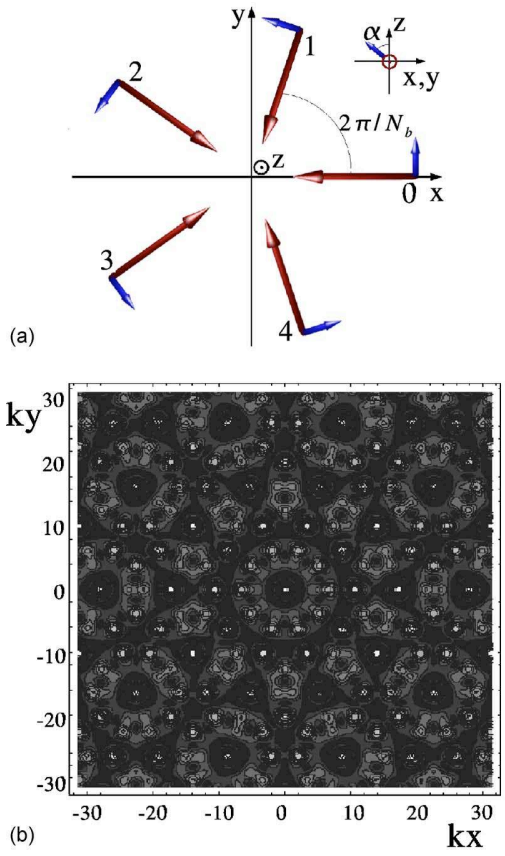

FIG. 1. (Color online) Left: The Laser arrangement (see the text for details). Right: A quasiperiodic lattice potential for $N_b=5$, $V_0<0$ and $\alpha_j=0$. The white points correspond to potential minima.

lattice displays potential wells which are clearly not periodically arranged. We also consider the configuration obtained by switching off lasers 1 and 4, which results in an anisotropic periodic lattice.

(a) Equilibrium properties. The stationary BEC wave function ψ_0 is obtained from evolution in imaginary time of the 2D Gross-Pitaevskii equation (GPE)

$$i\hbar\partial_t\psi=[-\hbar^2\vec{\nabla}^2/2M+V_{\rm ho}+V_{\rm latt}+g_{\rm 2D}|\psi|^2]\psi, \qquad (2)$$

where $g_{\rm 2D}=\sqrt{8\pi\hbar^3\omega_z/M}a_{\rm sc}$, with $a_{\rm sc}$ the s-wave scattering length. In order to elucidate the long-range order properties of the BEC, we compute the momentum distribution of ψ_0. In the periodic case [Fig. 2(a)], as expected, the momentum distribution displays discrete peaks corresponding to combinations of elementary basis vectors of the reciprocal lattice, $n_1\vec{\kappa}_1+n_2\vec{\kappa}_2$ with integer coefficients n_1 and n_2. As obtained in previous experimental works [24,25], this confirms the periodic long-range order of ψ_0. The quasiperiodic case [Fig. 2(b)] is more intriguing, resulting in a more complex structure. The momentum distribution also displays sharp peaks, being the signature of a long-range order which is quasiperiodic rather than periodic [26]. As in the periodic case, the positions of the peaks are linear combinations of integer numbers of $N_b=5$ wave vectors: $\Sigma_{j=0}^{N_b-1}n_j\vec{\kappa}_j$, where $\vec{\kappa}_0=\vec{k}_1-\vec{k}_0$ and $\vec{\kappa}_j=\mathcal{R}[\phi_j]\vec{\kappa}_0$ is the wave vector obtained by a

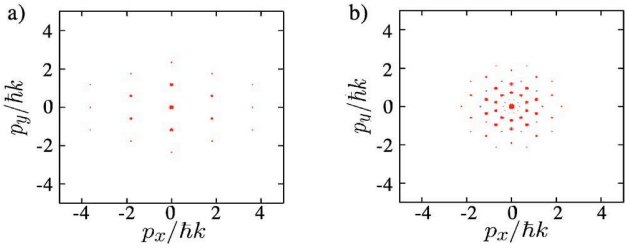

FIG. 2. (Color online) The matter-wave interference pattern of a BEC released from a combined OL and harmonic trap. (a) The periodic case; (b) The quasiperiodic case. Both correspond to ^{87}Rb and $V_0=-10E_{\rm R}$, where $E_{\rm R}=\hbar^2k^2/2M$ is the recoil energy.

rotation of angle $\phi_j=2\pi j/N_b$ of $\vec{\kappa}_0$. The reciprocal lattice thus clearly shows a fivefold rotation symmetry incompatible with any translation invariance [27]. This resembles the Penrose tiling [23] and the solid state QCs observed via Bragg diffraction [14].

The discussed momentum distribution can be *directly imaged* via matter-wave interferometry after a time-of-flight expansion [28]. Indeed, although the interactions are crucial for determining local populations of each potential well, they do not contribute significantly to the free BEC expansion after release from the trap [24]. Such measurements, standard in periodic OLs [24,25], can be easily extended to quasiperiodic ones.

(b) Quantum transport. Certainly, not all physical properties of optical QCs can be directly interpolated from the behavior of periodic lattices. Indeed, solid QCs show intriguing dynamical properties that are not yet completely understood [15]. In the following, we investigate dynamical properties of quasiperiodic lattices.

(b1) Coherent diffusion. Starting from the equilibrium wave function ψ_0, we consider the situation in which the harmonic trap is switched off at $t=0$, letting the BEC evolve in the OL. The BEC expansion is then computed using a Crank-Nicholson algorithm for the real time-dependent GPE (2). Figure 3 (inset) shows the time evolution of $\langle x^2\rangle$ and $\langle y^2\rangle$ of the interacting BEC along x and y, respectively. In the periodic case, the condensate expands coherently as one ex-

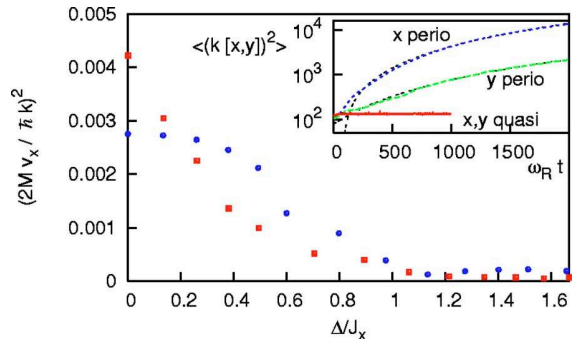

FIG. 3. (Color online) The crossover from ballistic to localization regimes with (squares) and without (circles) interactions, for $V_0=-7.5E_{\rm R}$. Inset: Coherent diffusion in periodic and quasiperiodic lattices for $V_0=-5E_{\rm R}$. Fits to $\langle r_j^2(t)\rangle=r_{j0}^2+2D_jt+v_j^2t^2$ in the periodic case are also shown.

pects from tunnel couplings between adjacent lattice sites. In order to infer a convenient fitting functional for the expansion of the interacting BEC, let us recall that in free space for large times $\langle r_j^2(t)\rangle \propto v_j^2 t^2$ with $v_j \propto 1/M$ [28]. In periodic lattices, the inertia is enhanced, and the expansion is expected to be as in free space but substituting the atomic mass M by an effective mass $M^* > M$. We thus expect $v_j \propto 1/M^*$ and $M/M^* \propto J$ where J is the site-to-site tunneling rate [29]. Numerical computations for various depths of the lattice potential V_0 show that v_j^2 decreases exponentially with V_0 as expected from the well-known exponential decay of J. Anisotropic ballistic expansion of the BEC reflects the anisotropy of our periodic lattice.

The behavior of the BEC in the quasiperiodic lattice is dramatically different, since after a short transient the BEC localizes [30] (inset of Fig. 3). This behavior strongly contrasts with the results obtained in the context of laser cooling where a similar classical normal expansion ($\langle r_j^2(t)\rangle \sim 2\tilde{D}_j t$) was found for both periodic and quasiperiodic OLs [19]. Here, spatial localization is a coherent effect induced by quasidisorder due to the lack of periodicity. Indeed, the BEC populates localized (Wannier-like) states centered on each lattice site. In the periodic case these states have all the same energy and are strongly coupled through quantum tunneling. On the contrary, in the quasiperiodic lattice, the sites have different energies. In particular, the typical difference of depths of adjacent sites (denoted Δ below) can be of the order of magnitude of (but smaller than) the potential depth. The tunneling is not resonant and the BEC localizes.

The remarkable flexibility of OLs [18] allows for the accurate study of the competition between tunneling and quasidisorder. By ramping up gradually the intensity of lasers 1 and 4 while keeping constant 0, 2, and 3, one turns continuously from an anisotropic periodic lattice to a fivefold symmetric quasiperiodic one, and hence from ballistic expansion to spatial localization. For small intensity of the control lasers 1 and 4, the quasiperiodicity is mainly *compositional* (the sites are still periodically displaced but the on-site energies are different from site to site). We define the quasidisorder Δ parameter as the variance of the differences of on-site energies in adjacent sites. From the previous discussion and to compare to the results of the nondegenerate case [19] we fit

$$\langle r_j^2(t)\rangle = \langle r_{j0}^2\rangle + 2D_j t + v_j^2 t^2. \tag{3}$$

In the considered range of parameters, all calculations fit well with Eq. (3) with a negligible diffusive term $2D_j t$. We characterize the expansion along the x direction through the ballistic velocity v_j. The behavior of v_x versus the quasidisorder parameter Δ is shown in Fig. 3 for the interacting BEC and it is compared to the noninteracting case. For the latter, we simultaneously switched off the interactions at $t=0$ [32]. In both cases, as expected, coherent diffusion dramatically decreases when quasidisorder increases. Spatial localization occurs for $\Delta \gtrsim J_x$, with J_x the tunneling rate between adjacent sites along the x direction [33]. This supports the interpretation that competition between coherent tunneling and inhomogeneities turns into localization as soon as tunneling becomes nonresonant.

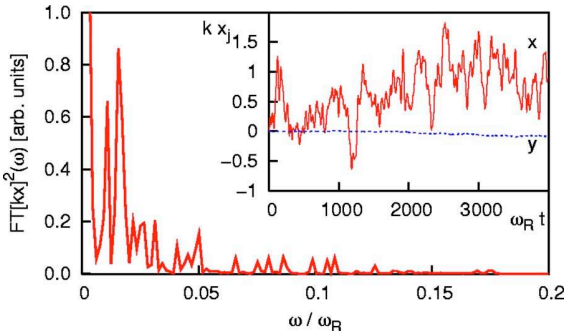

FIG. 4. (Color online) The Fourier transform of the mean position of a BEC in a periodic or quasiperiodic lattice. Inset: The time evolution of a BEC in a tilted quasiperiodic lattice. All beams have the same intensity, $V_0 = -2E_R$ and $V_{tilt} = 0.002E_R \times kx$.

To understand the effect of interactions that can help ($\Delta \lesssim 0.2J_x$ in Fig. 3) or hinder ($\Delta \gtrsim 0.2J_x$ in Fig. 3) diffusion, note first that two phenomena contribute to localization: (i) initial inhomogeneities (due to disorder and harmonic confinement) that appear in the dynamics through the interaction term $g_{2D}|\psi_0|^2$ [see Eq. (2)] and (ii) inhomogeneities associated to quasidisorder. Because of these inhomogeneities, quantum tunneling is not resonant and thus less efficient. However, during diffusion, the interaction energy is converted into kinetic energy and this tends to fasten the expansion. For small quasidisorder, the second phenomenon dominates so that interactions contribute to expansion whereas for larger quasidisorder, the inhomogenities significantly hinder tunneling so that interactions contribute to localization. The nontrivial interplay between disorder and interactions will be the subject of further research.

(b2) Quasiperiodic Bloch oscillations. One of the most appealing predictions of the quantum theory of solids [27] is that homogeneous static forces induce oscillatory rather than constant motion in periodic structures [34]. The corresponding Bloch oscillations have already been observed in superlattice superconductors [35] and on cold atoms in OLs [1,2]. It is a fundamental question whether such a phenomenon also exists in less ordered systems like QCs. Arguments based on general spectral properties of QCs [36] and numerical simulations of 1D Fibonacci lattices [37] support the existence of Bloch oscillations in quasiperiodic lattices. However, to the best of our knowledge, this effect has never been observed experimentally. Using accelerated lattices [1,2] or gravity [38] (we consider the latter), this question can be addressed experimentally in the discussed arrangement (Fig. 1). Starting from ψ_0 we switched off the harmonic trap and the interactions at time $t=0$ and tilt the quasiperiodic lattice in the x direction [39]. The latter evolution of the quantum gas is shown in the inset of Fig. 4. We find noisy-like oscillatory motion in the (tilted) x direction and no motion in the (nontilted) y direction. The oscillations in the x direction are clearly not periodic [40]. However, they definitely have an ordered structure, which is evidenced by the appearance of discrete sharp peaks in the time Fourier transform of the BEC mean position $\langle x(t)\rangle$ (Fig. 4), corresponding to a quasiperiodic motion [26].

The Bloch-like quasiperiodic oscillations can be interpreted as follows. Both in periodic and quasiperiodic lattices, the BEC wave function extends over many lattice wells, and can be decomposed into a sum of localized (Wannier-like) states. Due to the applied external force, these energy states are arranged in a Wannier-Stark ladder. In periodic lattices, the energy separation ΔE between the ladder states is fixed, leading to periodic Bloch oscillations of period $\propto \hbar/\Delta E$. However, for quasiperiodic lattices, a discrete set of different (noncommensurate) differences of on-site energies in adjacent wells occurs (i.e., a nonequally spaced Wannier-Stark ladder) leading to quasiperiodic (instead of periodic) oscillations. Purely random potentials would result in a continuous set of differences of on-site energies leading, as expected, to the disapearance of any sort of Bloch oscillations.

Summarizing, we have investigated the physics of BECs trapped in optical QCs. We have shown that (i) the equilibrium BEC wave function displays long-range quasiperiodic order and that (ii) quantum transport shares properties with both ordered and disordered systems. On the one hand, because of quasidisordered inhomogeneities, diffusion turns from ballistic to localization when quasiperiodicity is switched on. On the other hand, because of coherence extending over several lattice sites, quasiperiodic Bloch oscillations occur in quasiperiodic BECs.

The discussed arrangement can be easily generated using standard techniques, offering an exciting tool for controlled studies of the transition between periodic, quasiperiodic, and fully disordered systems in cold gases, a major topic of current experimental research [11–13]. In addition, the system can be used to address experimentally some unsolved issues on QCs, as, e.g., the application of the renormalization theory to the 2D case [15].

We thank P. Verkerk, M. Inguscio, P. Pedri, and H. Fehrmann for discussions. We acknowledge support from the Deutsche Forschungsgemeinschaft (Nos. SFB 407 and SPP1116), RTN Cold Quantum Gases, ESF PESC BEC2000+, the Humboldt Foundation, and CNRS.

[1] M. BenDahan, E. Peik, J. Reichel, Y. Castin, and C. Salomon, Phys. Rev. Lett. **76**, 4508 (1996); E. Peik, M. BenDahan, I. Bouchoule, Y. Castin, and C. Salomon, Phys. Rev. A **55**, 2989 (1997).

[2] O. Morsch, J. H. Muller, M. Cristiani, D. Ciampini, and E. Arimondo, Phys. Rev. Lett. **87**, 140402 (2001); M. Cristiani, O. Morsch, J. H. Muller, D. Ciampini, and E. Arimondo, Phys. Rev. A **65**, 063612 (2002).

[3] S. R. Wilkinson C. F. Bharucha, K. W. Madison, Q. Niu, and M. G. Raizen, Phys. Rev. Lett. **76**, 4512 (1996).

[4] B. P. Anderson and M. Kasevich, Science **282**, 1686 (1998); F. S. Cataliotti *et al.*, *ibid.* **293**, 843 (2001).

[5] D. Jaksch, C. Bruder, J. I. Cirac, C. W. Gardiner, and P. Zoller, Phys. Rev. Lett. **81**, 3108 (1998); M. Greiner *et al.*, Nature (London) **415**, 39 (2002).

[6] L.-M. Duan, E. Demler, and M. D. Lukin, Phys. Rev. Lett. **91**, 090402 (2003).

[7] L. Santos, M. A. Baranov, J. I. Cirac, H. U. Everts, H. Fehrmann, and M. Lewenstein, Phys. Rev. Lett. **93**, 030601 (2004).

[8] P. Horak, J.-Y. Courtois, and G. Grynberg, Phys. Rev. A **58**, 3953-3962 (1998).

[9] B. Paredes, C. Tejedor, and J. I. Cirac, Phys. Rev. A **71**, 063608 (2005).

[10] B. Damski, J. Zakrzewski, L. Santos, P. Zoller, and M. Lewenstein, Phys. Rev. Lett. **91**, 080403 (2003); R. Roth and K. Burnett, J. Opt. B: Quantum Semiclassical Opt. **5**, S50 (2003).

[11] J. E. Lye, L. Fallani, M. Modugno, D. S. Wiersma, C. Fort, and M. Inguscio, Phys. Rev. Lett. **95**, 070401 (2005); C. Fort, L. Fallani, V. Guarrera, J. Lye, M. Modugno, D. S. Wiersma, and M. Inguscio, Phys. Rev. Lett. **95**, 170410 (2005).

[12] D. Clément A. Varón, M. Hugbart, J. A. Retter, P. Bouyer, L. Sanlchez-Palencia, D. Gangardt, G.V. Shlyapnikov, and A. Aspect, Phys. Rev. Lett. **95**, 170409 (2005).

[13] T. Schulte S. Drenkelforth, J. Kruse, W. Ertmer, J. Arlt, K. Sacha, J. Zakrzewski, andM. Lewenstein, Phys. Rev. Lett. **95**, 170411 (2005).

[14] D. Shechtman, I. Blech, D. Gratias, and J. W. Cahn, Phys. Rev. Lett. **53**, 1951 (1984); D. Levine and P. J. Steinhardt, *ibid.* **53**, 2477 (1984).

[15] *The Physics of Quasicrystals*, edited by P. J. Steinhardt and S. Ostlund (World Scientific, Singapore, 1987); *Quasicrystals, the State of the Art*, edited by D. P. DiVincenzo and P. J. Steinhardt (World Scientific, Singapore, 1991); *Lectures on Quasicrystals*, edited by F. Hippert and D. Gratias (Les Editions de Physique, Paris, 1994).

[16] D. Levine and P. J. Steinhardt, Phys. Rev. B **34**, 596 (1986); M. J. Jarić, *ibid.* **34**, 4685 (1986).

[17] K. Ueda and H. Tsunetsugu, Phys. Rev. Lett. **58**, 1272 (1987); S. Martin *et al.*, *ibid.* **67**, 719 (1991); C. Berger *et al.*, Phys. Scr., T **35**, 90 (1991); B. Passaro, C. Sire, and V. G. Benza, Phys. Rev. B **46**, 13751 (1992); D. Mayou, C. Berger, F. Cyrot-Lackmann, T. Klein, and P. Lanco, Phys. Rev. Lett. **70**, 3915 (1993); F. S. Pierce *et al.*, Q. Guo, and S. J. Poon, *ibid.* **73**, 2220 (1994).

[18] G. Grynberg and C. Robilliard, Phys. Rep. **355**, 335 (2000).

[19] L. Guidoni, C. Triché, P. Verkerk, and G. Grynberg, Phys. Rev. Lett. **79**, 3363 (1997); L. Guidoni, B. Dépret, A. di Stefano, and P. Verkerk, Phys. Rev. A **60**, R4233 (1999).

[20] K. Drese and M. Holthaus, Phys. Rev. Lett. **78**, 2932 (1997).

[21] Y. Eksioglu *et al.*, e-print cond-mat/0405440.

[22] R. Grimm *et al.*, Adv. At., Mol., Opt. Phys. **42**, 95 (2000).

[23] R. Penrose, Bull. Inst. Math. Appl. **10**, 266 (1974).

[24] P. Pedri, L. Pitaevskii, S. Stringari, C. Fort, S. Burger, F. S. Cataliotti, P. Madaloni, F. Minardi, and M. Inguscio, Phys. Rev. Lett. **87**, 220401 (2001).

[25] M. Greiner, I. Bloch, O. Mandel, T. W. Hansch, and T. Esslinger, Phys. Rev. Lett. **87**, 160405 (2001).

[26] A function is said to be quasiperiodic whenever its Fourier transform is composed of discrete (numerable) peaks [15].

[27] N. W. Ashcroft and N. D. Mermin, *Solid State Physics* (Holt, Rinehart, and Winston, New York, 1976).
[28] J.-L. Basdevant and J. Dalibard, *Quantum Mechanics* (Springer, Berlin, 2002).
[29] M. Krämer, L. Pitaevskii, and S. Stringari, Phys. Rev. Lett. **88**, 180404 (2002).
[30] Note that because of the fivefold symmetry of the lattice, the system is now isotropic.
[31] S. Inouye *et al.*, Nature (London) **392**, 151 (1998); S. L. Cornish, N. R. Claussen, J. L. Roberts, E. A. Cornell, and C. E. Wieman, Phys. Rev. Lett. **85**, 1795 (2000).
[32] In this way we can indentify the effects of interaction during the expansion, starting both cases with the *same initial conditions*. In experiments, a_{sc} can be rigorously turned-off using Feshbach resonances [31].
[33] For small intensities of the control beams ($\Delta \ll V_0$), quasidisorder does not affect significantly J_x [10].
[34] F. Bloch, Z. Phys. **52**, 555 (1928); C. Zener, Proc. R. Soc. London, Ser. A **145**, 523 (1934).
[35] C. Waschke, H. G. Roskos, R. Schwedler, K. Leo, H. Kurz, and K. Kohler, Phys. Rev. Lett. **70**, 3319 (1993).
[36] C. Janot *et al.*, Phys. Lett. A **276**, 291 (2000).
[37] E. Diez, F. Dominguez-Adame, E. Macia, and A. Sanchez, Phys. Rev. B **54**, 16792 (1996).
[38] G. Roati, E. deMirandes, F. Ferliano, H. Ott, G. Modugno, and M. Inguscio, Phys. Rev. Lett. **92**, 230402 (2004).
[39] The interactions are switched off to simplify the analysis. However, this could turn out to be relevant in experiments, since the presence of interactions may smear out the discrete spectrum and hence lead to damping or even supression of the quasiperiodic Bloch oscillations.
[40] The amplitude of the quasiperiodic oscillations may be enhanced by reducing the intensity of beams one and four. This would increase the extension of the localized wave functions. Note, however, that the system would remain quasiperiodic.

Suppression of Transport of an Interacting Elongated Bose-Einstein Condensate in a Random Potential

D. Clément,[1] A. F. Varón,[1] M. Hugbart,[1] J. A. Retter,[1] P. Bouyer,[1] L. Sanchez-Palencia,[1] D. M. Gangardt,[2] G. V. Shlyapnikov,[2,3] and A. Aspect[1]

[1]*Laboratoire Charles Fabry, Institut d'Optique, Université Paris-Sud XI, 91403 Orsay Cedex, France*
[2]*Laboratoire de Physique Théorique et Modèles Statistiques, Université Paris-Sud XI, 91405 Orsay Cedex, France*
[3]*Van der Waals-Zeeman Institute, University of Amsterdam, Valckenierstraat 65/67, 1018 XE Amsterdam, The Netherlands*

(Received 24 June 2005; published 21 October 2005)

We observe the suppression of the 1D transport of an interacting elongated Bose-Einstein condensate in a random potential with an amplitude that is small compared to the typical energy per atom, dominated by the interaction energy. Numerical calculations reproduce our observations well. We propose a scenario for disorder-induced trapping of the condensate in agreement with our findings.

DOI: 10.1103/PhysRevLett.95.170409 PACS numbers: 03.75.Nt, 05.30.Jp

Atomic Bose-Einstein condensates (BECs) in optical potentials are a remarkable system in which to revisit standard problems of condensed matter physics, e.g., superfluidity and quantum vortices, the superfluid to Mott insulator transition, or Josephson arrays [1]. Another important topic in condensed matter physics is that of transport in disordered materials, with relevance to normal metallic conduction, superconductivity and superfluid flow in low temperature quantum liquids. This is a difficult problem and it has led to the introduction of intriguing and nonintuitive concepts, e.g., Anderson localization [2,3], percolation [4], and Bose [5] and spin [6] glasses. It also has a counterpart in wave physics, e.g., in optics and acoustics, specifically coherent diffusion in random media [7]. The main difficulty in understanding quantum transport arises from the subtle interplay of interference, scattering onto the potential landscape, and (whenever present) interparticle interactions.

Transport properties of BECs in periodic optical lattices have been widely investigated, showing lattice-induced reduction of mobility [8–10] and self-trapping [11]. Within the context of random potentials, most of the recent theoretical efforts [12] have considered disordered or quasidisordered optical lattices where a large variety of phenomena have been discussed, such as the Bose-glass phase transition [13], localization [13,14], and the formation of Fermi-glass, quantum percolating, and spin-glass phases in Fermi-Bose mixtures [12,15]. Effects of disorder on BECs have also been addressed in connection with superfluid flows in liquid helium in porous media [16]. In particular, the depletions of the condensate and of the superfluid fractions have been calculated in Ref. [17], and a significant shift and damping of sound waves have been predicted in Ref. [18]. Apart from the (undesired) fragmentation effect of a rough potential on trapped cold atoms and BECs on atom chips [19], there are few experiments on BECs in random potentials [20].

In this Letter we report on the strong reduction of mobility of atoms in an elongated BEC in a random potential [21]. Starting from a BEC in a 3D highly elongated harmonic trap, we turn off the axial trapping potential while maintaining strong transverse confinement, and we monitor both (i) the axial expansion driven by the repulsive interactions and (ii) the motion of the center of mass of the BEC. When the BEC is subjected to a 1D random potential created by laser speckle, the axial expansion is strongly inhibited and the BEC eventually stops expanding (see Fig. 1). The final rms size L decreases as the standard deviation σ_V of the random potential increases. The same effect has been observed for various realizations of the random potential. We also observe that the center of mass motion provoked by a longitudinal magnetic "kick" at the time of release is strongly damped and is stopped in about the same time (see Fig. 1). These

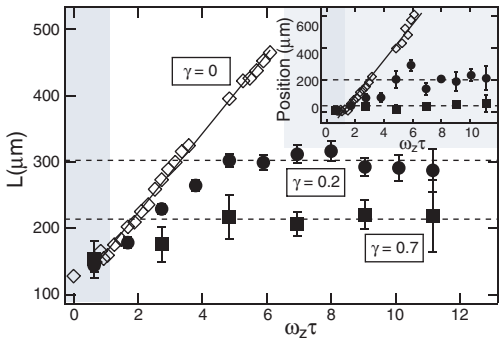

FIG. 1 (color online). Time evolution of the axial rms size L of the BEC, for various amplitudes σ_V of the random potential, all smaller than the chemical potential $\mu[\gamma = \sigma_V/\mu = 0\ (\diamond), 0.2\ (\bullet)$, and $0.7\ (\blacksquare)]$. The axial trapping frequency is initially $\omega_z/2\pi = 6.7$ Hz and is relaxed during the first 30 ms ($\omega_z\tau < 1.26$) of the expansion time (gray band). Each point corresponds to an average over three measurements; error bars represent 1 standard deviation. The solid lines are linear fits to the data and the dashed lines are guides to the eye. Inset: Motion of the center of mass of the BEC during axial expansion for the same values of γ. Both sets of data show a strong suppression of transport of the BEC in the presence of disorder.

observations are *not* made in a regime of tight binding; i.e., we observe this localization effect [22] for amplitudes of the random potential which are small compared to the chemical potential. One may wonder whether our observations can be interpreted in terms of Anderson localization [2]. In fact, in our situation, the interaction energy plays a crucial role, and the healing length is smaller than the typical distance between the speckle grains. This implies a different scenario, which we discuss in this Letter.

We create an elongated ^{87}Rb BEC in an iron-core electromagnet Ioffe-Pritchard trap [23,24] with oscillation frequencies, $\omega_\perp/2\pi = 660(4)$ Hz radially and $\omega_z/2\pi = 6.70(7)$ Hz axially. BECs of typically 3.5×10^5 atoms are obtained, with Thomas-Fermi (TF) half-length $L_{\mathrm{TF}} = 150$ μm and radius $R_{\mathrm{TF}} = 1.5$ μm, and chemical potential $\mu/2\pi\hbar \sim 5$ kHz [25]. The random potential is turned on at the end of the evaporative cooling ramp and we further evaporate during 200 ms to ensure that the BEC is in equilibrium in the combined harmonic plus random trap at the end of the sequence. To create the random potential, a $P \leq 150$ mW blue detuned laser beam with optical wavelength $\lambda \simeq 780$ nm, perpendicular to axis z, is shone through a scattering plate and projects a speckle pattern [28] on the BEC (see Fig. 2). The scattered beam diverges to an rms radius of 1.83 mm at the BEC.

A speckle field is defined by (i) a random intensity $I(\mathbf{r})$ with exponential statistical distribution for which the standard deviation equals the average intensity $\sigma_I = \langle I \rangle$ and (ii) an intensity correlation length Δz, defined as the "half-width" of the autocorrelation function [28]:

$$\Delta z = 1.22\lambda l/D, \tag{1}$$

where D is the beam diameter at the scattering plate and l is the distance from the lens to the BEC. We observe the speckle intensity distribution on a CCD camera placed at the same distance as the atoms. From this, we determine the autocorrelation function to obtain the grain size Δz for various beam diameters D. Taking into account the modulation transfer function [29] of the camera, we find that the measured grain size obeys Eq. (1) to within 2%. For our setup [$l = 140(5)$ mm and $D = 25.4(1)$ mm], Eq. (1) gives $\Delta z = 5.2(2)$ μm. This is much greater than the healing length $\xi = (8\pi na)^{-1/2} = 0.11$ μm of the trapped BEC. Since $R_{\mathrm{TF}} < \Delta z \ll L_{\mathrm{TF}}$, the optical potential is effectively 1D, with the trapped BEC spread over about 45–50 wells in the axial direction. We characterize the amplitude of the random potential σ_V with respect to the chemical potential μ by [30]

$$\gamma = \frac{\sigma_V}{\mu} = \frac{2}{3}\frac{\Gamma^2}{2\delta}\frac{\sigma_I}{I_{\mathrm{S}}}\frac{1}{\mu} = \frac{1}{\bar{\omega}}\frac{\Gamma^2}{6\delta}\frac{\sigma_I}{I_{\mathrm{S}}}\left(\frac{15aN}{\overline{a_{\mathrm{ho}}}}\right)^{-2/5} \tag{2}$$

with $\bar{\omega} = (\omega_z\omega_\perp^2)^{1/3}$ and $\overline{a_{\mathrm{ho}}} = (\hbar/m\bar{\omega})^{1/2}$, m the atomic mass, N the BEC atom number, $I_{\mathrm{S}} = 16.56$ W/m^2 the saturation intensity, $\Gamma/2\pi = 6.01$ MHz the linewidth, $a = 5.31$ nm the scattering length, and δ the laser detuning (between 0.15 nm and 0.39 nm in wavelength). The factor 2/3 accounts for the transition strength for π-polarized light. Taking into account our calibration uncertainty, we measure γ within $\pm 20\%$. For our parameters, the spontaneous scattering time $1/\Gamma_{\mathrm{sc}}$ is always larger than 1 s, i.e., much longer than the experiment.

To study the coherent transport of the BEC in the random potential, we open the axial magnetic trap while keeping the transverse confinement and the random potential unchanged. After lowering the current in the axial excitation coils, the axial trapping frequency $\omega_z/2\pi$ is smaller than 1 Hz [31]. Opening the trap abruptly induces atom loss and heating, therefore the trap is opened in 30 ms to avoid these processes. Once the current in the axial coils has reached its final value we have a BEC of $N \sim 2.5 \times 10^5$–3×10^5 atoms in the magnetic guide.

After a total axial expansion time τ (which includes the 30 ms opening time), we turn off all remaining fields (including the random potential) and wait a further 15 ms of free fall before imaging the atoms by absorption. During this time-of-flight, the axial rms size of the BEC does not increase more than 5%. From profiles of the absorption images we evaluate the axial rms size L [32] which we plot in Fig. 1 versus the axial expansion time τ. In the absence of the random potential ($\gamma = 0$), we observe that the rms size L grows linearly at a velocity $v_{\mathrm{rms}} \sim 2.47(3)$ mm s^{-1} in agreement with the scaling theory [33]. In the presence of the random potential, the expansion dynamics changes dramatically. For a sufficiently high amplitude, the expansion is significantly reduced and the BEC eventually stops expanding. In addition, we observe the damping of longitudinal motion of the center of mass of the BEC (see inset

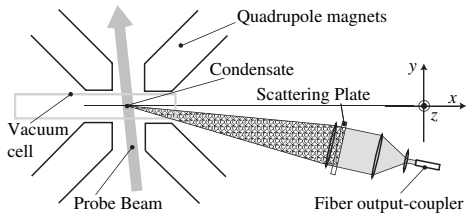

FIG. 2. Optical setup used to create the random speckle potential. The BEC is at the focus of the lens system with its long axis oriented along the z direction.

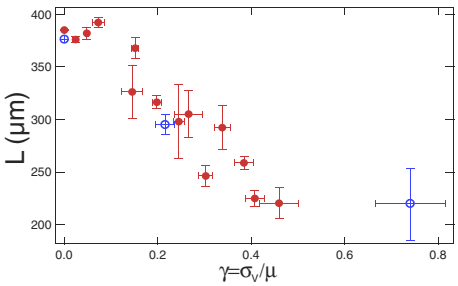

FIG. 3 (color online). rms size L of the BEC versus γ after an axial expansion time $\omega_z\tau = 4.84$ ($\tau = 115$ ms). The open circles correspond to the curves of Fig. 1.

of Fig. 1). This motion is triggered by an axial magnetic kick during the opening of the trap.

These results show a transition from noninhibited to inhibited transport as the speckle amplitude is increased. This is studied in further detail by measuring the BEC rms size after a fixed axial expansion time of 115 ms ($\omega_z\tau = 4.84$) for different amplitudes σ_V of the random potential. The results are shown in Fig. 3. We see that above a value $\gamma = 0.15$, the rms size decreases with γ.

From the absorption images, we also evaluate the density in the magnetic guide, after correcting for radial expansion during the time of flight. We observe that the density at the center of the BEC does not drop by more than a factor of 2 for $\gamma > 0.2$. Therefore, we conclude that the interaction energy dominates at the center of the BEC trapped by disorder, a point we discuss below.

To understand the disorder-induced suppression of expansion of the BEC, we have performed numerical calculations of the BEC dynamics in the Gross-Pitaevskii approach. We consider a BEC trapped in a cylindrically symmetric 3D-harmonic trap with frequencies $\omega_\perp$ and ω_z in the radial and axial directions, respectively. Assuming tight radial confinement ($\hbar\omega_\perp \gg \hbar\omega_z, \mu, k_B T$), the dynamics is reduced to 1D. In addition, the BEC is subjected to a static random potential $V(z) = \sigma_V v(z)$ where $v(z)$ is a numerically generated speckle pattern [28] with $\langle v\rangle^2 = \langle v^2\rangle/2 = 1$. This slightly differs from the experimental situation where the BEC is very elongated but not strictly 1D. However, in the experiment, the BEC is *guided* in a 1D random potential so that the radial size only slightly changes and, due to the different time scales in the axial ($1/\omega_z$) and radial ($1/\omega_\perp \ll 1/\omega_z$) directions, the radial size adapts adiabatically to the axial size. Thus we expect that the 1D simplified model captures the physics of the experiment. We consider parameters close to the experimental situation (see above). In particular, the healing length ($\xi \simeq 8 \times 10^{-4} L_{\rm TF}$) and the speckle correlation length ($\Delta z \simeq 0.049 L_{\rm TF}$) are much smaller than the size of the BEC.

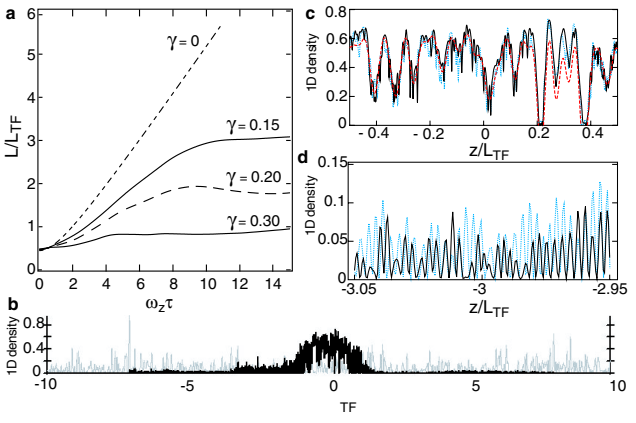

FIG. 4 (color online). (a) Time evolution of the rms size L of the BEC in the random potential $V(z)$ for various speckle amplitudes $\sigma_V = \gamma\mu$ as obtained from the numerical calculations. (b) Density profile (black) and random potential $V(z)/g_{1D}$ (gray) for $\gamma = 0.2$ at $\omega_z\tau = 10$. (c)–(d) Enlargement of density profile at $\omega_z\tau = 10$ (black solid) and $\omega_z\tau = 20$ [dotted (blue online)]. The dashed (red online) line in (c) is the TF prediction (see text).

We first compute the static 1D BEC wave function in the combined (harmonic plus random) trap. Because $\xi \ll \Delta z$, the density profile simply follows the modulations of the combined trap in the TF regime: $|\psi(z)|^2 = [\mu - m\omega_z^2 z^2/2 - V(z)]/g_{1D}$ in the region where $\mu > m\omega_z^2 z^2/2 + V(z)$ and $|\psi(z)|^2 = 0$ elsewhere. Here, m is the atomic mass and $g_{1D} = 2\hbar a \omega_\perp$ the 1D interaction parameter. At time $\tau = 0$, we suddenly switch off the axial harmonic confinement while keeping unchanged the interaction parameter g_{1D} and the random potential, and we compute the time evolution of the BEC. The results for the axial rms size L of the BEC are plotted in Fig. 4(a) for various amplitudes of the random potential. In the absence of disorder, the evolution of the BEC corresponds to self-similar expansion with scaling parameter $b(t) \sim \sqrt{2}\omega_z t$ [34]. In the presence of disorder ($\gamma \gtrsim 0.15$), after initial expansion, the BEC stops expanding. This is qualitatively the same behavior we observed in the experiment. The quantitative agreement is also reasonably good. For example, for $\gamma = 0.2$, the BEC expands by a factor of $\simeq 4$ in the numerics ($\simeq 3$ in the experiment) and is trapped after a transient expansion time of $\omega_z\tau \simeq 8$ ($\omega_z\tau \simeq 6$). This strong suppression of expansion corresponds to disorder-induced trapping of the BEC.

We now describe a scenario for disorder-induced trapping of the BEC. For small amplitudes of disorder, the initial stage of expansion can be described using the scaling theory [33]. According to this, the fast atoms populate the wings of the expanding BEC whereas the slow atoms are close to the center. It is thus tempting to distinguish two regions of the BEC: (i) the center where the interaction energy dominates the kinetic energy and trapping is due to the competition between interactions and disorder, and (ii) the wings where the kinetic energy exceeds the interactions and trapping is rather due to the competition between the kinetic energy and disorder.

In the center, the average density n_0 and thus the effective chemical potential $\bar{\mu}$ slowly decrease during the expansion stage. As the interaction energy is much larger than the kinetic energy, the local density adiabatically follows the instantaneous value of $\bar{\mu}$ in the TF regime: $|\psi(z)|^2 = [\bar{\mu} - V(z)]/g_{1D}$ in the region where $\bar{\mu} > V(z)$ and $|\psi(z)|^2 = 0$ elsewhere. This agrees with our numerical results [see Fig. 4(c)]. This evolution stops with fragmentation, i.e., when the BEC meets two peaks of the random potential with amplitudes larger than $\bar{\mu}$. Using the statistical properties of the random potential [28], we can estimate the probability of such large peaks and we conclude that this happens when n_0 reaches the value

$$n_0 \simeq 1.25\left(\frac{\sigma_V}{g_{1D}}\right)\ln\left[\frac{0.47 L_{\rm TF}}{\Delta z}\right]. \quad (3)$$

Because of the small density, the situation is different in the wings which are populated by almost free particles interacting with the disordered potential. The BEC thus undergoes disorder-induced multiple reflections and transmissions and is ultimately blocked by a large peak of the speckle potential. Therefore, the BEC is not in the TF regime and the local density is not stationary [see Fig. 4(d)]. Because of conservation of energy, the kinetic energy per particle ϵ is of the order of the typical energy in the initial BEC ($\epsilon \sim \mu$) so that the typical wavelength of the fluctuations in the wings is of the order of the healing length in the initial BEC $\lambda_w \sim \xi = \hbar/\sqrt{2m\mu}$.

This scenario is accurately supported by our numerical results [35]. In particular, the density profiles plotted in Fig. 4 show the static TF shape in the center with a density given by Eq. (3) and time-dependent fluctuations in the wings with typical wavelength $\lambda_w \sim \xi$.

In conclusion, we have experimentally investigated transport properties of an interacting BEC in a random potential. Controlling the strength of disorder, we have observed the transition from free expansion to absence of diffusion as disorder increases. We have presented numerical simulations that reproduce well the observed suppression of expansion and we have discussed a theoretical model that describes the scenario for disorder-induced trapping. In the future, it would be interesting to further investigate this highly controllable system, for example, by changing the correlation length of disorder or employing Bragg spectroscopy to probe the momentum spectrum of the BEC [24].

We are grateful to P. Chavel, J. Taboury, F. Gerbier, and C. Henkel for fruitful discussions. This work was supported by CNRS, Délégation Générale de l'Armement, Ministère de la Recherche (ACI Nanoscience 201), the European Union (Grants No. IST-2001-38863 and No. MRTN-CT-2003-505032) and INTAS (Contract No. 211-855). We acknowledge support from IXSEA-OCEANO (M. H.) and the Marie Curie Fellowship of the European Union (J. R.).

[1] For recent reviews, see J. R. Anglin and W. Ketterle, Nature (London) **416**, 211 (2002).
[2] P. W. Anderson, Phys. Rev. **109**, 1492 (1958).
[3] *Anderson Localization*, edited by Y. Nagaoka and H. Fukuyama, Springer Series in Solid State Sciences Vol. 39 (Springer, Berlin, 1982); *Anderson Localization*, edited by T. Ando and H. Fukuyama, Springer Proc. Phys. Vol. 28 (Springer, Berlin, 1988).
[4] A. Aharony and D. Stauffer, *Introduction to Percolation Theory* (Taylor & Francis, London, 1994).
[5] M. P. A. Fisher *et al.*, Phys. Rev. B **40**, 546 (1989).
[6] M. Mézard, G. Parisi, and M. A. Virasoro, *Spin Glass and Beyond* (World Scientific, Singapore, 1987).
[7] E. Akkermans and G. Montambaux, *Physique Mésoscopique des Électrons et des Photons* (EDP Science ed., Paris, 2004).
[8] S. Burger *et al.*, Phys. Rev. Lett. **86**, 4447 (2001).
[9] M. Krämer *et al.*, Phys. Rev. Lett. **88**, 180404 (2002).
[10] C. D. Fertig *et al.*, Phys. Rev. Lett. **94**, 120403 (2005).
[11] Th. Anker *et al.*, Phys. Rev. Lett. **94**, 020403 (2005); A. Trombettoni and A. Smerzi, *ibid.* **86**, 2353 (2001).
[12] V. Ahufinger *et al.*, cond-mat/0508042.
[13] B. Damski *et al.*, Phys. Rev. Lett. **91**, 080403 (2003).
[14] L. Sanchez-Palencia and L. Santos, cond-mat/0502529 [Phys. Rev. A (to be published)].
[15] A. Sanpera *et al.*, Phys. Rev. Lett. **93**, 040401 (2004).
[16] H. R. Glyde *et al.*, Phys. Rev. Lett. **84**, 2646 (2000).
[17] K. Huang and H. F. Meng, *ibid.* **69**, 644 (1992).
[18] S. Giorgini *et al.*, Phys. Rev. B **49**, 12 938 (1994).
[19] See for example J. Estève *et al.*, Phys. Rev. A **70**, 043629 (2004) and references therein.
[20] J. E. Lye *et al.*, Phys. Rev. Lett. **95**, 070401 (2005).
[21] While writing this paper, we have been informed that similar systems are currently studied in the groups of M. Inguscio at LENS and of W. Ertmer in Hannover (private communications).
[22] We use the word "localization" in its "working definition" of absence of diffusion, see B. van Tiggelen, in *Wave Diffusion in Complex Media*, Proceedings of Les Houches Summer School, edited by J. P. Fouque (Kluwer, Dordrecht, 1999).
[23] V. Boyer *et al.*, Phys. Rev. A **62**, 021601(R) (2000).
[24] S. Richard *et al.*, Phys. Rev. Lett. **91**, 010405 (2003).
[25] In elongated traps, thermal phase fluctuations may be important for large enough temperatures [26]. However, here, we estimate the temperature to be 150 nK [27] and therefore the phase coherence length [24] is $L_\phi \sim L_{TF}$, implying that the BEC is almost fully coherent.
[26] D. S. Petrov, G. V. Shlyapnikov, and J. T. M. Walraven, Phys. Rev. Lett. **87**, 050404 (2001).
[27] F. Gerbier *et al.*, Phys. Rev. A **70**, 013607 (2004).
[28] J. W. Goodman, in *Laser Speckle and Related Phenomena*, edited by J.-C. Dainty (Springer-Verlag, Berlin, 1975).
[29] M. Hugbart *et al.*, Eur. Phys. J. D **35**, 155 (2005).
[30] R. Grimm, M. Weidemüller, and Yu. B. Ovchinnikov, *Advances in Atomic, Molecular and Optical Physics*, edited by B. Bederson and H. Walther (Academic Press, London, 2000), Vol. 42, p. 95.
[31] From the variations of the dipole curvature with the current, we estimate the upper bound of $\omega_z/2\pi$ to be $\sim$500 mHz, which is compatible with the linear expansion observed in the absence of disorder (see Fig. 1).
[32] The rms axial size is defined $L = \sqrt{\langle (z - \langle z \rangle)^2 \rangle}$ where $\langle \cdot \rangle$ stands for the density-weighted average.
[33] Yu. Kagan, E. L. Surkov, and G. V. Shlyapnikov, Phys. Rev. A **54**, R1753 (1996); Y. Castin and R. Dum, Phys. Rev. Lett. **77**, 5315 (1996).
[34] Our findings are in excellent agreement with the analytic solution of the scaling equations of [33], $\sqrt{b(t)[b(t)-1]} + \ln[\sqrt{b(t)} + \sqrt{b(t)-1}] = \sqrt{2}\omega_z t$.
[35] A detailed analysis of these properties will be described in a future publication.

Anderson Localization of Expanding Bose-Einstein Condensates in Random Potentials

L. Sanchez-Palencia,[1] D. Clément,[1] P. Lugan,[1] P. Bouyer,[1] G. V. Shlyapnikov,[2,3] and A. Aspect[1]

[1]*Laboratoire Charles Fabry de l'Institut d'Optique, CNRS and Univ. Paris-Sud, Campus Polytechnique, RD 128, F-91127 Palaiseau cedex, France*

[2]*Laboratoire de Physique Théorique et Modèles Statistiques, Univ. Paris-Sud, F-91405 Orsay cedex, France*

[3]*Van der Waals-Zeeman Institute, Univ. Amsterdam, Valckenierstraat 65/67, 1018 XE Amsterdam, The Netherlands*

(Received 28 December 2006; published 23 May 2007)

We show that the expansion of an initially confined interacting 1D Bose-Einstein condensate can exhibit Anderson localization in a weak random potential with correlation length σ_R. For speckle potentials the Fourier transform of the correlation function vanishes for momenta $k > 2/\sigma_R$ so that the Lyapunov exponent vanishes in the Born approximation for $k > 1/\sigma_R$. Then, for the initial healing length of the condensate $\xi_{\rm in} > \sigma_R$ the localization is exponential, and for $\xi_{\rm in} < \sigma_R$ it changes to algebraic.

DOI: 10.1103/PhysRevLett.98.210401 PACS numbers: 05.30.Jp, 03.75.Kk, 03.75.Nt, 05.60.Gg

Disorder in quantum systems can have dramatic effects, such as strong Anderson localization (AL) of noninteracting particles in random media [1]. The main paradigm of AL is that the suppression of transport is due to a destructive interference of particles (waves) which multiply scatter from the modulations of a random potential. AL is thus expected to occur when interferences play a central role in the multiple scattering process [2]. In three dimensions, this requires the particle wavelength to be larger than the scattering mean free path, l, as pointed out by Ioffe and Regel [3]. One then finds a mobility edge at momentum $k_m = 1/l$, below which AL can appear. In one and two dimensions all single-particle quantum states are predicted to be localized [4–6], although for certain types of disorder one has an effective mobility edge in the Born approximation (see Ref. [7] and below). A crossover to the regime of AL has been observed in low dimensional conductors [8,9], and recently, evidences of AL have been obtained for light waves in bulk powders [10] and in 2D disordered photonic lattices [11]. The subtle question is whether and how the interaction between particles can cause delocalization and transport, and there is a long-standing discussion of this issue for the case of electrons in solids [12].

Ultracold atomic gases can shed new light on these problems owing to an unprecedented control of interactions, a perfect isolation from a thermal bath, and the possibilities of designing controlled random [13–17] or quasirandom [18] potentials. Of particular interest are the studies of localization in Bose gases [19,20] and the interplay between interactions and disorder in Bose and Fermi gases [21,22]. Localization of expanding Bose-Einstein condensates (BEC) in random potentials has been reported in Refs. [15–17]. However, this effect is *not* related to AL, but rather to the fragmentation of the core of the BEC, and to single reflections from large modulations of the random potential in the tails [15]. Numerical calculations [15,23,24] confirm this scenario for parameters relevant to the experiments of Refs. [15–17].

In this Letter, we show that the expansion of a 1D interacting BEC can exhibit AL in a random potential without large or wide modulations. Here, in contrast to the situation in Refs. [15–17], the BEC is not significantly affected by a single reflection. For this *weak disorder* regime we have identified the following localization scenario on the basis of numerical calculations and the toy model described below.

At short times, the disorder does not play a significant role, atom-atom interactions drive the expansion of the BEC and determine the long-time momentum distribution, $\mathcal{D}(k)$. According to the scaling theory [25], $\mathcal{D}(k)$ has a high-momentum cutoff at $1/\xi_{\rm in}$, where $\xi_{\rm in} = \hbar/\sqrt{4m\mu}$ and μ are the initial healing length and chemical potential of the BEC, and m is the atom mass. When the density is significantly decreased, the expansion is governed by the scattering of almost noninteracting waves from the random potential. Each wave with momentum k undergoes AL on a momentum-dependent length $L(k)$ and the BEC density profile will be determined by the superposition of localized waves. For speckle potentials the Fourier transform of the correlation function vanishes for $k > 2/\sigma_R$, where σ_R is the correlation length of the disorder, and the Born approach yields an effective mobility edge at $1/\sigma_R$. Then, if the high-momentum cutoff is provided by the momentum distribution $\mathcal{D}(k)$ (for $\xi_{\rm in} > \sigma_R$), the BEC is *exponentially* localized, whereas if the cutoff is provided by the correlation function of the disorder (for $\xi_{\rm in} < \sigma_R$) the localization is *algebraic*. These findings pave the way to observe AL in experiments similar to those of Refs. [15–17].

We consider a 1D Bose gas with repulsive short-range interactions, characterized by the 1D coupling constant g and trapped in a harmonic potential $V_{\rm ho}(z) = m\omega^2 z^2/2$. The finite size of the trapped sample provides a low-momentum cutoff for the phase fluctuations, and for weak interactions ($n \gg mg/\hbar^2$, where n is the 1D density), the gas forms a true BEC at low temperatures [26].

We treat the BEC wave function $\psi(z, t)$ using the Gross-Pitaevskii equation (GPE). In the presence of a superimposed random potential $V(z)$, this equation reads

$$i\hbar\partial_t\psi = \left[\frac{-\hbar^2}{2m}\partial_z^2 + V_{\rm ho}(z) + V(z) + g|\psi|^2 - \mu\right]\psi, \quad (1)$$

where ψ is normalized by $\int dz|\psi|^2 = N$, with N being the number of atoms. It can be assumed without loss of generality that the average of $V(z)$ over the disorder, $\langle V\rangle$, vanishes, while the correlation function $C(z) = \langle V(z')V(z'+z)\rangle$ can be written as $C(z) = V_R^2 c(z/\sigma_R)$, where the reduced correlation function $c(u)$ has unity height and width. So, $V_R = \sqrt{\langle V^2\rangle}$ is the standard deviation, and σ_R is the correlation length of the disorder.

The properties of the correlation function depend on the model of disorder. Although most of our discussion is general, we mainly refer to a 1D speckle random potential [27] similar to the ones used in experiments with cold atoms [13–17]. It is a random potential with a truncated negative exponential single-point distribution [27]:

$$\mathcal{P}[V(z)] = \frac{\exp[-(V(z)+V_R)/V_R]}{V_R}\Theta\left(\frac{V(z)}{V_R}+1\right), \quad (2)$$

where Θ is the Heaviside step function, and with a correlation function which can be controlled almost at will [17]. For a speckle potential produced by diffraction through a 1D square aperture [17,27], we have

$$C(z) = V_R^2 c(z/\sigma_R), \qquad c(u) = \sin^2(u)/u^2. \quad (3)$$

Thus the Fourier transform of $C(z)$ has a finite support:

$$\begin{aligned}\hat{C}(k) &= V_R^2\sigma_R\hat{c}(k\sigma_R),\\ \hat{c}(\kappa) &= \sqrt{\pi/2}(1-\kappa/2)\Theta(1-\kappa/2),\end{aligned} \quad (4)$$

so that $\hat{C}(k) = 0$ for $k > 2/\sigma_R$. This is actually a general property of speckle potentials, related to the way they are produced using finite-size diffusive plates [27].

We now consider the expansion of the BEC, using the following toy model. Initially, the BEC is assumed to be at equilibrium in the trapping potential $V_{\rm ho}(z)$ and in the absence of disorder. In the Thomas-Fermi regime (TF) where $\mu \gg \hbar\omega$, the initial BEC density is an inverted parabola, $n(z) = (\mu/g)(1 - z^2/L_{\rm TF}^2)\Theta(1 - |z|/L_{\rm TF})$, with $L_{\rm TF} = \sqrt{2\mu/m\omega^2}$ being the TF half-length. The expansion is induced by abruptly switching off the confining trap at time $t = 0$, still in the absence of disorder. Assuming that the condition of weak interactions is preserved during the expansion, we work within the framework of the GPE (1). Repulsive atom-atom interactions drive the short-time ($t \lesssim 1/\omega$) expansion, while at longer times ($t \gg 1/\omega$) the interactions are not important and the expansion becomes free. According to the scaling approach [25], the expanding BEC acquires a dynamical phase and the density profile is rescaled, remaining an inverted parabola:

$$\psi(z,t) = (\psi[z/b(t),0]/\sqrt{b(t)})\exp\{imz^2\dot{b}(t)/2\hbar b(t)\}, \quad (5)$$

where the scaling parameter $b(t) = 1$ for $t = 0$, and $b(t) \simeq \sqrt{2}\omega t$ for $t \gg 1/\omega$ [15].

We assume that the random potential is abruptly switched on at a time $t_0 \gg 1/\omega$. Since the atom-atom interactions are no longer important, the BEC represents a superposition of almost independent plane waves:

$$\psi(z,t) = \int \frac{dk}{\sqrt{2\pi}}\hat{\psi}(k,t)\exp(ikz). \quad (6)$$

The momentum distribution $\mathcal{D}(k)$ follows from Eq. (5). For $t \gg 1/\omega$, it is stationary and has a high-momentum cutoff at the inverse healing length $1/\xi_{\rm in}$:

$$\mathcal{D}(k) = |\hat{\psi}(k,t)|^2 \simeq \frac{3N\xi_{\rm in}}{4}(1-k^2\xi_{\rm in}^2)\Theta(1-k\xi_{\rm in}), \quad (7)$$

with the normalization condition $\int_{-\infty}^{+\infty} dk\mathcal{D}(k) = N$.

According to the Anderson theory [1], k waves will exponentially localize as a result of multiple scattering from the random potential. Thus, components $\exp(ikz)$ in Eq. (6) will become localized functions $\phi_k(z)$. At large distances, $\phi_k(z)$ decays exponentially, so that $\ln|\phi_k(z)| \simeq -\gamma(k)|z|$, with $\gamma(k) = 1/L(k)$ the Lyapunov exponent, and $L(k)$ the localization length. The AL of the BEC occurs when the independent k waves have localized. Assuming that the phases of the functions $\phi_k(z)$, which are determined by the local properties of the random potential and by the time t_0, are random uncorrelated functions for different momenta, the BEC density is given by

$$n_0(z) \equiv \langle|\psi(z)|^2\rangle = 2\int_0^\infty dk\mathcal{D}(k)\langle|\phi_k(z)|^2\rangle, \quad (8)$$

where we have taken into account that $\mathcal{D}(k) = \mathcal{D}(-k)$ and $\langle|\phi_k(z)|^2\rangle = \langle|\phi_{-k}(z)|^2\rangle$.

We now briefly outline the properties of the functions $\phi_k(z)$ from the theory of localization of single particles. For a weak random potential, using the phase formalism [28] the state with momentum k is written in the form

$$\phi_k(z) = r(z)\sin[\theta(z)], \qquad \partial_z\phi_k = kr(z)\cos[\theta(z)], \quad (9)$$

and the Lyapunov exponent is obtained from the relation $\gamma(k) = -\lim_{|z|\to\infty}\langle\log[r(z)]/|z|\rangle$. If the disorder is sufficiently weak, then the phase is approximately kz and solving the Schrödinger equation up to first order in $|\partial_z\theta(z)/k - 1|$, one finds [28],

$$\gamma(k) \simeq (\sqrt{2\pi}/8\sigma_R)(V_R/E)^2(k\sigma_R)^2\hat{c}(2k\sigma_R), \quad (10)$$

where $E = \hbar^2k^2/2m$. Such a perturbative (Born) approximation assumes the inequality

$$V_R\sigma_R \ll (\hbar^2k/m)(k\sigma_R)^{1/2}, \quad (11)$$

or equivalently $\gamma(k) \ll k$. Typically, Eq. (11) means that the random potential does not comprise large or wide peaks.

Deviations from a pure exponential decay of ϕ_k are obtained using diagrammatic methods [29], and one has

$$\langle|\phi_k(z)|^2\rangle = \frac{\pi^2\gamma(k)}{2}\int_0^\infty du\, u\sinh(\pi u)\left[\frac{1+u^2}{1+\cosh(\pi u)}\right]^2 \times \exp\{-2(1+u^2)\gamma(k)|z|\}, \quad (12)$$

where $\gamma(k)$ is given by Eq. (10). Note that at large distances

$(\gamma(k)|z| \gg 1)$, Eq. (12) reduces to $\langle|\phi_k(z)|^2\rangle \simeq (\pi^{7/2}/64\sqrt{2\gamma(k)}|z|^{3/2})\exp\{-2\gamma(k)|z|\}$.

The localization effect is closely related to the properties of the correlation function of the disorder. For the 1D speckle potential the correlation function $\hat{C}(k)$ has a high-momentum cutoff $2/\sigma_R$, and from Eqs. (4) and (10) we find

$$\gamma(k) = \gamma_0(k)(1 - k\sigma_R)\Theta(1 - k\sigma_R), \qquad \gamma_0(k) = \frac{\pi m^2 V_R^2 \sigma_R}{2\hbar^4 k^2}. \tag{13}$$

Thus, one has $\gamma(k) > 0$ only for $k\sigma_R < 1$ so that there is a mobility edge at $1/\sigma_R$ in the Born approximation. Strictly speaking, on the basis of this approach one cannot say that the Lyapunov exponent is exactly zero for $k > 1/\sigma_R$. However, direct numerical calculations of the Lyapunov exponent show that for $k > 1/\sigma_R$ it is at least 2 orders of magnitude smaller than $\gamma_0(1/\sigma_R)$ representing a characteristic value of $\gamma(k)$ for k approaching $1/\sigma_R$. For $\sigma_R \gtrsim 1\ \mu$m, achievable for speckle potentials [17] and for V_R satisfying Eq. (11) with $k \sim 1/\sigma_R$, the localization length at $k > 1/\sigma_R$ exceeds 10 cm which is much larger than the system size in the studies of quantum gases. Therefore, $k = 1/\sigma_R$ corresponds to an effective mobility edge in the present context. We stress that it is a *general* feature of optical speckle potentials, owing to the finite support of the Fourier transform of their correlation function.

We then use Eqs. (7), (12), and (13) for calculating the density profile of the localized BEC from Eq. (8). Since the high-momentum cutoff of $\mathcal{D}(k)$ is $1/\xi_{\rm in}$, and for the speckle potential the cutoff of $\gamma(k)$ is $1/\sigma_R$, the upper bound of integration in Eq. (8) is $k_c = \min\{1/\xi_{\rm in}, 1/\sigma_R\}$. As the density profile $n_0(z)$ is a sum of functions $\langle|\phi_k(z)|^2\rangle$ which decay exponentially with a rate $2\gamma(k)$, the long-tail behavior of $n_0(z)$ is mainly determined by the components with the smallest $\gamma(k)$, i.e., those with k close to k_c, and integrating in Eq. (8) we limit ourselves to leading order terms in Taylor series for $\mathcal{D}(k)$ and $\gamma(k)$ at k close to k_c.

For $\xi_{\rm in} > \sigma_R$, the high-momentum cutoff k_c in Eq. (8) is set by the momentum distribution $\mathcal{D}(k)$ and is equal to $1/\xi_{\rm in}$. In this case all functions $\langle|\phi_k(z)|^2\rangle$ have a finite Lyapunov exponent, $\gamma(k) > \gamma(1/\xi_{\rm in})$, and the whole BEC wave function is *exponentially localized*. For the long-tail behavior of $n_0(z)$, from Eqs. (7), (8), and (12) we obtain

$$n_0(z) \propto |z|^{-7/2}\exp\{-2\gamma(1/\xi_{\rm in})|z|\}, \qquad \xi_{\rm in} > \sigma_R. \tag{14}$$

Equation (14) assumes the inequality $\gamma(1/\xi_{\rm in})|z| \gg 1$, or equivalently $\gamma_0(k_c)(1 - \sigma_R/\xi_{\rm in})|z| \gg 1$.

For $\xi_{\rm in} < \sigma_R$, k_c is provided by the Lyapunov exponents of $\langle|\phi_k(z)|^2\rangle$ so that they do not have a finite lower bound. Then the localization of the BEC becomes *algebraic* and it is only *partial*. The part of the BEC wave function, corresponding to the waves with momenta in the range $1/\sigma_R < k < 1/\xi_{\rm in}$, continues to expand. Under the condition $\gamma_0(k_c)(1 - \xi_{\rm in}^2/\sigma_R^2)|z| \gg 1$ for the asymptotic density distribution of localized particles, Eqs. (8) and (12) yield

$$n_0(z) \propto |z|^{-2}, \qquad \xi_{\rm in} < \sigma_R. \tag{15}$$

Far tails of $n_0(z)$ will be always described by the asymptotic relations (14) or (15), unless $\xi_{\rm in} = \sigma_R$. In the special case of $\xi_{\rm in} = \sigma_R$, or for $\xi_{\rm in}$ very close to σ_R and at distances where $\gamma_0(k_c)|(1 - \xi_{\rm in}^2/\sigma_R^2)z| \ll 1$, still assuming that $\gamma_0(k_c)|z| \gg 1$ we find $n_0(z) \propto |z|^{-3}$.

Since the typical momentum of the expanding BEC is $1/\xi_{\rm in}$, according to Eq. (11), our approach is valid for $V_R \ll \mu(\xi_{\rm in}/\sigma_R)^{1/2}$. For a speckle potential, the typical momentum of the waves which become localized is $1/\sigma_R$ and for $\xi_{\rm in} < \sigma_R$ the restriction is stronger: $V_R \ll \mu(\xi_{\rm in}/\sigma_R)^2$. These conditions were not fulfilled, neither in the experiments of Refs. [15–17], nor in the numerics of Refs. [15,23,24].

We now present numerical results for the expansion of a 1D interacting BEC in a speckle potential, performed on the basis of Eq. (1). The BEC is initially at equilibrium in the combined random plus harmonic potential, and the expansion of the BEC is induced by switching off abruptly the confining potential at time $t = 0$ as in Refs. [15–17,20]. The differences from the model discussed above are that the random potential is already present for the initial stationary condensate and that the interactions are maintained during the whole expansion. This, however, does not significantly change the physical picture.

The properties of the initially trapped BEC have been discussed in Ref. [22] for an arbitrary ratio $\xi_{\rm in}/\sigma_R$. For $\xi_{\rm in} \ll \sigma_R$, the BEC follows the modulations of the random potential, while for $\xi_{\rm in} \gtrsim \sigma_R$ the effect of the random potential can be significantly smoothed. In both cases, the weak random potential only slightly modifies the density profile [22]. At the same time, the expansion of the BEC is strongly suppressed compared to the nondisordered case. This is seen from the time evolution of the rms size of the BEC, $\Delta z = \sqrt{\langle z^2\rangle - \langle z\rangle^2}$, in the inset of Fig. 1. At large times, the BEC density reaches an almost stationary pro-

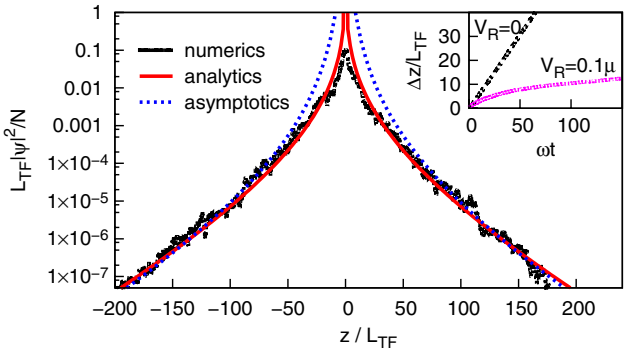

FIG. 1 (color online). Density profile of the localized BEC in a speckle potential at $t = 150/\omega$. Shown are the numerical data (black points), the fit of the result from Eqs. (7), (8), and (12) [red solid line], and the fit of the asymptotic formula (14) [blue dotted line]. Inset: Time evolution of the rms size of the BEC. The parameters are $V_R = 0.1\mu$, $\xi_{\rm in} = 0.01 L_{\rm TF}$, and $\sigma_R = 0.78\xi_{\rm in}$.

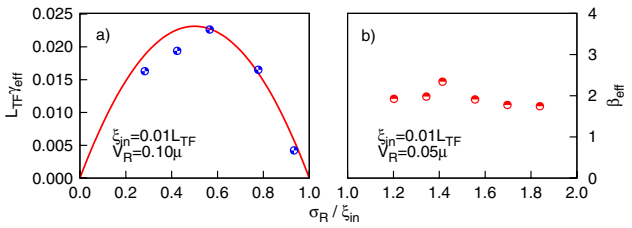

FIG. 2 (color online). (a) Lyapunov exponent γ_{eff} in units of $1/L_{\text{TF}}$ for the localized BEC in a speckle potential, in the regime $\xi_{\text{in}} > \sigma_R$. The solid line is $\gamma(1/\xi_{\text{in}})$ from Eq. (13). (b) Exponent of the power-law decay of the localized BEC in the regime $\xi_{\text{in}} < \sigma_R$. The parameters are indicated in the figure.

file. The numerically obtained density profile in Fig. 1 shows an excellent agreement with a fit of $n_0(z)$ from Eqs. (7), (8), and (12), where a multiplying constant was the only fitting parameter. Note that Eq. (8) overestimates the density in the center of the localized BEC, where the contribution of waves with very small k is important. This is because Eq. (13) overestimates $\gamma(k)$ in this momentum range, where the criterion (11) is not satisfied.

We have also studied the long-tail asymptotic behavior of the numerical data. For $\xi_{\text{in}} > \sigma_R$, we have performed fits of $|z|^{-7/2}e^{-2\gamma_{\text{eff}}|z|}$ to the data. The obtained γ_{eff} are in excellent agreement with $\gamma(1/\xi_{\text{in}})$ following from the prediction of Eq. (14), as shown in Fig. 2(a). For $\xi_{\text{in}} < \sigma_R$, we have fitted $|z|^{-\beta_{\text{eff}}}$ to the data. The results are plotted in Fig. 2(b) and show that the long-tail behavior of the BEC density is compatible with a power-law decay with $\beta_{\text{eff}} \simeq 2$, in agreement with the prediction of Eq. (15).

In summary, we have shown that in weak disorder the expansion of an initially confined interacting 1D BEC can exhibit Anderson localization. Importantly, the high-momentum cutoff of the Fourier transform of the correlation function for 1D speckle potentials can change localization from exponential to algebraic. Our results draw prospects for the observation of Anderson localization of matter waves in experiments similar to those of Refs. [15–17]. For $V_R = 0.2\mu$, $\xi_{\text{in}} = 3\sigma_R/2$, and $\sigma_R = 0.27$ μm, we find the localization length $L(1/\xi_{\text{in}}) \simeq 460$ μm. These parameters are in the range of accessibility of current experiments [17]. In addition, the localized density profile can be imaged directly, which allows one to distinguish between exponential and algebraic localization. Finally, we would like to raise an interesting problem for future studies. The expanding and then localized BEC is an excited Bose-condensed state as it has been made by switching off the confining trap. Therefore, the remaining small interaction between atoms should cause the depletion of the BEC and the relaxation to a new equilibrium state. The question is how the relaxation process occurs and to which extent it modifies the localized state.

We thank M. Lewenstein, S. Matveenko, P. Chavel, P. Leboeuf, and N. Pavloff for useful discussions. This work was supported by the French DGA, IFRAF, the Ministère de la Recherche (ACI Nanoscience 201), the European Union (FINAQS consortium and Grants No. IST-2001-38863 and No. MRTN-CT-2003-505032), the ANR (Grants No. NTOR-4-42586, No. NT05-2-42103, and No. 05-Nano-008-02), the ESF program QUDEDIS, and the Dutch Foundation FOM. LPTMS is a mixed research unit 8626 of CNRS and University Paris-Sud.

[1] P. W. Anderson, Phys. Rev. **109**, 1492 (1958).
[2] B. van Tiggelen, in *Wave Diffusion in Complex Media 1998*, edited by J. P. Fouque, Les Houches Lectures (Kluwer, Dordrecht, 1999).
[3] A. F. Ioffe and A. R. Regel, Prog. Semicond. **4**, 237 (1960).
[4] N. F. Mott and W. D. Towes, Adv. Phys. **10**, 107 (1961).
[5] D. J. Thouless, Phys. Rev. Lett. **39**, 1167 (1977).
[6] E. Abrahams *et al.*, Phys. Rev. Lett. **42**, 673 (1979).
[7] F. M. Izrailev and A. A. Krokhin, Phys. Rev. Lett. **82**, 4062 (1999); F. M. Izrailev and N. M. Makarov, J. Phys. A **38**, 10 613 (2005).
[8] Y. Imry, *Introduction to Mesoscopic Physics* (Oxford University, New York, 2002).
[9] M. E. Gershenson *et al.*, Phys. Rev. Lett. **79**, 725 (1997).
[10] C. M. Aegerter *et al.*, Europhys. Lett. **75**, 562 (2006).
[11] T. Schwartz *et al.*, Nature (London) **446**, 52 (2007).
[12] For a review, see: D. M. Basko, I. L. Aleiner, and B. L. Altshuler, Ann. Phys. (N.Y.) **321**, 1126 (2006).
[13] P. Horak *et al.*, Phys. Rev. A **58**, 3953 (1998); G. Grynberg *et al.*, Europhys. Lett. **49**, 424 (2000).
[14] J. E. Lye *et al.*, Phys. Rev. Lett. **95**, 070401 (2005).
[15] D. Clément *et al.*, Phys. Rev. Lett. **95**, 170409 (2005).
[16] C. Fort *et al.*, Phys. Rev. Lett. **95**, 170410 (2005).
[17] D. Clément *et al.*, New J. Phys. **8**, 165 (2006).
[18] L. Guidoni *et al.*, Phys. Rev. Lett. **79**, 3363 (1997).
[19] U. Gavish and Y. Castin, Phys. Rev. Lett. **95**, 020401 (2005); T. Paul *et al.*, Phys. Rev. A **72**, 063621 (2005); R. C. Kuhn *et al.*, Phys. Rev. Lett. **95**, 250403 (2005).
[20] L. Sanchez-Palencia and L. Santos, Phys. Rev. A **72**, 053607 (2005).
[21] B. Damski *et al.*, Phys. Rev. Lett. **91**, 080403 (2003); R. Roth and K. Burnett, Phys. Rev. A **68**, 023604 (2003); A. Sanpera *et al.*, Phys. Rev. Lett. **93**, 040401 (2004); V. Ahufinger *et al.*, Phys. Rev. A **72**, 063616 (2005); L. Fallani *et al.*, Phys. Rev. Lett. **98**, 130404 (2007); J. Wehr *et al.*, Phys. Rev. B **74**, 224448 (2006).
[22] L. Sanchez-Palencia, Phys. Rev. A **74**, 053625 (2006); P. Lugan *et al.*, Phys. Rev. Lett. **98**, 170403 (2007).
[23] M. Modugno, Phys. Rev. A **73**, 013606 (2006).
[24] E. Akkermans *et al.*, arXiv:cond-mat/0610579.
[25] Yu. Kagan *et al.*, Phys. Rev. A **54**, R1753 (1996); Y. Castin and R. Dum, Phys. Rev. Lett. **77**, 5315 (1996).
[26] D. S. Petrov *et al.*, Phys. Rev. Lett. **85**, 3745 (2000); D. S. Petrov *et al.*, J. Phys. IV (France) **116**, 3 (2004).
[27] J. W. Goodman, in *Statistical Properties of Laser Speckle Patterns*, edited by J.-C. Dainty, *Laser Speckle and Related Phenomena* (Springer-Verlag, Berlin, 1975).
[28] I. M. Lifshits *et al.*, *Introduction to the Theory of Disordered Systems* (Wiley, New York, 1988).
[29] A. A. Gogolin *et al.*, Sov. Phys. JETP **42**, 168 (1976); A. A. Gogolin, *ibid.* **44**, 1003 (1976).

Erratum: Anderson Localization of Expanding Bose-Einstein Condensates in Random Potentials [Phys. Rev. Lett. 98, 210401 (2007)]

L. Sanchez-Palencia, D. Clément, P. Lugan, P. Bouyer, G. V. Shlyapnikov, and A. Aspect

(Received 7 March 2011; published 4 April 2011)

DOI: 10.1103/PhysRevLett.106.149901 PACS numbers: 05.30.Jp, 03.75.Kk, 03.75.Nt, 05.60.Gg, 99.10.Cd

In this Letter, Eq. (12) contains an error. The correct formula, first obtained by Gogolin *et al.* [1], reads

$$\langle|\phi_k(z)|^2\rangle = \frac{\pi^2\gamma(k)}{8}\int_0^\infty du\, u\, \sinh(\pi u)\left[\frac{1+u^2}{1+\cosh(\pi u)}\right]^2 \exp\{-(1+u^2)\gamma(k)|z|/2\}, \tag{1}$$

and its large-distance limit ($\gamma(k)|z| \gg 1$) is $\langle|\phi_k(z)|^2\rangle \simeq (\pi^{7/2}/64\sqrt{\gamma(k)/2}|z|^{3/2})\exp\{-\gamma(k)|z|/2\}$. Correspondingly, Eq. (14) of our Letter becomes

$$n_0(z) \propto |z|^{-7/2}\exp\{-\gamma(1/\xi_{\rm in})|z|/2\}, \qquad \xi_{\rm in} > \sigma_R. \tag{2}$$

The same corrections apply to Ref. [2].

No other formula in the Letter is affected by the error. In particular, we stress that the calculation of the Lyapunov exponent $\gamma(k) = \lim_{|z|\to\infty}\langle\log[r(z)]\rangle/|z|$ using the phase formalism approach remains correct in the Letter as well as in all related works [3–5].

The numerical calculations reported in the Letter show an apparent agreement with the erroneous Eq. (12) of the same Letter. These calculations were performed in a limited space window and for a limited expansion time, which were chosen according to our numerical possibilities at that time. New numerical calculations performed in significantly larger systems and for significantly longer expansion times [6] show that in the regime $\xi_{\rm in} > \sigma_R$ the density profile first develops tails that are compatible with an exponential decay of rate $-2\gamma(1/\xi_{\rm in})$, in agreement with the behavior observed in the numerical study of the Letter. For short-enough distances, $|z| \lesssim 1/\gamma(1/\xi_{\rm in})$, relevant to the experiments of Ref. [7], this behavior persists in the long-time limit, so the theoretical prediction of Fig. 3 in Ref. [7] is not affected [8]. In the large-distance limit however, the numerical calculations of Ref. [6] show that the density profile evolves very slowly towards a new profile which is compatible with the correct Eq. (1). In the regime $\xi_{\rm in} < \sigma_R$, the conclusions of the Letter are not affected by the error and the new numerical calculations show density profiles with algebraic decay, $n(z) \sim 1/|z|^2$, as observed in the experiment of Ref. [7]. For details, see Ref. [6].

We thank Peter Schlagheck for drawing our attention to this issue and Marie Piraud for useful discussions.

[1] A. A. Gogolin, V. I. Mel'nikov, and E. I. Rashba, Sov. Phys. JETP **42**, 168 (1976); A. A. Gogolin, Sov. Phys. JETP **44**, 1003 (1976).
[2] L. Sanchez-Palencia, D. Clément, P. Lugan, P. Bouyer, and A. Aspect, New J. Phys. **10**, 045019 (2008).
[3] P. Lugan, D. Clément, P. Bouyer, A. Aspect, and L. Sanchez-Palencia, Phys. Rev. Lett. **99**, 180402 (2007).
[4] P. Lugan, A. Aspect, L. Sanchez-Palencia, D. Delande, B. Grémaud, C. A. Müller, and C. Miniatura Phys. Rev. A **80**, 023605 (2009).
[5] L. Sanchez-Palencia and M. Lewenstein, Nature Phys. **6**, 87 (2010).
[6] M. Piraud, P. Lugan, P. Bouyer, A. Aspect, and L. Sanchez-Palencia, Phys. Rev. A **83**, 031603(R) (2011).
[7] J. Billy, V. Josse, Z. Zuo, A. Bernard, B. Hambrecht, P. Lugan, D. Clément, L. Sanchez-Palencia, P. Bouyer, and A. Aspect, Nature (London) **453**, 891 (2008).
[8] In Ref. [7], localized density profiles are observed in a space window of the order of 1 mm, i.e., of the order of or less than $1/\gamma(1/\xi_{\rm in})$.

LETTERS

Direct observation of Anderson localization of matter waves in a controlled disorder

Juliette Billy[1], Vincent Josse[1], Zhanchun Zuo[1], Alain Bernard[1], Ben Hambrecht[1], Pierre Lugan[1], David Clément[1], Laurent Sanchez-Palencia[1], Philippe Bouyer[1] & Alain Aspect[1]

In 1958, Anderson predicted the localization[1] of electronic wavefunctions in disordered crystals and the resulting absence of diffusion. It is now recognized that Anderson localization is ubiquitous in wave physics[2] because it originates from the interference between multiple scattering paths. Experimentally, localization has been reported for light waves[3–7], microwaves[8,9], sound waves[10] and electron gases[11]. However, there has been no direct observation of exponential spatial localization of matter waves of any type. Here we observe exponential localization of a Bose–Einstein condensate released into a one-dimensional waveguide in the presence of a controlled disorder created by laser speckle[12]. We operate in a regime of pure Anderson localization, that is, with weak disorder—such that localization results from many quantum reflections of low amplitude—and an atomic density low enough to render interactions negligible. We directly image the atomic density profiles as a function of time, and find that weak disorder can stop the expansion and lead to the formation of a stationary, exponentially localized wavefunction—a direct signature of Anderson localization. We extract the localization length by fitting the exponential wings of the profiles, and compare it to theoretical calculations. The power spectrum of the one-dimensional speckle potentials has a high spatial frequency cutoff, causing exponential localization to occur only when the de Broglie wavelengths of the atoms in the expanding condensate are greater than an effective mobility edge corresponding to that cutoff. In the opposite case, we find that the density profiles decay algebraically, as predicted in ref. 13. The method presented here can be extended to localization of atomic quantum gases in higher dimensions, and with controlled interactions.

The transport of quantum particles in non-ideal material media (for example the conduction of electrons in an imperfect crystal) is strongly affected by scattering from the impurities in the medium. Even for weak disorder, semiclassical theories, such as those based on the Boltzmann equation for matter waves scattering from the impurities, often fail to describe transport properties[2], and fully quantum approaches are necessary. For example, Anderson localization[1], which predicts metal–insulator transitions, is based on interference between multiple scattering paths, leading to localized wavefunctions with exponentially decaying profiles. While Anderson's theory applies to non-interacting particles in static (quenched) disordered potentials[1], both thermal phonons and repulsive interparticle interactions significantly affect Anderson localization[14,15]. To our knowledge, no direct observation of exponentially localized wavefunctions in space has been reported in condensed matter.

Degenerate atomic quantum gases can be used to study a number of basic models in condensed matter theory experimentally, with unprecedented control and measurement possibilities (see refs 16, 17 and references therein). In investigating the behaviour of matter waves in disordered potentials[18], key advantages of atomic quantum gases are the possibility to implement systems in any dimension; the control of the interatomic interactions, either by density control or by Feshbach resonances; the possibility to design perfectly controlled and phonon-free disordered potentials; and the opportunity to measure *in situ* atomic density profiles via direct imaging. The quest for evidence of Anderson localization of Bose–Einstein condensates (BECs) in optical disordered potentials has thus attracted considerable attention in recent years[19–22]. Experiments using ultracold atoms have shown evidence of dynamical localization associated with a kicked rotor[23,24], which can be considered as a mapping onto momentum space of the Anderson localization phenomenon. Suppression of one-dimensional transport of BECs has been observed[19,20], but this occurred in a regime of strong disorder and strong interactions where localization is due to classical reflections from large peaks of the disordered potential. Here we report direct observation in real space of one-dimensional localization of a BEC in the regime of Anderson localization, that is, with weak disorder and negligible interatomic interactions.

Our experiment (sketched in Fig. 1a, b), starts with a small, elongated BEC (1.7×10^4 atoms of rubidium-87, with transverse and longitudinal radii of 3 μm and 35 μm, respectively, corresponding to the trapping frequencies given below, and a chemical potential of $\mu_{in}/h = 219$ Hz, where h is Planck's constant). The BEC is produced in an anisotropic opto-magnetic hybrid trap. A far-off-resonance laser beam (wavelength 1.06 μm, to be compared with the resonant wavelength of rubidium, 0.78 μm) creates an optical waveguide along the horizontal z axis[25], with a transverse harmonic confinement of frequency $\omega_\perp/2\pi = 70$ Hz. A shallow magnetic trap confines the BEC in the longitudinal direction ($\omega_z/2\pi = 5.4$ Hz).

The longitudinal confinement is switched off at $t = 0$, and the BEC starts to expand in the guide along the z direction under the effect of the initial repulsive interaction energy. A weakly anti-trapping magnetic field compensates the residual longitudinal trapping of the optical waveguide, so that the atoms can freely expand along the z direction over several millimetres. The expanding BEC can be imaged at any chosen time t after release by switching off the optical guide and irradiating the atoms with a resonant probe of duration 50 μs. An ultrasensitive electron-multiplying charge-coupled-device camera allows us to make an image of the fluorescing atoms with a resolution of 15 μm and a one-dimensional atomic density sensitivity of close to one atom per micrometre.

A disordered potential is applied to the expanding BEC using an optical speckle field produced by passing a laser beam (wavelength 0.514 μm) through a diffusing plate[22]. The detuning from the atomic frequency is great enough, and the intensity low enough, that spontaneous photon scattering on the atoms is negligible during the expansion, and we have a purely conservative disordered potential,

[1]Laboratoire Charles Fabry de l'Institut d'Optique, CNRS and Univ. Paris-Sud, Campus Polytechnique, RD 128, F-91127 Palaiseau cedex, France.

which extends 4 mm along the z direction. The three-dimensional autocorrelation of the disordered potential—that is, of the light intensity—is determined by diffraction from the diffusive plate onto the atoms' location[22].

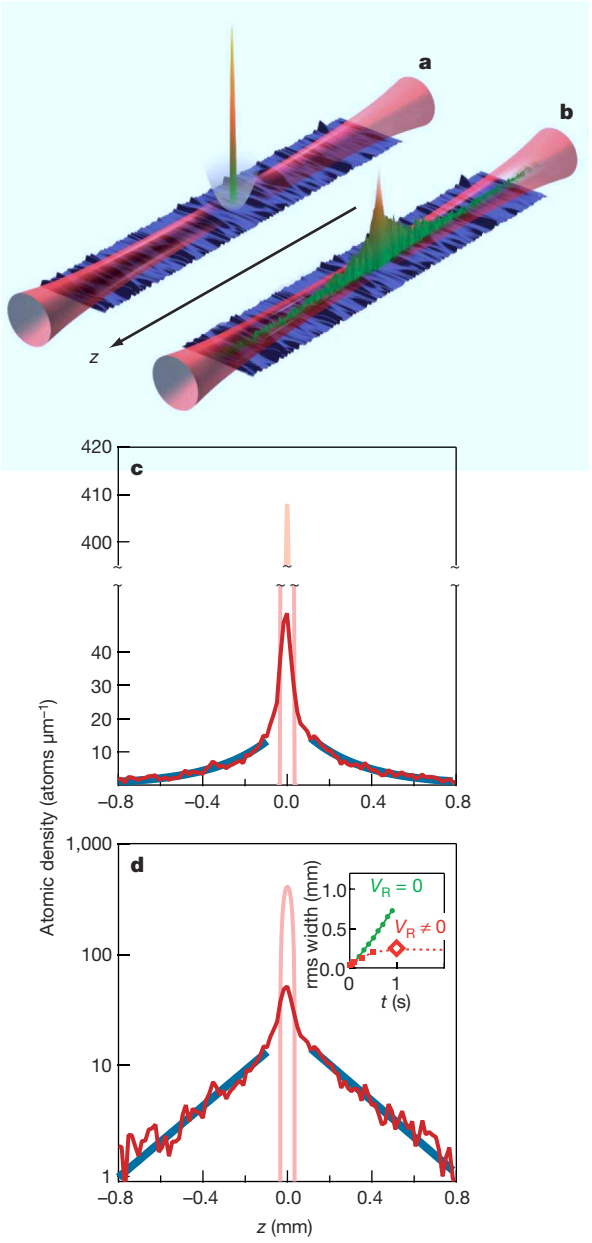

Figure 1 | Observation of exponential localization. **a**, A small BEC (1.7×10^4 atoms) is formed in a hybrid trap that is the combination of a horizontal optical waveguide, ensuring a strong transverse confinement, and a loose magnetic longitudinal trap. A weak disordered optical potential, transversely invariant over the atomic cloud, is superimposed (disorder amplitude V_R low in comparison with the chemical potential μ_{in} of the initial BEC). **b**, When the longitudinal trap is switched off, the BEC starts expanding and then localizes, as observed by direct imaging of the fluorescence of the atoms irradiated by a resonant probe. In **a** and **b**, false-colour images and sketched profiles are for illustration purposes; they are not exactly to scale. **c**, **d**, Density profiles (red) of the localized BEC one second after release, in linear (**c**) and semi-log (**d**) coordinates. In the inset in **d** we display the root-mean-square (rms) width of the profile versus time t, with ($V_R \neq 0$) and without ($V_R = 0$) disordered potential. This shows that the stationary regime is reached after 0.5 s. The diamond at $t = 1$ s corresponds to the data shown in **c** and the main panel of **d**. Blue lines in **c** are exponential fits to the wings, and correspond to the straight blue lines in **d**. The narrow central profiles (pink) represent the trapped condensate before release ($t = 0$ s).

Transversely, the correlation function (an ellipse with semi-axis lengths of 97 μm and 10 μm) is much wider than the atomic matter wave, and we can therefore consider the disorder as being one-dimensional for the BEC expanding along the z direction. Along this direction, the correlation function of the disordered potential is $V_R^2(\sin(z/\sigma_R)/(z/\sigma_R))^2$, where the correlation length $\sigma_R = 0.26 \pm 0.03$ μm (± 1 s.e.m.) is calculated knowing the numerical aperture of the optics, and V_R is the amplitude of the disorder. The corresponding speckle grain size is $\pi\sigma_R = 0.82$ μm. The power spectrum of this speckle potential is non-zero only for **k**-vectors lower in magnitude than a cutoff of $2/\sigma_R$. The amplitude of the disorder is directly proportional to the laser intensity[22]. The calibration factor is calculated knowing the geometry of the optical system and the properties of the rubidium-87 atoms.

When we switch off the longitudinal trapping in the presence of weak disorder, the BEC starts expanding, but the expansion rapidly stops, in stark contrast with the free expansion case (Fig. 1d inset, showing the evolution of the root-mean-square width of the observed profiles). Plots of the density profile in linear (Fig. 1c) and semi-log (Fig. 1d) coordinates then show clear exponential wings, a signature of Anderson localization. Our observations are made in a regime allowing Anderson localization, unlike in the experiments in refs 19 and 20. First, the disorder is weak enough ($V_R/\mu_{in} = 0.12$) that the initial interaction energy per atom is rapidly converted into a kinetic energy of the order of μ_{in} for atoms in the wings. This value is much greater than the amplitude of the disordered potential, so there is no possibility of a classical reflection from a potential barrier. Second, the atomic density in the wings is low enough (two orders of magnitude less than in the initial BEC) that the interaction energy is negligible in comparison with the atom kinetic energy. Last, we fulfil the criterion, emphasized in ref. 13, that the atomic matter wave **k**-vector distribution be bounded, with a maximum magnitude k_{max} of less than half the cutoff in the power spectrum of the speckle disordered potential used here, that is, $k_{max}\sigma_R < 1$. The value of k_{max} is measured directly by observing the free expansion of the BEC in the waveguide in the absence of disorder (see Methods). For the runs corresponding to Figs 1c, 1d, 2, and 3, we have $k_{max}\sigma_R = 0.65 \pm 0.09$ (± 2 s.e.m.).

An exponential fit to the wings of the density profiles yields the localization length L_{loc}, which we can compare to the theoretical value[13]

$$L_{loc} = \frac{2\hbar^4 k_{max}^2}{\pi m^2 V_R^2 \sigma_R (1 - k_{max}\sigma_R)} \quad (1)$$

valid only for $k_{max}\sigma_R < 1$ (m is the atomic mass). To ensure that the comparison is meaningful, we first check that we have reached a stationary situation, in which the fitted value of L_{loc} no longer evolves, as shown in Fig. 2. In Fig. 3, we plot the variation of L_{loc} with the disorder amplitude V_R, for the same number of atoms, that is, the same k_{max}. The dash–dot line is a plot of equation (1) for the values of k_{max} and σ_R determined as explained above. It shows quite a good agreement between our measurements and the theoretical predictions: with no adjustable parameters we obtain the correct magnitude and general shape. The shaded area reflects the envelope of the dash–dot line when we take into account the uncertainties in σ_R and k_{max}. The uncertainty in the calibration of V_R does not appear in Fig. 3. We estimate it to be no greater than 30%, which does not affect the agreement between theory and experiment.

An intriguing result of ref. 13 is the prediction of density profiles with algebraic wings when $k_{max}\sigma_R > 1$, that is, when the initial interaction energy is great enough that a fraction of the atoms have a **k**-vector greater in magnitude than $1/\sigma_R$, which plays the role of an effective mobility edge. We investigate this regime by repeating the experiment with a BEC containing more atoms (1.7×10^5 atoms, $\mu_{in}/h = 519$ Hz), for $V_R/\mu_{in} = 0.15$. Figure 4a shows the observed density profile in such a situation ($k_{max}\sigma_R = 1.16 \pm 0.14$ (± 2 s.e.m.)), and a log–log plot suggests a power-law decrease in the wings, with an

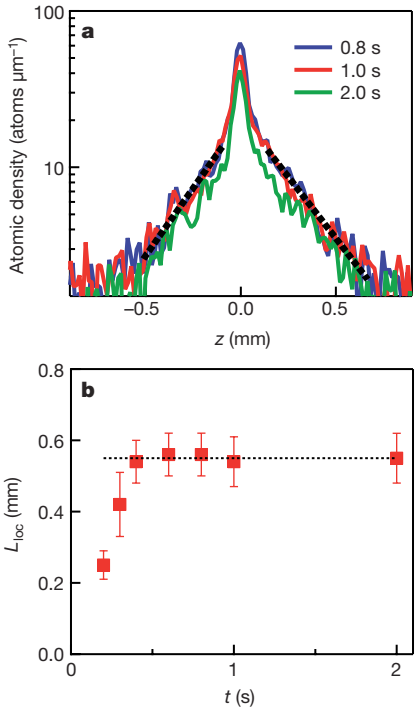

Figure 2 | Stationarity of the localized profile. **a**, Three successive density profiles, from which the localization length L_{loc} is extracted by fitting an exponential, $\exp(-2|z|/L_{loc})$ (dotted black lines), to the atomic density in the wings. **b**, Localization length L_{loc} versus expansion time t. Error bars, 95% confidence intervals for the fitted values (± 2 s.e.m.).

exponent of 1.95 ± 0.10 (± 2 s.e.m.), in agreement with the theoretical prediction that density decreases like $1/z^2$ in the wings. The semi-log plot (inset) confirms that an exponential would not work as well. For comparison, we present in Fig. 4b a log–log plot and a semi-log plot (inset) for the case with $k_{max}\sigma_R = 0.65$ and $V_R/\mu_{in} = 0.15$, where we conclude in favour of exponential rather than algebraic tails. These data support the existence of a crossover from an exponential to an algebraic regime in our speckle potential.

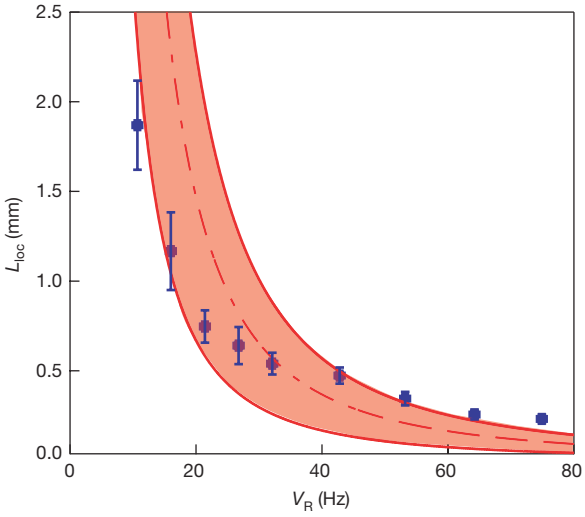

Figure 3 | Localization length versus amplitude of the disordered potential. L_{loc} is obtained by an exponential fit to the wings of the stationary localized density profiles, as shown in Fig. 2. Error bars, 95% confidence intervals for the fitted values (± 2 s.e.m.); 1.7×10^4 atoms ; $\mu_{in} = 219$ Hz. The dash–dot line is plotted using equation (1), where k_{max} is determined from the observed free expansion of the condensate (see Methods). The shaded area represents uncertainty associated with the evaluations of k_{max} and σ_R. We note that the limited extension of the disordered potential (4 mm) allows us to measure values of L_{loc} up to about 2 mm.

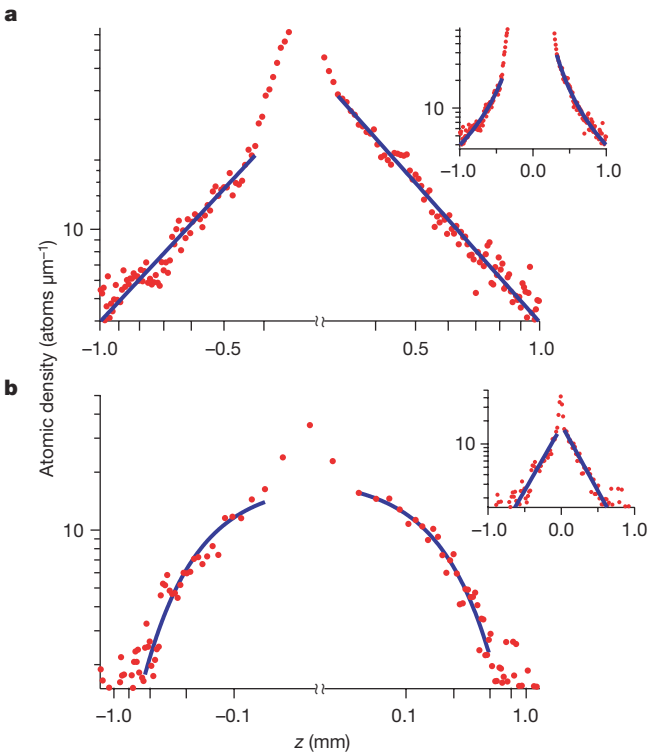

Figure 4 | Algebraic and exponential regimes in a one-dimensional speckle potential. Log–log and semi-log plots of the stationary atomic density profiles, showing the difference between the algebraic ($k_{max}\sigma_R > 1$) and exponential ($k_{max}\sigma_R < 1$) regimes. **a**, Density profile for $V_R/\mu_{in} = 0.15$ and $k_{max}\sigma_R = 1.16 \pm 0.14$ (± 2 s.e.m.). The momentum distribution of the released BEC has components beyond the effective mobility edge $1/\sigma_R$. The fit to the wings with a power-law decay $1/|z|^\beta$ yields $\beta = 1.92 \pm 0.06$ (± 2 s.e.m.) for the left-hand wing and $\beta = 2.01 \pm 0.03$ (± 2 s.e.m.) for the right-hand wing. The inset shows the same data in a semi-log plot, and confirms the non-exponential decay. **b**, For comparison, a similar set of plots (log–log and semi-log) in the exponential regime for the same $V_R/\mu_{in} = 0.15$ and $k_{max}\sigma_R = 0.65 \pm 0.09$ (± 2 s.e.m.).

Direct imaging of atomic quantum gases in controlled, optical disordered potentials is a promising technique to investigate a variety of open questions on disordered quantum systems. First, as in other problems of condensed matter simulated using ultracold atoms, direct imaging of atomic matter waves offers unprecedented possibilities to measure important properties, such as localization lengths. Second, our experiment can be extended to quantum gases with controlled interactions where localization of quasi-particles[26,27], Bose glass[14,15,28] and Lifshits glass[29] are expected, as well as to Fermi gases and to Bose–Fermi mixtures where rich phase diagrams have been predicted[30]. The reasonable quantitative agreement between our measurements and the theory of one-dimensional Anderson localization in a speckle potential demonstrates the high degree of control in our set-up. We thus anticipate that it can be used as a quantum simulator for investigating Anderson localization in higher dimensions[31,32], first to look for the mobility edge of the Anderson transition, and then to measure important features at the Anderson transition that are still under theoretical investigation, such as critical exponents. It will also become possible to investigate the effect of controlled interactions on Anderson localization.

METHODS SUMMARY

Momentum distribution of the expanding BEC. To compare measured localization lengths with those calculated from equation (1), we need to know k_{max}, the maximum amplitude of the **k**-vector distribution of the atoms, at the beginning of the expansion in the disordered potential. We measure k_{max} by releasing a BEC with the same number of atoms in the waveguide without disorder, and observing the density profiles at various times t. Density profiles are readily

converted into $\mathbf{k}$-vector distributions ($|\mathbf{k}| = \hbar^{-1} m\mathrm{d}z/\mathrm{d}t$). The key step in obtaining $k_{\max}$ is accurately determining the position $z_{\max}$ of the front edge of the profile. To do this, we fit the whole profile to an inverted parabola, which is the expected shape for the one-dimensional expansion of a BEC in the fundamental transverse mode of the waveguide. Actually, the BEC has an initial transverse profile that is slightly enlarged owing to interactions between atoms, but its density rapidly decreases during the expansion, and a numerical calculation using our experimental parameters shows that for expansion times greater than $t = 0.2$ s, an inverted parabola correctly approximates the atomic density profile and allows accurate determination of the front edge position. Using this procedure, we measure $z_{\max}$ every 0.1 s from $t = 0$ to $t = 1$ s, and find it to be proportional to t for $t > 0.2$ s. We estimate the uncertainty in $k_{\max}$ to about 6% and 9% for 1.7×10^5 atoms and 1.7×10^4 atoms, respectively.

Received 14 March; accepted 9 April 2008.

1. Anderson, P. W. Absence of diffusion in certain random lattices. *Phys. Rev.* **109,** 1492–1505 (1958).
2. Van Tiggelen, B. in *Wave Diffusion in Complex Media 1998* (ed. Fouque, J. P.) 1–60 (Kluwer, Dordrecht, 1999).
3. Wiersma, D. S., Bartolini, P., Lagendijk, A. & Righini, R. Localization of light in a disordered medium. *Nature* **390,** 671–673 (1997).
4. Scheffold, F., Lenke, R., Tweer, R. & Maret, G. Localization or classical diffusion of light? *Nature* **398,** 206–270 (1999).
5. Störzer, M., Gross, P., Aegerter, C. M. & Maret, G. Observation of the critical regime near Anderson localization of light. *Phys. Rev. Lett.* **96,** 063904 (2006).
6. Schwartz, T., Bartal, G., Fishman, S. & Segev, M. Transport and Anderson localization in disordered two-dimensional photonic lattices. *Nature* **446,** 52–55 (2007).
7. Lahini, Y. *et al.* Anderson localization and nonlinearity in one-dimensional disordered photonic lattices. *Phys. Rev. Lett.* **100,** 013906 (2008).
8. Dalichaouch, R., Armstrong, J. P., Schultz, S., Platzman, P. M. & McCall, S. L. Microwave localization by two-dimensional random scattering. *Nature* **354,** 53–55 (1991).
9. Chabanov, A. A., Stoytchev, M. & Genack, A. Z. Statistical signatures of photon localization. *Nature* **404,** 850–853 (2000).
10. Weaver, R. L. Anderson localization of ultrasound. *Wave Motion* **12,** 129–142 (1990).
11. Akkermans, E. & Montambaux, G. *Mesoscopic Physics of Electrons and Photons* (Cambridge Univ. Press, Cambridge, UK, 2006).
12. Goodman, J. W. *Speckle Phenomena in Optic*s (Roberts, Greenwood Village, Colorado, 2007).
13. Sanchez-Palencia, L. *et al.* Anderson localization of expanding Bose-Einstein condensates in random potentials. *Phys. Rev. Lett.* **98,** 210401 (2007).
14. Giamarchi, T. & Schulz, H. J. Anderson localization and interactions in one-dimensional metals. *Phys. Rev. B* **37,** 325–340 (1988).
15. Fisher, M. P. A., Weichman, P. B., Grinstein, G. & Fisher, D. S. Boson localization and the superfluid-insulator transition. *Phys. Rev. B* **40,** 546–570 (1989).
16. Bloch, I., Dalibard, J. & Zwerger, W. Many-body physics with ultracold atoms. *Rev. Mod. Phys.* (in the press); preprint at ⟨http://arxiv.org/abs/0704.3011⟩ (2007).
17. Lewenstein, M. *et al.* Ultracold atomic gases in optical lattices: mimicking condensed matter physics and beyond. *Adv. Phys.* **56,** 243–379 (2007).
18. Damski, B., Zakrzewski, J., Santos, L., Zoller, P. & Lewenstein, M. Atomic Bose and Anderson glasses in optical lattices. *Phys. Rev. Lett.* **91,** 080403 (2003).
19. Clément, D. *et al.* Suppression of transport of an interacting elongated Bose–Einstein condensate in a random potential. *Phys. Rev. Lett.* **95,** 170409 (2005).
20. Fort, C. *et al.* Effect of optical disorder and single defects on the expansion of a Bose–Einstein condensate in a one-dimensional waveguide. *Phys. Rev. Lett.* **95,** 170410 (2005).
21. Schulte, T. *et al.* Routes towards Anderson-like localization of Bose–Einstein condensates in disordered optical lattices. *Phys. Rev. Lett.* **95,** 170411 (2005).
22. Clément, D. *et al.* Experimental study of the transport of coherent interacting matter-waves in a 1D random potential induced by laser speckle. *N. J. Phys.* **8,** 165, doi:10.1088/1367-2630/8/8/165 (2006).
23. Moore, J. L., Robinson, J. C., Bharucha, C., Williams, P. E. & Raizen, M. G. Observation of dynamical localization in atomic momentum transfer: A new testing ground for quantum chaos. *Phys. Rev. Lett.* **73,** 2974–2977 (1994).
24. Chabé, J. *et al.* Experimental observation of the Anderson transition with atomic matter waves. Preprint available at ⟨http://arxiv.org/abs/0709.4320⟩ (2007).
25. Guerin, W. *et al.* Guided quasicontinuous atom laser. *Phys. Rev. Lett.* **97,** 200402 (2006).
26. Bilas, N. & Pavloff, N. Anderson localization of elementary excitations in a one-dimensional Bose–Einstein condensate. *Eur. Phys. J. D* **40,** 387–397 (2006).
27. Lugan, P., Clément, D., Bouyer, P., Aspect, A. & Sanchez-Palencia, L. Anderson localization of Bogolyubov quasiparticles in interacting Bose–Einstein condensates. *Phys. Rev. Lett.* **99,** 180402 (2007).
28. Fallani, L., Lye, J. E., Guarrera, V., Fort, C. & Inguscio, M. Ultracold atoms in a disordered crystal of light: towards a Bose glass. *Phys. Rev. Lett.* **98,** 130404 (2007).
29. Lugan, P. *et al.* Ultracold Bose gases in 1D-disorder: from Lifshits glass to Bose–Einstein condensate. *Phys. Rev. Lett.* **98,** 170403 (2007).
30. Sanpera, A., Kantian, A., Sanchez-Palencia, L., Zakrzewski, J. & Lewenstein, M. Atomic Fermi–Bose mixtures in inhomogeneous and random optical lattices: from Fermi glass to quantum spin glass and quantum percolation. *Phys. Rev. Lett.* **93,** 040401 (2004).
31. Kuhn, R. C., Miniatura, C., Delande, D., Sigwarth, O. & Müller, C. A. Localization of matter waves in two-dimensional disordered optical potentials. *Phys. Rev. Lett.* **95,** 250403 (2005).
32. Skipetrov, S. E., Minguzzi, A., van Tiggelen, B. A. & Shapiro, B. Anderson localization of a Bose-Einstein condensate in a 3D random potential. *Phys. Rev. Lett.* **100,** 165301 (2008).

Acknowledgements: The authors are indebted to P. Chavel, T. Giamarchi, M. Lewenstein and G. Shlyapnikov for many discussions, to P. Georges and G. Roger for assistance with the laser, and to F. Moron, A. Villing and G. Colas for technical assistance on the experimental apparatus. This research was supported by the Centre National de la Recherche Scientifique (CNRS), the Délégation Générale de l'Armement (DGA), the Ministère de l'Education Nationale, de la Recherche et de la Technologie (MENRT), the Agence Nationale de la Recherche (ANR), the Institut Francilien de Recherche sur les Atomes Froids (IFRAF) and IXSEA; by the STREP programme FINAQS of the European Union; and by the programme QUDEDIS of the European Science Foundation (ESF).

Author Information Reprints and permissions information is available at www.nature.com/reprints. Correspondence and requests for materials should be addressed to P.B. (philippe.bouyer@institutoptique.fr).

One-dimensional Anderson localization in certain correlated random potentials

P. Lugan, A. Aspect, and L. Sanchez-Palencia
Laboratoire Charles Fabry de l'Institut d'Optique, CNRS and Univ. Paris-Sud, Campus Polytechnique, RD 128, F-91127 Palaiseau Cedex, France

D. Delande
Laboratoire Kastler-Brossel, UPMC, ENS, CNRS, 4 Place Jussieu, F-75005 Paris, France

B. Grémaud
Laboratoire Kastler-Brossel, UPMC, ENS, CNRS, 4 Place Jussieu, F-75005 Paris, France and Centre for Quantum Technologies, National University of Singapore, 3 Science Drive 2, Singapore 117543, Singapore

C. A. Müller
Laboratoire Kastler-Brossel, UPMC, ENS, CNRS, 4 Place Jussieu, F-75005 Paris, France and Physikalisches Institut, Universität Bayreuth, D-95440 Bayreuth, Germany

C. Miniatura
Centre for Quantum Technologies, National University of Singapore, 3 Science Drive 2, Singapore 117543, Singapore and Institut Non Linéaire de Nice, UNS, CNRS, 1361 Route des Lucioles, F-06560 Valbonne, France

(Received 3 February 2009; revised manuscript received 4 June 2009; published 11 August 2009)

We study Anderson localization of ultracold atoms in weak one-dimensional speckle potentials using perturbation theory beyond Born approximation. We show the existence of a series of sharp crossovers (effective mobility edges) between energy regions where localization lengths differ by orders of magnitude. We also point out that the correction to the Born term explicitly depends on the sign of the potential. Our results are in agreement with numerical calculations in a regime relevant for experiments. Finally, we analyze our findings in the light of a diagrammatic approach.

DOI: 10.1103/PhysRevA.80.023605 PACS number(s): 03.75.−b, 05.60.Gg, 67.85.−d, 72.15.Rn

I. INTRODUCTION

Anderson localization (AL) of single electron wave functions [1], first proposed to understand certain metal-insulator transitions, is now considered an ubiquitous phenomenon, which can happen for any kind of waves propagating in a medium with random impurities [2,3]. It can be understood as a coherent interference effect of waves multiply scattered from random defects, yielding localized waves with exponential profile and resulting in complete suppression of the usual diffusive transport associated with incoherent wave scattering [4]. So far, AL has been reported for light waves in diffusive media [5,6] and photonic crystals [7,8], sound waves [9], or microwaves [10]. Ultracold atoms have allowed studies of AL in momentum space [11,12] and recently direct observation of localized atomic matter waves [13,14].

In one-dimensional (1D) systems, all states are localized, and the localization length is simply proportional to the transport mean-free path [15]. However, this strong property should not hide that long-range correlations can induce subtle effects in 1D models of disorder, in particular those whose power spectrum has a finite support [16,17]. Examples are random potentials resulting from laser speckle and used in experiments with ultracold atoms [13,18,19]. Indeed, by construction [20], speckles have no Fourier component beyond a certain value $2k_c$, and the Born approximation predicts no backscattering and no localization for atoms with momentum $\hbar k > \hbar k_c$. This defines an *effective mobility edge* at $k=k_c$ [17], clear evidence of which has been reported [13].

Beyond this analysis—relevant for systems of moderate size [13,17]—study of AL in correlated potentials beyond the effective mobility edge requires more elaborated approaches. In Ref. [21], disorder with symmetric probability distribution was studied, and examples were exhibited, for which exponential localization occurs even for $k>k_c$ although with a much longer localization length than for $k<k_c$. It was also concluded that for Gaussian disorder, there is a second effective mobility edge at $2k_c$, while for non-Gaussian disorder, it is generally not so. These results do not apply to speckle potentials whose probability distribution is *asymmetric*. Moreover, although speckle potentials are not Gaussian, they derive from the squared modulus of a Gaussian field, and as we will show, the conclusions of Ref. [21] must be reexamined. Hence, considering speckle potentials presents a twofold interest. First, they form an original class of non-Gaussian disorder which can inherit properties of an underlying Gaussian process. Second, they are easily implemented in experiments with ultracold atoms where the localization length can be directly measured [13].

In this work, we study AL in speckle potentials beyond the Born approximation using perturbation theory [22], numerical calculations, and diagrammatic methods. We find that there exist several effective mobility edges at $k_c^{(p)}=pk_c$ with integer p, such that AL in the successive intervals $k_c^{(p-1)}<k<k_c^{(p)}$ results from scattering processes of increasing order. Effective mobility edges are thus characterized by sharp crossovers in the k dependence of the Lyapunov exponent (see Fig. 1). We prove this for the first two effective mobility edges by calculating the three lowest-order terms

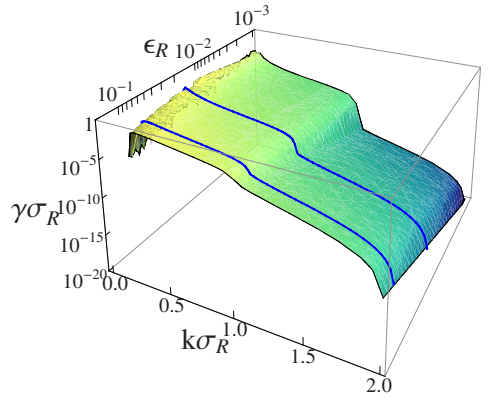

FIG. 1. (Color online) Lyapunov exponent γ calculated two orders beyond the Born approximation for particles in 1D speckle potentials created with a square diffusive plate versus the particle momentum $\hbar k$ and the strength of disorder $\epsilon_R = 2m\sigma_R^2 V_R/\hbar^2$ (V_R and σ_R are the amplitude and correlation length of the disorder). The solid blue lines correspond to $\epsilon_R = 0.1$ and $\epsilon_R = 0.02$.

and give general arguments for any p. In addition, we discuss the effect of odd terms that appear in the Born series due to the asymmetric probability distribution of speckle potentials.

II. SPECKLE POTENTIALS

Let us first recall the main properties of speckle potentials. Optical speckle is obtained by transmission of a laser beam through a medium with a random phase profile, such as a ground glass plate [20]. The resulting complex electric field $\mathcal{E}$ is a sum of independent random variables and forms a Gaussian process. In such a light field, atoms experience a random potential proportional to the intensity $|\mathcal{E}|^2$. Defining the zero of energies so that $\langle V\rangle = 0$, the random potential is thus

$$V(z) = V_R[|a(z/\sigma_R)|^2 - \langle |a(z/\sigma_R)|^2\rangle], \tag{1}$$

where the quantities $a(u)$ are complex Gaussian variables proportional to the electric field $\mathcal{E}$ and σ_R and V_R feature characteristic length and strength scales of the random potential (the precise definition of V_R and σ_R may depend on the model of disorder; see below). In contrast, $V(z)$ is not a Gaussian variable and its probability distribution is a decaying exponential, i.e., asymmetric. The sign of V_R is thus relevant and can be either positive or negative for "blue"- and "red"-detuned laser light, respectively. However, the random potential $V(z)$ inherits properties of the underlying Gaussian field $a(u)$. For instance, all potential correlators c_n are completely determined by the field correlator $c_a(u) = \langle a(0)^* a(u)\rangle$ via

$$\langle a_1^* \cdots a_p^* a_1 \cdots a_p\rangle = \sum_{\Pi} \langle a_1^* a_{\Pi(1)}\rangle \cdots \langle a_p^* a_{\Pi(p)}\rangle, \tag{2}$$

where $a_{p'} = a(z_{p'}/\sigma_R)$ and Π describes the $p!$ permutations of $\{1,\ldots,p\}$. Hence, $c_2(u) = |c_a(u)|^2$ and defining $a(u)$ so that $\langle |a(u)|^2\rangle = 1$, we have $\sqrt{\langle V(z)^2\rangle} = |V_R|$. Also, since speckle results from interference between light waves of wavelength λ_L coming from a finite-size aperture of angular width 2α, the Fourier transform of the field correlator has no component beyond $k_c = 2\pi \sin\alpha/\lambda_L$, and c_a has always a finite support:

$$\hat{c}_a(q) = 0 \quad \text{for } |q| > k_c\sigma_R \equiv 1. \tag{3}$$

As a consequence, the Fourier transform of the potential correlator also has a finite support: $\hat{c}_2(q) = 0$ for $|q| > 2$.

III. PHASE FORMALISM

Consider now a particle of energy E in a 1D random potential $V(z)$ with zero statistical average [$V(z)$ need not be a speckle potential here]. The particle wave function ϕ can be written in phase-amplitude representation

$$\phi(z) = r(z)\sin[\theta(z)]; \quad \partial_z\phi = kr(z)\cos[\theta(z)], \tag{4}$$

which proves convenient to capture the asymptotic decay of the wave function (here $k = \sqrt{2mE/\hbar^2}$ is the particle wave vector in the absence of disorder). It is easily checked that the Schrödinger equation is then equivalent to the coupled equations

$$\partial_z\theta(z) = k\{1 - [V(z)/E]\sin^2[\theta(z)]\}, \tag{5}$$

$$\ln[r(z)/r(0)] = k\int_0^z dz'[V(z')/2E]\sin[2\theta(z')]. \tag{6}$$

Since Eq. (5) is a closed equation for the phase θ, it is straightforward to develop the perturbation series of θ in increasing powers of V. Reintroducing the solutions at different orders into Eq. (6) yields the corresponding series for the amplitude $r(z)$ and the Lyapunov exponent:

$$\gamma(k) = \lim_{|z|\to\infty} \frac{\langle \ln[r(z)]\rangle}{|z|} = \sum_{n\geq 2} \gamma^{(n)}(k). \tag{7}$$

The nth-order term $\gamma^{(n)}$ is thus expressed as a function of the n-point correlator $C_n(z_1,\ldots,z_{n-1}) = \langle V(0)V(z_1)\cdots V(z_{n-1})\rangle$ of the random potential, which we write $C_n(z_1,\ldots,z_{n-1}) = V_R^n c_n(z_1/\sigma_R,\ldots,z_{n-1}/\sigma_R)$. Up order $n=4$, we find

$$\gamma^{(n)} = \sigma_R^{-1}\left(\frac{\epsilon_R}{k\sigma_R}\right)^n f_n(k\sigma_R), \tag{8}$$

where $\epsilon_R = 2m\sigma_R^2 V_R/\hbar^2$ and

$$f_2(\kappa) = +\frac{1}{4}\int_{-\infty}^{0} du c_2(u)\cos(2\kappa u), \tag{9}$$

$$f_3(\kappa) = -\frac{1}{4}\int_{-\infty}^{0} du \int_{-\infty}^{u} dv c_3(u,v)\sin(2\kappa v), \tag{10}$$

$$f_4(\kappa) = -\frac{1}{8}\int_{-\infty}^{0} du \int_{-\infty}^{u} dv \int_{-\infty}^{v} dw c_4(u,v,w)\{2\cos(2\kappa w) + \cos[2\kappa(v+w-u)]\}. \tag{11}$$

Note that the compact form (11) is valid provided that oscillating terms, which may appear from terms in c_4 that can be factorized as c_2 correlators, are appropriately regularized at

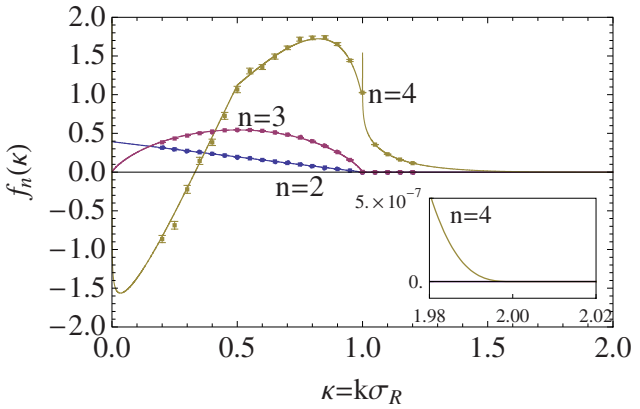

FIG. 2. (Color online) Functions f_n for $n=2$, 3, and 4 for a speckle potential created with a square diffusive plate [solid lines; see Eqs. (12) and (13) and the Appendix] and comparison with numerical calculations (points with error bars). The inset is a magnification of function f_4 around $\kappa=2$.

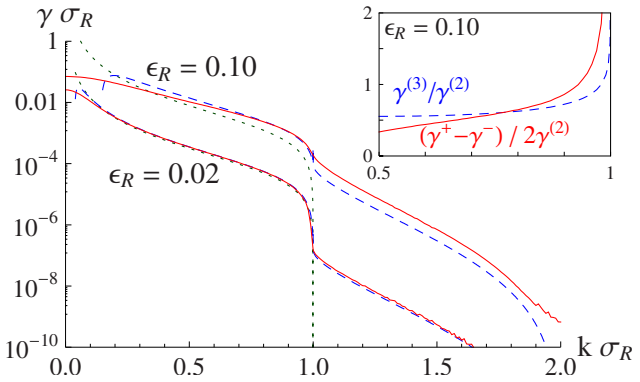

FIG. 3. (Color online) Lyapunov exponent $\gamma(k)$ versus the particle momentum k as determined numerically (solid red lines) and by perturbation theory up to order 4 (dashed blue lines) for a speckle potential created with a square plate. The dotted green lines are the Born term. Inset: comparison of odd and even contributions in the Born series for $\epsilon_R=0.1$.

infinity. Note also that in Eq. (8), the coefficients $(\epsilon_R/k\sigma_R)^n$ diverge for $k\to0$, while the exact $\gamma(k)$ remains finite for any ϵ_R [23]. This signals a well-known breakdown of the perturbative approach. Conversely, the perturbative expansion is valid when $\gamma(k)\ll k$ (for $k\to0$), i.e., when the localization length exceeds the particle wavelength, a physically satisfactory criterion.

IV. ONE-DIMENSIONAL ANDERSON LOCALIZATION IN SPECKLE POTENTIALS

A. Analytic results

Let us now examine the consequences of the peculiar properties of speckle potentials in the light of the above perturbative approach. For clarity, we restrict ourselves to 1D speckle potentials created by square diffusive plates as in Refs. [13,18] for which $c_a(u)=\sin(u)/u$ and $\hat{c}_a(q)\propto\Theta(1-|q|)$, where Θ is the Heaviside step function [24]. Using Eqs. (9) and (10), we find

$$f_2(\kappa)=\frac{\pi}{8}\Theta(1-\kappa)(1-\kappa), \tag{12}$$

$$f_3(\kappa)=-\frac{\pi}{4}\Theta(1-\kappa)[(1-\kappa)\ln(1-\kappa)+\kappa\ln(\kappa)]. \tag{13}$$

The functions f_2 and f_3 are simple and vanish for $\kappa\geq1$ (see Fig. 2). This property is responsible for the existence of the first effective mobility edge at $k=k_c$ [17], such that $\gamma(k)\sigma_R\sim(\epsilon_R/k\sigma_R)^2$ for $k\lesssim\sigma_R^{-1}$ while $\gamma(k)\sigma_R=O(\epsilon_R/k\sigma_R)^4$ for $k\gtrsim\sigma_R^{-1}$. The fact that f_3 vanishes in the same interval $(\kappa\geq1)$ as f_2 exemplifies the general property that odd-n terms cannot be leading terms in any range of k because $\gamma(k)$ must be positive whatever the sign of V_R. For $\kappa<1$ however, $f_3(\kappa)$ is not identically zero owing to the asymmetric probability distribution in speckle potentials. The term $\gamma^{(3)}$ can thus be either positive or negative depending on the sign of V_R [22].

The function f_4 is found similarly from Eq. (11). While its expression is quite complicated (see the Appendix), its behavior is clear when plotted (see Fig. 2). Let us emphasize some of its important features. First, there is a discontinuity of the derivative of f_4 at $\kappa=1/2$. Second, we find a very narrow logarithmic divergence, $f_4(\kappa)\sim-(\pi/32)\ln|1-\kappa|$ at $\kappa=1$, which signals a singularity of the perturbative approach (note that it does not appear in Fig. 1 due to finite resolution of the plot). Finally, the value $\kappa=2$ corresponds to the boundary of the support of f_4, showing explicitly the existence of a second effective mobility edge at $k=2\sigma_R^{-1}$. Hence, while $\gamma(k)\sigma_R\sim(\epsilon_R/k\sigma_R)^4$ for $k\lesssim2\sigma_R^{-1}$, we have $\gamma(k)\sigma_R=O(\epsilon_R/k\sigma_R)^6$ for $k\gtrsim2\sigma_R^{-1}$, since $f_4(\kappa)$ as well as $f_5(\kappa)$ vanish for $\kappa\geq2$.

B. Numerics

In order to test the validity of the perturbative approach for experimentally relevant parameters, we have performed numerical calculations using a transfer matrix approach. The results are plotted in Fig. 3: $\epsilon_R=0.02$ corresponds to $V_R/\hbar=2\pi\times16$ Hz in Fig. 3 of Ref. [13] and $\epsilon_R=0.1$ to $V_R/\hbar=2\pi\times80$ Hz in Fig. 3 and to Fig. 4 of Ref. [13]. For $\epsilon_R=0.02$, the agreement between analytical and numerical results is excellent. The effective mobility edge at $k=\sigma_R^{-1}$ is very clear: we find a sharp step for $\gamma(k)$ of about 2 orders of magnitude. For $\epsilon_R=0.1$, we find the same trend but with a smoother and smaller step (about one order of magnitude). In this case, although the Born term for $k\lesssim\sigma_R^{-1}$ and the fourth-order term for $k\gtrsim\sigma_R^{-1}$ provide reasonable estimates (within a factor of 2), higher-order terms—which may depend on the sign of V_R—contribute significantly.

The contribution of the odd terms can be extracted by taking $\gamma^+-\gamma^-$, where $\gamma^\pm$ are the Lyapunov exponents obtained for positive and negative disorder amplitude of same modulus $|V_R|$, respectively. As shown in the inset of Fig. 3, the odd terms range from 30% to 70% of the Born term for $0.6\lesssim k\sigma_R\lesssim0.9$ and $\epsilon_R=0.1$ and are of the order of $\gamma^{(3)}$ in weak disorder and away from the divergence at $k=\sigma_R^{-1}$. This shows that the first correction $\gamma^{(3)}$ to the Born term can be relevant in experiments.

For completeness, we have calculated the $f_n(\kappa)$ as the coefficients of fits in powers of $\epsilon_R/k\sigma_R$ using series of calculations of $\gamma(k)$ at fixed k and various ϵ_R. As shown in Fig. 2, the agreement with the analytic formulas is excellent. In particular, the numerics reproduce the predicted kink at $\kappa=1/2$. The logarithmic singularity around $\kappa=1$ being very narrow, we did not attempt to study it.

V. DIAGRAMMATIC ANALYSIS

Let us finally complete our analysis using diagrammatic methods, which allow us to exhibit momentum exchange in scattering processes as compact graphics and thus to identify effective mobility edges in a quite general way. In 1D, the localization length can be calculated from the backscattering probability of $\langle|\psi|^2\rangle$ using quantum transport theory. The irreducible diagrams of elementary scattering processes in speckle potentials have been identified in Ref. [25].

To lowest order in ϵ_R (Born approximation), the average intensity of a plane wave with wave vector k backscattered by the random potential is described by

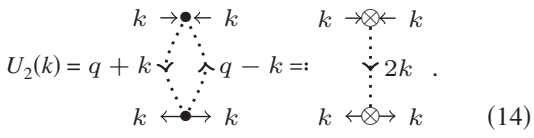

$$U_2(k) = \quad , \tag{14}$$

The upper part of the diagram represents ψ (particle) and the lower part its conjugate ψ^* (hole). The dotted line $\bullet\cdots\overset{q}{\rightarrow}\cdots\bullet = \epsilon_R\hat{c}_a(q)$ represents the field correlator; simple closed loops over field correlations can be written as a potential correlation $\otimes\cdots\cdots\otimes$. Backscattering requires diagram (14) to channel a momentum $2k$, entering at the particle, down along the potential correlations to the hole. Therefore, the diagram vanishes for $k\sigma_R>1$.

At order ϵ_R^3, the only possible contribution is

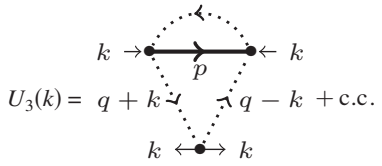

$$U_3(k) = \quad , \tag{15}$$

The straight black line stands for the particle propagator $[E_k-E_p+i0]^{-1}$ at intermediate momentum p. Diagram (15) features two vertical field correlation lines, just as diagram (14), and thus vanishes at the same threshold $k=\sigma_R^{-1}$. Evaluating two-loop diagram (15), we recover precisely contribution (13).

Many diagrams contribute to order ϵ_R^4. First there are the usual backscattering contributions with pure intensity correlations [Figs. 4(a)–4(c)]. Both Figs. 4(a) and 4(c) have a single vertical intensity correlation and vanish for $k>\sigma_R^{-1}$. In contrast, the crossed diagram [Fig. 4(b)] has two vertical intensity correlation lines and can thus accommodate momenta up to $k=2\sigma_R^{-1}$. Performing the integration, we find that this diagram reproduces those contributions to $f_4(\kappa)$ for $\kappa\in[1,2]$ that contain factorized correlators (see the Appendix). Second, there are nine more diagrams, all with nonfactorizable field correlations [25]. A single one has not two, but four vertical field correlation lines, shown in Fig. 4(d), and contributes for $k\sigma_R\in[1,2]$. Carrying out the three-loop integration, we recover exactly the nonfactorizable contributions to $f_4(\kappa)$ for $\kappa\in[1,2]$.

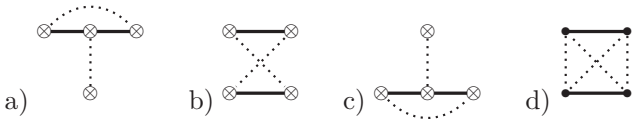

FIG. 4. Relevant fourth-order backscattering contributions. Contrary to the case of uncorrelated potentials [26,27], the sum of diagrams (a)–(c) *does not* give zero for speckle potentials; only diagrams (b) and (d) contribute for $k\sigma_R\in[1,2]$.

VI. CONCLUSION

We have developed perturbative and diagrammatic approaches beyond the Born approximation, suitable to study 1D AL in correlated disorder with possibly asymmetric probability distribution. In speckle potentials, the k dependence of the Lyapunov exponent exhibits sharp crossovers (effective mobility edges) separating regions where AL is due to scattering processes of increasing order. We have shown it explicitly for $k=\sigma_R^{-1}$ and $k=2\sigma_R^{-1}$, and we infer that there is a series of effective mobility edges at $k=p\sigma_R^{-1}$ with integer p since, generically, diagrams with $2p$ field correlations or p intensity correlations can contribute up to $k=p\sigma_R^{-1}$. This is because, although speckles are not Gaussian, they derive from a Gaussian field. Finally, exact numerics support our analysis for experimentally relevant parameters and indicate the necessity to use higher-order terms in the Born series even for $k<\sigma_R^{-1}$. Hence, important features that we have pointed out, such as odd terms in the Born series for $k<\sigma_R^{-1}$ and exponential localization for $k>\sigma_R^{-1}$, should be observable experimentally.

ACKNOWLEDGMENTS

Stimulating discussions with P. Bouyer, V. Josse, T. Giamarchi, and B. van Tiggelen are acknowledged. This research was supported by the French Centre National de la Recherche Scientifique (CNRS), Agence Nationale de la Recherche (ANR), Ministère de l'Education Nationale, de la Recherche et de la Technologie (MENRT), Triangle de la Physique, and Institut Francilien de Recherche sur les Atomes Froids (IFRAF).

APPENDIX

Here, we give the explicit formula of the function $f_4(\kappa)$ for a speckle potential created by a square diffusive plate, such that the fourth-order term in the Born expansion of the Lyapunov exponent γ reads

$$\gamma^{(4)} = \sigma_R^{-1}\left(\frac{\epsilon_R}{k\sigma_R}\right)^4 f_4(k\sigma_R).$$

The function $f_4(\kappa)$ is the sum of three terms with different supports:

$$f_4(\kappa) = f_4^{[0,1/2]}(\kappa) + f_4^{[0,1]}(\kappa) + f_4^{[1,2]}(\kappa),$$

where $f_4^{[\alpha,\beta]}(\kappa)$ lives on the interval $\kappa \in [\alpha,\beta]$ and

$$f_4^{[0,1/2]}(\kappa) = -\frac{\pi^3}{16}(1-2\kappa),$$

$$\begin{aligned} f_4^{[0,1]}(\kappa) = \frac{\pi}{16}\Bigg\{ & 4 - 6\kappa - \frac{10\pi^2}{3}(1-2\kappa) - (4-2\kappa)\ln(\kappa) - \left(\frac{5}{\kappa} - 3\kappa\right)\ln(1-\kappa) + \left(\frac{1}{\kappa} + \kappa\right)\ln(1+\kappa) - (4-8\kappa)\ln^2(\kappa) \\ & + 22(1-\kappa)\ln^2(1-\kappa) + (18+14\kappa)\ln^2(1+\kappa) - 16(1-\kappa)\ln(1-\kappa)\ln(\kappa) - 4(1-\kappa)\ln(1-\kappa)\ln(1+\kappa) \\ & - 32(1+\kappa)\ln(\kappa)\ln(1+\kappa) - 24(1+\kappa)\mathrm{Li}_2(\kappa) + 32(1+\kappa)\mathrm{Li}_2\left(\frac{\kappa}{1+\kappa}\right) - 8\kappa\mathrm{Li}_2\left(\frac{2\kappa}{1+\kappa}\right) - 8(1-2\kappa)\mathrm{Li}_2\left(2 - \frac{1}{\kappa}\right)\Bigg\}, \end{aligned}$$

$$f_4^{[1,2]}(\kappa) = \frac{\pi}{32}\left\{-2 + \left(1 + \frac{\pi^2}{3}\right)\kappa + 4\kappa\mathrm{Li}_2(1-\kappa) - \left(\frac{2}{\kappa} - 2 + \kappa\right)\ln(\kappa-1) - 2(\kappa-1) - \ln^2(\kappa-1) + 4\kappa\ln(\kappa-1)\ln(\kappa)\right\},$$

where $\mathrm{Li}_2(z) = \int_z^0 dt\, \ln(1-t)/t = \sum_{k=1}^{\infty} z^k/k^2$ is the dilogarithm function.

[1] P. W. Anderson, Phys. Rev. **109**, 1492 (1958).

[2] E. Akkermans and G. Montambaux, *Mesoscopic Physics of Electrons and Photons* (Cambridge University Press, New York, 2006).

[3] B. van Tiggelen, in *Wave Diffusion in Complex Media*, edited by J. P. Fouque, Lecture Notes at Les Houches 1998, NATO Science (Kluwer, Dordrecht, 1999).

[4] P. A. Lee and T. V. Ramakrishnan, Rev. Mod. Phys. **57**, 287 (1985).

[5] D. S. Wiersma, P. Bartolini, A. Lagendijk, and R. Righini, Nature (London) **390**, 671 (1997).

[6] M. Störzer, P. Gross, C. M. Aegerter, and G. Maret, Phys. Rev. Lett. **96**, 063904 (2006).

[7] T. Schwartz, G. Bartal, S. Fishman, and M. Segev, Nature (London) **446**, 52 (2007).

[8] Y. Lahini, A. Avidan, F. Pozzi, M. Sorel, R. Morandotti, D. N. Christodoulides, and Y. Silberberg, Phys. Rev. Lett. **100**, 013906 (2008).

[9] H. Hu, A. Strybulevytch, J. H. Page, S. E. Skipetrov, and B. A. van Tiggelen, Nat. Phys. **4**, 945 (2008).

[10] A. A. Chabanov, M. Stoytchev, and A. Z. Genack, Nature (London) **404**, 850 (2000).

[11] F. L. Moore, J. C. Robinson, C. F. Bharucha, B. Sundaram, and M. G. Raizen, Phys. Rev. Lett. **75**, 4598 (1995).

[12] J. Chabé, G. Lemarié, B. Grémaud, D. Delande, P. Szriftgiser, and J. C. Garreau, Phys. Rev. Lett. **101**, 255702 (2008).

[13] J. Billy, V. Josse, Z. Zuo, A. Bernard, B. Hambrecht, P. Lugan, D. Clément, L. Sanchez-Palencia, P. Bouyer, and A. Aspect, Nature (London) **453**, 891 (2008).

[14] G. Roati, C. D'Errico, L. Fallani, M. Fattori, C. Fort, M. Zaccanti, G. Modugno, M. Modugno, and M. Inguscio, Nature (London) **453**, 895 (2008).

[15] C. W. J. Beenakker, Rev. Mod. Phys. **69**, 731 (1997).

[16] F. M. Izrailev and A. A. Krokhin, Phys. Rev. Lett. **82**, 4062 (1999).

[17] L. Sanchez-Palencia, D. Clément, P. Lugan, P. Bouyer, G. V. Shlyapnikov, and A. Aspect, Phys. Rev. Lett. **98**, 210401 (2007); L. Sanchez-Palencia, D. Clément, P. Lugan, P. Bouyer, and A. Aspect, New J. Phys. **10**, 045019 (2008).

[18] D. Clément, A. F. Varón, J. A. Retter, L. Sanchez-Palencia, A. Aspect, and P. Bouyer, New J. Phys. **8**, 165 (2006).

[19] L. Fallani, C. Fort, and M. Inguscio, Adv. At., Mol., Opt. Phys. **56**, 119 (2008).

[20] J. W. Goodman, *Speckle Phenomena in Optics: Theory and Applications* (Roberts and Co., Englewood, 2007).

[21] L. Tessieri, J. Phys. A **35**, 9585 (2002).

[22] See also E. Gurevich and O. Kenneth, Phys. Rev. A **79**, 063617 (2009).

[23] B. Derrida and E. Gardner, J. Phys. **45**, 1283 (1984).

[24] Our results can be extended to any 1D random potential that fulfill conditions (1)–(3) with similar conclusions.

[25] R. C. Kuhn, C. Miniatura, D. Delande, O. Sigwarth, and C. A. Müller, New J. Phys. **9**, 161 (2007).

[26] I. V. Gornyi, A. D. Mirlin, and D. G. Polyakov, Phys. Rev. B **75**, 085421 (2007).

[27] A. Cassam-Chenai, and B. Shapiro, J. Phys. I (France) **4**, 1527 (1994).

Editorial Note: One-dimensional Anderson localization in certain correlated random potentials [Phys. Rev. A 80, 023605 (2009)]

P. Lugan, A. Aspect, L. Sanchez-Palencia, D. Delande, B. Grémaud, C. A. Müller, and C. Miniatura

(Received 27 June 2011; published 11 July 2011)

DOI: 10.1103/PhysRevA.84.019902 PACS number(s): 03.75.−b, 05.60.Gg, 67.85.−d, 72.15.Rn, 99.10.Np

This paper was published on 11 August 2009 with mistakes that were inadvertently introduced during the production cycle. The expressions of $f_4^{[0,1]}$ and $f_4^{[1,2]}$ in the Appendix of the article were published with typographical errors. The formulas should read

$$
\begin{aligned}
f_4^{[0,1]}(\kappa) = \frac{\pi}{64}\Bigg\{ & 4 - 6\kappa - \frac{10\pi^2}{3}(1-2\kappa) - (4-2\kappa)\ln(\kappa) - \left(\frac{5}{\kappa} - 3\kappa\right)\ln(1-\kappa) + \left(\frac{1}{\kappa} + \kappa\right)\ln(1+\kappa) \\
& - (4-8\kappa)\ln^2(\kappa) + 22(1-\kappa)\ln^2(1-\kappa) + (18+14\kappa)\ln^2(1+\kappa) - 16(1-\kappa)\ln(1-\kappa)\ln(\kappa) \\
& - 4(1-\kappa)\ln(1-\kappa)\ln(1+\kappa) - 32(1+\kappa)\ln(\kappa)\ln(1+\kappa) - 24(1+\kappa)\mathrm{Li}_2(\kappa) \\
& + 32(1+\kappa)\mathrm{Li}_2\left(\frac{\kappa}{1+\kappa}\right) - 8\kappa\,\mathrm{Li}_2\left(\frac{2\kappa}{1+\kappa}\right) - 8(1-2\kappa)\mathrm{Li}_2\left(2 - \frac{1}{\kappa}\right)\Bigg\}, \\
f_4^{[1,2]}(\kappa) = \frac{\pi}{32}\Bigg\{ & -2 + \left(1 + \frac{\pi^2}{3}\right)\kappa + 4\kappa\,\mathrm{Li}_2(1-\kappa) - \left(\frac{2}{\kappa} - 2 + \kappa\right)\ln(\kappa-1) - 2(\kappa-1)\ln^2(\kappa-1) \\
& + 4\kappa\ln(\kappa-1)\ln(\kappa)\Bigg\}.
\end{aligned}
$$

These typographical errors introduced during the production process do not affect the figures and results presented in the article, which are all based on the correct equations.

Chapter 3

BOSE GASES AT EQUILIBRIUM IN DISORDERED POTENTIALS: LOCALIZATION AND INTERACTIONS

In brief – *The interplay of interactions and disorder is a major problem in quantum physics. It leads to a variety of effects, which depend crucially on the specific problem at hand. We have addressed this question for bosons with repulsive interactions in the meanfield regime at equilibrium in a disordered potential. We eventually worked out a generic quantum-state diagram, which shows a variety of states resulting from the interplay of interactions and disorder.*

- *For strong meanfield interactions, the Bose gas forms a connected condensate. It is weakly affected by the disorder and is thus extended. We actually showed that repulsive interactions smooth the disordered potential. In this regime, time-of-flight images display anomalously large density modulations, which we explain by the dynamics of the time-of-flight process.*
- *For weak interactions, the Bose gas forms a Lifshits-Anderson glass in strong disordered potentials, which is described as a Fock state of single-particle localized states. In this regime, relevant quantities are the single-particle density of states and the participation length. The equation of state relating this quantities is derived.*
- *For intermediate interactions, the Bose gas separates in a number of fragments. The corresponding fragmented condensate is the weak-interaction counterpart of the Bose glass, which is characterized by insulting properties and absence of a gap.*

Beyond the meanfield background, the dynamical behavior of interacting systems is primarily governed by collective excitations. For strong meanfield interactions, the latter are Bogolyubov quasi-particles. We demonstrated many-body Anderson localization of these quasi-particles in interacting Bose gases. This effect offers an original viewpoint on localization in interacting quantum systems.

3.1 Combined interactions and disorder in quantum systems

In quantum physics, both repulsive interactions and disorder induce localization effects, which spark fluid / insulator transitions. The Mott localization –which is driven by interactions in disorder-free systems– and the Anderson localization –which is driven by disorder in noninteracting systems– are the most fundamental aspects of these transitions in condensed-matter physics (see Sec. 2.1.1). Both are reasonably well understood, and have been observed independently in ultracold atomic systems. In many systems however, both particle-particle interactions and disorder play significant roles, and an even more difficult question arises: How does the interplay of particle-particle interactions and disorder affect metal-insulator transitions ? This question proved very puzzling from the earliest times of Anderson localization (Anderson, 1977) and is actually still widely open. As we will show, the combined effects of interactions and disorder leads a variety of phenomena, which crucially depend on the characteristics of the system under consideration. For instance, we will see that interactions may either hamper or favor localization in disordered systems, depending in particular on the quantum statistics, the dimension and the strength of interactions.

In condensed-matter physics, all these aspects may be relevant in various systems, and several theoretical and/or experimental works unveil intriguing effects, which are not fully understood.

- Dirty bosons are relevant to experiments on ^{4}He in porous media. Landmark experiments by Reppy and coworkers show that helium films absorbed on porous substrates undergo suppression of superfluidity when the density increases (Reppy, 1984; Crowell *et al.*, 1995; 1997). This result suggests that in strongly-interacting Bose systems, there exists a critical density above which repulsive interactions cooperate with disorder to favor localization, which lead to the key concept of the *Bose glass* (Hertz *et al.*, 1979; Giamarchi and Schulz, 1987; 1988; Fisher *et al.*, 1989).
- Weakly-interacting fermions are relevant to certain dirty electronic systems. In particular, experiments performed on metal-oxide semiconductor field effect transistors (MOSFETs) show an intriguing metal-insulator transition in two dimensions (Kravchenko *et al.*, 1994; Kravchenko *et al.*, 1995). This observation is usually interpreted by arguing that in dimension two –which, according to the scaling theory (Abrahams *et al.*, 1979), is the marginal dimension for Anderson localization– very weak interactions may be sufficient to modify the scaling flow of the dimensionless conductance so as to give $\beta(g = +\infty)$ a finite positive value, thus leading to delocalization (see Sec. 2.1.2). This interpretation is however still strongly debated (Abrahams, 2001).
- Effects of disorder in superconductors are also of major importance. For weak interactions, the Fermi superfluid is well described by the Bardeen-Schrieffer-Cooper (BCS) theory (Bardeen *et al.*, 1957) and formation of spatially extended Cooper pairs consisting of two fermions of opposite spins and momenta. The famous Anderson theorem indicates that disorder should not affect very much the BCS superfluid owing to the long-range and overlapping nature of the Cooper pairs (Anderson, 1959). Surprisingly, d-wave superconductors are very robust to disorder (Balatsky *et al.*, 2006), which may have several reasons: (i) disorder lies off the CuO2 planes in the spacer layers, (ii) the short coherence length in cuprates leads to a very local response to impurities (Nachumi *et al.*, 1996; Ghosal *et al.*, 2000), and (iii) the effect of disorder is suppressed by strong correlations (Garg *et al.*, 2008).

In most condensed-matter physics systems, disorder modifies simultaneously several ingredients in the system, such as the Coulomb interaction, electron-phonon couplings, and density of

states. Control of disorder (Clément *et al.*, 2006; Fallani *et al.*, 2008) and interactions (Roati *et al.*, 2007; Pollack *et al.*, 2009) in ultracold atomic systems offer particularly promising routes to address the interplay of disorder and interactions. Let us briefly comment on the role of interactions in the early studies of Anderson localization with Bose-Einstein condensates (Billy *et al.*, 2008; Roati *et al.*, 2008). In the experiments at LENS (Roati *et al.*, 2008), the interactions where almost exactly cancelled using Feshbach resonance techniques, so they do not play any role. Conversely, in the experiment at Institut d'Optique (Billy *et al.*, 2008), the interactions do play a crucial role as they determine the momentum distribution of the expanding condensate (see comments at the end of page 49). They however do not play a significant role in the Anderson localization process of the k-waves which are supposed to be independent from each other (Sanchez-Palencia *et al.*, 2007).

In contrast, stronger interactions may play a non-negligible role. Common belief is that even weak interactions strongly affect or even destroy localization. The question is how will they affect it ? This question seems relatively simple and well posed. It is not so and actually, even in most recent works, it appears that different approaches provide apparently contradicting answers in different transport schemes. For instance, recent numerical calculations (Pikovsky and Shepelyansky, 2008; Palpacelli and Succi, 2008) suggest that for expanding condensates [as in the experiment at Institut d'Optique (Billy *et al.*, 2008)], repulsive interactions destroy localization above a given threshold. Conversely, other recent results (Kopidakis *et al.*, 2008) predict that localization should persist even in the presence of interactions. Finally, in transmission experiments[1], perturbative calculations and numerical results indicate that repulsive interactions decrease the localization length before completely destroying localization, giving rise to strong temporal fluctuations (Paul *et al.*, 2007).

In the following, we adopt a different approach to the interplay of particle-particle interactions and disorder, which proves fruitful, and actually more tractable from a theoretical perspective. Instead of studying the effects of interactions in transport schemes, we now wonder what is the quantum state of a zero-temperature gas at equilibrium in a finite, closed box, in the presence of a disordered potential and of interactions. In orther words, we wonder what is the many-body ground state and possibly the excitations of the many-body, d-dimensional Hamiltonian (1.1).

3.2 Effects of weak short-range interactions in disordered, Bose and Fermi systems

In the remainder of this chapter, we restrict ourselves to weak short-range interactions. Strong interactions also have very interesting effects. A satisfying description of the latter would however require a complete chapter, and we chose to avoid a too long discussion.

As can be easily anticipated, the effect of interactions significantly depends on the quantum statistics (Bose or Fermi). A simple analysis actually shows that the difference is not only quantitative, but even qualitative.

[1] A transmission scheme consists in throwing a mono-kinetic wavepacket to a disordered region of finite length and measure the transmission probability. It is thus also a transport scheme but it however significantly differs from the expansion scheme. Although the two are equivalent for non-interacting particles, it is not clear that interactions preserve the equivalence.

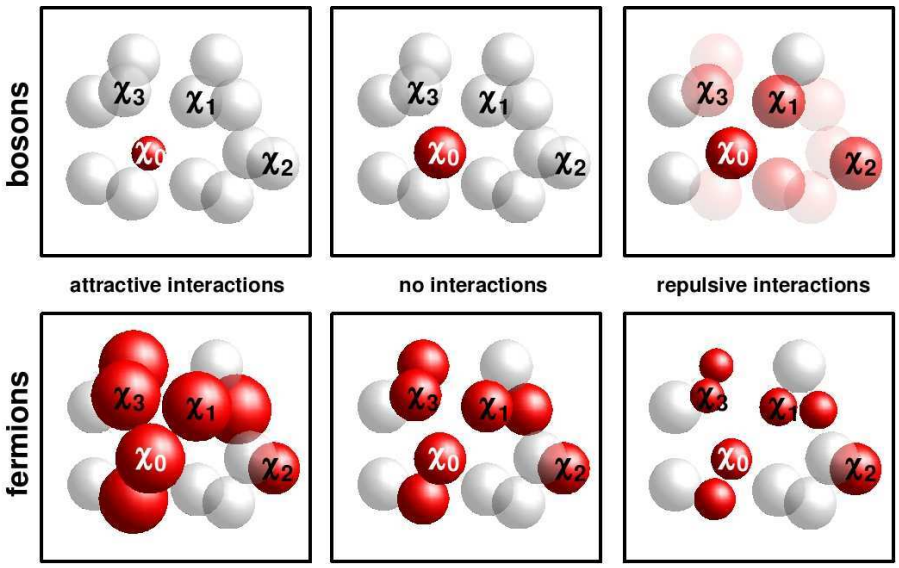

Figure 3.1 | **Effect of interactions in disordered gases.** The gas is described using the single-particle states $|\chi_\nu\rangle$. In the presence of disorder, localized states (represented by the spheres; in red when they are populated) are distributed around. **Bose gas:** For non-interacting bosons (top, central panel), the ground state, $|\chi_0\rangle$, only is populated. Attractive interactions (top, left panel) contract this state, thus favoring localization. Conversely, repulsive interactions (top, right panel) work against localization by populating more and more $|\chi_\nu\rangle$ states. **Fermi gas:** In the absence of interactions, a gas of N fermions populates the N lowest-energy $|\chi_\nu\rangle$ states (bottom, central panel). Then, each state tends to extend under the action of attractive interactions as for maximizing the overlap between different populated $|\chi_\nu\rangle$ states (bottom, left panel). Conversely, for repulsive interactions, they tend to minimize their mutual overlap, thus favoring localization (bottom, right panel) [from (Sanchez-Palencia and Lewenstein, 2010)].

Bosons (upper panel of Fig. 3.1) For vanishing interactions and zero temperature, a gas of identical bosons populates the single-particle ground state, $|\chi_0\rangle$. Very weak attractive interactions are expected to favor localization by contracting the Bose gas, but also induce strong instabilities for moderate attractive interactions, pretty much like those leading to the collapse of trapped Bose-Einstein condensates (Dalfovo *et al.*, 1999; Pitaevskii and Stringari, 2003). Conversely, weak to moderate repulsive interactions do not affect much the stability, but work against localization, by populating an increasing number of single-particle states, $|\chi_\nu\rangle$. Weak repulsive interactions populate significantly only the lowest-energy states. Since they are strongly bound in rare, low-energy modulations of the potential (Lifshitz, 1964), their mutual overlap is small.

Fermions (lower panel of Fig. 3.1) - Consider now a Fermi gas. In the absence of interactions, the gas of N fermions populates the N lowest single-particle states. For low atomic densities (*i.e.* $nP^d \ll 1$, where P is the typical linear size of a localized single-particle state, for instance the participation length), short-range interactions do not play a significant role as the populated states are spatially separated. For large-enough density however, they do overlap. Then, for repulsive interactions, each populated state tends to contract to minimize its overlap with other populated states, thus favoring localization. This was first pointed out in the context of (repulsive) Coulomb interactions in (fermionic) electronic dirty systems (Altshuler *et al.*, 1980; Aleiner *et al.*, 1999). Conversely, for attractive interactions, the populated states tend to extend to maximize their

overlap, thus favoring delocalization.

Hence, strikingly, weak interactions have opposite effects on localization of bosons and fermions.

3.3 Disordered Bose-Einstein condensates in the presence of repulsive interactions

In this and the following sections, we review our contributions to the field. We have studied the interplay of interactions and disorder in weakly-interacting Bose gases. This section is devoted to the study of Bose-Einstein condensates in the meanfield regime, while the next sections discuss beyond meanfield properties.

3.3.1 Condensate wave-function

▷ *see paper reprinted on page 103*

Introducing disorder, even of small amplitude (in particular in low-dimensional systems) can have strong consequences on the behavior of non-interacting particles. Hence, interference of multiply-scattered linear waves from impurities leads to Anderson localization, that is exponential decay of the wavefunction (Anderson, 1958). What does happen in a Bose-Einstein condensate with weak repulsive interactions ?

In the meanfield regime, for a very weak disordered potential and strong interactions, the Bose gas is expected to form a connected quantum fluid (Lee and Gunn, 1990), *i.e.* a Bose-Einstein condensate in three dimensions or possibly a quasi-condensate in lower dimensional systems (Popov, 1972). In this regime, the quantum state is determined by the minimization of the grand-canonical energy functional

$$E[n,\theta] = \int d\mathbf{r} \left[\frac{\hbar^2 |\nabla\theta(\mathbf{r})|^2}{2m} n_c(\mathbf{r}) + \frac{\hbar^2 |\nabla\sqrt{n_c(\mathbf{r})}|^2}{2m} + V(\mathbf{r})\, n_c(\mathbf{r}) + \frac{g}{2} n_c(\mathbf{r})^2 - \mu\, n_c(\mathbf{r}) \right], \quad (3.1)$$

where $V(\mathbf{r})$ is the disordered potential (supposed to be of zero average), m is the atomic mass and g is the coupling parameter. Since the phase, $\theta(\mathbf{r})$, and density, $n(\mathbf{r})$, fields are separated in Eq. (3.1), we immediately see that the energy is minimum for $\theta(\mathbf{r}) = cst$, irrespective to the behavior of $n(\mathbf{r})$. While in low dimensions, phase fluctuations are strong (Mermin and Wagner, 1966; Hohenberg, 1967), in three dimensions, they are suppressed and $\psi(\mathbf{r}) = \sqrt{n_c(\mathbf{r})}$ up to an homogeneous (unphysical) phase. In both cases, the density profile $n_c(\mathbf{r})$ is governed by the Gross-Pitaevskii equation (Pitaevskii and Stringari, 2003):

$$\mu = \frac{-\hbar^2\nabla^2\sqrt{n_c(\mathbf{r})}}{2m\sqrt{n_c(\mathbf{r})}} + V(\mathbf{r}) + g n_c(\mathbf{r}). \quad (3.2)$$

As pointed out in Sec. 2.1.2, for non-interacting atoms ($g = 0$), the solutions of Eq. (3.2) are not trivial, in particular because a simple perturbation approach in powers of V_R/μ in the form $\psi = \psi_0 + \delta\psi$ usually diverges, and one should rely on more subtle perturbation theory, for instance the phase formalism approach (Lifshits *et al.*, 1988). Surprisingly enough, for finite repulsive interactions, the nonlinear term, $g n_c(\mathbf{r})$, simplifies the problem and it turns out that the

perturbation series does not show similar divergence. Then, using standard perturbation theory, the solution of Eq. (3.2) reads (Sanchez-Palencia, 2006)

$$n_{\rm c}(\mathbf{r}) = \frac{\mu - \widetilde{V}(\mathbf{r})}{g} \tag{3.3}$$

where, to lowest order[2],

$$\widetilde{V}(\mathbf{r}) = \int {\rm d}\mathbf{r}' G_\xi(\mathbf{r}') V(\mathbf{r}-\mathbf{r}') \tag{3.4}$$

is the convolution of the bare disordered potential $V(\mathbf{r})$ and of the function $G_\xi(\mathbf{r})$, the Fourier transform of which reads $G_\xi(\mathbf{q}) = \frac{(2\pi)^{-d/2}}{1+(|\mathbf{q}|\xi)^2}$, with $\xi = \hbar/\sqrt{2m\mu}$ the healing length. Equation (3.3) holds for weak disorder, *i.e.* $\widetilde{V}_{\rm R} \ll \mu$.

Turning to Fourier space, we find that $\widetilde{V}(\mathbf{q}) = \frac{V(\mathbf{q})}{1+(|\mathbf{q}|\xi)^2}$. In this form, it can be easily seen that $\widetilde{V}(\mathbf{r})$ reproduces the long-wavelength ($|\mathbf{q}| \ll 1/\xi$) components of $V(\mathbf{r})$ while suppressing the short wavelengths ($|\mathbf{q}| \gg 1/\xi$) components. Therefore, the potential $\widetilde{V}(\mathbf{r})$ is called the *smoothed potential* (Sanchez-Palencia, 2006). For very strong meanfield interactions ($\xi \ll \sigma_{\rm R}$), $\widetilde{V}(\mathbf{r}) \simeq V(\mathbf{r})$ and Eq. (3.3) is the Thomas-Fermi solution, *i.e.* the spatial modulations of the density profile exactly follow those of the disordered potential. For weaker interactions ($\xi \gtrsim \sigma_{\rm R}$), the solution (3.3) resembles the Thomas-Fermi solution except that the smoothed potential $\widetilde{V}(\mathbf{r})$ takes the place of the bare disordered potential $V(\mathbf{r})$. It can be easily checked that homogeneity of the bare disordered potential implies homogeneity of the smoothed disordered potential[3]. Therefore, the density profile (3.3) is extended, *i.e.* it does not show Anderson localization, in strong contrast to non-interacting particles, even for $\xi > \sigma_{\rm R}$. Recovering localization requires extremely weak interactions, but then, the Gross-Pitaevskii approach is no longer sufficient (see Sec. 3.4).

These results can be easily extended to disordered (quasi-)condensates in weak harmonic traps by applying local density approximation, which amounts to replace the healing length by a position-dependent healing length, $\xi = \hbar/\sqrt{2mgn_{\rm c}^0(\mathbf{r})}$, where $n_{\rm c}^0(\mathbf{r})$ is the density in the absence of disorder (Sanchez-Palencia, 2006). These calculations are illustrated in Fig. 3.2 for the one-dimensional case.

3.3.2 Density modulations in time-of-flight images of disordered Bose-Einstein condensates

▷ *see paper reprinted on page 111*

Ultracold atoms offer a number of measuring techniques to probe the properties of Bose-Einstein condensates. One of the most routinely used is time-of-flight (TOF) imaging, which consists in releasing the gas from its trap and let it expand (Ketterle *et al.*, 1999; Ketterle and Zwerlein, 2008). The TOF dynamics is very well known in various situations, which allows to reconstruct key features of the initially-trapped gas. For instance, in the absence of interactions, the expansion is ballistic, which allows one to directly measure the initial momentum distribution [see for instance (Basdevant and Dalibard, 2002)]. For strong meanfield interactions (Thomas-Fermi regime) and

[2]For detailed calculations beyond the lowest order, see the PhD thesis of Pierre Lugan (2010).

[3]A disordered potential is said to be homogeneous if all statistical averages (*e.g.* $\langle V(\mathbf{r})\rangle$, $C_2(\mathbf{r}) = \langle V(\mathbf{r}'+\mathbf{r})V(\mathbf{r}')\rangle - \langle V\rangle^2$) are independent of the position $\mathbf{r}$ (Lifshits *et al.*, 1988).

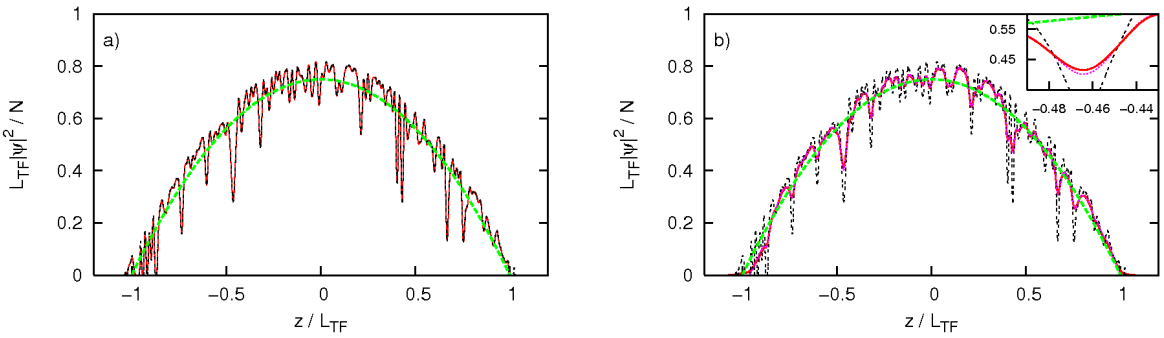

Figure 3.2 | Density profiles of a trapped, interacting Bose-Einstein (quasi-)condensate in the presence of a disordered potential. The dashed black lines correspond to the Thomas-Fermi solution, $n(z) = [\mu - V(z)]/g$, and the dotted purple lines to the smoothed potential, $n(z) = [\mu - \widetilde{V}(z)]/g$. The solid red lines are obtained from numerical solutions of the Gross-Pitaevskii equation The dashed green line if the inverted parabola corresponding to the density profile in the absence of disorder (the condensate of N atoms has a Thomas-Fermi half-length L_{TF}). **a) Regime where $\xi < \sigma_R$.** In this case, the density profile follows the modulations of the disordered potential, $V(z)$ (the curves are hardly distinguished). **b) Regime where $\xi > \sigma_R$.** In this case, the density profile does not follow the modulations of the bare disordered potential, but rather those of a smoothed potential, $\tilde{V}(z)$ (the solid red line is hardly distinguished from the dotted purple curve, except at very small scale shown in the inset) [from (Sanchez-Palencia, 2006)].

a harmonic trap, the expansion is self-similar, so that one can access the initial density profile and reveal small-scale features, such as vortex cores for instance (Fetter, 2009).

Then, what does happen for a condensate created in a disordered potential ? Let us consider a three-dimensional condensate in the Thomas-Fermi regime and in the presence of a one-dimensional disordered potential, $V(z)$. We define the relative modulations $\eta(z)$ of the one-dimensional density profile, $n_{1D}(z) = \int d\rho\ n_{3D}(\rho)$ with $\rho = (x,y)$ is the transverse coordinate, such that $n_{1D}(z) = n^0_{1D}(z)[1+\eta(z)]$ where n^0_{1D} is the density profile in the absence of disorder. In the trap center, we expect that the root mean square value of η is $\Delta\eta \simeq 2V_R/\mu$ (Sanchez-Palencia, 2006)[4]. Experimental results obtained at LENS, Institut d'Optique and Rice University however show significantly larger density modulations (Lye *et al.*, 2005; Clément *et al.*, 2008; Chen *et al.*, 2008). A possible explanation that was first raised is that disorder may enhance thermal or quantum phase fluctuations in the initially-trapped condensate. It is indeed known that initial phase fluctuations develop density fluctuations in TOF images of elongated (non-disordered) quasi-condensates (Dettmer *et al.*, 2001; Richard *et al.*, 2003). A couple of evidences lead us to conclude that it is not a correct interpretation in the present case. The most striking one is that exactly the same modulated density profile is observed for different realizations of the TOF process but with the same realization of the disordered potential. Therefore, the observed modulations cannot emanate from thermal or quantum fluctuations.

In fact, we have shown that the disorder does not significantly enhance the initial phase fluctuations but that it is the TOF process itself that enhances the density modulations, at least for the experimental parameters of (Lye *et al.*, 2005; Clément *et al.*, 2008; Chen *et al.*, 2008). We have first performed numerical calculations within the time-dependent Gross-Pitaevskii approach. The

[4]Note that for the experimental parameters of (Lye *et al.*, 2005; Clément *et al.*, 2008; Chen *et al.*, 2008), $\xi \ll \sigma_R$, so that the smoothing effect is negligible. In a d-dimensional condensate, one finds a root mean square value of V_R/μ (see Sec. 3.3.1). Here the multiplying factor 2 results from the integration over the radial coordinates.

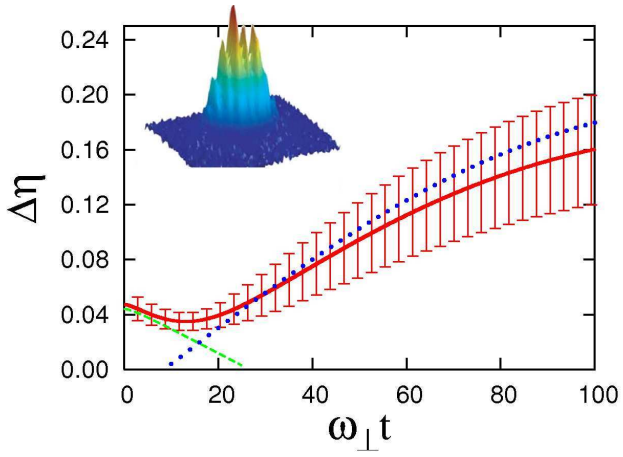

Figure 3.3 | Dynamics of density modulations during time-of-flight of a disordered, elongated Bose-Einstein condensate. The main figure shows the root mean square of the density modulations as a function of time. The solid red line with errorbars is the result of numerical calculations, and the dashed green and dotted blue lines to analytical calculations for short and long times respectively. The inset shows an experimental one-dimensional profile imaged after an expansion time of 17ms for $V_R/\mu \simeq 0.4$ [adapted from (Clément *et al.*, 2008)].

numerical results reproduce quantitatively and qualitatively the experimental observations, thus confirming that initial phase fluctuations –which are not included in the numerics– are not relevant. In turn, we have elaborated the following two-stage scenario.

– When the trap and the disordered potential are switched off at time $t = 0$, the expansion of the elongated condensate is essentially radial. The small initial density modulations (of the order of $2V_R/\mu$), which are longitudinal, are thus frozen. They correspond to an inhomogeneous local chemical potential $\mu - gn(z)$, since the disordered potential and the trap are now switched off. In the Thomas-Fermi regime, it induces an inhomogeneous phase, which reads $\theta(z) \simeq \frac{\mu - gn(z)}{g}\frac{t}{\hbar} = \frac{V(z)t}{\hbar}$ at short times ($t \ll 1/\omega_\perp$) and saturates to the final value $\theta(z) \simeq \frac{\pi}{2}\frac{V(z)}{\hbar\omega_\perp}$ in the long times limit.

– This produces a strong disorder-induced modulation of the phase in the expanding condensate, of root mean square value of the order of $(\pi/2)(V_R/\hbar\omega_\perp)$. In a later stage, the phase modulations –which correspond to an inhomogeneous velocity gradient in the longitudinal direction– are converted into (time-dependent) density modulations along z, $\Delta\eta \propto V_R/\hbar\omega_\perp$.

This mechanism, which is just outlined here [see (Clément *et al.*, 2008) as well as (Chalker and Shapiro, 2009) for details], allows for analytical calculations in good agreement with numerical results, as illustrated in Fig. 3.3. In brief, we find that $\Delta\eta(t)$ is initially $2V_R/\mu$, as expected. Then $\Delta\eta(t)$ slightly decreases because, when released from the disordered potential, the condensates tends to fill its holes. Finally, $\Delta\eta(t)$ strongly increases as a result of the development of density modulations induced by the inhomogeneous phase produced during the initial (radial) expansion stage.

We have hence shown that the large modulations observed at LENS, Institut d'Optique and Rice University in TOF images of disordered condensates *do not* rely on initial disorder-induced phase fluctuations. They actually result from the TOF process of a condensate with small initial density modulations but without phase fluctuations. These results do not exclude that in other regimes, phase fluctuations are enhanced by disorder. This may happen for instance in a regime of Anderson localization of Bogolyubov excitations (Lugan *et al.*, 2007b). Our work actually shows that revealing this possible effect via TOF images as in (Dettmer *et al.*, 2001; Richard *et al.*, 2003) requires taking into account the phase modulation which develops during the first stage of the TOF.

3.4 Localization versus interactions in ultracold Bose gases: A schematic quantum-state diagram

▷ *see paper reprinted on page 117 (collaboration with Maciej Lewenstein)*

The analysis of Sec. 3.3.1 performed in the framework of the Gross-Pitaevskii equation shows that strong repulsive interactions in the meanfield regime suppress Anderson localization. It has been addressed by considering the perturbative effect of disorder on a (quasi-)condensate with a given amount of interactions. We then found that the condensate density is modulated by the disordered potential, inducing in particular troughs in the vicinity of local maxima of the disordered potential. This analysis is expected to break down when the amplitude of disorder (possibly corrected by the smoothing effect) becomes of the order of magnitude of the interaction energy per particle. Ultimately, for vanishing interactions, one should recover an Anderson-localized state. In this section, we interpolate between the two regimes with the aim of drawing a clear physical picture illustrated by a schematic quantum-state diagram.

3.4.1 Quantum states

Let us consider a Bose gas in dimension d with repulsive interactions in a disordered potential, which, in three dimensions, we assume sufficiently strong that the lowest-energy states are localized. We assume that the gas is confined in a large[5] flat box of d-dimensional volume Ω and consider the many-body ground-state properties. Our point of view is to fix the disordered potential and then discuss the main features of the quantum states that can appear when increasing the strength of interactions.

Anderson-Lifshits glass (weak interactions) - In the absence of interactions, all N bosons condense into the ground state $|\chi_0\rangle$ of a single particle in the disordered potential, which is assumed to be localized. The N-body wavefunction of the Bose gas is thus the Fock state $|\Psi\rangle = (N!)^{-1/2}(\hat{b}_0^\dagger)^N|\emptyset\rangle$ where $\hat{b}_0^\dagger$ is the creation operator of a boson in state $|\chi_0\rangle$. This state is however strongly instable against even very weak interactions, at least in large systems. This can be intuitively understood: In a homogeneous disordered potential of large size[5], the ground state $|\chi_0\rangle$ will have many similar low-energy partners $|\chi_\nu\rangle$ –*i.e.* with energy and spatial extension similar to those of $|\chi_0\rangle$– but far apart. Then, distributing the atoms among these states does not significantly change the kinetic and potential energy but significantly lowers the interaction energy.

The many-body quantum state of the Bose gas is hence determined by the distribution of the N bosons in the lowest-energy single-particle eigenstates, $\{|\chi_\nu\rangle, \nu \in \mathbb{N}\}$, of the disordered potential. This is represented by the Fock state

$$|\Psi\rangle \;=\; \prod_{\nu\geqslant 0} \frac{1}{\sqrt{N_\nu!}}\,(b_\nu^\dagger)^{N_\nu}|\emptyset\rangle, \tag{3.5}$$

where the number N_ν of bosons in the single-particle eigenstate $|\chi_\nu\rangle$ results from the competition between the single-particle energies ε_ν and the self-interaction energies, $U_\nu = gP_\nu^{-1}$, where

[5]Here, 'large' means much larger than the typical spatial extension of the lowest-energy single-particle states in the disordered potential.

$P_\nu^{-1} = \int d\mathbf{r}|\chi_\nu(\mathbf{r})|^4$ is the inverse participation volume, of all populated localized states. This description is expected to hold as long as the populated states are sufficiently far apart that the inter-state interaction terms, proportional to $g\int d\mathbf{r}\ |\chi_{\nu_1}(\mathbf{r})|^2|\chi_{\nu_2}(\mathbf{r})|^2$, are negligible (se below). Then, minimization of the energy corresponding to the state (3.5), provides the number of atoms in each single-particle state:

$$\begin{aligned} N_\nu &= [\mu-\varepsilon_\nu]/U_\nu \quad \text{for } \mu > \varepsilon_\nu \\ N_\nu &= 0 \quad \text{otherwise,} \end{aligned} \tag{3.6}$$

where μ is the chemical potential[6]. This equation allows us to determine the equation of state

$$g\bar{n}_c = \int_{-\infty}^{\mu} \mathrm{d}\varepsilon\ \mathcal{D}(\varepsilon)(\mu-\varepsilon)P(\varepsilon), \tag{3.7}$$

where $\bar{n}_c = N/\Omega$ is the average density, and $\mathcal{D}(\varepsilon)$ is the density of states per unit volume. Further numerical calculations confirm this equation of state which is characteristic of the Anderson-Lifshits glass (Lugan *et al.*, 2007a).

In this regime, the main effect of repulsive interactions is thus to delocalize the Bose gas by populating more and more single-particle states $|\chi_\nu\rangle$ located at different positions, but each $|\chi_\nu\rangle$ is not significantly changed. This regime is sometimes called the Anderson glass (Scalettar *et al.*, 1991; Damski *et al.*, 2003; Roth and Burnett, 2003). We stress however that, in this regime, the exponential decay of the localized states $|\chi_\nu\rangle$ –which is the most celebrated characteristics of Anderson localization (see Chap. 2)– is not the most relevant quantity. Conversely, the above analysis shows that the relevant quantities are i) the density of states $\mathcal{D}(\varepsilon)$ and ii) the participation volume $P(\varepsilon)$ in the so-called Lifshits tail (Lugan *et al.*, 2007a). In turn, the localization length, which characterizes the exponential decay of the low-amplitude far tails of $|\chi_\nu\rangle$, significantly differs from the participation length $P_\nu^{1/d}$, which characterizes the typical size of $|\chi_\nu\rangle$ and is mainly determined by its high-amplitude core. We thus rather call this regime the *Anderson-Lifshits glass regime*.

Bose-Einstein condensate (strong meanfield interactions) - When the interaction strength is very large, the number of populated Lifshits states is so large that they significantly overlap. It is thus no longer convenient to work in the basis of the Lifshits states. Rather, we expect to recover the *connected condensate regime*, which is described by a single-particle wavefunction, governed by the Gross-Pitaevskii equation (see Sec. 3.3.1). Then, for $\mu \gg \widetilde{V}_R$, the density profile of the Bose gas is given by Eq. (3.3): $n_c(\mathbf{r}) = [\mu - \widetilde{V}(\mathbf{r})]/g$. Since the average value of the disordered potential V has been assumed to be zero (without loss of generality), the average value of the smoothed disordered potential $\widetilde{V}$ vanishes, and the equation of state of the (quasi-)condensate immediately follows from Eq. (3.3):

$$g\bar{n}_c \simeq \mu. \tag{3.8}$$

This equation of state drastically differs from that of the Anderson-Lifshits glass, in particular, it only weakly depends on the disordered potential (Lugan *et al.*, 2007a).

[6]Interestingly, Eq. (3.6) is formally equivalent to a Thomas-Fermi profile where ν would be a position, ε_ν the potential, and $N_\nu P_\nu^{-1}$ the local density. This is due to the fact that the single-particle states $|\chi_\nu\rangle$ are strictly eigenstates of the non-interacting Hamiltonian. Therefore, the tunneling between two states is strictly zero, *i.e.* the kinetic energy vanishes as in the usual Thomas-Fermi limit.

Using the definition of the smoothed potential, given by Eq. (3.4), we find that the standard deviation of the smoothed potential is

$$\widetilde{V}_{\rm R} = \sqrt{\frac{1}{(2\pi)^{d/2}} \int {\rm d}\mathbf{q}\, \frac{\widehat{C}(\mathbf{q})}{\left[1+(\xi|\mathbf{q}|)^2\right]^2}} \tag{3.9}$$

where $C(\mathbf{r}) = \langle V(\mathbf{r}+\mathbf{r}')V(\mathbf{r}')\rangle$ is the two-point correlation function of the bare disordered potential, the typical width of which is the correlation length $\sigma_{\rm R}$, and $\widehat{C}(\mathbf{q}) = (2\pi)^{-d/2}\int d^d\mathbf{r}\, C(\mathbf{r}){\rm e}^{-i\mathbf{q}.\mathbf{r}}$ is the Fourier transform. From the relations $\mu \propto 1/\xi^2$ and $\widehat{C}(\mathbf{q}) \propto \langle|\widehat{V}(\mathbf{q})|^2\rangle \geq 0$, we then find that the modulations of the density profile, $\Delta n_{\rm c} = \sqrt{\langle (n_{\rm c}(\mathbf{r})-\overline{n}_{\rm c})^2\rangle} = \widetilde{V}_{\rm R}$, increase when the chemical potential increases (up to a saturation value of $V_{\rm R}$). However, the relative modulations of the density profile, $\Delta n_{\rm c}/\overline{n}_{\rm c} = \widetilde{V}_{\rm R}/\mu$, decrease when the chemical potential μ increases. More precisely, we find

$$\frac{\Delta n_{\rm c}}{\overline{n}_{\rm c}} = \frac{\widetilde{V}_{\rm R}}{\mu} \simeq \frac{V_{\rm R}}{\mu} \qquad \text{for } \mu \gg E_{\rm R} \text{ (\textit{i.e.} for } \xi \ll \sigma_{\rm R}) \tag{3.10}$$

and

$$\frac{\Delta n_{\rm c}}{\overline{n}_{\rm c}} = \frac{\widetilde{V}_{\rm R}}{\mu} \propto \frac{V_{\rm R}}{\mu^{1-d/4} E_{\rm R}^{d/4}} \qquad \text{for } \mu \ll E_{\rm R} \text{ (\textit{i.e.} for } \xi \gg \sigma_{\rm R}), \tag{3.11}$$

where $E_{\rm R} = \hbar^2/2m\sigma_{\rm R}^2$ is the energy associated to the disorder correlation length. These relations are universal in the sense that they do not depend on the details of the disordered potential. Equation (3.10) corresponds to the regime of negligible smoothing. In turn, Eq. (3.11) corresponds to a situation where the correlation length of the disordered potential is much smaller than the other typical length scale of the problem (the healing length ξ), and thus corresponds to the white-noise limit ($\sigma_{\rm R} \to 0$ and $V_{\rm R}^2\sigma_{\rm R}^d = cst$).

Fragmented condensate (intermediate interactions) - The intermediate regime is more difficult to describe, and precise analytical predictions are difficult to make, mainly because the effects of disorder and interactions are of the same order of magnitude. In the Anderson-Lifshits regime, disorder dominates: It determines the shape of the separated islands (the Lifshits states), and the role of increasing interactions is just to populate more and more states, without significantly affecting the shape of each islands. In the connected condensate regime, the interactions dominate: There is a single island, the shape of which depends on the interaction strength, and as discussed above, the relative modulations actually decrease when the interaction strength increases. The intermediate regime interpolates between these two regimes, and it is then not possible to separate the role of disorder and interactions any longer. Then, the Bose gas separates in various fragments, the number, the shapes and the populations of each are all determined by the complex interplay of disorder and interactions. In turn, it is possible to estimate the boundaries of this regime –which we call *fragmented condensate regime*– from the breakdown of the Anderson-Lifshits description on one hand, and of the connected condensate regime on the other hand (see Sec. 3.4.2).

The above description relies on a microscopic approach, which allowed us to discriminate between the various states of the system. If we now rely on macroscopic features, we can easily

see that there are only two different phases: (i) a gapless insulator, *i.e.* a Bose glass phase (Giamarchi and Schulz, 1988; Fisher *et al.*, 1989), which corresponds to the Anderson-Lifshits and fragmented condensate regimes, and (ii) a fluid (coherent in 3D) phase, which corresponds to the connected condensate regime.

In the Anderson-Lifshits glass regime, the Bose gas forms a Fock state of localized states. It is thus an insulator. In addition, it is compressible owing to the gapless distribution of the single-particle energies ε_ν in infinite systems. The fragmented condensate regime also corresponds to an insulator, due to fragmentation into disconnected islands. It is compressible because each fragment smoothly adapts to a slight increase of the interaction strength, just like in a single condensate. Only the connected condensate regime corresponds to a superfluid phase. This picture is valid as long as the Bose gas remains in the weakly-interacting regime. For stronger interactions, it may suffer a second transition to an insulating Bose glass phase (Giamarchi and Schulz, 1988; Fisher *et al.*, 1989).

3.4.2 Quantum-state diagram

Drawing the quantum-state diagram of an interacting, disordered Bose gas is not straightforward. On one hand, the interaction strength g does not directly determine the various states. We will thus rather use the chemical potential μ. First, it can serve as a measure of the interaction strength as it is expected to be an increasing function of g. This can be easily checked from Eq. (3.7) in the Anderson-Lifshits regime, and from Eq. (3.8) in the connected condensate regime. Although, it remains to be checked, it is reasonable to assume that it is still valid in the fragmented condensate regime. Second, we will show that μ is a convenient parameter to determine the quantum state of the interacting, disordered Bose gas. On the other hand, the disorder is determined by several quantities, *i.e.* its amplitude, its correlation length, and the model under consideration (*e.g.* uncorrelated impurity potential, blue- or red-detuned speckle potentials, ...). Here we choose the amplitude V_R as a measure of the disorder strength. We will then show that it is convenient to fix the parameter $\alpha_R = \hbar^2/2m\sigma_R^2 V_R$, *i.e.* when changing the amplitude V_R, the correlation length σ_R changes accordingly. This leads to the schematic diagram of Fig. 3.4a, which we comment below. Let us fix the disordered potential and change the interaction strength (*i.e.* we travel along a horizontal line in the diagram).

Forbidden region - Depending on the model of disorder, the density of states $\mathcal{D}(\varepsilon)$ may vanish for $\varepsilon < \varepsilon_{\min}$. For instance, this occurs when the disordered potential is bounded below (*i.e.* $V(\mathbf{r}) \geq V_{\min}$), an example of which is the case of blue-detuned speckle potentials (see Box 1, page 43). Then, the chemical potential μ cannot be smaller than $\varepsilon_{\min}$. This defines a forbidden region (hatched gray in Fig. 3.4a). Scaling arguments that we do not repeat here, show that $\varepsilon_{\min} \propto V_R$ (Lugan *et al.*, 2007a). The multiplying coefficient only depends on α_R, which we have fixed in the diagram, and is negative since we assume that $\langle V \rangle = 0$. Should it exist, the forbidden region is thus bounded by a straight line with a negative slope in the diagram. If the density of states does not vanish for $\varepsilon \to -\infty$, the forbidden region simply does not exist.

Anderson-Lifshits regime - For weak interactions, the Bose gas is in the Anderson-Lifshits regime (green in Fig. 3.4a). In this regime, when the strength of interactions increases, the number of populated Lifshits states, $\mathcal{N}_{LS} = \Omega \int_{-\infty}^{\mu} d\varepsilon\, \mathcal{D}(\varepsilon)$, increase. When this number becomes too large, some Lifshits states start to overlap, so that the mutual interaction terms, $g \int d\mathbf{r}\, |\chi_{\nu_1}(\mathbf{r})|^2 |\chi_{\nu_2}(\mathbf{r})|^2$,

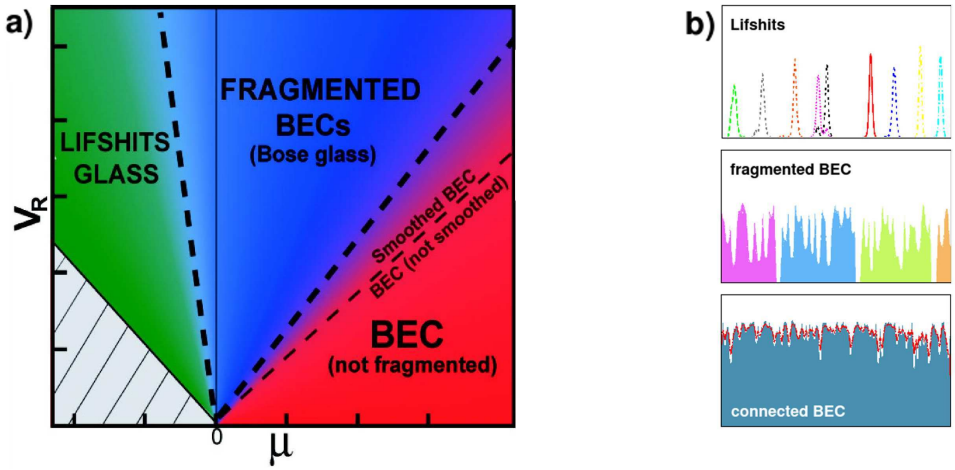

Figure 3.4 | Quantum states of a Bose gas with repulsive interactions in a disordered potential. a) Schematic quantum-state diagram. The crossovers between the various regimes are controlled by the single parameter $\alpha_R = \hbar^2/2m\sigma_R^2 V_R$ which is fixed in the figure (*i.e.* moving along the vertical axis, σ_R changes together with V_R so that the product $V_R\sigma_R^2$ does not change). The hatched part corresponds to a forbidden zone ($\mu < V_{\rm min}$). Note that the smoothed condensate regime exists only in the quantum disorder regimes, *i.e.* when $\alpha_R \gtrsim 1$ [from (Lugan *et al.* 2007a)]. **b) Representations of the quantum states in the different regimes.** From up to bottom: single-particle Lifshits states (they are strongly localized states; the interactions determine their populations without changing significantly their shapes); fragmented Bose-Einstein condensate; connected (quasi-)condensate (the blue area represents the Thomas-Fermi solution: $n_c(\mathbf{r}) = [\mu - V(\mathbf{r})]/g$ and the red line the smoothing solution, Eq. (3.3) for $\xi \simeq \sigma_R$).

cannot be neglected any longer, and the equation of state (3.7) breaks down. Although a precise typical boundary of the Anderson-Lifshits regime can strongly depend on the model of disorder, a simple upper bound is given by estimating the volume occupied by the populated Lifshits states, assuming that they do not overlap significantly, *i.e.* $\Omega \int_{-\infty}^{\mu} d\varepsilon\ \mathcal{D}(\varepsilon)P(\varepsilon)$. When this volume exceed the total volume, the populated Lifshits states have to overlap. The Bose gas then enters the fragmented condensate regime when $\int_{-\infty}^{\mu} d\varepsilon\ \mathcal{D}(\varepsilon)P(\varepsilon) \sim 1$. Again, scaling arguments discussed in (Lugan *et al.*, 2007a) show that $\mathcal{D}(\varepsilon) = (V_R\sigma_R^d)^{-1}\ \zeta_{\alpha_R}(\varepsilon/V_R)$ and $P(\varepsilon) = \sigma_R^d\ \pi_{\alpha_R}(\varepsilon/V_R)$, where the functions ζ_{α_R} and π_{α_R} depend on the parameter α_R and on the model of disorder. Then, the above large-interaction boundary of the Anderson-Lifshits regime reduces to

$$\int_{-\infty}^{\mu/V_R} du\ \zeta_{\alpha_R}(u)\pi_{\alpha_R}(u) \sim 1, \tag{3.12}$$

which again is a straight line in the diagram, the slope of which depends on α_R and the model of disorder. We remind that this estimate is in principle just an upper bound. We expect it is actually quite good for a one-dimensional blue-detuned speckle potential, because the lowest-energy Lifshits states spread over quite homogeneously (see Fig. 3.4b, upper panel).

(Quasi-)condensate regime - For large interactions, the Bose gas forms a connected condensate (red in Fig. 3.4a). In this regime, when the strength of interactions decreases, the relative modulations of the density profile increase. Then, the Bose gas separates into fragments (blue in Fig. 3.4a), when the modulations Δn_c are of the order of the average density itself, $\overline{n}_c$, *i.e.*

when $\widetilde{V}_{\rm R} \sim \mu$. The boundary between the connected and fragmented condensate regimes is fully analytical so that one can draw it easily on any diagram. According to Eqs. (3.10) and (3.11), it corresponds to

$$V_{\rm R} \sim \mu \qquad \text{for } \xi \ll \sigma_{\rm R} \tag{3.13}$$

and

$$V_{\rm R} \sim \mu^{1-d/4} E_{\rm R}^{d/4} \qquad \text{for } \xi \gg \sigma_{\rm R}. \tag{3.14}$$

For the diagram of Fig. 3.4a where the parameter $\alpha_{\rm R}$ is fixed, it can be found using Eq. (3.9) and the scaling $C(\mathbf{r}) = V_{\rm R}^2 c(\mathbf{r}/\sigma_{\rm R})$, where $c(\mathbf{u})$ is the reduced correlation function of the disorder, which only depends on the model of disorder. We then find the boundary between the two regimes:

$$\frac{V_{\rm R}}{\mu} \sqrt{\frac{1}{(2\pi)^{d/2}} \int \mathrm{d}\kappa \, \frac{\widehat{c}(\kappa)}{\left[1 + \left(\frac{V_{\rm R}}{\mu}\right) \alpha_{\rm R} |\kappa|^2\right]^2}} \quad \sim \quad 1. \tag{3.15}$$

Again, this boundary is a straight line in the diagram, the slope of which depends on $\alpha_{\rm R}$ and the model of disorder. Note that this boundary can be regarded as a classical percolation threshold for the smoothed potential $\widetilde{V}(\mathbf{r})$, the existence of which can depend on the spatial dimension and on the model of disorder.

3.4.3 Numerical and experimental investigations

In this section, we discuss some recent numerical and experimental investigations of the quantum-state diagram in the context of ultracold atoms.

Numerical results - Numerical calculations performed within the Gross-Pitaevskii approach confirm the above description, both qualitatively and quantitatively. Schulte *et al.* (2005; 2006) and Lye *et al.* (2007) studied the delocalization of a Bose gas by repulsive interactions in a one-dimensional quasi-periodic lattice. A principal lattice serves to create a deep periodic potential, so that the atomic dynamics is governed by the Bose-Hubbard Hamiltonian, *i.e.* Eq (1.3) for a single bosonic species. Then, pseudo-disorder is introduced with the help of one or two weak additional lattices, with incommensurate lattice spacings. This indeed produces a suitable pseudo-random potential in finite-size systems (Sokoloff, 1985; Damski *et al.*, 2003; Roth and Burnett, 2003). The numerical solutions of the Gross-Pitaevskii, taking into account the full polychromatic lattice, show a single strongly localized density peak in the absence of interactions. When the interaction strength grows, several peaks appear. The atoms redistribute in all, but the shape of each does not significantly change. This is consistent with the above description of the Anderson-Lifshits regime. For larger interactions, the density peaks merge, forming a single delocalized condensate, the relative density modulations of which decrease. This is consistent with the condensate regime.

In collaboration with Maciej Lewenstein, we have performed a more quantitative study. We have used a similar numerical approach but for a one-dimensional blue-detuned speckle potential. Our results confirm those obtained for quasi-periodic lattices. Moreover, we have studied the behavior of the chemical potential μ versus the strength of interactions $g\bar{n}_{\rm c}$. The results are reported on Fig. 3.5, together with analytical predictions in the Anderson-Lifshits [Eq. (3.7)] and condensate [Eq. (3.8)] regimes. A crossover between the two regimes is clearly observed. It is worth stressing that in principle the Gross-Pitaevskii approach is not sufficient to treat the problem

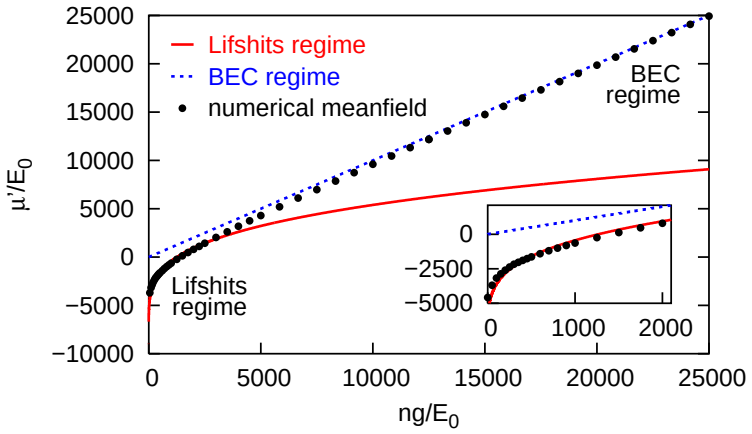

Figure 3.5 | Crossover from Lifshits to condensate regimes. Chemical potential of a 1D Bose gas in a speckle potential versus interactions. The black points are numerical solutions of the Gross-Pitaevskii equation; the solid red and dotted blue lines are the analytic predictions (3.7) and (3.8) in the Lifshits and condensate regimes. Here $E_0 = \hbar^2/2mL^2$ with L the box size [from (Lugan *et al.*, 2007a)].

because it relies on a single-orbital description where all particles a described by a single classical field $\psi(z)$ (or $n(z)$ here, since we do not consider the phase). This is expected to be wrong in the Anderson-Lifshits and fragmented condensate regimes, where the bosons occupy various orbitals. The Gross-Pitaevskii equation is however still reliable to study local variables, such as the density profile or the chemical potential, which are expected to be weakly affected by taking into account more orbitals because they are spatially separated. Conversely, this approach completely breaks down when studying non-local quantities, such as momentum distributions or correlation functions.

The behavior of the correlations in a disordered, interacting Bose gas provides further insight on the quantum-state diagram. For instance, in one dimension, it is expected that the one-body correlation function, $G(z,z') = \langle \Psi^\dagger(z)\Psi(z')\rangle$, decays algebraically in the extended quasi-condensate regime (Schwartz, 1977; Andersen *et al.*, 2002; Mora and Castin, 2003). Conversely, in the Bose glass regime, long-range correlations should be suppressed and one rather expects that $G(z,z')$ decays exponentially (Giamarchi and Schulz, 1988; Fisher *et al.*, 1989). Fontanesi *et al.* (2009; 2010) have studied the fluid-insulator transition in a one-dimensional Bose gas at zero temperature, using the Bogolyubov approach. By analyzing the behavior of the one-body correlation function, they confirmed the scaling of the boundary line between connected and fragmented condensate regimes (Lugan *et al.*, 2007a). More precisely, Fontanesi *et al.* found that the boundary corresponds to $V_R \sim \mu^\gamma$, where $\gamma \simeq 0.75 \pm 0.03$ in a regime where $\xi > \sigma_R$, and $\gamma \simeq 1$ in a regime where $\xi < \sigma_R$. These numerical results are in very good agreement with our predictions of Eqs. (3.13) and (3.14) in dimension $d = 1$.

Experiments - Experimental investigations of the effect of repulsive interactions on localization in Bose gases at equilibrium have been performed in the group of Massimo Inguscio at LENS (Deissler *et al.*, 2010). The experiment slightly differs from our analysis (Lugan *et al.*, 2007a), mainly because a bichromatic lattice is used, instead of a continuous disordered potential. First, the system is discretized owing to the strong primary lattice potential. Second, quasi-disorder is introduced by the use of a weak secondary lattice with a period, incommensurate with that of the primary lattice, thus realizing the Harper-Aubry-André model (Harper, 1955; Aubry and André, 1980). We stress that the description of the quantum-state diagram of Fig. 3.4 mainly rely on the existence of isolated, strongly-localized low-energy single-particle states. As demonstrated

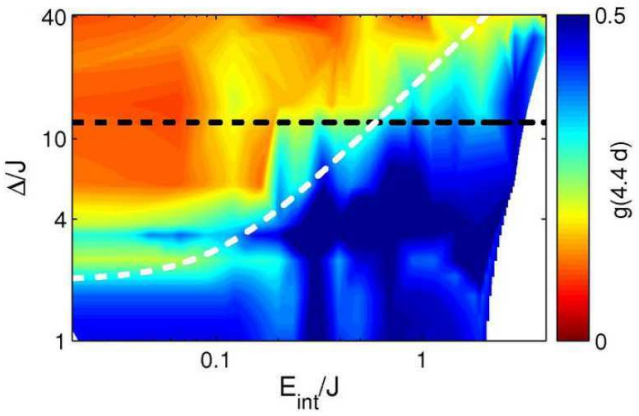

Figure 3.6 | Phase coherence of an interacting Bose gas in a one-dimensional bichromatic lattice. Shown is the expectation value of the one-body density matrix at $4.4d$ –*i.e.* the distance separating neighboring single-particle localized states– as a function of interactions ($E_{\rm int}$) and disorder (Δ). The white dashed line enlightens the crossover from strong to weak correlations and the black dashed line corresponds to $\Delta/J = 12$ [from (Deissler *et al.*, 2010)].

by Roati *et al.* (2008), the bi-chromatic lattice Bose gas does sustain such strong localization of low-energy single-particle states. Our diagram is thus also applicable to this case. The main difference compared to the above description, which holds for a truly disordered potential, is that the density of states does not display Lifshits tails in the bichromatic lattice, and the strong disorder, low-interaction state should rather be referred to as the Anderson glass.

For the parameters of the experiment by Deissler *et al.* (2010), the single-particle localized states are separated by a distance of about $\sim 4.4d$ (d is the principal lattice spacing). Then coherence or absence of coherence between adjacent localized states can be probed by measuring the expectation value of the one-body density matrix at this distance, $g(4.4d)$. In the experiment, this is done by Fourier analysis of momentum distributions obtained from time-of-flight images[7]. Measurements of the value of $g(4.4d)$ as a function of the interaction ($E_{\rm int}$) and disorder (Δ) is reproduced in Fig. 3.6. In the absence of interactions ($E_{\rm int} = 0$), Deissler *et al.* (2010) found a crossover from strong correlations for $\Delta/J \lesssim 2$ to strong correlations for $\Delta/J \gtrsim 2$. This is consistent with the expected metal-insulator transition associated to the one-dimensional Aubry-André model (Aubry and André, 1980). In the presence of repulsive interactions ($E_{\rm int} > 0$), the crossover is shifted towards larger values of the disorder strength. This is consistent with the idea that localized single-particle states merge, thus building up coherence of neighbor states, when repulsive interactions increase. Deissler *et al.* (2010) found a crossover scaling consistent with the expected $E_{\rm int} \propto \Delta$ for $\Delta \gg 2J$.

3.5 Many-body Anderson localization in interacting Bose-Einstein condensates

▷ *see papers reprinted on pages 121 and 125* .

In Secs. 3.3 and 3.4, we have discussed the ground state properties of a Bose gas at equilibrium in a disordered potential, which results from the competition between repulsive particle-particle interactions and single-particle localization. In this section, we adopt a different point of view and look for traces of *Anderson localization* at the many-body level. In other words, we no

[7]The time-of-flight expansion is performed after switching off the interactions via a Feshbach resonance technique. Its dynamics thus do not affect the measurement of momentum distributions in the lattice.

longer study localization of single particles, but rather localization of collective states, which the relevant states in interacting systems (Basko *et al.*, 2006). Let us consider a Bose gas in a weak disordered potential with repulsive binary interactions, weak-enough to be in the meanfield regime but strong-enough that the ground state is in the non-fragmented condensate regime (for any ratio ξ/σ_R, *i.e.* with or without smoothing). In this case, the ground state of the Bose gas has an extended density profile owing to the strong interactions (see Sec. 3.3). Then, collective effects emerge when, going beyond the Gross-Pitaevskii approach (Dalfovo *et al.*, 1999; Pitaevskii and Stringari, 2003), one considers the excitations of the Bose gas. The latter are strongly affected by the interactions and correspond to nearly non-interacting Bogolyubov quasiparticles, which can be regarded as bare particles surrounded by a halo representing the main contributions of the interaction terms with neighboring particles (Fetter and Walecka, 2002).

The quasiparticle spectrum is found from the Bogolyubov perturbation theory in the Popov form, which is valid for condensates as well as quasi-condensates (Bogolyubov, 1947; Bogolyubov, 1958; Popov, 1983). We write the field operator $\hat{\Psi}(\mathbf{r}) = e^{i\hat{\theta}(\mathbf{r})}\sqrt{\hat{n}(\mathbf{r})}$ with $\hat{n}(\mathbf{r}) = n_c(\mathbf{r}) + \delta\hat{n}(\mathbf{r})$ where $n_c = \langle\hat{n}\rangle$ and

$$\hat{\theta}(\mathbf{r}) = \frac{-i}{2\sqrt{n_c(\mathbf{r})}}\sum_\nu [f_\nu^+(\mathbf{r})\,\hat{b}_\nu - \text{h.c.}] \tag{3.16}$$

$$\delta\hat{n}(\mathbf{r}) = \sqrt{n_c(\mathbf{r})}\sum_\nu [f_\nu^-(\mathbf{r})\,\hat{b}_\nu + \text{h.c.}] \tag{3.17}$$

are the phase and density fluctuations operators. Then, expanding the grand-canonical, many-body Hamiltonian

$$\hat{H} = \int d\mathbf{r}\,\hat{\Psi}^\dagger(\mathbf{r})\left[-\frac{\hbar^2\nabla^2}{2m} + V(\mathbf{r}) - \mu\right]\hat{\Psi}(\mathbf{r}) + \frac{g}{2}\int d\mathbf{r}\,\hat{\Psi}^\dagger(\mathbf{r})\hat{\Psi}^\dagger(\mathbf{r})\hat{\Psi}(\mathbf{r})\hat{\Psi}(\mathbf{r}) \tag{3.18}$$

in the limit of small phase gradients ($\hbar^2|\nabla\hat{\theta}|^2/2m \ll \mu$) and small density fluctuations ($\delta\hat{n} \ll n_c$), we end up with the Bogolyubov-de Gennes equations (de Gennes, 1966):

$$\left[\frac{-\hbar^2\nabla^2}{2m} + V + \;\; gn_c - \mu\right] f_\nu^+ = \varepsilon_\nu f_\nu^- \tag{3.19}$$

$$\left[\frac{-\hbar^2\nabla^2}{2m} + V + 3gn_c - \mu\right] f_\nu^- = \varepsilon_\nu f_\nu^+ . \tag{3.20}$$

where n_c is the (quasi-)condensate background density, which is governed by the Gross-Pitaevskii equation (3.2). The behavior of the Bogolyubov quasiparticles is then determined by the shape of the amplitudes $f_\mathbf{k}^\pm(\mathbf{r})$. For instance exponential decays of their envelope in the presence of disorder would signal collective Anderson localization.

As it is well known (Pitaevskii and Stringari, 2003), in a homogeneous Bose gas ($V(\mathbf{r}) \equiv 0$), the Bogolyubov quasiparticles are plane waves of wave vector $\mathbf{k}$ with the dispersion relation $\varepsilon_\mathbf{k} = \sqrt{E_\mathbf{k}(E_\mathbf{k} + 2\mu)}$ where $E_\mathbf{k} = \hbar^2k^2/2m$ is the energy of a non-interacting particle with $k = |k|$. The spectrum thus crosses over from phonons at low momenta ($\varepsilon_\mathbf{k} \simeq \sqrt{\mu/m}\hbar k$ for $k \ll 1/\xi$) to free particles at large momenta ($\varepsilon_\mathbf{k} \simeq \mu + E_\mathbf{k}$ for $k \gg 1/\xi$). In the presence of weak disorder ($V(\mathbf{r}) \ll \mu$), several approaches can be used to solve the Bogolyubov-de Gennes equations (3.19) and (3.20). For instance, Bilas and Pavloff (2006) used the hydrodynamic and transfer matrix techniques for one-dimensional uncorrelated disorder, and Gurarie *et al.* (2008) used renormalization group

theory of the uncorrelated Bose-Hubbard model. Here, we present a more general approach, which is valid for weak, correlated disordered potentials in any dimension (Lugan *et al.*, 2007b).

Under appropriate conditions which mainly reduce to weak disorder –see (Lugan and Sanchez-Palencia, 2011) for details– the Bogolyubov-de Gennes equations can be mapped onto the following Schrödinger-like equation:

$$\frac{-\hbar^2\nabla^2}{2m}g_{\mathbf{k}}^{+} + \mathcal{V}_k(\mathbf{r})g_{\mathbf{k}}^{+} \simeq \frac{\hbar^2k^2}{2m}g_{\mathbf{k}}^{+}, \tag{3.21}$$

where the function $g_{\mathbf{k}}^{+}(\mathbf{r}) = \sqrt{\rho_k}\ f_{\mathbf{k}}^{+}(\mathbf{r}) + (1/\sqrt{\rho_k})\ f_{\mathbf{k}}^{-}(\mathbf{r})$, with $\rho_k = \sqrt{1+1/(k\xi)^2}$, is a linear combination of the Bogolyubov quasiparticle amplitudes $f_{\mathbf{k}}^{\pm}(\mathbf{r})$ and

$$\mathcal{V}_k(\mathbf{r}) = V(\mathbf{r}) - \frac{1+4(k\xi)^2}{1+2(k\xi)^2}\widetilde{V}(\mathbf{r}) \tag{3.22}$$

is a screened potential. Note that in the presence of disorder, the energy ε of a quasiparticle is well-defined quantum quantity, in contrast to k. As for the phase-formalism of bare particles (see Sec. 2.1.2), we formally define the quantity k from the dispersion relation for non-disorder quasiparticles, $\varepsilon = \sqrt{(\hbar^2k^2/2m)[(\hbar^2k^2/2m)+2\mu]}$, which has a unique solution in k.

Since Eq. (3.21) is formally equivalent to a Schrödinger equation for bare particles of wavevector $\mathbf{k}$ in a disordered potential $\mathcal{V}_k(\mathbf{r})$, one can expect Anderson localization of Bogolyubov quasiparticles and apply standard techniques to determine the localization properties of a non-interacting particle with a given energy, in any spatial dimension. It is however worth stressing that the screened disordered potential $\mathcal{V}_k(\mathbf{r})$ is a k-dependent linear combination of the bare disordered potential $V(\mathbf{r})$ and of the smoothed disordered potential $\widetilde{V}(\mathbf{r})$, which accounts for disorder-induced density modulations of the (quasi-)condensate background (see Sec. 3.3). This has important consequences and the localization properties of Bogolyubov quasiparticles turn out to significantly differ from those of non-interacting particles (Bilas and Pavloff, 2006; lugan *et al.*, 2007b; Gurarie *et al.*, 2008; Lugan and Sanchez-Palencia, 2011). While for usual disordered potentials –*i.e.* when the power spectrum is a decreasing function k–, the localization length of non-interacting particles increases with the energy $E_k = \hbar^2k^2/2m$, the localization length of Bogolyubov quasiparticles versus k (or equivalently versus ε) shows a non-monotonic behavior. For a one-dimensional disordered potential, we found a general relation between the Lyapunov exponents (inverse localization length) of a Bogolyubov quasiparticle (Γ_k) and of a bare particle (γ_k) of same k:

$$\Gamma_k = [\mathcal{S}(k\xi)]^2\ \gamma_k \tag{3.23}$$

where $\mathcal{S}(k\xi) = 2(k\xi)^2/[1+2(k\xi)^2]$ is the screening function. In the *phonon regime* (*i.e.* for $k \ll 1/\xi$), the disordered potential is strongly screened and the Lyapunov exponent of a Bogolyubov quasiparticle is much smaller than that of a bare particle with the same wavenumber ($\Gamma_k \ll \gamma_k$) and Γ_k increases with the Bogolyubov quasiparticle energy ε (*i.e.* with k). This behavior is similar to that of phonons in elastic media (Ishii, 1973). Conversely, in the *free-particle regime* (*i.e.* for $k \gg 1/\xi$), the relevant Fourier component of the disordered potential is hardly screened[8]. Then,

[8] We recall that Anderson localization in one dimension relies on back-scattering processes, which is determined by the sole Fourier component at $2k$ of the disordered potential (see Sec. 2.1.2). Now, since $\widetilde{V}(q) = \frac{V(q)}{1+(q\xi)^2}$, we see from Eq. (3.22) that $\mathcal{V}_k(2k) = V(2k) - \frac{1+4(k\xi)^2}{1+2(k\xi)^2}\frac{\widetilde{V}(2k)}{1+(2k\xi)^2} = \mathcal{S}(k\xi)V(2k)$. Therefore, in the free-particle regime ($k \gg 1/\xi$), one finds $\mathcal{V}_k(2k) \simeq V(2k)$.

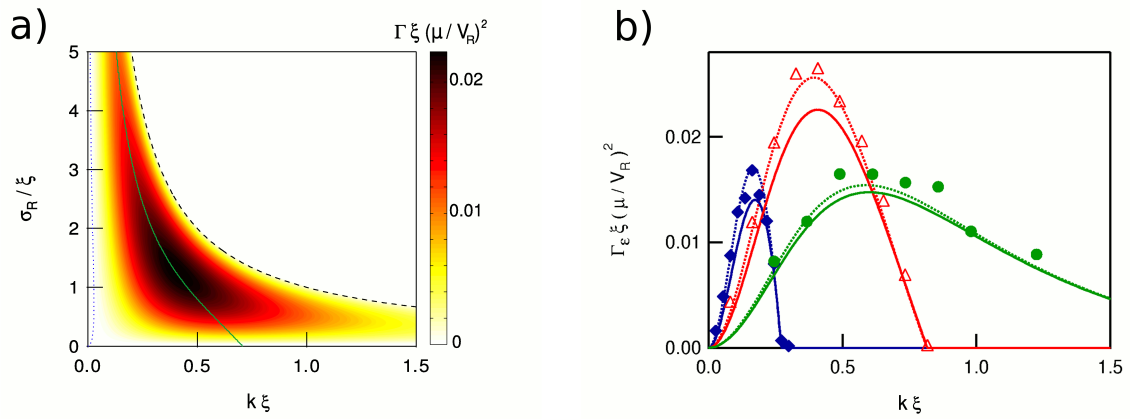

Figure 3.7 | Anderson localization of Bogolyubov quasiparticles for one-dimensional quasi-condensates in a speckle potential. a) Contour plot of the Lyapunov exponent of the Bogolyubov quasiparticles in a speckle potential, as given by Eq. (3.24). The black dashed line corresponds to the effective mobility edge, beyond which the lowest order terms of the Lyapunov exponent vanish. The green solid line represents the wave-vector of maximum localization for each ratio σ_R/ξ. **b)** Numerically-calculated Lyapunov exponents of the Bogolyubov quasiparticles in a one-dimensional speckle potential for $\sigma_R = 3.7\xi$ (blue diamonds), $\sigma_R = \sqrt{3/2}\xi$ (red open triangles), and $\sigma_R = 0.4\xi$ (green dots), and $V_R/\mu = 0.05$. The solid lines correspond to Eq. (3.24), and the dashed lines to small corrections of the order of V_R^3 [not described in this document; for details, see (Lugan and Sanchez-Palencia, 2011)].

as expected, the Lyapunov exponent of a Bogolyubov quasiparticle approximately equals that of a bare particle with the same wavenumber ($\Gamma_k \simeq \gamma_k$) which decays as a function of k.

For a one-dimensional speckle potential created by a square aperture, we find the explicit formula (Lugan *et al.*, 2007b):

$$\Gamma_k = \frac{\pi}{8}\left(\frac{V_R}{\mu}\right)^2 \frac{\sigma_R k^2(1-k\sigma_R)}{[1+2(k\xi)^2]^2}\Theta(1-k\sigma_R) \tag{3.24}$$

which is plotted in Fig. 3.7a as a function of k and the ratio σ_R/ξ. We have performed direct numerical integration of the Gross-Pitaevskii equation (3.2) and of the Bogolyubov-de Gennes equations (3.19) and (3.20), and shown evidence of exponentially decaying functions $g_{\mathbf{k}}^+$ (or equivalently of $f_{\mathbf{k}}^{\pm}(\mathbf{r})$) with localization lengths in good agreement with the analytic prediction (3.24), as shown in Fig. 3.7b.

Hence, while the (quasi-)condensate background is extended as a result of the competition between repulsive interactions and single-particle localization, the Bogolyubov quasiparticles show evidence of many-body exponential localization. This is a striking example of Anderson localization in the presence of strong interactions. A possibly useful extension of our work for experimental purposes would be to include the effect of harmonic trapping. Experimentally, Anderson localization of Bogolyubov quasiparticles has not been observed yet and it remains an important challenge to excite and detect single-mode Bogolyubov quasiparticles in the bulk of a condensate. One possibility would be to imprint a moving quasi-plane wave in a small region of the condensate and observe localization, *i.e.* suppression of transport. Another possibility would be to use Bragg spectroscopy which has been developed to measure the Bogolyubov spectrum of three-dimensional condensates (Stamper-Kurn *et al.*, 1999; Steinhauer *et al.*, 2003) and coherence lengths in elongated quasi-condensates (Richard *et al.*, 2003). Estimates using reasonable

experimental parameters indicate that the localization length of a Bogolyubov quasiparticle can be of the order of 300μm, which should be measurable using this technique.

3.6 Reprints of papers associated with the chapter

1. SANCHEZ-PALENCIA L., *Smoothing effect and delocalization of interacting Bose-Einstein condensates in random potentials*, Phys. Rev. A **74**, 053625 (2006); ▷ ***page 103***.

2. CLÉMENT D., BOUYER P., ASPECT A., and SANCHEZ-PALENCIA L., *Density modulations in an elongated Bose-Einstein condensate released from a disordered potential*, Phys. Rev. A **77**, 033631 (2008); ▷ ***page 111***.

3. LUGAN P., CLÉMENT D., BOUYER P., ASPECT A., LEWENSTEIN M., and SANCHEZ-PALENCIA L., *Ultracold Bose gases in 1D disorder: From Lifshits glass to Bose-Einstein condensate*, Phys. Rev. Lett. **98**, 170403 (2007); ▷ ***page 117***.

4. LUGAN P., CLÉMENT D., BOUYER P., ASPECT A., and SANCHEZ-PALENCIA L., *Anderson localization of Bogolyubov quasiparticles in interacting Bose-Einstein condensates*, Phys. Rev. Lett. **99**, 180402 (2007); ▷ ***page 121***.

5. LUGAN P. and SANCHEZ-PALENCIA L., *Localization of Bogoliubov quasiparticles in interacting Bose gases with correlated disorder*, Phys. Rev. A **84**, 013612 (2011); ▷ ***page 125***.

Smoothing effect and delocalization of interacting Bose-Einstein condensates in random potentials

L. Sanchez-Palencia
Laboratoire Charles Fabry de l'Institut d'Optique, CNRS and Univ. Paris-Sud XI, Campus Polytechnique, RD 128, F-91127 Palaiseau cedex, France[*]

(Received 1 September 2006; published 29 November 2006)

We theoretically investigate the physics of interacting Bose-Einstein condensates at equilibrium in a weak (possibly random) potential. We develop a perturbation approach to derive the condensate wave function for an amplitude of the potential smaller than the chemical potential of the condensate and for an arbitrary spatial variation scale of the potential. Applying this theory to disordered potentials, we find in particular that, if the healing length is smaller than the correlation length of the disorder, the condensate assumes a delocalized Thomas-Fermi profile. In the opposite situation where the correlation length is smaller than the healing length, we show that the random potential can be significantly smoothed and, in the mean-field regime, the condensate wave function can remain delocalized, even for very small correlation lengths of the disorder.

DOI: 10.1103/PhysRevA.74.053625 PACS number(s): 03.75.Hh, 79.60.Ht

I. INTRODUCTION

Ultracold atomic gases are currently attracting a lot of attention from both experimental and theoretical viewpoints. Taking advantage of the recent progress in cooling and trapping of neutral atoms [1], dilute atomic Bose-Einstein condensates (BEC's) [2] and degenerate Fermi gases (DFG's) [3–6] are now routinely produced at the laboratory. Using various techniques, space-dependent potentials can be designed almost on demand in these systems. For example, one can produce periodic [7,8], quasiperiodic [9–11], or random potentials [12–17] by using optical means. For these reasons and due to unique control and analysis possibilities, ultracold gases constitute a favorite playground for revisiting standard problems of condensed matter (CM) physics [18–21].

Most current experiments with BEC's lie in the mean-field regime where the Bose gas is described by a single wave function ψ governed by the (nonlinear) Gross-Pitaevskii equation [22]. Due to the interplay between the kinetic energy term and the interaction term, it is usually difficult to derive an exact solution of this equation. The importance of interactions can be characterized by the *healing length* ξ, which defines the typical distance below which the spatial variations of ψ significantly contribute to the energy of the BEC via the kinetic energy term [22]. In the Thomas-Fermi (TF) regime—i.e., when ξ is significantly smaller than the typical variation scale σ_R of the potential $V(\mathbf{r})$ to which the BEC is subjected—the kinetic term is negligible and the BEC density simply follows the spatial variations of the potential:[1]

$$|\psi(\mathbf{r})|^2 \propto \mu - V(\mathbf{r}). \tag{1}$$

In the opposite situation ($\xi > \sigma_R$), the kinetic term should be taken into account and the exact BEC wave function usually cannot be found analytically.

Besides a general interest, the question of determining the BEC wave function for an arbitrary ratio σ_R/ξ has direct applications to the case where $V(\mathbf{r})$ is a random potential. The physics of quantum systems in the presence of disorder is central in CM [23–25], owing to unavoidable defects in "real-life systems." One of the major paradigms of disordered quantum systems is due to Anderson who has shown that the eigenstates of single-quantum particles in arbitrary weak random potentials can be localized; i.e., ψ shows an exponential decay at large distances[2] [26]. Recent experiments have studied the onset of strong or weak localization effects of light waves [27,28] and microwaves [29,30]. Ultracold matter waves are also widely considered as promising candidates to investigate Anderson localization in random [31–33] or quasirandom structures [10,31,34] and more generally to investigate the effects of disorder in various quantum systems (for a recent review, see Ref. [35] and references therein). It is expected that the dramatic versatility of ultracold gases would allow for a direct comparison with theoretical studies of quantum-disordered systems.

A key peculiarity of BEC's is that interactions usually cannot be neglected and interaction-induced delocalization can compete with disorder-induced localization effects [15–17]. Generally, the interplay between the kinetic energy, the interactions, and the disorder is still a open question that has motivated many works [36–40]. It is clear from Eq. (1) that, in the TF regime ($\sigma_R \gg \xi$), where the interaction forces the wave function to adapt to the random potential, a BEC will not localize. Indeed, if $V(\mathbf{r})$ is a *homogeneous* random

[*]URL: http://www.atomoptic.fr

[1]This is standard in the case of a harmonic confinement, $V(\mathbf{r}) = m\omega^2\mathbf{r}^2/2$. Although there is no intrinsic typical variation scale, one can define σ_R as $m\omega^2\sigma_R^2/2 = \mu$—i.e., $\sigma_R = L_{TF}$—the usual TF half size of the condensate and the validity of the TF regime reads $\xi \ll L_{TF}$. For periodic, quasiperiodic, or random potentials, σ_R is the spatial period or the correlation length (see Sec. III for details).

[2]In one-dimensional (1D) and 2D systems, all eigenstates are usually localized, while in 3D, they are localized below the so-called *mobility edge*.

function[3] [41], so is the BEC wave function ψ, which, therefore, cannot decay at large distances. This has been confirmed in recent experiments [15–17]. The question thus arises as to understand whether, as a naive transcription of the Ioffe-Regel criterion [42] would suggest, localization can happen when $\sigma_R < \xi$.

In this paper, we show that this criterion is actually not sufficient for BEC's at equilibrium if the interactions are non-negligible (i.e., if $\xi \ll L$, where L is the size of the system). We indeed show that interaction-induced delocalization still overcomes localization effects even when $\xi \gg \sigma_R$. In fact, due to the *smoothing* of the random potential [43], the effect of disorder turns out to be reduced when ξ/σ_R increases.

In the following, we develop a general formalism based on perturbation theory (see Sec. II) to determine the BEC wave function in any given weak potential $V(\mathbf{r})$ for an arbitrary ratio σ_R/ξ. We find that the BEC density $|\psi|^2$ is still given by Eq. (1), except that the potential $V(\mathbf{r})$ has to be replaced by a *smoothed potential* $\tilde{V}(\mathbf{r})$. We derive an exact formula for the smoothed potential up to first order in the perturbation series. We then apply our results to the case where $V(\mathbf{r})$ is a 1D homogeneous random potential (see Sec. III) and derive the statistical properties of the smoothed random potential $\tilde{V}(\mathbf{r})$. From this, we conclude that an interacting BEC remains delocalized, even for $\xi \gg \sigma_R$ (if $\xi \ll L$).

II. SMOOTHING EFFECT IN INTERACTING BOSE-EINSTEIN CONDENSATES

Consider a low-temperature Bose gas in d dimensions with contact atom-atom interactions, $g_{dD}\delta^{(d)}(\mathbf{r})$, where g_{dD} is the d-dimensional interaction parameter. In 3D geometries, $g_{3D}=4\pi\hbar^2 a_{sc}/m$, where a_{sc} is the scattering length [22] and m is the atomic mass. Low-dimensional geometries (1D or 2D) can be realized in ultracold atomic samples using a tight radial confinement, so that the radial wave function is frozen to zero-point oscillations in the form $\varphi_\perp^0(\mathbf{r}_\perp)$, where $\mathbf{r}_\perp$ is the radial coordinate vector. In this case, $g_{dD}=g_{3D}\int d\mathbf{r}_\perp |\varphi_\perp^0(\mathbf{r}_\perp)|^4$. For instance, one finds $g_{1D}=2\hbar\omega_\perp a_{sc}$, for a 2D harmonic radial confinement of frequency $\omega_\perp$. In addition, the Bose gas is assumed to be subjected to a given potential $V(\mathbf{r})$, with a typical amplitude V_R and a typical variation scale σ_R. Possibly, the potential $V(\mathbf{r})$ may have various length scales. In this case, we assume that σ_R is the smallest. Assuming weak interactions—i.e., $\bar{n}^{2/d-1} \gg m g_{dD}/\hbar^2$, where $\bar{n}$ the mean density [44,45]—we treat the BEC in the mean-field approach [22] and we use the Gross-Pitaevskii equation (GPE)

$$\mu\psi(\mathbf{r}) = \left[\frac{-\hbar^2\nabla^2}{2m} + V(\mathbf{r}) + g_{dD}|\psi(\mathbf{r})|^2\right]\psi(\mathbf{r}), \tag{2}$$

where μ is the BEC chemical potential and where the wave function ψ is normalized to the total number of condensed atoms, $\int d\mathbf{r}|\psi(\mathbf{r})|^2 = N$. Note that ψ minimizes the N-body energy functional so that ψ is necessary a real function (up to a nonphysical uniform phase). In 1D and 2D geometries and in the absence of trapping, no true BEC can exist due to significant long-wavelength phase fluctuations [46]. In this case, no macroscopic wave function ψ can be defined. However, because density fluctuations are strongly suppressed in the presence of interactions, the Bose gas forms a *quasicondensate* [46] and the density n can be treated as a classical field. It turns out that $\sqrt{n}$ is governed by Eq. (2). Therefore, even though we only refer to BEC wave functions in the following, our formalism also applies to quasicondensates, after replacing ψ by $\sqrt{n}$.

A. Thomas-Fermi regime

In the simplest situation, the healing length of the BEC is much smaller than the typical length scale of the potential ($\xi \ll \sigma_R$). Therefore, the kinetic energy term in the GPE (2) is small and the BEC density $|\psi|^2$ simply follows the spatial modulations of the potential:

$$|\psi(\mathbf{r})|^2 = [\mu - V(\mathbf{r})]/g_{dD} \quad \text{for } \mu > V(\mathbf{r}),$$
$$|\psi(\mathbf{r})|^2 = 0 \quad \text{otherwise}. \tag{3}$$

This corresponds to the TF regime. Note that for $V_R \ll \mu$, one has

$$\psi(z) \simeq \psi_0 - \frac{V(\mathbf{r})\psi_0}{2\mu}, \tag{4}$$

with $\psi_0 = \sqrt{\mu/g_{dD}}$ being the BEC wave function at $V(\mathbf{r})=0$. Therefore, the BEC wave function itself follows the modulations of the potential $V(\mathbf{r})$.

B. Beyond the Thomas-Fermi regime: The smoothing effect

The situation changes when the healing length is of the order of, or larger than, the typical length scale of the potential ($\xi > \sigma_R$). Indeed, the kinetic contribution limits the smallest variation length of the spatial modulations of a BEC wave function to a finite value of the order of the healing length [22]. Therefore, the BEC can only follow modulations of the potential on a length scale typically larger than ξ and Eq. (3) no longer holds.

For a weak amplitude of the potential,[4] we can use perturbation theory techniques. We thus write the BEC wave function as $\psi(\mathbf{r}) = \psi_0 + \delta\psi(\mathbf{r})$ where we assume that $\delta\psi \ll \psi_0$ and ψ_0 is the zeroth-order solution of the GPE (2):

$$\mu\psi_0 = -\frac{\hbar^2}{2m}\nabla^2\psi_0 + g_{dD}\psi_0^3. \tag{5}$$

Since the BEC is homogeneous at zero order, one has $\psi_0 = \sqrt{\mu/g_{dD}}$. Then, the first order term of the perturbation series is given by

$$-\frac{\hbar^2}{2m}\nabla^2(\delta\psi) - [\mu - 3g_{dD}\psi_0^2]\delta\psi = -V(\mathbf{r})\psi_0. \tag{6}$$

[3] In this context, the term "homogeneous" means that all local statistical properties of the random potential are independent of the position.

[4] A precise condition for the validity of the perturbative approach will be given later [see Eq. (16)].

Since $\mu - 3g_{dD}\psi_0^2 = -2\mu$, we are left with the equation

$$-\frac{\xi^2}{2}\nabla^2(\delta\psi) + \delta\psi = -\frac{V(\mathbf{r})\psi_0}{2\mu}, \tag{7}$$

where $\xi = \hbar/\sqrt{2m\mu}$ is the healing length of the BEC. We straightforwardly find the solution of Eq. (7), which reads

$$\delta\psi(\mathbf{r}) = -\int d\mathbf{r}' G(\mathbf{r}-\mathbf{r}')\frac{V(\mathbf{r}')\psi_0}{2\mu}, \tag{8}$$

where $G(\mathbf{r})$ is the Green function of Eq. (7), defined as the solution of

$$\left[-\frac{\xi^2}{2}\nabla^2 + 1\right]G(\mathbf{r}) = \delta^{(d)}(\mathbf{r}) \tag{9}$$

or, equivalently, in Fourier space

$$\left[\frac{\xi^2}{2}|\mathbf{k}|^2 + 1\right]\hat{G}(\mathbf{k}) = 1/(2\pi)^{d/2}, \tag{10}$$

where $\hat{G}(\mathbf{k}) = \frac{1}{(2\pi)^{d/2}}\int d\mathbf{r} G(\mathbf{r}) e^{-i\mathbf{k}\cdot\mathbf{r}}$ is the Fourier transform of G. In contrast to the case of single particles, the Green function $\hat{G}(\mathbf{k})$ has no singularity point so that the perturbative approach can be safely applied for any wave vector $\mathbf{k}$.

The explicit formula for the Green function G depends on the dimension of the system. After some simple algebra, we find

$$\text{in 1D,} \quad G(z) = \frac{1}{\sqrt{2}\xi}\exp\left(-\frac{|z|}{\xi/\sqrt{2}}\right), \tag{11}$$

$$\text{in 2D,} \quad G(\rho) = \frac{1}{\pi\xi^2}K_0\left(+\frac{|\rho|}{\xi/\sqrt{2}}\right), \tag{12}$$

$$\text{in 3D,} \quad G(\mathbf{r}) = \frac{1}{2\pi\xi^2|\mathbf{r}|}\exp\left(-\frac{|\mathbf{r}|}{\xi/\sqrt{2}}\right), \tag{13}$$

where K_0 is the modified Bessel function. Finally, up to first order in the perturbation series, the BEC wave function reads

$$\psi(\mathbf{r}) \simeq \psi_0 - \frac{\tilde{V}(\mathbf{r})\psi_0}{2\mu}, \tag{14}$$

with

$$\tilde{V}(\mathbf{r}) = \int d\mathbf{r}' G(\mathbf{r}')V(\mathbf{r}-\mathbf{r}'). \tag{15}$$

Interestingly enough, the Green function in any dimension shows a exponential decay, with a typical attenuation length, ξ, and is normalized to unity,[5] $\int d\mathbf{r} G(\mathbf{r}) = 1$. Therefore, $G(\mathbf{r})$ can be seen as a *smoothing function* with a typical width ξ. Indeed, it should be noted that Eq. (14) is similar to Eq. (4), except that the potential $V(\mathbf{r})$, which is relevant in the case $\xi \ll \sigma_R$, changes to the potential $\tilde{V}(\mathbf{r})$ for $\xi > \sigma_R$. The potential $\tilde{V}(\mathbf{r})$ is a convolution of $V(\mathbf{r})$ with a function which has a typical width ξ and thus corresponds to a *smoothed potential* with an amplitude smaller than V_R. In addition, if σ_R corresponds to the width of the correlation function of a random potential V, the correlation length of the smoothed random potential $\tilde{V}$ is of the order of $\max(\sigma_R, \xi)$ [for details, see Sec. III].[6]

Note that, for $\xi \ll \sigma_R$, $G(\mathbf{r})$ can be approximated by $\delta^{(d)}(\mathbf{r})$ in Eq. (15) and $\tilde{V}(\mathbf{r}) \simeq V(\mathbf{r})$. We thus recover the results of Sec. II A, valid for the TF regime.

The validity condition of the perturbation approach directly follows from Eq. (14):

$$\tilde{V}(\mathbf{r}) \ll \mu. \tag{16}$$

Note that if $\xi \gg \sigma_R$, the potential can be significantly smoothed so that the above condition can be less restrictive than the *a priori condition* $V(\mathbf{r}) \ll \mu$.

The results of this section show that the potential $V(\mathbf{r})$ can be significantly smoothed in interacting BEC's. We stress that this applies to any kind of potentials provided that $\xi \ll L$ and $\tilde{V}(\mathbf{r}) \ll \mu$. In the next section, we present an illustration of the smoothing effect in the case of a random potential.

III. APPLICATION TO A TRAPPED INTERACTING BOSE-EINSTEIN CONDENSATE IN A 1D RANDOM POTENTIAL

A. Trapped 1D Bose-Einstein condensate in a random potential

In this section, we consider a 1D Bose gas subjected to a weak homogeneous random potential $V(z)$, with a vanishing average value ($\langle V \rangle = 0$), a standard deviation V_R, and a spatial correlation length σ_R, significantly smaller than the size of the system. In addition, we assume that the gas is trapped in a confining harmonic trap,[7] $V_h(z) = m\omega^2 z^2/2$, as in almost all current experiments on disordered BEC's [14–17]. We consider a situation such that $\hbar\omega \ll n g_{1D} \ll \hbar^2 n^2/m$—i.e., the Bose gas lies in the mean-field regime—and in the absence of disorder, the interactions dominate over the kinetic energy.[8] The situation mimics the experimental conditions of Ref. [15,17]. The presence of the harmonic confinement introduces a low-momentum cutoff for the phase fluctuations

[5] This property follows directly from the definition (10) of the Green function. Indeed, $\int d\mathbf{r} G(\mathbf{r}) = (2\pi)^{d/2}\hat{G}(\mathbf{k}=0) = 1$.

[6] In contrast, for example in the case of a deterministic periodic potential $V(z) = V_R\cos(kz)$, the variation scale $\sigma_R = 2\pi/k$ corresponds to the period of the potential, and we find $\tilde{V}(z) = \frac{V_R\cos(kz)}{1+k^2\xi^2}$. The potential is indeed smoothed as the amplitude of $\tilde{V}$ is smaller than that of V. Nevertheless, the period of the smoothed potential $\tilde{V}$ is the same as that of the bare potential V.

[7] All results also apply if there is no trapping. In this case, all zeroth-order terms simply do not depend on z.

[8] This corresponds to the usual TF regime for confined BEC's in the absence of disorder [22]. However, no restriction is imposed for the ratio σ_R/ξ, so that the BEC can be out of the TF regime as defined in Sec. I.

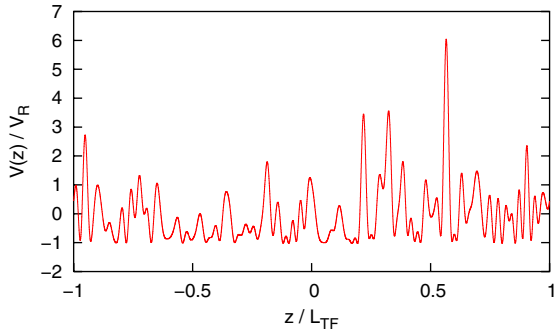

FIG. 1. (Color online) Example of the realization of a speckle random potential with $\sigma_R \simeq 10^{-2} L_{TF}$.

so that the 1D Bose gas forms a true condensate at low temperatures [44,45]. In this case, the BEC wave function is

$$\psi_0 = \sqrt{\mu_0(z)/g_{1D}}, \tag{17}$$

where $\mu_0(z)=\mu-m\omega^2 z^2/2$ is the local chemical potential. This corresponds to an inverted parabolic density profile with a half-size $L_{TF}=\sqrt{2\mu/m\omega^2}$, where the chemical potential is $\mu=\mu_{TF}=\frac{\hbar\omega}{2}\left(\frac{3Nmg_{1D}l}{2\hbar^2}\right)^{2/3}$, with $l=\sqrt{\hbar/m\omega}$ being the extension of the ground state of the harmonic oscillator.

As $L_{TF} \gg (\xi, \sigma_R)$, it is legitimate to use the local density approximation (LDA) [22]; i.e., in a region significantly smaller than L_{TF}, the quantities ψ_0 and μ_0 can be considered as uniform. We can thus directly apply the results of Sec. II B. From Eqs. (14)–(17), we immediately find that

$$n(z) \simeq n_0(z) - \frac{\tilde{V}(z)}{g_{1D}}, \tag{18}$$

where

$$\tilde{V}(z) = \int dz' \frac{\exp\left(\frac{-|z'|}{\xi_0(z)/\sqrt{2}}\right)}{\sqrt{2}\xi_0(z)} V(z-z') \tag{19}$$

is the smoothed potential, with $\xi_0(z)=\hbar/\sqrt{2m\mu_0(z)}$ being the local healing length. The density profile of the BEC is thus expected to follow the modulations of a *smoothed random potential*.

Note that the total number of condensed atoms is $N=\int dz|\sqrt{n_0(z)}+\delta\psi|^2 \simeq \int dz[n_0(z)-\tilde{V}(z)/g_{1D}]$ up to first order in $\tilde{V}/\mu$. Since $\langle\tilde{V}\rangle=0$, one has $\langle N\rangle \simeq \int dz n_0(z)$, owing to the assumed self-averaging property of the potential [41]. In addition, we have $\mu=\mu_{TF}$.

We now compare our predictions to the exact solutions of the GPE (2) as obtained numerically. For the sake of concreteness, we consider a speckle random potential [47] similar to the one used in recent experiments [14–17] (see Fig. 1). Briefly, a speckle pattern consists in a random intensity distribution and is characterized by its statistical properties. First, the single-point amplitude distribution is a negative exponential

$$\mathcal{P}[V(z)] = \frac{\exp\{-[V(z)+V_R]/V_R\}}{|V_R|} \quad \text{if } \frac{V(z)}{V_R} \geqslant -1,$$

$$\mathcal{P}[V(z)] = 0 \quad \text{otherwise}, \tag{20}$$

corresponding to the average value $\langle V\rangle=0$ and the standard deviation $\Delta V=\sqrt{\langle[V(z)-\langle V\rangle]^2\rangle}=|V_R|$. Second, the spatial correlations are characterized by the autocorrelation function $C(\Delta z)=\langle V(\Delta z)V(0)\rangle$, the correlation length of which is denoted σ_R and can be chosen at will [17,47]. For the numerical calculations, we numerically generate a 1D speckle pattern using a method similar to the one described in Ref. [48] in 1D and corresponding to the correlation function

$$C(\Delta z) = V_R^2 |\mathrm{sinc}(\sqrt{3}\Delta z/\sqrt{2}\sigma_R)|^2, \tag{21}$$

where $\mathrm{sinc}(x)=\sin(x)/x$. For the sake of simplicity, it is useful to approximate $C(\Delta z)$ to a Gaussian function (see, for example, Sec. III B). Up to second order in $\Delta z/\sigma_R$, we have $C(\Delta z) \simeq V_R^2 \exp(-\Delta z^2/2\sigma_R^2)$.

Numerical solutions of the GPE (2) are presented in Fig. 2 for two values of the ratio σ_R/ξ, where ξ is the BEC healing length at the trap center. In the first case [Fig. 2(a)], we have $\xi \ll \sigma_R$ and the density simply follows the modulations of the bare random potential, according to Eq. (3). In the second case [Fig. 2(b)], we have $\xi > \sigma_R$, and as expected, the BEC wave function does not follow the modulations of the bare random potential $V(z)$ but actually follows smoother modulations of the smoothed potential $\tilde{V}(z)$. Figure 2(b) (and the inset) shows that the numerically computed density can hardly be distinguished from Eq. (18). This supports the validity of our approach.

B. Statistical properties of the smoothed random potential

It is useful to compute the statistical properties of the smoothed random potential $\tilde{V}(z)$ as they will be imprinted on the BEC density profile according to Eq. (18). From Eq. (15), we immediately find that (i) $\tilde{V}(z)$ is a random *homogeneous* potential, (ii) the average value of $\tilde{V}$ vanishes,

$$\langle\tilde{V}\rangle = \langle V\rangle = 0, \tag{22}$$

and (iii) the correlation function of $\tilde{V}$ is given by

$$\tilde{C}_z(\Delta z) = \int du\, dv\, C[\Delta z + (v-u)] G_z(u) G_{z+\Delta z}(v), \tag{23}$$

where $C(\Delta z)=\langle V(\Delta z)V(0)\rangle$ is the correlation function of the bare potential V and $G_z(u)$ is given by Eq. (11) with ξ replaced by $\xi_0(z)$. In the following, we assume that $\Delta z \ll L_{TF}$ so that $G_z \simeq G_{z+\Delta z}$ and we omit the subscripts. Assuming for simplicity a Gaussian correlation function for the bare random potential, $C(\Delta z) \simeq V_R^2 \exp(-\Delta z^2/2\sigma_R^2)$, we find after some algebra

$$\tilde{C}(\Delta z) = V_R^2 \Sigma\left(\frac{\sigma_R}{\xi_0}, \frac{\Delta z}{\xi_0}\right), \tag{24}$$

with

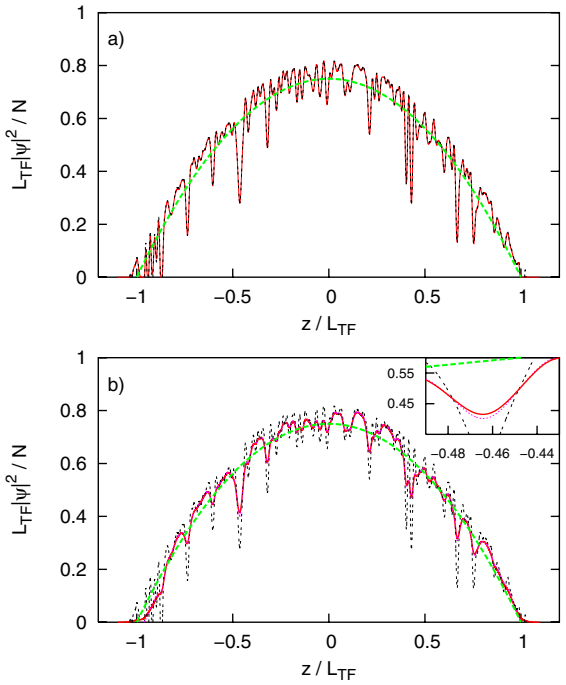

FIG. 2. (Color online) Density profiles of a BEC confined in a combined harmonic plus random potential ($V_R=0.1\mu$, $\sigma_R=7.5\times10^{-3}\,L_{TF}$). The solid (red online) line corresponds to the numerically computed BEC wave function, the dashed (green online) line is the TF profile in the absence of disorder, and the black dotted line is a plot of the disordered TF profile [Eq. (3)]. (a) Case where the healing length at the trap center, ξ, is smaller than the correlation length of the random potential: $\sigma_R/\xi\simeq10$. In this case, the density profile follows the modulations of the random potential according to Eq. (3). (b) Opposite situation: $\sigma_R/\xi\simeq0.5$. In this case, the BEC density profile, obtained numerically, significantly differs from Eq. (3), but can hardly be distinguished from Eq. (18) [also plotted in Fig. 2(b) as a dotted (purple online) line]. The inset shows a magnification of the plot in a very small region of the BEC.

$$\Sigma(\bar{\sigma}_R,\overline{\Delta z}) = \bar{\sigma}_R^2 \exp\left(-\frac{\overline{\Delta z}^2}{2\bar{\sigma}_R^2}\right) + \frac{\sqrt{\pi}}{4}\bar{\sigma}_R(1-2\bar{\sigma}_R^2 - \sqrt{2\overline{\Delta z}})\exp(\bar{\sigma}_R^2 + \sqrt{2\overline{\Delta z}})\mathrm{erfc}\left(\frac{2\bar{\sigma}_R^2+\sqrt{2\overline{\Delta z}}}{2\bar{\sigma}_R}\right) + \frac{\sqrt{\pi}}{4}\bar{\sigma}_R(1-2\bar{\sigma}_R^2+\sqrt{2\overline{\Delta z}})\exp(\bar{\sigma}_R^2 - \sqrt{2\overline{\Delta z}})\mathrm{erfc}\left(\frac{2\bar{\sigma}_R^2-\sqrt{2\overline{\Delta z}}}{2\bar{\sigma}_R}\right), \quad (25)$$

where $\bar{\sigma}_R=\sigma_R/\xi_0$, $\overline{\Delta z}=\Delta z/\xi_0$, and $\mathrm{erfc}(x)=\frac{2}{\sqrt{\pi}}\int_x^\infty dt e^{-t^2}$ is the complementary error function. The correlation function $\Sigma\left(\frac{\sigma_R}{\xi_0},\frac{\Delta z}{\xi_0}\right)$ is plotted in Fig. 3.

This function Σ clearly decreases with σ_R/ξ_0, indicating the onset of an increasing smoothing effect. At $\Delta z=0$, we have a simple asymptotic expression for $\sigma_R\gg\xi_0$:

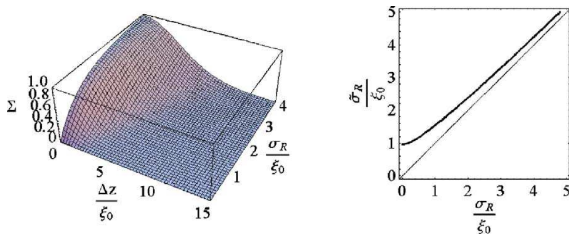

FIG. 3. (Color online) Left: plot of the correlation function $\Sigma\left(\frac{\sigma_R}{\xi_0},\frac{\Delta z}{\xi_0}\right)$. Right: width at $1/\sqrt{e}$ of the normalized correlation function $\Sigma\left(\frac{\sigma_R}{\xi_0},\frac{\Delta z}{\xi_0}\right)\Big/\Sigma\left(\frac{\sigma_R}{\xi_0},0\right)$.

$$\Sigma(\sigma_R/\xi_0,0) \simeq 1-\left(\frac{\xi_0}{\sigma_R}\right)^2, \quad \sigma_R \gg \xi_0. \quad (26)$$

So, as expected, $\Sigma(\sigma_R/\xi_0,0)\to1$ as $\sigma_R/\xi_0\to\infty$; i.e., the random potential is hardly smoothed. For $\sigma_R\ll\xi_0$,

$$\Sigma(\sigma_R/\xi_0,0) \simeq \frac{\sqrt{\pi}}{2}\frac{\sigma_R}{\xi_0}, \quad \sigma_R \ll \xi_0. \quad (27)$$

So $\Sigma(\sigma_R/\xi_0,0)\to0$ as $\sigma_R/\xi_0\to0$; i.e., the amplitude of the smoothed random potential is significantly reduced compared to the amplitude of the bare random potential. Generally speaking, from Eq. (24), we have $\langle\tilde{V}^2\rangle=\tilde{C}(0)=V_R^2\Sigma(\sigma_R/\xi_0,0)$. It follows that $\langle\tilde{V}^2\rangle$ is an increasing function of σ_R/ξ_0 and that $\langle\tilde{V}^2\rangle\ll V_R^2$. This is consistent with the idea of a *smoothing* of the random potential.

In addition, the correlation length $\tilde{\sigma}_R$ of the smoothed random potential $\tilde{V}$ is given by the width at $1/\sqrt{e}$ of the function $\Delta z\to\Sigma(\bar{\sigma}_R/\xi_0,\Delta z/\xi_0)$. At $\sigma_R\gg\xi_0$, the smoothing is weak and $\tilde{\sigma}_R\simeq\sigma_R$. For $\sigma_R<\xi_0$, the smoothing is significant, so that $\tilde{\sigma}_R$ saturates at $\tilde{\sigma}_R\simeq\xi_0$, as expected. Roughly speaking, we have $\tilde{\sigma}_R\sim\max(\sigma_R,\xi_0)$ (see Fig. 3).

C. Effect of disorder in interacting Bose-Einstein condensates

We finally discuss the properties of the BEC wave function in the presence of disorder. It follows from Eq. (18) that the BEC density follows the modulations of a random potential $\tilde{V}$. In the TF regime ($\xi\ll\sigma_R$), $\tilde{V}\simeq V$, while when $\xi>\sigma_R$, $\tilde{V}$ is smoothed. Since $\tilde{V}$ is a homogeneous random potential, there is no decay of the wave function. In particular, Anderson localization does not occur, even for $\xi\gg\sigma_R$. In the case when $\xi>\sigma_R$, it turns out that the BEC density is actually less affected by the random potential than in the TF regime ($\xi\ll\sigma_R$). This is in striking contrast with the case of noninteracting particles where localization effects are usually stronger at low energy [41].

More quantitatively, using the statistical properties of the smoothed random potential $\tilde{V}$, one can easily compute the fluctuations $\Delta n(z)=\sqrt{\langle[n(z)-n_0(z)]^2\rangle}$ of the BEC density around the average value $n_0(z)=[\mu-m\omega^2z^2/2]/g_{1D}$. From Eq. (18), we find $\Delta n^2\simeq\tilde{C}(0)/g_{1D}^2$. Note that Δn^2 depends on the displacement from the trap center through the dependence of ξ_0 on z. At the trap center, we find

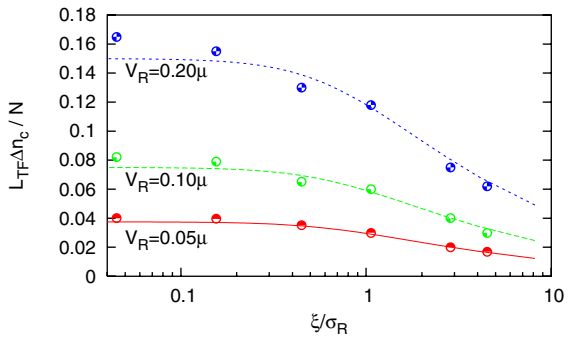

FIG. 4. (Color online) Amplitude of the fluctuations of the BEC density at the trap center, Δn_c, in the combined harmonic plus random potential as a function of the ratio of the healing length to the correlation length of the disorder for several amplitudes of the random potential. The dots correspond to exact numerical results in the Gross-Pitaevskii approach [Eq. (2)], and the lines show the theoretical prediction [Eq. (28)].

$$\Delta n_c = \frac{V_R}{g_{1D}} \sqrt{\Sigma(\sigma_R/\xi, 0)}. \tag{28}$$

We recall that $\xi = \xi_0(0) = \hbar/\sqrt{2m\mu}$ is the BEC healing length in the trap center.

We have numerically extracted the fluctuations of the density in the trap center, according to the formula $\Delta n_c \simeq \sqrt{\frac{1}{L_{TF}/2}\int_{-L_{TF}/4}^{+L_{TF}/4} dz[n(z)-n_0(z)]^2}$. This provides a good estimate of Δn_c as $\xi_0(z)$ changes by less than 3% in the range $[-L_{TF}/4, +L_{TF}/4]$. As shown in Fig. 4, the numerical results perfectly agree with Eq. (28) over a large range of the ratio ξ/σ_R. The numerical calculations are performed for the speckle potential described in Sec. III B and no fitting parameter has been used. In addition, note that we have used a single realization of the random potential for each point in Fig. 4. Averaging over disorder turned out to have little importance, since the random potential is almost self-averaging in the range $[-L_{TF}/4, +L_{TF}/4]$, if $\sigma_R \ll L_{TF}$.

Finally, we find from Eq. (16) that the perturbative approach that we have performed is valid whenever $\Delta n \ll n_0$—i.e., whenever

$$V_R \sqrt{\Sigma(\sigma_R/\xi_0, 0)} \ll \mu. \tag{29}$$

Note that this effect is more restrictive in the trap center where ξ_0 is minimum.

IV. CONCLUSION

In summary, we have presented an analytical technique, based on the perturbation theory, to compute the static wave function of an interacting BEC subjected to a weak potential. This applies to the case where both the healing length of the BEC (ξ) and the spatial scale of the potential (σ_R) are much smaller than the size of the system (L), but without restriction for the ratio ξ/σ_R. In particular, we have shown that when the healing length is larger than the space scale of the potential, the BEC is sensitive to a *smoothed potential* which can be determined within our framework.

Applying these results to the case of a 1D random potential, we have shown that the wave function of a static interacting BEC is delocalized, similarly as in the TF regime [15]. This is confirmed by numerical calculations. The results of this analysis show that, for an interacting BEC at equilibrium, the larger the healing length, the smaller the perturbation induced by the disorder. It is worth noting that the conclusions of the present work hold for *static* BEC's in the *mean-field regime* and when the interaction energy dominates over the kinetic energy in the absence of disorder—i.e., when the healing length is significantly smaller than the BEC half size ($\xi \ll L$). Going beyond the mean-field regime, it is interesting to study the interplay of interactions, disorder, and kinetic energy in a Bose gas for interactions ranging from zero (where localization is expected) to the TF regime (where the BEC is delocalized as shown in this work). This question is addressed in Ref. [49].

Finally, we note that the transport properties of a BEC can show significantly different physics. For instance, localization has been studied in matter-wave beams [33] and in the expansion of an interacting BEC [15–17]. In the latter two cases, localization indeed does occur although non-negligible interactions can modify the usual picture of localization [15,17,33].

ACKNOWLEDGMENTS

We are indebted to G. Shlyapnikov, A. Aspect, M. Lewenstein, D. Gangardt, and P. Bouyer for many stimulating discussions. We thank D. Clément and P. Lugan for discussions and useful comments on the manuscript. This work was supported by the Centre National de la Recherche Scientifique (CNRS), the Délégation Générale de l'Armement, the Agence Nationale de la Recherche (Contract No. NTOR-4-42586), the European Union (Grant Nos. IST-2001-38863 and MRTN-CT-2003-505032), and INTAS (Contract No. 211-855). The Atom Optics group at LCFIO is a member of the Institut Francilien de Recherche sur les Atomes Froids (IFRAF).

[1] S. Chu, Rev. Mod. Phys. **70**, 685 (1998); C. Cohen-Tannoudji, *ibid.* **70**, 707 (1998); W. D. Phillips, *ibid.* **70**, 721 (1998).

[2] E. A. Cornell and C. E. Wieman, Rev. Mod. Phys. **74**, 875 (2002); W. Ketterle, *ibid.* **74**, 1131 (2002).

[3] A. G. Truscott, K. E. Strecker, W. I. McAlexander, G. B. Partridge, and R. G. Hulet, Science **291**, 2570 (2001).

[4] F. Schreck, L. Khaykovich, K. L. Corwin, G. Ferrari, T. Bourdel, J. Cubizolles, and C. Salomon, Phys. Rev. Lett. **87**,

080403 (2001).
[5] Z. Hadzibabic, C. A. Stan, K. Dieckmann, S. Gupta, M. W. Zwierlein, A. Görlitz, and W. Ketterle, Phys. Rev. Lett. **88**, 160401 (2002).
[6] G. Roati, F. Riboli, G. Modugno, and M. Inguscio, Phys. Rev. Lett. **89**, 150403 (2002).
[7] G. Grynberg and C. Robilliard, Phys. Rep. **355**, 335 (2000).
[8] P. Verkerk, B. Lounis, C. Salomon, C. Cohen-Tannoudji, J.-Y. Courtois, and G. Grynberg, Phys. Rev. Lett. **68**, 3861 (1992).
[9] L. Guidoni, C. Triché, P. Verkerk, and G. Grynberg, Phys. Rev. Lett. **79**, 3363 (1997).
[10] L. Sanchez-Palencia and L. Santos, Phys. Rev. A **72**, 053607 (2005).
[11] T. Schulte, S. Drenkelforth, J. Kruse, W. Ertmer, J. Arlt, K. Sacha, J. Zakrzewski, and M. Lewenstein, Phys. Rev. Lett. **95**, 170411 (2005).
[12] P. Horak, J.-Y. Courtois, and G. Grynberg, Phys. Rev. A **58**, 3953 (1998).
[13] G. Grynberg, P. Horak, and C. Mennerat-Robilliard, Europhys. Lett. **49**, 424 (2000).
[14] J. E. Lye, L. Fallani, M. Modugno, D. S. Wiersma, C. Fort, and M. Inguscio, Phys. Rev. Lett. **95**, 070401 (2005).
[15] D. Clément, A. F. Varón, M. Hugbart, J. A. Retter, P. Bouyer, L. Sanchez-Palencia, D. M. Gangardt, G. V. Shlyapnikov, and A. Aspect, Phys. Rev. Lett. **95**, 170409 (2005).
[16] C. Fort, L. Fallani, V. Guarrera, J. E. Lye, M. Modugno, D. S. Wiersma, and M. Inguscio, Phys. Rev. Lett. **95**, 170410 (2005).
[17] D. Clément, A. F. Varón, J. A. Retter, L. Sanchez-Palencia, A. Aspect, and P. Bouyer, New J. Phys. **8**, 165 (2006).
[18] J. R. Anglin and W. Ketterle, Nature (London) **416**, 211 (2002).
[19] D. Jaksch and P. Zoller, Ann. Phys. (N.Y.) **315**, 52 (2005).
[20] T. Giamarchi, e-print cond-mat/0605472.
[21] M. Lewenstein, A. Sanpera, V. Ahufinger, B. Damski, A. Sen (De), and U. Sen, e-print cond-mat/0606771.
[22] L. P. Pitaevskii and S. Stringari, *Bose-Einstein Condensation* (Clarendon Press, Oxford, 2004).
[23] *Anderson Localization*, edited by Y. Nagaoka and H. Fukuyama, *Springer Series in Solid State Sciences*, Vol. 39 (Springer, Berlin, 1982).
[24] *Anderson Localization*, edited by T. Ando and H. Fukuyama, Springer Proceedings in Physics, Vol. 28 (Springer, Berlin, 1988).
[25] B. van Tiggelen, in *Wave Diffusion in Complex Media*, 1998 Les Houches Lectures, edited by J. P. Fouque (Kluwer, Dordrecht, 1999).
[26] P. W. Anderson, Phys. Rev. **109**, 1492 (1958).
[27] D. S. Wiersma, P. Bartolini, A. Lagendijk, and R. Righini, Nature (London) **390**, 671 (1997).
[28] G. Labeyrie, F. de Tomasi, J.-C. Bernard, C. A. Müller, Ch. Miniatura, and R. Kaiser, Phys. Rev. Lett. **83**, 5266 (1999).
[29] R. Dalichaouch, J. P. Amstrong, S. Schultz, P. M. Platzman, and S. L. McCall, Nature (London) **354**, 53 (1991).
[30] A. A. Chabanov, M. Stoytchev, and A. Z. Genack, Nature (London) **404**, 850 (2000).
[31] B. Damski, J. Zakrzewski, L. Santos, P. Zoller, and M. Lewenstein, Phys. Rev. Lett. **91**, 080403 (2003).
[32] U. Gavish and Y. Castin, Phys. Rev. Lett. **95**, 020401 (2005).
[33] T. Paul, P. Leboeuf, N. Pavloff, K. Richter, and P. Schlagheck, Phys. Rev. A **72**, 063621 (2005).
[34] R. Roth and K. Burnett, Phys. Rev. A **68**, 023604 (2003).
[35] V. Ahufinger, L. Sanchez-Palencia, A. Kantian, A. Sanpera, and M. Lewenstein, Phys. Rev. A **72**, 063616 (2005).
[36] T. Giamarchi and H. J. Schulz, Phys. Rev. B **37**, 325 (1988).
[37] M. P. A. Fisher, P. B. Weichman, G. Grinstein, and D. S. Fisher, Phys. Rev. B **40**, 546 (1989).
[38] O. N. Dorokhov, Sov. Phys. JETP **71**, 360 (1990).
[39] D. L. Shepelyansky, Phys. Rev. Lett. **73**, 2607 (1994).
[40] R. Graham and A. Pelster, e-print cond-mat/0508306.
[41] I. M. Lifshits, S. A. Gredeskul, and L. A. Pastur, *Introduction to the Theory of Disordered Systems* (Wiley, New York, 1988).
[42] A. F. Ioffe and A. R. Regel, Prog. Semicond. **4**, 237 (1960).
[43] Note that smoothing effects have also been discussed in lattice Bose gases with uncorrelated random potentials by D. K. K. Lee and J. M. F. Gunn, J. Phys.: Condens. Matter **2**, 7753 (1990).
[44] D. S. Petrov, G. V. Shlyapnikov, and J. T. M. Walraven, Phys. Rev. Lett. **85**, 3745 (2000).
[45] D. S. Petrov, D. M. Gangardt, and G. V. Shlyapnikov, J. Phys. IV **116**, 5 (2004).
[46] V. N. Popov, Theor. Math. Phys. **11**, 565 (1972); *Functional Integrals in Quantum Field Theory and Statistical Physics* (Reidel, Dordrecht, 1983).
[47] J. W. Goodman, in *Statistical Properties of Laser Speckle Patterns*, in *Laser Speckle and Related Phenomena*, edited by J.-C. Dainty (Springer-Verlag, Berlin, 1975).
[48] J. M. Huntley, Appl. Opt. **28**, 4316 (1989).
[49] P. Lugan, D. Clément, P. Bouyer, A. Aspect, M. Lewenstein, and L. Sanchez-Palencia, e-print cond-mat/0610389.

Density modulations in an elongated Bose-Einstein condensate released from a disordered potential

D. Clément, P. Bouyer, A. Aspect, and L. Sanchez-Palencia
Laboratoire Charles Fabry de l'Institut d'Optique, CNRS and Univ. Paris-Sud, Campus Polytechnique, RD 128, F-91127 Palaiseau cedex, France
(Received 12 October 2007; published 31 March 2008)

We observe large density modulations in time-of-flight images of elongated Bose-Einstein condensates, initially confined in a harmonic trap and in the presence of weak disorder. The development of these modulations during the time of flight and their dependence with the disorder are investigated. We render an account of this effect using numerical and analytical calculations. We conclude that the observed large density modulations originate from the weak initial density modulations induced by the disorder and not from initial phase fluctuations (thermal or quantum).

DOI: 10.1103/PhysRevA.77.033631 PACS number(s): 03.75.Hh, 03.75.Kk, 64.60.Cn

Gaseous Bose-Einstein condensates (BECs) in disordered potentials [1–5] offer controllable systems to study open basic questions on the effects of disorder in quantum media [6]. In this respect, a still debated question relies on the nature of the disorder-induced superfluid-insulator transitions [7] which can originate from strong fluctuations of either the density or the phase. This question can be addressed experimentally with gaseous BECs in optical disorder [1–5] as both density and phase can be measured directly [8]. In addition to its fundamental interest, this study is important for BECs on chips [9] and can also shed some light on the physics of dirty superconductors [10] and granular metals [11].

In the presence of repulsive interactions, Anderson localization is suppressed in a stationary BEC and weak disorder results in small density modulations [12]. However, one may wonder whether weak disorder *may* significantly affect the coherence of a connected BEC and entail large phase fluctuations. It has been suggested [1,13], by analogy with elongated (nondisordered) quasi-BECs, that the observation of large fringes in *time-of-flight* (TOF) images of disordered BECs (see Fig. 1 and [1,14,15]) may signal strong initial phase fluctuations [16–18]. For quasi-BECs, such fringes in TOF images are *indeed* a signature of initial phase fluctuations [17]. However, for disordered BECs, no systematic study of these fringes has been reported so far and their relation to disorder-induced phase fluctuations is still unclear.

In this paper, we report a detailed study of the density modulations in the TOF images of an elongated, nonfragmented three-dimensional (3D) BEC initially placed in a weak 1D disordered potential. Our main experimental result is that the fringes in the TOF images are reproduced from shot to shot when using the *same* realization of the disorder. This excludes disorder-induced phase fluctuations (thermal or quantum) in the trapped BEC as the origin of the fringes observed after TOF for the parameter range of the experiment (relevant also for [1,14,15]). Using analytical and numerical calculations, which do not include initial phase fluctuations, we show that the fringes actually develop during the TOF according to the following scenario. Just after release, the initial weak density modulations (induced by the disorder onto the trapped BEC) imprint a phase with axial modulations and transversal invariance. Then, the resulting axial phase modulations are converted into large axial density modulations.

The experiment is detailed in Refs. [2,5]. We form a cigar-shaped BEC of ^{87}Rb atoms in an Ioffe-Pritchard trap of frequencies $\omega_z/2\pi=6.7$ Hz and $\omega_\perp/2\pi=660$ Hz. The BEC atom number is $N_0\sim 3\times 10^5$, the length $2L_{\mathrm{TF}}\simeq 300$ μm, and the chemical potential $\mu/2\pi\hbar\simeq 4.5$ kHz. We create a 1D speckle (disordered) potential along the z axis. The correlation function is $C(z)=V_{\mathrm{R}}^2\,\mathrm{sinc}^2(z/\sigma_{\mathrm{R}})$ where both amplitude V_{R} and correlation length σ_{R} down to 0.33 μm can be controlled [2,5]. The results presented in this work correspond to $\sigma_{\mathrm{R}}\simeq 1.7$ μm [19]. In the experiment, we wait 300 ms for the BEC to reach equilibrium in the presence of disorder and then switch off abruptly both magnetic and speckle potentials. We then take absorption images of the expanding cloud after a variable time of flight t_{TOF} with typical images shown in Fig. 1.

These images show large density modulations along the axis z of the disorder. To measure their amplitude, we first extract a 1D axial density $n_{1\mathrm{D}}(z)$ by integrating the column density over the second transverse direction x. We then define $\eta(z)$ as the normalized deviations of the 1D density from the 1D parabolic Thomas-Fermi (TF) profile $n_{1\mathrm{D}}^0(z)$ which fits best the data (red line in Fig. 1), so that

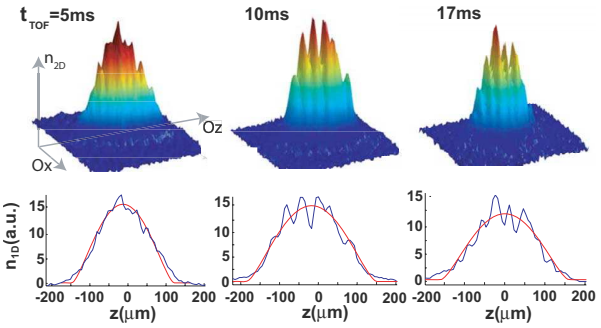

FIG. 1. (Color online) Upper panel: TOF images of an expanding disordered BEC for three different times of flight. The vertical axis represents the column density along the y axis. Lower panel: axial 1D density profiles $n_{1\mathrm{D}}(z)$ (column density integrated along the x axis, blue) and 1D TF parabolic profiles $n_{1\mathrm{D}}^0(z)$ (red). The amplitude of the disorder is $\gamma=V_{\mathrm{R}}/\mu=0.41$.

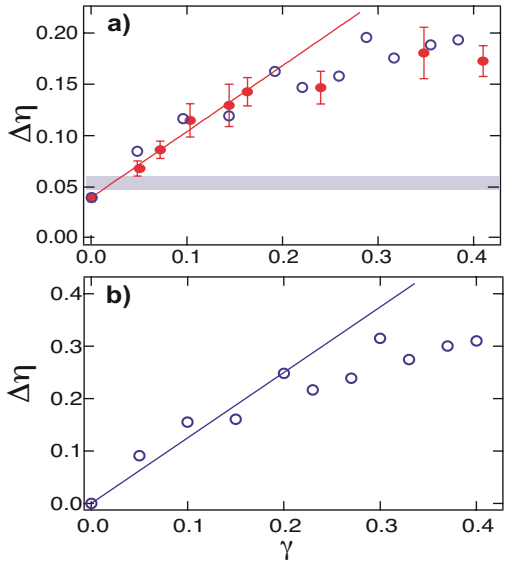

FIG. 2. (Color online) (a) Experimental results (red points) for the density modulations at $\omega_\perp t_{\mathrm{TOF}}=62.2$ versus the amplitude of the disorder. The shaded area corresponds to phase fluctuations in our initial elongated BEC, as calculated in Ref. [17] (the error bar reflects the uncertainty on the temperature). (b) Corresponding numerical results, taking into account the finite resolution of our optics, but not the misalignment of the probe beam. The open blue circles in (a) show the same data including an offset accounting for the small initial phase fluctuations and the correction corresponding to the probe angle.

$n_{1\mathrm{D}}(z)=n^0_{1\mathrm{D}}(z)[1+\eta(z)]$. Finally, we calculate the standard deviation of $\eta(z)$ over a given length L: $\Delta\eta=\sqrt{\frac{1}{L}\int_L dz\ \eta^2(z)}$ [here $\int_L dz\ \eta(z)=0$]. The calculation of $\Delta\eta$ is restricted to 70% of the BEC total length ($L=1.4L_{\mathrm{TF}}$) to avoid the edges where thermal atoms are present. Two imperfections reduce the measured $\Delta\eta$ compared to the real value. First, our imaging system has a finite resolution $L_{\mathrm{res}}=8.5\ \mu$m, larger than the variation scale σ_{R} of the disorder. This effect is quantified by measuring the modulation transfer function (MTF) of the imaging system. Second, a slight misalignment of the probe beam—which is not exactly perpendicular to axis z—also reduces the contrast of the fringes [17]. This effect is more difficult to quantify as angles smaller than our uncertainty on the probe angle (1°) can drastically reduce the contrast. We find that numerics reproduce our experimental results assuming a misalignment of 0.33°.

We first study the amplitude of the normalized density modulations, $\Delta\eta$, as a function of the amplitude of the disorder $\gamma=V_{\mathrm{R}}/\mu$ at a given time of flight $t_{\mathrm{TOF}}=15.3$ ms ($\omega_\perp t_{\mathrm{TOF}}=62.2$) with experimental results plotted in Fig. 2(a). In the absence of disorder, we observe nonvanishing density modulations ($\Delta\eta_0\simeq 0.037$) larger than the noise in the background of the images ($\Delta\eta_{\mathrm{n}}\simeq 0.015$). They are interpreted as small but nonzero phase fluctuations initially present in our elongated BEC [16]. The calculation of their contribution to the density modulations in the TOF images as determined in Ref. [17] agrees with our data [see Figs. 2(a)]. In the presence of disorder, we find that, for small values of γ (typically $\gamma<0.2$), $\Delta\eta$ grows with γ as $\Delta\eta=\Delta\eta_0+0.64(3)\gamma$. For larger values of γ, the disordered BEC is fragmented either in the trap or during the expansion, and $\Delta\eta$ has a maximum value of $\Delta\eta\simeq 0.17$ in the experiment [20].

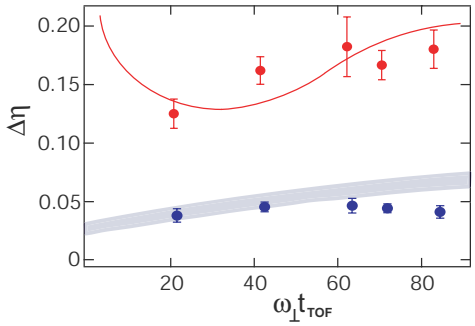

FIG. 3. (Color online) Time evolution of the measured density modulations $\Delta\eta$ during a TOF for $\gamma=0$ (no disorder, blue points) and $\gamma=0.41$ (with disorder, red points). The shaded area corresponds to the calculation of Ref. [17], taking into account the uncertainty on the temperature. The solid red line is the result of numerical calculations for $\gamma=0.4$ (see text).

We also perform numerical integrations of the 3D Gross-Pitaevskii equation (GPE) for the expanding disordered BEC and extract $\Delta\eta$ as in the experiments. The numerics do not include any initial phase fluctuations. We find a linear dependence of $\Delta\eta$ versus γ, $\Delta\eta\simeq 3.5\gamma$ for the bare numerical results and $\Delta\eta\simeq 1.23\gamma$ if we take into account the finite resolution of the imaging system, but not the misalignment of the probe [see Fig. 2(b)]. In fact, we find that the numerics agree with the experiments if, in addition to an offset $\Delta\eta_0$ to mimic the small initial phase fluctuations, we include the systematic correction associated to a probe angle of 0.33° [see Fig. 2(a)].

We now examine the TOF dynamics of the disordered BEC and plot $\Delta\eta$ versus t_{TOF} in Fig. 3. In the presence of disorder, the observed density modulations (red points) are clearly enhanced compared to those in the absence of disorder (blue points). We also observe that the density modulations first develop and then saturate. The dynamics of their development is reproduced well by our numerical calculations (solid red line) if we take into account all imperfections of our imaging system.

After correcting all experimental imperfections, the density modulations in the TOF images turn out to be larger ($\Delta\eta\simeq 3.5\gamma$) than the ones of the trapped BEC before TOF ($\Delta\eta=2\gamma$) [21]. One may wonder whether these large density modulations in the TOF images reveal phase fluctuations induced by the disorder in the initial BEC [1,13]. Actually, several arguments lead us to conclude that it is not so. First, our numerics, which reproduce the experimental data, do *not* include initial phase fluctuations. Second, the numerical diagonalization of the Bogolyubov equations indicates that the disorder hardly affect the excitation spectrum of a 1D BEC for the experimental parameters [22]. Last but not least, we have observed identical density modulations in successive experiments performed with the *same* realization of the disorder (see also Refs. [14,15]). Hence, averaging over various images taken with the same realization of the disorder does not wash out the fringes [23] and this excludes initial random fluctuations, quantum or thermal [19].

We now develop an analytical model for the evolution of the BEC density profile during the TOF, which shows explicitly how a weak disorder leads to large density modulations after a long-enough TOF, *without initial phase fluctuations*. Although the probability of fragmentation is small for weak-enough disorder, it may happen that the BEC is fragmented into a small number of fragments. However, for the considered $t_{\mathrm{TOF}} \lesssim 1/\omega_z$, the fragments will only weakly overlap as the axial expansion is small. Therefore, we neglect fragmentation in our model.

In the absence of disorder, the TOF expansion of a BEC initially trapped in a harmonic potential in the Thomas-Fermi regime is self-similar [24], so that

$$\psi(\vec{r},t) = \left[\prod\nolimits_j b_j(t)\right]^{-1/2} \phi(\{x_j/b_j(t)\},t) e^{i\theta_0(\vec{r},t)}, \tag{1}$$

with $j=1,\ldots,3$ the spatial directions, $\theta_0(\vec{r},t)=(m/2\hbar)\times\Sigma_j(\dot{b}_j/b_j)x_j^2$ the dynamical phase, and ϕ the (time-independent) wave function of the BEC in the trap. The scaling factors $b_j(t)$ are governed by the equations $\ddot{b}_j = \omega_j^2/(b_j\Pi_k b_k)$ with the initial conditions $b_j(0)=1$ and $\dot{b}_j(0)=0$ [24]. In the presence of disorder, we use the scaling (1) and we write the (now time-dependent) wave function $\phi(\rho,z,t)=\sqrt{\tilde{n}(\rho,z,t)}e^{i\tilde{\theta}(\rho,z,t)}$ where $\rho=\sqrt{x^2+y^2}$ is the radial coordinate. In the absence of phase fluctuations, $\phi(\rho,z,t=0)$ is real (up to a homogeneous phase) as it is the ground state of the trapped, disordered BEC. The TOF dynamics is then governed by two coupled equations for the density $\tilde{n}$ and the phase $\tilde{\theta}$ which are equivalent to the complete time-dependent GPE.

Let us introduce now a couple of approximations. First, in elongated 3D BECs, the expansion for $\omega_z t \lesssim 1$ is mainly radial and $b_z(t)\simeq 1$. Second, we assume not too large perturbation of the density, so that $\tilde{n}=\tilde{n}_0+\delta\tilde{n}$ with $\tilde{n}_0$, the density in the absence of disorder, and $\delta\tilde{n}\ll\tilde{n}_0$. Using the local density approximation, we can neglect all the spatial derivatives of $\tilde{n}_0$. We also neglect the radial derivatives of $\delta\tilde{n}$ since the 1D disorder induces short-range spatial inhomogeneities mainly along the z axis. We are thus left with the equations

$$\partial_t \delta\tilde{n} = -(\hbar/m)\tilde{n}_0\partial_z^2\tilde{\theta}, \tag{2}$$

$$-\hbar\partial_t\tilde{\theta} = g\delta\tilde{n}/b_\perp^2 + (\hbar^2/2m)[|\partial_z\tilde{\theta}|^2 - \partial_z^2\delta\tilde{n}/2\tilde{n}_0]. \tag{3}$$

In a first stage, the initial small inhomogeneities of the density induced by the 1D disordered potential before TOF, $\delta\tilde{n}\simeq -V(z)/g$ [12], hardly evolve since $\partial_t\delta\tilde{n}(t=0)=0$. They are, however, crucial as they act as an inhomogeneous potential which induces the development of a phase modulation $\tilde{\theta}(z,t)$ at the beginning of the TOF [25]. From Eqs. (2) and (3), we find

$$\tilde{\theta}(z,t) \simeq \arctan(\omega_\perp t)[V(z)/\hbar\omega_\perp], \tag{4}$$

$$\delta\tilde{n} \simeq -V(z)/g - [\tilde{n}_0\partial_z^2 V(z)/m\omega_\perp^2]F(\omega_\perp t), \tag{5}$$

where $F(\tau)=\int_0^\tau d\tau'\arctan(\tau')=\tau\arctan(\tau)-\ln\sqrt{1+\tau^2}$. From Eq. (5), we then find

$$\Delta\eta(t) \simeq 2\left(\frac{V_{\mathrm{R}}}{\mu}\right)\left[1-\frac{2}{3}\left(\frac{\mu}{\hbar\omega_\perp}\right)^2\left(\frac{\xi}{\sigma_{\mathrm{R}}}\right)^2 F(\omega_\perp t)\right]. \tag{6}$$

Hence, $\Delta\eta$ first slightly decreases. It is easily understood as an interacting BEC initially at rest will tend to fill its holes when released from the disordered potential. The solution [Eqs. (4) and (5)] is valid as long as the contribution of the last two terms in Eq. (3) remains small [i.e., for $\omega_\perp t \ll (\sigma_{\mathrm{R}}/\xi)^2$ and $\omega_\perp t \ll (\sigma_{\mathrm{R}}/\xi)(\hbar\omega_\perp/\sqrt{V_{\mathrm{R}}\mu})$]. In addition, it requires that the density modulations not vary much [i.e., the second term on the right-hand side (rhs) of Eq. (5) is small compared to the first one]. For the experimental parameters, the last condition is the most restrictive. It defines a typical time $t_0=(1/\omega_\perp)F^{-1}[(\sigma_{\mathrm{R}}/\xi)^2(\hbar\omega_\perp/\mu)^2/2]$ during which the radial expansion imprints a phase modulation due to the initial inhomogeneities of the BEC density created by the disorder before the TOF. In particular, if $t_0 \gg 1/\omega_\perp$, the phase modulations freeze at $\tilde{\theta}(z)\simeq(\pi/2)[V(z)/\hbar\omega_\perp]$.

In a second stage, the phase modulations are converted into density modulations similarly as thermal phase fluctuations do during the TOF of an elongated quasi-BEC [17]. For $t \gtrsim t_1$ where t_1 is a typical time much longer than $1/\omega_\perp$ (see below), the scaling parameter $b_\perp(t)$ becomes large so that the first term on the rhs of Eq. (3) can now be neglected. Assuming small phase gradients, we are left with the equation $\partial_t^2\delta\tilde{n}_k+\hbar^2k^4\delta\tilde{n}_k/4m^2=0$ where $\delta\tilde{n}_k(\rho,t)$ is the 1D Fourier transform of $\delta\tilde{n}$ along z and whose solution reads $\delta\tilde{n}_k(t)=\delta\tilde{n}_k(t_1)\cos[(\hbar k^2/2m)(t-t_1)]+[2m\delta\dot{\tilde{n}}_k(t_1)/\hbar k^2]\sin[(\hbar k^2/2m)\times(t-t_1)]$. If $t_0 \gg 1/\omega_\perp$, we can take $1/\omega_\perp \ll t_1 \leq t_0$ and the exact value of t_1 does not matter much (we use $t_1=t_0$). If $t_0 \lesssim 1/\omega_\perp$, the determination of t_1 is not straightforward, but can be found through fitting procedures, for instance. Then, according to Eq. (5), $\delta\tilde{n}_k(t_1)\simeq -V(z)/g$ is mainly determined by the initial density modulations of the trapped BEC while $\delta\dot{\tilde{n}}_k(t_1)\simeq -[\tilde{n}_0\partial_z^2V(z)/m\omega_\perp]\arctan(\omega_\perp t_1)$ results from the phase modulations created in the first stage of the TOF. For $\hbar\omega_\perp \ll \mu$ as in the experiment, the cosine term can be neglected and we find

$$\Delta\eta(t) \simeq \sqrt{8}(V_{\mathrm{R}}/\hbar\omega_\perp)\arctan(\omega_\perp t_1) I(\sigma_{\mathrm{R}}, t-t_1), \tag{7}$$

where $I(\sigma_{\mathrm{R}},t)=\sqrt{\int_0^1 d\kappa(1-\kappa)\sin^2[(2\hbar t/m\sigma_{\mathrm{R}}^2)\kappa^2]}$ for a speckle potential.

Numerical integrations of the complete 3D GPE confirm the expected behavior of $\Delta\eta$ during the TOF at short [Eq. (6)] and long [Eq. (7)] times as shown in Fig. 4. This validates our scenario in a quantitative manner.

Three remarks are in order. First, we find that, due to the development of phase modulations in the first stage of the TOF, the density modulations in the expanded BEC ($\Delta\eta \propto V_{\mathrm{R}}/\hbar\omega_\perp$) can be larger than those in the trapped BEC ($\Delta\eta \propto V_{\mathrm{R}}/\mu$) if $\mu > \hbar\omega_\perp$. Second, the density pattern is completely determined by the realization of the disorder. Third, Eq. (7) shows that the density modulations saturate at $\Delta\eta \simeq \sqrt{2}(V_{\mathrm{R}}/\hbar\omega_\perp)\arctan(\omega_\perp t_1)$ for very long times t [26]. These properties are in qualitative agreement with the experimental observations.

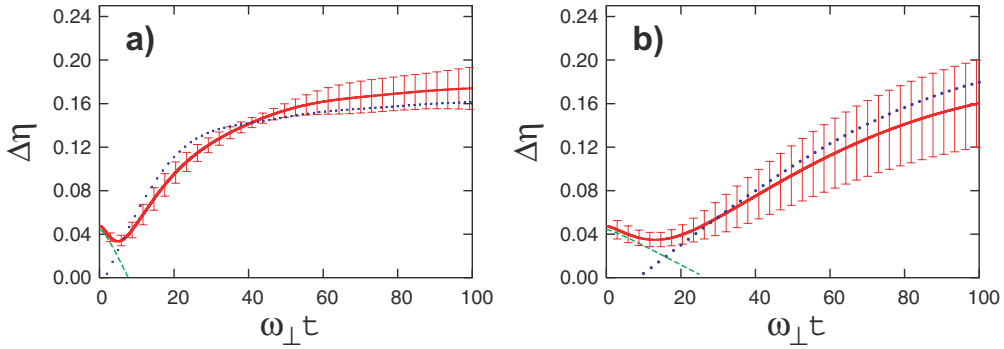

FIG. 4. (Color online) Dynamics of density modulations as obtained numerically (solid red line with error bars) and comparisons with Eq. (6) (green dashed line) and Eq. (7) (blue dotted line). (a) The parameters are the same as in the experiment (in particular, $\sigma_R = 1.7\ \mu$m) with $V_R = 0.02\mu$. Here $\omega_\perp t_0 \simeq 3$ and we have used $t_1 = 0.5t_0$. (b) Same as (a), but with $\sigma_R = 3.4\ \mu$m. Here, $\omega_\perp t_0 \simeq 8.5 \gg 1$, so that we have used $t_1 = t_0$ (see text).

In conclusion, we have shown that the large fringes observed in this work and Refs. [1,14,15] in TOF images of disordered BECs *do not* rely on initial disorder-induced phase fluctuations. They actually result from the TOF process of a BEC with small initial density modulations, but without phase fluctuations. A phase modulation determined by the weak initial modulations of the BEC density first develops and is later converted into large density modulations. Our analytical calculations based on this scenario agree with numerical calculations and experimental observations. Nevertheless, our results do not exclude that, in different regimes, disorder might enhance phase fluctuations. This question is crucial in connection to the nature of superfluid-insulator transitions in the presence of disorder. Dilute BECs can help answering it as their phase coherence can be probed with accuracy [17,18]. Revealing this possible effect via TOF images requires taking into account the phase modulation which develops during the first stage of the TOF as demonstrated here.

We thank P. Chavel for useful discussions and J. Retter and A. Varon for their help in the early stage of the experiment. This work was funded by the French DGA, MENRT, ANR, and IFRAF and by the ESF program QUDEDIS.

[1] J. E. Lye, L. Fallani, M. Modugno, D. S. Wiersma, C. Fort, and M. Inguscio, Phys. Rev. Lett. **95**, 070401 (2005).
[2] D. Clément, A. F. Varon, M. Hugbart, J. A. Retter, P. Bouyer, L. Sanchez-Palencia, D. M. Gangardt, G. V. Shlyapnikov, and A. Aspect, Phys. Rev. Lett. **95**, 170409 (2005).
[3] C. Fort, L. Fallani, V. Guarrera, J. E. Lye, M. Modugno, D. S. Wiersma, and M. Inguscio, Phys. Rev. Lett. **95**, 170410 (2005).
[4] T. Schulte, S. Drenkelforth, J. Kruse, W. Ertmer, J. Arlt, K. Sacha, J. Zakrzewski, and M. Lewenstein, Phys. Rev. Lett. **95**, 170411 (2005).
[5] D. Clément, A. F. Varon, J. A. Retter, L. Sanchez-Palencia, A. Aspect, and P. Bouyer, New J. Phys. **8**, 165 (2006).
[6] B. Damski, J. Zakrzewski, L. Santos, P. Zoller, and M. Lewenstein, Phys. Rev. Lett. **91**, 080403 (2003); A. Sanpera, A. Kantian, L. Sanchez-Palencia, J. Zakrzewski, and M. Lewenstein, *ibid.* **93**, 040401 (2004); R. C. Kuhn, C. Miniatura, D. Delande, O. Sigwarth, and C. A. Muller, *ibid.* **95**, 250403 (2005); L. Sanchez-Palencia, D. Clément, P. Lugan, P. Bouyer, G. V. Shlyapnikov, and A. Aspect, *ibid.* **98**, 210401 (2007); P. Lugan, D. Clément, P. Bouyer, A. Aspect, M. Lewenstein, and L. Sanchez-Palencia, *ibid.* **98**, 170403 (2007); A. Niederberger, T. Schulte, J. Wehr, M. Lewenstein, L. Sanchez-Palencia, and K. Sacha, *ibid.* **100**, 030403 (2008); S. E. Skipetrov *et al.*, e-print arXiv:0801.3631.
[7] P. Phillips and D. Dalidovich, Science **302**, 243 (2003).
[8] See, for instance, J. R. Anglin and W. Ketterle, Nature (London) **416**, 211 (2002) and references therein.
[9] See, for instance, R. Folman, P. Krüger, J. Schmiedmayer, J. Denschlag, and C. Henkel, Adv. At., Mol., Opt. Phys. **48**, 263 (2002); J. Estève, C. Aussibal, T. Schumm, C. Figl, D. Mailly, I. Bouchoule, C. I. Westbrook, and A. Aspect, Phys. Rev. A **70**, 043629 (2004); J. Fortàgh and C. Zimmermann, Rev. Mod. Phys. **79**, 235 (2007) and references therein.
[10] M. P. A. Fisher, Phys. Rev. Lett. **65**, 923 (1990); A. F. Hebard and M. A. Paalanen, *ibid.* **65**, 927 (1990); M. A. Paalanen, A. F. Hebard, and R. R. Ruel, *ibid.* **69**, 1604 (1992); T. Cren *et al.*, Europhys. Lett. **54**, 84 (2001); Y. Dubi *et al.*, Nature (London) **449**, 876 (2007).
[11] I. S. Beloborodov, A. V. Lopatin, V. M. Vinokur, and K. B. Efetov, Rev. Mod. Phys. **79**, 469 (2007).
[12] L. Sanchez-Palencia, Phys. Rev. A **74**, 053625 (2006).
[13] M. Lewenstein, A. Sanpera, V. Ahufinger, B. Damski, A. Sen(de), and U. Sen, Adv. Phys. **56**, 243 (2007).
[14] Y. P. Chen, J. Hitchcock, D. Dries, M. Junker, C. Welford, and R. G. Hulet, following paper, Phys. Rev. A **77**, 033632 (2008).
[15] J. Arlt (private communication).
[16] D. S. Petrov, G. V. Shlyapnikov, and J. T. M. Walraven, Phys. Rev. Lett. **87**, 050404 (2001).

[17] S. Dettmer, D. Hellweg, P. Ryytty, J. J. Arlt, W. Ertmer, K. Sengstock, D. S. Petrov, G. V. Shlyapnikov, H. Kreutzmann, L. Santos, and M. Lewenstein, Phys. Rev. Lett. **87**, 160406 (2001).

[18] S. Richard, F. Gerbier, J. H. Thywissen, M. Hugbart, P. Bouyer, and A. Aspect, Phys. Rev. Lett. **91**, 010405 (2003).

[19] We found similar experimental results for $\sigma_R = 0.33$ μm.

[20] For stronger disorder ($\gamma > 0.5$), quantum fluctuations of the phases of the BEC fragments may reduce the contrast of the fringes in TOF images.

[21] For 1D BECs, one finds $\Delta\eta = \gamma$ [12]. Here, the factor of 2 is due to the integration over the two radial directions.

[22] Nevertheless, significant localization of Bogolyubov excitations can be obtained for different parameters; see P. Lugan, D. Clément, P. Bouyer, A. Aspect, and L. Sanchez-Palencia, Phys. Rev. Lett. **99**, 180402 (2007).

[23] The pictures of Fig. 1 are actually averaged over six TOF images with the same disordered potential.

[24] Y. Kagan, E. L. Surkov, and G. V. Shlyapnikov, Phys. Rev. A **54**, R1753 (1996); Y. Castin and R. Dum, Phys. Rev. Lett. **77**, 5315 (1996).

[25] This effect shares some analogy with the phase-imprinting methods: Ł. Dobrek, M. Gajda, M. Lewenstein, K. Sengstock, G. Birkl, and W. Ertmer, Phys. Rev. A **60**, R3381 (1999); S. Burger, K. Bongs, S. Dettmer, W. Ertmer, K. Sengstock, A. Sanpera, G. V. Shlyapnikov, and M. Lewenstein, Phys. Rev. Lett. **83**, 5198 (1999); J. Denschlag, J. E. Simsarian, D. L. Feder, C. W. Clark, L. A. Collins, J. Cubizolles, L. Deng, E. W. Hagley, K. Helmerson, W. P. Reinhardt, S. L. Rolston, B. I. Schneider, and W. D. Phillips, Science **287**, 97 (2000).

[26] This is valid for $t < 1/\omega_z$. However, at even longer times, the axial expansion of the BEC may reduce $\Delta\eta$.

Ultracold Bose Gases in 1D Disorder: From Lifshits Glass to Bose-Einstein Condensate

P. Lugan,[1] D. Clément,[1] P. Bouyer,[1] A. Aspect,[1] M. Lewenstein,[2] and L. Sanchez-Palencia[1]

[1]*Laboratoire Charles Fabry de l'Institut d'Optique, CNRS and Univ. Paris-Sud, Campus Polytechnique, RD 128, F-91127 Palaiseau cedex, France*

[2]*ICREA and ICFO-Institut de Ciències Fotòniques, Parc Mediterrani de la Tecnologia, E-08860 Castelldefels (Barcelona), Spain*

(Received 15 October 2006; published 27 April 2007)

We study an ultracold Bose gas in the presence of 1D disorder for repulsive interatomic interactions varying from zero to the Thomas-Fermi regime. We show that for weak interactions the Bose gas populates a finite number of localized single-particle Lifshits states, while for strong interactions a delocalized disordered Bose-Einstein condensate is formed. We discuss the schematic quantum-state diagram and derive the equations of state for various regimes.

DOI: 10.1103/PhysRevLett.98.170403 PACS numbers: 05.30.Jp, 03.75.Hh, 64.60.Cn, 79.60.Ht

Disorder is present in nearly all condensed-matter systems due to unavoidable defects of the sustaining media. It is known not only to impair quantum flows but also to lead to spectacular effects such as Anderson localization [1–3]. In contrast to condensed-matter systems, ultracold atomic gases can be realized in the presence of controlled disorder [4], opening possibilities for investigations of localization effects [5–9] (for a review, see Ref. [10]). The first experimental studies of localization in disordered interacting Bose gases have been reported in Refs. [11–16].

One of the most fundamental issues in this respect concerns the interplay between localization and interactions in many-body quantum systems at zero temperature. Without interactions, a quantum gas in a random potential populates localized states [1], either a single state (in the case of bosons), or many (fermions). Weak repulsive interactions lead to delocalization, but strong interactions in confined geometries lead to Wigner-Mott-like localization [17]. Surprisingly, even for weakly interacting Bose gases, where the mean-field Hartree–Fock–Gross–Pitaevskii–Bogolyubov–de Gennes (HFGPBdG) description is expected to be valid, there exists no clear picture of the localization-delocalization scenario. Numerical calculations using the Gross-Pitaevskii equation (GPE) suggest that the Bose gas wave function at low densities is a superposition of localized states [15]. It is thus natural to seek the true ground state in the form of generalized HFGPBdG states, for which the Bose gas populates various low-energy single-atom states. In the presence of disorder, they correspond to so-called Lifshits states (LS) [18].

In this Letter we consider a d-dimensional (dD) Bose gas at zero temperature with repulsive interactions, and placed in a 1D random potential with arbitrary amplitude and correlation length. We show that generalized HFGPBdG states indeed provide a very good description of the many-body ground state for interactions varying from zero to the Thomas-Fermi (TF) regime [19]. We stress that the solution we find is different from that of noninteracting fermions which at zero temperature form a Fermi glass and occupy a large number of localized single-particle levels [10]. In contrast, many bosons may occupy the same level and thus populate only a finite number of LSs forming what we call a Lifshits glass. In the following, we discuss the quantum states of the system as a function of the strength of interactions and the amplitude and correlation length of the random potential, and we draw the schematic quantum-state diagram (see Fig. 1). In the limit of weak interactions, the Bose gas is in the Lifshits glass state, whereas for stronger interactions the gas forms a (possibly smoothed) delocalized disordered Bose-Einstein condensate (BEC) [20]. Our theoretical treatment provides us with a novel, physically clear, picture of disordered, weakly interacting, ultracold Bose gases. This is the main result of this work. In addition, we derive analytical formulas for the boundaries (corresponding to crossovers) in the quantum-state diagram and for the equations of state in the various regimes. We illustrate our results using a speckle random potential [21].

Consider a dD ultracold Bose gas with weak repulsive interactions, i.e., such as $n^{1-2/d} \ll \hbar^2/mg$, where m is the atomic mass, n the density, and g the dD coupling constant.

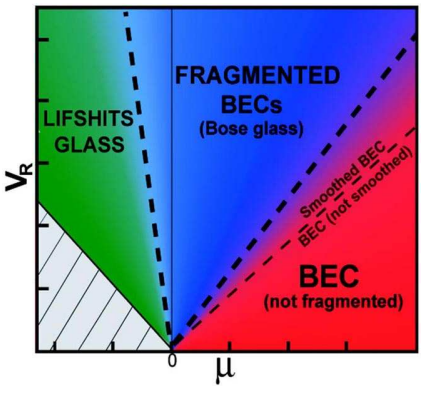

FIG. 1 (color online). Schematic quantum-state diagram of an interacting ultracold Bose gas in 1D disorder. The dashed lines represent the boundaries (corresponding to crossovers) which are controlled by the parameter $\alpha_R = \hbar^2/2m\sigma_R^2 V_R$ (fixed in the figure, see text), where V_R and σ_R are the amplitude and correlation length of the random potential. The hatched part corresponds to a forbidden zone ($\mu < V_{\min}$).

The gas is assumed to be axially confined to a box of length $2L$ in the presence of a 1D random potential $V(z)$, and trapped radially in a 2D harmonic trap with frequency $\omega_\perp$. We assume that the random potential is bounded below [$V_{\min} = \min(V)$] and we use the scaling form $V(z) = V_R v(z/\sigma_R)$, where $v(u)$ is a random function with both typical amplitude and correlation length equal to unity [22].

For illustration, we will consider a 1D speckle potential [21] similar to that used in Refs. [11–14]. In brief, $v(u)$ is random with the probability distribution $\mathcal{P}(v) = \Theta(v+1)\exp[-(v+1)]$, where Θ is the Heaviside function. Thus v is bounded below by $v_{\min} = -1$ and we have $\langle v\rangle = 0$ and $\langle v^2\rangle = 1$. In addition, for a square aperture, the correlation function reads $\langle v(u)v(u')\rangle = \mathrm{sinc}^2[\sqrt{3/2}(u-u')]$.

Below, we discuss the quantum states of the Bose gas, which are determined by the interplay of interactions and disorder.

BEC regime.—For strong repulsive interactions the Bose gas is delocalized and forms a BEC [12,20] (possibly quasi-BEC in 1D or elongated geometries [23]). The density profile is then governed by the GPE,

$$\mu = -\hbar^2\nabla^2(\sqrt{n})/2m\sqrt{n} + m\omega_\perp^2\rho^2/2 + V(z) + gn(\mathbf{r}), \tag{1}$$

where ρ is the radial coordinate and μ the chemical potential. This regime has been studied in the purely 1D case in Ref. [20]. Here, we focus on the case of a shallow radial trap ($\hbar\omega_\perp \ll \mu$) such that the radial profile is a TF inverted parabola. Proceeding as in Ref. [20], we find that the BEC density has a generalized TF profile [24]

$$\sqrt{n(\rho,z)} \simeq \sqrt{\mu(\rho)/g}[1 - \tilde{V}(\rho,z)/2\mu(\rho)], \tag{2}$$

where $\mu(\rho) = \mu[1-(\rho/R_\perp)^2]$ is the local chemical potential, $R_\perp = \sqrt{2\mu/m\omega_\perp^2}$ is the radial TF half-size and $\tilde{V}(\rho,z) = \int dz' G(\rho,z')V(z-z')$ is a smoothed potential [20] with $G(\rho,z) = \frac{1}{\sqrt{2}\xi(\rho)}\exp(-\frac{\sqrt{2}|z|}{\xi(\rho)})$, and $\xi(\rho) = \hbar/\sqrt{2m\mu(\rho)}$ being the local healing length. For $\xi(\rho) \ll \sigma_R$, i.e., for

$$\mu(\rho) \gg \hbar^2/2m\sigma_R^2, \tag{3}$$

we have $\tilde{V}(\rho,z) \simeq V(z)$, and the BEC density follows the modulations of the random potential in the TF regime. For $\xi(\rho) \gtrsim \sigma_R$, the kinetic energy cannot be neglected and competes with the disorder and the interactions. The random potential is therefore smoothed [20]: $\Delta\tilde{V}(\rho) < \Delta V$, where ΔV [$\Delta\tilde{V}(\rho)$] is the standard deviation of the (smoothed) random potential. The solution (2) corresponds to a delocalized disordered BEC.

The perturbative approach is valid when $\mu(\rho) \gg \Delta\tilde{V}(\rho)$. From the expression for $\tilde{V}$, we write $\Delta\tilde{V}(\rho) = V_R\sqrt{\Sigma^0(\sigma_R/\xi(\rho))}$. For the speckle potential, we can approximate the correlation function to $V_R^2\exp(-z^2/2\sigma_R^2)$ and we find [20]

$$\Sigma^0(\tilde{\sigma}_R) = \tilde{\sigma}_R^2 + (1-2\tilde{\sigma}_R^2)\tilde{\sigma}_R e^{\tilde{\sigma}_R^2}\int_{\tilde{\sigma}_R}^{\infty} d\theta e^{-\theta^2}, \tag{4}$$

with $\tilde{\sigma}_R = \sigma_R/\xi(\rho)$. In the center, i.e. $\rho = 0$ or in 1D, the validity condition of the BEC regime thus reduces to

$$\mu \gg V_R\sqrt{\Sigma^0(\sigma_R/\xi)} \quad \text{with} \quad \xi = \xi(0). \tag{5}$$

If condition (5) is not fulfilled, the Bose gas will form a fragmented BEC. The latter is a compressible insulator and thus can be identified with a Bose glass [17].

Noninteracting regime.—In the opposite situation, for vanishing interactions, the problem is separable and the radial wave function is the ground state of the radial harmonic oscillator. We are thus left with the eigenproblem of the single-particle 1D Hamiltonian $\hat{h} = -\hbar^2\partial_z^2/2m + V(z)$. In the presence of disorder, the eigenstates χ_ν are all localized [2] and are characterized by [18] (i) a finite localization length, (ii) a dense pure point density of states $\mathcal{D}_{2L}$, and (iii) a small participation length $P_\nu = 1/\int dz|\chi_\nu(z)|^4$ [25]. If $V(z)$ is bounded below, so is the spectrum and the low energy states belong to the so-called Lifshits tail, which is characterized by a stretched exponential cumulative density of states (cDOS), $\mathcal{N}_{2L}(\epsilon) = \int^\epsilon d\epsilon'\mathcal{D}_{2L}(\epsilon') \sim \exp(-c\sqrt{\frac{V_R}{\epsilon - V_{\min}}})$, in 1D [26].

Numerical results for the speckle potential are shown in Fig. 2. As expected the cDOS shows a stretched exponential form, the lowest LSs are spatially localized, and $P(\epsilon)$ increases with energy indicating a weaker localization. However, $P(\epsilon)$ is almost constant at low energy. Note also that the lowest LSs hardly overlap if their extension is much smaller than the system size.

Lifshits regime.—We turn now to the regime of finite but weak interactions, where the chemical potential μ lies in the Lifshits tail of the spectrum. Owing to the fact that the lowest single-particle LSs hardly overlap, it is convenient to work in the basis of the LSs, $\{\chi_\nu, \nu \in \mathbb{N}\}$. These can be regarded as trapping microsites populated with N_ν bosons in the quantum state $\phi_\nu(\rho)\chi_\nu(z)$, where the longitudinal motion is frozen to χ_ν and ϕ_ν accounts for the radial extension in the microsite ν. Therefore, the many-body wave function is the Fock state

$$|\Psi\rangle = \prod_{\nu\geq 0}(N_\nu!)^{-1/2}(b_\nu^\dagger)^{N_\nu}|\mathrm{vac}\rangle, \tag{6}$$

where $b_\nu^\dagger$ is the creation operator in the state $\phi_\nu(\rho)\chi_\nu(z)$ [27]. Each ϕ_ν can be a transverse 2D BEC for $N_\nu \gg 1$. However, the quantum state (6) does not correspond generally to a single 3D BEC since it does not reduce to $(N!)^{-1/2}(b_0^\dagger)^N|\mathrm{vac}\rangle$. Rather, the Bose gas splits into several fragments whose longitudinal shapes are those of the LSs, χ_ν, and are hardly affected by the interactions.

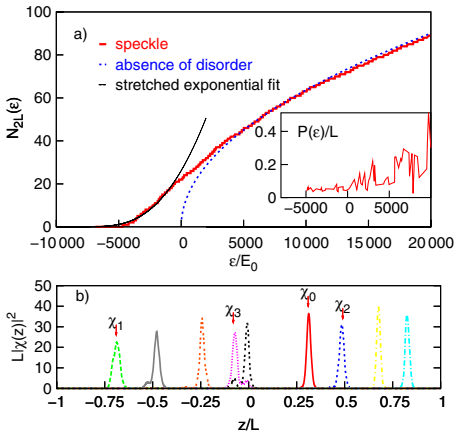

FIG. 2 (color online). (a) Cumulative density of states of single particles in a speckle potential with $\sigma_R = 2 \times 10^{-3} L$ and $V_R = 10^4 E_0$, where $E_0 = \hbar^2/2mL^2$ ($V_{\min} = -V_R$). Inset: Participation length [25]. (b) Low-energy Lifshits eigenstates. For the considered realization of disorder, $\epsilon_0 \simeq -5 \times 10^3 E_0$.

The mean-field energy associated with state (6) reads

$$E[\Psi] = \sum_\nu N_\nu \int d\rho \phi_\nu^* \left(\frac{-\hbar^2 \nabla_\perp^2}{2m} + \frac{m\omega_\perp^2 \rho^2}{2} + \epsilon_\nu \right) \phi_\nu + \sum_\nu \frac{N_\nu^2}{2} \int d\rho U_\nu |\phi_\nu|^4, \tag{7}$$

where $U_\nu = g \int dz |\chi_\nu(z)|^4 = g P_\nu^{-1}$ is the local interaction energy in the LS χ_ν. Minimizing $E[\Psi]$ for a fixed number of atoms ($E[\Psi] - \mu \sum_\nu N_\nu \to \min$), we find the equation

$$(\mu - \epsilon_\nu)\phi_\nu = [-\hbar^2 \nabla_\perp^2/2m + m\omega_\perp^2 \rho^2/2 + N_\nu U_\nu |\phi_\nu|^2] \phi_\nu. \tag{8}$$

Solving the 2D GPE (8) for each microsite ν, one finds the atom numbers N_ν and the wave functions ϕ_ν. As μ increases, $|\phi_\nu|^2$ will turn continuously from a Gaussian (for $\hbar\omega_\perp \gg \mu$) into an inverted parabola (for $\hbar\omega_\perp \ll \mu$).

To discuss the validity condition of the Lifshits regime let us call $\nu^{\max}$ the index of the highest LS such that all lower LSs hardly overlap. The Lifshits description requires the chemical potential μ to be small enough so that the number of populated LSs is smaller than $\nu^{\max}$, i.e., if

$$\mathcal{N}_{2L}(\mu) \leq \nu^{\max}. \tag{9}$$

If condition (9) is not fulfilled, several populated LSs will overlap and the Bose gas will start to form a fragmented BEC. Each fragment will be a superposition of LSs, and its shape will be modified by the interactions.

Although both $\mathcal{N}_{2L}$ and $\nu^{\max}$ may have complex dependencies versus V_R, σ_R and the model of disorder, general properties can be obtained using scaling arguments. We write the single-particle equation as

$$(\epsilon_\nu/V_R)\varphi_\nu(u) = -\alpha_R \partial_u^2 \varphi_\nu(u) + v(u)\varphi_\nu(u), \tag{10}$$

where $u = z/\sigma_R$, $\varphi_\nu(u) = \sqrt{\sigma_R}\chi_\nu(z)$ and $\alpha_R = \hbar^2/2m\sigma_R^2 V_R$. Thus, all characteristics of the spectrum depend only on the parameter α_R after renormalization of energies and lengths. Scaling arguments show that in the Lifshits tail

$$\mathcal{N}_{2L}(\epsilon) = (L/\sigma_R)\zeta(\alpha_R, \epsilon/V_R) \quad \text{and} \quad \nu^{\max} = (L/\sigma_R)\eta(\alpha_R), \tag{11}$$

where ζ and η are v-dependent functions. Finally, inserting these expressions into Eq. (9) and solving formally, we obtain the validity condition of the Lifshits regime:

$$\mu \leq V_R F(\alpha_R), \tag{12}$$

where F is the solution of $\zeta[\alpha_R, F(\alpha_R)] = \eta(\alpha_R)$, which can be computed numerically, for example.

We are now able to draw the schematic quantum-state diagram of the zero-temperature Bose gas as a function of μ and V_R (see Fig. 1). From the discussion above, it is clearly fruitful to fix the parameter α_R while varying V_R. The boundaries between the various regimes (Lifshits, fragmented BEC, BEC, and smoothed BEC) result from the competition between the interactions and the disorder and are given by Eqs. (3), (5), and (12). We stress that they are crossovers rather than phase transitions. Interestingly, all these boundaries are straight lines with slopes depending on the parameter α_R. This is clear from Eq. (12) for the boundary between the Lifshits and the fragmented regimes. In addition, since $V_R = (\hbar^2/2m\sigma_R^2)/\alpha_R$, the nonsmoothing condition (3) reduces to $\mu \gg \alpha_R V_R$. Finally, since $\mu = \hbar^2/2m\xi^2$ and thus $\sigma_R/\xi = \frac{1}{\sqrt{\alpha_R}}\sqrt{\mu/V_R}$, the nonfragmented BEC condition (5) also corresponds to a straight line α_R in Fig. 1.

To finish with, we derive the equations of state of the Bose gas in the identified quantum states. It is important to relate the chemical potential μ which governs the crossovers between the various regimes to the mean atomic density $\bar{n} = N/2L$ and the coupling constant g. Both can be controlled in experiments with ultracold atoms.

Tight radial confinement.—For $\mu' - \epsilon_\nu \ll \hbar\omega_\perp$ where $\mu' = \mu - \hbar\omega_\perp$, the radial wave functions are frozen to zero-point oscillations, $\phi_\nu(\rho) = \exp(-\rho^2/2l_\perp^2)/\sqrt{\pi} l_\perp$ with $l_\perp = \sqrt{\hbar/m\omega_\perp}$ the width of the radial oscillator.

In the BEC regime, $\mu' \gg \Delta\tilde{V}$, we find from Eq. (2),

$$\mu' = \bar{n} g. \tag{13}$$

In the Lifshits regime, we find

$$N_\nu = [\mu' - \epsilon_\nu]/U_\nu \quad \text{for} \quad \mu' > \epsilon_\nu \quad \text{and} \quad N_\nu = 0 \quad \text{otherwise}, \tag{14}$$

by inserting the above expression for $\phi_\nu(\rho)$ into Eq. (8). Turning to a continuous formulation and using the normalization condition, $N = \int d\epsilon \mathcal{D}_{2L}(\epsilon) N(\epsilon)$, we deduce the equation of state of the Bose gas in the Lifshits regime:

$$Ng = \int_{-\infty}^{\mu'} d\epsilon \mathcal{D}_{2L}(\epsilon)(\mu' - \epsilon) P(\epsilon), \tag{15}$$

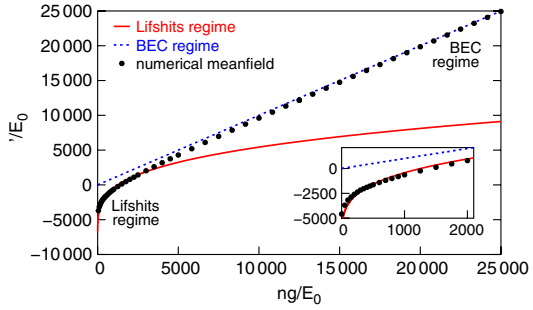

FIG. 3 (color online). Chemical potential of a Bose gas in a speckle potential with the same parameters as in Fig. 2, in the case of a tight radial confinement ($\mu' - \epsilon_\nu \ll \hbar\omega_\perp$). The points are given by numerical calculations; the solid and dotted lines represent the analytical formulas Eqs. (13) and (16) derived for the Lifshits and BEC regime, respectively.

which relates the chemical potential μ' to the coupling constant g. The relation is in general nonuniversal. In the case of a speckle potential, $\mathcal{N}_{2L}(\epsilon) = A(\alpha_R)(L/\sigma_R) \times \exp[-c(\alpha_R)/\sqrt{\epsilon/V_R + 1}]$, and assuming that the participation length $P_\nu = \sigma_R p_\nu(\alpha_R)$ is independent of the energy in the Lifshits tail, we find

$$\tilde{n}g \simeq A(\alpha_R)c^2(\alpha_R)p_0(\alpha_R)V_R\Gamma(-2, c(\alpha_R)/\sqrt{\mu'/V_R + 1}), \tag{16}$$

where Γ is the incomplete gamma function and $A(\alpha_R)$, $c(\alpha_R)$, and $p_0(\alpha_R)$ can be determined numerically.

Using a numerical minimization of the energy functional (7) in the Gross-Pitaevskii formulation, we compute the chemical potential of the Bose gas in a wide range of interactions. The result shown in Fig. 3 indicates a clear crossover from the Lifshits regime to the BEC regime as the interaction strength increases. The numerically obtained chemical potential μ agrees with our analytical formulas in both Lifshits and BEC regimes.

Shallow radial confinement.—The equations of state can also be obtained in the case of shallow radial confinement ($\mu - \epsilon_\nu \gg \hbar\omega_\perp$). In the BEC regime, for $\xi \ll \sigma_R$, we find $\mu \simeq \sqrt{\tilde{n}gm\omega_\perp^2/\pi - V_R^2}$. In the Lifshits regime the 2D wave functions $\phi_\nu(\rho)$ are in the TF regime, $|\phi_\nu(\rho)|^2 = \frac{\mu-\epsilon_\nu}{N_\nu U_\nu}(1 - \rho^2/R_\nu^2)$, where $R_\nu = \sqrt{2(\mu - \epsilon_\nu)/m\omega_\perp^2}$ is the 2D-TF radius and $N_\nu = \pi(\mu - \epsilon_\nu)^2/m\omega_\perp^2 U_\nu$ for $\mu > \epsilon_\nu$ (0 otherwise). Proceeding as in the 1D case, we find

$$Ng = \frac{\pi}{m\omega_\perp^2}\int_{-\infty}^{\mu} d\epsilon \mathcal{D}_{2L}(\epsilon)(\mu - \epsilon)^2 P(\epsilon). \tag{17}$$

Applying this formula to the relevant model of disorder allows us to compute the populations N_ν of the various LSs χ_ν and the corresponding radial extensions ϕ_ν.

In summary, we have presented a complete picture of the quantum states of an interacting Bose gas in the presence of 1D disorder, including the novel description of the weakly interacting Lifshits glass state. We have provided analytical formulas for the boundaries (crossovers) in the quantum-state diagram and shown that they are determined by the coupling constant. Since this coupling constant can be controlled in cold gases, future experiments should be able to explore the whole diagram.

We thank G. Shlyapnikov, L. Santos, D. Gangardt, C. Mora, R. Hulet, and R. Nyman for useful discussions. This work was supported by the French DGA, MENRT, IFRAF, and ANR, the Spanish MEC Programs, DUQUAG, QOIT, and the European Union, QUDEDIS and IP SCALA.

[1] P. W. Anderson, Phys. Rev. **109**, 1492 (1958).
[2] N. F. Mott and W. D. Towes, Adv. Phys. **10**, 107 (1961).
[3] E. Abrahams *et al.*, Phys. Rev. Lett. **42**, 673 (1979).
[4] G. Grynberg *et al.*, Europhys. Lett. **49**, 424 (2000); L. Guidoni *et al.*, Phys. Rev. Lett. **79**, 3363 (1997).
[5] B. Damski *et al.*, Phys. Rev. Lett. **91**, 080403 (2003); R. Roth and K. Burnett, Phys. Rev. A **68**, 023604 (2003).
[6] U. Gavish and Y. Castin, Phys. Rev. Lett. **95**, 020401 (2005); R. C. Kuhn *et al.*, *ibid.* **95**, 250403 (2005).
[7] L. Sanchez-Palencia and L. Santos, Phys. Rev. A **72**, 053607 (2005).
[8] T. Paul *et al.*, Phys. Rev. A **72**, 063621 (2005).
[9] L. Sanchez-Palencia *et al.*, cond-mat/0612670.
[10] V. Ahufinger *et al.*, Phys. Rev. A **72**, 063616 (2005).
[11] J. E. Lye *et al.*, Phys. Rev. Lett. **95**, 070401 (2005).
[12] D. Clément *et al.*, Phys. Rev. Lett. **95**, 170409 (2005).
[13] C. Fort *et al.*, Phys. Rev. Lett. **95**, 170410 (2005).
[14] D. Clément *et al.*, New J. Phys. **8**, 165 (2006).
[15] T. Schulte *et al.*, Phys. Rev. Lett. **95**, 170411 (2005).
[16] L. Fallani *et al.*, Phys. Rev. Lett. **98**, 130404 (2007).
[17] M. P. A. Fisher *et al.*, Phys. Rev. B **40**, 546 (1989); R. T. Scalettar *et al.*, Phys. Rev. Lett. **66**, 3144 (1991).
[18] I. M. Lifshits *et al.*, *Introduction to the Theory of Disordered Systems* (Wiley, New York, 1988).
[19] Here, the TF regime corresponds to a situation where the kinetic energy is negligible compared to the interaction energy; see L. P. Pitaevskii and S. Stringari, *Bose-Einstein Condensation* (Clarendon, Oxford, 2004).
[20] L. Sanchez-Palencia, Phys. Rev. A **74**, 053625 (2006).
[21] J. W. Goodman, in *Statistical Properties of Laser Speckle Patterns*, edited by J.-C. Dainty, Laser Speckle and Related Phenomena (Springer-Verlag, Berlin, 1975).
[22] The random potential $V(z)$ is thus characterized by a typical amplitude V_R and a typical correlation length σ_R.
[23] D. S. Petrov, G. V. Shlyapnikov, and J. T. M. Walraven, Phys. Rev. Lett. **85**, 3745 (2000); **87**, 050404 (2001).
[24] Equation (2) is valid also in the 1D case where $\rho = 0$ [20].
[25] The participation length scales as the width of the wave function and thus decreases for stronger localization.
[26] I. M. Lifshits, Adv. Phys. **13**, 483 (1964); T. P. Eggarter, Phys. Rev. B **5**, 3863 (1972); J. M. Luttinger and H. K. Sy, Phys. Rev. A **7**, 701 (1973).
[27] Similar ansatz have been used in L. S. Cederbaum and A. I Streltsov, Phys. Lett. A **318**, 564 (2003); O. E. Alon and L. S. Cederbaum, Phys. Rev. Lett. **95**, 140402 (2005).

Anderson Localization of Bogolyubov Quasiparticles in Interacting Bose-Einstein Condensates

P. Lugan, D. Clément, P. Bouyer, A. Aspect, and L. Sanchez-Palencia

Laboratoire Charles Fabry de l'Institut d'Optique, CNRS and Univ. Paris-Sud, Campus Polytechnique, RD 128, F-91127 Palaiseau cedex, France

(Received 18 July 2007; published 2 November 2007; corrected 14 November 2007)

We study the Anderson localization of Bogolyubov quasiparticles in an interacting Bose-Einstein condensate (with a healing length ξ) subjected to a random potential (with a finite correlation length σ_R). We derive analytically the Lyapunov exponent as a function of the quasiparticle momentum k, and we study the localization maximum $k_{\max}$. For 1D speckle potentials, we find that $k_{\max} \propto 1/\xi$ when $\xi \gg \sigma_R$ while $k_{\max} \propto 1/\sigma_R$ when $\xi \ll \sigma_R$, and that the localization is strongest when $\xi \sim \sigma_R$. Numerical calculations support our analysis, and our estimates indicate that the localization of the Bogolyubov quasiparticles is accessible in experiments with ultracold atoms.

DOI: 10.1103/PhysRevLett.99.180402 PACS numbers: 05.30.Jp, 03.75.Hh, 64.60.Cn, 79.60.Ht

An important issue in mesoscopic physics concerns the effects of disorder in systems where both quantum interference and particle-particle interactions play crucial roles. Multiple scattering of noninteracting quantum particles from a random potential leads to strong Anderson localization (AL) [1], characterized by an exponential decay of the quantum states over a typical distance, the localization length. AL occurs for arbitrarily weak disorder in 1D and 2D, and for strong-enough disorder in 3D [2]. The problem is more involved in the presence of interactions. Strong disorder in repulsively interacting Bose gases induces novel insulating quantum states, such as the Bose [3] and Lifshits [4] glasses. For moderate disorder and interactions, the system forms a Bose-Einstein condensate (BEC) [4–6], where the disorder induces a depletion of the condensed and superfluid fractions [7] and the shift and damping of sound waves [8].

These studies have direct applications to experiments on liquid ^{4}He in porous media [9], in particular as regards the understanding of the absence of superfluidity. Moreover, the realization of disordered gaseous BECs [10–14] has renewed the issue due to an unprecedented control of the experimental parameters. Using optical speckle fields [15], for instance, one can control the amplitude and design the correlation function of the random potential almost at will [14], opening possibilities for experimental studies of AL [16,17]. Earlier studies related to localization in the context of ultracold atoms include dynamical localization in δ-kicked rotors [18] and spatial diffusion of laser-cooled atoms in speckle potentials [19].

Transport processes in repulsively interacting BECs can exhibit AL [17,20]. However, for BECs at equilibrium, interaction-induced delocalizing effects dominate disorder-induced localization, except for very weak interactions [5,6]. The ground state of an interacting BEC at equilibrium is thus extended. Beyond, one may wonder how the many-body (collective) excitations of the BEC behave in weak disorder. In dilute BECs, these excitations correspond to quasiparticles (particle-hole pairs) described by the Bogolyubov theory [21]. In this case, the interplay of interactions and disorder is subtle, and strong arguments indicate that the Bogolyubov quasiparticles (BQP) experience a random potential *screened* by the BEC density [5]. This problem has been addressed in the idealized case of uncorrelated disorder (random potentials with a delta correlation function) in Ref. [22].

In this Letter, we present a general quantitative treatment of the localization of the BQPs in an interacting BEC with healing length ξ in a weak random potential with arbitrary correlation length σ_R. For weak disorder, we introduce a transformation that maps rigorously the many-body Bogolyubov equations onto the Schrödinger equation for a noninteracting particle in a screened random potential, which we derive analytically. We calculate the Lyapunov exponent Γ_k (inverse localization length) as a function of the BQP wave number k for 1D speckle potentials. For a given ratio ξ/σ_R, we determine the wave number $k_{\max}$ for which Γ_k is maximum: We find $k_{\max} \sim 1/\xi$ for $\xi \gg \sigma_R$, and $k_{\max} \sim 1/\sigma_R$ for $\xi \ll \sigma_R$. The absolute maximum appears for $\xi \sim \sigma_R$ so that the finite-range correlations of the disorder need to be taken into account. Numerical calculations support our analysis. Finally, possibilities to observe the AL of BQPs in BECs placed in speckle potentials are discussed.

We consider a d-dimensional Bose gas in a potential $V(\mathbf{r})$ with weak repulsive short-range atom-atom interactions, characterized by the coupling constant g. Its physics is governed by the many-body Hamiltonian

$$\hat{H} = \int d\mathbf{r}\{(\hbar^2/2m)[(\nabla\hat{\theta})^2\hat{n} + (\nabla\sqrt{\hat{n}})^2] + V(\mathbf{r})\hat{n} + (g/2)\hat{n}^2 - \mu\hat{n}\} \quad (1)$$

where m is the atomic mass, μ is the chemical potential, and $\hat{\theta}$ and $\hat{n}$ are the phase and density operators, which obey the commutation relation $[\hat{n}(\mathbf{r}), \hat{\theta}(\mathbf{r}')] = i\delta(\mathbf{r} - \mathbf{r}')$. According to the Bogolyubov-Popov theory [21,23,24], for small phase gradients ($\hbar^2|\nabla\theta|^2/2m \ll \mu$) and small density fluctuations ($\delta\hat{n} \ll n_c$, where $n_c = \langle\hat{n}\rangle$ and $\delta\hat{n} = \hat{n} - n_c$), Hamiltonian (1) can be diagonalized up to second

order as $\hat{H} = E_0 + \sum_\nu \epsilon_\nu \hat{b}_\nu^\dagger \hat{b}_\nu$, where $\hat{b}_\nu$ is the annihilation operator of the excitation (BQP) of energy ϵ_ν. The many-body ground state of the Bose gas is a BEC with a uniform phase and a density governed by the Gross-Pitaevskii equation (GPE):

$$\mu = -\hbar^2\nabla^2(\sqrt{n_c})/2m\sqrt{n_c} + V(\mathbf{r}) + g n_c(\mathbf{r}). \quad (2)$$

Expanding the density and phase in the basis of the excitations, $\hat{\theta}(\mathbf{r}) = [-i/2\sqrt{n_c(\mathbf{r})}]\sum_\nu [f_\nu^+(\mathbf{r})\hat{b}_\nu - \text{H.c.}]$ and $\delta\hat{n}(\mathbf{r}) = \sqrt{n_c(\mathbf{r})}\sum_\nu [f_\nu^-(\mathbf{r})\hat{b}_\nu + \text{H.c.}]$, the Hamiltonian reduces to the above diagonal form provided that $f_\nu^\pm$ obey the Bogolyubov–de Gennes equations (BdGE) [25]:

$$[-(\hbar^2/2m)\nabla^2 + V + g n_c - \mu] f_\nu^+ = \epsilon_\nu f_\nu^- \quad (3)$$

$$[-(\hbar^2/2m)\nabla^2 + V + 3g n_c - \mu] f_\nu^- = \epsilon_\nu f_\nu^+, \quad (4)$$

with the normalization $\int d\mathbf{r}\, [f_\nu^+ f_{\nu'}^{-*} + f_\nu^- f_{\nu'}^{+*}] = 2\delta_{\nu,\nu'}$. Equations (2)–(4) form a complete set to calculate the ground state (BEC) and excitations (BQPs) of the Bose gas, from which one can compute all properties of finite temperature or time-dependent BECs.

Here, we analyze the properties of the BQPs in the presence of weak disorder. According to Eqs. (3) and (4), they are determined by the interplay of the disorder V and the BEC density background n_c. Let $V(\mathbf{r})$ be a weak random potential ($\tilde{V} \ll \mu$, see below) with a vanishing average and a finite-range correlation function, $C(\mathbf{r}) = V_R^2 c(\mathbf{r}/\sigma_R)$, where $V_R = \sqrt{\langle V^2 \rangle}$ is the standard deviation, and σ_R the correlation length of V. As shown in Refs. [4–6], the BEC density profile is extended for strong-enough repulsive interactions (i.e., for $\xi \ll L$, where $\xi = \hbar/\sqrt{4m\mu}$ is the healing length and L the size of the BEC). More precisely, up to first order in V_R/μ, the GPE (2) yields

$$n_c(\mathbf{r}) = [\mu - \tilde{V}(\mathbf{r})]/g \quad (5)$$

where $\tilde{V}(\mathbf{r}) = \int d\mathbf{r}' G_\xi(\mathbf{r} - \mathbf{r}') V(\mathbf{r}')$, and G_ξ, the Green function of the linearized GPE [4,6], reads $G_\xi(\mathbf{q}) = (2\pi)^{-d/2}/[1 + (|\mathbf{q}|\xi)^2]$ in Fourier space [26]. Then,

$$\tilde{V}(\mathbf{q}) = V(\mathbf{q})/[1 + (|\mathbf{q}|\xi)^2]. \quad (6)$$

Thus, ξ is a threshold in the response of the density n_c to the potential V, as $\tilde{V}(\mathbf{q}) \simeq V(\mathbf{q})$ for $|\mathbf{q}| \ll \xi^{-1}$, while $\tilde{V}(\mathbf{q}) \ll V(\mathbf{q})$ for $|\mathbf{q}| \gg \xi^{-1}$. The potential $\tilde{V}(\mathbf{r})$ is a smoothed potential [6]. If V is a homogeneous random potential, so is $\tilde{V}$, and according to Eq. (5), the BEC density profile n_c is random but extended [4,6].

Solving the BdGEs (3) and (4) is difficult in general because they are strongly coupled. Yet, we show that for a weak (possibly random) potential $V(\mathbf{r})$, this hurdle can be overcome by using appropriate linear combinations $g_\mathbf{k}^\pm$ of the $f_\mathbf{k}^\pm$ functions, namely $g_\mathbf{k}^\pm = \pm\rho_k^{\pm 1/2} f_\mathbf{k}^+ + \rho_k^{\mp 1/2} f_\mathbf{k}^-$, with $\rho_k = \sqrt{1 + 1/(k\xi)^2}$ and $k = |\mathbf{k}|$. For $V = 0$, the equations for $g_\mathbf{k}^\pm$ are uncoupled [see Eqs. (7) and (8)] and we recover the usual plane-wave solutions of wave vector $\mathbf{k}$ and energy $\epsilon_k = \rho_k(\hbar^2k^2/2m)$ [21]. For weak but finite V, inserting Eq. (5) into Eqs. (3) and (4), we find

$$\frac{\hbar^2k^2}{2m} g_\mathbf{k}^+ = -\frac{\hbar^2}{2m}\nabla^2 g_\mathbf{k}^+ - \frac{2\rho_k \tilde{V}}{1+\rho_k^2} g_\mathbf{k}^- + \left[V - \frac{3+\rho_k^2}{1+\rho_k^2}\tilde{V}\right] g_\mathbf{k}^+ \quad (7)$$

$$-\rho_k^2 \frac{\hbar^2k^2}{2m} g_\mathbf{k}^- = -\frac{\hbar^2}{2m}\nabla^2 g_\mathbf{k}^- - \frac{2\rho_k \tilde{V}}{1+\rho_k^2} g_\mathbf{k}^+ + \left[V - \frac{1+3\rho_k^2}{1+\rho_k^2}\tilde{V}\right] g_\mathbf{k}^-. \quad (8)$$

Equations (7) and (8), which are coupled at most by a term of the order of V [since $|\tilde{V}| \le |V|$ and $2\rho_k/(1+\rho_k^2) \le 1$], allow for perturbative approaches. Note that the functions $g_\mathbf{k}^+$ and $g_\mathbf{k}^-$ have very different behaviors owing to the signs in the left-hand side terms in Eqs. (7) and (8). Equation (8) can be solved to the lowest order in $\tilde{V}_R/\mu$ with a Green kernel defined in Ref. [6]: we find $g_\mathbf{k}^-(\mathbf{r}) \simeq \frac{2/\epsilon_k}{1+\rho_k^2} \times \int d\mathbf{r}' G_{\xi_k}(\mathbf{r} - \mathbf{r}')\tilde{V}(\mathbf{r}')g_\mathbf{k}^+(\mathbf{r}')$, where $\xi_k = \xi/\sqrt{1 + (k\xi)^2}$. Equation (7) cannot be solved using the same method because the perturbation series diverges. Nevertheless, from the solution for $g_\mathbf{k}^-$, we find that $|g_\mathbf{k}^-/g_\mathbf{k}^+| \lesssim \frac{2/\epsilon_k}{1+\rho_k^2}|\tilde{V}| < |\tilde{V}|/\mu \ll 1$. The coupling term in Eq. (7) can thus be neglected to first order in $\tilde{V}_R/\mu$, and we are left with the closed equation

$$-(\hbar^2/2m)\nabla^2 g_\mathbf{k}^+ + \mathcal{V}_k(\mathbf{r}) g_\mathbf{k}^+ \simeq (\hbar^2k^2/2m) g_\mathbf{k}^+, \quad (9)$$

where

$$\mathcal{V}_k(\mathbf{r}) = V(\mathbf{r}) - \frac{1 + 4(k\xi)^2}{1 + 2(k\xi)^2}\tilde{V}(\mathbf{r}). \quad (10)$$

Equation (9) is formally equivalent to a Schrödinger equation for noninteracting bare particles with energy $\hbar^2k^2/2m$, in a random potential $\mathcal{V}_k(\mathbf{r})$. This mapping allows us to find the localization properties of the BQPs using standard methods for bare particles in 1D, 2D, or 3D [27]. However, since $\mathcal{V}_k(\mathbf{r})$ depends on the wave vector $\mathbf{k}$ itself, the localization of the BQPs is dramatically different from that of bare particles as discussed below.

In the remainder of the Letter, we restrict ourselves to the 1D case, for simplicity, but also because AL is expected to be stronger in lower dimensions [2]. The Lyapunov exponent Γ_k is a self-averaging quantity in infinite 1D systems, which can be computed in the Born approximation using the phase formalism [27] (see also Ref. [17]). We get $\Gamma_k = (\sqrt{2\pi}/8)(2m/\hbar^2k)^2 \mathcal{C}_k(2k)$, where $\mathcal{C}_k(q)$ is the Fourier transform of the correlation function of $\mathcal{V}_k(z)$, provided that $\Gamma_k \ll k$ [16,17,27]. Since $\mathcal{C}_k(q) \propto \langle|\mathcal{V}_k(q)|^2\rangle$, the component of $\mathcal{V}_k$ relevant for the calculation of Γ_k is $\mathcal{V}_k(2k)$. From Eqs. (6) and (10), we find

$$\mathcal{V}_k(2k) = \mathcal{S}(k\xi)V(2k); \qquad \mathcal{S}(k\xi) = \frac{2(k\xi)^2}{1+2(k\xi)^2}, \quad (11)$$

and the Lyapunov exponent of the BQP reads

$$\Gamma_k = [\mathcal{S}(k\xi)]^2\gamma_k \quad (12)$$

where $\gamma_k = (\sqrt{2\pi}/32)(V_R/\mu)^2(\sigma_R/k^2\xi^4)c(2k\sigma_R)$ is the Lyapunov exponent for a bare particle with the same wave number k [17,27].

Let us summarize the validity conditions of the perturbative approach presented here. It requires (i) the smoothing solution (5) to be valid (i.e., $\tilde{V}_R \ll \mu$), (ii) the coupling term proportional to g_k^- in Eq. (7) to be negligible (which is valid if $\tilde{V}_R \ll \mu$), and (iii) the phase formalism to be applicable. The latter requires $\Gamma_k \ll k$, i.e., $(V_R/\mu)\times(\sigma_R/\xi)^{1/2} \ll (k\xi)^{3/2}[1+1/2(k\xi)^2]$, which is valid for any k if $(V_R/\mu)(\sigma_R/\xi)^{1/2} \ll 1$.

Applying Eq. (12) to uncorrelated potentials [$C(z) = 2D\delta(z)$ with $\sigma_R \to 0$, $V_R \to \infty$ and $2D = V_R^2\sigma_R \int dx c(x) = cst$], one recovers the formula for Γ_k found in Ref. [22]. Our approach generalizes this result to potentials with finite-range correlations, which proves useful since uncorrelated random potentials are usually crude approximations of realistic disorder, for which σ_R can be significantly large. We show below that if $\xi \lesssim \sigma_R$, as, e.g., in the experiments of Refs. [10–14], the behavior of Γ_k versus k is dramatically affected by the finite-range correlations of the disorder.

Let us discuss the physical content of Eqs. (9) and (10). According to Eqs. (3) and (4), the properties of the BQPs are determined by both the bare random potential V and the BEC density n_c in a nontrivial way. Equation (9) makes their roles more transparent. As the occurrence of the smoothed potential $\tilde{V}(z)$ in Eq. (10) is reminiscent of the presence of the meanfield interaction gn_c in the BdGEs (3) and (4), it appears that the random potential $\mathcal{V}_k(z)$ results from the *screening* of the random potential $V(z)$ by the BEC density background [5]. More precisely, the expression (11) for the Fourier component $\mathcal{V}_k(2k)$, relevant for the Lyapunov exponent of a BQP, shows that the screening strength depends on the wave number k. In the *free-particle regime* ($k \gg 1/\xi$), we find that the Lyapunov exponent of a BQP equals that of a bare particle with the same wave number ($\Gamma_k \simeq \gamma_k$), as expected. In the *phonon regime* ($k \ll 1/\xi$), the disorder is strongly screened, and we find $\Gamma_k \ll \gamma_k$, as in models of elastic media [28]. Here, the localization of a BQP is strongly suppressed by the repulsive atom-atom interactions, as compared to a bare particle in the same bare potential. These findings agree with and generalize the results obtained from the transfer matrix method, which applies to potentials made of a 1D random series of δ-scatterers [22].

Our approach applies to any weak random potential with a finite correlation length. We now further examine the case of 1D speckle potentials used in quantum gases [10–14]. Inserting the corresponding reduced correlation functions, $c(\kappa) = \sqrt{\pi/2}(1-\kappa/2)\Theta(1-\kappa/2)$ where Θ is the Heaviside function [17], into Eq. (12), we find

$$\Gamma_k = \frac{\pi}{8}\left(\frac{V_R}{\mu}\right)^2 \frac{\sigma_R k^2(1-k\sigma_R)}{[1+2(k\xi)^2]^2}\Theta(1-k\sigma_R) \quad (13)$$

which is plotted in Fig. 1. To test our general approach on the basis of this example, we have performed numerical calculations using a direct integration of the BdGEs (3) and (4) in a finite but large box of size L. The Lyapunov exponents are extracted from the asymptotic behavior of $\log[r_k(z)/r_k(z_k)]/|z-z_k|$, where z_k is the localization center and $r_k(z)$ is the envelope of the function g_k^+, obtained numerically. The numerical data, averaged over 40 realizations of the disorder, are in excellent agreement with formula (13) as shown in Fig. 2. These results validate our approach. It should be noted, however, that our numerical calculations return BQP wave functions that can be strongly localized for very small momenta k. This will be discussed in more details in a future publication [29].

Of special interest are the maxima of Γ_k, which denote a maximum localization of the BQPs. It is straightforward to show that, for a fixed set of parameters $(V_R/\mu, \xi, \sigma_R)$, Γ_k is nonmonotonic and has a single maximum, $k_{\max}$, in the range $[0, 1/\sigma_R]$ (see Fig. 2). This contrasts with the case of bare particles, for which the Lyapunov exponent γ_k decreases monotonically as a function of k, provided that $c(2k\sigma_R)$ decreases versus k (which is valid for a broad class of random potentials [27]). The existence of a localization maximum with respect to the wave number k is thus specific to the BQPs and results from the strong screening of the disorder in the phonon regime. In general, the value of $k_{\max}$, plotted in the inset of Fig. 2 versus the correlation length of the disorder, depends on both ξ and σ_R. For $\sigma_R \ll \xi$, we find $k_{\max} \simeq \frac{1}{\sqrt{2}\xi}(1-\frac{\sigma_R/\xi}{2\sqrt{2}})$, so that the localization is maximum near the crossover between the phonon and the free-particle regimes as for uncorrelated potentials [22]. For $\sigma_R \gg \xi$, however, we find $k_{\max} \simeq 2/3\sigma_R$ so that $k_{\max}$ is no longer determined by the healing length but rather by the correlation length of the disorder, and lies deep in the phonon regime. For $k > 1/\sigma_R$, Γ_k vanishes. This defines an *effective mobility edge* due to long-range

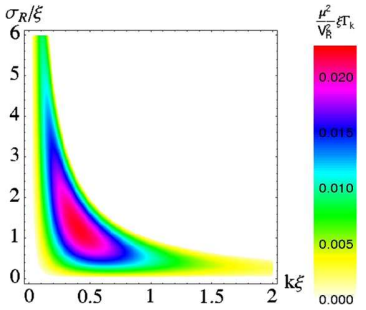

FIG. 1 (color online). Density plot of the Lyapunov exponent of the BQPs for a 1D speckle potential.

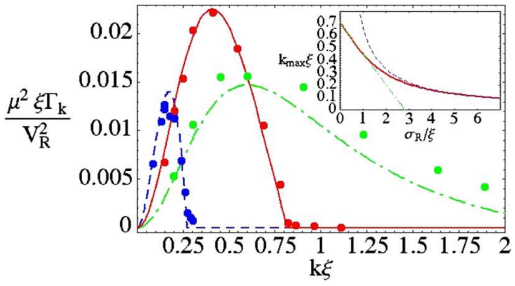

FIG. 2 (color online). Lyapunov exponent of the BQPs for a 1D speckle potential. The lines correspond to Eq. (13), and the points to numerical results for $\xi = 1.25 \times 10^{-5} L$, $V_R = 0.075\mu$, and $\sigma_R = \sqrt{3/2}\xi$ (solid line), $\sigma_R = 3.7\xi$ (dashed line), $\sigma_R = 0.4\xi$ (dash-dotted line). Inset: localization maximum versus the ratio of the correlation length of the disorder to the healing length of the BEC (the dash-dotted and dashed lines correspond to the limits $\sigma_R \ll \xi$ and $\sigma_R \gg \xi$ respectively; see text).

correlations in speckle potentials, as for bare particles [17,30].

Finally, let us determine the absolute localization maximum. The Lyapunov exponent Γ_k decreases monotonically versus ξ and V_R/μ. However, for fixed values of V_R/μ and ξ, Γ_k has a maximum at $\sigma_R = \sqrt{3/2}\xi$ and $k = \xi^{-1}/\sqrt{6}$ (see Fig. 1), and we find the corresponding localization length ($L_{\max} = 1/\Gamma_{\max}$):

$$L_{\max}(\xi) = (512\sqrt{6}/9\pi)(\mu/V_R)^2\xi. \qquad (14)$$

At the localization maximum, we have $\sigma_R \sim \xi$ so that the disorder cannot be modeled by an uncorrelated potential, and the long-range correlations must be accounted for as in our approach. For $\sigma_R = 0.3\ \mu$m [14] and $V_R = 0.2\ \mu$, we find $L_{\max} \simeq 280\ \mu$m, which can be smaller than the system size in disordered, ultracold gases [11,14,31].

In conclusion, we have presented a general treatment for the AL of BQPs in an interacting BEC subjected to a random potential with finite-range correlations. We have calculated the Lyapunov exponents for a 1D speckle potential, and we have shown that the localization is strongest when $\sigma_R \sim \xi$. We have found that the localization length can be smaller than the size of the BEC for experimentally accessible parameters. We expect that the AL of BQPs could be observed directly, for instance as a broadening of the resonance lines in Bragg spectroscopy, a well mastered technique in gaseous BECs [32].

We thank M. Lewenstein, G. Shlyapnikov, S. Stringari, and W. Zwerger for stimulating discussions during the Workshop on Quantum Gases at the Institut Henri Poincaré—Centre Emile Borel. This work was supported by the French DGA, MENRT and ANR, and the ESF QUDEDIS program. The Atom Optics group at LCFIO is a member of the Institut Francilien de Recherche sur les Atomes Froids (IFRAF).

[1] P. W. Anderson, Phys. Rev. **109**, 1492 (1958).
[2] E. Abrahams *et al.*, Phys. Rev. Lett. **42**, 673 (1979).
[3] T. Giamarchi and H. J. Schulz, Phys. Rev. B **37**, 325 (1988); M. P. A. Fisher *et al.*, *ibid.* **40**, 546 (1989); R. T. Scalettar *et al.*, Phys. Rev. Lett. **66**, 3144 (1991); S. Rapsch *et al.*, Europhys. Lett. **46**, 559 (1999).
[4] P. Lugan *et al.*, Phys. Rev. Lett. **98**, 170403 (2007).
[5] D. K. K. Lee and J. M. F. Gunn, J. Phys. Condens. Matter **2**, 7753 (1990).
[6] L. Sanchez-Palencia, Phys. Rev. A **74**, 053625 (2006).
[7] K. Huang and H. F. Meng, Phys. Rev. Lett. **69**, 644 (1992); K. G. Singh and D. S. Rokhsar, Phys. Rev. B **49**, 9013 (1994); G. E. Astrakharchik *et al.*, Phys. Rev. A **66**, 023603 (2002).
[8] L. Zhang, Phys. Rev. B **47**, 14364 (1993); S. Giorgini, L. Pitaevskii, and S. Stringari, *ibid.* **49**, 12938 (1994).
[9] J. D. Reppy, J. Low Temp. Phys. **87**, 205 (1992).
[10] J. E. Lye *et al.*, Phys. Rev. Lett. **95**, 070401 (2005).
[11] D. Clément *et al.*, Phys. Rev. Lett. **95**, 170409 (2005).
[12] C. Fort *et al.*, Phys. Rev. Lett. **95**, 170410 (2005).
[13] T. Schulte *et al.*, Phys. Rev. Lett. **95**, 170411 (2005).
[14] D. Clément *et al.*, New J. Phys. **8**, 165 (2006).
[15] J. W. Goodman, in *Statistical Properties of Laser Speckle Patterns*, edited by J.-C. Dainty, Laser Speckle and Related Phenomena (Springer-Verlag, Berlin, 1975).
[16] R. C. Kuhn *et al.*, Phys. Rev. Lett. **95**, 250403 (2005); R. C. Kuhn *et al.*, New J. Phys. **9**, 161 (2007).
[17] L. Sanchez-Palencia *et al.*, Phys. Rev. Lett. **98**, 210401 (2007).
[18] R. Graham *et al.*, Phys. Rev. A **45**, R19 (1992); F. L. Moore *et al.*, Phys. Rev. Lett. **73**, 2974 (1994).
[19] P. Horak *et al.*, Phys. Rev. A **58**, 3953 (1998); G. Grynberg *et al.*, Europhys. Lett. **49**, 424 (2000).
[20] T. Paul *et al.*, Phys. Rev. Lett. **98**, 210602 (2007).
[21] N. N. Bogolyubov, J. Phys. (USSR) **11**, 23 (1947); Sov. Phys. JETP **7**, 41 (1958).
[22] N. Bilas and N. Pavloff, Eur. Phys. J. D **40**, 387 (2006).
[23] V. N. Popov, Theor. Math. Phys. (Engl. Transl.) **11**, 565 (1972); *Functional Integrals in Quantum Field Theory and Statistical Physics* (Reidel, Dordrecht, 1983).
[24] D. S. Petrov, G. V. Shlyapnikov, and J. T. M. Walraven, Phys. Rev. Lett. **85**, 3745 (2000); **87**, 050404 (2001).
[25] P.-G. de Gennes, *Superconductivity of Metals and Alloys* (Benjamin, New York, 1966).
[26] Here, we define $G_\xi(\mathbf{q}) = \int \frac{d\mathbf{r}}{(2\pi)^{d/2}} G_\xi(\mathbf{r}) \exp(-i\mathbf{q}\cdot\mathbf{r})$.
[27] I. M. Lifshits *et al.*, *Introduction to the Theory of Disordered Systems* (Wiley, New York, 1988).
[28] K. Ishii, Prog. Theor. Phys., Suppl. **53**, 77 (1973).
[29] P. Lugan *et al.* (to be published).
[30] Beyond the Born approximation, Γ_k and γ_k may not strictly vanish for $k > 1/\sigma_R$. However, the localization length can be several orders of magnitude larger than the system size in studies of quantum gases [17].
[31] One-millimeter-long disordered BECs have been produced at Rice University; R. Hulet and Y. Chen (private communication).
[32] D. M. Stamper-Kurn *et al.*, Phys. Rev. Lett. **83**, 2876 (1999); J. Steinhauer *et al.*, *ibid.* **90**, 060404 (2003); S. Richard *et al.*, *ibid.* **91**, 010405 (2003).

Localization of Bogoliubov quasiparticles in interacting Bose gases with correlated disorder

P. Lugan[1,2] and L. Sanchez-Palencia[1]

[1]*Laboratoire Charles Fabry de l'Institut d'Optique, CNRS and Univ. Paris-Sud, Campus Polytechnique, RD 128, F-91127 Palaiseau cedex, France*

[2]*Physikalisches Institut, Albert-Ludwigs-Universität, Hermann-Herder Strasse 3, D-79104 Freiburg, Germany*

(Received 3 May 2011; published 22 July 2011)

We study the Anderson localization of Bogoliubov quasiparticles (elementary many-body excitations) in a weakly interacting Bose gas of chemical potential μ subjected to a disordered potential V. We introduce a general mapping (valid for weak inhomogeneous potentials in any dimension) of the Bogoliubov–de Gennes equations onto a single-particle Schrödinger-like equation with an effective potential. For disordered potentials, the Schrödinger-like equation accounts for the scattering and localization properties of the Bogoliubov quasiparticles. We derive analytically the localization lengths for correlated disordered potentials in the one-dimensional geometry. Our approach relies on a perturbative expansion in V/μ, which we develop up to third order, and we discuss the impact of the various perturbation orders. Our predictions are shown to be in very good agreement with direct numerical calculations. We identify different localization regimes: For low energy, the effective disordered potential exhibits a strong screening by the quasicondensate density background, and localization is suppressed. For high-energy excitations, the effective disordered potential reduces to the bare disordered potential, and the localization properties of quasiparticles are the same as for free particles. The maximum of localization is found at intermediate energy when the quasicondensate healing length is of the order of the disorder correlation length. Possible extensions of our work to higher dimensions are also discussed.

DOI: 10.1103/PhysRevA.84.013612 PACS number(s): 03.75.Hh, 05.30.Jp, 64.60.Cn, 79.60.Ht

I. INTRODUCTION

Disorder in ultracold quantum gases is attracting a growing interest due to unprecedented possibilities of controlling disorder and atom-atom interactions for bosons, fermions, or mixtures of atomic species created in one-, two-, or three-dimensional traps [1–4]. So far much attention has been devoted to studies of the disorder-induced damping of motion in Bose [5–10] and Fermi [11] gases, classical localization [12–20], spatial diffusion [19–25], and Anderson localization in regimes where interactions can be neglected [18,21,24,26–39]. The effects of disorder in interacting quantum systems have also been studied in a variety of contexts, such as transport in weakly interacting Bose-Einstein condensates [40–48], interacting Bose gases at equilibrium [26,49–72], strongly interacting Fermi gases [73–76], and coupled two-component gases [77–83].

The interplay of disorder and interactions in quantum systems is an issue of fundamental importance to understand the behaviors of superfluid ^{4}He in porous media [84–88], dirty superconductors [89–93], and ultracold gases in optical disorder [55,66–68,70]. Although a number of questions are open, in particular regarding the fate of Anderson localization, general behaviors can be found in various situations. For instance, weak repulsive interactions in a Bose gas at zero temperature in a disordered potential generally lead to delocalization [53,60,63,94]: In the absence of interactions, all bosons condense into the single-particle ground state, which is localized [95]. This kind of N-body Fock state is highly unstable in an infinite system where an infinity of spatially-separated single-particle states coexist at arbitrarily close energies [96]. Then, for weak repulsive interactions, the Bose gas fragments into a number of low-energy, localized single-particle states, so as to minimize the interaction energy [53,60,63]. The Bose gas forms a gapless compressible insulating phase, known as the Bose glass [94,97–103]. For increasing mean-field interactions, the fragments merge and form a single extended condensate, which restores superfluidity [53,60,63,104–108]. Finally, in the strongly interacting regime, repulsive interactions can finally destroy again superfluidity, forming Tonks-Girardeau gases in 1D [99,109–111] or disordered Mott insulators in lattice gases [100–102].

The above results lead to the conclusion that, at zero temperature where only the ground state plays a role, repulsive interactions destroy Anderson localization in Bose gases for moderate interaction strengths that are compatible with the mean-field approach [53,94,104]. At nonzero temperature however, important properties, such as the correlation functions, phase coherence, and long-range order [105,112], are determined by the excitations of the Bose gas, which are populated thermally. It is thus of prime importance to determine how disorder affects the behavior of the latter. These excitations of the many-body system are of collective nature. They can be viewed as quasiparticles, scattering on the disordered potential. In contrast to the mean-field background, which is extended, the Bogoliubov quasiparticles of a weakly interacting Bose gas can be localized in the presence of a disordered potential [51,54,58,71,72].

In this paper, following the approach of Ref. [54], we present a detailed theory of the Anderson localization of Bogoliubov quasiparticles in weakly interacting Bose gases subjected to correlated disordered potentials. On the one hand, this approach applies to any kind of weak disordered potentials with short- or long-range correlations and offers a unified theory valid all along the crossover from the phonon regime to the free particle regime. On the other hand, it permits a straightforward interpretation of the effect of repulsive interactions in terms of a screening of the disorder by the density background. In Sec. II, the grand-canonical Hamiltonian of the interacting many-body system is expanded up to second order in phase and

density fluctuations. The reduced Hamiltonian is quadratic and can be diagonalized by following the standard Bogoliubov-Popov approach. The excitations are the solutions of the Bogoliubov–de Gennes equations, which consist in a set of two coupled differential equations of order two. In Sec. III, we then introduce a general mapping, valid for weak inhomogeneous potentials in any dimension, of the Bogoliubov–de Gennes equations onto a single-particle Schrödinger-like equation with a screened potential. For disordered potentials, the effective Schrödinger-like equation describes the scattering and localization properties of the Bogoliubov quasiparticles. In Sec. IV, we apply this approach to study the Anderson localization of Bogoliubov quasiparticles in one-dimensional disorder. We derive analytical formulas for the localization length of the Bogoliubov quasiparticles up to third order in perturbation theory and compare our predictions to direct numerical calculations. Our results exhibit different localization regimes: For low energy, the effective disordered potential accounts for a strong screening by the quasicondensate density background and Anderson localization is suppressed. For high energy excitations, the screening is small; the effective disordered potential reduces to the bare disordered potential and the localization properties of quasiparticles are the same as for free particles. The maximum of localization is found at intermediate energy when the quasicondensate healing length is of the order of the disorder correlation length. Finally, in Sec. V, we summarize our results and discuss possible extensions of our work, in particular toward higher dimensions.

II. ELEMENTARY (BOGOLIUBOV) EXCITATIONS IN A BOSE GAS WITH WEAK DENSITY FLUCTUATIONS

We consider a d-dimensional, ultracold, dilute gas of bosons with weak repulsive interactions, in a potential $V(\mathbf{r})$. The system is described by the grand-canonical Hamiltonian

$$\begin{aligned}\hat{K} &= \hat{H} - \mu\hat{N} \\ &= \int d\mathbf{r}\left\{\frac{\hbar^2}{2m}[(\nabla\hat{\theta})^2\hat{n} + (\nabla\sqrt{\hat{n}})^2]\right. \\ &\quad \left. + V(\mathbf{r})\hat{n} + \frac{g}{2}\hat{n}^2 - \mu\hat{n}\right\}, \end{aligned} \tag{1}$$

where the short-range atom-atom interactions are modeled by a contact potential with coupling constant $g > 0$, m is the atomic mass, $\hat{n}$ and $\hat{\theta}$ are the density and phase operators, which satisfy the commutation relation $[\hat{n}(\mathbf{r}),\hat{\theta}(\mathbf{r}')] = \mathrm{i}\delta(\mathbf{r}-\mathbf{r}')$ [113], and μ is the chemical potential. In the full form (1), solving $\hat{K}$ for eigenstates is difficult in general. Yet, for small density fluctuations around $n_c = \langle\hat{n}\rangle$ (i.e., for $|\delta\hat{n}| \ll n_c$, where $|\delta\hat{n}|$ is the typical value of $\delta\hat{n} = \hat{n} - n_c$ in the state of the system) and for small phase gradient ($\hbar^2|\nabla\hat{\theta}|^2/2m \ll \mu$), the operator $\hat{K}$ can be expanded around the classical field n_c, $\nabla\hat{\theta} = 0$, following the Bogoliubov-Popov approach [114–119].[1] In the zeroth-order expansion the ground-state density profile is found by minimizing the grand-canonical energy functional associated with the Hamiltonian (1) with respect to the variation of $n_c(\mathbf{r})$. This yields the Gross-Pitaevskii equation (GPE)

$$\left[-\frac{\hbar^2}{2m}\nabla^2 + V(\mathbf{r}) + gn_c(\mathbf{r}) - \mu\right]\sqrt{n_c(\mathbf{r})} = 0. \tag{2}$$

Then, retaining only the leading terms in the expansion of the density fluctuations $\delta\hat{n}$ and phase gradients $\nabla\hat{\theta}$, the Hamiltonian (1) is cast into the form $\hat{K} = E_0 + \sum_\nu \epsilon_\nu \hat{b}_\nu^\dagger\hat{b}_\nu$, where $\hat{b}_\nu^\dagger$ and $\hat{b}_\nu$ are the bosonic creation and annihilation operators of an excitation [Bogoliubov quasiparticle (BQP)] of energy ϵ_ν.[2] The phase and density operators are expanded as

$$\hat{\theta}(\mathbf{r}) = \frac{-i}{2\sqrt{n_c(\mathbf{r})}}\sum_\nu [f_\nu^+(\mathbf{r})\,\hat{b}_\nu - \text{H.c.}], \tag{3}$$

$$\delta\hat{n}(\mathbf{r}) = \sqrt{n_c(\mathbf{r})}\sum_\nu [f_\nu^-(\mathbf{r})\,\hat{b}_\nu + \text{H.c.}], \tag{4}$$

where the Bogoliubov wave functions $f_\nu^\pm(\mathbf{r})$ are solutions of the Bogoliubov–de Gennes equations (BdGEs) [122]

$$\left[-\frac{\hbar^2}{2m}\nabla^2 + V(\mathbf{r}) + gn_c(\mathbf{r}) - \mu\right] f_\nu^+(\mathbf{r}) = \epsilon_\nu f_\nu^-(\mathbf{r}), \tag{5}$$

$$\left[-\frac{\hbar^2}{2m}\nabla^2 + V(\mathbf{r}) + 3gn_c(\mathbf{r}) - \mu\right] f_\nu^-(\mathbf{r}) = \epsilon_\nu f_\nu^+(\mathbf{r}) \tag{6}$$

with the normalization

$$\int d\mathbf{r}[f_\nu^+(\mathbf{r})f_{\nu'}^{-*}(\mathbf{r}) + f_\nu^-(\mathbf{r})f_{\nu'}^{+*}(\mathbf{r})] = 2\delta_{\nu,\nu'}. \tag{7}$$

Equations (3) and (4) reveal the simple physical meaning of the functions $f_\nu^+(\mathbf{r})$ and $f_\nu^-(\mathbf{r})$. Up to the factor $\sqrt{n_c(\mathbf{r})}$, they describe the spatial dependence of the phase and density fluctuations associated with the BQPs, respectively. Notice that, as first pointed out by Popov [116,117], the above derivation of the BdGEs in the phase-density representation provides an extension of the usual Bogoliubov–de Gennes theory. In the latter, the starting point consists in applying the usual Bogoliubov shift to the field operator, $\hat{\Psi} = \sqrt{n_c} + \delta\hat{\Psi}$, and expanding $\hat{K}$ up to quadratic terms in the fluctuation $\delta\hat{\Psi}$ [114,115,122]. This approach assumes weak phase and density fluctuations around a unique classical field $\sqrt{n_c}$ which breaks the $U(1)$ phase symmetry of the Hamiltonian. On the contrary, the phase-density picture used in this work does not rely on this assumption. In particular, it provides a satisfactory description

[1] The definition of a phase operator requires special care. A suitable definition can be found in Ref. [118], where a lattice model is used for a rigorous formulation of the Bogoliubov-Popov theory for quasicondensates. The equations derived in this lattice model coincide with the continuous formulation of Eqs. (2), (5), and (6) upon replacement of the coupling constant g by an effective coupling constant that depends on the lattice spacing l, and converges to g in the limit $l \to 0$ in 1D [118,119].

[2] We discard in the canonical form of $\hat{K}$ and in Eqs. (3) and (4) the contribution of the $\hat{P}$ and $\hat{Q}$ operators which arise in Bogoliubov approaches without particle number conservation [120,121], as these operators play no role in the elementary excitations of the Bose gas and vanish in number-conserving approaches. Note also that the orthogonal projection of the Bogoliubov modes, as used in conserving approaches [118,121], does not alter the results presented here.

of the mean-field ground state $n_c(\mathbf{r})$ and the excitations of Bose gases in the quasicondensate regime [123,124].

Within the above formalism, Eqs. (2), (5), and (6) form a closed set which describes noninteracting, bosonic quasiparticles. Interactions between these quasiparticles only arise with higher-order terms in the expansion of $\hat{K}$, which we neglect here. Therefore, to study the low-temperature properties of the Bose gas in the external potential $V(\mathbf{r})$, we are left with the sole modes defined by the GPE (2) and BdGEs (5) and (6). Still, the set of equations (2), (5), and (6) remains difficult to solve in general, as the GPE (2) is nonlinear, and the two coupled second-order BdGEs (5) and (6) themselves amount to a differential problem of order four. In the following, we develop a perturbative approach, valid in the limit of a weak potential $V(\mathbf{r})$, which enables us to solve Eqs. (2), (5), and (6) rigorously, and to interpret the underlying physics in simple terms.

III. A SCHRÖDINGER-LIKE EQUATION FOR BOGOLIUBOV EXCITATIONS IN WEAK POTENTIALS

From now on, we assume that $V(\mathbf{r})$ is a weak external potential with a vanishing average ($\overline{V} = 0$),[3] and a typical amplitude V_R,[4] such that $V_R^2 = \overline{V^2}$. While a less stringent weakness criterion can be derived (see below and Ref. [104]), $|V_R| \ll \mu$ is a sufficient assumption to start with. Note that, although we will focus on the case of a disordered potential in the following, the perturbative approach introduced here is general, and V need not be a disordered potential. In any case, we write the autocorrelation function of V, $C_2(\mathbf{r}' - \mathbf{r}) = \overline{V(\mathbf{r})V(\mathbf{r}')}$, in the dimensionless form

$$C_2(\mathbf{r}) = V_R^2 c_2(\mathbf{r}/\sigma_R), \tag{8}$$

where σ_R is a characteristic length scale of V, which will be precisely defined below when needed. In the following paragraphs, we solve the GPE (2) for the ground-state density n_c (Sec. III A), and we use the result to reduce the BdGEs (5) and (6) to a single Schrödinger-like equation (Secs. III B and III C).

A. The (quasi-)BEC density background

In the regime where the repulsive interactions are strong enough (while remaining compatible with the mean-field regime), i.e., when the healing length

$$\xi = \frac{\hbar}{\sqrt{4m\mu}} \tag{9}$$

is much smaller than the size of the system L, the density profile n_c is homogeneous in the absence of an external potential, and remains extended (delocalized) for a weak potential V, owing to the nonlinear term in the GPE (2) [53,94,104]. It then proves useful to write the mean-field density term in the form

$$n_c(\mathbf{r}) = \frac{\mu + \Delta - \widetilde{V}(\mathbf{r})}{g}, \tag{10}$$

where

$$\widetilde{V}(\mathbf{r}) = g\overline{n_c} - g n_c(\mathbf{r}) \tag{11}$$

contains the inhomogeneous part such that $\overline{\widetilde{V}} = 0$, and

$$\Delta = g\overline{n_c} - \mu \tag{12}$$

represents the mean deviation from the mean-field equation of state $\mu = g n_c$ that holds in the homogeneous case ($V = 0$). The quantities $\widetilde{V}$ and Δ both vanish for $V = 0$, and are expected to remain small for a weak external potential V and repulsive interactions that are strong enough. We then write the perturbation expansions of these quantities in increasing powers of V_R/μ:

$$\widetilde{V}(\mathbf{r}) = \widetilde{V}^{(1)}(\mathbf{r}) + \widetilde{V}^{(2)}(\mathbf{r}) + \cdots, \tag{13}$$

$$\Delta = \Delta^{(1)} + \Delta^{(2)} + \cdots. \tag{14}$$

The various terms can be calculated by generalizing the approach of Ref. [104] beyond the first order. Details of these calculations are presented in Appendix A (see also Ref. [72]). Below, we only discuss the main results.

1. First correction to the mean-field equation of state

The first-order term $\Delta^{(1)}$ in the deviation Δ vanishes [104]. The leading term is thus provided by $\Delta^{(2)}$, which depends explicitly on the potential V and on the healing length ξ through [see Eq. (A16) in Appendix A]:

$$\Delta^{(2)} = \frac{V_R^2 \sigma_R^d}{2(2\pi)^{d/2}\mu} \int d\mathbf{q}\, \frac{(|\mathbf{q}|\xi)^2}{[1 + (|\mathbf{q}|\xi)^2]^2} \hat{c}_2(\mathbf{q}\sigma_R), \tag{15}$$

where $\hat{c}_2$ is the Fourier transform[5] of the reduced autocorrelation function c_2 defined in Eq. (8). As $\hat{c}_2$ is a positive function by virtue of the Wiener-Khinchin theorem, we always have $\Delta^{(2)} > 0$, i.e., $\mu < g\overline{n_c}$ in the presence of an external potential (see also Ref. [94]). In Fig. 1, Eq. (15) is compared to exact numerical calculations of Δ for a disordered potential and a monochromatic lattice potential, with various values of the ratio σ_R/ξ, in a 1D geometry. As expected, the agreement is good for values of V_R/μ as low as in Fig. 1. We checked that the small discrepancy between $\Delta^{(2)}$ and Δ in the disordered case is due to contributions of the order of V_R^3, which are absent in a monochromatic lattice. This validates the perturbative approach.

[3] When V is a disordered potential, we assume *spatial homogeneity*, so that the spatial average of V coincides with its statistical average [96]. For non-disordered potentials, $\overline{V}$ denotes the spatial average of V.

[4] The sign of V_R becomes relevant in the description of disordered potentials with asymmetric single-point probability distribution (see, e.g., Ref. [1]).

[5] Throughout the paper, the Fourier transform is defined as $f(\mathbf{q}) = (2\pi)^{-d/2} \int \mathbf{d}\mathbf{r}\, f(\mathbf{r}) e^{-i\mathbf{q}\cdot\mathbf{r}}$. The notation $\hat{f}$ is used for the Fourier transform of functions f with dimensionless arguments.

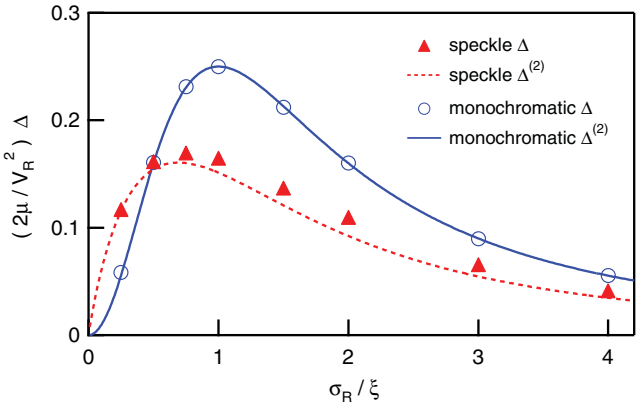

FIG. 1. (Color online) Comparison of the leading-order correction $\Delta^{(2)}$ to the mean-field equation of state with numerical computations of Δ for a 1D speckle potential with a reduced autocorrelation function $c_2(u) = \sin(u)^2/u^2$ as used in experiments [12,15,29] and for a 1D periodic lattice $V(z) = V_R\sqrt{2}\cos(z/\sigma_R)$. Here $V_R = 0.1\mu$.

Let us examine some limiting cases. In the Thomas-Fermi limit, $\xi \ll \sigma_R$, we find

$$\Delta^{(2)} \simeq \frac{V_R^2}{2(2\pi)^{d/2}\mu}\left(\frac{\xi}{\sigma_R}\right)^2 \int d\boldsymbol{\kappa}\ |\boldsymbol{\kappa}|^2 \hat{c}_2(\boldsymbol{\kappa}), \tag{16}$$

so that $\Delta^{(2)}/\mu \propto (V_R/\mu)^2(\xi/\sigma_R)^2 \ll (V_R/\mu)^2$. The opposite limit, $\xi \gg \sigma_R$, corresponds in principle to the white-noise limit which is obtained by letting the ratio σ_R/ξ vanish while keeping the product $V_R^2\sigma_R^d$ constant. Then, the Fourier transform of the reduced autocorrelation function may be approximated by a constant, $\hat{c}_2(\boldsymbol{\kappa}) \simeq \hat{c}_2(\mathbf{0})$. In fact, we find that the white-noise limit of expression (15) is correctly defined only in 1D, for which we obtain

$$\Delta^{(2)} \simeq \frac{\sqrt{\pi}V_R^2\sigma_R}{4\sqrt{2}\mu\xi}\hat{c}_2(0), \tag{17}$$

so that $\Delta^{(2)}/\mu \propto (V_R/\mu)^2(\sigma_R/\xi) \ll (V_R/\mu)^2$. In dimension higher than one, this limit cannot be defined because the integrand $d\mathbf{q}\ (|\mathbf{q}|\xi)^2/[1+(|\mathbf{q}|\xi)^2]^2$ scales as $q^{d-3}dq$ for high momenta ($q \gg \xi^{-1}$). The integral in Eq. (15) would thus be plagued by an ultraviolet divergence for $d \geqslant 2$ and a constant $\hat{c}_2(\boldsymbol{\kappa}) = \hat{c}_2(\mathbf{0})$. In other words, for $d \geqslant 2$, the quantity $\Delta^{(2)}$ depends crucially on the precise form of the reduced autocorrelation function c_2.

2. *Inhomogeneous part of the (quasi-)BEC density*

In contrast to the mean deviation Δ, the leading contribution to the inhomogeneous part of the density profile is provided by the first-order term, which reads

$$\widetilde{V}^{(1)}(\mathbf{r}) = \int d\mathbf{r}' G_\xi(\mathbf{r}-\mathbf{r}')V(\mathbf{r}'), \tag{18}$$

where G_ξ is the Green function associated with the differential operator $-\xi^2\nabla^2 + 1$ (see Ref. [104] and Eq. (A15) in Appendix A). In Fourier space we have

$$G_\xi(\mathbf{q}) = \frac{(2\pi)^{-d/2}}{1+(|\mathbf{q}|\xi)^2}, \tag{19}$$

so that

$$\widetilde{V}^{(1)}(\mathbf{q}) = \frac{V(\mathbf{q})}{1+(|\mathbf{q}|\xi)^2}. \tag{20}$$

The healing length ξ clearly appears as a threshold length scale in the response of the density $n_c(\mathbf{r})$ to the external potential $V(\mathbf{r})$. Indeed, we have $\widetilde{V}^{(1)}(\mathbf{q}) \simeq V(\mathbf{q})$ for $|\mathbf{q}| \ll \xi^{-1}$, whereas $\widetilde{V}^{(1)}(\mathbf{q}) \ll V(\mathbf{q})$ for $|\mathbf{q}| \gg \xi^{-1}$. In other words, the potential $\widetilde{V}^{(1)}(\mathbf{r})$ follows the spatial modulations of $V(\mathbf{r})$ while evening out the high-frequency components. It also follows from the Parseval-Plancherel theorem that $|\widetilde{V}_R^{(1)}| \leqslant |V_R|$, where $|\widetilde{V}_R^{(1)}|$ is the standard deviation of $\widetilde{V}^{(1)}$ and the sign of $\widetilde{V}_R^{(1)}$ is chosen to be the same as that of V_R. The potential $\widetilde{V}^{(1)}(\mathbf{r})$ is thus termed a *smoothed* potential [104].

If $V(\mathbf{r})$ is a homogeneous disordered potential, that is, a disordered potential whose statistical properties do not depend on the position $\mathbf{r}$ [96], then so is $\widetilde{V}^{(1)}(\mathbf{r})$. If $V(\mathbf{r})$ is a periodic potential, $\widetilde{V}^{(1)}(\mathbf{r})$ is also periodic with the same period, but a smoothed Bloch amplitude in each periodic cell, and simply rescaled Fourier components, as shown in Fig. 2. In either case, Eq. (10) implies that, if $V(\mathbf{r})$ is a homogeneous potential, the density profile n_c is extended [53,104]. Note also that the first-order term $\widetilde{V}^{(1)}$ is indeed a small perturbation of the homogeneous density profile whenever $|\widetilde{V}_R^{(1)}| \ll \mu$, which loosens the initial weakness criterion $|V_R| \ll \mu$.

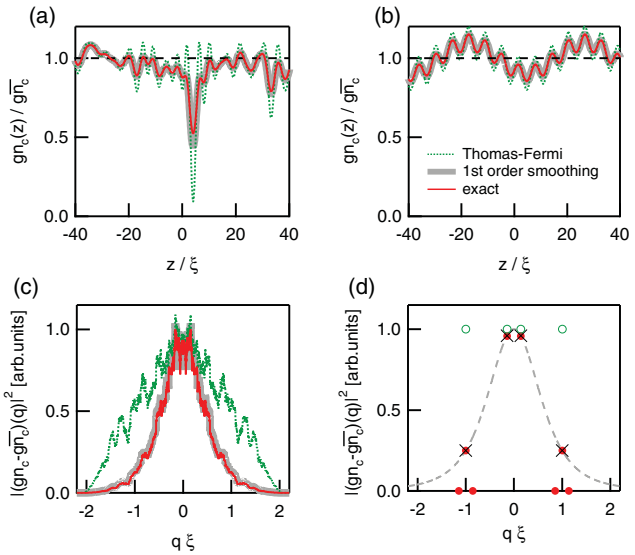

FIG. 2. (Color online) Comparison of the first-order smoothing solution [Eq. (10) with $\Delta = 0$ and $\widetilde{V} = \widetilde{V}^{(1)}$] and exact numerical computations of the density profile in the cases of (a,c) a 1D speckle potential with reduced autocorrelation function $c(u) = \sin(u)^2/u^2$ and correlation length $\sigma_R = \xi$ and of (b,d) a 1D bichromatic periodic potential. The periodic potential reads $V(z) = V_R[\cos(k_0 z) + \cos(k_0 z/7)]$ with $k_0\xi = 1$. In both cases, $V_R = 0.1\mu$. (a,b) The analytical expression $g\overline{n_c} - \widetilde{V}^{(1)}(z)$ (broad gray line) is hardly distinguishable from $gn_c(z)$ as obtained numerically (red solid line). The average density $g\overline{n_c}$ (black dashed line) and the Thomas-Fermi limit $g\overline{n_c} - V(z)$ (green dotted line) are shown as references. (c,d) Corresponding power spectra of the modulations of $gn_c(z)$ (red solid line/red dots), $\widetilde{V}^{(1)}(z)$ (broad gray line/black crosses), and $V(z)$ (green dotted line/green circles). The gray dashed line in (d) is a plot of $1/[1+(q\xi)^2]^2$.

The smoothing solution (10) at first order ($\Delta = 0$ and $\widetilde{V} = \widetilde{V}^{(1)}$) is compared to exact numerical computations of the density profile in Fig. 2, both for a disordered and a bichromatic periodic potential, in coordinate and Fourier spaces. For the sake of clarity, the power spectra for the disordered potential [Fig. 2(c)] have been smoothed by a running average of width 0.1 in $q\xi$ units. The agreement between the first-order smoothing solution and the numerical results is good, especially when compared to the Thomas-Fermi limit [for which $\widetilde{V}^{(1)}(z) = V(z)$]. For the bichromatic periodic potential, the appearance of red dots around $q\xi = \pm 1$ in Fig. 2(d) results from the admixture of the two components of the bichromatic lattice potential due to the nonlinearity of the GPE, as described by the first nonlinear correction $\widetilde{V}^{(2)}$ (see Appendix A). The other higher-order components, which are several orders of magnitude smaller, are not shown.

B. Bogoliubov–de Gennes equations in the decoupling basis

With the BEC background solution $n_c(\mathbf{r})$ at hand, we can now solve the BdGEs (5) and (6). Using Eq. (10), these equations can be cast into

$$\left[-\frac{\hbar^2}{2m}\nabla^2 + V + \Delta - \widetilde{V}\right] f_\nu^+ = \epsilon_\nu f_\nu^-, \quad (21)$$

$$\left[-\frac{\hbar^2}{2m}\nabla^2 + 2\mu + V + 3\Delta - 3\widetilde{V}\right] f_\nu^- = \epsilon_\nu f_\nu^+, \quad (22)$$

where Δ, $V(\mathbf{r})$, and $\widetilde{V}(\mathbf{r})$ are small compared to μ. As $n_c(\mathbf{r})$ is the *ground-state* solution of the GPE (2), the (quasi-), condensate is dynamically stable (see, e.g., Refs. [125,126]), and we need only consider real-valued, strictly positive eigenvalues of the BdGEs. Now, given such an eigenvalue ϵ_ν, we are interested in the properties of the corresponding mode $\{f_\nu^+(\mathbf{r}), f_\nu^-(\mathbf{r})\}$. Following the approach developed in Ref. [54], we take advantage of the structure of the eigenmodes before perturbation by a weak potential and introduce an alternative representation of the BQPs in terms of the components $\{g_\nu^+(\mathbf{r}), g_\nu^-(\mathbf{r})\}$, where the functions $g^\pm$ and $f^\pm$ are related by the linear transformation

$$g_\nu^\pm(\mathbf{r}) = \pm\rho_\nu^{\pm 1/2} f_\nu^+(\mathbf{r}) + \rho_\nu^{\mp 1/2} f_\nu^-(\mathbf{r}), \quad (23)$$

with

$$\rho_\nu = \frac{\mu}{\epsilon_\nu} + \sqrt{1 + \left(\frac{\mu}{\epsilon_\nu}\right)^2}. \quad (24)$$

Expression (24) defines ρ_ν as a function of the eigenvalue ϵ_ν which does not depend on the details of the specific mode under consideration. The linear transformation (23), derived in Appendix B, is chosen is such a way that the coupling between $g_\nu^+(\mathbf{r})$ and $g_\nu^-(\mathbf{r})$ vanishes in the homogeneous case $V = 0$. As such, it offers a convenient starting point for a perturbation expansion in the case of weak potentials, as shown below.

In the basis of the $g_\nu^\pm(\mathbf{r})$ functions, the BdGEs take the exact form [see Eqs. (B13) and (B14) in Appendix B]:

$$\frac{\hbar^2 k_\nu^2}{2m} g_\nu^+ = -\frac{\hbar^2}{2m}\nabla^2 g_\nu^+ - \frac{2\rho_\nu}{1+\rho_\nu^2}(\widetilde{V} - \Delta) g_\nu^- + \left[V - \frac{3+\rho_\nu^2}{1+\rho_\nu^2}(\widetilde{V} - \Delta)\right] g_\nu^+, \quad (25)$$

$$-\frac{\hbar^2 \beta_\nu^2}{2m} g_\nu^- = -\frac{\hbar^2}{2m}\nabla^2 g_\nu^- - \frac{2\rho_\nu}{1+\rho_\nu^2}(\widetilde{V} - \Delta) g_\nu^+ + \left[V - \frac{1+3\rho_\nu^2}{1+\rho_\nu^2}(\widetilde{V} - \Delta)\right] g_\nu^-, \quad (26)$$

where

$$\frac{\hbar^2 k_\nu^2}{2m} = \sqrt{\mu^2 + \epsilon_\nu^2} - \mu, \quad (27)$$

$$\frac{\hbar^2 \beta_\nu^2}{2m} = \sqrt{\mu^2 + \epsilon_\nu^2} + \mu. \quad (28)$$

Both k and β are real-valued functions of the energy ϵ. As a consequence, the associated g_ν^+ and g_ν^- functions are essentially of the oscillating and the evanescent type, respectively, owing to the signs of the left-hand side (l.h.s.) terms in Eqs. (25) and (26). This is consistent with the limit of a vanishing external potential ($V = 0$, and thus $\widetilde{V} = 0$, $\Delta = 0$), where the equations for g_ν^+ and g_ν^- are decoupled. It the latter case, the quantity k can be identified with the wave number $|\mathbf{k}|$ of an oscillating, plane-wave BQP mode of energy ϵ_k, and Eq. (27) is equivalent to the usual Bogoliubov dispersion relation

$$\epsilon_k = \sqrt{\frac{\hbar^2 k^2}{2m}\left(\frac{\hbar^2 k^2}{2m} + 2\mu\right)}. \quad (29)$$

The β coefficients, on the other hand, characterize a subset of solutions to the BdGEs that are forbidden when $V = 0$, as the boundary conditions imposed on the system (e.g., periodic or homogeneous Dirichlet boundary conditions) preclude monotonously growing or decreasing BQP components.

C. Effective Schrödinger equation

While the g_ν^- function vanishes identically in the absence of an external potential, this is no longer true when V couples g_ν^- to g_ν^+ via Eqs. (25) and (26). For a weak external potential, however, all the terms introduced by g_ν^- in Eq. (25) are at least of second order in V_R [see Eq. (B16) and the discussion below], so that we can neglect the second term on the right-hand side (r.h.s.) of Eq. (25). Besides, the terms proportional to Δ in Eqs. (25) and (26) are at least of second order in the disorder amplitude V_R (see Sec. III A 1), and can also be neglected in a first-order approach. We are thus left with the following closed equation for g_ν^+, which is valid to first order in V_R:

$$-\frac{\hbar^2}{2m}\nabla^2 g_\nu^+(\mathbf{r}) + \mathcal{V}_{k_\nu}(\mathbf{r}) g^+(\mathbf{r}) \simeq \frac{\hbar^2 k_\nu^2}{2m} g_\nu^+(\mathbf{r}), \quad (30)$$

where

$$\mathcal{V}_{k_\nu}(\mathbf{r}) = V(\mathbf{r}) - \frac{3+\rho_\nu^2}{1+\rho_\nu^2}\widetilde{V}^{(1)}(\mathbf{r}). \quad (31)$$

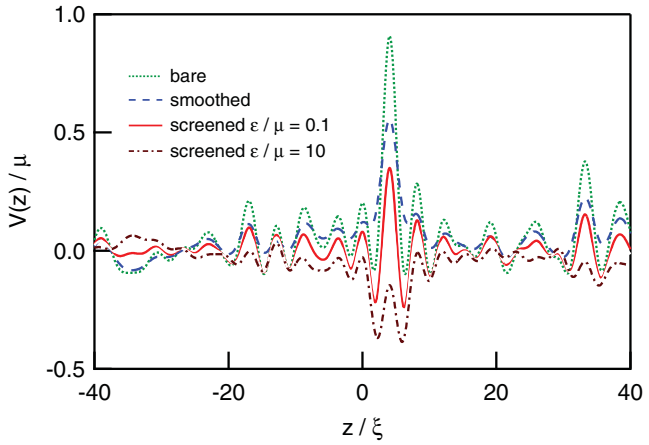

FIG. 3. (Color online) Plot of the screened potential $\mathcal{V}_k(z)$ for the same 1D speckle potential ($\sigma_R = \xi$, $V_R/\mu = 0.1$) as in Fig. 2(a), with $\epsilon/\mu = 0.1$ (i.e., $k\xi \simeq 0.05$) and $\epsilon/\mu = 10$ (i.e., $k\xi \simeq 2$). The bare potential $V(z)$ and the smoothed potential $\widetilde{V}(z)$ are shown for comparison.

Equation (30) is formally equivalent to a Schrödinger equation for a bare particle of energy $\hbar^2 k_\nu^2/2m$ in an effective potential $\mathcal{V}_{k_\nu}(\mathbf{r})$.[6] The potential $\mathcal{V}_{k_\nu}(\mathbf{r})$ differs from both the bare potential $V(\mathbf{r})$ and the smoothed potential $\widetilde{V}(\mathbf{r})$ and explicitly depends on the BQP energy ϵ_ν via the parameter ρ_ν. These features are illustrated in Fig. 3 where we plot a given realization of a 1D speckle potential $V(z)$, together with the corresponding smoothed potential $\widetilde{V}(z)$ and effective potential $\mathcal{V}_{k_\nu}$ (hereafter named *screened* potential on grounds explained below), for two values of the BQP energy.

For further convenience, the dependence of the effective potential on the BQP energy ϵ_ν is expressed by the subscript k_ν, with the understanding that k_ν is defined by Eq. (27). Combining Eqs. (24) and (27), we find

$$\rho_\nu = \sqrt{1 + \frac{1}{(k_\nu \xi)^2}}, \tag{32}$$

and hence

$$\mathcal{V}_{k_\nu}(\mathbf{r}) = V(\mathbf{r}) - \frac{1 + 4(k_\nu\xi)^2}{1 + 2(k_\nu\xi)^2}\widetilde{V}^{(1)}(\mathbf{r}). \tag{33}$$

To gain more insight into the properties of $\mathcal{V}_{k_\nu}(\mathbf{r})$, let us turn to Fourier space where, by virtue of Eq. (20), the effective potential reads

$$\mathcal{V}_{k_\nu}(\mathbf{q}) = V(\mathbf{q})\left[1 - \frac{1 + 4(k_\nu\xi)^2}{1 + 2(k_\nu\xi)^2}\frac{1}{1 + (|\mathbf{q}|\xi)^2}\right]. \tag{34}$$

Upon inspection, this expression shows that we have $|\mathcal{V}_{k_\nu}(\mathbf{q})| \leqslant |V(\mathbf{q})|$ for any Fourier component $\mathbf{q}$ and any BQP energy ϵ_ν. Note also that, by construction of $\widetilde{V}^{(1)}$, the potential $\mathcal{V}_{k_\nu}$ has a vanishing average. Hence, keeping in mind that $\mathcal{V}_{k_\nu}$ results from the competition of the bare potential V and the BEC background n_c in the BdGEs, we term $\mathcal{V}_{k_\nu}$ a *screened* potential. The screening thus affects all Fourier components of the external potential in any dimension.

Once Eq. (30) has been solved (possibly self-consistently) for g_ν^+, the function g_ν^- can be computed from g_ν^+. Indeed, since $\hbar^2\beta_\nu^2/2m > \mu$ [see Eq. (28)] and for $|V_R| \ll \mu$, the last term in the r.h.s. of Eq. (26) can be neglected, and we find

$$g_\nu^-(\mathbf{r}) \simeq \frac{2m}{\hbar^2\beta_\nu^2}\frac{2\rho_\nu}{1+\rho_\nu^2}\int d\mathbf{r}' G_{1/\beta}(\mathbf{r}-\mathbf{r}')\widetilde{V}^{(1)}(\mathbf{r}')g_\nu^+(\mathbf{r}'), \tag{35}$$

where $G_{1/\beta}(\mathbf{q}) = \frac{(2\pi)^{-d/2}}{1+(|\mathbf{q}/\beta|)^2}$ is the Green function associated with the differential operator $-(1/\beta)^2\nabla^2 + 1$, written in Fourier space.

For analytical purposes, the $g_\nu^\pm$ functions hence usefully replace the physically meaningful quantities $f_\nu^\pm$, which can readily be recovered by inverting transformation (23). In particular, as far as asymptotic localization properties in disordered potentials are concerned, Eq. (35) tells us that the typical amplitude of g_ν^- evolves parallel to the amplitude of g_ν^+ on intermediate to long length scales, if $\widetilde{V}$ is homogeneous. In this respect, the benefit of the mapping of the exact BdGEs onto Eqs. (30) and (31) is that we can apply standard techniques for *bare* Schrödinger particles in weak disordered potentials, in any dimension, as long as these are consistent with the lowest-order approximation used to derive the effective equation (30). Yet, BQPs differ substantially from usual bare particles in their scattering and localization properties, because of the peculiar features of the screened potential $\mathcal{V}_{k_\nu}(\mathbf{r})$.

IV. LOCALIZATION OF BOGOLIUBOV QUASIPARTICLES IN ONE DIMENSION

The formalism developed in Sec. III is valid for any weak potential. It is particularly fruitful when applied to disordered potentials as known theories developed for single (noninteracting) particles can be directly applied to the effective Schrödinger-like equation (30). In this section, we focus on the one-dimensional geometry using the so-called phase formalism [96], which allows for an exact perturbative calculation of the Lyapunov exponent (inverse localization length). This procedure can be straightforwardly extended to higher dimensions, applying appropriate single-particle theories to Eq. (30), for instance the self-consistent theory of localization [127,128].

A. Phase formalism in the Born approximation

In 1D, the Lyapunov exponent γ_k of a bare particle of energy E_k in a disordered potential $V(z)$ is simply related to the backscattering amplitude of the particle from the inhomogeneities of V. For a weak disorder, the Lyapunov exponent can be extracted from a perturbation expansion $\gamma_k = \gamma_k^{(2)} + \gamma_k^{(3)} + \cdots$ in powers of the disorder amplitude V_R. For $\gamma_k \ll k$, this approach yields the following result in the lowest-order (Born) approximation [96]:

$$\gamma_k^{(2)} = \frac{\sqrt{2\pi}}{8k^2}\left(\frac{2m}{\hbar^2}\right)^2 C_2(2k), \tag{36}$$

[6]Note that the effective energy $\hbar^2 k_\nu^2/2m$ appearing in the Schrödinger-like equation (30) differs from the actual energy ϵ_ν of the BQP under consideration, as shown by Eq. (27).

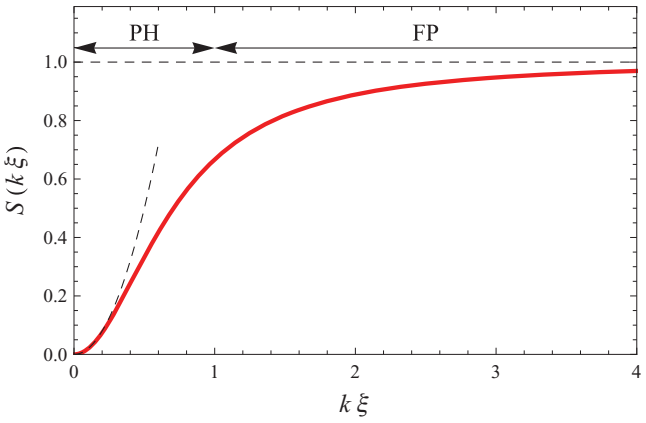

FIG. 4. (Color online) Screening function $\mathcal{S}$. The dashed lines show the asymptotic behaviors in the phonon regime [$\mathcal{S}(k\xi) \simeq 2(k\xi)^2$ for $k\xi \ll 1$ or, equivalently, $\epsilon \ll \mu$] and free-particle regime [$\mathcal{S}(k\xi) \simeq 1$ for $k\xi \gg 1$ or, equivalently, $\epsilon \gg \mu$].

where $C_2(q)$ is the Fourier transform of $C_2(z)$, evaluated at $q = 2k$. In this formulation, $V(z)$ has a vanishing average, and k, explicitly defined as $k = \sqrt{2mE_k}/\hbar$, stands for the typical wave vector of the particle under consideration. As such, the parameter k, rather than the related energy E_k, is the meaningful quantity in the interference effect that causes Anderson localization. Applying this result to the Schrödinger-like equation (30), we derive the Lyapunov exponent Γ_k of a BQP in the Born approximation $\Gamma_k \simeq \Gamma_k^{(2)}$:

$$\Gamma_k^{(2)} = \frac{\sqrt{2\pi}}{8k^2}\left(\frac{2m}{\hbar^2}\right)^2 \mathcal{C}_{2,k}(2k), \tag{37}$$

where $\mathcal{C}_{2,k}(q)$ is the Fourier transform of the two-point correlator $\mathcal{C}_{2,k}(z) = \overline{\mathcal{V}_k(z')\mathcal{V}_k(z'+z)}$, and k depends on the energy ϵ through Eq. (27) as we are now dealing with BQPs. From the Wiener-Khinchin theorem, we have $\mathcal{C}_{2,k}(q) \propto \overline{|\mathcal{V}_k(q)|^2}$, so that, according to Eq. (31), the relevant Fourier component of $\mathcal{V}_k$ for the calculation of $\Gamma_k^{(2)}$ is

$$\mathcal{V}_k(2k) = V(2k) - \frac{1+4(k\xi)^2}{1+2(k\xi)^2}\widetilde{V}^{(1)}(2k). \tag{38}$$

Then, inserting Eq. (20) into Eq. (38), we obtain

$$\mathcal{V}_k(2k) = \mathcal{S}(k\xi)V(2k), \tag{39}$$

where

$$\mathcal{S}(k\xi) = \frac{2(k\xi)^2}{1+2(k\xi)^2}. \tag{40}$$

Finally, Eq. (37) can be rewritten as

$$\Gamma_k^{(2)} = [\mathcal{S}(k\xi)]^2\gamma_k^{(2)}, \tag{41}$$

where

$$\gamma_k^{(2)} = \frac{\sqrt{2\pi}}{32}\left(\frac{V_R}{\mu}\right)^2 \frac{\sigma_R}{k^2\xi^4}\hat{c}_2(2k\sigma_R). \tag{42}$$

Equation (41), together with Eqs. (27), (40), and (42), completely determines the Lyapunov exponent of a BQP of energy ϵ in a weak, correlated, 1D disordered potential.

Remarkably, Eq. (41) shows that the Lyapunov exponent of a BQP can be simply related to that of a bare Schrödinger particle with the same average wave vector k [54]. The effects of interactions, in particular, are entirely absorbed in the term $\mathcal{S}(k\xi)$ defined in Eq. (40), which we call *screening* function on the basis of the analysis presented in Sec. IV B below. This function is shown in Fig. 4 and displays two regimes which can be traced back to the nature of the elementary excitations of the interacting Bose gas in the absence of disorder. In the homogeneous case ($V = 0$), the elementary (BQP) excitations of the Bose gas undergo a crossover from a regime of pair excitations with linear dispersion relation for $\epsilon \ll \mu$, $\epsilon_k \simeq \hbar ck$ with $c = \sqrt{\mu/m}$ the speed of sound [phonon regime (PH)], to a regime of single-particle excitations with a quadratic dispersion relation $\epsilon_k \simeq E_k = (\hbar^2/2m)k^2$ for $\epsilon \gg \mu$ [free-particle regime (FP)]. Hence, while the localization of single particles merely results from the competition of their kinetic energy with the disorder amplitude and correlation [33], the localization of BQPs also crucially depends on interaction-induced particle correlations.

B. Localization regimes

Summarizing the results of the previous section, we find that the Lyapunov exponent of BQPs in weak 1D disordered potentials is given by the expression

$$\Gamma_k^{(2)} = \frac{\sqrt{2\pi}}{8}\left(\frac{V_R}{\mu}\right)^2 \frac{k^2\sigma_R}{[1+2(k\xi)^2]^2}\hat{c}_2(2k\sigma_R), \tag{43}$$

obtained by combining Eqs. (40), (41), and (42). In this expression, the quadratic dependence on the potential amplitude V_R is characteristic of the Born approximation. The scaled Lyapunov exponent $(\mu/V_R)^2\Gamma_k^{(2)}\xi$ depends only on the two parameters $k\xi$ and σ_R/ξ. Expression (43) nevertheless contains contributions of three distinct physical origins, which appear more clearly in Eqs. (41) and (42): i) a $1/k^2$ term which is representative of the kinetic energy of a bare particle, ii) the squared screening function $\mathcal{S}(k\xi)^2$ which accounts for particle interactions, and iii) the spectral density of disorder $V_R^2\sigma_R\hat{c}_2(2k\sigma_R)$ at the wave vector $2k$. The role of these various contributions is discussed below.

1. Screening in the phonon regime

The interplay of the first two contributions is best understood by studying the case of a white-noise potential, which is obtained in the limit $\sigma_R \to 0$, $|V_R| \to \infty$, with $V_R^2\sigma_R = \text{const}$. In this limit, the spectral density $\hat{c}_2$ uniformly approaches a flat distribution with an amplitude of the order of one. Then, in the free-particle regime $\epsilon \gg \mu$ (i.e., $k\xi \gg 1$), we have $\mathcal{S}(k\xi) \simeq 1$ and $\Gamma_k^{(2)} \sim 1/k^2 \sim 1/\epsilon$. In other words, BQPs localize exactly like bare Schrödinger particles in this regime, as expected. In the phonon regime, on the contrary, the kinetic term is dominated by the $\mathcal{S}(k\xi)^2$ factor, which is approximately quartic in k (or ϵ). We then get the scaling $\Gamma_k^{(2)} \sim k^2 \sim \epsilon^2$ [51,54], which is consistent with known results on the localization of acoustic phonons in 1D [129–132].

Interestingly, Eq. (41) combines the two limiting models in a unified picture, and provides a physical interpretation for the decreasing localization of phonon modes with decreasing

energy. The function $\mathcal{S}(k\xi)$ reflects the competition of the bare external potential V and the interaction of the BQPs with the quasi-BEC density background gn_c, which appears here as $\widetilde{V}$. In particular, the strong decay of $\mathcal{S}(k\xi)$ in the phonon regime can be interpreted as an increasing screening of the external potential by the static quasi-BEC background, which adapts to the long-wavelength modulations of the disordered potential (see Sec. III A 2).

2. *Correlated disordered potentials*

To analyze the role of the correlation length σ_R in Eq. (43), we consider optical speckle potentials, which are now widely used with ultracold atoms for their tunability and truly random properties, as a model of correlated disorder [5,6,9,12,13,15,19,29,66,67,133]. In the simplest case where the speckle pattern is obtained at the back focal plane of a lens with rectangular aperture and uniform illumination (see, e.g., Ref. [15]), the reduced autocorrelation function reads

$$c_2(u) = \sin(u)^2/u^2, \tag{44}$$

where $u = z/\sigma_R$. The corresponding Fourier spectrum is

$$\hat{c}_2(k\sigma_R) = \sqrt{\frac{\pi}{2}}\left(1 - \frac{k\sigma_R}{2}\right)\Theta\left(1 - \frac{k\sigma_R}{2}\right), \tag{45}$$

where Θ is the Heaviside step function. Then, Eq. (43) reads

$$\Gamma_k^{(2)} = \frac{\pi}{8}\left(\frac{V_R}{\mu}\right)^2 \frac{k^2\sigma_R(1-k\sigma_R)}{[1+2(k\xi)^2]^2}\Theta(1-k\sigma_R), \tag{46}$$

which is shown in Fig. 5. Such disorder correlations introduce several features, which we discuss below.

Effective mobility edge. Equation (46) shows that the Lyapunov exponent in the Born approximation, $\Gamma_k^{(2)}$, vanishes identically for $k\sigma_R > 1$ (see also Figs. 5 and 6). This feature

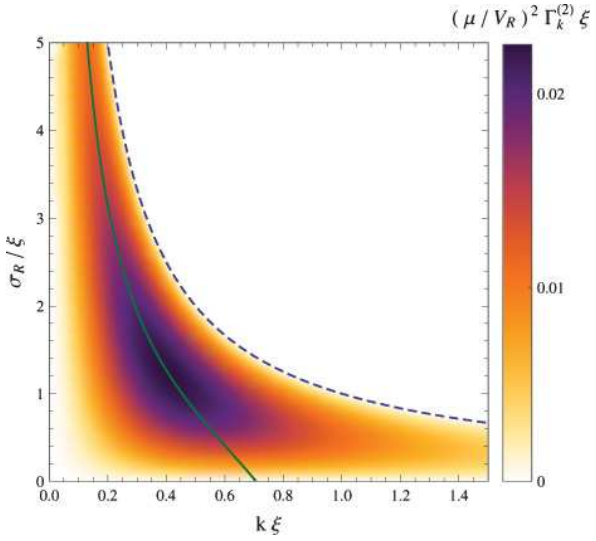

FIG. 5. (Color online) Contour plot of the Lyapunov exponent of BQPs in a speckle potential, as given by Eq. (46). Beyond $k\sigma_R = 1$ (black dashed line), the Lyapunov exponent vanishes completely in the Born approximation, due to the finite support of the speckle power spectrum. The green solid line represents the wave vector of maximum localization for each ratio σ_R/ξ.

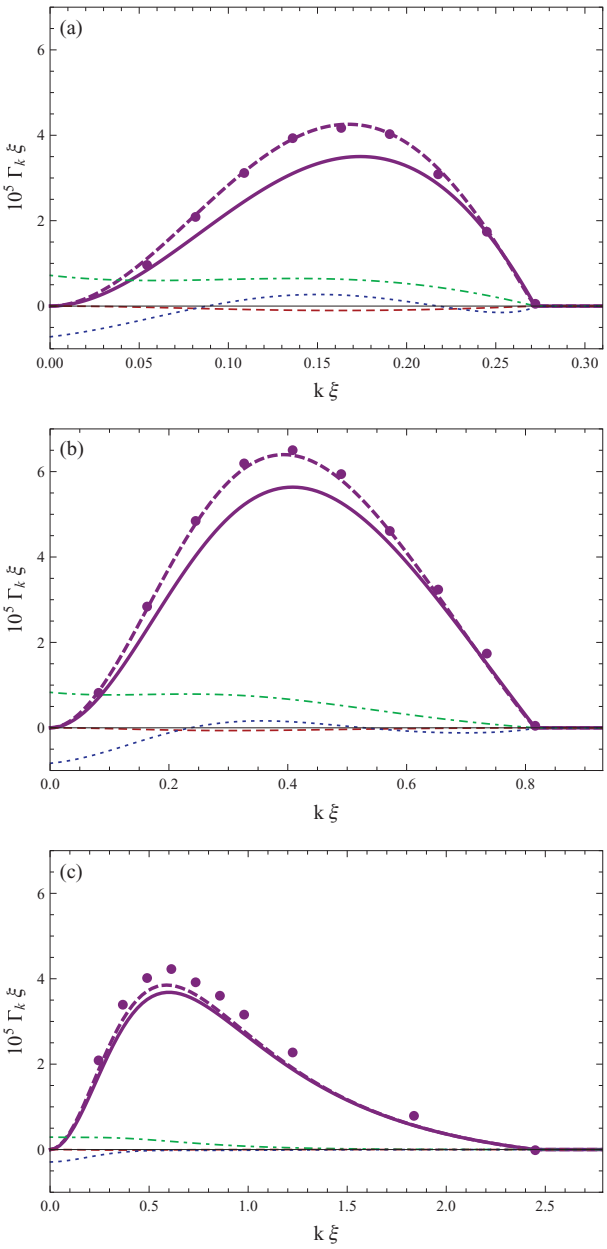

FIG. 6. (Color online) Lyapunov exponent of BQPs in 1D speckle potentials with the statistical properties described in Sec. IV B 2, with $V_R/\mu = 0.05$, and for a) $\sigma_R = 3.7\,\xi$, b) $\sigma_R = \sqrt{3/2}\,\xi$, and c) $\sigma_R = 0.4\,\xi$. The thick solid lines correspond to the Born term $\Gamma_k^{(2)}$ given by Eq. (46). The thick purple dashed lines correspond to the next-order expansion $\Gamma_k \simeq \Gamma_k^{(2)} + \Gamma_k^{(3)}$ (see Sec. IV E). The term $\Gamma_k^{(3)}$ scales as V_R^3, and results from the addition of three contributions: $\Gamma^{(3)}_{\mathcal{V}_k,\mathcal{V}_n}$ (green dash-dotted), $\Gamma^{(3)}_{\mathcal{V}_k,\mathcal{V}_-}$ (red dashed), and $\Gamma^{(3)}_{\mathcal{V}_k,\mathcal{V}_k,\mathcal{V}_k}$ (blue dotted). The dots are the numerical data obtained with the procedure described in Sec. IV D.

originates from the special correlation properties of speckle potentials, the power spectrum of which has a high-momentum cutoff [see Eq. (45)], i.e., contains no $2k$ component able to backscatter a wave traveling with wave vector $k > 1/\sigma_R$ according to the elastic process $+k \to -k$ at the level of the Born approximation [18,27]. The Born approximation consists in truncating the perturbation series in powers of V_R

used to derive Lyapunov exponents after the leading order, proportional to V_R^2. In agreement with the understanding of localization in 1D, whereby single particles are localized (i.e., $\gamma_k > 0$) at all energies under fairly general assumptions [95], higher-order terms in the perturbation expansions of γ_k and Γ_k are expected to carry contributions which do not all vanish identically for $k\sigma_R > 1$. However, the larger power dependence on the small parameter V_R/μ makes these terms negligible in the limit of weak disorder. In this limit, the Lyapunov exponents thus experience a sharp crossover and drop by orders of magnitude when k is varied through the value $1/\sigma_R$. Such a crossover characterizes an *effective* mobility edge which strongly affects localization properties in finite-size systems. As a matter of fact, the third-order contribution to Γ_k, proportional to V_R^3, can be shown to vanish abruptly for momenta above the same cutoff at $1/\sigma_R$ (see Sec. IV E), so that corrections to Eq. (46) beyond that cutoff scale as V_R^4 at least.[7] This behavior is specific to potentials with cutoffs in their Fourier-transformed correlation functions [27,32,33,134,135].

Localization maxima. In the white-noise limit, the BQPs localize best for $k\xi = 1/\sqrt{2}$ (i.e., $\epsilon = \sqrt{3}\mu$), that is, in the crossover region between the phonon and the free-particle regime [51]. This behavior results from the competition of bare kinetic energy and mean-field interactions via the screening effect, as discussed above. With correlations, however, the detailed statistical properties of the disorder play a role as well, and the wave vector of maximum localization k_{max} decreases with increasing correlation length σ_R. More generally, it can be checked from Eq. (43) that for any correlated disorder with monotonously decreasing power spectrum akin to model (45), the wave vector of maximum localization is shifted to lower values than the corresponding white-noise value. The locus of k_{max} as a function of the correlation and healing lengths is plotted in green solid line in Fig. 5. For each σ_R/ξ ratio, we indeed find a unique maximum k_{max} with

$$k_{max} \simeq \frac{1}{\sqrt{2}\,\xi}\left(1 - \frac{\sigma_R/\xi}{2\sqrt{2}}\right), \quad \sigma_R \ll \xi, \tag{47}$$

$$k_{max} \simeq \frac{2}{3\,\sigma_R}, \quad \sigma_R \gg \xi. \tag{48}$$

These asymptotic expressions show that k_{max} is controlled by the longest length scale in the problem. Finally, we find an absolute maximum at fixed ξ for $\sigma_R = \sqrt{3/2}\,\xi$ and $k\xi = 1/\sqrt{6}$, which yields a localization length

$$L_{max}(\xi) = \Gamma_{max}^{-1}(\xi) = \frac{512\sqrt{6}}{9\pi}\left(\frac{\mu}{V_R}\right)^2 \xi. \tag{49}$$

Current experiments with ultracold atoms implement disordered potentials with correlation lengths of the order of $\sigma_R \simeq 0.25\,\mu$m [19,29,66,67], which yields $L_{max} \simeq 230\,\mu$m for $V_R = 0.2\mu$. Since this value can be of the order of or even smaller than the system size, we conclude that localization of BQPs in ultracold Bose gases is relevant for present-day experiments.

C. Validity of the leading-order result

Before turning to some numerical tests, let us review the conditions of validity of the results discussed above. The Born approximation for BQPs, which yields $\Gamma_k \simeq \Gamma_k^{(2)} = [\mathcal{S}(k\xi)]^2\gamma_k^{(2)}$, requires (i) the first-order smoothing solution [Eq. (10) with $\widetilde{V}$ replaced by $\widetilde{V}^{(1)}$ as given by Eq. (18)], (ii) the first-order decoupling of the g^+ and g^- modes that leads to Eq. (30), and (iii) the Born approximation $\gamma_k \simeq \gamma_k^{(2)}$ to be valid. The *weak disorder* condition $|\widetilde{V}_R| \ll \mu$ alone ensures (i) and (ii). Note that this criterion of weak disorder appears less stringent on the amplitude V_R of the bare potential, since smoothing reduces the amplitude of $\widetilde{V}$ with respect to V. The regime of validity of the Lyapunov exponent derived for *Schrödinger* particles in a weak-disorder expansion is in itself a subtle issue, as the successive terms in the perturbation series all depend on the disorder amplitude and the energy of the particle. The resulting asymptotic series is well-behaved in the high-energy limit. A precise inspection of the low-energy limit, where the terms of the series blow up, is necessary to exhibit a rigorous criterion for the validity of a truncated perturbation expansion (see, e.g., Ref. [136]). For single particles, $\gamma_k \ll k$ is usually retained [96]. In physical terms, the localization length should exceed the typical wavelength of the particle. This sets a V_R-dependent lower bound on the single-particle energies for which the perturbative result is meaningful. Translating the above criterion to BQPs ($\Gamma_k \ll k$), we obtain

$$\frac{|V_R|}{\mu}\sqrt{\frac{\sigma_R}{\xi}}\sqrt{\hat{c}_2(2k\sigma_R)} \ll (k\xi)^{3/2} + \frac{1}{2(k\xi)^{1/2}}. \tag{50}$$

This condition of validity resembles the corresponding one for Schrödinger particles: $(|V_R|/\mu)\sqrt{(\sigma_R/\xi)}\sqrt{\hat{c}_2(2k\sigma_R)} \ll (k\xi)^{3/2}$. As expected, the two coincide in the FP regime ($k \gg 1/\xi$). However, they differ significantly in the PH regime ($k \ll 1/\xi$). Indeed, for free particles, perturbation theory always breaks down at low energy (i.e., for $k \to 0$). Conversely, for BQPs in the PH regime, the strong screening of the disordered potential leads to a completely different condition: $(|V_R|/\mu)\sqrt{(\sigma_R/\xi)}\sqrt{\hat{c}_2(2k\sigma_R)} \ll 1/(k\xi)^{1/2}$. The latter is always valid at low energy, with the assumption that $\hat{c}_2(2k\sigma_R)$ is of the order of unity at most. We thus find that the validity condition (50) is easily satisfied on the whole spectrum by a potential that is weak enough, i.e., for $(|V_R|/\mu)\sqrt{(\sigma_R/\xi)} \ll 1$.

D. Numerical calculations

In order to test the accuracy of our perturbative approach, we performed numerical calculations of the Lyapunov exponent of BQPs in a 1D speckle potential, for various ratios σ_R/ξ. The first step consisted in determining the ground-state solution n_c of the GPE (2), using a propagation scheme in imaginary time. As a precise determination of $n_c(z)$ is required for a correct calculation of the low-energy eigenmodes of the BdGEs (5) and (6), we compared the result of this procedure

[7] For a complete discussion in the framework of the pure Schrödinger particles in speckle potentials, see, for instance, Refs. [32,33].

with the smoothing expansion including up to ten perturbation orders (see Appendix A). The values of Δ computed with the two methods for $\sigma_R = \sqrt{3/2}\,\xi$ agreed within a relative difference $\delta\Delta/\Delta$ of 0.3% for $V_R = 0.05\mu$, while the r.m.s. difference of the computed density profiles typically amounted to a few $10^{-4} V_R/g$. Homogeneous Dirichlet boundary conditions were imposed in the calculations, i.e., both the density profile n_c and the BQP components f^+ and f^- were constrained to vanish at the system boundaries.[8] We used system sizes of the order of a few 10^5 healing lengths, so that the corrections to the equation of state $\mu = g\overline{n_c}$ solely due to kinetic terms at the boundaries of the system were negligible,[9] in particular as compared to the corrections introduced by the disordered potential, described in Sec. III A 1.

In a second step, the profile $n_c(z)$ obtained as described above was included into the exact BdGEs (5) and (6), and the Bogoliubov modes were computed by solving the associated discretized eigenvalue problem. Eigenvalues and eigenvectors of the resulting large, non-Hermitian band matrices were obtained for a limited set of target energies using standard ARPACK routines.[10] The Lyapunov exponent Γ_k was then obtained by computing estimators of

$$-\lim_{z\to\infty} \frac{\overline{\ln[r(z)/r(z_0)]}}{|z-z_0|}, \tag{51}$$

where $r = \sqrt{(g^+)^2 + (\partial_z g^+/k)^2}$ defines the envelope of g^+ (see, e.g., Refs. [33,96]), and the abscissa z_0 refers to the localization center of each eigenstate. In order to obtain accurate estimates of the average value of the logarithm of $r(z)$ at infinity for a wide range of σ_R/ξ and $k\xi$ parameters, the numerical calculations were carried out in a large box of size $L = 3.2\times 10^5\xi$ (i.e., $10^5 - 10^6\sigma_R$), and disorder averaging was performed over 200 randomly generated 1D speckle patterns. We checked that, as expected, using $r(z) = |g^+(z)|$ in expression (51) produces the same results but requires more extensive disorder averaging, owing to the divergence of $\ln|g^+(z)/g^+(z_0)|$ at the nodes of g^+. We also found that replacing g^+ by one of the functions f^+, f^- or g^- in the expression of r leaves our numerical estimates of the Lyapunov exponent (51) unchanged, within a relative difference of less than 5% for all the parameters in this study.

On the whole spectral range which spans the phonon and free-particle regimes, the numerical data (filled points) shown in Fig. 6 are in excellent qualitative and fair quantitative agreement with the analytic prediction of Eq. (46) (thick solid lines), which corresponds to second-order perturbation theory. The choice of the value of V_R/μ was motivated by experimental relevance and, as aforesaid, by numerical tractability for an entire set of σ_R/ξ and $k\xi$ parameters.

Still, for this intermediate value of V_R/μ, we find slight deviations between the numerical data and Eq. (46). As discussed in Sec. IV E, this small difference can be attributed mostly to third-order terms which contribute to the exact Lyapunov exponent Γ_k. Hence, the observed deviations are expected to be negligible for lower values of V_R/μ. We also find that, even if these deviations cannot be completely neglected for $V_R \simeq 0.05\mu$, they do not change the qualitative behavior of Γ_k. Finally, note that for comparable parameters the deviations appear smaller in the data of Ref. [54] compared to those of the present work. The present results are actually more accurate as only a lowest-order smoothing expansion was used to compute the density n_c in Ref. [54].

E. Beyond the Born approximation

While the screened potential $\mathcal{V}_k$ of Eq. (30) and the Lyapunov exponent $\Gamma_k^{(2)}$ of Eq. (41) accurately account for the scattering and localization properties of BQPs in the limit of weak potentials, going beyond the leading-order (Born) approximation used to derive them is interesting in several respects. First, it should allow us to address the question of localization beyond cutoffs in the Lyapunov exponent $\Gamma_k^{(2)}$ such as the one arising in speckle potentials at wave number $1/\sigma_R$, described in Sec. IV B 2. Second, studying the localization properties of BQPs for stronger disorder or weaker interactions is of particular importance, since with increasing V_R/μ ratio the interacting Bose gas moves away from the deep superfluid (quasi-)BEC regime and into the weakly interacting fragmented Bose-glass phase [53,98,99,105,112]. While recent studies [58,105,112] have shown that the low-energy scaling of the inverse participation length of BQPs (which characterizes their short-range localization properties) is modified through the phase transition, the impact of strong disorder on the long-range localization properties of BQPs remains an open issue.

We now briefly address the localization properties of the Bogoliubov quasiparticles beyond the Born approximation by an inspection of the next-order terms of the weak-disorder expansion. While details of the derivation can be found in Appendix C, here we just outline the approach. The starting point is again the set of BdGEs (25) and (26) in the decoupling basis $g^\pm$. Retaining terms up to second order in the potential amplitude V_R, we find a new approximate Schrödinger-like equation for g^+:

$$\frac{\hbar^2k^2}{2m}g^+ \simeq -\frac{\hbar^2}{2m}\nabla^2 g^+ + [\mathcal{V}_k(\mathbf{r}) + \mathcal{V}_n(\mathbf{r}) + \mathcal{V}_-(\mathbf{r})]g^+, \tag{52}$$

where $\mathcal{V}_k$ is the screened potential of Eq. (30), proportional to V_R. The two additional terms $\mathcal{V}_n$ and $\mathcal{V}_-$ scale as V_R^2, and account for the second-order modulations of the density profile n_c and for the coupling of g^+ and g^-, respectively. Their expressions are given in Eqs. (C3) and (C4). Although Eq. (52) is valid *a priori* only in the regime $k \ll \min(1/\sigma_R, 1/\xi)$ (see Appendix C), we found it to provide a rather good approximation over a wider range of parameters (see Fig. 6 and below). On the basis of the Schrödinger-like equation (52),

[8] Periodic boundary conditions were found to complicate the analysis of the asymptotic localization properties of BQP modes, due to the periodic regrowths of the localized states in space.

[9] In a 1D box of length L, the relative correction to the equation of state associated with the Dirichlet boundary conditions scales as $\sqrt{2E_L/g\overline{n_c}} \simeq 2\xi/L$ for $g\overline{n_c}/E_L \gg 1$, where $E_L = \hbar^2/2mL^2$.

[10] This approach was preferred over other traditional methods for boundary-value problems, such as shooting algorithms [137], since the propagation of initial data by a differential operator $\xi\partial_z$ diverges exponentially on the length scale of a few healing lengths due to the coupling into evanescent modes in the case of Bogoliubov excitations (see Appendix B).

we calculate the third-order contributions to the Lyapunov exponent following the approach of Ref. [33]. We find

$$\Gamma_k^{(3)} = \Gamma_{\mathcal{V}_k,\mathcal{V}_n}^{(3)} + \Gamma_{\mathcal{V}_k,\mathcal{V}_-}^{(3)} + \Gamma_{\mathcal{V}_k,\mathcal{V}_k,\mathcal{V}_k}^{(3)}, \tag{53}$$

where $\Gamma_{\mathcal{V}_k,\mathcal{V}_n}^{(3)}$ (respectively, $\Gamma_{\mathcal{V}_k,\mathcal{V}_-}^{(3)}$) stems from the cross-correlator of $\mathcal{V}_k$ with $\mathcal{V}_n$ (respectively, $\mathcal{V}_-$), and the last term involves the three-point autocorrelation function of $\mathcal{V}_k$ [see Eqs. (C9) to (C11)]. These various contributions are plotted in Fig. 6 for a speckle potential and various σ_R/ξ ratios. We find an excellent agreement between the numerical data and the analytical result $\Gamma_k^{(2)} + \Gamma_k^{(3)}$. For the smallest value of σ_R/ξ however, the third order term $\Gamma_k^{(3)}$ does not fully account for the small difference between the Born approximation $\Gamma_k^{(2)}$ and the numerical data [see Fig. 6(c)]. This may be due to the fact that the criterion $k \ll 1/\xi$ is not met or to contributions of higher order in Γ_k. Let us now discuss the properties of the terms appearing in Eq. (53).

Note first that the third-order contributions scale as V_R^3. They are thus nonzero only for potentials which do not possess symmetric statistics under the transformation $V \to -V$. This holds for speckle potentials as used in experiments with ultracold atoms [33].

A generic feature of the contributions to $\Gamma_k^{(3)}$ is that they are all of the form

$$\Gamma_i^{(3)} \propto \int dq\, F_i(q) \hat{c}_3(q, 2k\sigma_R), \tag{54}$$

where i is an index labeling any of the terms in Eq. (53), F_i is some function, and $\hat{c}_3(q,q')$ is the Fourier transform of the reduced three-point autocorrelation function of the bare potential V. Thus, we find that if $\hat{c}_3$ has a compact support, $\Gamma_k^{(3)}$ vanishes over an extended part of the spectrum, as in the single-particle case [32,33]. In particular, in the case of speckle potentials, one finds a high-momentum cutoff that is identical to the cutoff in $\hat{c}_2$, whereby $\Gamma_k^{(3)}$ vanishes identically for $k > 1/\sigma_R$, just as $\Gamma_k^{(2)}$ does. This result is consistent with the argument that no odd power of V_R can provide the leading-order term in a given part of the spectrum, since the Lyapunov exponent is a non-negative quantity [33]. Note that this feature emerges from the analysis of the terms in Eq. (53) although the region $k \approx 1/\sigma_R$ *a priori* lies outside the regime of validity of Eq. (52).

Figure 6 shows that the magnitude of $\Gamma_{\mathcal{V}_k,\mathcal{V}_-}^{(3)}$, which originates from the coupling of g^+ and g^-, is small compared to the other terms in $\Gamma_k^{(3)}$. This further legitimizes the use of the $g^\pm$ basis and suggests that the difference between the analytical and the numerical results in Fig. 6(c) are likely to be due to higher-order terms rather than the violation of criterion $k \ll \xi$. We also note that, remarkably, the contributions $\Gamma_{\mathcal{V}_k,\mathcal{V}_n}^{(3)}$ and $\Gamma_{\mathcal{V}_k,\mathcal{V}_k,\mathcal{V}_k}^{(3)}$ tend to constant values at zero energy which turn out to be opposite and thus cancel out in the calculation of $\Gamma_k^{(3)}$. This cancellation between two terms that seem to have different origins in the perturbation expansion is certainly not accidental, and must be due to the $g^\pm$ representation chosen to set it up. Finally, an inspection of the low-energy limit of expression (53) in the case of the above speckle potential yields the scaling $\Gamma_k^{(3)} \sim k^2 \sim E^2$, a feature which is likely to be generic for disordered potentials with $\hat{c}_3(0,0) \neq 0$.

V. CONCLUSION

In this work, we presented a general approach, valid in any dimension, to describe a weakly interacting Bose gas of chemical potential μ subjected to a weak inhomogeneous potential $V(\mathbf{r})$. This approach relies on a two-step perturbative expansion of the Gross-Pitaevskii equation (GPE) and the Bogoliubov–de Gennes equations (BdGE), which govern the (quasi)condensate background and elementary excitations (Bogoliubov quasiparticles) of the Bose gas, respectively. In the first step, we calculate the mean-field density profile using a perturbative expansion of the GPE in V/μ. In the second step, the result is incorporated into the BdGEs. Turning to an adapted basis for the Bogoliubov wave functions, we then show that the BdGEs can be approximately mapped onto a Schrödinger-like equation, with an effective potential $\mathcal{V}_k$ which depends on the bare potential V, the condensate density background, and the quasiparticle wave vector k.

Our approach is well suited to study the effects of disorder in interacting Bose gases and, in particular, to examine the Anderson localization of Bogoliubov quasiparticles. On the one hand, it applies to any kind of weak, correlated disordered potentials. We stress that it is not limited to i) Gaussian disorder, ii) (uncorrelated) white-noise potentials, or iii) models of non-overlapping impurities. In particular, it applies to speckle potentials as used in many experiments with ultracold atoms. On the other hand, the only small parameter of the perturbative expansion is the ratio of the disorder amplitude V_R over the chemical potential μ. Our approach differs in this respect from standard approximations used in various other works: (i) the approximation of the BdGEs by hydrodynamical equations, which confine the theory to excitations of typical wavelength $\lambda \gg \xi$, where ξ is the healing length of the condensate [51,125], (ii) the Thomas-Fermi approximation of the background density profile, which is valid only under the assumption $\xi \ll \sigma_R$, where σ_R is the typical (minimal) length scale on which the external potential varies [51], (iii) the white-noise approximation which requires at least $\sigma_R \ll \lambda$ [51,138]. Conversely, the approach developed here holds for any ordering of the length scales ξ, σ_R, and λ.

Although our approach can be used to describe the scattering and localization properties of Bogoliubov quasiparticles in any dimension, we focused in this work on the one-dimensional case, which leads to the strongest localization effects [54]. In the low-energy limit and at the leading and next-leading orders in the disorder amplitude, we found a quadratic scaling of the Lyapunov exponent with the quasiparticle energy, $\Gamma_k \sim \epsilon^2 \propto k^2$. This finding is consistent with known results on the localization of phonons [129–132] and studies in the white-noise limit [51]. The effective potential $\mathcal{V}_k$ derived in our approach provides a physical interpretation of this suppression of localization in the low-energy phonon regime ($k\xi \ll 1$) in terms of an efficient screening of the long-wavelength modulations of the external potential by the background density of the Bose gas. In the free-particle regime ($k\xi \gg 1$), the Lyapunov exponent asymptotically approaches the exponent of a bare Schrödinger particle, $\Gamma_k \simeq \gamma_k$. For

uncorrelated potentials, the Lyapunov exponent of Bogoliubov quasiparticles thus falls off as $\Gamma_k \sim 1/\epsilon \propto 1/k^2$ in the high-energy limit. For correlated disorder, the high-energy decay of the Lyapunov exponent strongly depends on the large k behavior of the disorder power spectrum, $\Gamma_k \sim C_2(2k)/k^2$. If $C_2(2k)$ has a finite support as for speckle potentials for instance [18,27,33], effective mobility edges arise as for bare particles [32,33,134,135].

Most importantly, our approach covers the crossover between the phonon and free particle regimes. We find that localization (Γ_k) is maximum at a given energy ϵ. For uncorrelated potentials, this maximum lies around $E \simeq \mu$ (i.e., $k\xi \simeq 1$), at the crossover between the phonon and free-particle regimes [51,54]. For correlated potentials, the strength of localization is also determined by the detailed power spectrum of the potential and the energy of strongest localization depends on both the quasicondensate healing length ξ and the disorder correlation length σ_R.

Finally, let us discuss some possible extensions of our work. On the experimental side, the observation of localized Bogoliubov excitations appears as a challenge. It would be interesting to search for evidence of localization in the broadening of the dynamic structure factor, as measured in Bragg spectroscopy experiments [139–141]. Such broadenings have been measured to characterize coherence lengths of a couple hundred micrometers in elongated quasicondensates [141]. We infer therefrom that Bragg spectroscopy should allow the measurement of localization lengths of the same order of magnitude. On the theoretical side, the localization properties of Bogoliubov quasiparticles in two and three dimensions are expected to exhibit an even richer phenomenology. In particular, as pointed out previously [72,142], the screening of disorder by interactions is expected to lead to the possible occurrence of two mobility edges in three dimensions. In such a scenario, a first delocalization transition would occur at high energy, as for bare particles, and a second one would occur at low energies, as the effect of disorder is suppressed in the limit of vanishing quasiparticle energy [131]. The localized states would then reside around $k\xi \simeq 1$. Below a critical amount of disorder however, no quasiparticle states should be localized at all. As the screened potential derived here accurately describes scattering in higher dimensions as well, it may offer a simple avenue for the description of such a phenomenology.

ACKNOWLEDGMENTS

We thank A. Aspect, P. Bouyer, D. Clément, T.-L. Dao, L. Fontanesi, C. Gaul, V. Gurarie, C. A. Müller, V. Savona, and M. Wouters for fruitful discussions. This research was supported by CNRS, the European Research Council (FP7/2007-2013 Grant Agreement No. 256294), Agence Nationale de la Recherche (Contract No. ANR-08-blan-0016-01), RTRA-Triangle de la Physique, and the Alexander von Humboldt Foundation (Grant No. 1139948). We acknowledge the use of the computing facility cluster GMPCS of the LUMAT federation (FR LUMAT 2764). Laboratoire Charles Fabry de l'Institut d'Optique (LCFIO) is a member of the Institut Francilien de Recherche sur les Atomes Froids (IFRAF).

APPENDIX A: PERTURBATION SERIES OF THE SMOOTHING SOLUTION

In this appendix, we calculate explicitly the leading terms of the modulations $\widetilde{V}(\mathbf{r}) = g\overline{n_c} - gn_c(\mathbf{r})$ of the mean-field interaction term $gn_c(\mathbf{r})$ and the deviation $\Delta = g\overline{n_c} - \mu$ from the homogeneous equation of state. We consider the limit of a weak external potential V and strong interactions which is relevant to our study (see Sec. III A). Working along the lines of Ref. [104], the weakness of V suggests an expansion of the square root of the density in powers of V_R/μ, which we write as

$$\sqrt{n_c(\mathbf{r})} = \sqrt{\frac{\mu}{g}}\,[\phi^{(0)}(\mathbf{r}) + \phi^{(1)}(\mathbf{r}) + \phi^{(2)}(\mathbf{r}) + \cdots], \quad \text{(A1)}$$

where $\phi^{(0)}(\mathbf{r}) = 1$ is the solution in the absence of disorder [143] and the functions $\phi^{(n)}(\mathbf{r})$ are real valued. We thus have

$$n_c(\mathbf{r}) = \frac{\mu}{g}\sum_{i,j}\phi^{(i)}(\mathbf{r})\phi^{(j)}(\mathbf{r}) \quad \text{(A2)}$$

and the quantities of interest at any order in the expansion series are readily obtained by collecting the terms at the corresponding order:

$$\Delta^{(0)} = 0, \quad \text{(A3)}$$

$$\Delta^{(n)} = \mu \sum_{\substack{0\leqslant i,j\leqslant n\\ i+j=n}} \overline{\phi^{(i)}\phi^{(j)}}, \qquad \text{for } n \geqslant 1, \quad \text{(A4)}$$

and

$$\widetilde{V}^{(0)}(\mathbf{r}) = 0, \quad \text{(A5)}$$

$$\widetilde{V}^{(n)}(\mathbf{r}) = \Delta^{(n)} - \mu \sum_{\substack{0\leqslant i,j\leqslant n\\ i+j=n}} \phi^{(i)}(\mathbf{r})\phi^{(j)}(\mathbf{r}), \qquad \text{for } n \geqslant 1. \quad \text{(A6)}$$

The functions $\phi^{(n)}(\mathbf{r})$ are determined by inserting the perturbation series (A1) into the GPE (2), which is equivalently written as

$$\left[-2\xi^2\nabla^2 - 1 + \frac{V(\mathbf{r})}{\mu} + \frac{gn_c(\mathbf{r})}{\mu}\right]\sqrt{n_c(\mathbf{r})} = 0, \quad \text{(A7)}$$

and by collecting the terms of order n. The explicit calculation of $\phi^{(n)}$ becomes increasingly tedious as the number of terms involved grows like n^2. Yet, the above perturbation hierarchy produces a simple recursion formula which can be used in analytical or numerical calculations. Following the procedure outlined above, for all $n \geqslant 1$, we obtain

$$\phi^{(n)} = -\frac{1}{2}G_\xi * \left[\frac{V}{\mu}\phi^{(n-1)} + \sum_{\substack{i+j+k=n\\ 0\leqslant i,j,k\leqslant n-1}} \phi^{(i)}\phi^{(j)}\phi^{(k)}\right], \quad \text{(A8)}$$

where $G_\xi(\mathbf{r})$ is the Green function associated with the operator $-\xi^2\nabla^2 + 1$, which is best written in Fourier space as

$$G_\xi(\mathbf{q}) = \frac{(2\pi)^{-d/2}}{1 + (|\mathbf{q}|\xi)^2}, \quad \text{(A9)}$$

and the convolution product is defined as

$$(f * g)(\mathbf{r}) = \int d\mathbf{r}'\; f(\mathbf{r} - \mathbf{r}')g(\mathbf{r}'). \quad \text{(A10)}$$

Applying the recursive procedure up to second order, we find

$$\phi^{(0)} = 1, \tag{A11}$$

$$\phi^{(1)} = -\frac{1}{2\mu} G_\xi * V, \tag{A12}$$

$$\phi^{(2)} = \frac{1}{4\mu^2} G_\xi * \left[V(G_\xi * V) - \frac{3}{2}(G_\xi * V)^2 \right]. \tag{A13}$$

Then, using Eqs. (A4) and (A6), we find

$$\Delta^{(1)} = 0, \tag{A14}$$

$$\widetilde{V}^{(1)} = G_\xi * V = \int d\mathbf{r}'\, G_\xi(\mathbf{r} - \mathbf{r}') V(\mathbf{r}'), \tag{A15}$$

and

$$\begin{aligned}\Delta^{(2)} &= \frac{1}{4\mu}\overline{\{G_\xi * [2V(G_\xi * V) - 3(G_\xi * V)^2] + (G_\xi * V)^2\}} \\ &= \frac{V_R^2 \sigma_R^d}{2(2\pi)^{d/2}\mu} \int d\mathbf{q}\, \frac{(|\mathbf{q}|\xi)^2}{[1 + (|\mathbf{q}|\xi)^2]^2} \hat{c}_2(\mathbf{q}\sigma_R),\end{aligned} \tag{A16}$$

$$\begin{aligned}\widetilde{V}^{(2)} &= \Delta^{(2)} - \frac{1}{4\mu}\{G_\xi * [2V(G_\xi * V) - 3(G_\xi * V)^2] \\ &\quad + (G_\xi * V)^2\}.\end{aligned} \tag{A17}$$

Finally, let us make two comments on the above perturbative solution of the GPE. First, for the perturbation expansion be valid, the mean-field density profile n_c must be weakly perturbed around the homogeneous value μ/g. While the original small parameter is V_R/μ, Eq. (A8) shows that

$$\left|\widetilde{V}_R^{(1)}\right| \ll \mu \tag{A18}$$

with

$$\widetilde{V}_R^{(1)} = \mathrm{sgn}(V_R)\sqrt{\overline{\widetilde{V}^{(1)2}}} \tag{A19}$$

is a somewhat looser criterion for the successive terms of the expansion to be small. The rms amplitude $|\widetilde{V}_R^{(1)}|$ [see Eq. (A19)] can be calculated explicitly from Eq. (A15):

$$\left|\widetilde{V}_R^{(1)}\right| = \sqrt{\frac{V_R^2 \sigma_R^d}{(2\pi)^{d/2}} \int d\mathbf{q} \frac{\hat{c}_2(\mathbf{q}\sigma_R)}{[1 + (|\mathbf{q}|\xi)^2]^2}}. \tag{A20}$$

Second, Eq. (A8) can be used to show by induction that, whenever the potential V is extended, then so are all the perturbation orders $\phi^{(n)}$ and $\widetilde{V}^{(n)}$. In the disordered case, these simple considerations show how localization can be destroyed in a regime of weak interactions compatible with the mean-field approach.

APPENDIX B: DECOUPLING BASIS FOR BOGOLIUBOV–DE GENNES EQUATIONS IN WEAK POTENTIALS

In this appendix, we motivate the introduction of the functions g^+ and g^- (see Sec. III B) to solve the BdGEs (5) and (6), and justify the use of the Schrödinger-like equation (30) for weak potentials. Throughout the paper, we assume that the system lies in a box whose dimensions eventually tend to infinity to emulate the continuum limit, and we impose periodic or homogeneous Dirichlet boundary conditions on the functions f^+ and f^-. In the latter case, the density n_c and the BQP components f^+ and f^- vanish at the system boundaries. However, in the limit $\xi/L \to 0$, where L is the system size, and the absence of an external potential, the system can be regarded as homogeneous. Together with these boundary conditions, the BdGEs form the differential problem to be solved. The system of coupled equations (21) and (22) can be rewritten as a differential problem in matrix form:

$$\xi^2 \nabla^2 F(\mathbf{r}) = H_\epsilon(\mathbf{r}) F(\mathbf{r}), \tag{B1}$$

where

$$F(\mathbf{r}) = \begin{pmatrix} f^+(\mathbf{r}) \\ f^-(\mathbf{r}) \end{pmatrix}, \tag{B2}$$

and $H_\epsilon(\mathbf{r}) = H_\epsilon^{(0)} + W(\mathbf{r})$ is a real-valued symmetric matrix, which depends on the energy ϵ and the position $\mathbf{r}$, with[11]

$$H_\epsilon^{(0)} = \begin{pmatrix} 0 & -\epsilon/2\mu \\ -\epsilon/2\mu & 1 \end{pmatrix}, \tag{B3}$$

$$W(\mathbf{r}) = \frac{1}{2\mu}\begin{pmatrix} V + \Delta - \widetilde{V} & 0 \\ 0 & V + 3\Delta - 3\widetilde{V} \end{pmatrix}, \tag{B4}$$

where the position dependence of V and $\widetilde{V}$ was dropped for conciseness. The two differential equations on f^+ and f^- associated with Eq. (B1) are strongly coupled via the off-diagonal terms in $H_\epsilon^{(0)}$. Since W is small (at most of first order in V_R), it is worth working in the basis that diagonalizes $H_\epsilon^{(0)}$. Indeed, although the change of basis may introduce off-diagonal (coupling) terms in W, these terms will remain small. We will then show that this approach is suitable for the setup of a perturbation expansion.

1. Bogoliubov–de Gennes equations in the decoupling basis

In the absence of an external potential ($V = 0$), the matrix W vanishes identically. Then, the matrix $H_\epsilon = H_\epsilon^{(0)}$ has two eigenvalues,

$$\frac{1 - \sqrt{1 + (\epsilon/\mu)^2}}{2} \equiv -k^2\xi^2, \tag{B5}$$

$$\frac{1 + \sqrt{1 + (\epsilon/\mu)^2}}{2} \equiv +\beta^2\xi^2, \tag{B6}$$

associated to the eigenvectors

$$F_k \propto \begin{pmatrix} \sqrt{\rho} \\ +1/\sqrt{\rho} \end{pmatrix} \quad \text{and} \quad F_\beta \propto \begin{pmatrix} -1/\sqrt{\rho} \\ \sqrt{\rho} \end{pmatrix}, \tag{B7}$$

respectively, where

$$\rho = \frac{\mu}{\epsilon} + \sqrt{1 + \left(\frac{\mu}{\epsilon}\right)^2}. \tag{B8}$$

For simplicity, let us restrict our discussion to the 1D case.[12] Since Eq. (B1) is of second order, each eigen-subspace

[11] In an equivalent formulation, H_ϵ can be regarded as an operator acting on two-vectors of functions f^+ and f^-. The position representation of Eq. (B1) is adopted here for simplicity.

[12] The conclusions are naturally extended in higher dimensions.

corresponds to two possible solutions of the BdGEs. First, the solutions corresponding to $+\beta^2\xi^2$ are $e^{\pm\beta z}F_\beta$, which either grow or decrease exponentially. These modes are the *evanescent* modes discussed below Eq. (28), which thus appear naturally in this formulation. Since no solution of Eq. (B1) in the subspace spanned by these eigenvectors can satisfy the boundary conditions on both boundaries, these modes are forbidden in the case of vanishing V. Second, the solutions corresponding to $-k^2\xi^2$ are $e^{\pm ikz}F_k$, which are *oscillating* (plane wave) modes. Since solutions of Eq. (B1) that satisfy the boundary conditions can be built with linear combinations of these eigenvectors, these modes are allowed for $V = 0$. They correspond to the well-known physical solutions of the BdGEs (5) and (6).

The procedure above allowed us to decouple the BdGEs in homogeneous space. Let us introduce now the external potential $V(\mathbf{r})$. Rewriting Eq. (B1) in the eigenbasis of $H_\epsilon^{(0)}$, we find

$$\xi^2\nabla^2 G(\mathbf{r}) = H'_\epsilon(\mathbf{r})G(\mathbf{r}), \tag{B9}$$

where $G(\mathbf{r}) = P^{-1}F(\mathbf{r})$, and

$$P^{-1} = \begin{pmatrix} +\sqrt{\rho} & +1/\sqrt{\rho} \\ -1/\sqrt{\rho} & +\sqrt{\rho} \end{pmatrix} \tag{B10}$$

is the inverse of the transformation matrix from the F basis to the G basis. The term $H'_\epsilon = H'^{(0)}_\epsilon + W'$, which is the analog of H_ϵ in the G basis, contains a homogeneous part

$$H'^{(0)}_\epsilon = \begin{pmatrix} -k^2\xi^2 & 0 \\ 0 & \beta^2\xi^2 \end{pmatrix}, \tag{B11}$$

and a potential-dependent part

$$W'(\mathbf{r}) = P^{-1}W(\mathbf{r})P = \frac{1}{2\mu}\begin{pmatrix} V - \frac{3+\rho^2}{1+\rho^2}(\widetilde{V}-\Delta) & -\frac{2\rho}{1+\rho^2}(\widetilde{V}-\Delta) \\ V - \frac{2\rho}{1+\rho^2}(\widetilde{V}-\Delta) & -\frac{1+3\rho^2}{1+\rho^2}(\widetilde{V}-\Delta) \end{pmatrix}. \tag{B12}$$

Note that the BQP energy ϵ is here embedded in the dependence of k, β, and ρ on ϵ [see Eqs. (B5), (B6), and (B8)].

For the sake of clarity, let us write explicitly the two coupled equations associated to Eq. (B9) in terms of the components $g^\pm$ of $G(\mathbf{r}) = (g^+(\mathbf{r}), g^-(\mathbf{r}))^{\mathrm{T}}$:

$$\frac{\hbar^2k^2}{2m}g^+ = -\frac{\hbar^2}{2m}\nabla^2 g^+ - \frac{2\rho}{1+\rho^2}(\widetilde{V}-\Delta)g^- + \left[V - \frac{3+\rho^2}{1+\rho^2}(\widetilde{V}-\Delta)\right]g^+, \tag{B13}$$

$$-\frac{\hbar^2\beta^2}{2m}g^- = -\frac{\hbar^2}{2m}\nabla^2 g^- - \frac{2\rho}{1+\rho^2}(\widetilde{V}-\Delta)g^+ + \left[V - \frac{1+3\rho^2}{1+\rho^2}(\widetilde{V}-\Delta)\right]g^-, \tag{B14}$$

where

$$g^\pm_\nu(\mathbf{r}) = \pm\rho_\nu^{\pm 1/2}f^+_\nu(\mathbf{r}) + \rho_\nu^{\mp 1/2}f^-_\nu(\mathbf{r}). \tag{B15}$$

These equations are equivalent to the BdGEs, without any approximation. The benefit of the transformation we have used is that, for a weak external potential, the terms appearing in W' are all small. In particular, the terms coupling g^+ and g^- in Eqs. (B13) and (B14) are at most of the order of V [as $|\widetilde{V}_\mathrm{R}| \simeq |\widetilde{V}^{(1)}_\mathrm{R}| \leqslant |V_\mathrm{R}|$ and $2\rho/(1+\rho^2) \leqslant 1$]. The G basis thus offers a suitable starting point, which takes into account the full structure of the BdGEs, and which allows for a perturbative approach in the regime of weak disorder.

2. Leading-order terms: Mapping the Bogoliubov–de Gennes equations onto a Schrödinger-like equation

Let us now develop the perturbation expansion of the BdGEs in the G basis. Since Eqs. (B13) and (B14) are weakly coupled, we can resort to the following self-consistent approach. Assuming that g^- is vanishingly small compared to g^+ for small V_R, we neglect the third term on the right-hand side of Eq. (B14). Then, solving for g^- and retaining only the leading-order term in V_R, we obtain[13]

$$g^-(\mathbf{r}) \simeq \frac{2m}{\hbar^2\beta^2}\frac{2\rho}{1+\rho^2}\int d\mathbf{r}' G_{1/\beta}(\mathbf{r}-\mathbf{r}')\widetilde{V}^{(1)}(\mathbf{r}')g^+(\mathbf{r}'), \tag{B16}$$

where $G_{1/\beta}(\mathbf{q}) = \frac{(2\pi)^{-d/2}}{1+(|\mathbf{q}|/\beta)^2}$ is the Green function associated with the differential operator $-(1/\beta)^2\nabla^2 + 1$, written in Fourier space. The positive smoothing function $G_{1/\beta}$ satisfies $\int \mathrm{d}\mathbf{r}' G_{1/\beta}(\mathbf{r}') = 1$, and decays on the length scale $1/\beta$, which is smaller than the healing length ξ and than $1/k$, i.e., the typical length scale over which g^+ varies (see Fig. 7). Thus, owing to the fact that $2m/(\hbar^2\beta^2) < 1/\mu$ and $2\rho/(1+\rho^2) < 1$, we can safely write

$$|g^-(\mathbf{r})| < \frac{1}{\mu}\int d\mathbf{r}' G_{1/\beta}(\mathbf{r}-\mathbf{r}')|\widetilde{V}^{(1)}(\mathbf{r}')||g^+(\mathbf{r}')|. \tag{B17}$$

Then, in terms of orders of magnitude,

$$|g^-| \lesssim \frac{|\widetilde{V}^{(1)}_\mathrm{R}|}{\mu}|g^+|\int d\mathbf{r}' G_{1/\beta}(\mathbf{r}-\mathbf{r}') \lesssim \frac{|\widetilde{V}^{(1)}_\mathrm{R}|}{\mu}|g^+| \ll |g^+|, \tag{B18}$$

which is consistent with our initial assumption, i.e., g^- is small compared to g^+. In Fig. 7 we show numerical results which corroborate expression (B16) and the fact that g^- is a term of order $\widetilde{V}^{(1)}_\mathrm{R}/\mu$ at most to g^+.

From the upper bound (B18), we infer that the second term on the right-hand side of Eq. (B13) is of the order of $(\widetilde{V}^2_\mathrm{R}/\mu)|g^+|$ at most, while the third term contains terms scaling as $|V_\mathrm{R}g^+|$. Hence, we neglect the former contribution, and obtain a closed equation for g^+ which is valid up to first order in V_R/μ:

$$-\frac{\hbar^2}{2m}\nabla^2 g^+ + \mathcal{V}_k(\mathbf{r})g^+ \simeq \frac{\hbar^2k^2}{2m}g^+, \tag{B19}$$

where

$$\mathcal{V}_k(\mathbf{r}) = V(\mathbf{r}) - \frac{3+\rho^2}{1+\rho^2}\widetilde{V}^{(1)}(\mathbf{r}). \tag{B20}$$

[13]Note that Δ is of second order in V_R (see Sec. III A or Appendix A).

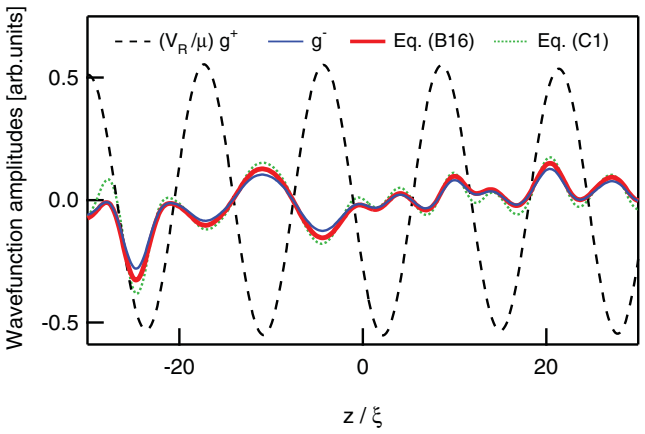

FIG. 7. (Color online) BQP mode in the $g^{\pm}$ basis. This eigenmode was computed at energy $\epsilon \simeq 1.1\mu$ for a speckle potential with $V_R = 0.05\mu$ and $\sigma_R/\xi = \sqrt{3/2}$. The mode is displayed here over a few healing lengths, while the size of the box used for the calculation is $L = 3.2 \times 10^5 \xi$. The g^+ and g^- components obtained numerically are given by the black dashed line and the blue solid line, respectively. The thick red line represents the convolution formula (B16), and the green dotted line the somewhat cruder approximation (C1) to g^-. Note that the g^+ component has been rescaled by V_R/μ in this figure for better comparison with the various representations of g^-. With the above parameters, $\widetilde{V}_R^{(1)} \simeq 0.6\, V_R$.

These are the expressions reproduced in Eqs. (30) and (31), which form the basis of our approach to calculate the BQP modes in leading-order perturbation theory. The advantage of the $g^{\pm}$ representation is that, at this level of approximation, the coupled equations (21) and (22) reduce to a simple closed equation for g^+, the solution of which also determines g^- via Eq. (B16).

APPENDIX C: LYAPUNOV EXPONENT OF BOGOLIUBOV QUASIPARTICLES BEYOND THE BORN APPROXIMATION

In this appendix, the perturbation expansion of the Lyapunov exponent of BQPs is extended one order beyond the leading-order (Born) approximation, so as to include terms scaling as V_R^3. To this aim, we consider explicitly the terms in Eq. (B13) that are of second order in V_R.

The third term on the right-hand side of Eq. (B13) contains both an inhomogeneous term $\widetilde{V}^{(2)}$ and an offset $\Delta^{(2)}$ that are proportional to V_R^2, and for which explicit expressions are given in Appendix A. Elements of order V_R^2 are also introduced into Eq. (B13) by the cross-term $\widetilde{V} g^-$, where g^- may be replaced by expression (B16). If g^+ varies on a length scale larger than that of the other quantities in the integrand of Eq. (B16), we can use the approximation

$$g^-(\mathbf{r}) \simeq \frac{2m}{\hbar^2\beta^2}\frac{2\rho}{1+\rho^2} g^+(\mathbf{r}) \int d\mathbf{r}' G_{1/\beta}(\mathbf{r}-\mathbf{r}')\widetilde{V}(\mathbf{r}'). \quad \text{(C1)}$$

While Eq. (C1) is justified for $k \ll \min(1/\sigma_R, 1/\xi)$, we found that it is actually a good approximation on a broader range of parameters (see Sec. IV E). For instance, this approximation shows good agreement with direct numerical results for g^- for the parameters of Fig. 7. Hence, we get a new closed equation for g^+, which now comprises all the terms up to order V_R^2 and is legitimate in the low-energy limit:

$$\frac{\hbar^2 k^2}{2m} g^+ \simeq -\frac{\hbar^2}{2m}\nabla^2 g^+ + [\mathcal{V}_k(\mathbf{r}) + \mathcal{V}_n(\mathbf{r}) + \mathcal{V}_-(\mathbf{r})]g^+, \quad \text{(C2)}$$

where $\mathcal{V}_k$ is the screened potential (B20), and the terms $\mathcal{V}_n$ and $\mathcal{V}_-$ are potentials proportional to V_R^2:

$$\mathcal{V}_n(\mathbf{r}) = -\frac{3+\rho^2}{1+\rho^2}[\widetilde{V}^{(2)}(\mathbf{r}) - \Delta^{(2)}], \quad \text{(C3)}$$

$$\mathcal{V}_-(\mathbf{r}) = -\frac{8m\rho^2}{\hbar^2\beta^2(1+\rho^2)^2}\int d\mathbf{r}' G_{1/\beta}(\mathbf{r}-\mathbf{r}')\widetilde{V}^{(1)}(\mathbf{r})\widetilde{V}^{(1)}(\mathbf{r}'). \quad \text{(C4)}$$

The potential term $\mathcal{V}_n$ follows from a second-order expansion of the ground-state density profile, and $\mathcal{V}_-$ originates from the coupling between g^+ and g^-. Both $\mathcal{V}_n$ and $\mathcal{V}_-$ have a nonvanishing average. These nonvanishing averages suggest an evaluation of the correlation functions at a wave vector off the energy shell (29) in the fourth-order Lyapunov exponent $\Gamma^{(4)}$. However, these averages play no role in the correlation functions contributing to $\Gamma_k^{(3)}$ (see below), and can thus be disregarded at this level of approximation.

For Schrödinger particles of energy $E = \hbar^2 k^2/2m$ in a 1D disordered potential V, the leading orders of the weak-disorder expansion of the Lyapunov exponent read [33]

$$\gamma_k^{(2)} = \frac{1}{4k^2}\left(\frac{2m}{\hbar^2}\right)^2 \int_{-\infty}^{0} dz C_2(z)\cos(2kz), \quad \text{(C5)}$$

with $C_2(z) = \overline{V(0)V(z)}$ and

$$\gamma_k^{(3)} = -\frac{1}{4k^3}\left(\frac{2m}{\hbar^2}\right)^3 \mathcal{P}\int dq \frac{C_3(q,2k) + C_3(-q,-2k)}{2q} = -\frac{1}{4k^3}\left(\frac{2m}{\hbar^2}\right)^3 \int_{-\infty}^{0} dz \int_{-\infty}^{z} dz' C_3(z,z')\sin(2kz'), \quad \text{(C6)}$$

where $\mathcal{P}$ denotes a Cauchy principal value, $C_3(z,z') = \overline{V(0)V(z)V(z')}$ is the three-point correlation function and $C_3(q,q')$ is its Fourier transform. Replacing V in these formulas by the sum of the potential terms appearing in Eq. (C2) and collecting the different terms according to their order in V_R, up to V_R^3, we find

$$\Gamma_k \simeq \Gamma^{(2)}_{\mathcal{V}_k,\mathcal{V}_k} + \Gamma^{(3)}_{\mathcal{V}_k,\mathcal{V}_n} + \Gamma^{(3)}_{\mathcal{V}_k,\mathcal{V}_-} + \Gamma^{(3)}_{\mathcal{V}_k,\mathcal{V}_k,\mathcal{V}_k}, \quad \text{(C7)}$$

where

$$\Gamma^{(2)}_{\mathcal{V}_k,\mathcal{V}_k} = \frac{1}{4k^2}\left(\frac{2m}{\hbar^2}\right)^2 \int_{-\infty}^{0} dz \overline{\mathcal{V}_k(0)\mathcal{V}_k(z)}\cos(2kz) \quad \text{(C8)}$$

corresponds to result (37), obtained in the Born approximation, and the remaining terms are the three contributions to the

third-order Lyapunov exponent of BQPs:

$$\Gamma^{(3)}_{\mathcal{V}_k,\mathcal{V}_n} = \frac{1}{4k^2}\left(\frac{2m}{\hbar^2}\right)^2 \int_{-\infty}^{0} dz[\overline{\mathcal{V}_k(0)\mathcal{V}_n(z)} + \overline{\mathcal{V}_n(0)\mathcal{V}_k(z)}]\cos(2kz), \quad \text{(C9)}$$

$$\Gamma^{(3)}_{\mathcal{V}_k,\mathcal{V}_-} = \frac{1}{4k^2}\left(\frac{2m}{\hbar^2}\right)^2 \int_{-\infty}^{0} dz[\overline{\mathcal{V}_k(0)\mathcal{V}_-(z)} + \overline{\mathcal{V}_-(0)\mathcal{V}_k(z)}]\cos(2kz), \quad \text{(C10)}$$

$$\Gamma^{(3)}_{\mathcal{V}_k,\mathcal{V}_k,\mathcal{V}_k} = -\frac{1}{4k^3}\left(\frac{2m}{\hbar^2}\right)^3 \int_{-\infty}^{0} dz \times \int_{-\infty}^{z} dz'\overline{\mathcal{V}_k(0)\mathcal{V}_k(z)\mathcal{V}_k(z')}\sin(2kz'). \quad \text{(C11)}$$

Note that, since $\overline{\mathcal{V}_k} = 0$, the nonvanishing mean values of $\mathcal{V}_n$ and $\mathcal{V}_-$ play no role in the various contributions to $\Gamma^{(3)}$, and can subtracted from $\mathcal{V}_n$ and $\mathcal{V}_-$ in Eqs. (C9) and (C11). As the expressions of contributions (C9) to (C11) in Fourier space are quite involved, we do not reproduce them here. We refer to Fig. 6 and to Sec. IV E, which provide a discussion of the behavior of these terms.

[1] L. Sanchez-Palencia and M. Lewenstein, Nature Phys. **6**, 87 (2010).
[2] G. Modugno, Rep. Prog. Phys. **73**, 102401 (2010).
[3] A. Aspect and M. Inguscio, Phys. Today **62**, 30 (2009).
[4] L. Fallani, C. Fort, and M. Inguscio, Adv. At. Mol. Opt. Phys. **56**, 119 (2008).
[5] J. E. Lye, L. Fallani, M. Modugno, D. S. Wiersma, C. Fort, and M. Inguscio, Phys. Rev. Lett. **95**, 070401 (2005).
[6] Y. P. Chen, J. Hitchcock, D. Dries, M. Junker, C. Welford, and R. G. Hulet, Phys. Rev. A **77**, 033632 (2008).
[7] M. Albert, T. Paul, N. Pavloff, and P. Leboeuf, Phys. Rev. Lett. **100**, 250405 (2008).
[8] S. G. Bhongale, P. Kakashvili, C. J. Bolech, and H. Pu, Phys. Rev. A **82**, 053632 (2010).
[9] D. Dries, S. E. Pollack, J. M. Hitchcock, and R. G. Hulet, Phys. Rev. A **82**, 033603 (2010).
[10] Z. Wu and E. Zaremba, Phys. Rev. Lett. **106**, 165301 (2011).
[11] L. Pezzé, B. Hambrecht, and L. Sanchez-Palencia, Europhys. Lett. **88**, 30009 (2009).
[12] D. Clément, A. F. Varón, M. Hugbart, J. A. Retter, P. Bouyer, L. Sanchez-Palencia, D. M. Gangardt, G. V. Shlyapnikov, and A. Aspect, Phys. Rev. Lett. **95**, 170409 (2005).
[13] C. Fort, L. Fallani, V. Guarrera, J. E. Lye, M. Modugno, D. S. Wiersma, and M. Inguscio, Phys. Rev. Lett. **95**, 170410 (2005).
[14] T. Schulte, S. Drenkelforth, J. Kruse, W. Ertmer, J. Arlt, K. Sacha, J. Zakrzewski, and M. Lewenstein, Phys. Rev. Lett. **95**, 170411 (2005).
[15] D. Clément, A. F. Varón, J. A. Retter, L. Sanchez-Palencia, A. Aspect, and P. Bouyer, New J. Phys. **8**, 165 (2006).
[16] M. Modugno, Phys. Rev. A **73**, 013606 (2006).
[17] E. Akkermans, S. Ghosh, and Z. H. Musslimani, J. Phys. B **41**, 045302 (2008).
[18] L. Sanchez-Palencia, D. Clément, P. Lugan, P. Bouyer, and A. Aspect, New J. Phys. **10**, 045019 (2008).
[19] M. Robert-de Saint-Vincent, J.-P. Brantut, B. Allard, T. Plisson, L. Pezzé, L. Sanchez-Palencia, A. Aspect, T. Bourdel, and P. Bouyer, Phys. Rev. Lett. **104**, 220602 (2010).
[20] L. Pezzé, M. Robert-de Saint-Vincent, T. Bourdel, J.-P. Brantut, B. Allard, T. Plisson, A. Aspect, P. Bouyer, and L. Sanchez-Palencia, e-print arXiv:1103.2294.
[21] R. C. Kuhn, C. Miniatura, D. Delande, O. Sigwarth, and C. A. Müller, Phys. Rev. Lett. **95**, 250403 (2005).
[22] L. Sanchez-Palencia and L. Santos, Phys. Rev. A **72**, 053607 (2005).
[23] B. Shapiro, Phys. Rev. Lett. **99**, 060602 (2007).
[24] R. C. Kuhn, O. Sigwarth, C. Miniatura, D. Delande, and C. A. Müller, New J. Phys. **9**, 161 (2007).
[25] L. Beilin, E. Gurevich, and B. Shapiro, Phys. Rev. A **81**, 033612 (2010).
[26] B. Damski, J. Zakrzewski, L. Santos, P. Zoller, and M. Lewenstein, Phys. Rev. Lett. **91**, 080403 (2003).
[27] L. Sanchez-Palencia, D. Clément, P. Lugan, P. Bouyer, G. V. Shlyapnikov, and A. Aspect, Phys. Rev. Lett. **98**, 210401 (2007).
[28] S. E. Skipetrov, A. Minguzzi, B. A. van Tiggelen, and B. Shapiro, Phys. Rev. Lett. **100**, 165301 (2008).
[29] J. Billy, V. Josse, Z. Zuo, A. Bernard, B. Hambrecht, P. Lugan, D. Clément, L. Sanchez-Palencia, P. Bouyer, and A. Aspect, Nature (London) **453**, 891 (2008).
[30] G. Roati, C. D'Errico, L. Fallani, M. Fattori, C. Fort, M. Zaccanti, G. Modugno, M. Modugno, and M. Inguscio, Nature (London) **453**, 895 (2008).
[31] J. Chabé, G. Lemarié, B. Grémaud, D. Delande, P. Szriftgiser, and J. C. Garreau, Phys. Rev. Lett. **101**, 255702 (2008).
[32] E. Gurevich and O. Kenneth, Phys. Rev. A **79**, 063617 (2009).
[33] P. Lugan, A. Aspect, L. Sanchez-Palencia, D. Delande, B. Grémaud, C. A. Müller, and C. Miniatura, Phys. Rev. A **80**, 023605 (2009).
[34] G. Lemarié, H. Lignier, D. Delande, P. Szriftgiser, and J. C. Garreau, Phys. Rev. Lett. **105**, 090601 (2010).
[35] M. Antezza, Y. Castin, and D. A. W. Hutchinson, Phys. Rev. A **82**, 043602 (2010).
[36] L. Pezzé and L. Sanchez-Palencia, Phys. Rev. Lett. **106**, 040601 (2011).
[37] M. Piraud, P. Lugan, P. Bouyer, A. Aspect, and L. Sanchez-Palencia, Phys. Rev. A **83**, 031603(R) (2011).
[38] M. Piraud, A. Aspect, and L. Sanchez-Palencia, e-print arXiv:1104.2314.
[39] M. Moratti and M. Modugno, e-print arXiv:1102.5299.
[40] T. Paul, P. Schlagheck, P. Leboeuf, and N. Pavloff, Phys. Rev. Lett. **98**, 210602 (2007).
[41] A. S. Pikovsky and D. L. Shepelyansky, Phys. Rev. Lett. **100**, 094101 (2008).
[42] G. Kopidakis, S. Komineas, S. Flach, and S. Aubry, Phys. Rev. Lett. **100**, 084103 (2008).

[43] S. Palpacelli and S. Succi, Phys. Rev. E **77**, 066708 (2008).
[44] T. Paul, M. Albert, P. Schlagheck, P. Leboeuf, and N. Pavloff, Phys. Rev. A **80**, 033615 (2009).
[45] S. Flach, D. O. Krimer, and C. Skokos, Phys. Rev. Lett. **102**, 024101 (2009).
[46] M. Albert, T. Paul, N. Pavloff, and P. Leboeuf, Phys. Rev. A **82**, 011602 (2010).
[47] Y. Hu, Z. Liang, and B. Hu, Phys. Rev. A **81**, 053621 (2010).
[48] E. Lucioni, B. Deissler, L. Tanzi, G. Roati, M. Modugno, M. Zaccanti, M. Inguscio, and G. Modugno, Phys. Rev. Lett. **106**, 230403 (2011).
[49] R. Roth and K. Burnett, Phys. Rev. A **68**, 023604 (2003).
[50] V. Gurarie and J. T. Chalker, Phys. Rev. B **68**, 134207 (2003).
[51] N. Bilas and N. Pavloff, Eur. Phys. J. D **40**, 387 (2006).
[52] V. I. Yukalov and R. Graham, Phys. Rev. A **75**, 023619 (2007).
[53] P. Lugan, D. Clément, P. Bouyer, A. Aspect, M. Lewenstein, and L. Sanchez-Palencia, Phys. Rev. Lett. **98**, 170403 (2007).
[54] P. Lugan, D. Clément, P. Bouyer, A. Aspect, and L. Sanchez-Palencia, Phys. Rev. Lett. **99**, 180402 (2007).
[55] L. Fallani, J. E. Lye, V. Guarrera, C. Fort, and M. Inguscio, Phys. Rev. Lett. **98**, 130404 (2007).
[56] B. Horstmann, J. I. Cirac, and T. Roscilde, Phys. Rev. A **76**, 043625 (2007).
[57] V. I. Yukalov, E. P. Yukalova, K. V. Krutitsky, and R. Graham, Phys. Rev. A **76**, 053623 (2007).
[58] V. Gurarie, G. Refael, and J. T. Chalker, Phys. Rev. Lett. **101**, 170407 (2008).
[59] G. Roux, T. Barthel, I. P. McCulloch, C. Kollath, U. Schollwöck, and T. Giamarchi, Phys. Rev. A **78**, 023628 (2008).
[60] T. Nattermann and V. L. Pokrovsky, Phys. Rev. Lett. **100**, 060402 (2008).
[61] C. Gaul and C. A. Müller, Europhys. Lett. **83**, 10006 (2008).
[62] V. Yukalov, E. Yukalova, and V. Bagnato, Laser Physics **19**, 686 (2009).
[63] G. M. Falco, T. Nattermann, and V. L. Pokrovsky, Europhys. Lett. **85**, 30002 (2009).
[64] L. Pollet, N. V. Prokof'ev, B. V. Svistunov, and M. Troyer, Phys. Rev. Lett. **103**, 140402 (2009).
[65] V. Gurarie, L. Pollet, N. V. Prokof'ev, B. V. Svistunov, and M. Troyer, Phys. Rev. B **80**, 214519 (2009).
[66] M. White, M. Pasienski, D. McKay, S. Q. Zhou, D. Ceperley, and B. DeMarco, Phys. Rev. Lett. **102**, 055301 (2009).
[67] M. Pasienski, D. McKay, M. White, and B. DeMarco, Nature Phys. **6**, 677 (2010).
[68] B. Deissler, M. Zaccanti, G. Roati, C. D'Errico, M. Fattori, M. Modugno, G. Modugno, and M. Inguscio, Nature Phys. **6**, 354 (2010).
[69] I. L. Aleiner, B. L. Altshuler, and G. V. Shlyapnikov, Nature Phys. **6**, 900 (2010).
[70] B. Deissler, E. Lucioni, M. Modugno, G. Roati, L. Tanzi, M. Zaccanti, M. Inguscio, and G. Modugno, New J. Phys. **13**, 023020 (2011).
[71] C. Gaul and C. A. Müller, e-print arXiv:1009.5448.
[72] C. Gaul and C. A. Müller, Phys. Rev. A **83**, 063629 (2011).
[73] G. Orso, Phys. Rev. Lett. **99**, 250402 (2007).
[74] K. Byczuk, W. Hofstetter, and D. Vollhardt, Phys. Rev. Lett. **102**, 146403 (2009).
[75] K. Byczuk, W. Hofstetter, and D. Vollhardt, Int. J. Mod. Phys. B **24**, 1727 (2010).
[76] L. Han and C. A. R. Sá de Melo, New J. Phys. **13**, 055012 (2011).
[77] A. Sanpera, A. Kantian, L. Sanchez-Palencia, J. Zakrzewski, and M. Lewenstein, Phys. Rev. Lett. **93**, 040401 (2004).
[78] V. Ahufinger, L. Sanchez-Palencia, A. Kantian, A. Sanpera, and M. Lewenstein, Phys. Rev. A **72**, 063616 (2005).
[79] J. Wehr, A. Niederberger, L. Sanchez-Palencia, and M. Lewenstein, Phys. Rev. B **74**, 224448 (2006).
[80] A. Niederberger, T. Schulte, J. Wehr, M. Lewenstein, L. Sanchez-Palencia, and K. Sacha, Phys. Rev. Lett. **100**, 030403 (2008).
[81] A. Niederberger, J. Wehr, M. Lewenstein, and K. Sacha, Europhys. Lett. **86**, 26004 (2009).
[82] A. Niederberger, M. M. Rams, J. Dziarmaga, F. M. Cucchietti, J. Wehr, and M. Lewenstein, Phys. Rev. A **82**, 013630 (2010).
[83] F. Crépin, G. Zaránd, and P. Simon, Phys. Rev. Lett. **105**, 115301 (2010).
[84] M. Bretz, Phys. Rev. Lett. **31**, 1447 (1973).
[85] J. D. Reppy, Physica B+C **126**, 335 (1984).
[86] J. D. Reppy, J. Low Temp. Phys. **87**, 205 (1992).
[87] P. A. Crowell, F. W. Van Keuls, and J. D. Reppy, Phys. Rev. Lett. **75**, 1106 (1995).
[88] P. A. Crowell, F. W. Van Keuls, and J. D. Reppy, Phys. Rev. B **55**, 12620 (1997).
[89] A. A. Abrikosov and L. P. Gorkov, Sov. Phys. JETP **8**, 1090 (1958).
[90] A. A. Abrikosov and L. P. Gorkov, Sov. Phys. JETP **9**, 220 (1959).
[91] P. W. Anderson, J. Phys. Chem. Sol. **11**, 26 (1959).
[92] P. A. Lee and T. V. Ramakrishnan, Rev. Mod. Phys. **57**, 287 (1985).
[93] D. Belitz and T. R. Kirkpatrick, Rev. Mod. Phys. **66**, 261 (1994).
[94] D. K. K. Lee and J. M. F. Gunn, J. Phys. Condens. Matter **2**, 7753 (1990).
[95] E. Abrahams, P. W. Anderson, D. C. Licciardello, and T. V. Ramakrishnan, Phys. Rev. Lett. **42**, 673 (1979).
[96] I. M. Lifshits, S. Gredeskul, and L. Pastur, *Introduction to the Theory of Disordered Systems* (Wiley, New York, 1988).
[97] M. Ma, B. I. Halperin, and P. A. Lee, Phys. Rev. B **34**, 3136 (1986).
[98] T. Giamarchi and H. J. Schulz, Europhys. Lett. **3**, 1287 (1987).
[99] T. Giamarchi and H. J. Schulz, Phys. Rev. B **37**, 325 (1988).
[100] M. P. A. Fisher, P. B. Weichman, G. Grinstein, and D. S. Fisher, Phys. Rev. B **40**, 546 (1989).
[101] R. T. Scalettar, G. G. Batrouni, and G. T. Zimanyi, Phys. Rev. Lett. **66**, 3144 (1991).
[102] W. Krauth, N. Trivedi, and D. Ceperley, Phys. Rev. Lett. **67**, 2307 (1991).
[103] K. Huang and H.-F. Meng, Phys. Rev. Lett. **69**, 644 (1992).
[104] L. Sanchez-Palencia, Phys. Rev. A **74**, 053625 (2006).
[105] L. Fontanesi, M. Wouters, and V. Savona, Phys. Rev. A **81**, 053603 (2010).
[106] E. Altman, Y. Kafri, A. Polkovnikov, and G. Refael, Phys. Rev. B **81**, 174528 (2010).
[107] L. Fontanesi, M. Wouters, and V. Savona, Phys. Rev. A **83**, 033626 (2011).
[108] R. Vosk and E. Altman, e-print arXiv:1104.2063.
[109] J. A. Hertz, L. Fleishman, and P. W. Anderson, Phys. Rev. Lett. **43**, 942 (1979).

[110] A. De Martino, M. Thorwart, R. Egger, and R. Graham, Phys. Rev. Lett. **94**, 060402 (2005).
[111] J. Radić, V. Bačić, D. Jukić, M. Segev, and H. Buljan, Phys. Rev. A **81**, 063639 (2010).
[112] L. Fontanesi, M. Wouters, and V. Savona, Phys. Rev. Lett. **103**, 030403 (2009).
[113] S. M. Barnett and P. M. Radmore, *Methods in Theoretical Quantum Optics* (Clarendon, Oxford, 1997).
[114] N. N. Bogolyubov, J. Phys. USSR **11**, 23 (1947).
[115] N. N. Bogolyubov, Sov. Phys. JETP **7**, 41 (1958).
[116] V. M. Popov, Theor. Math. Phys. **11**, 72 (1972).
[117] V. M. Popov, *Functional Integrals in Quantum Field Theory and Statistical Physics* (Reidel, Dordrecht, 1983).
[118] C. Mora and Y. Castin, Phys. Rev. A **67**, 053615 (2003).
[119] Y. Castin, J. Phys. IV (France) **116**, 89 (2004).
[120] M. Lewenstein and L. You, Phys. Rev. Lett. **77**, 3489 (1996).
[121] Y. Castin and R. Dum, Phys. Rev. A **57**, 3008 (1998).
[122] P.-G. de Gennes, *Superconductivity of Metals and Alloys* (Addison-Wesley, Reading, MA, 1995).
[123] D. S. Petrov, M. Holzmann, and G. V. Shlyapnikov, Phys. Rev. Lett. **84**, 2551 (2000).
[124] D. S. Petrov, G. V. Shlyapnikov, and J. T. M. Walraven, Phys. Rev. Lett. **85**, 3745 (2000).
[125] Y. Castin, in *Coherent Atomic Matter Waves*, edited by R. Kaiser, C. Westbrook, and F. David, Proceedings of the Les Houches Summer School of Theoretical Physics, Vol. LXXII (EDP Sciences/Springer-Verlag, Berlin, 2001), Chap. "Bose-Einstein condensates in atomic gases: simple theoretical results."
[126] D. V. Skryabin, Phys. Rev. A **63**, 013602 (2000).
[127] D. Vollhardt and P. Wölfle, Phys. Rev. Lett. **45**, 842 (1980).
[128] D. Vollhardt and P. Wölfle, Phys. Rev. B **22**, 4666 (1980).
[129] K. Ishii, Prog. Theor. Phys., Suppl. **53**, 77 (1973).
[130] J. Jäckle, Solid State Commun. **39**, 1261 (1981).
[131] S. John, H. Sompolinsky, and M. J. Stephen, Phys. Rev. B **27**, 5592 (1983).
[132] M. Y. Azbel, Phys. Rev. B **28**, 4106 (1983).
[133] D. Clément, P. Bouyer, A. Aspect, and L. Sanchez-Palencia, Phys. Rev. A **77**, 033631 (2008).
[134] F. M. Izrailev and A. A. Krokhin, Phys. Rev. Lett. **82**, 4062 (1999).
[135] L. Tessieri, J. Phys. A **35**, 9585 (2002).
[136] B. Derrida and E. Gardner, J. Phys. (France) **45**, 1283 (1984).
[137] W. H. Press, S. A. Teukolsky, W. T. Vetterling, and B. P. Flannery, *Numerical Recipes*, 3rd ed. (Cambridge University Press, Cambridge, 2007).
[138] S. Giorgini, L. Pitaevskii, and S. Stringari, Phys. Rev. B **49**, 12938 (1994).
[139] J. Stenger, S. Inouye, A. P. Chikkatur, D. M. Stamper-Kurn, D. E. Pritchard, and W. Ketterle, Phys. Rev. Lett. **82**, 4569 (1999).
[140] J. Steinhauer, R. Ozeri, N. Katz, and N. Davidson, Phys. Rev. Lett. **88**, 120407 (2002).
[141] S. Richard, F. Gerbier, J. H. Thywissen, M. Hugbart, P. Bouyer, and A. Aspect, Phys. Rev. Lett. **91**, 010405 (2003).
[142] P. Lugan, Ph.D. thesis, Ecole Polytechnique, Palaiseau (2010), [http://tel.archives-ouvertes.fr/tel-00468888/en/].
[143] L. P. Pitaevskii and S. Stringari, *Bose-Einstein Condensation* (Clarendon Press, Oxford, 2004).

Chapter 4

TWO-COMPONENT ULTRACOLD GASES: EXTENDED HUBBARD AND SPIN MODELS

In brief – *Ultracold atomic systems offer fascinating possibilities to investigate the effects of disorder in complex systems. For instance, one can realize multi-component gases of bosons, fermions or mixtures of several species, with controlled parameters. This allows design of new Hamiltonians, paving the way to investigations of new effects of disorder in ultracold atoms.*

Under fairly general assumptions, the dynamics of two-component, strongly-correlated gases in optical lattices can be mapped onto that of single-component composite particles governed by extended Hubbard-like models. Disorder in these systems induces a plethora of phenomena. In Fermi-Bose mixtures, weak disorder leads to composite fermions with random tunneling and random interactions between nearest-neighbor sites, which can be all attractive, all repulsive, or randomly attractive and repulsive. It is then possible to form a non-interacting Fermi gas, a weakly-interacting Fermi liquid, a checker-board insulator or a domain insulator. For strong on-site inhomogeneities, it is possible to map the Hamiltonian onto a disordered Ising-like model, which realizes the analogue of the very debated spin glasses.

Lattice spin Hamiltonians can also be realized with Bose-Bose mixtures in optical lattices. Then, weak disorder allows to simulate controlled random magnetic fields, paving the way to interesting effects. For instance, the so-called random-field induced order (RFIO) corresponds to situations where, counter-intuitively, disorder favors spin ordering. RFIO is however very weak in optical lattice systems. Alternatively, one can use coupled Bose-Einstein condensates (in the absence of a lattice), which sustain the continuous counterpart of RFIO. This is signaled by a fixed relative phase and in this case, the effect is very strong and robust.

▷ The work presented in this chapter has been performed first in the group of Maciej Lewenstein in Hannover with Anna Sanpera, Veronica Ahufinger, Adrian Kantian and Jakub Zakrzewski, and then in collaboration with Maciej Lewenstein, Jan Wehr, Krzysztof Sacha, Thomas Schulte and Armand Niederberger.

4.1 Two-component lattice gases in the strongly-correlated regime: Effective Hamiltonian for composite particles

In this section, we consider a two-species (binary) mixture of ultracold atoms in a deep optical lattice. We assume that one of the species (b) is bosonic, while the other (B) can be either bosonic or fermionic. As we will see, the discussion of this section does not depend much on the quantum statistics of the B-species. We will thus mainly refer to the case of bosons, which is slightly more general, and point out specific differences in the case of fermions.

4.1.1 Two-component Hamiltonian

The dynamics of a two-component gas confined in a deep optical lattice at low temperature is governed by the Bose-Bose Hubbard model [see (Lewenstein *et al.*, 2007) and Eq. (1.3) in Sec. 1.1]:

$$\begin{aligned}\hat{H} &= -\sum_{\langle j,l\rangle}\left[\left(\tau_{\rm b}\hat{b}_j^\dagger\hat{b}_l+\tau_{\rm B}\hat{B}_j^\dagger\hat{B}_l\right)+\text{h.c.}\right]+\sum_j\left(v_j\hat{n}_j+V_j\hat{N}_j\right) \\ &\quad+\sum_j\left[\frac{U_{\rm bb}}{2}\,\hat{n}_j(\hat{n}_j-1)+\frac{U_{\rm BB}}{2}\,\hat{N}_j(\hat{N}_j-1)+U_{\rm bB}\,\hat{n}_j\hat{N}_j\right]\end{aligned} \tag{4.1}$$

where $\hat{b}_j$ and $\hat{B}_j$ are the annihilation operators of an atom in the lattice site j for the b and B species respectively, $\hat{n}_j=\hat{b}_j^\dagger\hat{b}_j$ and $\hat{N}_j=\hat{B}_j^\dagger\hat{B}_j$ are the corresponding number operators, and $\langle j,l\rangle$ denotes a pair of nearest-neighbor lattice sites. The on-site energies v_j and V_j are assumed to be site-dependent. They may include a harmonic component due to trapping and/or a random component of zero average, which can be generated with incommensurate lattices (Fallani *et al.*, 2007; Roati *et al.*, 2008; Deissler *et al.*, 2010) or speckle lasers (White *et al.*, 2009; Pasienski *et al.*, 2010). Note that in the case where the B-species is fermionic[1], the interaction term proportional to $\hat{N}_j(\hat{N}_j-1)$ vanishes in the Fermi sub-space, owing to the anti-commutation relation $\{\hat{f}_j,\hat{f}_j^\dagger\}=1$. The value of $U_{\rm BB}$, which is unrelevant for fermions, can thus be chosen arbitrary. As we will see, it is convenient to choose $U_{\rm BB}=\infty$.

4.1.2 The composite-particle picture

Consider now the strongly-correlated regime, such that $0<\tau_{\rm b},\tau_{\rm B}\ll U_{\rm bb},U_{\rm BB},U_{\rm bB}$. In order to construct a relevant Hilbert sub-space, let us first consider the bosonic b-species alone in the lattice. Neglecting the tunneling, the b-bosons form a Mott insulator with $n_j=\left\lfloor\frac{\mu_{\rm b}-v_j}{U_{\rm bb}}\right\rfloor$, where $\lfloor\,.\,\rfloor$ stands for the integer part and $\mu_{\rm b}$ is the chemical potential of the b-bosons in the absence of the second species. For the sake of simplicity, we assume that $\mu_{\rm b}=U_{\rm bb}/2$ and $|v_j|<U_{\rm bb}/2$, so that the b-Bose gas forms a Mott insulator with $n_j=1$ particle per site[2,3]. If the values v_j are bounded, this state is gaped by an excitation energy $U_{\rm bb}-\Delta v$, where Δv is the width of the distribution of the v_j's.

[1] For explicit reference to fermions, we use the notation f instead of B.

[2] We discuss various cases in (Sanpera *et al.*, 2004) and (Ahufinger *et al.*, 2005). Here we restrict to a case that turns out to be quite generic and rich.

[3] Physically, this state can be produced with the help of a smooth harmonic trap, close to the trap center (Greiner *et al.*, 2002).

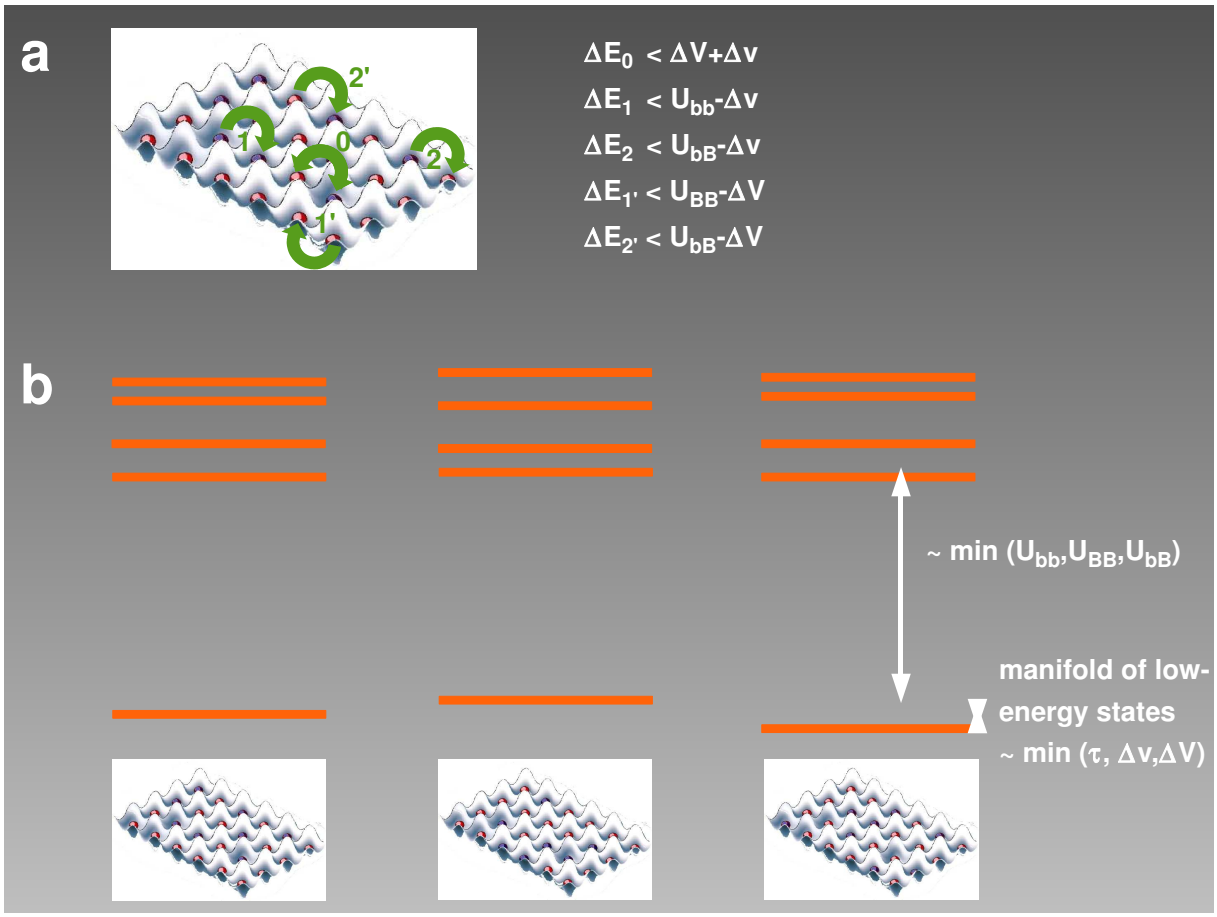

Figure 4.1 | Typical energy spectrum of two-component lattice gases in the strongly-correlated regime. Blue balls represent b-particles, while red balls represent B-particles. **a)** Excitation processes and associated typical energies. While the process 0 keeps the state in the low-energy manifold, the other ones transfer it to higher-energy states. **b)** Energy spectrum of a two-component lattice gas with strong interactions. The low-lying states correspond to all configurations of the two atomic species with one atom per lattice site. The higher-energy excitations correspond to transitions towards states with at least one site with two particles.

Let us now add the second species, particle per particle. Each B-particle can be added in any lattice site j. The first one is included into a site that necessarily contains a b-particle, which costs the energy $U_{bB}+V_j$ if the b-particle stays, while exchanging the b-particle for the B-particle would cost the energy $V_j - v_j$. For $U_{bB} \gtrsim \Delta v$, it is thus energetically favorable to exchange the particles[2]. Let us now add more B-particles. Similarly as before, if we add a B-particle in a site that contains a b-particle, it replaces it. If we try to add the B-particle in a site that already contains a B-particle, it would cost the energy $U_{BB}+V_j$. Then, for $U_{BB} > \Delta v, \Delta V$, this process is not energetically favorable. Note that if the B-particles are fermionic, it is just forbidden by the Pauli principle, which is equivalent to the case of hard-core bosons, *i.e.* $U_{BB} = \infty$.

Hence, for $U_{bb}, U_{BB}, U_{bB} > \Delta v, \Delta V$, we have constructed a binary system whose ground state is a Fock state $\prod_j |n_j, N_j\rangle$, where for any lattice site j, (n_j, N_j) is either $(1,0)$ or $(0,1)$. The exact ground state depends on the total number of b- and B-particles, and on the configuration of the inhomogeneous fields $\{v_j\}$ and $\{V_j\}$. There are two kinds of excitations (see Fig. 4.1a). The first

kind consists in moving a single particle from one site to another (processes 1, 1′, 2, and 2′ in the figure). This costs the interaction energy U_{bb}, U_{BB} or U_{bB} and on-site energies of the order of Δv or ΔV or smaller. The second kind consists in exchanging a b-particle in a given site and a B-particle in another site (process 0 in the figure). This costs an energy of the order of $\Delta v + \Delta V$ or smaller.

Here, we consider a situation where the interaction terms exceed the other relevant energy scales, *i.e.* temperature and tunneling rates and on-site energies. We can thus restrict the Hilbert space to the subspace $\mathcal{E}_0$ generated by $\{\prod_j |n_j, N_j\rangle,\ n_j + N_j = 1 \text{ for all j}\}$. This corresponds to a manifold of low-energy states formed by all possible configurations with only one particle (b or B) per lattice site (see Fig. 4.1b). Then, the physics of the mixture can be regarded as the one of *composite particles* made of one B-particle and a bosonic b-hole (Lewenstein *et al.*, 2004; Sanpera *et al.*, 2004). The vacuum thus corresponds to one b-boson in each lattice site. The annihilation and creation operators of the composite particles depend on the nature of the B-particles:

– For bosonic B-particles, the annihilation and creation operators of the composites are

$$\hat{\mathcal{B}}_j = \hat{b}_j^\dagger \hat{B}_j \mathcal{P} \tag{4.2}$$

$$\hat{\mathcal{B}}_j^\dagger = \mathcal{P} \hat{B}_j^\dagger \hat{b}_j \tag{4.3}$$

where $\mathcal{P}$ is the projection operator onto $\mathcal{E}_0$. One can check that these operators verify the bosonic commutation relations in different sites and fermionic anti-commutation relations in the same site. The composite particles are thus so called Schwinger (*i.e.* hard-core) bosons (Auerbach, 1994).

– For fermionic f-particles[1], the annihilation and creation operators of the composites are

$$\hat{\mathcal{F}}_j = \hat{b}_j^\dagger \hat{f}_j \mathcal{P} \tag{4.4}$$

$$\hat{\mathcal{F}}_j^\dagger = \mathcal{P} \hat{f}_j^\dagger \hat{b}_j. \tag{4.5}$$

These operators verify the fermionic anti-commutation relations, and the composite particles are thus fermions.

4.1.3 Effective Hamiltonian

So far, we restricted the analysis to the on-site terms $\hat{H}_0$ in Eq. (4.1), and excluded the coupling terms $\hat{H}_1$ corresponding to the first sum in Eq. (4.1). However, since the manifold of low-energy states that generates the subspace $\mathcal{E}_0$ is quasi-degenerate, the coupling terms can strongly couple the corresponding states of the manifold. Extending the process outlined by Kuklov and Svistunov (2003) to include inhomogeneous on-site energies, we used resolvent perturbation theory restricted to the Hilbert subspace $\mathcal{E}_0$ and include the coupling terms. The effective Hamiltonian thus reads

$$\langle \text{out}|\hat{H}_{\text{eff}}|\text{in}\rangle = \langle \text{out}|\hat{H}_0|\text{in}\rangle + \langle \text{out}|H_1|\text{in}\rangle - \frac{1}{2}\langle \text{out}|\hat{H}_1 \left(\frac{1}{\hat{H}_0 - E_{\text{in}}} + \frac{1}{\hat{H}_0 - E_{\text{out}}} \right) \hat{H}_1 |\text{in}\rangle, \tag{4.6}$$

where $|\text{in}\rangle$ and $|\text{out}\rangle$ lie in the subspace $\mathcal{E}_0$. The Hamiltonian (4.1) then reduces to (Sanpera *et al.*, 2004; Ahufinger *et al.*, 2005; Wehr *et al.*, 2006)

$$H_{\text{eff}} = -\sum_{\langle j,l \rangle} \left(J_{j,l}\ \hat{\mathcal{B}}_j^\dagger \hat{\mathcal{B}}_l + \text{h.c} \right) + \sum_{\langle j,l \rangle} K_{j,l}\ \hat{\mathcal{N}}_j \hat{\mathcal{N}}_l + \sum_j \mathcal{V}_j\ \hat{\mathcal{N}}_j \tag{4.7}$$

where $\hat{\mathcal{N}}_j = \hat{\mathcal{B}}_j^\dagger \hat{\mathcal{B}}_j$ is the number operator of a composite particle. Hamiltonian $H_{\rm eff}$ contains (i) a hopping term $J_{j,l}$, (ii) an interaction term between neighbor sites $K_{j,l}$, and (iii) inhomogeneous on-site energies $\mathcal{V}_j$. The coupling parameters in Hamiltonian (4.7) read

$$J_{j,l} = \frac{\tau_{\rm b}\tau_{\rm B}}{U_{\rm bB}}\left[\frac{1}{1-\left(\frac{\delta_{j,l}}{U_{\rm bB}}\right)^2}+\frac{1}{1-\left(\frac{\Delta_{j,l}}{U_{\rm bB}}\right)^2}\right] \tag{4.8}$$

$$K_{j,l} = -\frac{4\tau_{\rm b}^2/U_{\rm bb}}{1-\left(\frac{\delta_{j,l}}{U_{\rm bb}}\right)^2}+\frac{2\tau_{\rm b}^2/U_{\rm bB}}{1-\left(\frac{\delta_{j,l}}{U_{\rm bB}}\right)^2}+\frac{2\tau_{\rm B}^2/U_{\rm bB}}{1-\left(\frac{\Delta_{j,l}}{U_{\rm bB}}\right)^2}-\frac{4\tau_{\rm B}^2/U_{\rm BB}}{1-\left(\frac{\Delta_{j,l}}{U_{\rm BB}}\right)^2} \tag{4.9}$$

$$\mathcal{V}_j = V_j - v_j + \sum_{\langle j,l\rangle}\left[\frac{4\tau_{\rm b}^2/U_{\rm bb}}{1-\left(\frac{\delta_{j,l}}{U_{\rm bb}}\right)^2}-\frac{\tau_{\rm b}^2/U_{\rm bB}}{1-\frac{\delta_{j,l}}{U_{\rm bB}}}-\frac{\tau_{\rm B}^2/U_{\rm bB}}{1+\frac{\Delta_{j,l}}{U_{\rm bB}}}+\frac{4\tau_{\rm B}^2/U_{\rm BB}}{1-\left(\frac{\Delta_{j,l}}{U_B}\right)^2}\right], \tag{4.10}$$

where $\delta_{j,l} = v_j - v_l$ and $\Delta_{j,l} = V_j - V_l$. In principle, these relations hold only in the case where the B-particles are bosons (Wehr *et al.*, 2006). In fact, all denominators in Eqs. (4.8)-(4.10) result from virtual hopping of particles from one site to a neighboring one. Some of these process, which exist when the B-particles are bosons are forbidden for fermions (*e.g.* hopping of a fermion towards a site that already contains a fermion). The latter process do not contribute to the hopping term (4.8), but they do contribute to the interaction terms and to the on-site energies, through the last term in Eqs. (4.9) and (4.10). Since these terms vanish, in the hard-core limit, the above equation actually also holds for fermions, provided that we use the convention $U_{\rm ff} = U_{\rm BB} = \infty$ (Sanpera *et al.*, 2004; Ahufinger *et al.*, 2005).

4.2 Fermi-Bose mixtures

▷ *see papers reprinted on pages 161 and 165*

Using the composite-particle picture, we have analyzed the physics of Fermi-Bose mixtures in disordered, deep optical lattices. The zoology of quantum phases is extremely wide as described in details in (Sanpera *et al.*, 2004; Ahufinger *et al.*, 2005). Here, we restrict our discussion to a small part of the phase diagram which illustrates the richness of the system.

4.2.1 Expected phases in the presence of weak disorder

Consider the case described in Sec. 4.1.2 where composites are formed of a f-fermion plus a b-bosonic hole. For the discussion below, we assume that $\tau_{\rm b} = \tau_{\rm f}$. As can be seen from Eqs. (4.8)-(4.10), apart from multiplying parameters (scaling as squared tunneling divided by interaction terms), the parameters of the effective Hamiltonian (4.7) strongly depend on the on-site energies v_j and V_j of the two bare particle species. Hence, the physics depends on how the two species react to external fields, *i.e.* trapping and/or disordered potentials.

Case where $V_j = 0$ - Let us first consider the case where $V_j = 0$, *i.e.* the fermionic species is not subjected to any external field. The coupling constants $J_{j,l}$ and $K_{j,l}$ are plotted on Fig. 4.2a-b as a function of $\delta_{j,l}$. The hopping amplitudes $J_{j,l}$ are all positive, but may vary quite significantly with

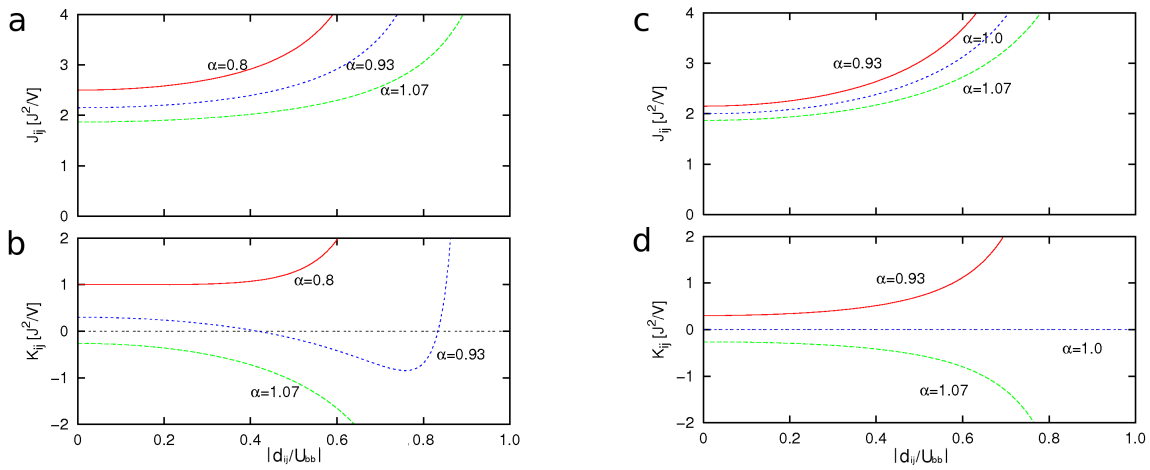

Figure 4.2 | Coupling parameters for composite fermions in inhomogeneous lattices. The figures show the tunneling, $J_{j,l}$, and nearest-neighbor couplings, $K_{j,l}$, for composites made of one bare fermion and one bosonic hole as a function of $\delta_{j,l}$, and for different boson-fermion interactions, $\alpha = U_{\rm bf}/U_{\rm bb}$. Figures a) and b) correspond to the case $V_j = 0$, while figures c) and d) correspond to the case $V_j = v_j$.

inhomogeneities, especially when $\delta_{j,l}$ approaches $U_{\rm bf}$. For $\alpha \equiv U_{\rm bf}/U_{\rm bb} > 1$, we have $K_{j,l} \leq 0$ and we deal with attractive (although inhomogeneous) interactions. For α sufficiently smaller than unity, we have $K_{j,l} \geq 0$ and the interactions between composites are repulsive. For $\alpha \lesssim 1$, we find that $K_{j,l}$ might take positive or negative values depending on the value of $\delta_{j,l}$. Hence, in the latter case, the qualitative character of interactions can be controlled by the inhomogeneity (Sanpera *et al.*, 2004).

Let us discuss the case of on-site energies v_j generated by a disordered potential. For weak disorder, we neglect the contributions of $\delta_{j,l}$ to $J_{j,l}$ and $K_{j,l}$, and keep only the leading contribution in $\mathcal{V}_j$, *i.e.* the first term in Eq. (4.10). For $K \ll J$, the system forms a *Fermi glass* phase, *i.e.* an Anderson localized (and possibly many-body corrected) phase where single-particle states are occupied according to the Fermi-Dirac distribution (Freedman and Hertz, 1977; Imry, 1995; von Oppen and Wettig, 1995; Jacoud and Shepelyansky, 1997). The latter always holds in one- and two-dimensional systems, and in three dimensions for sufficiently strong disorder, leading to Anderson localization of single particles (Abrahams *et al.*, 1979). For strong repulsive interactions ($K > 0$ and $K \gg J$), the ground state forms a Mott insulator-like phase and the composite fermions are pinned for large-enough filling factors. In particular, for half filling factor, one expects the ground state to be in the form of a checker-board. For intermediate values of K/J and still for $K > 0$, delocalized metallic phases with enhanced persistent currents have been predicted (Schmitteckert *et al.*, 1998; Benenti *et al.*, 1999; Waintal *et al.*, 2000; Gambetti-Césare *et al.*, 2002), which would be interesting to search for. Similarly, for weak attractive interactions (*i.e.* $K < 0$ and $|K|/J < 1$), one expects competition between pairing of fermions and disorder, *i.e.* a 'dirty' superfluid phase. Finally, for strong, attractive interactions ($K < 0$ and $|K| \gg J$, the fermions form a domain insulator, *i.e.* the fermions group together in $N_{\rm f}$ adjacent sites. These various phases are schematically depicted on Fig. 4.3.

Case where $V_j = v_j$ - The situation differs if the fermions are also subjected to external fields. Consider now the case where the two species are equally sensitive to the disorder, that is the on-

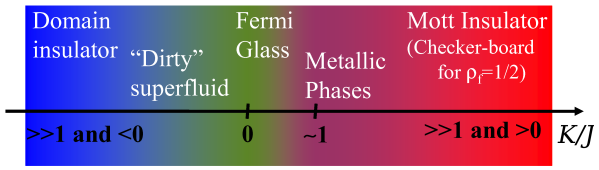

Figure 4.3 | Schematic phase diagram of fermionic composites in a weak disordered potential. The diagram represents the expected phases as a function of the nearest-neighbor interaction strength for composites made of one bare fermion and one bosonic hole in weak disorder ($\delta_{j,l} \ll U_{bb}, U_{bf}$) and for vanishing fermionic on-site energies ($V_j \equiv 0$) [from (Ahufinger *et al.*, 2005)].

site energies are equal for bosons and fermions in each lattice site, $V_j = v_j$. The coupling constants $J_{j,l}$ and $K_{j,l}$ are plotted on Fig. 4.2c and d as a function of $\delta_{j,l} = \Delta_{j,l}$. The hopping amplitudes $J_{j,l}$ are all positive and do not differ very significantly from the previous case. In contrast to the case where the bosons only are subjected to the disorder, here the sign of the interactions between the composites is governed by the interactions between bosons and fermions *alone*. Since $\delta_{j,l} = \Delta_{j,l}$ for all couples of adjacent sites (and since we assume $\tau_b = \tau_f$), we immediately see from Eq. (4.9) that $K_{j,l} = 0$ for $\alpha = 1$ (*i.e.* $U_{bf} = U_{bb}$). For $\alpha > 1$, the effective interactions are always negative, and the composites experience random attractive interactions, as in the previous case. Conversely, for $\alpha < 1$, the effective interactions are always positive, and we thus deal with random repulsive interactions.

In the presence of a weak disordered potential, we expect the appearance of similar phases as in the previous case.

4.2.2 Numerical calculations within the Gutzwiller approach

In order to gain insight to this physics, we have performed numerical calculations that give evidences of (i) formation of composite particles, and (ii) existence of different quantum phases in disordered lattices and in the presence of a harmonic trap. Mean field theory provides appropriate –although not exact– properties of Hubbard models (Sachdev, 1999). We used the Gutzwiller variational meanfield approach (Fisher *et al.*, 1989; Rokhsar and Kotliar, 1991; Krauth *et al.*, 1992; K. Sheshadri *et al.*, 1993). In brief, the Gutzwiller approach neglects site-to-site quantum coherence so that the many-body ground state is written as a product of N states, each one being localized in a different lattice site (N being the total number of lattice sites). Each localized state is a superposition of different Fock states $|n,m\rangle_j$ with exactly n bosons and m fermions on the j-th lattice site :

$$|\psi_{GA}\rangle = \prod_{j=1}^{N} \left[\sum_{n\geq 0} \sum_{m=0,1} g_{n,m}^{(j)} |n,m\rangle_j \right]. \tag{4.11}$$

In practice, the sum over n is limited to a finite value n_{max} which is chosen large-enough that the numerical results are not affected by n_{max}. The $g_{n,m}^{(j)}$ are complex coefficients proportional to the amplitude of finding n bosons and m fermions in the j-th lattice site, and consequently we can impose, without loss of generality, these coefficients to satisfy $\sum_{n,m} |g_{n,m}^{(j)}|^2 = 1$. For the sake of simplicity, we neglect the anticommutation relation of fermionic creation ($\hat{f}_j$) and annihilation ($\hat{f}_j^\dagger$) operators in different lattice sites. However the Pauli principle is taken into account (*i.e.* $m_j \in \{0,1\}, \forall j$). Inserting $|\psi_{GA}\rangle$ in the Schrödinger equation associated to the two-species Fermi-Bose Hamiltonian (4.1), we can compute the ground state and dynamical evolution of the Fermi-

Bose mixture. Technical details are provided in (Ahufinger *et al.*, 2005).

Non-disordered phases - Let us first focus on the case where the inhomogeneity is only provided by confining harmonic traps: $v_j = U_{\rm bb}\omega_{\rm b} \times l(j)^2$ and $V_j = U_{\rm bb}\omega_{\rm f} \times l(j)^2$, where $l(j)$ is the distance of site j to the center of the trap.

The ground state is first calculated for independent bosons and fermions ($U_{\rm bf} = 0$) with $N_{\rm b} = 60$ bosons and $N_{\rm f} = 40$ fermions, $\tau_{\rm b} = \tau_{\rm f} = 0.02U_{\rm bb}$ and $\omega_{\rm b} = 10^{-7}$ and $\omega_{\rm f} = 5 \times 10^{-7}$ in a 10×10 two-dimensional square lattice. Under these conditions, the bosons strongly interact but do not significantly feel the harmonic trap, which is very weak. Due to non-integer filling factor (0.6), they thus form a superfluid (Fisher *et al.*, 1989; Jaksch *et al.*, 1998). Similarly, the fermions are not much affected by the trap and distribute almost uniformly in the lattice. This is illustrated in Fig. 4.4a which shows, for all sites j, the probability of having no boson and one fermion in the various sites, $g^{(j)}_{n=0,m=1}$.

For sufficiently large interactions between the bosons and the fermions, the composites form, which is evidenced by the fact the only non-zero probabilities are: (i) $|g^{(j)}_{n=1,m=0}|^2$ (one boson and no fermion, *i.e.* absence of a composite), or (ii) $|g^{(j)}_{n=0,m=1}|^2$ (no boson and one fermion, *i.e.* presence of a composite). In particular, the probabilities of having neither a boson nor a fermion or of having one boson and one fermion are negligible. The probability density of the composites, $|g^{(j)}_{n=0,m=1}|^2$, is shown in Figs. 4.4b-d for increasing values of the fermion-boson interaction $U_{\rm bf}$. It worth noting that the energy scales of the composites are much smaller than the corresponding energies for bare bosons and fermions ($J, K \ll \tau_{\rm b}, \tau_{\rm f}, U_{\rm bb}, U_{\rm bf}$). The effect of inhomogeneities is hence much larger for composites than it is for bare fermions and bosons. A direct consequence is that the harmonic trap is significant for the composite, while it was negligible for independent bare particles.

For $U_{\rm bf} = 0.5U_{\rm bb}$, which corresponds to repulsive interactions between composites $K = J =$

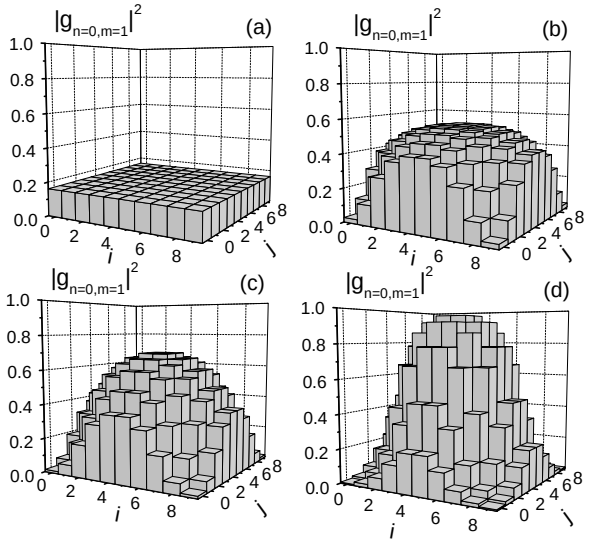

Figure 4.4 | Non-disordered phases of composite fermions in a harmonic trap. Probability of having one fermion and zero boson at each lattice site in a 10×10 2D lattice for a Fermi-Bose mixture with $N_{\rm b} = 60$, $N_{\rm f} = 40$, $\tau_{\rm b} = \tau_{\rm f} = 0.02U_{\rm bb}$ and in the presence of harmonic traps characterized by $\omega_{\rm b} = 10^{-7}$ and $\omega_{\rm f} = 5 \times 10^{-7}$. The interaction strength between fermions and bosons is (a) $U_{\rm bf} = 0$ corresponding to independent bare bosons and fermions, (b) $U_{\rm bf} = 0.5U_{\rm bb}$ corresponding to a composite Fermi liquid, (c) $U_{\rm bf} = U_{\rm bb}$ corresponding to ideal composite Fermi gas and (d) $U_{\rm bf} = 10U_{\rm bb}$ corresponding to composite Fermi domain insulator, respectively [from (Ahufinger *et al.*, 2005)].

1.6×10^{-3}, the ground state is a delocalized (non-ideal) *Fermi liquid*. For $U_{bf} = U_{bb}$, the system reaches the point where the interactions between composites cancel ($K = 0$) and forms an ideal *Fermi gas* phase. For $U_{bf} > U_{bb}$, the interactions between composites are attractive ($K < 0$) and the composite fermions form a *fermionic Mott insulator domain* in the vicinity of the trap center. For strong enough effective attraction ($|K| \gg J$), the probability of having composite fermions in the center of the trap reaches nearly unity (see Fig. 4.4d).

Disordered phases - Let us now consider the effect of disorder. We assume here that only the bosons are subjected to the disordered potential (*i.e.* $\Delta_{j,l} = 0$), so that the on-site energy v_j has a random component which is independent from site to site with standard deviation, Δ. In the numerics, we start from one of the phases described above (for a given set of parameters τ_b, τ_f, U_{bb} and U_{bf}) and we slowly ramp up the disorder from 0 to its nominal value Δ.

Let us start with an ideal *Fermi gas* in the absence of disorder (corresponding to Fig. 4.5b). As discussed above, the composite fermions are delocalized although confined near the center of the effective harmonic potential $[U_{bb}(\omega_f - \omega_b) \times l(j)^2]$. In particular, we find that the population of each lattice site fluctuates around $\langle m_j \rangle \simeq N_f/N = 0.4$ with $\sqrt{\langle (m_j - \langle m_j \rangle)^2 \rangle} \simeq 0.43$ (see the value on the left-hand side of Fig. 4.5a). While slowly increasing the amplitude of disorder, the composite fermions get more and more localized in the lattice sites, which is evidenced by the decrease of the fluctuations in composite number, $\sqrt{\langle (m_j - \langle m_j \rangle)^2 \rangle}$, shown in Fig. 4.5a. For $\Delta = 5 \times 10^{-4}$, the composite fermions are pinned in random sites (see Fig. 4.5c). As expected from the diagram of Fig. 4.3, the system thus enters a *Fermi glass* phase where the N_f composite fermions populate the N_f sites with minimal V_j.

It should be noted that in the absence of interactions between bosons and fermions (*i.e.* when the composites are not formed), no effect of disorder is observed. This again shows the formation of composites with typical energies significantly smaller than those of bare particles. Besides, similar calculations starting from a different initial state, namely the domain insulator, also show strong reduction of the fluctuations in composite number indicating localization by the disorder. In this case however, it is very difficult to reach the ground state numerically due to reduced mobility of the composites (Ahufinger *et al.*, 2005).

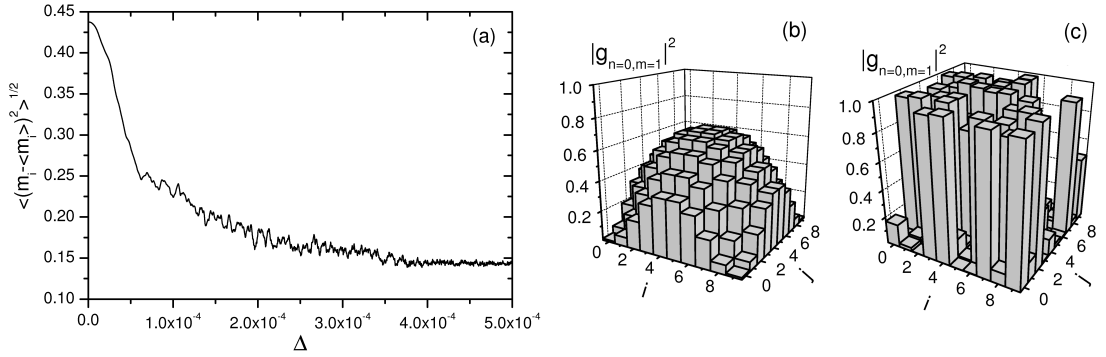

Figure 4.5 | **Dynamical crossover from Fermi gas to disordered Fermi glass.** (a) Variance of the number of fermions per lattice site, averaged over all sites as a function of the disorder strength Δ. (b) Probability of having one composite (one fermion and a bosonic hole) for all lattice sites in the absence of disorder and (c) after ramping up adiabatically diagonal disorder with strength $\Delta = 5 \times 10^{-4} U_{bb}$. The parameters are the same as in Fig. 4.4c [from (Ahufinger *et al.*, 2005)].

4.3 Simulating disordered spin systems with two-component ultracold gases

A major worthwhile feature of ultracold atoms is their ability to simulate basic models of theoretical condensed-matter physics. Jaksch *et al.* have shown in a pioneering work that atoms in deep optical lattices directly realize the celebrated Hubbard model (Jaksch *et al.*, 1998), which plays a major role in strongly-correlated Bose or Fermi systems (Lewenstein *et al.*, 2007; Georges, 2008; Bloch *et al.*, 2008). It was soon realized that, applying canonical transformations, one can simulate other classes of generic models of condensed-matter physics, for instance spin models (Jaksch and Zoller, 2005; Micheli *et al.*, 2006). In this section, we discuss possibilities to investigate the physics of disordered spin models with two-component mixtures of ultracold gases.

4.3.1 Spin glasses

▷ *see papers reprinted on pages 161 and 165*

Consider again Fermi-Bose mixtures as discussed in Sec. 4.2, where composites made of one fermion and one bosonic hole are formed and where the inhomogeneities apply only to the bosonic species (*i.e.* for $\Delta_{j,l} = 0$). In this case, the effective nearest-neighbor interaction $K_{j,l}$ strongly depends on the boson inhomogeneity $\delta_{j,l}$ for $\alpha = U_{\rm bf}/U_{\rm bb} \simeq 1$. For instance, Fig. 4.2(b) shows that, for $\alpha = 0.93$, the effective interaction $K_{j,l}$ turns from negative to positive values at $|\delta_{\rm c}| \simeq 0.84 U_{\rm bb}$. Since this value is smaller than $U_{\rm bb}$ and $U_{\rm bf}$, the composite picture is still valid (see Fig. 4.1), although it requires very small temperature because $\delta_{\rm c}$ is not very far from $U_{\rm bb}$ and $U_{\rm bf}$.

This situation can be exploited using an optical superlattice with a spatial period twice as large as the main lattice period to, alone, set $\delta_{j,l} = \pm\delta_{\rm c}$. Then, adding a very weak disordered potential induces small random fluctuations of $\delta_{j,l}$ around $\pm\delta_{\rm c}$, which translates into strong fluctuations of $K_{j,l}$. In this limit, the tunneling can be neglected in Eq. (4.7) since it becomes non-resonant. Applying the canonical transformation $\hat{S}_j \equiv 1/2 - \hat{\mathcal{N}}_j$, the composite Hamiltonian (4.7) can be mapped onto a new Hamiltonian:

$$H_{\rm eff} = \sum_{\langle j,l \rangle} K_{j,l}\, \hat{S}_j \cdot \hat{S}_l - \sum_j h_j \cdot \hat{S}_j, \tag{4.12}$$

where we have dropped a constant energy of $\frac{1}{4}\sum_{\langle j,l\rangle} K_{j,l} + \frac{1}{2}\sum_j \mathcal{V}_j$, and $h_j = \mathcal{V}_j + \frac{1}{2}\sum_{\langle j,l\rangle} K_{j,l}$ (in the formula for h_j, $\sum_{\langle j,l\rangle}$ denotes summation over all neighbors of the considered site j). This Hamiltonian resembles the celebrated Edwards-Anderson model, which describes spins located at the nodes of a cubic lattice, with random spin exchange coupling (Binder and Young, 1986; Mézard *et al.*, 1987). It however differs from the usual Edwards-Anderson model since, on one hand, it incorporates an additional random magnetic field h_j, which is correlated to the random coupling term $K_{j,l}$ and, on the other hand, has to satisfy the constraint of fixed magnetization, $m = 1/2 - N_{\rm f}/N$, as the number of fermions in the underlying Fermi-Bose-Hubbard model is conserved. In spite of this remark, Hamiltonian (4.12) shares basic characteristics with the Edwards-Anderson model. In particular, it provides bond frustration, which is crucial for the appearance of the *spin glass* phase in this model. The experimental study of this limit could thus present a way to address various open questions on spin glass physics concerning the nature of spin order in the ground state and possibly in metastable states, broken symmetry and dynamics

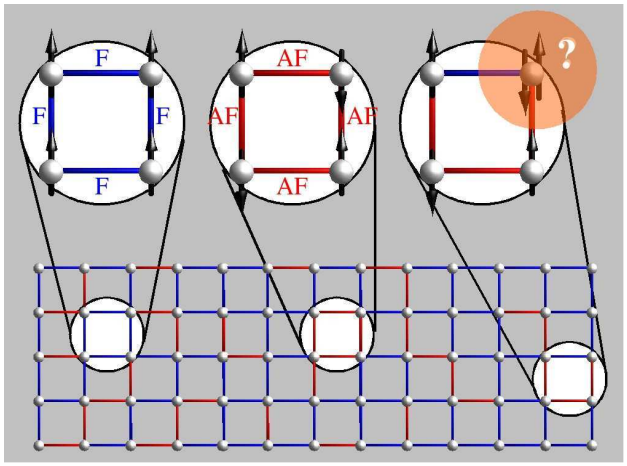

Figure 4.6 | The spin glass problem. Spins located at the nodes of a cubic lattice interact with exchange couplings that are randomly distributed, and can be either ferromagnetic (blue bonds) or anti-ferromagnetic (red bonds). In some plaquetes of four sites, local minimization of the exchange energy is easy, for instance when all bonds are ferromagnetic (left disk) or anti-ferromagnetic (central disk). In some other ones, it leads to frustration, for instance for odd numbers of bonds of each kind (right disk). In the latter case, at least one spin is frustrated, *i.e.* its orientation does not allow minimization the energy of each bond.

in classical (in absence of hopping) and quantum (with small, but nevertheless present hopping) spin glasses (Sachdev, 1999; Georges *et al.*, 2001).

Spin order in disordered systems such as that governed by Hamiltonian (4.12) is characterized by two order parameters: the magnetization, $m \equiv \overline{\langle s_j \rangle_T}$ where $\overline{\ .\ }$ denotes averaging over disorder and $\langle\ .\ \rangle_T$ thermodynamic averaging, and the Edwards-Anderson order parameter, $q_{\text{E-A}} \equiv \overline{\langle s_j \rangle_T^2}$, which measures local magnetization, irrespective to its local orientation. Then, experimental observations suggest three equilibrium phases, which are (i) an unordered paramagnetic phase, with $m = 0$ and $q_{\text{E-A}} = 0$; (ii) an ordered spin glass phase with $m = 0$ and $q_{\text{E-A}} \neq 0$ which is separated from the paramagnetic phase by a second order phase transition[4]; and (iii) an ordered ferromagnetic phase with $m \neq 0$ and $q_{\text{E-A}} \neq 0$. It is believed that the critical dimension for the onset of the spin glass phase is two, so that physically they exist only in dimension three.

Spin glasses were initially introduced to describe the physics of alloys where a few number of magnetic impurities are randomly displaced in space and interact via exchange coupling terms. The coupling between two impurities can be large or small and attractive or negative, depending on the distance separating two impurities. Various theoretical models have been proposed to describe these systems. The most paradigmatic model is an Ising-like model where spins located on a hypercubic lattice interact via ferro or anti-ferromagnetic bonds, which are randomly distributed, and are subjected to a constant magnetic field. The presence of random coupling terms makes the physics of these systems extraordinary complex, the major source of which is the appearance of bond frustration, *i.e.* existence of many loops such that it is not possible to choose the orientations of the spins without frustrating at least one bond (see Fig. 4.6). A consequence is that there exists a huge manifold of metastable states with very similar energies separated by large free-energy barriers, and spin glasses exhibit non trivial thermodynamic and dynamic features, much richer than their non-disordered counterpart (Binder and Young, 1986; Mézard *et al.*, 1987; Dotsenko *et al.*, 1990; Fischer and Hetz, 1991; Weissman, 1993).

Such models not only became paradigms of disorder in spin systems, but also turned out to have counterparts in many other fields such as neurology, computer science, economy or biology. However, the difficulty in choosing the correct distribution of couplings (short range or long

[4]The lower critical dimension for this transition to happen at non-zero T is believed to be two [see (Newman and Stein, 2003) and references therein]

range) have lead to controversies because different models lead to different predictions for the phase diagram and the nature of spin ordering of even classical spin glass models. Two main pictures of spin glasses have been proposed.

The Fisher-Huse 'droplet' picture - A most natural assumption is that the properties of spin glasses are crucially determined by short-range spatial correlations between the spins (Fisher and Huse, 1986; Bray and Moore, 1987; Fisher and Huse, 1988), which leads to the so-called Edwards-Anderson model:

$$H_{\text{E-A}} = \sum_{\langle j,l \rangle} K_{j,l}\, \hat{S}_j \cdot \hat{S}_l - \sum_j h \cdot \hat{S}_j, \tag{4.13}$$

where spin exchange coupling is limited to nearest neighbor spins, as for Hamiltonian (4.12), and where the magnetic field is homogeneous. The so-called *droplet picture* assumes that the ground state is unique up to obvious symmetries. Then, an excitation of the spin glass corresponds to a spin configuration where a complete block (droplet) of spins is turned upside down with respect to the ground state configuration, just like in usual magnets. In an ordered magnet, the excitation energy scales as the surface of the droplet, *i.e.* $E \sim L^{d-1}$. Here however, frustration strongly affects this scaling law, because in the ground state, not all couplings are satisfied and the energy cost associated to flipping all spins of a droplet is lower. The natural guess that E might scale as the square root of the surface –which would hold for fully random distributions of spins– is actually an overestimate. This is because the droplets may acquire a complex (*e.g.* fractal) surface so as to adapt to the actual spin configuration and lower their activation energy, thus leading to $\theta < (d-1)/2$. The very existence of droplets with a wide distribution of sizes, with non-negligible probability of low activation energy (below $k_{\text{B}}T$) is believed to sustain the wide spectrum of relaxation times in spin glasses.

The Mézard-Parisi 'ultrametric' picture - A completely different picture assumes in contrast that frustration does not only change the energy scale for activation energy of droplets but also profoundly modifies the spectrum, leading to an infinite number of Gibbs states that are not related by simple symmetries. In this case, complexity is mainly driven by the connection between the Gibbs states, which is a complex function of all spin couplings. The site-to-site coupling between the spins may hence be unrelevant, so that one may use the so-called Sherrington-Kirkpatrick (complete graph) model (Sherrington and Kirkpatrick, 1975):

$$H_{\text{S-K}} = \sum_{(j,l)} K_{j,l}\, \hat{S}_j \cdot \hat{S}_l - \sum_j h \cdot \hat{S}_j, \tag{4.14}$$

which differs from the Edwards-Anderson model only by the assumption that all pairs (j,l) of spins interact with equal probability, irrespective to their mutual distance. This simplification turns out to be very convenient to meanfield approaches and the problem was solved by Parisi and co-workers under some approximations and latter given a rigorous proof (Parisi, 1980). The connection between the various Gibbs states is characterized by an ultrametric topology, which can be represented as a hierarchical tree (Weissman, 1993). This complex topology leads to hierarchical kinetic pictures and to a wide range of relaxation times, although with different scaling compared to the droplet picture. The spin glass transition is then characterized by replica symmetry breaking, which chooses a pure state configuration that alone describes the low-temperature properties of the spin glass.

4.3.2 Random-field induced order: Coupled lattice Bose gases

▷ *see paper reprinted on page 191*

As seen in Sec. 4.3.1, an important drawback of two-component ultracold gases to simulate spin systems and study unbiased magnetism is that the average magnetization along the z-axis is fixed by the average number of composites, that is the average difference of numbers of b- and B-particles, which is usually a conserved quantity. It is however possible to release this constraint if the b- and B-particles correspond to the same atomic species in different internal states. Then, it is possible to introduce a term $\sum_j \left(\frac{\Omega_j}{2}\,\hat{B}_j^\dagger \hat{b}_j + \text{h.c.}\right)$ in Hamiltonian (4.1), using a two-photon Raman process for instance (Wehr *et al.*, 2006). If the coupling term Ω is smaller than all other relevant energy scales, it does not significantly affect the state of the system. In turn, it can convert a b-particle into a B-particle (and reciprocally). Hence, while the total number of particles is conserved, the numbers of b- and B-particles are not. In other words, the coupling term allows chemical equilibrium between the two 'species', which releases the constraint of a fixed magnetization along z.

Let us come back to the effective Hamitonian (4.7) for the composites, to which we have to add the coupling term, $\sum_j \left(\frac{\Omega_j}{2}\,\hat{\mathcal{B}}_j^\dagger + \text{h.c.}\right)$. Since the commutation relations of $\hat{\mathcal{B}}_j$ and $\hat{\mathcal{B}}_j^\dagger$ are those of Schwinger bosons, we can directly turn to the spin representation by defining $\hat{S}_j^x = (\hat{\mathcal{B}}_j + \hat{\mathcal{B}}_j^\dagger)/2$, $\hat{S}_j^y = (\hat{\mathcal{B}}_j - \hat{\mathcal{B}}_j^\dagger)/2i$, and $\hat{S}_j^z = 1/2 - \hat{\mathcal{N}}_j$. It can be checked easily that the $\hat{\mathbf{S}}_j$ operators indeed verify the commutation relations of spins (Auerbach, 1994). For weak inhomogeneities ($\delta_{j,l} = v_j - v_l, \Delta_{j,l} = V_j - V_l \ll U_{\text{bb}}, U_{\text{BB}}, U_{\text{bB}}$), Hamiltonian H_{eff} is then equivalent to the anisotropic Heisenberg XXZ model in a random field:

$$H_{\text{eff}} = -J_\perp \sum_{\langle j,l\rangle} \left(\hat{S}_j^x \hat{S}_l^x + \hat{S}_j^y \hat{S}_l^y\right) \;-\; J_z \sum_{\langle j,l\rangle} \hat{S}_j^z \hat{S}_l^z \;-\; \sum_j \left(h_j^x \hat{S}_j^x + h_j^y \hat{S}_j^y + h_j^z \hat{S}_j^z\right) \tag{4.15}$$

where

$$J_\perp = \frac{4\tau_{\text{b}}\tau_{\text{B}}}{U_{\text{bB}}} \tag{4.16}$$

$$J_z = 2\left(\frac{2\tau_{\text{b}}^2}{U_{\text{bb}}} + \frac{2\tau_{\text{B}}^2}{U_{\text{BB}}} - \frac{\tau_{\text{b}}^2 + \tau_{\text{B}}^2}{U_{\text{bB}}}\right) \tag{4.17}$$

$$h_j^x = \Omega_j^{\text{R}} \quad ; \quad h_j^y = -\Omega_j^{\text{I}} \quad ; \quad h_j^z = \mathcal{V}_j - \zeta J_z/2\,, \tag{4.18}$$

with ζ the lattice coordination number, $\mathcal{V}_j = V_j - v_j + \zeta[4\tau_{\text{b}}^2/U_{\text{bb}} + 4\tau_{\text{B}}^2/U_{\text{BB}} - (\tau_{\text{b}}^2 + \tau_{\text{B}}^2)/U_{\text{bB}}]$ and Ω_j^{R} and Ω_j^{I} the real and imaginary parts of Ω_j. In atomic systems, all these (possibly site-dependent) terms can be controlled almost at will (Sanpera *et al.*, 2004; Lewenstein *et al.*, 2007). For instance, by employing various control tools, one can design the Heisenberg ferromagnet ($J_\perp = J_z$) and the XY ($J_z = 0$) models (Duan *et al.*, 2003; Imambekov *et al.*, 2003; Altman *et al.*, 2003; Jaksch and Zoller, 2005).

Consider the classical ferromagnetic XY model in a two-dimensional square lattice, the energy functional of which reads

$$E[\{\theta_j\}] \;=\; -J \sum_{\langle j,l\rangle} \mathbf{S}_j \cdot \mathbf{S}_l \;-\; \sum_j \mathbf{h}_j \cdot \mathbf{S}_j, \tag{4.19}$$

where the spins are unit two-dimensional vectors in the XY plane, $\mathbf{S}_j \propto (\cos\theta_j, \sin\theta_j)$, and $\mathbf{h}_j$ represents an inhomogeneous magnetic field. For $\mathbf{h} = 0$ the system does not magnetize[5]. This is a direct consequence of the Mermin-Wagner-Hohenberg theorem which states that spin or field-theoretic systems with continuous symmetry in dimensions $d \leq 2$ cannot exhibit long-range order (Mermin and Wagner, 1966; Hohenberg, 1967). In the presence of a symmetrically-distributed random magnetic field, magnetization is even more strongly suppressed, *i.e.* there is no spontaneous magnetization in dimensions $d \leq 4$ (Imry and Ma, 1975; Aizenman and Wehr, 1989; Aizenman and Wehr, 1990).

In the presence of a uniaxial random magnetic field however, the system sustains a striking effect, namely random-field induced order (RFIO) (Aharony, 1978; Minchau and Pelcovits, 1985; Feldman, 1998). RFIO is a general phenomenon where weak, uniaxial random fields break a continuous symmetry, thus making the Mermin-Wagner-Hohenberg theorem inapplicable. Then, counter-intuitively weak disorder can favor ordering. This effect has been reported in graphene quantum Hall ferromagnets (Abanin *et al.*, 2007), ^{3}He$-$A in aerogel and amorphous ferromagnets (Fomin, 2005; 2007; Volovik, 2005), and hard-core Bose systems (Lee *et al.*, 2006). Here, a uniaxial random magnetic field breaks the continuous $U(1)$ symmetry and in dimension $d = 2$, the system spontaneously magnetizes with a non-zero component of the magnetization perpendicular to the random field. Jan Wehr has given a rigorous proof of this at zero temperature and developed strong arguments that the effect persists at small temperatures (Wehr *et al.*, 2006). Hereafter, we just give a simple argument, which contains the essential physics of the disorder-induced magnetization effect.

The essence of the Mermin-Wagner-Hohenberg argument is that, for strictly zero field, if one chooses a certain direction for magnetization, spin-wave excitations are not thermally suppressed for $d \leq 2$, leading to absence of magnetization. Let us consider now a weak, random magnetic field of zero average and choose a given direction θ_0 for magnetization. The random field does not significantly affect the spin-wave energies, since it averages to zero[6]. If the random field is uniaxial along the x-axis however, there are configurations that significantly lower the total energy: Consider a distribution of angles $\theta_j = \theta_0 + \delta\theta_j$ with $\delta\theta_j \ll 2\pi$. The exchange energy cost is $\delta E_\mathrm{J} \sim JN\zeta(\delta\theta)^2/2$ where N is the number of lattice sites, while the magnetic energy cost is $\delta E_\mathrm{h} \simeq +\sum_j h_j(\sin\theta_0)\delta\theta_j$. If the $\delta\theta_j$ are of the order of $\delta\theta$ with a fixed or random sign, then $\delta E_\mathrm{h} \sim \sqrt{N}\Delta h(\sin\theta_0)\delta\theta$. Conversely, if we choose $\delta\theta_j$ of the order of $\delta\theta$ but with a sign such that $h_j(\sin\theta_0)\delta\theta_j$ is negative for all sites, then $\delta E_\mathrm{h} \sim -N\Delta h|\sin\theta_0|\delta\theta$. If now we choose $1/\sqrt{N} \ll \delta\theta \ll \Delta h/J\zeta, 2\pi$, then δE_h exceeds the ferromagnetic energy and the fluctuations of the magnetic energy[6]. The energy is thus minimized for $|\sin\theta_0| = +1$, *i.e.* $\theta_0 = \pm\pi/2$. We thus expect that the system spontaneously magnetizes along the direction perpendicular to the direction of the magnetic field. Note that spin-wave excitations are now thermally suppressed because they cost an energy of the order of δE_h.

In order to study quantitatively the RFIO effect, we have used the ALPS routines (Troyer *et al.*, 1998; Alet *et al.*, 2005) to numerically compute the magnetization of the classical 2D-XY model versus temperature in a 200×200 square lattice with axial random magnetic fields. In such finite-size systems, magnetic effects are usually obscured by long-range power-law decay of cor-

[5] In higher dimensions, however, the system does magnetize at low temperature (Zinn-Justin, 1989; Fröhlich *et al.*, 1976; Balaban, 1995; Balaban, 1996).

[6] The magnetic energy depends on the exact realization of the $\mathbf{h}$-field. Assuming independent magnetic components $\mathbf{h}_j$, the fluctuations of the magnetic energy is $\sqrt{N}\Delta h\cos(\theta_0)$.

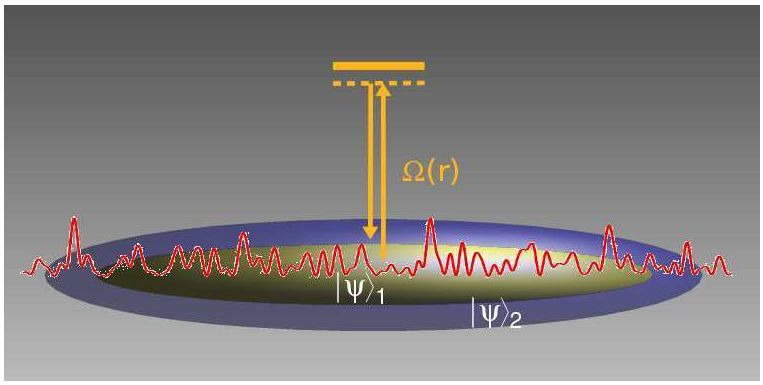

Figure 4.7 | Bose-Einstein condensates coupled by a random Raman field. Two condensates $|\psi_1\rangle$ and $|\psi_2\rangle$ are confined in harmonic traps. They are made of the same atomic species in two different internal states, with repulsive inter- and intra-species interactions. A two-photon Raman field with a fixed phase but inhomogeneous amplitude couples them.

relations, which, for instance, are known to induce finite magnetization even in the absence of disorder (Bramwell and Holdsworth, 1994). We then expect that RFIO results in an increase of the magnetization at finite temperature. We indeed demonstrated the effect, although it turns out to be very weak. It is signaled by a maximum increase of magnetization of 1.6% at $T = 0.7J/k_B$ (Wehr *et al.*, 2006).

4.3.3 Random-field induced order: Coupled Bose-Einstein condensates

▷ *see paper reprinted on page 199*

As shown above, RFIO is rather weak in two-dimensional optical lattices of reasonable sizes. Fortunately, it is a general effect, which is relevant in nearly any system with a $U(1)$ symmetry broken by disorder. In collaboration with the group of Maciej Lewenstein, Jan Wehr and Krzysztof Sacha, we have considered a trapped two-component Bose gas with repulsive interactions and coupled by a (quasi-)random real-valued Raman field $\Omega(\mathbf{r})$ of zero average (see Fig. 4.7). The meanfield energy functional associated to the condensate fields $\psi_j(\mathbf{r}) = e^{i\theta_j(\mathbf{r})}\sqrt{\rho_j(\mathbf{r})}$ reads

$$\begin{aligned} E &= \int d\mathbf{r} \left[\frac{\hbar^2}{2m}|\nabla\psi_1|^2 + V_1(\mathbf{r})|\psi_1|^2 + \frac{g_1}{2}|\psi_1|^4 + \frac{\hbar^2}{2m}|\nabla\psi_2|^2 + V_2(\mathbf{r})|\psi_2|^2 + \frac{g_1}{2}|\psi_2|^4 \right] \\ &\quad + \int d\mathbf{r} \left[g_{12}|\psi_1|^2|\psi_2|^2 + \frac{\hbar\Omega(\mathbf{r})}{2}\left(\psi_1^*\psi_2 + \psi_2^*\psi_1\right) \right]. \end{aligned} \tag{4.20}$$

where we assume weak coupling terms (Ω, g_{12}). For vanishing coupling $\Omega = 0$ and strong-enough intra-species interactions (for g_1, $g_2 > g_{12}$ when $V_1 = V_2$), the condensates are in the Thomas-Fermi regime and miscible (Ho and Shenoy, 1996), with densities $\rho_j(\mathbf{r})$. A weak Raman coupling does not noticeably affect the densities, but breaks the continuous $U(1)$ symmetry associated to the relative phase $\theta = \theta_1 - \theta_2$ of the condensates. Then, the energy functional reduces to the phase terms:

$$E = E_0 + \int d\mathbf{r} \left[\frac{\hbar^2}{2m} \frac{\rho_1(\mathbf{r})^2 + \rho_2(\mathbf{r})^2}{\left(\rho_1(\mathbf{r}) + \rho_2(\mathbf{r})\right)^2} \left(\nabla\theta\right)^2 + \sqrt{\rho_1(\mathbf{r})\rho_2(\mathbf{r})}\, \hbar\Omega(\mathbf{r}) \cos\left(\theta(\mathbf{r})\right) \right]. \tag{4.21}$$

In Eq. (4.21), we have not included the term associated to the absolute phase $\Theta = (\rho_1\theta_1 + \rho_2\theta_2)/(\rho_1 + \rho_2)$ which can be easily shown to vanish in the ground state (Niederberger *et al.*, 2008). For homogeneous condensates (*i.e.* ρ_1 and ρ_2 independent of the position), Eq. (4.21) is

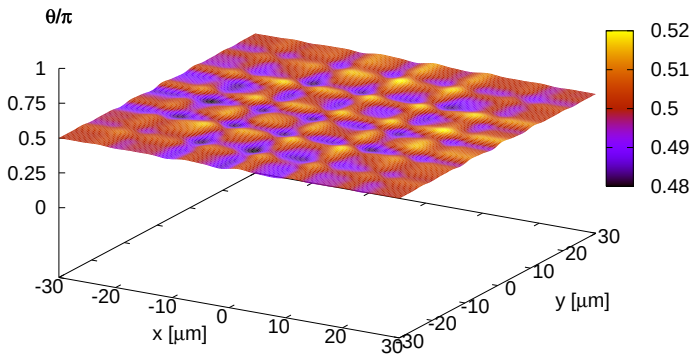

Figure 4.8 | Random-field induced order in coupled Bose-Einstein condensates. The figure shows the relative phase θ in the plane $z = 0$ in units of π. Here, we have used two identical condensates in a spherically symmetric harmonic trap and a quasi-random Raman coupling $\Omega(x,y,z) \propto \Omega_R \sum_{u\in\{x,y,z\}} [\sin(u/\lambda_R) + \sin(u/(1.71\lambda_R))]$ with $\hbar\Omega_R \simeq 5\times 10^{-3}\mu$ [from (Niederberger *et al.*, 2008)].

equivalent to the classical field description of the spin model (4.19) in the continuous limit, where the relative phase $\theta(\mathbf{r})$ represents the spin angle and the Raman coupling $\Omega(\mathbf{r})$ plays the role of the random, uniaxial magnetic field. We thus expect RFIO (Wehr *et al.*, 2006) to show up in the form $\cos\theta \simeq 0$ for weak random $\Omega(\mathbf{r})$. For condensates in smooth harmonic traps, Eq. (4.21) is no longer strictly equivalent to the continuous spin model. However, we can use a local-density approximation (LDA) argument and infer that RFIO should show up as well.

We have numerically calculated the ground state properties of two coupled condensates in a weak, random, real-valued Raman field using the Gross-Pitaevskii approach. We indeed found that RFIO shows up, the signature of which is a fixed relative phase $\theta \simeq \pm\pi/2$. An example, corresponding to two three-dimensional condensates in a spherically-symmetric harmonic trap subjected to a quasi-random Raman field of $\hbar\Omega \sim 10^{-2}\mu$ with μ the chemical potential of the coupled Bose-Einstein condensates, is shown in Fig. 4.8. The density modulations are found to be negligible, but, even for this low value of $\hbar\Omega$, the relative phase is fixed around $\theta \simeq \pm\pi/2$ with small fluctuations (the sign of θ is random and determined by spontaneous breaking of the $\theta \to -\theta$ symmetry). In contrast to the two-component lattice Bose gases (see Sec. 4.3.2), we found that the RFIO effect is very robust. We indeed demonstrated it in one-, two- and three-dimensional gases, for quasi-random or purely random Raman fields (Niederberger *et al.*, 2008), and further investigations extended it to superfluid Fermi-Bose mixtures (Niederberger *et al.*, 2009).

Let us finally make a brief comment. Random-field induced order is one example where simulating condensed-matter physics –namely lattice XY models in random magnetic fields– with ultracold atoms allows for direct evidence of some generic effects. If one strictly stands on classic models, it may happen that interesting effects are too weak to be observed and are thus unrelevant. This is the case of RFIO in lattice XY models of reasonable size (Wehr *et al.*, 2006). Going beyond toy models allows us not only to study the exact physics of ultracold atoms, but also to explore new situations, in which counterparts of basic effects are relevant and robust. As shown above, extension of RFIO to continuous space, namely in coupled condensates is a striking example, which paves the way to direct evidence of this counter-intuitive effect (Niederberger *et al.*, 2008).

4.4 Reprints of papers associated with the chapter

1. SANPERA A., KANTIAN A., SANCHEZ-PALENCIA L., ZAKREWSKI J., and LEWENSTEIN M., *Atomic Fermi-Bose mixtures in inhomogeneous and random optical lattices: From Fermi glass to quantun spin glass and quantum percolation*, Phys. Rev. Lett. **93**, 040401 (2004); ▷ *page 161*.

2. AHUFINGER V., SANCHEZ-PALENCIA L., KANTIAN A., SANPERA A., and LEWENSTEIN M., *Disordered ultracold atomic gases in optical lattices: A case study of Fermi-Bose mixtures*, Phys. Rev. A **72**, 063616 (2005); ▷ *page 165*.

3. WEHR J., NIEDERBERGER A., SANCHEZ-PALENCIA L., and LEWENSTEIN M., *Disorder versus the Mermin-Wagner-Hohenberg effect: From classical spin systems to ultracold atomic gases*, Phys. Rev. B **74**, 224448 (2006); ▷ *page 191*.

4. NIEDERBERGER A., SCHULTE T., WEHR J., LEWENSTEIN M., SANCHEZ-PALENCIA L., and SACHA K., *Disorder-induced order in two-component Bose-Einstein condensates*, Phys. Rev. Lett. **100**, 030403 (2008); ▷ *page 199*.

Atomic Fermi-Bose Mixtures in Inhomogeneous and Random Lattices: From Fermi Glass to Quantum Spin Glass and Quantum Percolation

A. Sanpera,[1,2] A. Kantian,[2] L. Sanchez-Palencia,[2] J. Zakrzewski,[3] and M. Lewenstein[1,2]

[1]*Institut de Ciències Fotòniques, 08034 Barcelona, Spain*

[2]*Institut für Theoretische Physik, Universität Hannover, D-30167 Hannover, Germany*

[3]*Instytut Fizyki, Uniwersytet Jagielloński, PL-30-059 Kraków, Poland*

(Received 13 February 2004; published 20 July 2004)

We investigate strongly interacting atomic Fermi-Bose mixtures in inhomogeneous and random optical lattices. We derive an effective Hamiltonian for the system and discuss its low temperature physics. We demonstrate the possibility of controlling the interactions at local level in inhomogeneous but regular lattices. Such a control leads to the achievement of Fermi glass, quantum Fermi spin-glass, and quantum percolation regimes involving bare and/or composite fermions in random lattices.

DOI: 10.1103/PhysRevLett.93.040401 PACS numbers: 03.75.Kk, 03.75.Lm, 05.30.Jp, 64.60.Cn

Fermi-Bose (FB) mixtures attract considerable interest in the physics of ultracold atomic and molecular gases, comparable with the interest in molecular Bose-Einstein condensation [1], or Bardeen-Cooper-Schrieffer transition [2] in ultracold Fermi mixtures. The reason for interest in FB systems is threefold. First, they are very fundamental systems without direct analogues in condensed matter. Second, these systems can be efficiently cooled using sympathetic cooling down to very low temperatures (tens of nK) [3–6]. Finally, their physics is extremely rich and not yet fully understood.

FB mixtures have been intensively studied in traps [7], but the experimental observation of the superfluid to Mott-insulator (MI) transition in bosonic gases [14], predicted in Ref. [15], has triggered the interest in the physics of FB mixtures in optical lattices [16]. Under appropriate conditions such mixtures are described by the Fermi-Bose Hubbard model (FBH) [17]. A particularly appealing feature of the FBH model is the possibility to produce novel quantum phases [18], fermion-boson induced superfluidity [19], and composite fermions, which for attractive (repulsive) interactions between fermions and bosons, are formed by a fermion and bosons (bosonic holes) as shown in [20] (see also [21,22]).

FB mixtures in the limit of strong atom-atom interactions (strong coupling regime) show a very rich variety of quantum phases in periodic optical lattices [21]. They include the mentioned composite fermions, and range from a normal Fermi liquid, a density wave, a superfluid liquid, to an insulator with fermionic domains. The phase diagram of the system has been determined in Ref. [23] by means of mean-field theory [24]. These studies have been generalized recently to inhomogeneous lattices [25] to include the effects of the lattice and of a possible trap potential. So far, only the case of strong interactions and vanishing hopping has been considered.

In the present Letter we study the low temperature physics of FB mixtures in optical lattices with local and random inhomogeneities in the strong interactions limit but including tunneling as a perturbation. We show that interactions and tunneling may be controlled at the local level in inhomogeneous lattices [26]. This control gives access to a wide variety of regimes and we derive the corresponding effective Hamiltonians. We then show how to achieve Fermi glass, fermionic spin-glass, and quantum percolation regimes involving bare and/or composite fermions in random lattices.

We consider a sample of ultracold bosonic and (polarized) fermionic atoms (e.g., ^{7}Li-^{6}Li or ^{87}Rb-^{40}K) trapped in an optical lattice. At low temperature, the atoms occupy only the lowest energy band and it is convenient to work in the corresponding Wannier basis [15]. Note that a fermion number N_F strictly smaller than the number of lattice sites N is required here. The Hamiltonian of the system reads [17,27]:

$$H_{\mathrm{FBH}} = -\sum_{\langle ij\rangle}(J_B b_i^\dagger b_j + J_F f_i^\dagger f_j + \mathrm{H.c.}) + \sum_i\left[\frac{1}{2}Vn_i(n_i-1) + Un_i m_i - \mu_i^B n_i - \mu_i^F m_i\right], \quad (1)$$

where b_j, f_j are the bosonic and fermionic annihilation operators, $n_i = b_i^\dagger b_i$ and $m_i = f_i^\dagger f_i$. The FBH model describes: (i) nearest neighbor (nn) boson (fermion) hopping, with an associated negative energy, $-J_B$ ($-J_F$); (ii) on-site repulsive boson-boson interactions with an energy V; (iii) on-site boson-fermion interactions with an energy U, which is positive (negative) for repulsive (attractive) interactions, (iv) and, finally, interactions with the optical potential, with energies μ_i^B and μ_i^F. In the following, we consider only the case $J_B = J_F = J$ and the regime of strong interactions ($V, U \gg J$).

In a periodic optical lattice, $\mu_i^{B,F}$ is simply the (bosons or fermions) chemical potential and is independent of the site i. It is, however, possible to add a laser field independent of the lattice to modify the depths of the optical

potential wells in a site-dependent way [28]. In this case, the local potential depth has to be added to $\mu_i^{\mathrm{B,F}}$, which may now be inhomogeneous. If the added field is periodic and if the spatial period is commensurate with the lattice period, $\mu_i^{\mathrm{B,F}}$ is periodic; if the spatial periods are incommensurate, $\mu_i^{\mathrm{B,F}}$ is quasiperiodic. One can also add a random speckle field, so that $\mu_i^{\mathrm{B,F}}$ is random. Experimental techniques offer full possibilities to control such periodic, quasiperiodic, or disordered $\mu_i^{\mathrm{B,F}}$ [29]. Note, that the additional inhomogeneous potential might, but does not have to, act equally on both atomic species. Here, we study the case $\mu_i^{\mathrm{F}} = 0$, $\mu_i^{\mathrm{B}} = \mu_i V$.

In Ref. [21] we have used the method of degenerate second order perturbation theory to derive an effective Hamiltonian by projecting the wave function onto the multiply degenerate ground state of the system in the absence of tunneling. This can be extended to the present situation, where there are very many states with similar energies. It is thus reasonable to project the wave function on the manifold of "ground states." These states are local minima of energy, since at least some of hopping acts increase their energy by V or $|U|$.

Let us consider first $J = 0$, and the case $0 \leq \mu_i < 1$. In the absence of a fermion one expects one boson per site, i.e., $n_i = 1$ [30]. We shall consider here only the case of repulsive interactions, i.e., $\alpha = U/V > 0$.

It is useful to divide the sites into (i) A sites, for which $\mu_i - \alpha \geq 0$, and fermions do not push bosons out, and (ii) B sites, for which $\mu_i - \alpha < 0$, and the fermion pushes the boson out forming a composite fermion-bosonic hole. Energetically, the second situation is favorable, so for a given set of N^A of A sites, and $N^B = N - N^A$ of B sites, the fermions will first occupy the B sites until $N_{\mathrm{F}} = N^B$, and then they will start to occupy the A sites. We construct the corresponding projector operators P, $Q = 1 - P$, which depend on N^{A} and N_{F}. The operator P describes the projection onto the manifold of quasidegenerated states in which the fermions occupy the B sites stripped of bosons and some A sites only if $N_{\mathrm{F}} \geq N^B$. In this case there is a boson in any A site and if $N_{\mathrm{F}} < N^B$ there is also a boson in the B sites which do not contain fermions. We use second order time dependent perturbation theory [32], and project the Schrödinger equation, $i\hbar\partial_t|\psi(t)\rangle = (H_0 + H_1)|\psi(t)\rangle$, onto the manifold of states spanning P. The "zeroth-order" part H_0 contains the atomic interactions and terms proportional to the chemical potential and commutes with P. H_1 represents the tunneling terms. The effective equation for $|\psi_P\rangle = P|\psi\rangle$ reads then $i\hbar\partial_t|\psi_P(t)\rangle = H_{\mathrm{eff}}|\psi_P(t)\rangle$, where

$$\langle \mathrm{out}|H_{\mathrm{eff}}|\mathrm{in}\rangle = \langle \mathrm{out}|H_0|\mathrm{in}\rangle + \langle \mathrm{out}|PH_1P|\mathrm{in}\rangle - \frac{1}{2}\langle \mathrm{out}|PH_1Q\left(\frac{1}{H_0 - E_{\mathrm{in}}} + \frac{1}{H_0 - E_{\mathrm{out}}}\right) \times QH_1P|\mathrm{in}\rangle. \quad (2)$$

The effective Hamiltonian H_{eff} has the form

$$H_{\mathrm{eff}} = \sum_{\langle ij\rangle}[-(d_{ij}F_i^\dagger F_j + \mathrm{H.c.}) + K_{ij}M_iM_j] + \sum_i \tilde{\mu}_i M_i, \quad (3)$$

where F_i is the (composite) fermionic annihilation operator, and $M_i = F_i^\dagger F_i$. The hopping amplitudes d_{ij} and the nn couplings K_{ij} [which might be repulsive (>0) or attractive (<0)] are of the order of J^2/V. The couplings depend on α, $\tilde{\mu}_i$, $\tilde{\mu}_j$, and J, and have to be determined carefully for different cases, as discussed below. Note, however, that the hopping $i \rightarrow j$, or back causes the energy change $\pm(\Delta_{ij} = \mu_i - \mu_j)$ in units of V, i.e., is highly nonresonant and inefficient for $\Delta_{ij} \simeq 1$; it first leads to jump rates of order $O(J^4/V^3)$. Additionally, composite fermions may feel the local energy $\tilde{\mu}_i$.

I. All sites are of type B.—In this case we have a gas of composites flowing within the MI with one boson per site. The couplings are

$$d_{ij} = \frac{J^2}{V}\left(\frac{\alpha}{\alpha^2 - (\Delta_{ij})^2} + \frac{1}{\alpha}\right), \quad (4)$$

$$K_{ij} = -\frac{J^2}{V}\left(\frac{4}{1 - (\Delta_{ij})^2} - \frac{2}{\alpha} - \frac{2\alpha}{\alpha^2 - (\Delta_{ij})^2}\right). \quad (5)$$

The chemical potential $\tilde{\mu}_i/V \simeq \mu_i$ up to corrections of order $O(J^2/V)$. The hopping amplitudes d_{ij} are for this case always positive, although may vary quite significantly with disorder, especially when $\Delta_{ij} \simeq \alpha$. As shown in Fig. 1, for $\alpha > 1$, $K_{ij} \leq 0$ and we deal with attractive (although random) interactions. For $\alpha < 1$, but close to 1, K_{ij} might take positive or negative values for Δ_{ij} small or $\Delta_{ij} \simeq \alpha$. In this case *the qualitative character of interactions is controlled by inhomogeneity.*

The physics of the system depends on the relation between μ_i's and α. For small inhomogeneities, we may neglect the contributions of Δ_{ij} to $d_{ij} \simeq d$ and $K_{ij} \simeq K$, and keep only the leading disorder contribution in $\tilde{\mu}_i$. Note, that the latter contribution is relevant in 1D and 2D leading to Anderson localization of single particles [33].

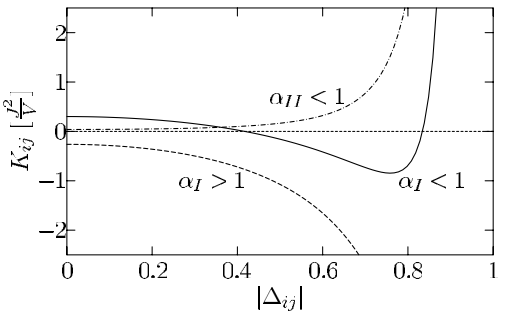

FIG. 1. Nearest neighbor couplings K_{ij} as a function of Δ_{ij}. Solid line: Coupling in case I, with $\alpha_{\mathrm{I}} = 0.93$. Dashed line: Same expression with $\alpha_{\mathrm{I}} = 1.07$. Dash-dotted line: Coupling in case II with $\alpha_{\mathrm{II}} = 0.03$.

When $K \ll d$ one will have a Fermi glass phase, i.e., Anderson localized (and many-body corrected) single particle states will be occupied according to the Fermi-Dirac rules [34]. For repulsive interactions and $K \gg d$, the ground state will be a Mott insulator for large enough filling factors. In particular, for filling factor $1/2$ a checkerboard phase is expected. For intermediate values of K/d delocalized metallic phases with enhanced persistent currents are possible [35]. Similarly, for attractive interactions ($K < 0$) and $|K| < d$ one expects competition between pairing of fermions and disorder; for $|K| \gg d$, the fermions will form a domain insulator.

Another interesting limit is when $|\Delta_{ij}| \simeq \alpha \simeq 1$. The tunneling becomes then nonresonant and negligible, while the couplings K_{ij} fluctuate strongly. We end up with the (fermionic) Ising spin glass model [36] described by the Edwards-Anderson model [37]:

$$H_{\text{E-A}} = \frac{1}{4}\sum_{\langle ij\rangle} K_{ij} s_i s_j + \sum_i \tilde{\mu}_i s_i/2, \tag{6}$$

with $s_i = 2M_i - 1 = \pm 1$. The above Hamiltonian is well approximated by a random one with Gaussian and independent distributions for $K_{ij}/4$ and $\tilde{\mu}_i/2$ with mean 0 (H), and variances K (h), respectively. In this limit the system may be used to study various open questions of spin-glass physics, concerning the nature of ordering (Parisi's [37] versus "droplet" picture [38]), broken symmetry and dynamics in classical (in the absence of hopping) and quantum (with small, but nevertheless present hopping) spin glasses [24,39]. The predictions of Parisi's mean field theory for the model (6) can be obtained by replacing the model by the corresponding Sherrington-Kirkpatrick model, and employing the standard method of replica trick [37]. The calculations differ from the standard ones in that the constraint of fixed mean number of fermions is applied, and one deals simultaneously with random couplings and "magnetic fields" $\tilde{\mu}_i$. Following the de Almeida and Thouless (AT) approach [40], we obtain the AT surface separating the stable paramagnetic state from the "true" spin-glass state, characterized by replica symmetry breaking, and ultrametrically arranged ground states. The paramagnetic state is stable for

$$\left(\frac{k_{\text{B}}T}{K}\right)^2 > \left\langle\left\langle \text{sech}^4\left(\frac{x\sqrt{K^2 q + h^2} + H}{k_{\text{B}}T}\right)\right\rangle\right\rangle_x, \tag{7}$$

where $q = \langle\langle \tanh^2[(x\sqrt{K^2 q + h^2} + H)/k_{\text{B}}T]\rangle\rangle_x$, the constraint is $m = \langle\langle \tanh[(x\sqrt{K^2 q + h^2} + H)/k_{\text{B}}T]\rangle\rangle_x$, with $m = 2N_{\text{F}}/N - 1$ and $\langle\langle . \rangle\rangle_x$ denotes averaging over normally distributed random variable x which represents disorder within the replica method [37]. Note, that according to the predictions of the alternative "droplet" model [38], applied to (6), no AT surface is expected.

II. All sites are of type A.—In this case $\alpha < 1$, and we have a gas of bare fermions flowing over the MI with one boson per site. The coefficients are

$$\begin{aligned} d_{ij} &= J, \\ K_{ij} &= -\frac{J^2}{V}\left[\frac{8}{1-(\Delta_{ij})^2} - \frac{4(1+\alpha)}{(1+\alpha)^2-(\Delta_{ij})^2}\right. \\ &\qquad \left. - \frac{4(1-\alpha)}{(1-\alpha)^2-(\Delta_{ij})^2}\right], \end{aligned} \tag{8}$$

and $\tilde{\mu}_i \simeq 0$ up to corrections of order $O(J^2/V)$. The couplings K_{ij} are positive, and for $\alpha \simeq 0$, $K_{ij} \simeq O(\alpha^2)$, and both the repulsive interactions, and disorder are very weak, leading to a Fermi liquid behavior at low T. For finite α, and $\Delta_{ij} \simeq 1 - \alpha$, however, the fluctuations of K_{ij} might be quite large. Note, that for $\alpha \simeq 1$, this will occur even for small disorder. Assuming for simplicity that K_{ij} take either very large, or zero value, we see that the physics of bond percolation [41] will play a role. The bonds will form a "weak" and "strong" clusters, each of which may be percolating. The fermions will hope freely in the "weak" cluster; only one fermion per bond will be allowed in the "strong" cluster.

III. Both N^{A} and N^{B} of order $N/2$—In this case the physics of site percolation [41] will be relevant. If $N_{\text{F}} \leq N^{\text{B}}$ the composite fermions will move within a cluster of B sites. When N^{B} is above the classical percolation threshold, this cluster will be percolating. The expressions Eqs. (4) and (5) will still be valid, except that they will connect only the B sites.

The physics of the system will be similar as in case I, but it will occur now on the percolating cluster. For small disorder, and $K \ll d$ the system will be a Fermi glass in which the interplay between the Anderson localization of single particles due to fluctuations of μ_i and quantum percolation effects (randomness of the B-sites cluster) will occur. For repulsive interactions and $K \gg d$, the ground state will be a Mott insulator on the cluster for large filling factors. It is an open question whether the delocalized metallic phases with enhanced persistent current of the kind discussed in Ref. [35] might exist in this case. Similarly, it is an open question whether for attractive interactions ($K < 0$) and $|K| < d$ pairing of (perhaps localized) fermions will take place. If $|K| \gg d$, we expect the fermions to form a domain insulator on the cluster.

In the "spin-glass" limit $\Delta_{ij} \simeq \alpha \simeq 1$, we deal with the Edwards-Anderson spin glass on the cluster. Such systems are of interest in condensed matter physics [42], and again questions connected to the nature of spin-glass ordering may be studied in this case.

When $N_{\text{F}} > N^{\text{B}}$, all B sites will be filled, and the physics will occur on the cluster of A sites. For $\alpha \simeq 0$, we shall deal with a gas with very weak repulsive interactions, and no significant disorder on the random cluster. This is an ideal test ground to study quantum percolation at low T. For finite α, and $\Delta_{ij} \simeq 1 - \alpha$, the interplay

between the fluctuating repulsive K_{ij}'s and quantum percolation might be studied.

Summarizing, we have studied atomic Fermi-Bose mixtures in optical lattices in the strong interaction limit, and in the presence of an inhomogeneous, or random on-site potential. We have derived the effective Hamiltonian describing the low temperature physics of the system, and shown that an inhomogeneous potential may be efficiently used to control the nature and strength of (boson mediated) interactions in the system. Using a random potential, one is able to control the system in such a way that its physics corresponds to a whole variety of quantum disordered systems: Fermi glass, fermionic spin-glass, and quantum percolation systems.

We thank M. Baranov, H.-P. Büchler, A. Georges, J. Wehr, J. Parrondo, and P. Zoller for fruitful discussions. We acknowledge support from the Deutsche Forschungsgemeinschaft (SFB 407 and SPP1116), the RTN Cold Quantum Gases, ESF PESC BEC2000+, the Alexander von Humboldt Foundation, and KBN Grant No. PBZ-MIN-008/P03/2003 (J. Z.).

[1] S. Jochim *et al.*, Sci. Express **302**, 2101 (2003); M. Greiner, C. A. Regal, and D. S. Jin, Nature (London) **426**, 537 (2003); M. W. Zwierlein *et al.*, Phys. Rev. Lett. **91**, 250401 (2003).
[2] G. V. Shlyapnikov, in *Proceedings of the XVIII International Conference on Atomic Physics*, edited by H.R- Sadeghpour, D. E. Pritchard, and E. J. Heller (World Scientific, Singapore, 2002).
[3] A. G. Truscott *et al.*, Science **291**, 2570 (2001).
[4] F. Schreck *et al.*, Phys. Rev. Lett. **87**, 080403 (2001).
[5] Z. Hadzibabic *et al.*, Phys. Rev. Lett. **91**, 160401 (2003).
[6] G. Modugno *et al.*, Science **297**, 2240 (2002).
[7] The studies of trapped FB gases concerned, in particular, FB phase separation [8,9], the phase diagram [10], novel collective modes [9,11], Fermi-Fermi interactions mediated by bosons [9,12], the collapse of the Fermi cloud in the presence of attractive FB interactions [6], or the effects characteristic for 1D FB mixtures [13].
[8] K. Mølmer, Phys. Rev. Lett. **80**, 1804 (1998).
[9] M. J. Bijlsma, B. A. Heringa, and H. T. C. Stoof, Phys. Rev. A **61**, 053601 (2000); H. Pu, W. Zhang, M. Wilkens, and P. Meystre, Phys. Rev. Lett. **88**, 070408 (2002).
[10] R. Roth, Phys. Rev. A **66**, 013614 (2002).
[11] P. Capuzzi and E. S. Hernández, Phys. Rev. A **64**, 043607 (2001); X.-J. Liu and H. Hu, *ibid.* **67**, 023613 (2003).
[12] A. Albus *et al.*, Phys. Rev. A **65**, 053607 (2002); L. Viverit and S. Giorgini, *ibid.* **66**, 063604 (2002); H. Heiselberg, C. J. Pethick, H. Smith, and L. Viverit, Phys. Rev. Lett. **85**, 2418 (2000).
[13] K. K. Das, Phys. Rev. Lett. **90**, 170403 (2003); M. A. Cazalilla and A. F. Ho, *ibid.* **91**, 150403 (2003).
[14] M. Greiner *et al.*, Nature (London) **415**, 39 (2002).
[15] D. Jaksch *et al.*, Phys. Rev. Lett. **81**, 3108 (1998).
[16] G. Modugno *et al.*, Phys. Rev. A **68**, 011601(R) (2003).
[17] A. Albus, F. Illuminati, and J. Eisert, Phys. Rev. A **68**, 023606 (2003).
[18] H. P. Büchler and G. Blatter, Phys. Rev. Lett. **91**, 130404 (2003); R. Roth and K. Burnett, Phys. Rev. A **68**, 023604 (2003).
[19] F. Illuminati and A. Albus, cond-mat/0311248.
[20] A. B. Kuklov and B. V. Svistunov, Phys. Rev. Lett. **90**, 100401 (2003).
[21] M. Lewenstein, L. Santos, M. A. Baranov, and H. Fehrmann, Phys. Rev. Lett. **92**, 050401 (2004).
[22] This phenomenon, related to the appearance of counterflow superfluidity in Ref. [20], may occur also in the absence of the optical lattice, M. Yu. Kagan, D. V. Efremov, and A. V. Klaptsov, cond-mat/0209481.
[23] H. Fehrmann *et al.*, cond-mat/0307635.
[24] S. Sachdev, *Quantum Phase Transitions* (Cambridge University Press, Cambridge, 1999).
[25] M. Cramer, J. Eisert, and F. Illuminati, cond-mat/0310705.
[26] For control in other context, see L.-M. Duan, E. Demler, and M. D. Lukin, Phys. Rev. Lett. **91**, 090402 (2003).
[27] A. Auerbach, *Interacting Electrons and Quantum Magnetism* (Springer, New York, 1994).
[28] B. Damski *et al.*, Phys. Rev. Lett. **91**, 080403 (2003).
[29] L. Guidoni and P. Verkerk, Phys. Rev. A **57**, 1501(R) (1999); L. Guidoni, C. Triché, P. Verkerk, and G. Grynberg, Phys. Rev. Lett. **79**, 3363 (1997); P. Horak, J.-Y. Courtois, and G. Grynberg, Phys. Rev. A **58**, 3953 (1998).
[30] In current experiments [14], the exact commensurate filling factor 1 appears in the central region of the lattice due to the presence of a weak confining potential [31].
[31] G. Batrouni *et al.*, Phys. Rev. Lett. **89**, 117203 (2002).
[32] C. Cohen-Tannoudji, J. Dupont-Roc, and G. Grynberg, *Atom-Photon Interactions: Basic Processes and Applications* (Wiley, New York, 1992).
[33] E. Abrahams, P. W. Anderson, D. C. Licciardello, and T. V. Ramakrishnan, Phys. Rev. Lett. **42**, 673 (1979).
[34] R. Freedman and J. A. Hertz, Phys. Rev. B **15**, 2384 (1977).
[35] G. Benenti, X. Waintal, and J.-L. Pichard, Phys. Rev. Lett. **83**, 1826 (1999); E. Gambeti-Césare *et al.*, Europhys. Lett. **60**, 120 (2002).
[36] R. Oppermann and D. Sherrington, Phys. Rev. B **67**, 245111 (2003).
[37] M. Mézard, G. Parisi, and M. A. Virasoro, *Spin Glass and Beyond* (World Scientific, Singapore, 1987).
[38] D. S. Fisher and D. A. Huse, Phys. Rev. Lett. **56**, 1601 (1986); A. J. Bray and M. A. Moore, *ibid.* **58**, 57 (1987); C. M. Newman and D. L. Stein, J. Phys. Condens. Matter **15**, R1319 (2003).
[39] A. Georges, O. Parcollet, and S. Sachdev, Phys. Rev. B **63**, 134406 (2001).
[40] J. R. L. de Almeida and D. J. Thouless, J. Phys. A **11**, 983 (1978).
[41] A. Aharony and D. Stauffer, *Introduction to Percolation Theory* (Taylor & Francis, London, 1994).
[42] P. H. R. Barbosa, E. P. Raposo, and M. D. Coutinho-Filho, Phys. Rev. Lett. **91**, 197207 (2003).

Disordered ultracold atomic gases in optical lattices: A case study of Fermi-Bose mixtures

V. Ahufinger,[1,2] L. Sanchez-Palencia,[2,3] A. Kantian,[2,4,5] A. Sanpera,[2,6,*] and M. Lewenstein[2,7,*]
[1]*Grup d'Òptica, Departament de Física, Universitat Autònoma de Barcelona, E-08193 Belaterra, Barcelona, Spain*
[2]*Institut für Theoretische Physik, Universität Hannover, D-30167 Hannover, Germany*
[3]*Laboratoire Charles Fabry, Institut d'Optique Théorique et Appliquée, Université Paris-Sud XI, F-91403 Orsay Cedex, France*
[4]*Institut für Quantenoptik und Quanteninformation der Österreichischen, Akademie der Wissenschaften, A-6020 Innsbruck, Austria*
[5]*Institut für Theoretische Physik, Universität Innsbruck, A-6020 Innsbruck, Austria*
[6]*Grup de Física Teòrica, Departament de Física, Universitat Autònoma de Barcelona, E-08193 Belaterra, Barcelona, Spain*
[7]*Institut de Ciències Fotòniques, E-08034 Barcelona, Spain*
(Received 7 September 2005; published 21 December 2005)

We present a review of properties of ultracold atomic Fermi-Bose mixtures in inhomogeneous and random optical lattices. In the strong interacting limit and at very low temperatures, fermions form, together with bosons or bosonic holes, *composite fermions*. Composite fermions behave as a spinless interacting Fermi gas, and in the presence of local disorder they interact via random couplings and feel effective random local potential. This opens a wide variety of possibilities of realizing various kinds of ultracold quantum disordered systems. In this paper we review these possibilities, discuss the accessible quantum disordered phases, and methods for their detection. The discussed quantum phases include Fermi glasses, quantum spin glasses, "dirty" superfluids, disordered metallic phases, and phases involving quantum percolation.

DOI: 10.1103/PhysRevA.72.063616 PACS number(s): 03.75.Kk, 03.75.Lm, 05.30.Jp, 64.60.Cn

I. INTRODUCTION

A. Disordered systems

Since the discovery of the quantum localization phenomenon by Anderson in 1958 [1], disordered and frustrated systems have played a central role in condensed matter physics. They have been involved in some of the most challenging open questions concerning many body systems (cf. [2–4]). Quenched (i.e., frozen on the typical time scale of the considered systems) disorder determines the physics of various phenomena, from transport and conductivity, through localization effects and metal-insulator transition (cf. [5]), to spin glasses (cf. [6–8]), neural networks (cf. [9]), percolation [10,11], high T_c superconductivity (cf. [12]), or quantum chaos [13]. One of the reasons why disordered systems are very hard to describe and simulate is related to the fact that, usually, in order to characterize the system, one should calculate the relevant physical quantities averaged over a particular realization of the disorder. Analytical approaches require the averaging of, for instance, the free energy, which (being proportional to the logarithm of the partition function in the canonical ensemble) is a very highly nonlinear function of the disorder. Averaging requires then the use of special methods, such as the replica trick (cf. [6]), or supersymmetry method [14]. In numerical approaches this demands either simulating very large samples to achieve "self-averaging," or numerous repetitions of simulations of small samples. Obviously, this difficulty is particularly important for quantum disordered systems. Systems which are not disordered but frustrated (i.e., unable to fulfill simultaneously all the constrains imposed by the Hamiltonian), lead very often to similar difficulties, because quite often they are characterized at low temperature by an enormously large number of low energy excitations (cf. [15]). It is thus desirable to ask whether atomic, molecular physics, and quantum optics may help to understand such systems. In fact, very recently, it has been proposed how to overcome the difficulty of quenched averaging by encoding quantum mechanically in a superposition state of an auxiliary system, all possible realizations of the set of random parameters [16]. In this paper we propose a more direct approach to the study of disorder: direct realization of various disordered models using cold atoms in optical lattices.

B. Disordered ultracold atomic gases

In recent years there has been enormous progress in the studies of ultracold weakly interacting [17], as well as strongly correlated, atomic gases. In fact, present experimental techniques allow one to design, realize, and control in the laboratory various types of ultracold interacting Bose or Fermi gases, as well as their mixtures. Such ultracold gases can be transferred to optical lattices and form a, practically perfect, realization of various Hubbard models [18]. This observation, suggested in the seminal theory paper by Jaksch *et al.* [19] in 1998, and confirmed then by the seminal experiments of Greiner *et al.* [20], has triggered enormous interest in the studies of strongly correlated quantum systems in the context of atomic and molecular lattice gases.

It soon became clear that one can introduce local disorder and/or frustration to such systems in a controlled way using various experimentally feasible methods. Local quasidisorder potentials may be created by superimposing superlattices incommensurable with the main one to the system. Although strictly speaking such a superlattice is not disordered, its effects are very similar to those induced by the genuine random potentials [21–23]. Controlled local truly random poten-

*Also at Institució Catalana de Recerca i Estudis Avançats.

tials can be created by placing a speckle pattern on the main lattice [24,25]. As shown in Ref. [21], for a system of strongly correlated bosons located in such a disordered lattice, both methods should permit one to achieve an Anderson-Bose glass [26], provided that the correlation length of the disorder L_{dis} is much smaller than the size of the system. Unfortunately, it is difficult to have L_{dis} smaller than a few microns using speckles. Thus, L_{dis} is typically larger than the condensate healing length $l_{heal}=1/\sqrt{8\pi na}$, where n is the condensate density, and a the atomic scattering length. Due to this fact, i.e., due to the effects resulting from the nonlinear interactions, it is difficult to achieve the Anderson localization regime with weakly interacting Bose-Einstein condensates (BECs) [27,28]. We have shown, however, that quantum localization should be experimentally feasible using the quasidisorder created by several lasers with incommensurable frequencies [29]. Random local disorder appears also, naturally, in magnetic microtraps and atom chips as a result of roughness of the underlying surface ([30], for theory see [31,32]).

One can also create disorder using a second atomic species, by rapidly quenching it from the superfluid to the localized Mott phase. After such a process, different lattice sites are populated by a random number of atoms of the second species, which act effectively as random scatterers for the atoms of the first species [33]. Last, but not least it is possible to use Feschbach resonances in fluctuating or inhomogeneous magnetic fields in order to induce a type of disorder that corresponds to random, or at least inhomogeneous, nonlinear interaction couplings [34] (for theory in one-dimensional (1D) systems see [35,36]). It has been also been proposed [37] that tunneling induced interactions in systems with local disorder results in controllable disorder on the level of next-neighbor interactions. That opens a possible path for the realization of quantum spin glasses [37]. As we have already mentioned, several experimental groups have already achieved [27–29], or are soon going to realize [33,34] disordered potentials using these methods. It is worth mentioning here a very recent attempt to create controlled disorder using optical tweezers methods [38].

There are also several ways to realize nondisordered but frustrated systems with atomic lattice gases. One is to create such gases in "exotic" lattices, such as the Kagomé lattice [39], another is to induce and control the nature and range of interactions by adjusting the external optical potentials, such as, for instance, proposed in Ref. [40]. Another example of such a situation is provided for instance by atomic gases in a two-dimensional lattice interacting via dipole-dipole interactions with dipole moment polarized parallel to the lattice [41].

Finally, there are also several ideas concerning the possibility of realizing various types of complex systems using atomic lattice gases or trapped ion chains. Particularly interesting here are the possibilities of producing long range interactions (falling off as inverse of the square, or cube of the distance) [42], systems with several metastable energy minima, and last, but not least systems in designed external magnetic [43], or even non-Abelian gauge fields [44].

C. Quantum information with disordered systems

One important theoretical aspect that should be considered in this context deals with the role of entanglement in quantum statistical physics in general (where it concerns quantum phase transitions, entanglement correlation length, and scaling [45]), and characterization of various types of distributed entanglement. This aspect is particularly interesting in theoretical and experimental studies of disordered systems. The question which one is tempted to ask is, to what extent can one realize quantum information processing in (i) disordered systems, (ii) nondisordered systems with long range interactions, and (iii) nondisordered frustrated systems.

At the first sight, the answer to this question is negative. Disordered quantum information processing sounds like *contradictio in adjecto*. But, one should not neglect the possible advantages offered by the systems under investigation. First, such systems have typically a significant number of (local) energy minima, as, for instance, happens in spin glasses. Such metastable states might be employed to store information distributed over the whole system, as in neural network models. The distributed storage implies redundancy similar to the one used in error correcting protocols [46]. Second, in the systems with long range interactions the stored information is usually robust: metastable states have large basins of attraction thermodynamically, and destruction of a part of the system does not destroy the metastable states (for the preliminary studies see Refs. [47,48]). Third, and perhaps the most important aspect for the present paper, is that atomic ultracold gases offer a unique opportunity to realize special purpose quantum computers (quantum simulators) to simulate quantum disordered systems. The importance of the experimental realizations of such quantum simulators will without doubts forward our understanding of quantum disordered systems enormously. In particular, we can think about large scale quantum simulations of the Hubbard model for spin $1/2$ fermions with disorder, which lies at the heart of the present-day-understanding of high T_c superconductivity. The impact of this possibility for physics and technology is hard to overestimate. Fourth, very recently, several authors have used the ideas of quantum information theory to develop novel algorithms for efficient simulations of quantum systems on classical computers [49]. Applications of these novel algorithms to disordered systems are highly desired.

D. Fermi-Bose mixtures

The present paper deals with the above formulated questions, which lie at the frontiers of modern theoretical physics, and concern not only atomic, molecular, and optical (AMO) physics and quantum optics, but also condensed matter physics, quantum field theory, quantum statistical physics, and quantum information. This interdisciplinary theme is one of the most hot current subjects of the physics of ultracold gases. In particular, we present here the study of a specific example of disordered ultracold atomic gases: Fermi-Bose (FB) mixtures in optical lattices in the presence of additional inhomogeneous and random potentials.

In the absence of disorder and in the limit of strong atom-atom interactions such systems can be described in terms of

composite fermions consisting of a bare fermion, or a fermion paired with one boson (bosonic hole), or two bosons (bosonic holes), etc. [50]. The physics of Fermi-Bose mixtures in this regime has been studied by us recently in a series of papers [52–54]; for contributions of other groups to the studies of FB mixtures in traps and in optical lattices see Ref. [55] and for the studies of strongly correlated FB mixtures in lattices see Ref. [63], respectively. In particular, the validity of the effective Hamiltonian for fermionic composites in 1D was studied using exact diagonalization and the density matrix renormalization group method in Ref. [64]. The effects of inhomogeneous trapping potential on FB lattice mixtures has been for the first time discussed by Cramer *et al.* [65]. The physics of disordered FB lattice mixtures was studied by us in Ref. [37], which has essentially demonstrated that this system may serve as a paradigm fermionic system to study a variety of disordered phases and phenomena: from Fermi glass to quantum spin glass and quantum percolation.

E. Plan of the paper

The main goal of the present paper is to present the physics of the disordered FB lattice gas in more detail, and in particular to investigate conditions for obtaining various quantum phases and quantum states of interest.

The paper is organized as follows. Section II describes the "zoology" of disordered systems and disordered phases known from condensed matter physics. We pay particular attention to the systems realizable with cold atoms on one side, and particularly interesting from the other. This latter phrase means that we consider here the systems that concern important open questions and challenges of the physics of disordered systems. In this sense this section is thought as a list of such challenging open questions that can be perhaps addressed by the cold gases community. This section is thus directed to the cold gases experts, and is supposed to motivate and stimulate their interest in the physics of ultracold disordered systems.

In Sec. III, we introduce the composite fermions formalism, first discussing it for the case of homogeneous lattices, and then for disordered ones. We derive here the explicit formulas for the effective Hamiltonian, and for various types of disorder. One of the results of this section concerns the generalizations of the results of Ref. [37], that implies that *local* disorder on the level of the Fermi-Bose Hubbard model leads to randomness of the nearest neighbor tunneling and coupling coefficients for the composite fermions. Obviously, these tunneling and coupling coefficients arise in effect of tunneling mediated interactions between the composites.

In Sec. IV, we present our numerical results in the weak disorder limit, based on the time dependent Gutzwiller ansatz. These results concern mainly the physics of composites, the realization of Fermi glass, and the transition from Fermi liquid to Fermi glass.

The results for the case of strong disorder, spin glasses, are discussed in Sec. V. The problem of detection of the phenomena predicted in this paper is addressed in Sec. VI, whereas we conclude in Sec. VII.

II. DISORDERED SYSTEMS: THE OLD AND NEW CHALLENGES FOR AMO PHYSICS

In this section we present a list of problems and challenges of the physics of disordered systems that may, in our opinion, be realized and addressed in the context of physics of ultracold atomic or molecular gases. We concentrate here mainly on fermionic systems. This section is written on an elementary level and addressed to nonexperts in the physics of disordered systems.

A. Anderson localization

One of the most spectacular effects of disorder concerns single particles. The spectrum of a Hamiltonian of a free particle in free space or in a periodic lattice is continuous and the corresponding eigenfunctions are extended (plane waves or Bloch functions). Introduction of disorder may drastically change this situation. The basic knowledge about these phenomena comes from the famous scaling theory formulated by the "gang of four" ([66,5]).

The scaling theory predicts that in 1D infinitesimally small disorder leads to exponential localization of all eigenfunctions. The localization length (defined as the width of the exponentially localized states) is a function of the ratio between the potential and the kinetic (tunneling) energies of the eigenstate and the disorder strength. For the case of discrete systems with constant tunneling rates and local disorder distributed according to a Lorentzian distribution (Lloyd's model, cf. [13]) the exact expression for the localization length is known. In general, an exact relation between the density of states and the range of localization in 1D has been provided by Thouless [67]. Hard core bosons with strong repulsion in 1D chains, described by the *XY* model in a random transverse field, can be mapped using the Wigner-Jordan transformation to 1D noninteracting fermions in a random local potential, which in turn maps the bosonic problem onto the problem of Anderson localization [68].

In 2D, following the scaling theory, it is believed that localization occurs also for arbitrarily small disorder, but its character interpolates smoothly between algebraic for weak disorder, and exponential for strong disorder. There are, however, no rigorous arguments to support this belief, and several controversies arose about this subject over the years. It would be evidently challenging to shed more light on this problem using cold atoms in disordered lattices.

3D scaling theory predicts a critical value of disorder, above which every eigenfunction exponentially localizes, and this fact has found strong evidence in numerical simulations.

In the area of AMO physics, effects of disorder have been studied in the context of weak localization of light in random media [69], which is believed to be a precursor of Anderson localization, and in the form of the so-called dynamical localization, that inhibits diffusion over the energy levels ladder in periodically driven quantum chaotic systems, such as kicked rotor [70], microwave driven hydrogenlike atom (see [13] and references therein), or cold atoms kicked by optical lattices [71].

It is also worth mentioning at this point the existing large literature on unusual band structure and conductance properties in systems with incommensurate periodic potentials [72]. The famous Harper's equation describing electron's hopping in a $\cos(\cdot)$ potential in 1D [73] may have, depending on the strength of the potential, only localized, or only extended states due to the, so-called, Aubry self-duality. In more complicated cases without self-dual property, and/or in higher dimensions coexistence of localized and extended states is very frequent.

B. Localization in Fermi liquids

The effects of disorder in electronic gases (i.e., Fermi gases with repulsive interactions) were in the center of interest over many decades. Originally, it was believed that weak disorder should not modify essentially the Fermi liquid quasiparticle picture of Landau. Altshuler and Aronov [74], and independently Fukuyama [75], have shown, however, that even weak disorder leads to surprisingly singular corrections to electronic density of states near the Fermi surface, and to transport properties.

As we discussed above, for sufficient disorder in 3D all states are localized, and the standard Fermi liquid theory is not valid. One can use then a Fermi-liquid-like theory using localized quasiparticle states. The system enters then an insulating *Fermi glass* state [76], termed often also as Anderson insulator, in which most of the interaction effects are included in the properties of the Landau's quasiparticles.

In 1994 Shepelyansky [77] stimulated further discussion about the role of interactions by considering two interacting particles (TIP) in a random potential. He argued that two repulsing or attracting particles can propagate coherently on a distance much larger than the one-particle localization length. Several groups have tried to study these effects of interplay between the disorder and (repulsive) interactions in more detail in the regime when Fermi liquid becomes unstable as the Mott insulator state is approached by increasing the interactions. Numerical studies performed for spinless fermions with nearest-neighbor (NN) interactions in a disordered mesoscopic ring; for spin $1/2$ electrons in a ring, described by the half-filled Hubbard-Anderson model; for spinless fermions with Coulomb repulsion (reduced to NN repulsion) in 2D, etc. ([78,79]) show that as interactions become comparable with disorder, delocalization takes places. In a 1D ring it leads to the appearance of persistent currents, in 2D the delocalized state exhibits also an ordered flow of persistent currents, which is believed to constitute a novel quantum phase corresponding to the metallic phase observed in experiments, for instance, with a gas of holes in GaAs heterostructures for the similar range of parameters.

Another intensive subject of investigation concerns metal (Fermi liquid)-insulator transition driven by disorder in 3D. Theoretical description of this phenomenon goes back to the seminal works of Efros and Shklovskii [80] and McMillan [81]. In this context, particularly impressive are the recent results of experiments on disordered alloys, such as amorphous NbSi [82], where the evidence for scaling and quantum critical behavior was found. Weakly doped semiconductors provide a good model of a disordered solid, and their critical behavior at the metal-insulator transition has been intensively studied (cf. [83]). Very interesting results concerning in particular various forms of electronic glass: from Fermi glass, with negligible effects of Coulomb repulsion, to Coulomb glass [84], dominated by the electronic correlations were obtained in the group of Dressel [85].

Although there exists experimental evidence for delocalization, enhanced persistent currents, and novel metallic phases at the frontier between the Fermi glass and Mott insulator, the further experimental models that physics of cold atoms might provide are highly welcomed. Especially, since the cold atoms Hubbard toolbox should allow one to design with great fidelity the models studied by theorists: spinless fermions extended Hubbard model in 1D, 2D, and 3D, and spin $1/2$ Hubbard model in a disordered potential, or even more exotic systems such as Fermi systems with SU(N) "flavor" symmetry [86]. Perhaps a less ambitious, but still interesting challenge is to use ultracold atomic gases to create both Fermi glass and a fermionic Mott insulator, and investigate their properties in detail.

C. Localization in Bose systems

At this point it is also worth mentioning the existing literature on the influence of repulsive interactions on Anderson localization in bosonic systems. In the weakly interacting case, one observes at low temperatures the phenomenon of Bose-Einstein condensation (BEC), but to the eigenstates of the random potential (which are Anderson localized). Strong nonlinear interactions tend, however, to destroy the localization effects by introducing screening of disorder by the nonlinear mean field potential [87,88]. This happens as soon as the disorder localization length, L_{dis}, becomes larger than the healing length, l_{heal}. Such destruction of localization by weak nonlinearity occurs also in the context of chaos, as discussed in 1993 by Shepelyansky [89]. Several experiments, aiming at observation of localization with BECs have been recently performed with elongated condensates in the presence of a speckle pattern and 1D optical lattices [27–29]. In particular, transport suppression has been observed in the Orsay and Lens experiments, whereas, as we have shown in the Hannover setup [29], conditions for Anderson localization can be achieved using additional incommensurate superlattices. As the nonlinearity (i.e., number of atoms) grows the condensate wave function becomes a superposition of exponentially localized modes of comparably low energies. Overlapping of those modes signifies the onset of the screening regime. We believe that similar effects hold in the strongly interacting limit in optical lattices, when they occur at the crossover from the Anderson glass (in the weak interacting regime) to Bose glass (in the strong interacting regime) behavior (see [21], and also [90]).

D. Localization in superconductors

Obviously, the effects of disorder on superconductivity were studied practically from the very beginning of the theory of superconductors. Already in the late 1950's Anderson and Gorkov considered "dirty" superconductors [91].

For a weak disorder, Bardeen-Cooper-Schrieffer (BCS) theory is still valid, but must be modified; the critical temperature is reduced by the localization effects [92].

The situation is more complex in the case of strong disorder. For example, in 2D superconductors the superconducting state exists only for sufficiently small values of the disorder. This state is often termed a superconducting vortex glass. Cooper pairs in this state condense and form a delocalized "Bose" condensate. This condensate contains a large number of quantum vortices that are immobile and localized in the random potential energy minima associated with disorder [93]. As disorder grows, the system enters the insulating phase, which is a Bose glass of Copper pairs (for general theory see [26]). Finally, for even stronger values of the disorder the system enters the insulating Fermi glass phase, when the Cooper pairs break down. Obviously, this picture becomes even more complex at the BCS-BEC crossover.

Superconductor-insulator transition has been recently intensively studied in thin metal films on Ge or Sb substrates, that induce disorder on the atomic scale. For not too thin films, transition to superconduting state occurs via Kosterlitz-Thouless-Berezinsky mechanism, whereas for ultrathin films localization effects suppress superconductivity [94,95]. In particular, scaling behavior and scaling exponent were studied in thin bismuth films [96].

As before, the physics of cold gases might contribute here significantly to our understanding of the influence of quenched disorder on the phenomenon of superconductivity.

E. Localization and percolation

Percolation is a classical phenomenon that is very closely related to localization [2]. Percolation provides a very general paradigm for a lot of physical problems ranging from disordered electric devices [97], forest fires, and epidemics [10,98], to ferromagnetic ordering [8]. In lattices, one considers site and bond percolation, and asks the following question: given a probability of filling a lattice site (filling a bond), and given a layer of the lattice of linear width L, does a percolating cluster of filled sites (bonds) that connects the walls of the layer exist?

Obviously, a percolating medium with a percolating cluster of empty sites is an example of a medium consisting of randomly distributed scatterers. One has to expect that Anderson localization will occur if quantum waves will propagate and scatter in such a medium. An interplay between percolation and localization has been a subject of intensive studies in recent years. On one hand, when a classical flow is possible, the quantum one might be suppressed due to the destructive interferences and Anderson mechanism. On the other hand, quantum mechanics offers a possibility of tunneling through the classically forbidden regions, and may thus allow for a classically forbidden flow. It turns out that this latter mechanism is very weak, and one typically observes three regimes of localization-delocalization behavior: classical localization below the percolation limit, quantum localization above the percolation limit, and quantum delocalization sufficiently above the percolation limit [99,100]. Quantum percolation plays a role of mechanism responsible for quantum Hall effect [101]. Obviously, interactions in the presence of quantum percolation introduce additional complexity into the phenomenon.

Atomic Fermi-Bose mixtures and atomic gases in general offer an interesting possibility to study quantum percolation in a controlled way. One should stress that quenching atoms as random scatterers in a lattice (below percolation threshold) would be one of the methods itself to generate random local potentials.

F. Random field Ising model

Particularly interesting are those disordered systems, in which arbitrarily small disorder causes large qualitative effects, with Anderson localization in 1D and, most presumably, in 2D being paradigm examples. Other examples are provided by classical systems that exhibit long range order at the lower critical dimension. In such systems, addition of an arbitrary small local potential (magnetic field), that has a distribution assuming the same symmetry as the considered model, destroys long range order.

The first example of such behavior has been shown by Imry and Ma [102], using the domain wall argument; it concerns random field Ising model in 2D, for which magnetization vanishes in a random magnetic field in the Ising spin direction with symmetric distribution (Z_2 symmetry). This result was soon after proven rigorously [103], and even generalized to XY, Heisenberg, or Potts models (provided that the corresponding "field" assumes the same symmetry as the model, i.e., U(1), SU(2), etc. [104]).

One should note that most of the above discussed effects concern abstract spin models, and have no direct experimental realizations in condensed matter systems. Cold atoms offer here a unique possibility of both feasible realization of classical models, and of studying quantum effects in those systems. Equally interesting in this context could be spin models in which the random magnetic field breaks the symmetry, such as, for instance, XY model in 2D in the random field directed in, say, the X direction. Such field breaks the U(1) symmetry and changes the universality class of the model to the Ising class. Simultaneously, it prevents spontaneous magnetization in the X direction. In effect, the system attains the macroscopic magnetization in the Y direction [105]. We have recently studied these kinds of systems and proved this result at $T=0$ rigorously. We expect in fact finite T transition (as in Ising model), but a detailed analysis of that case goes beyond the scope of the present paper [106].

G. Spin glasses: Parisi's theory and the "droplet" model

Spin glasses are spin systems interacting via random couplings, that can be both ferro- or antiferromagnetic. Such variations of the couplings lead typically to frustration. Spin glass models may thus exhibit many local minima of the free energy. For this reason, spin glasses remain one of the challenges of the statistical physics and, in particular, the question of the nature of their ordering is still open. According to Parisi's picture, the spin glass phase consists of very many pure thermodynamic phases. The order parameter of a spin glass becomes thus a function characterizing the probability

of overlaps between the distinct pure phases [6]. According to the so-called "droplet" picture, developed by Huse-Fisher and Bray-Moore [7,107] there are (for Ising spin glasses) just two pure phases (up to Z_2 symmetry), and what frustration does is to change very significantly the spectrum of excitations (domain walls, droplets) close to the equilibrium. While the Parisi's picture (related also to the replica symmetry breaking) is most presumably valid for long range spin glass models, such as Sherrington-Kirkpatrick model [108], the "droplet" model is formulated as a scaling theory, and has a lot of numerical support for short range models, such as the Edwards-Anderson [109] model. For more details of these two pictures relevant for our actual study see Sec. V.

III. DYNAMICS OF COMPOSITE FERMIONS IN THE STRONG COUPLING REGIME

In this section we begin our detailed discussion of the low temperature physics of the Fermi-Bose mixtures. In particular we consider a mixture of ultracold bosons (b) and spinless (or spin-polarized) fermions (f), for example ^{7}Li-^{6}Li or ^{87}Rb-^{40}K, trapped in an optical lattice. In the following, we will first consider the case of an homogeneous optical lattice, where all lattice sites are equivalent, and we will review previous results focusing on the formation of composite fermions and the quantum phase diagram [52]. Second, we shall extend the analysis to the case of inhomogeneous optical lattices. We consider on-site inhomogeneities consisting of a harmonic confining potential and/or diagonal disorder. In all cases considered below, the temperature is assumed to be low enough and the potential wells deep enough so that only quantum states in the fundamental Bloch band for bosons or fermions are populated. Note that this requires that the filling factor for fermions ρ_f, is smaller than 1, i.e., the total number of fermions, N_f, is smaller than the total number of lattice sites N.

In the tight-binding regime, it is convenient to project wave functions on the Wannier basis of the fundamental Bloch band, corresponding to wave functions well localized in each lattice site [110,111]. This leads to the Fermi-Bose Hubbard (FBH) Hamiltonian [8,12,19,63]:

$$H_{\mathrm{FBH}} = -\sum_{\langle ij\rangle}\left[J_b b_i^\dagger b_j + J_f f_i^\dagger f_j + \mathrm{H.c.}\right] + \sum_i \left[\frac{V}{2} n_i(n_i-1) + U n_i m_i\right] + \sum_i \left[-\mu_i^b n_i - \mu_i^f m_i\right], \tag{1}$$

where $b_i^\dagger$, b_i, $f_i^\dagger$, and f_i are bosonic and fermionic creation-annihilation operators of a particle in the ith localized Wannier state of the fundamental band and $n_i=b_i^\dagger b_i$, $m_i=f_i^\dagger f_i$ are the corresponding on-site number operators. The FBH model describes: (i) nearest-neighbor (NN) boson (fermion) hopping, with an associated negative energy, $-J_b(-J_f)$; (ii) on-site boson-boson interactions with an energy V, which is supposed to be positive (i.e., repulsive) in the reminder of the paper; (iii) on-site boson-fermion interactions with an energy U, which is positive (negative) for repulsive (attractive) interactions; and (iv) on-site energy due to interactions with a possibly inhomogeneous potential, with energies $-\mu_i^b$ and $-\mu_i^f$; eventually, $-\mu_i^b$ and $-\mu_i^f$ also contain the chemical potentials in grand canonical description. For the sake of simplicity, we shall focus, in the following, on the case of equal hopping for fermions and bosons, $J_b=J_f=J$ and we shall assume the strong coupling regime, i.e., $V,U \gg J$. Generalization to the case $J_b \neq J_f$ is just straightforward.

A. Quantum phases in homogeneous optical lattices

Before turning to inhomogeneous optical lattices, let us briefly review here the results presented in [52] for homogeneous lattices at zero temperature, when all sites are translationally equivalent. In the limit of vanishing hopping ($J=0$) with finite repulsive boson-boson interaction V, and in the absence of interactions between bosons and fermions ($U=0$), the bosons are in a Mott insulator (MI) phase with exactly $\tilde{n}=\lceil\tilde{\mu}^b\rceil+1$ bosons per site, where $\tilde{\mu}^b=\mu^b/V$ and $\lceil x\rceil$ denotes the integer part of x. In contrast, the fermions can be in any set of Wannier states, since for vanishing tunneling, the energy is independent of their configuration. The situation changes when the interparticle interactions between bosons and fermions, U, are turned on. In the following, we define $\alpha=U/V$ and we consider the case of a bosonic MI phase with $\tilde{n}$ bosons per site. The presence of a fermion in site i may attract $-s>0$ bosons or equivalently expel $s\leqslant\tilde{n}$ boson(s) depending on the sign of U. The on-site energy gain in attracting $-s$ bosons or expelling s bosons from site i is $\Delta E_i=(V/2)s(s-2\tilde{n}+1)-Us+\mu^b s$. Minimizing ΔE_i it clearly appears energetically favorable to expel $s=\lceil\alpha-\tilde{\mu}^b\rceil+\tilde{n}$ bosons. Within the occupation number basis, excitations correspond to having $\tilde{n}-s\pm1$ bosons in a site with a fermion, instead of $\tilde{n}-s$ and, therefore, the corresponding excitation energy is $\sim V$. In the following, we assume that the temperature is smaller than V so that the population of the abovementioned excitations can be neglected. It follows that tunneling of a fermion is necessarily accompanied by the tunneling of $-s$ bosons (if $s<0$) or opposed-tunneling of s bosons (if $s\geqslant0$). The dynamics of our Fermi-Bose mixture can thus be regarded as the one of composite fermions made of one fermion plus $-s$ bosons (if $s<0$) or one fermion plus s bosonic holes (if $s\geqslant0$). The annihilation operators of the composite fermions are [52]

$$F_i = \sqrt{\frac{(\tilde{n}-s)!}{\tilde{n}!}}(b_i^\dagger)^s f_i \quad \text{for } s \text{ bosonic holes}, \tag{2}$$

$$F_i = \sqrt{\frac{\tilde{n}!}{(\tilde{n}-s)!}}(b_i)^{-s} f_i \quad \text{for } -s \text{ bosons}. \tag{3}$$

These operators are fermionic in the sub-Hilbert space generated by $|n\text{-}ms,m\rangle$ with $m=0,1$ in each lattice. Note that within the picture of fermionic composites, the vacuum state corresponds to the MI phase with $\tilde{n}$ boson per site. At this point, different composite fermions appear depending on the values of α, $\tilde{n}$, and $\tilde{\mu}^b$ as detailed in Fig. 1 [52]. The different composites are denoted by Roman numbers *I*, *II*, *III*, etc, which denote the total number of particles that form the corresponding composite fermion. Additionally, a bar over a Ro-

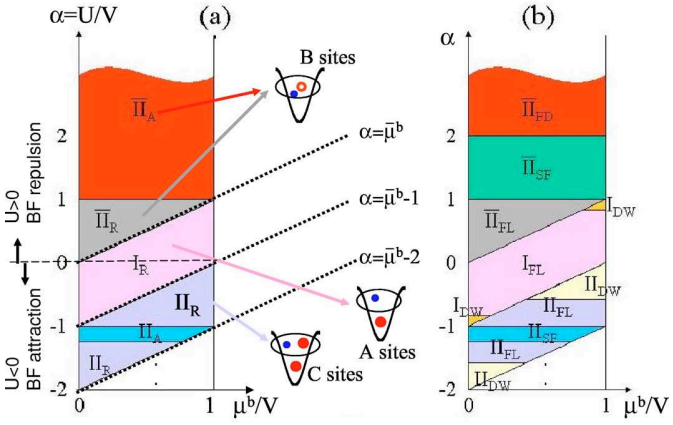

FIG. 1. (Color online) Quantum phase diagrams of Fermi-Bose mixtures in a homogeneous optical lattice as functions of $\tilde{\mu}^{\mathrm{b}}$ and $\alpha=U/V$, for $\rho_{\mathrm{f}}=0.4$ and $J/V=0.02$. Roman numbers denote the total number of particles that form the composite and a bar means that the composite is formed by bosonic holes rather than bosons. (a) Diagram of composites where the filled small (blue) dots symbolize fermions, large (red) dots symbolize bosons, and empty (red) dots, bosonic holes. The subindex A (R) indicates attractive (repulsive) composites interactions. (b) Detailed quantum phase diagram of fermionic composites. The subindices denote here different phases: DW (density wave), FL (fermi liquid), SF (superfluid), and FD (fermionic domains). The strongly correlated phases for small but finite J are surrounded by characteristic lobs [53], beyond which bosons become superfluid. Therefore there are thin regions of bosonic superfluid between the various composite phases [112]. The general explanation of the figure appears in Sec. III A while the numerical calculations of some of the possible phases are reported, for the case of sites B, in Sec. IV B. A detailed explanation of the phases exhibited by composites $\bar{I}\bar{I}$ (B sites), composites I (A sites), and composites II (C sites) in the presence of disorder can be found in Secs. III C–III E, respectively.

man number indicates composite fermions formed by one bare fermion and bosonic holes, rather than bosons. For the sake of simplicity, we shall consider only bosonic MI phases with $\tilde{n}=1$ boson per site (i.e., $0<\tilde{\mu}^{\mathrm{b}}\leqslant 1$) in the following parts of this paper [113].

If $\alpha-\tilde{\mu}^{\mathrm{b}}>0$, a fermion in site i pushes the boson out of the site. We will call the sites with this property B-sites. This notation will become particularly important in the presence of disorder (local $\tilde{\mu}^{\mathrm{b}}$). The composites, in this case, correspond to one fermion plus one bosonic hole [this phase is called $\bar{I}\bar{I}$ in Fig. 1(a)]. If $-1<\alpha-\tilde{\mu}^{\mathrm{b}}<0$, we have bare fermions as composites (this corresponds to phase I). The sites with this property will be called A-sites. Finally, if $-2<\alpha-\tilde{\mu}^{\mathrm{b}}<-1$, the composites are made of one fermion plus one boson (phase II). The sites with the latter property will be called C-sites. Because all sites are equivalent for the fermions, the ground state is highly $[N!/(N_{\mathrm{f}})!(N-N_{\mathrm{f}})!]$-degenerated, so the manifold of ground states is strongly coupled by fermion or boson tunneling. We assume now that the tunneling rate J is small but finite. Using time-dependent degenerate perturbation theory [114], we derive an effective Hamiltonian [12] for the fermionic composites:

$$H_{\mathrm{eff}}=-d_{\mathrm{eff}}\sum_{\langle i,j\rangle}(F_i^{\dagger}F_j+\mathrm{H.c.})+K_{\mathrm{eff}}\sum_{\langle i,j\rangle}M_iM_j-\bar{\mu}_{\mathrm{eff}}\sum_i M_i, \tag{4}$$

where $M_i=F_i^{\dagger}F_i$ and $\bar{\mu}_{\mathrm{eff}}$ is the chemical potential, whose value is fixed by the total number of composite fermions. The nearest neighbor hopping for the composites is described by $-d_{\mathrm{eff}}$ and the nearest neighbor composite-composite interactions are given by K_{eff}, which may be repulsive (>0) or attractive (<0). This effective model is equivalent to that of spinless interacting fermions. The interaction coefficient K_{eff} originates from second order terms in perturbative theory and can be written in the general form:

$$K_{\mathrm{eff}}=\frac{-2J^2}{V}\left[(2\tilde{n}-s)(\tilde{n}+1)-s(\tilde{n}-s)-\frac{(\tilde{n}-s)(\tilde{n}+1)}{1+s-\alpha}-\frac{(\tilde{n}-s+1)\tilde{n}}{1-s+\alpha}-\frac{1}{s\alpha}\right]. \tag{5}$$

This expression is valid in all the cases but when $s=0$ the last term $(1/s\alpha)$ should not be taken into account. d_{eff} originates from $(|s|+1)$-th order terms in perturbative theory and thus presents different forms in different regions of the phase diagram of Fig. 1. For instance in region I, $d_{\mathrm{eff}}=J$, in region $\bar{I}\bar{I}$ $d_{\mathrm{eff}}=2J^2/U$, and in region II, $d_{\mathrm{eff}}=4J^2/|U|$.

The physics of the system is determined by the ratio $K_{\mathrm{eff}}/d_{\mathrm{eff}}$ and the sign of K_{eff}. In Fig. 1(a), the subindex A/R denotes attractive ($K_{\mathrm{eff}}<0$)/repulsive ($K_{\mathrm{eff}}>0$) composites interactions. Figure 1(b) shows the quantum phase diagram of composites for fermionic filling factor $\rho_{\mathrm{f}}=0.4$ and tunneling $J/V=0.02$. As an example, let us consider the case of repulsive interactions between bosons and fermions, $\alpha>0$. Once the fermion-bosonic hole composites $\bar{I}\bar{I}$ have been created ($\alpha>\tilde{\mu}^{\mathrm{b}}$), the relation $K_{\mathrm{eff}}/d_{\mathrm{eff}}=-2(\alpha-1)$ applies. Consequently, if one increases the interactions between bosons and fermions adiabatically, the system evolves through different quantum phases. For $\tilde{\mu}^{\mathrm{b}}<\alpha<1$, the interactions between composite fermions are repulsive and of the same order of the tunneling; the system exhibits delocalized metallic phases. For $\alpha\simeq 1$, the interactions between composite fermions vanish and the system shows up the properties of an ideal Fermi gas. Growing further the repulsive interactions between bosons and fermions, the interactions between composite fermions become attractive. For $1<\alpha<2$, one expects the system to show superfluidity, and for $\alpha>2$ fermionic insulator domains are predicted.

In the reminder of the paper, we shall generalize these results to the case of inhomogeneous optical lattices. We shall assume diagonal inhomogeneities, i.e., site-dependent local energies ($\mu_i^{\mathrm{b,f}}$ depends on site i but the tunneling rate J and interactions U and V do not). Diagonal inhomogeneities may account for (i) overall trapping potential (usually harmonic), which is usually underlying in experiments on ultracold atoms, and (ii) disorder that may be introduced in different ways in ultracold samples (see Sec. VI for details).

B. Composites in disordered lattices: Effective Hamiltonian

In this section we include on-site energy inhomogeneities in the optical lattice and we derive a generalized effective Hamiltonian for the composite fermions. Strictly speaking, in the presence of disorder the hopping terms should depend on the site under consideration. Nevertheless, for weak enough disorder one can assume site independent tunneling for both bosons or fermions [21]. In the following we will restrict ourselves to the case where the hopping rates of bosons and fermions are equal and site-independent, $J_b=J_f=J$ and to the strong coupling regime, $V,U\gg J$, where the tunneling can be considered as a perturbation, as in Sec. III A.

For homogeneous lattices (see Sec. III A), following the lines of Refs. [51,52], we have used the method of degenerate second order perturbation theory to derive the effective Hamiltonian (4) by projecting the wave function onto the multiply degenerated ground state of the system in the absence of tunneling.

In the inhomogeneous case, this approach cannot be applied since even for $J=0$ there exists a well-defined single ground state determined by the values of the local chemical potentials. Nevertheless, in general, there will be a manifold of many states with similar energies. The differences of energy inside a manifold are of the order of the difference of chemical potential in different sites, whose random distribution is bounded, i.e., $0\leqslant\tilde{\mu}_i^{\mathrm{b}}$, $\tilde{\mu}_i^{\mathrm{f}}\leqslant 1$. Moreover, the lower energy manifold is separated from the exited states by a gap given by the boson-boson interaction, V. Therefore one can apply a form of quasidegenerate perturbation theory by projecting onto the manifold of near-ground states [114].

As it is described in Ref. [114] and briefly summarized in Appendix A, we construct an effective Hamiltonian that describes the slow, low-energy perturbation induced within the manifold of unperturbed ground states by means of a unitary transformation applied to the total Hamiltonian (1). By denoting with P the projector on the manifold and $Q=1-P$ its complement, the expression of the effective Hamiltonian can be written as

$$\langle out|H_{\mathrm{eff}}|in\rangle=\langle out|H_0|in\rangle+\langle out|PH_{int}P|in\rangle-\frac{1}{2}\langle out|PH_{int}Q\times\left(\frac{1}{H_0-E_{\mathrm{in}}}+\frac{1}{H_0-E_{\mathrm{out}}}\right)QH_{int}P|in\rangle. \tag{6}$$

As second order theory can only connect states that differ on one set of two adjacent sites, the effective Hamiltonian H_{eff} can only contain nearest-neighbor hopping and interactions as well as on-site energies $\bar{\mu}_i$ [37]:

$$H_{\mathrm{eff}}=\sum_{\langle i,j\rangle}\left[-d_{ij}F_i^\dagger F_j+\mathrm{H.c.}\right]+\sum_{\langle i,j\rangle}K_{ij}M_iM_j+\sum_i\bar{\mu}_iM_i, \tag{7}$$

where M_i, F_i are defined as in Eq. (4). The explicit calculation of the coefficients d_{ij}, K_{ij}, and $\bar{\mu}_i$ depends on the concrete type of composites. In the three following sections we address the cases of fermion-bosonic hole composites ($\bar{II}$), bare fermion composites (I), and fermion-boson composites (II).

C. Fermion-Bosonic hole composites

In this section, we assume that all sites are B-sites, i.e., $\alpha-\tilde{\mu}_i^{\mathrm{b}}>0$, so that composite fermions $\bar{II}$ are created. This means that each site contains either one boson or one fermion plus a bosonic hole. Thus the manifold of low lying states comprises all possible configurations of N_{f} fermions on an N-site lattice, with no fermion occupied sites filled by bosons.

Within the manifold of ground states, a fermion jump from site i to site j can only occur if the boson that was initially in site j jumps back to site i into the hole the fermion leaves behind. Therefore the number operator for fermions and bosons are related with the number operator of composites, i.e., $M_i=m_i=1-n_i$. Note that the composite model is expressed in terms of the composite fermionic operators $F_i=b_i^\dagger f_i$ and thus $M_i=f_i^\dagger f_ib_ib_i^\dagger$. To determine the coefficients in Eq. (7), one looks at two adjacent sites with indices i and j and uses a vector notation $|1_{\mathrm{b}},1_{\mathrm{f}}\rangle$ which would correspond to one boson on site i and one fermion on site j. In the composite fermion picture this would be denoted as $|0,1\rangle^c$, i.e., one composite fermion on site j and no composite fermion on site i. With this notation tunneling rates and nearest-neighbor interactions are calculated from Eq. (6) as

$$\langle 1_{\mathrm{f}},1_{\mathrm{b}}|H_{\mathrm{eff}}|1_{\mathrm{b}},1_{\mathrm{f}}\rangle=-\frac{1}{2}\frac{J^2}{V}\left(\frac{1}{\alpha-\Delta_{ij}^{\mathrm{b}}}+\frac{1}{\alpha+\Delta_{ij}^{\mathrm{b}}}+\frac{1}{\alpha-\Delta_{ij}^{\mathrm{f}}}+\frac{1}{\alpha+\Delta_{ij}^{\mathrm{f}}}\right)\equiv{}^c\langle 1,0|F_i^\dagger F_j|0,1\rangle^c, \tag{8}$$

$$\langle 1_{\mathrm{b}},1_{\mathrm{b}}|H_{\mathrm{eff}}|1_{\mathrm{b}},1_{\mathrm{b}}\rangle=-\frac{1}{2}\frac{J^2}{V}\left(\frac{2}{1-\Delta_{ij}^{\mathrm{b}}}+\frac{2}{1+\Delta_{ij}^{\mathrm{b}}}+\frac{2}{1-\Delta_{ij}^{\mathrm{b}}}+\frac{2}{1+\Delta_{ij}^{\mathrm{b}}}\right)\equiv{}^c\langle 0,0|(1-M_i)(1-M_j)|0,0\rangle^c, \tag{9}$$

$$\langle 1_{\mathrm{f}},1_{\mathrm{b}}|H_{\mathrm{eff}}|1_{\mathrm{f}},1_{\mathrm{b}}\rangle=-\frac{1}{2}\frac{J^2}{V}\left(\frac{2}{\alpha-\Delta_{ij}^{\mathrm{b}}}+\frac{2}{\alpha+\Delta_{ij}^{\mathrm{f}}}\right)\equiv{}^c\langle 1,0|M_i(1-M_j)|1,0\rangle^c, \tag{10}$$

$$\langle 1_{\mathrm{b}},1_{\mathrm{f}}|H_{\mathrm{eff}}|1_{\mathrm{b}},1_{\mathrm{f}}\rangle=-\frac{1}{2}\frac{J^2}{V}\left(\frac{1}{\alpha+\Delta_{ij}^{\mathrm{b}}}+\frac{1}{\alpha-\Delta_{ij}^{\mathrm{f}}}\right)\equiv{}^c\langle 1,0|M_i(1-M_j)|1,0\rangle^c. \tag{11}$$

Summing these terms up yields the coefficients for Eq. (7):

$$d_{ij}=\frac{J^2}{V}\left(\frac{\alpha}{\alpha^2-(\Delta_{ij}^{\mathrm{b}})^2}+\frac{\alpha}{\alpha^2-(\Delta_{ij}^{\mathrm{f}})^2}\right), \tag{12}$$

$$K_{ij}=-\frac{J^2}{V}\left(\frac{4}{1-(\Delta_{ij}^{\mathrm{b}})^2}-\frac{2\alpha}{\alpha^2-(\Delta_{ij}^{\mathrm{f}})^2}-\frac{2\alpha}{\alpha^2-(\Delta_{ij}^{\mathrm{b}})^2}\right), \tag{13}$$

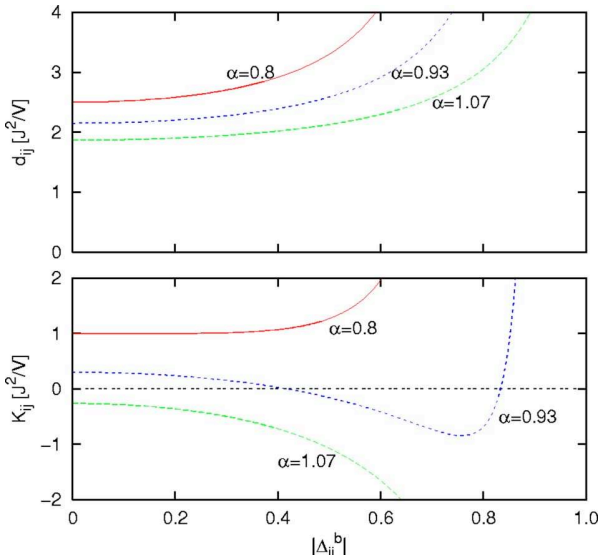

FIG. 2. (Color online) Tunneling, d_{ij}, and nearest-neighbor couplings, K_{ij}, of type $\overline{II}$ composites as a function of disorder Δ_{ij}^{b}, and for different boson-fermion interactions, α, in the case $\mu_i^f=0$.

$$\bar{\mu}_i = \mu_i^b - \mu_i^f + \frac{J^2}{V}\left[\sum_{\langle i,j\rangle}\frac{4}{1-(\Delta_{ij}^b)^2} - \frac{1}{\alpha-\Delta_{ij}^b} - \frac{1}{\alpha+\Delta_{ij}^f}\right], \tag{14}$$

with $\Delta_{ij}^{f,b}=\tilde{\mu}_i^{f,b}-\tilde{\mu}_j^{f,b}$. Here, $\langle i,j\rangle$ represents all neighbor sites of i. We shall now consider separately two limiting cases: (i) $\mu_i^f=0$ and $\mu_i^b=\mu_i V$, and (ii) $\mu_i^f=\mu_i^b=\mu_i V$.

1. Case where $\mu_i^f=0$

In the first case, we assume that the on-site energy for fermions vanishes. We assume also that all sites are B-sites, i.e., $\alpha-\tilde{\mu}_i^b>0$ everywhere. In this case, the hopping amplitudes d_{ij} are always positive, although may vary quite significantly with disorder, especially when $\Delta_{ij}^b\simeq\alpha$. As shown in Fig. 2, for $\alpha>1$, $K_{ij}\leqslant 0$ and we deal with attractive (although random) interactions. For $\alpha<1$, $K_{ij}\geqslant 0$ and the interactions between composites are repulsive. For $\alpha<1$, but close to 1, K_{ij} might take positive or negative values for Δ_{ij}^b small or $\Delta_{ij}^b\simeq\alpha$. In this case, the *qualitative character of interactions* may be *controlled by inhomogeneity* [37]. At low temperatures the physics of the system will depend on the relation between $\tilde{\mu}_i^b$'s and α.

(a) Small disorder limit. For small disorder, we may neglect the contributions of Δ_{ij}^b to $d_{ij}\simeq d$ and $K_{ij}\simeq K$, and keep only the leading disorder contribution in $\bar{\mu}_i$, i.e., the first term in Eq. (14). Note that the latter contribution is relevant in 1D and 2D leading to Anderson localization of single particles [66]. When $K/d\ll 1$ the system will then be in the Fermi glass phase, i.e., Anderson localized (and many-body corrected) single particle states will be occupied according to the Fermi-Dirac rules [76]. For repulsive interactions and $K/d\gg 1$, the ground state will be a Mott insulator and the composite fermions will be pinned for large filling factors. In particular, for filling factor $\rho_f=1/2$, one expects the ground state to be in the form of a checkerboard. For intermediate values of K/d, with $K>0$, delocalized metallic phases with enhanced persistent currents are possible [78]. Similarly, for attractive interactions $(K<0)$ and $|K|/d<1$ one expects competition between pairing of fermions and disorder, i.e., a "dirty" superfluid phase while for $|K|/d\gg 1$, the fermions will form a domain insulator. Figure 3 shows a schematic representation of expected disordered phases of the type $\overline{II}$ fermionic composites for small disorder, and vanishing fermionic on-site chemical potential.

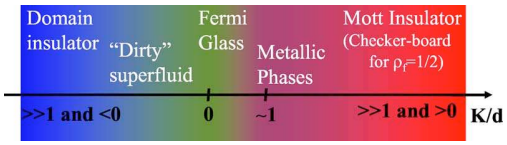

FIG. 3. (Color online) Schematic phase diagram of type $\overline{II}$ fermionic composites for low disorder $(\Delta_{ij}^b\ll 1,\alpha)$ and vanishing fermionic on-site energy $(\mu_i^f=0)$ as a function of the ratio between NN interactions and tunneling for the composites.

(b) Spin glass limit. Another interesting limit corresponds to the case $\Delta_{ij}^b\simeq\alpha\simeq 1$. Such a situation can be achieved by combining a superlattice potential with a spatial period twice as large as the one of the lattice (which alone induces $|\Delta_{ij}^b|=1$) and a random potential to induce site-to-site fluctuations. The tunneling becomes then nonresonant and can be neglected in Eq. (7), while the couplings K_{ij} fluctuate strongly as shown in Fig. 2. We end up then with the (fermionic) Ising spin glass model [37] described by the Edwards-Anderson model with $s_i=2M_i-1=\pm 1$. This case is studied in more detail in Sec. V.

2. Case where $\mu_i^f=\mu_i^b$

Let us now consider that the chemical potential is equal for bosons and fermions at each lattice site, $\mu_i^f=\mu_i^b=\mu_i V$. All sites are still assumed to be B-sites.

The effective interactions are for $\alpha>1$ always negative, and therefore the composites experience random attractive interactions (as in the previous case), while for $\alpha<1$, $K_{ij}>0$, and therefore we deal with random repulsive interactions. For $\alpha=1$, the interactions between composites vanish for all the values of the amplitude of the disorder.

In this case the sign of the interactions between composites is governed by the interactions between bosons and fermions *alone*. Note that this is not possible when one considers only disorder for the bosons. Figure 4 shows the tunneling and the nearest-neighbor couplings for different values of α. We expect here the appearance of similar phases, as in the previously discussed case.

D. Bare Fermion composites

In this section we now assume that all sites are A-sites and correspond to type I fermionic composites, i.e., $-1<\alpha-\tilde{\mu}_i^b<0$. This means that composite fermions reduce to bare fermions $(F_i=f_i)$ flowing on the top of a MI phase with $\tilde{n}=1$ boson per site. Each site now contains one boson plus eventually one fermion. From application of perturbation theory as described in Sec. III B [see Eq. (6)], one finds that the

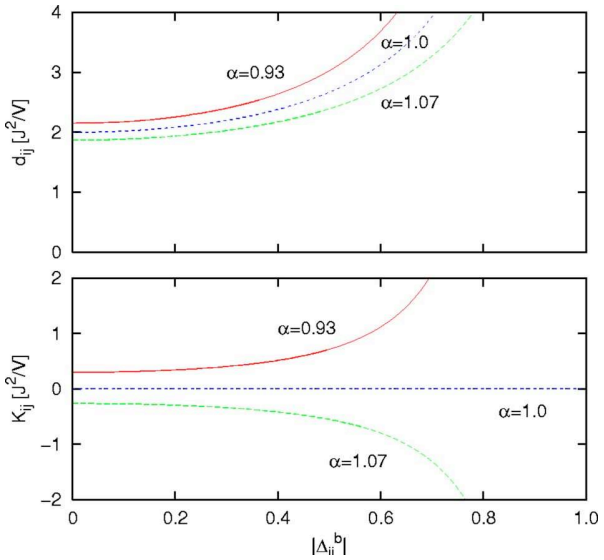

FIG. 4. (Color online) Tunneling, d_{ij}, and nearest-neighbor couplings, K_{ij}, of type $\overline{II}$ composites as a function of disorder Δ_{ij}^{b}, and for different boson-fermion interactions, α, in the case $\mu_i^{\mathrm{f}}=\mu_i^{\mathrm{b}}=\mu_i V$.

coefficients of the effective Hamiltonian (7) are

$$d_{ij}=J, \tag{15}$$

$$K_{ij}=-\frac{J^2}{V}\left(\frac{8}{1-(\Delta_{ij}^{\mathrm{b}})^2}-\frac{4(1+\alpha)}{(1+\alpha)^2-(\Delta_{ij}^{\mathrm{b}})^2}-\frac{4(1-\alpha)}{(1-\alpha)^2-(\Delta_{ij}^{\mathrm{b}})^2}\right), \tag{16}$$

$$\bar{\mu}_i=-\mu_i^{\mathrm{f}}+\frac{J^2}{V}\sum_{\langle i,j\rangle}\left[\frac{4}{1-(\Delta_{ij}^{\mathrm{b}})^2}-\frac{1}{\Delta_{ij}^{\mathrm{f}}}-\frac{4}{1-(\alpha-\Delta_{ij}^{\mathrm{b}})^2}\right]. \tag{17}$$

We observe that the inhomogeneities for fermions (site-dependent μ_i^{f}) neither perturb the effective tunneling, nor the effective interaction parameter, while $\bar{\mu}_i\simeq-\mu_i^{\mathrm{f}}$ up to corrections of the order of $O(J^2/V)$ for type *I* composite (bare) fermions. In this case, composite tunneling d_{ij} originates from the first order term, while the nearest-neighbor interaction originates from second order perturbation. It should be noted that in the case of type *I* composites, the hopping d_{ij} and interaction K_{ij} parameters in Eq. (7) do not depend on the sign of the fermion-boson interaction α.

The couplings K_{ij} are always positive, and for $\alpha\simeq 0$, $K_{ij}\simeq O(\alpha^2)$, and both the repulsive interactions and disorder are very weak, leading to an almost ideal Fermi liquid behavior at low temperature. For finite α, and $\Delta_{ij}^{\mathrm{b}}\simeq 1-|\alpha|$, however, the fluctuations of K_{ij} might be quite large as shown in Fig. 5. Note that for $|\alpha|\simeq 1$, this will occur even for small disorder. It is interesting to note that the dynamics of type *I* composites in our system resembles *quantum bond percolation*. As suggested from Fig. 5, one can assume in a somehow simplified view that the interaction parameter K_{ij} takes either very large, or zero values. The lattice decomposes into two sublattices (see Fig. 6): a "weak" bond sublattice (corresponding to $K_{ij}\ll d_{ij}$) in which fermions flow as in an almost ideal Fermi liquid, and a "strong" sublattice (corresponding to $K_{ij}\gg d_{ij}$), where only one fermion per bond is allowed ($M_iM_j=0$ for all nearest neighbors in the "strong" cluster). Therefore we see that the physics of bond percolation [10,97] will play a role. For $p>p_{\mathrm{c}}$, where p is the density of weak bonds and $p_{\mathrm{c}}\simeq 0.50$ (in two-dimensional square lattices) and $p_{\mathrm{c}}\simeq 0.25$ (in three-dimensional cubic lattices), the weak bond sublattice will be percolating, i.e., there exists a large cluster of weak bonds which spans the lattice from one side to the other. The question arises as to determine the quantum bond percolation threshold p_{Q}, i.e., for which minimal value of p, the eigenstates of the quantum gas will be delocalized over the extension of the system. Although it is clear that $p_{\mathrm{Q}}>p_{\mathrm{c}}$, it is still an open question to determine the exact value for the quantum percolation threshold p_{Q} [99,115–118]. Therefore experimental realization of our system may be of considerable interest for addressing this general question.

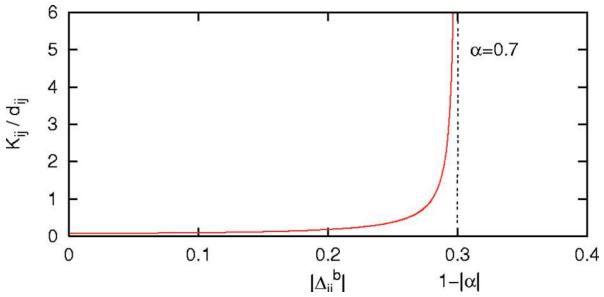

FIG. 5. (Color online) Ratio of nearest-neighbor coupling and tunneling K_{ij}/d_{ij} as a function of disorder Δ_{ij}^{b} for $\alpha=0.7$ and $J/V=0.01$ in the case of type *I* composite fermions.

E. Fermion-Boson composites

We finally consider in this section the case, when all sites are *C*-sites, so that type *II* composites corresponding to $-2<\alpha-\tilde{\mu}_i^{\mathrm{b}}<-1$ are formed. The composites are made of one fermion and one boson. This means that each lattice site

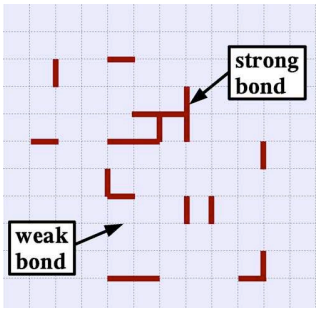

FIG. 6. (Color online) Schematic representation of connecting bonds in type *I* composite systems. The bonds are separated in two types: (i) the weak bonds in which two composites do not interact and (ii) the strong bonds where only one composite can stay. The short lines represent the bonds and the crossing points of the bonds are the lattice sites.

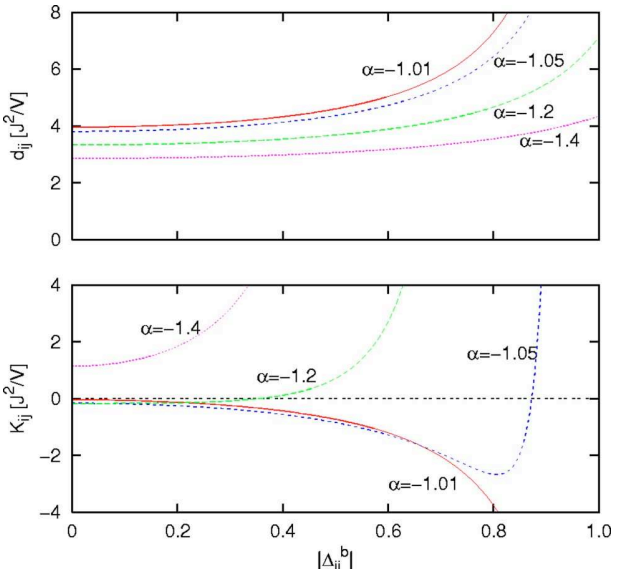

FIG. 7. (Color online) Tunneling, d_{ij}, and nearest-neighbor couplings, K_{ij}, of type *II* composites as a function of disorder Δ_{ij}^{b} and for different boson-fermion interactions, α, in the case $\mu_i^{\mathrm{f}}=0$.

is populated by either one boson or one fermion plus two bosons. Tunneling as well as nearest-neighbor interaction of composites arise from second order terms in perturbative theory [see Sec. III B and Eq. (6) for details]. Along the lines of Sec. III B, we find the following expressions:

$$d_{ij}=\frac{J^2}{V}\left(\frac{2|\alpha|}{|\alpha|^2-(\Delta_{ij}^{\mathrm{b}})^2}+\frac{2|\alpha|}{|\alpha|^2-(\Delta_{ij}^{\mathrm{f}})^2}\right), \tag{18}$$

$$K_{ij}=\frac{-J^2}{V}\left(\frac{16}{1-(\Delta_{ij}^{\mathrm{b}})^2}-\frac{2|\alpha|}{|\alpha|^2-(\Delta_{ij}^{\mathrm{f}})^2}-\frac{8|\alpha|}{|\alpha|^2-(\Delta_{ij}^{\mathrm{b}})^2}-\frac{6(2-|\alpha|)}{(2-|\alpha|)^2-(\Delta_{ij}^{\mathrm{b}})^2}\right), \tag{19}$$

$$\bar{\mu}_i=-\mu_i^{\mathrm{f}}-\mu_i^{\mathrm{b}}+\frac{J^2}{V}\sum_{\langle i,j\rangle}\left[\frac{4}{1-(\Delta_{ij}^{\mathrm{b}})^2}-\frac{4}{|\alpha|+\Delta_{ij}^{\mathrm{b}}}-\frac{3}{2-|\alpha|-\Delta_{ij}^{\mathrm{b}}}-\frac{1}{|\alpha|+\Delta_{ij}^{\mathrm{f}}}\right]. \tag{20}$$

Different scenarios also arise in this case. In the following, we shall consider the case $\mu_i^{\mathrm{f}}=0$ and $\mu_i^{\mathrm{b}}=\mu_i V$. The other extreme case, $\mu_i^{\mathrm{f}}=\mu_i^{\mathrm{b}}=\mu_i V$, leads to qualitatively similar conclusions.

Case where $\mu_i^{\mathrm{f}}=0$

We assume here that the on-site energy for fermions is $\mu_i^{\mathrm{f}}=0$. As for Fig. 2, we plot the effective tunneling and interaction parameter versus inhomogeneity parameter Δ_{ij}^{b} in Fig. 7. The general behavior of d_{ij} and K_{ij} is qualitatively the same as in the case of type $\overline{II}$ composites. For type *II* composites, and for small disorder, we find $K/d=1-4|\alpha|+3/(2-|\alpha|)$ with $1<|\alpha|<2$. The inhomogeneity is now given, for type *II* composites, by $\bar{\mu}_i=-\mu_i^{\mathrm{b}}$. The regimes, where $K\ll d$ corresponding to an almost ideal Fermi gas (in the absence of disorder), or to a Fermi glass (in the presence of disorder), can be reached in the region $\alpha\simeq-5/4$. The opposite regimes of strong effective interactions, where $K\gg d$ appears for $\alpha\gtrsim-2$ and corresponds to repulsive interactions $K>0$. In this region, the fermionic checkerboard phase if the filling factor is 1/2 (for vanishing disorder) and the repulsive Fermi glass phase (in the presence of disorder) are expected. Here, no strong attractive interactions regime occurs since K/d reaches a minimum of $\simeq-0.07$ for $\alpha=\sqrt{3}/2-2$. Therefore, in contrast to type $\overline{II}$ composites, for type *II* composites: (i) due to weakness of attractive interactions, the domain insulator phase does not appear, and even the "dirty" superfluid phase may be washed out; and (ii) arbitrary strong repulsive interactions can be used to generate a Mott insulator, which might be difficult for $\overline{II}$ composites, where K/d is limited to 2, suggesting that Fermi liquid, Fermi glass behavior will prevail.

As shown in Fig. 7, the spin glass limit can also be reached, for example, for $\alpha\simeq-1.05$ and $|\Delta_{ij}^{\mathrm{f}}|\simeq0.9$. In this regime, the tunneling is nonresonant due to strong disorder and the nearest-neighbor interaction fluctuates strongly from negative to positive values. See Sec. V for further study of the spin glass limit.

F. Optical lattices with different types of sites

Sites A and B

Obviously, the situation becomes much more complex when we deal with different types of sites in the lattice. Again there are infinitely many possibilities, and the simplest ones are, for instance: (i) coexistence of *A*- and *B*-sites, or (ii) *A*- and *C*-sites, or (iii) *A*-, *B*-, and *C*-sites, etc. In the following we shall consider only the case (i) with $\mu_i^{\mathrm{f}}=0$ and $\mu_i^{\mathrm{b}}=\mu_i V$, since the other cases lead to qualitatively similar effects.

Let us assume that the numbers of *A*- and *B*-sites are macroscopic, i.e., of the order of *N*. More precisely, we will consider that N_A (number of *A*-sites) and N_B (number of *B*-sites) of order $N/2$. In this case the physics of site percolation [10] will play a role. If $N_{\mathrm{f}}\leqslant N_B$ the composite fermions will move within a cluster of *B*-sites. When N_B will be above the classical percolation threshold, this cluster will be percolating. The expressions Eq. (12) and Eq. (13) will still be valid, except that they will connect only the *B*-sites. The physics of the system will be similar as in the case of type *I* composites), but it will occur now on the percolating cluster. For small disorder, and $K/d\ll1$, the system will be in a Fermi glass phase in which the interplay between the Anderson localization of single particles due to fluctuations of μ_i^{b} and quantum percolation effects, that is randomness of the *B*-sites cluster, will occur. For repulsive interactions and $K/d\gg1$, the ground state will be a Mott insulator on the cluster and the composite fermions will be pinned (in particular for half-filling of the cluster). It is an open question whether the delocalized metallic phases with enhanced persistent current of the kind discussed in Ref. [78] might exist in this case. Similarly, it is an open question whether for

attractive interactions ($K<0$) and $|K|/d<1$ pairing of (perhaps localized) fermions will take place. In the case of $|K|/d \gg 1$, we expect that the fermions will form a domain insulator on the cluster.

In the spin glass limit $\Delta_{ij}^{\mathrm{b}} \simeq \alpha \simeq 1$, we will deal with the Edward-Anderson spin glass on the cluster. Such systems are of interest in condensed matter physics (cf. [11]), and again questions connected to the nature of spin glass ordering may be studied in this case.

When $N_{\mathrm{f}} > N_B$, all B-sites will be filled, and the physics will occur on the cluster of A-sites. For $\alpha \simeq 0$, we will deal with a gas with very weak repulsive interactions, and no significant disorder on the random cluster; this is an ideal test to study quantum percolation at low T. For finite α, and $\Delta_{ij}^{\mathrm{b}} \simeq 1-\alpha$, the interplay between the fluctuating repulsive K_{ij}'s and quantum percolation might be studied.

IV. NUMERICAL ANALYSIS USING GUTZWILLER ANSATZ

A. Numerical method

In this section, we present numerical results that give evidences of (i) formation of composite particles in Fermi-Bose mixtures in optical lattices and (ii) existence of different quantum phases for various sets of composite tunneling and interaction parameters and inhomogeneities. We mainly focus on type *II* composites. Mean-field theory provides appropriate although not exact properties of Hubbard models [8]. In the following, we consider a variational mean field approach provided by the Gutzwiller ansatz (GA) [26,119]. In particular, the GA ansatz has been successfully employed for bosonic systems to study the superfluid to Mott insulator transition [19,26] in nondisordered lattices, and the Anderson and Bose glass transitions in the presence of disorder [21,26].

Briefly, the Gutzwiller approach neglects site-to-site quantum coherences so that the many-body ground state is written as a product of N states, each one being localized in a different lattice site. Each localized state is a superposition of different Fock states $|n,m\rangle_i$ with exactly n bosons and m fermions on the ith lattice site:

$$|\psi_{\mathrm{MF}}\rangle = \prod_{i=1}^{N} \left(\sum_{n=0}^{n_{\max}} \sum_{m=0,1} g_{n,m}^{(i)} |n,m\rangle_i \right), \tag{21}$$

where $n_{\max}$ is an arbitrary maximum occupation number of bosons in each lattice site [120].

The $g_{n,m}^{(i)}$ are complex coefficients proportional to the amplitude of finding n bosons and m fermions in the ith lattice site, and consequently we can impose, without loss of generality, these coefficients to satisfy $\Sigma_n \Sigma_m |g_{n,m}^{(i)}|^2 = 1$. For the sake of simplicity, we neglect the anticommutation relation of fermionic creation (f_i) and annihilation ($f_j^{\dagger}$) operators in different lattice sites. However, Pauli principle applies in each lattice site ($m_i \leqslant 1 \, \forall \, i$). Since GA neglects correlations between different sites, this procedure is expected to be safe and is commonly used within the Gutzwiller approach [53].

Inserting $|\psi_{\mathrm{MF}}\rangle$ in the Schrödinger equation with the two-species Fermi-Bose Hamiltonian (1), we were able to determine the ground state and to compute the dynamical evolution of the Fermi-Bose mixture.

1. Ground state calculations

Employing a standard conjugate-gradient downhill method [121], we minimize the total energy $\langle \psi_{MF}|H_{\mathrm{FBH}}|\psi_{MF}\rangle$ with H_{FBH} given by Eq. (1) under the constraint of fixed total numbers of fermions N_{f} and bosons N_{b} [122]:

$$\langle \psi_{\mathrm{MF}}|H_{\mathrm{FBH}}|\psi_{\mathrm{MF}}\rangle - \Lambda_{\mathrm{f}} \left(\langle \psi_{\mathrm{MF}}| \sum_i m_i |\psi_{\mathrm{MF}}\rangle - N_{\mathrm{f}} \right)^2 - \Lambda_{\mathrm{b}} \left(\langle \psi_{\mathrm{MF}}| \sum_i n_i |\psi_{\mathrm{MF}}\rangle - N_{\mathrm{b}} \right)^2 \to \min. \tag{22}$$

The numerical procedure is as follows: (i) We minimize the energy of the mixture (eventually) in the presence of smooth trapping potentials and with nonzero tunneling for bosons and fermions, but assuming vanishing interactions between bosons and fermions ($U=0$). During the minimization the normalization ($\Sigma_n \Sigma_m |g_{n,m}|^2 = 1$) should be imposed. (ii) After this initial minimization, we ramp up adiabatically the interactions between bosons and fermions using the dynamical Gutzwiller approach (see below). In this way, we end up with the ground state of the mixture in the presence of tunneling J, nonvanishing interactions U and V, and eventually in the presence of a smooth trapping potential.

This two-step procedure is indeed necessary because in the presence of interactions between bosons and fermions finite numbers of bosons and fermions correspond to a saddle point of Eq. (22), and no true minimum can be found within direct minimization of the total Hamiltonian [54].

2. Time-dependent calculations

Using the time-dependent variational principle ($\langle \psi_{\mathrm{MF}}|i\hbar\partial_t - H_{\mathrm{FBH}}(t)|\psi_{\mathrm{MF}}\rangle \to \min$) with Hamiltonian H_{FBH} given by Eq. (1) and eventually time-dependent parameters $J_{\mathrm{f,b}}$, U, V, $\mu_i^{\mathrm{f,b}}$, we end up with the following dynamical equation for the Gutzwiller coefficients [54,123]:

$$\begin{aligned} i\hbar \partial_t g_{n,m}^{(i)} = & \left[\frac{V}{2} n(n-1) + Unm - \mu_i^{\mathrm{b}} n - \mu_i^{\mathrm{f}} m \right] g_{n,m}^{(i)} \\ & - (\Sigma_i^{\mathrm{b}}) \sqrt{n} g_{n-1,m}^{(i)} - (\Sigma_i^{\mathrm{b}})^* \sqrt{n+1} g_{n+1,m}^{(i)} - (\Sigma_i^{\mathrm{f}}) g_{n,m-1}^{(i)} \\ & - (\Sigma_i^{\mathrm{f}})^* g_{n,m+1}^{(i)}, \end{aligned} \tag{23}$$

where

$$\Sigma_i^{\mathrm{b}} = \sum_{\langle i,j \rangle} J_{\mathrm{b}} \left[\sum_n \sum_{m=0,1} \sqrt{n+1} g_{n,m}^{(j)*} g_{n+1,m}^{(j)} \right], \tag{24}$$

$$\Sigma_i^{\mathrm{f}} = \sum_{\langle i,j \rangle} J_{\mathrm{f}} \left[\sum_n g_{n,0}^{(j)*} g_{n,1}^{(j)} \right]. \tag{25}$$

Note that these equations are valid under the hypothesis of neglecting anticommutation relations for fermionic operators in different sites. Equations (23)–(25) preserve both normalization of the wave function and the mean particle numbers.

In the following, the dynamical Gutzwiller approach will be used for (i) computing the ground state of the mixture in

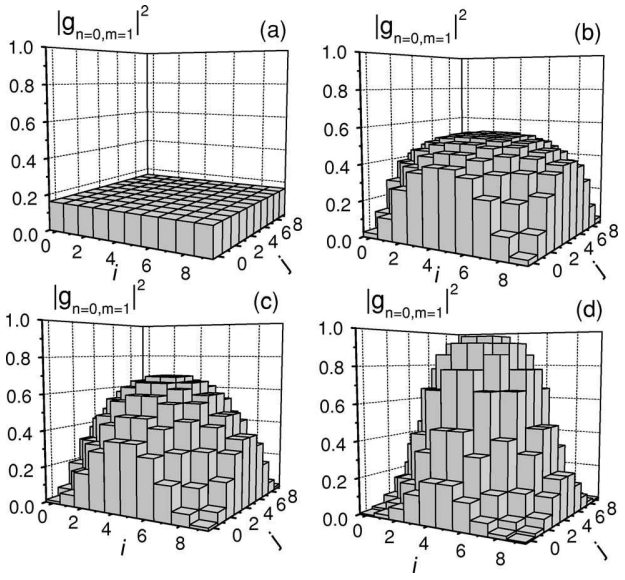

FIG. 8. Probability of having one fermion and zero boson at each lattice site for the $N=100$ sites in a Fermi-Bose mixture with $N_b=60$, $N_f=40$, $J_b/V=J_f/V=0.02$ and in the presence of harmonic traps for bosons and fermions characterized by $\omega_b=10^{-7}$ and $\omega_f=5\times10^{-7}$, respectively. The interaction between fermions and bosons is (a) $\alpha=0$ (independent bosonic MI and Fermi gas), (b) $\alpha=0.5$ (Fermi liquid), (c) $\alpha=1$ (ideal Fermi gas), and (d) $\alpha=10$ (fermionic insulator domain).

the presence of interactions between bosons and fermions (see above) and (ii) to ramp up adiabatically disorder in the optical lattice potential.

B. Numerical results

We have considered a 2D optical lattice with $N=10\times10$ sites to perform the simulations of the different quantum phases that appear for type $\bar{II}$ composites in the presence of a very shallow harmonic trapping potential $[\tilde{\mu}_i^{b,f}=\omega^{b,f}\times l(i)^2$, where $l(i)$ is the distance from site i to the central site in cell size units], with different amplitudes for bosons and fermions. The harmonic on-site energy simulates shallow magnetic or optical trapping. The confining potential is experimentally of vital importance in order to see Mott insulator phases that require commensurate filling [20,124,125]. It plays the role of a local chemical potential, and it has been predicted that it modifies some properties of strongly correlated phases [126]. Additionally, this breaks the equivalence of all lattice sites and makes it more obvious the different phases that one can achieve (see below). We first calculate the ground state of the system considering $N_b=60$ bosons, $N_f=40$ fermions, $J_b/V=J_f/V=0.02$, $U=0$ in the presence of harmonic traps characterized by $\omega^b=10^{-7}$ and $\omega^f=5\times10^{-7}$.

Under these conditions, we find that, as expected, the bosons are well inside the MI phase with $\tilde{n}=1$ boson per site [19,26]. Due to the very small values of ω^f and ω^b neither the bosons nor the fermions feel significantly the confining trap as shown in Fig. 8(a).

1. Nondisordered phases

Starting with this ground state we adiabatically grow the repulsive interactions between bosons and fermions, U, keeping the repulsion between bosons, V, constant, i.e., growing effectively α in order to create the composites. Once the composites appear, the only nonzero probabilities are (i) $|g^{(i)}_{n=1,m=0}|^2$ to have one boson and zero fermion (i.e., no composite), or (ii) $|g^{(i)}_{n=0,m=1}|^2$ to have zero boson and one fermion (i.e., one composite). This proves the formation of type $\bar{II}$ composites [128]. In Fig. 8(b), we show the probability of having one composite $|g^{(i)}_{n=0,m=1}|^2$ (i.e., one fermion and zero boson) at each lattice site for $\alpha=0.5$, which corresponds to repulsive interactions between composites $K_{eff}=d_{eff}=1.6\times10^{-3}$. Due to the important value of the composite tunneling d_{eff}, the ground state is delocalized and corresponds to a (nonideal) *Fermi liquid*.

Increasing further the fermion-boson interaction parameter, α, the system reaches the point where the interactions between composites are negligible corresponding to the region of an ideal *Fermi gas* phase ($\alpha\simeq1$). Figure 8(c) displays the probability of having a composite in each lattice site in the case where the interactions between composites exactly vanish, i.e., $\alpha=1$. Increasing again the interaction parameter α, one reaches for $\alpha>1$ the region where the interactions between composites are attractive ($K_{eff}<0$). In this region, composite *fermionic insulator domains* are predicted. Due to the attractive interactions, the probability of having composite fermions in the center of the trap increases reaching nearly one for high enough effective attractive interactions as shown in Fig. 8(d).

It is also worth noticing that the energies involving the composites are at least three orders of magnitude smaller than the corresponding energies for bosons and fermions ($d_{eff}, K_{eff} \ll J, U, V$). As a consequence, the effect of inhomogeneities is much larger for composites than it is for bare bosons and fermions. This is exemplified in Fig. 8. For no interaction between bosons and fermions ($\alpha=0$), the bare particles are not significantly affected by the harmonic trap on the 10×10 lattice [see Fig. 8(a)]. On the contrary, as soon as composites $\bar{II}$ are created, the harmonic trapping clearly reflects in inhomogeneous population of the lattice sites [see Figs. 8(b)–8(d)]. Another important consequence is that large time scales are necessary in time evolution processes in order to fulfill the adiabaticity condition.

2. Disordered phases

We now consider disordered optical lattices for the bosons. The on-site energy μ_i^b is assumed to be random with time-dependent standard deviation $\sqrt{\langle(\tilde{\mu}_i^b)^2\rangle-(\langle\tilde{\mu}_i^b\rangle)^2}=\Delta(t)$ and independent from site to site. For this, we create type $\bar{II}$ composites in different regimes (this is controlled by the value of α as shown before) and we slowly ramp up the disorder from 0 to its final value Δ.

Let us first consider a *Fermi gas* in the absence of disorder [see Fig. 9(b)]. Because of effective tunneling, d_{ij}, the composite fermions are delocalized although confined near the center of the effective harmonic potential $[(\omega_f-\omega_b)\times l(i)^2]$. In particular, the population of each lattice site fluctuates around $\langle m_i\rangle\simeq0.4$ with $\sqrt{\langle(m_i-\langle m_i\rangle)^2\rangle}\simeq0.43$. While slowly increasing the amplitude of disorder, the composite

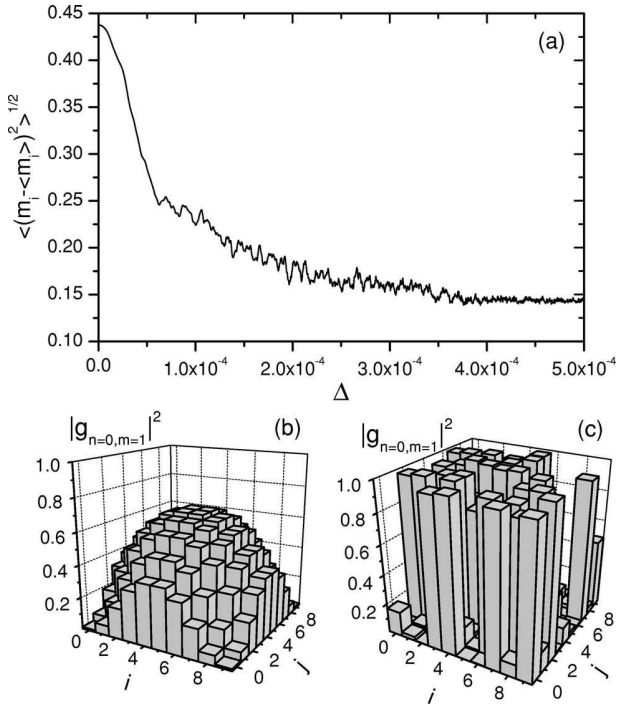

FIG. 9. Dynamical crossover from the Fermi gas to the Fermi glass phases. The parameters are the same as in Fig. 8(c). (a) Variance of the number of fermions per lattice site as a function of the amplitude of the disorder Δ. (b) Probability of having one composite (one fermion and zero boson) at each lattice site for the N sites in the absence of disorder and (c) after ramping up adiabatically diagonal disorder with amplitude $\Delta=5\times10^{-4}$.

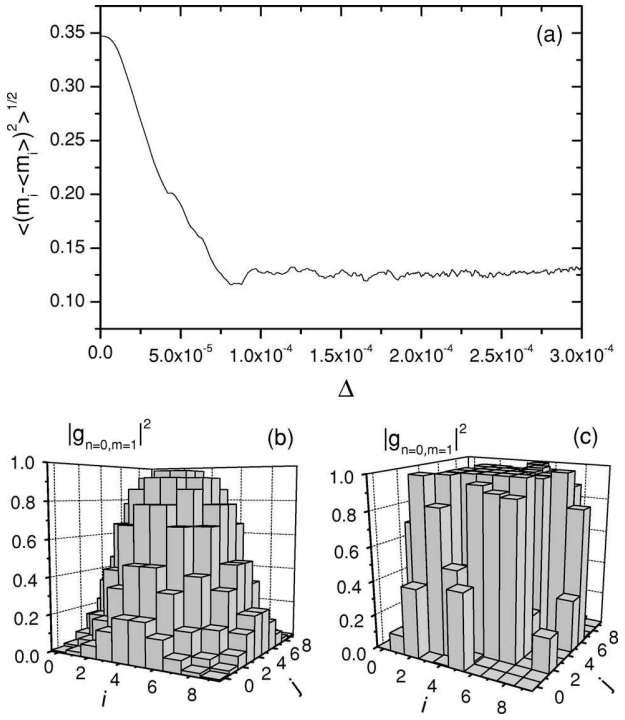

FIG. 10. Dynamical crossover from the fermionic domain insulator to a disordered insulating phase. The parameters correspond to Fig. 8(d). (a) Variance of the number of fermions per lattice site as a function of the amplitude of the disorder. (b) Probability of having one composite (one fermion and zero boson) in each lattice site in the absence of disorder and (c) after ramping up adiabatically the disorder with amplitude $\Delta=3\times10^{-4}$.

fermions become more and more localized in the lattice sites to form a *Fermi glass*. Indeed, Fig. 9(a) shows that the fluctuations in composite number are significantly reduced as the amplitude of the disorder increases. For $\Delta=5\times10^{-4}$, the composite fermions are pinned in random sites as shown in Fig. 9(c). As expected, the N_{f} composite fermions populate the N_{f} sites with minimal $\tilde{\mu}_i^{\mathrm{b}}$.

It should be noted that in the absence of interactions between bosons and fermions (i.e., when the composites are not formed), no effect of disorder is observed. This again shows the formation of composites with typical energies significantly smaller than those of bare particles.

We now consider the *Fermi insulator domain* phase [see Fig. 10(b)] with slowly increasing disorder. In the *Fermi insulator domain* (in the absence of disorder), the composite fermions are pinned in the central part of the confining potential. In addition, there is a ring of delocalized fermions and this gives finite fluctuations on the atom number per site $[\sqrt{\langle(m_i-\langle m_i\rangle)^2\rangle}\simeq0.35]$. As shown in Fig. 10(a), while ramping up the amplitude of disorder, the fluctuations decrease fast and reach $\sqrt{\langle(m_i-\langle m_i\rangle)^2\rangle}\simeq0.13$ for $\Delta>10^{-4}$. This indicates that the composite fermions are pinned in different lattice sites. This is confirmed in Fig. 10(c) where we plot the population of the composites fermions in each lattice site for $\Delta=5\times10^{-4}$. Contrary to what happens for the transition from *Fermi gas* to *Fermi glass*, the composites mostly populate the central part of the confining potential. The reason for that is twofold. First, with our parameters, the attractive interaction between composites is of the order of $K\simeq-1.4\times10^{-3}$ and can compete with disorder $\Delta=3\times10^{-4}$. This explains the central insulator domain. Second, because tunneling is small ($d\simeq8\times10^{-5}$) and because disorder breaks the symmetry of lattice sites in the ring around the domain, the atoms in this region get pinned. The populated sites match the lowest $\tilde{\mu}_i^{\mathrm{b}}$.

V. SPIN GLASSES

In this section we discuss in more detail the possible realization of the Edwards-Anderson spin glass Fermi-Bose mixtures as discussed in Sec. III C. Strictly speaking, since the system is quantum it allows for realization of fermionic spin glass [129]. The main goal of such an investigation is to study the nature of the spin glass ordering and to compare the predictions of the Mézard-Parisi and "droplet" pictures.

Although we work along the lines of the original papers [6], it is necessary to reformulate the standard Mézard-Parisi mean field description of our system. The main difference appears because the Ising spins are coded as presence or absence of a composite at a given site. This leads to a fixed magnetization due to the fixed number of particles in the system. For this we repeat very shortly the Sherrington-Kirkpatrick calculations [108] here, adapted to our case.

A. Edwards-Anderson model for composite fermions

The spin glass limit obtained in Sec. III C with large disorder derives of the composite fermionic model (7) with vanishing hopping due to strong site-to-site energy fluctuations and NN interactions, K_{ij}. By appropriate choice of Δ_{ij}^{b}, K_{ij} fluctuate around mean zero with random positive and negative values [see Fig. 2(b)]. Replacing the composite number operators with a classical Ising spin variable $s_i := 2M_i - 1 = \pm 1$, one ends up with the Hamiltonian:

$$H_{\mathrm{E-A}} = \frac{1}{4}\sum_{\langle ij\rangle} K_{ij} s_i s_j + \frac{1}{2}\sum_i \bar{\mu}_i s_i. \tag{26}$$

It describes an (fermionic) Ising spin glass [129], which differs from the Edwards-Anderson model [6,130] in that it has an additional random magnetic field $\bar{\mu}_i$ and, moreover, has to satisfy the constraint of fixed magnetization value, $m = 2N_{\mathrm{f}}/N - 1$, as the number of fermions in the underlying FBH model is conserved. It, however, shares the basic characteristics with the Edwards-Anderson model as being a spin Hamiltonian with random spin exchange terms K_{ij}. In particular, this provides bond frustration, which in this model is essential for the appearance of a spin glassy phase. The experimental study of this limit thus could present a way to address various open questions of spin glass physics concerning the nature and the ordering of its ground and possibly metastable states (the Mézard-Parisi picture [6] versus the "droplet" picture [7,107]), broken symmetry, and dynamics in classical (in the absence of hopping) and quantum (with small, but nevertheless present hopping) spin glasses [8,131].

For sufficiently large systems, Eq. (26) is well approximated by assuming K_{ij} and $\bar{\mu}_i$ to be independent random variables with Gaussian distribution, with mean 0 and H, respectively, and variances $K/\sqrt{N}$ and h, respectively [132]. This approximation will be used in the following calculations.

Before employing the mean field approach for Edwards-Anderson-like models in Sec. V E for the Hamiltonian (26), a very basic outline of the different phases of the short-range Ising models with bond frustration is given and the two competing physical pictures for the spin glass phase are briefly summarized in this section.

The experimental observations have led to the identification of three equilibrium phases, which are characterized by two order parameters (for zero external magnetic field): $M := \overline{\langle s_i \rangle_T}$ is the magnetization, i.e., the order parameter for magnetic ordering, and $Q_{EA} := \overline{\langle s_i \rangle_T^2}$ is the Edwards-Anderson order parameter for spin glass ordering. Here, $\langle\cdot\rangle_T$ denotes the Gibbs ensemble average and $\bar{\cdot}$ the disorder average. The three phases are (i) an unordered paramagnetic phase, with $M=0$ and $Q_{EA}=0$; (ii) an ordered spin glass phase with $M=0$ and $Q_{EA}\neq 0$ that is separated from the paramagnetic phase by a second order phase transition [133]; and (iii) dependent on the mean value of K_{ij}, an ordered ferromagnetic phase with $M\neq 0$ and $Q_{EA}=0$. It should be pointed out that there are additional questions—different from, but of course connected to the ones discussed in the following—about the nature of the equilibrium spin glass state that stem from the intrinsic problems that are associated in this system with separating equilibrium from nonequilibrium effects such as metastability, hysteresis, and others (see [134] and references therein).

B. Mézard-Parisi picture

The *Mézard-Parisi* (MP) picture is fundamentally guided by the results of the mean-field theory. On the level of statistical physics, the Gibbs equilibrium distribution of the spin system in the MP picture at temperature T and for a particular disorder configuration K can be written as a unique convex combination of infinitely many pure equilibrium state distributions [7,135],

$$\rho_{T,K} = \sum_\alpha w_{T,K}^\alpha \rho_{T,K}^\alpha, \quad \text{with} \sum_\alpha w_{T,K}^\alpha = 1, \tag{27}$$

where the overlap between two pure states is defined as

$$Q_{\alpha\beta} \equiv \Omega^{-1}\sum_i \langle s_i\rangle_{T,K}^\alpha \langle s_i\rangle_{T,K}^\beta, \tag{28}$$

where Ω denotes the size of the system. The mean-field version of $Q_{\alpha\beta}$ emerges naturally from the calculation in the next section and motivates definition (28).

In the MP picture, the spin glass transition is interpreted akin to the transition from an Ising paramagnet to a ferromagnet. There, the Gibbs distribution is written as a sum of only two pure states, corresponding to the two possible fully spin-polarized ferromagnetic ground states. As the temperature of the system decreases, the Z_2 symmetry of the system is broken, and a phase transition to a ferromagnetic phase occurs, whose equilibrium properties are not described by the Gibbs state, but by the relevant pure state distribution alone [6]. Analogously, the spin glass transition is characterized by the breaking of the infinite index symmetry, called replica symmetry breaking in the mean-field case, by which one pure state distribution $\rho_{T,K}^\alpha$ is chosen and alone describes the low-temperature properties of the system [6]. However, unlike the Ising ferromagnet, the pure states of the spin glass are not related to each other by a symmetry of the Hamiltonian, but rather by an accidental, infinite degeneracy of the ground state caused by the randomness of the bonds and the frustration effects. This picture can be interpreted as the system getting frozen into one particular state out of infinitely many different ground or metastable states of the system. These states are all taken to be separated by free energy barriers, whose height either diverges with the system size or it is finite but still so large that the decay into a "true" ground state does not occur on observable time scales. Thus fluctuations around one of these ground states can only sample excited states within one particular free energy valley. Consequently, Q_{EA} in the spin glass phase must be redefined as $Q_{EA} := Q_{\alpha\alpha}$, the self-overlap of the state, whereas it remains unchanged for the paramagnetic phase.

C. de Almeida-Thouless plane

Based on the results of mean-field theory, one of the predictions of the MP picture concerns the order of the infinitely

many spin glass ground states, which is ultrametric [6,136], as can be seen from the joint probability distribution of three different ground state overlaps, $P_K(Q_{12},Q_{13},Q_{23})$. Upon choosing independently three pure states 1, 2, and 3 from the decomposition (27), one should find that with probability 1/4, $Q_{12}=Q_{13}=Q_{23}$ and with probability 3/4 two of the overlaps are equal and smaller than the third. Ultrametricity then follows from the canonical distance function $D_{\alpha\beta}=Q_{EA}-Q_{\alpha\beta}$. The mean-field theory, both with and without a magnetic field, predicts the existence of a plane in the space of the Hamiltonian parameters, called the de Almeida-Thouless (dAT) plane [137], below which the naive ansatz for the spin glass phase becomes invalid and the system is characterized by the transition to this ultrametrically ordered infinite manifold of ground states. It should be pointed out that the clear occurrence of such a dAT plane in the finite range Edwards-Anderson model would be an important indicator for the validity of the MP picture in these systems. As we discuss in Sec. V D, this conclusion has to be drawn with great care.

D. "Droplet" model

The very applicability of the MP model for finite-range systems is, however, still unproven. It is both challenged by a rival theory, the so-called *droplet* model [107], as well as by mathematical analysis (cf. [7] and references therein) that questions the validity of transferring a picture developed for the infinite-range mean-field case to the short-range model. Being a phenomenological theory based on scaling arguments and numerical results, the droplet model describes the ordered spin glass phase below the transition as one of just two possible pure states, connected by spin-flip symmetry, analogous to the ferromagnet mentioned above. Consequently there can be no infinite hierarchy of any kind, and thereby no ultrametricity. Excitations over the ground state are regions with a fractal boundary—the droplets—in which the spins are in the configuration of the opposite ground-state. The free energy of droplets of diameter L is taken to scale as $\sim L^{\theta}$, with $\theta<0$ at and below the critical dimension, which is generally taken to be two. So three is the only physical dimension where the spin glass transition is stable with nonzero transition temperature, with $\theta\sim 0.2$ in this case. The free energy barriers for the creation and annihilation of a droplet scales in 3D as $\sim L^{\psi}$, with $\theta\leqslant\psi\leqslant 2$.

Although there can be no dAT plane in the strict sense in the droplet-model, for an external magnetic field the system can be kept from equilibration on experimental time scales for parameters below a line that scales just like the dAT line. This phenomenon might mimic the effects of the replica symmetry breaking in the MP picture (see [107] for further details).

E. Replica-symmetric solution for fixed magnetization

This section serves to show that the mean-field version of the effective Hamiltonian (26) with random magnetic field and magnetization constraint exhibits replica symmetry breaking just as for the pure Edwards-Anderson model, and would therefore be a candidate to examine the validity of the MP or droplet picture in a realistic short-ranged spin glass model. Following Sherrington and Kirkpatrick (SK) [6], the mean-field model is given by

$$H_{\mathrm{SK}}=\frac{1}{4}\sum_{(i,j)}K_{ij}s_is_j+\frac{1}{2}\sum_i\bar{\mu}_is_i, \tag{29}$$

where the round brackets $(\cdot,\cdot)$ are generally used to denote sums over all pairs of different indices. This model differs from Eq. (26) by the long-range spin exchange. As the mean of $\bar{\mu}_i$, H is generally nonzero this model will not exhibit a phase transition, which, however, is not a concern, as the number of (quasi-)ground states will be the quantity of interest. Following the analysis of SK, we aim at finding the free energy, ground state overlap and magnetization constraint. Then we will use the de Almeida and Thouless approach [6] to show that the obtained solution is unstable in a certain parameter region, that lies below the so-called dAT-plane of stability. The type of instability that emerges is then well-known to require the replica symmetry breaking solution of Parisi [6].

As the disorder is quenched (static on experimental time scales), one cannot average directly over disorder in the partition function as would be done for annealed disorder, but one must rather average the free energy density, $\bar{f}=-\beta\overline{\ln Z}$ using the "replica trick:" We form n identical copies of the system (the replicas) and the average is calculated for an integer n and a finite number of spins N. Then, using the general formula $\ln x=\lim_{n\to 0}(x^n-1)/n$, $\ln Z$ is obtained from the analytic continuation of $\overline{Z^n}$ for $n\to 0$. Finally, we take the thermodynamic limit $N\to\infty$. Explicitly, $\overline{Z^n}$ is given by

$$\overline{Z^n}=\sum_{\{s_i^{\alpha}=\pm 1\}}\exp[-\beta\overline{H_{\mathrm{SK}}[s_i^{\alpha},n]}], \tag{30}$$

where $\overline{H_{\mathrm{SK}}[s_i^{\alpha},n]}$ is the sum of n independent and indentical spin Hamiltonians (29), averaged over the Gaussian disorder, with Greek indices now numbering the n replicas.

Executing the average over the Gaussian distributions for K_{ij} and $\bar{\mu}_i$ leads to coupling between spin-spin interactions of different replicas. As the mean-field approach means that the double sum over the site indices in Eq. (29) can be simplified into a square using $(s_i^{\alpha})^2=1$, one finds:

$$\begin{aligned}\overline{f_N^n}=-(Nn\beta)^{-1}\Bigg\{&e^{Nn(\beta K)^2/4}e^{-n^2(\beta K)^2/2+n(\beta h)^2/2}\\&\times\sum_{\{s_i^{\alpha}=\pm 1\}}\exp\Bigg[\frac{N(\beta K)^2}{2}\sum_{\alpha<\beta}\Bigg(\sum_i\frac{s_i^{\alpha}s_i^{\beta}}{N}\Bigg)^2\\&+(\beta h)^2\sum_{\alpha<\beta}\sum_i s_i^{\alpha}s_i^{\beta}-\beta H\sum_{\alpha}\sum_i s_i^{\alpha}\Bigg]-1\Bigg\},\end{aligned} \tag{31}$$

where the prefactor $e^{-n^2(\beta K)^2/2+n(\beta h)^2 n/2}$ becomes irrelevant in the limit $n\to 0$ and is subsequently dropped. As in the standard procedure, the square of the operator sum $\Sigma_i s_i^{\alpha}s_i^{\beta}$ is decoupled by introducing auxiliary operators $q_{\alpha\beta}$ via a Hubbard-Stratonovitch (HS) transformation [6].

$$\overline{f_N^n} = -(Nn\beta)^{-1}\left\{ e^{Nn(\beta K)^2/4}\int_{-\infty}^{\infty}\left[\prod_{\alpha<\beta} dq_{\alpha\beta}\left(\frac{N}{2\pi}\right)^{1/2}\beta K\right] \times \exp\left[-\frac{N(\beta K)^2}{2}\sum_{\alpha<\beta} q_{\alpha\beta}^2 + N \times \ln\left(\sum_{\{s^\alpha=\pm1\}} \exp[L(q_{\alpha\beta})]\right)\right] - 1\right\}, \quad (32)$$

where the functional $L(q_{\alpha\beta})$ is

$$L(q_{\alpha\beta}) = \beta^2 \sum_{\alpha<\beta} (K^2 q_{\alpha\beta} + h^2) s^\alpha s^\beta - \beta H \sum_\alpha s^\alpha \quad (33)$$

and the configuration sum of $\exp[L(q_{\alpha\beta})]$ now only goes over the n spins s^α in $L(q_{\alpha\beta})$, the HS transformation having made it possible to decouple the configuration sum over Nn spins in Eq. (31) into a N-fold product of n-spin sums. Assuming that the thermodynamic limit ($N\to\infty$) can be taken before $n\to 0$, i.e., that the usual limiting process can be inverted, then Eq. (32) can be evaluated by the method of steepest descent, as the exponent is proportional to N. According to this method, the free energy per spin in the thermodynamic limit is the maximum of the $q_{\alpha\beta}$-dependent function in the exponent:

$$-\beta\bar{f} = \lim_{n\to 0} \max\left\{ \frac{(\beta K)^2}{4}\left(1 - \frac{1}{n}\sum_{(\alpha,\beta)} q_{\alpha\beta}^2\right) + \frac{1}{n}\ln\left(\sum_{\{s^\alpha=\pm1\}} \exp[L(q_{\alpha\beta})]\right)\right\} \quad (34)$$

(with $\bar{f} := \lim_{n\to 0}\overline{f^n}$) with the self-consistency condition:

$$\frac{\partial \bar{f}}{\partial q_{\alpha\beta}} = 0 \Leftrightarrow q_{\alpha\beta} = \langle s^\alpha s^\beta\rangle_L \quad (35)$$

and the magnetization:

$$m = -\frac{1}{\beta}\frac{\partial \bar{f}}{\partial H} = \langle s^\alpha\rangle_L = 2N_F/N - 1 \quad (36)$$

where the average $\langle(\cdot)\rangle_L$ is defined as

$$\langle(\cdot)\rangle_L = \lim_{n\to 0} \frac{\sum_{\{s^\alpha=\pm1\}}(\cdot)\exp[L(q_{\alpha\beta})]}{\sum_{\{s^\alpha=\pm1\}}\exp[L(q_{\alpha\beta})]}. \quad (37)$$

The mean-field approach has allowed a decoupling of the spins and a reduction of the problem to a single-site model with "Hamiltonian" $L[q_{\alpha\beta}]$. For this new problem, the overlap parameter emerges naturally, albeit in a self-consistent manner. To push the calculation further some assumption for $q_{\alpha\beta}$ has to be made. Naively, from the requirement that the result should be independent of the replica-indices, the most natural choice for q is to consider all identical overlaps between the replicas, $q_{\alpha\beta}=q$, which is the SK ansatz. Thus the double sum over the replicas $\Sigma_{(\alpha,\beta)} s^\alpha s^\beta$ in Eq. (33) can be written as a square, keeping $(s^\alpha)^2=1$ in mind. Another Hubbard-Stratonovitch transformation with auxiliary variable z then decouples the square and yields an expression for the free energy density, which has to be evaluated self-consistently and in which the limit $n\to 0$ can be easily calculated:

$$-\beta\bar{f}_{SK} = \lim_{n\to 0}\left\{ \frac{(\beta K)^2}{4}[1-(n-1)q^2] + \frac{1}{n}\ln\left(\frac{1}{\sqrt{2\pi}}\int_{-\infty}^{\infty} dz \exp\left[-\frac{z^2}{2}\right] \times\left(\exp\left[-\frac{\beta^2(K^2q+h^2)}{2}\right] \times\sum_{s=\pm1}\exp[\beta\sqrt{K^2q+h^2}s - \beta H s]\right)^n\right)\right\} \quad (38)$$

$$\Rightarrow \beta\bar{f}_{SK} = \frac{(\beta K)^2}{4}(1-q)^2 - \frac{(\beta h)^2}{2} + \left(\frac{1}{2\pi}\right)^{1/2}\int_{-\infty}^{\infty} dz e^{-z^2/2}\ln\{2\cosh[A(z)]\}, \quad (39)$$

with $A(z) := \beta\sqrt{K^2q+h^2} - \beta H$. The overlap (35) and the magnetization constraint (36) can also be evaluated in the same way:

$$q = \frac{1}{\sqrt{2\pi}}\int_{-\infty}^{\infty} dz e^{-z^2/2}\tanh^2[A(z)], \quad (40)$$

$$m = \frac{1}{\sqrt{2\pi}}\int_{-\infty}^{\infty} dz e^{-z^2/2}\tanh[A(z)] = 2N_F/N - 1. \quad (41)$$

A well-known problem with the SK ansatz for $q_{\alpha\beta}$ is that it yields negative entropy for low temperatures and thus becomes unphysical. This is due to a fundamental technical problem with the replica trick: For the method of steepest descent to be valid, the SK solution must be a maximum of the exponent in Eq. (32) and must *stay* a maximum as the replica limit $n\to 0$ is taken. But there is *no* unique way of choosing the zero-dimensional limit of the matrix $q_{\alpha\beta}$. The SK solution just corresponds to one possible choice for this limit. Thus the question arises whether the SK solution for the free energy is still a good, i.e., maximal choice in the replica limit.

To answer this question, one proceeds analogous to the de Almeida and Thouless procedure [137] to analyze the fluctuations around the SK solution, while taking the magnetization constraint into account (see Appendix B for details). Developing Eqs. (34) and (36) to second and first order, respectively, around $q_{\alpha\beta}=q$ one finds that in the replica limit $n\to 0$ there is an eigenvalue λ_2 of the matrix $\partial^2\bar{f}/\partial q_{\alpha\beta}\partial q_{\gamma\delta}$ that can have both negative values and respects the constraint, yielding the condition

$$\lambda_2 = \frac{1}{(\beta K)^2} - \frac{1}{\sqrt{2\pi}} \int_{-\infty}^{\infty} dz e^{-z^2/2} \mathrm{sech}^4[A(z)] > 0, \quad (42)$$

which is violated for low enough T/K, H/K, and h/K. The plane in parameter space below which this happens is the so-called dAT surface. This instability is rectified by a much more involved ansatz for $q_{\alpha\beta}$ that breaks the symmetry of the replicas and leads to the phenomena described in Sec. V A.

VI. EXPERIMENTAL INSIGHTS

Experimental creation and detection of the phenomena discussed in this paper poses a major problem and deserves a lot of creative thinking and separate publications. In this section we will just sketch what in our opinion are the most obvious ways of addressing these problems. In this section we do not address the questions concerning experimental realization of ultracold FB mixtures and composite fermions—these questions are discussed in Ref. [53].

The first question thus to be addressed is what are the best ways to create quenched disorder in a controlled way. Roth and Burnett [22] and the authors [21] have suggested that the use of pseudorandom disorder induced by noncommensurate optical lattices should work as well as the use of the genuine random lattices. Indeed the latter can be only (so far) achieved using speckle radiation, i.e., disorder correlation length of order of a few microns. If we work with systems of size of mm's, such disorder would definitely be enough to induce localization in 1D or 2D. Unfortunately, the size of the systems in question is typically of the order of hundred of microns, and that is one of the reasons why it is difficult to observe Anderson localization with BECs [27,28].

The analysis performed by us in this context implies clearly that it will be much easier to achieve the desired properties of the disorder using pseudodisordered, i.e., overlapped incommensurable optical lattices [29]. One should also stress the equally promising look to the proposals formulated recently to use the optical tweezers techniques [38] and a random distribution of impurity atoms pinned in different lattice sites [33].

Another variety of problems is related to the detection of the quantum phases discussed in this paper. Below we list basic methods that have been already successfully applied to ultracold atomic gases in optical lattices.

(1) *Imaging of the atomic cloud after ballistic expansion*. This (perhaps the most standard method) has been used in Ref. [20] to distinguish the bosonic SF phase from the MI phase. It allows for measurement of the quasimomentum distribution of atoms obtained after initial expansion caused by interactions [138], i.e., it detects first order coherence (interference pattern), present, for instance, in the SF phase.

(2) *Monitoring the density profile*. Using phase contrast imaging [139] it is possible to perform a direct and nondestructive observation of the spatial distribution of the condensate *in situ*. This kind of measurement allows the direct observation of superfluidity [140] and can be therefore applied to characterize the fluid and superfluid phases.

(3) *Tilting or acceleration of the lattice*. This method was used in Ref. [141] to detect the gap in the MI phase. It allows, in principle, to distinguish gapless from gapped phases, provided the continuum of low energy states can be achieved via tilting. Fluidity, superfluidity, and in general extended, nonlocalized excitations should allow one to detect Bloch oscillations [142].

(4) *Absorption of energy via modulation of the lattice*. This method was also designed to detect the gap in the MI phase [124]. Similarly as tilting, it provides a way of probing excitations in the systems.

(5) *Bragg spectroscopy*. This method, one of the first proposed [143], is also a way of probing a certain kind of excitations in the system [144].

(6) *Cooper pair spectroscopy*. This method is particularly useful to detect Fermi superfluids [145]. Its theoretical aspects are discussed in Ref. [146], while for experiments see Ref. [147].

(7) *Trap shaking and nonlinear dynamics*. Yet another way to probe excitations could correspond to analysis of the response of the system upon sudden shaking of the trap [32].

(8) *Observations of vortices, solitons, etc*. This method provides a direct way to detect superfluidity (for vortices in Bose superfluid see, for instance, Ref. [148], for vortices in Fermi superfluid see [149]).

(9) *Spatial quantum noise interferometry*. The last, but not the least method discussed here allows for practically direct measurement of the density-density correlation and second order coherence. It has been proposed in Ref. [150] (see also [151]), and used with great success to detect the bosonic Mott insulator [152] and the Fermi superfluid [153]. It has capabilities of detecting and measuring relevant properties of various phases and structures ranging from supersolids, charge-density wave phases, and even Luttinger liquids in 1D. In the Fourier frequency and momentum domain it corresponds to measurements of the dynamic structure factor (for a discussion in the context of cold gases see Ref. [154]).

There are of course more methods than the ones discussed above, but combined applications of those discussed should allow for clear detection and characterization of the quantum phases discussed in this paper.

Let us start this discussion with ideal Fermi gas, Fermi liquid, and metallic phases between Fermi glass and glassy Mott insulator. All of them are fluids, i.e., will respond consequently to perturbations. They are gapless and differ in this sense from the Fermi superfluids. All of them should lead to a nontrivial Fermi surface imaging in ballistic expansion. The difference between ideal and interacting phases is here rather quantitative, and as such can be measured. Quantities such as the effective mass can be recovered from the measurements. Influence of disorder on these phases will be seen as a gradual decrease of their "conducting" properties. A similar scenario is expected to take place with "dirty" superfluids; here measurements of the gap (using any of the excitation probing methods) should reveal a rapid gap decrease with the increasing disorder.

Disordered and glassy phases, such as Femi glass or glassy Mott insulator, are more difficult to detect. Obviously they will tend to give blurred images in the measurement of the first order coherence. Spatial noise interferometry should reveal some information about the glassy Mott insulator, especially in the region of parameters where it will incorporate

domains of checkerboard phase. Although the glassy phases are gapless, the states forming the spectral quasicontinuum at low energies may be very difficult to achieve in simple excitation measurements, since they may lie far away one from another in the phase space. Probing of one of such states would thus allow one to study excitations accesible locally in the phase, which most presumably will be gapped. The character of excitations, and in particular their spectrum should, however, be a very sensitive function of how one excites them, and how one detects them (compare [32]). On the other hand, the domain insulator phase should be visible by the "naked eye," and independent of detection of bosons and composites. Also, the noise interferometry should reveal information about the presence of the lattice, similarly as in the standard Mott insulator phase [152].

Finally, a separate problem concerns detection of the fermionic spin glass phase and its properties, as well as distinction between the possible adequacy of the Parisi versus droplet model. Repeated preparation of the system in the lattice with the same disorder (or even direct comparison and measurement of overlap of replicas [155]) will shed some light on the latter problem. In many other aspects, response of the spin glass to excitations will be similar to that of Fermi glasses and glassy Mott insulator.

VII. CONCLUSIONS

Summarizing, we have studied atomic Fermi-Bose mixtures in optical lattices in the strong interacting limit, and in the presence of an inhomogeneous, or random on-site potential. We have derived the effective Hamiltonian describing the low temperature physics of the system, and shown that an inhomogeneous potential may be efficiently used to control the nature and strength of (boson mediated) interactions in the system. Using a random potential, one is able to control the system in such a way that its physics corresponds to a wide variety of quantum disordered systems. It is worth mentioning that the physics discussed in this paper is very much analogous to the one of Bose-Bose mixtures in the limit of hard core bosons (when both species exhibit strong intraspecies repulsion).

We end this section with a general comment on quantum complex systems. In our opinion quantum degenerate gases offer an absolutely unique possibility to study various models of physics of disorder systems, such as Bose and Fermi glasses, quantum percolating systems, "dirty" superfluids, domain and Mott insulators, quantum spin glasses, systems exhibiting localization-delocalization phenomena, etc. The summary of predictions of this paper is schematically shown in the following list of quantum phases, obtained for the case of only one type of sites, and $\mu_i^{\mathrm{f}}=0$, or $\mu_i^{\mathrm{f}}=\mu_i^{\mathrm{b}}$:

(1) composites *I*—Fermi liquid, Fermi glass, quantum bond percolation;

(2) composites *II*—ideal Fermi gas, Fermi glass, Fermi liquid, Mott insulator, fermionic spin glass; and

(3) composites $\bar{I}\bar{I}$—domain insulator, "dirty" superfluid, Fermi glass, metallic phase, Mott insulator, fermionic spin glass.

Additionally, for the case of lattices with different types of sites, physics of quantum site percolation will become relevant. Complex systems such as quantum cellular automata or neural networks can also be realized in this way. In fact, we and other authors have several times already stressed the fascinating possibility of using the ultracold lattice gases as quantum simulators of complex systems. But, the proposed systems go beyond just repeating what is known from the other kinds of physics; they allow one to create novel quantum phases and novel quantum behaviors.

ACKNOWLEDGMENTS

We thank M. Baranov, H.-P. Büchler, B. Damski, M. Dressel, A. Georges, A. Niederberger, J. Parrondo, L. Santos, A. Sen (De), U. Sen, G.V. Shlyapnikov, J. Wehr, and P. Zoller for fruitful discussions. We acknowledge support from the Deutsche Forschungsgemeinschaft (SFB 407, SPP1116 436POL), the RTN Cold Quantum Gases, ESF PESC QUDEDIS, the Alexander von Humboldt Foundation, and Ministerio de Ciencia y Tecnologia (BFM-2002-02588). V.A. acknowledges support from the European Community (MEIF-CT-2003 -501075) and from the Spanish Ministerio de Educación y Ciencia.

APPENDIX A: EFFECTIVE HAMILTONIAN TO SECOND ORDER

The Hamiltonian of our two-species system described in Sec. III B splits into two components: H_0 and H_{int}. The Hamiltonian H_0 has known eigenstates that are grouped in blocks (or manifolds) of states close in energy while the differences between states from two different blocks are much larger than the intrablock spacing. In the case of Sec. III B, this corresponds to the manifold of near-ground states, separated in energy by terms of order $\Delta_{ij}^{\mathrm{b,f}}$, which is separated from other blocks of higher excited states (two or more bosons in one site) by terms of the order V. Generally, the projector on each block space is denoted by P_α where α is the block index, and the ith state in any block is denoted by $|\alpha,i\rangle$. Note that $P_\alpha H_0 P_\beta=0$ holds for $\alpha\neq\beta$.

The second component is a Hamiltonian, H_{int}, that couples to H_0 via a factor J, where J is considered to be small, to form the complete Hamiltonian of the system, $H=H_0+JH_{int}$. The interaction Hamiltonian is now considered to introduce couplings between block α and β, i.e., $P_\alpha H_{int} P_\beta\neq 0$ for $\alpha\neq\beta$.

Following the technique detailed, e.g., in [114], we construct an effective Hamiltonian, H_{eff}, from H such that it describes the slow, low-energy perturbation-induced tunneling *strictly within* each manifold of unperturbed block states, i.e., $P_\alpha H_{eff} P_\beta=0$ for $\alpha\neq\beta$, and has the same eigenvalues as H. Tunneling between different blocks is thus neglected, as this corresponds to fast, high-frequency processes which we neglect here. Technically, the requirements for H_{eff} are

(1) H_{eff} is Hermitian, with the same eigenvalues and the same degeneracies as H. To achieve this, one defines $T:=e^{iS}$, with S Hermitian, $S=S^\dagger$, and chosen such that:

$$H_{eff}=THT^\dagger. \tag{A1}$$

(2) H_{eff} does not couple states from different manifolds:

$$P_\alpha H_{eff} P_\beta = 0, \quad \alpha \neq \beta. \tag{A2}$$

(3) As the first two conditions still allow for an infinite number of unitary transformations (all UT are still possible, U being any unitary transformation acting only *within* the manifolds), the following additional condition is imposed:

$$P_\alpha S P_\alpha = 0 \quad \text{for any } \alpha. \tag{A3}$$

Expanding the first condition using the Baker-Hausdorff formula, one obtains:

$$H_{eff} = H + [iS,H] + \frac{1}{2!}[iS,[iS,H]] + \frac{1}{3!}[iS,[iS,[iS,H]]] + \cdots . \tag{A4}$$

Making a power-series ansatz in S,

$$S = JS_1 + J^2 S_2 + J^3 S_3 + \cdots , \tag{A5}$$

and employing $H = H_0 + JH_{int}$ one obtains from Eq. (A4) to second order

$$H_{eff} = H_0 + J\overbrace{([iS_1,H_0] + H_{int})}^{H^1_{eff}} + J^2\overbrace{\left([iS_2,H_0] + [iS_1,H_{int}] + \frac{1}{2}[iS_1,[iS_1,H_0]]\right)}^{H^2_{eff}}. \tag{A6}$$

This is a power series for H_{eff}, with its moments denoted by H^1_{eff}, H^2_{eff},…, where H^n_{eff} generally depends on all S_j with $1 \leqslant j \leqslant n$. This allows for a systematic evaluation of the matrix elements $\langle \alpha,i|iS_j|\beta,j\rangle$, and consequently delivers matrix expressions for the H^j_{eff} and H_{eff}.

To start with this, one considers the expansions (A6) and (A5) up to first order, i.e., $H_{eff} = H_0 + JH^1_{eff}$ and $S = JS_1$. Using the second and third conditions, as well as $P_\alpha H_0 P_\beta = 0$ and the expression for H^1_{eff} in Eq. (A6), one finds:

$$\langle \alpha,i|iS_1|\beta,j\rangle(E_{\beta j} - E_{\alpha i}) + \langle \alpha,i|H_{int}|\beta,j\rangle = 0 \tag{A7}$$

$$\Rightarrow \langle \alpha,i|iS_1|\beta,j\rangle = \begin{cases} \dfrac{\langle \alpha,i|H_{int}|\beta,j\rangle}{E_{\alpha i} - E_{\beta j}}, & \alpha \neq \beta \\ 0, & \alpha = \beta. \end{cases} \tag{A8}$$

Thus the effective Hamiltonian within the α manifold depends only on the interaction term and not on S_1, i.e., $\langle \alpha,i|H^1_{eff}|\alpha,j\rangle = \langle \alpha,i|H_{int}|\alpha,j\rangle$. A general result for any n is that $\langle \alpha,i|H^n_{eff}|\alpha,j\rangle$ is independent of S_n, based on the third condition, and on the observation that S_n enters the expression for H^n_{eff} only in the commutator with H_0, which is diagonal in the manifold index.

Thus when continuing to second order, the term $[iS_2,H_0]$ in the expression for H^2_{eff} can be dropped. Of the two remaining terms defining H^2_{eff} in Eq. (A6), the second one can be simplified by observing that according to Eq. (A7) the operator $[iS_1,H_0]$ is purely nondiagonal in the manifold index, with values opposite to those of the nondiagonal part of the interaction Hamiltonian. Thus $\frac{1}{2}[iS_1,[iS_1,H_0]] = -\frac{1}{2}[iS_1,H^{nd}_{int}]$. Now inserting the identity between the operators in the still untreated second term in H^2_{eff}, $[iS_1,H_{int}]$, one sees that due to S_1 being nondiagonal in α, again only the nondiagonal part of H_{int} can contribute: $[iS_1,H_{int}] = [iS_1,H^{nd}_{int}]$. Therefore one has

$$H^2_{eff} = [iS_1,H^{nd}_{int}] + \frac{1}{2}[iS_1,\overbrace{[iS_1,H_0]}^{-H^{nd}_{int}}] = \frac{1}{2}[iS_1,H^{nd}_{int}]. \tag{A9}$$

Collecting all terms relevant for $\langle \alpha,i|H_{eff}|\alpha,j\rangle$ to second order in J, and introducing the notation $Q_{\alpha i} := \Sigma_{k,\gamma\neq\alpha}[|\gamma,k\rangle \times \langle \gamma,k|/(E_{\gamma k} - E_{\alpha i})]$, one finds

$$\langle \alpha,i|H_{eff}|\alpha,j\rangle = E_{\alpha i}\delta_{ij} + J\langle \alpha,i|H_{int}|\alpha,j\rangle - \frac{J^2}{2}(\langle \alpha,i|H_{int}[Q_{\alpha i} + Q_{\alpha j}]H_{int}|\alpha,j\rangle), \tag{A10}$$

where the identity operator has been inserted in the final expression for H^2_{eff} in formula (A9), and then evaluated using formula (A8), which naturally leads one to define the operator $Q_{\alpha i}$ as above. Note that this construction can be generalized to arbitrary orders in J in a straightforward manner, as detailed in [114].

APPENDIX B: STABILITY OF THE SK SOLUTION

The Taylor expansion of Eq. (34) around $q_{\alpha\beta} = q$ yields the correction $-\frac{1}{2}\delta\bar{f}$ to the free energy, with

$$\delta\bar{f} = \sum_{[\alpha,\beta][\gamma,\delta]} \underbrace{\left.\frac{\partial^2 \bar{f}}{\partial q_{\alpha\beta}\partial q_{\gamma\delta}}\right|_{SK}}_{:=G_{(\alpha\beta)(\gamma\delta)}} \delta q_{\alpha\beta}\delta q_{\gamma\delta} = \sum_{[\alpha,\beta][\gamma,\delta]} [\delta_{(\alpha,\beta)(\gamma,\delta)} - (\beta K)^2(\langle s^\alpha s^\beta s^\gamma s^\delta\rangle^{SK}_L - \langle s^\alpha s^\beta\rangle^{SK}_L\langle s^\gamma s^\delta\rangle^{SK}_L]\,\delta q_{\alpha\beta}\delta q_{\gamma\delta}, \tag{B1}$$

where $[\cdot,\cdot]$ denotes a sum over all distinct index pairs irrespective of the order, the index SK denotes evaluation at $q_{\alpha\beta} = q$, and, analogous to Eqs. (40) and (41), $\langle s^\alpha s^\beta s^\gamma s^\delta\rangle_L|_{SK} = (1/2\pi)^{1/2}\int_{-\infty}^{\infty} dz e^{-z^2/2}\tanh^4[A(z)]$.

If the SK solution really corresponds to a maximum, this symmetric quadratic form must be positive definite. To check this, one calculates the eigenvalues of the $\frac{1}{2}n(n-1)$-dimensional matrix $G_{(\alpha\beta)(\gamma\delta)}$ in terms of its three distinct matrix elements:

$$P \equiv G_{(\alpha\beta)(\alpha\beta)} = 1 - (\beta K)^2(1 - \langle s^\alpha s^\beta\rangle^2_L)|_{SK},$$

$$Q \equiv G_{(\alpha\beta)(\alpha\gamma)} = -(\beta K)^2(\langle s^\beta s^\gamma\rangle_L - \langle s^\alpha s^\beta\rangle^2_L)|_{SK},$$

$$R \equiv G_{(\alpha\beta)(\gamma\delta)} = -(\beta K)^2(\langle s^\alpha s^\beta s^\gamma s^\delta\rangle_L - \langle s^\alpha s^\beta\rangle^2_L)|_{SK}.$$

As becomes apparent from this, there are just three distinct classes of transformations that leave $G_{(\alpha\beta)(\gamma\delta)}$ invariant: those

that permute no index acting on the P's; those that permute a single index acting on the Q's; and those that permute two indices acting on the R's. Thus there are only three eigenspaces to distinct eigenvalues and the linearly independent eigenvectors within each of these eigenspaces can naturally be chosen by considering a group of vectors that is invariant under the corresponding permutation transformation.

1. No index permutation

The ansatz for the eigenvalue is trivially given by

$$\delta q_{\alpha\beta} = c, \quad \text{for all } (\alpha\beta), \tag{B2}$$

which is nondegenerate. With this ansatz, the eigenvalue equation is

$$\left[P + 2(n-2)Q + \frac{1}{2}(n-2)(n-3)R - \lambda_1 \right] c = 0 \tag{B3}$$

from which λ_1 can immediately be read off.

2. Permutation of a single index

Again, the ansatz for the eigenvectors is naturally given by

$$\delta q_{\alpha\beta} = c \quad \text{for } \alpha \text{ or } \beta = \theta, \quad \delta q_{\alpha\beta} = d \quad \text{for } \alpha, \beta \neq \theta. \tag{B4}$$

The ansatz still contains the previous case, as the requirement of the eigenvectors (B2) and (B4) being orthogonal still has to be fulfilled. This yields $c = (1-n/2)d$ and a degeneracy of $n-1$ for the eigenvalue. The eigenvalue equation then becomes

$$[P + (n-4)Q + (n-3)R - \lambda_1']d = 0 \tag{B5}$$

from which λ_1' is again immediately obvious.

3. Permutation of both indices

The ansatz is

$$\delta q_{\theta\nu} = c, \quad \delta q_{\theta\alpha} = \delta q_{\nu\alpha} = d \quad \text{for } \alpha \neq \theta, \nu,$$

$$\delta q_{\alpha\beta} = e \quad \text{for } \alpha, \beta \neq \theta, \nu. \tag{B6}$$

Orthogonality to the previous eigenspaces requires $c = (2-n)$, $d = (3-n)/2$, and results in the final eigenvalue equation:

$$[P - 2Q + R - \lambda_2]e = 0 \tag{B7}$$

with λ_2 having degeneracy $\frac{1}{2}n(n-3)$.

Taking the naive replica limit again the first two eigenvalues coincide:

$$\lim_{n\to 0} \lambda_1 = \lim_{n\to 0} \lambda_1' = P - 4Q - 3R. \tag{B8}$$

As de Almeida and Thouless report [137], a region in parameter-space where this limiting value took a negative value could not be found. Thus, calculating λ_2 explicitly, the relevant stability condition reads

$$\lambda_2 = \frac{1}{(\beta K)^2} - \frac{1}{\sqrt{2\pi}} \int_{-\infty}^{\infty} dz e^{-z^2/2} \operatorname{sech}^4[A(z)] > 0. \tag{B9}$$

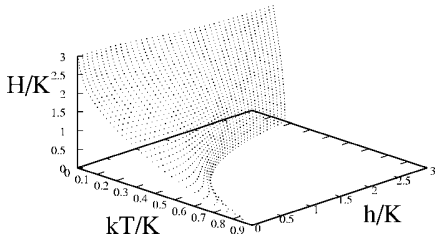

FIG. 11. Almeida-Thouless plane in the reduced variables kT/K, h/K, and H/K. The constraint on the magnetization (41) has been effectively neglected for this, as it is a parameter in the experiment as well.

Solving the coupled equations (39)–(41) for $\lambda_2 = 0$ yields the dAT plane (cf. Fig. 11). Above it, the SK solution is still valid, and below it λ_2 takes negative value and the SK solution breaks down.

This can of course only happen if eigenvectors to λ_2 are compatible with the magnetization constraint (36). To see this, one has to check that small fluctuations around $q_{\alpha\beta} = q$ do not lead to a deviation from the value for m, i.e., that

$$\delta m = \sum_{[\alpha,\beta]} \left. \frac{\partial \langle s^\lambda \rangle_L}{\partial q_{\alpha\beta}} \right|_{SK} \delta q_{\alpha\beta} = 0 \tag{B10}$$

holds, with

$$\left. \frac{\partial \langle s^\lambda \rangle_L}{\partial q_{\alpha\beta}} \right|_{SK} = \begin{cases} [(K\beta)^2 \langle s^\lambda \rangle_L - \langle s^\alpha s^\beta \rangle_L \langle s^\lambda \rangle_L]|_{SK}, & \alpha \text{ or } \beta = \lambda \\ [(K\beta)^2 \langle s^\lambda s^\alpha s^\beta \rangle_L - \langle s^\alpha s^\beta \rangle_L \langle s^\lambda \rangle_L)|_{SK}, & \alpha, \beta \neq \lambda \end{cases}. \tag{B11}$$

Inserting any eigenvector of λ_2 into Eq. (B10) will, however, yield the desired result. As is clearly seen from Eq. (B11) $\partial \langle s^\lambda \rangle_L / \partial q_{\alpha\beta}$ evaluated at $q_{\alpha\beta} = q$ is an eigenvector to λ_1', and thus $\delta m = 0$ is fulfilled.

The magnetization constraint is thereby compatible with the instability $\lambda_2 < 0$, and replica-symmetry breaking is expected to occur. From the calculations it has become clear that the presence of the random magnetic field would not change the occurrence of replica symmetry breaking, and all properties like infinitely degenerate ground-states and ultrametricity would be expected to occur in this model as well, provided the Mézard-Parisi approach can be applied to the finite range spin glass at all.

[1] P. W. Anderson, Phys. Rev. **109**, 1492 (1958).
[2] N. E. Cusack, *The Physics of Structurally Disordered Matter* (Adam Hilger, Bristol, 1987).
[3] *Ill-Condensed Matter*, edited by R. Balian, R. Maynard, and G. Toulouse (North-Holland, Amsterdam, 1979).
[4] D. Chowdhury, *Spin Glasses and Other Frustrated Systems* (Wiley, New York, 1986).
[5] *Anderson Localization*, edited by Y. Nagaoka and H. Fukuyama, Vol. 39 of Springer Series in Solid State Sciences (Springer, Heidelberg, 1982); *Anderson Localization*, edited by T. Ando and H. Fukuyama, Vol. 28 of Springer Proceedings in Physics (Springer, Heidelberg, 1988); P. A. Lee and R. V. Ramakrishan, Rev. Mod. Phys. **57**, 287 (1985).
[6] M. Mézard, G. Parisi, and M. A. Virasoro, *Spin Glass Theory and Beyond* (World Scientific, Singapore, 1987).
[7] C. M. Newman and D. L. Stein, J. Phys.: Condens. Matter **15**, R1319 (2003).
[8] S. Sachdev, *Quantum Phase Transitions* (Cambridge University Press, Cambridge, England, 1999).
[9] D. J. Amit, *Modelling Brain Function* (Cambridge University Press, Cambridge, England, 1989).
[10] A. Aharony and D. Stauffer, *Introduction to Percolation Theory* (Taylor & Francis, London, 1994).
[11] P. H. R. Barbosa, E. P. Raposo, and M. D. Coutinho-Filho, Phys. Rev. Lett. **91**, 197207 (2003).
[12] A. Auerbach, *Interacting Electrons and Quantum Magnetism* (Springer, New York, 1994).
[13] F. Haake, *Quantum Signatures of Chaos* (Springer, Berlin, 2004).
[14] K. Efetov, *Supersymmetry in Disorder and Chaos* (Cambridge University Press, Cambridge, England, 1997).
[15] G. Misguich and C. Lhuillier, in *Frustrated Spin Systems*, edited by H. T. Diep (World Scientific, Singapore, 2004).
[16] B. Paredes, F. Verstraete, and J. I. Cirac, Phys. Rev. Lett. **95**, 140501 (2005).
[17] L. P. Pitaevskii and S. Stringari, *Bose-Einstein Condensation* (Oxford University Press, Oxford, 2004); A. J. Leggett, Rev. Mod. Phys. **73**, 307 (2001).
[18] D. Jaksch and P. Zoller, Ann. Phys. **315**, 52 (2005).
[19] D. Jaksch, C. Bruder, J. I. Cirac, C. W. Gardiner, and P. Zoller, Phys. Rev. Lett. **81**, 3108 (1998).
[20] M. Greiner, O. Mandel, T. Esslinger, T. W. Hänsch, and I. Bloch, Nature (London) **415**, 39 (2002).
[21] B. Damski, J. Zakrzewski, L. Santos, P. Zoller, and M. Lewenstein, Phys. Rev. Lett. **91**, 080403 (2003).
[22] R. Roth and K. Burnett, J. Opt. B: Quantum Semiclassical Opt. **5**, S50 (2003); Phys. Rev. A **68**, 023604 (2003).
[23] L. Sanchez-Palencia and L. Santos, Phys. Rev. A **72**, 053607 (2005).
[24] L. Guidoni and P. Verkerk, Phys. Rev. A **57**, R1501 (1999); L. Guidoni, C. Triché, P. Verkerk, and G. Grynberg, Phys. Rev. Lett. **79**, 3363 (1997); P. Horak, J.-Y. Courtois, and G. Grynberg, Phys. Rev. A **58**, 3953 (1998).
[25] J. C. Dainty, *Laser Speckle and Related Phenomena* (Springer, Berlin, 1975).
[26] M. P. A. Fisher, P. B. Weichman, G. Grinstein, and D. S. Fisher, Phys. Rev. B **40**, 546 (1989).
[27] J. E. Lye, L. Fallani, M. Modugno, D. S. Wiersma, C. Fort, and M. Inguscio, Phys. Rev. Lett. **95**, 070401 (2005); C. Fort, L. Fallani, V. Guarrera, J. E. Lye, M. Modugno, D. S. Wiersma, and M. Inguscio, *ibid.* **95**, 170410 (2005).
[28] D. Clément, A. F. Varón, M. Hugbard, J. A. Retter, P. Bouyer, L. Sanchez-Palencia, D. M. Gangardt, G. V. Shlyapnikov, and A. Aspect, Phys. Rev. Lett. **95**, 170409 (2005).
[29] T. Schulte, S. Drenkelforth, J. Kruse, W. Ertmer, J. Arlt, K. Sacha, J. Zakrzewski, and M. Lewenstein, Phys. Rev. Lett. **95**, 170411 (2005).
[30] R. Folman, P. Kruger, J. Schmiedmayer, J. Denschlag, and C. Henkel, Adv. At., Mol., Opt. Phys. **48**, 263 (2002); for the latest results see Y. J. Wang, D. Z. Anderson, V. M. Bright, E. A. Cornell, Q. Diot, T. Kishimoto, M. Prentiss, R. A. Saravanan, S. R. Segal, and S. J. Wu, Phys. Rev. Lett. **94**, 090405 (2005); T. Schumm, J. Esteve, C. Figl, J. B. Trebbia, C. Aussibal, H. Nguyen, D. Mailly, I. Bouchoule, C. I. Westbrook, and A. Aspect, Eur. Phys. J. D **32**, 171 (2005); J. Fortagh and C. Zimmermann, Science **307**, 860 (2005); P. Hommelhoff, W. Hansel, T. Steinmetz, T. W. Hänsch, and J. Reichel, New J. Phys. **7**, Art. No. 3 (2005); L. Feenstra, L. M. Andersson, and J. Schmiedmayer, Gen. Relativ. Gravit. **36**, 2317 (2004).
[31] C. Henkel, P. Krüger, R. Folman, and J. Schmiedmayer, Appl. Phys. B: Lasers Opt. **76**, 173 (2003).
[32] D.-W. Wang, M. D. Lukin, and E. Demler, Phys. Rev. Lett. **92**, 076802 (2004).
[33] P. Zoller, H. P. Büchler, and I. Bloch (private communication); U. Gavish and Y. Castin, Phys. Rev. Lett. **95**, 020401 (2005).
[34] J. Schmiedmayer (private communication).
[35] A. Kantian, Diploma thesis, Universität Hannover, 2004.
[36] H. Gimperlein, S. Wessel, J. Schmiedmayer, and L. Santos, Phys. Rev. Lett. **95**, 170401 (2005).
[37] A. Sanpera, A. Kantian, L. Sanchez-Palencia, J. Zakrzewski, and M. Lewenstein, Phys. Rev. Lett. **93**, 040401 (2004).
[38] M. G. Raizen (private communication).
[39] L. Santos, M. A. Baranov, J. I. Cirac, H.-U. Everts, H. Fehrmann, and M. Lewenstein, Phys. Rev. Lett. **93**, 030601 (2004); B. Damski, H.-U. Everts, A. Honecker, H. Fehrmann, L. Santos, and M. Lewenstein, *ibid.* **95**, 060403 (2005).
[40] L. M. Duan, E. Demler, and M. D. Lukin, Phys. Rev. Lett. **91**, 090402 (2003).
[41] K. Góral, L. Santos, and M. Lewenstein, Phys. Rev. Lett. **88**, 170406 (2002).
[42] F. Mintert and C. Wunderlich, Phys. Rev. Lett. **87**, 257904 (2001); D. Porras and J. I. Cirac, *ibid.* **92**, 207901 (2004).
[43] D. Jaksch, and P. Zoller, New J. Phys. **5**, Art. No. 56 (2003); E. J. Mueller, Phys. Rev. A **70**, 041603(R) (2004); A. S. Sorensen, E. Demler, and M. D. Lukin, Phys. Rev. Lett. **94**, 086803 (2005).
[44] K. Osterloh, M. Baig, L. Santos, P. Zoller, and M. Lewenstein, Phys. Rev. Lett. **95**, 010403 (2005); J. Ruseckas, G. Juzeliunas, P. Öhberg, and M. Fleischhauer, *ibid.* **95**, 010404 (2005).
[45] A. Osterloh, L. Amico, G. Falci, and R. Fazio, Nature (London) **416**, 608 (2002); F. Verstraete, M. Popp, and J. I. Cirac, Phys. Rev. Lett. **92**, 027901 (2004); J. I. Latorre, E. Rico, and G. Vidal, Quantum Inf. Comput. **1**, 48 (2004).
[46] C. H. Bennett, D. P. DiVincenzo, J. A. Smolin, and W. K. Wootters, Phys. Rev. A **54**, 3824 (1996); A. Steane, Rep. Prog. Phys. **61**, 117 (1998); E. Knill and R. Laflamme, Phys. Rev. A **55**, 900 (1997).
[47] W. Dür, L. Hartmann, M. Hein, M. Lewenstein, and H. J. Briegel, Phys. Rev. Lett. **94**, 097203 (2005); A. Sen (De), U. Sen, V. Ahufinger, H. J. Briegel, A. Sanpera, and M. Lewenstein, e-print quant-ph/0507172.

[48] M. LL. Pons, V. Ahufinger, A. Sanpera, C. Wunderlich, and M. Lewenstein (unpublished).
[49] G. Vidal, Phys. Rev. Lett. **91**, 147902 (2003); F. Verstraete, D. Porras, and J. I. Cirac, *ibid.* **93**, 227205 (2004); A. J. Daley, C. Kollath, U. Schollwöck, and G. Vidal, J. Stat. Mech.: Theory Exp. 2004, P04005; F. Verstraete and J. I. Cirac, Phys. Rev. A **70**, 060302(R) (2004).
[50] This phenomenon, related to the appearance of counterflow superfluidity in Ref. [51], may also occur in the absence of the optical lattice; see M. Yu. Kagan, I. V. Brodsky, D. V. Efremov, and A. V. Klaptsov, e-print cond-mat/0209481; Phys. Met. Metallogr. **99**, 225 (2005); Phys. Rev. A **70**, 023607 (2004).
[51] A. B. Kuklov and B. V. Svistunov, Phys. Rev. Lett. **90**, 100401 (2003).
[52] M. Lewenstein, L. Santos, M. A. Baranov, and H. Fehrmann, Phys. Rev. Lett. **92**, 050401 (2004).
[53] H. Fehrmann, M. A. Baranov, B. Damski, M. Lewenstein, and L. Santos, Opt. Commun. **243**, 23 (2004).
[54] H. Fehrmann, M. A. Baranov, M. Lewenstein, and L. Santos, Opt. Express **12**, 55 (2004).
[55] The studies of trapped FB gases concerned in particular FB phase separation [56,57], the phase diagram [58], novel types of collective modes [57,59], Fermi-Fermi interactions mediated by bosons [57,60], collapse of the Fermi cloud in the presence of attractive FB interactions [61], or the effects characteristic for the 1D FB mixtures [62].
[56] K. Mølmer, Phys. Rev. Lett. **80**, 1804 (1998).
[57] M. J. Bijlsma, B. A. Heringa, and H. T. C. Stoof, Phys. Rev. A **61**, 053601 (2000); H. Pu, W. Zhang, M. Wilkens, and P. Meystre, Phys. Rev. Lett. **88**, 070408 (2002).
[58] R. Roth, Phys. Rev. A **66**, 013614 (2002).
[59] P. Capuzzi and E. S. Hernández, Phys. Rev. A **64**, 043607 (2001); X.-J. Liu and H. Hu, *ibid.* **67**, 023613 (2003).
[60] A. P. Albus, S. A. Gardiner, F. Illuminati, and M. Wilkens, Phys. Rev. A **65**, 053607 (2002); L. Viverit and S. Giorgini, *ibid.* **66**, 063604 (2002); H. Heiselberg, C. J. Pethick, H. Smith, and L. Viverit, Phys. Rev. Lett. **85**, 2418 (2000).
[61] G. Modugno, G. Roati, F. Riboli, F. Ferlaino, R. J. Brecha, and M. Inguscio, Science **297**, 2240 (2002); M. Modugno, F. Ferlaino, F. Riboli, G. Roati, G. Modugno, and M. Inguscio, Phys. Rev. A **68**, 043626 (2003).
[62] K. K. Das, Phys. Rev. Lett. **90**, 170403 (2003); M. A. Cazalilla and A. F. Ho, *ibid.* **91**, 150403 (2003).
[63] A. Albus, F. Illuminati, and J. Eisert, Phys. Rev. A **68**, 023606 (2003); H. P. Büchler and G. Blatter, Phys. Rev. Lett. **91**, 130404 (2003); R. Roth and K. Burnett, Phys. Rev. A **69**, 021601(R) (2004); J. Phys. B **37**, 3893 (2004); F. Illuminati and A. Albus, Phys. Rev. Lett. **93**, 090406 (2004).
[64] A. Mehring, U. Schollwöck, and M. Fleischhauer, Verhandlungen der Deutschen Physicalischen Gesellshaft, 69th Jahrestagung Berlin 2005, Kurzfassungen der Vorträge, Q32.6.
[65] M. Cramer, J. Eisert, and F. Illuminati, Phys. Rev. Lett. **93**, 190405 (2004).
[66] E. Abrahams, P. W. Anderson, D. C. Licciardello, and T. V. Ramakrishnan, Phys. Rev. Lett. **42**, 673 (1979).
[67] D. J. Thouless, J. Phys. C **5**, 77 (1972).
[68] A. De Martino, M. Thorwart, R. Egger, and R. Graham, Phys. Rev. Lett. **94**, 060402 (2005).
[69] G. Labeyrie, D. Delande, C. A. Muller, C. Miniatura, and R. Kaiser, Opt. Commun. **243**, 157 (2004); J. Bertolotti, S. Gottardo, D. S. Wiersma, M. Ghulinyan, and L. Pavesi, Phys. Rev. Lett. **94**, 113903 (2005).
[70] S. Fishman, D. R. Grempel, and R. E. Prange, Phys. Rev. Lett. **49**, 509 (1982).
[71] F. L. Moore, J. C. Robinson, C. Bharucha, P. E. Williams, and M. G. Raizen, Phys. Rev. Lett. **73**, 2974 (1994).
[72] J. B. Sokoloff, Phys. Rep. **126**, 189 (1985).
[73] P. G. Harper, Proc. Phys. Soc., London, Sect. A **68**, 874 (1955); see also D. R. Hofstadter, Phys. Rev. B **14**, 2239 (1976).
[74] B. L. Altshuler and A. G. Aronov, Solid State Commun. **30**, 115 (1079); Sov. Phys. JETP **50**, 968 (1979).
[75] H. Fukuyama, J. Phys. Soc. Jpn. **48**, 2169 (1980).
[76] R. Freedman and J. A. Hertz, Phys. Rev. B **15**, 2384 (1977); Y. Imry, Europhys. Lett. **30**, 405 (1995); F. von Oppen and T. Wettig, *ibid.* **32**, 741 (1995); Ph. Jacquod and D. L. Shepelyansky, Phys. Rev. Lett. **78**, 4986 (1997).
[77] D. L. Shepelyansky, Phys. Rev. Lett. **73**, 2607 (1994).
[78] P. Schmitteckert, R. A. Jalabert, D. Weinmann, and J.-L. Pichard, Phys. Rev. Lett. **81**, 2308 (1998); E. Gambeti-Césare, D. Weinmann, R. A. Jalabert, and Ph. Brune, Europhys. Lett. **60**, 120 (2002); G. Benenti, X. Waintal, and J.-L. Pichard, Phys. Rev. Lett. **83**, 1826 (1999); X. Waintal, G. Benenti, and J.-L. Pichard, Europhys. Lett. **49**, 466 (2000).
[79] For very recent results of dynamical mean-field theory applied to half filled Hubbard-Anderson model, see K. Byczuk, W. Hofstetter, and D. Vollhardt, Phys. Rev. Lett. **94**, 056404 (2005).
[80] A. L. Efros, Sov. Phys. JETP **54**, 218 (1981); A. L. Efros and B. I. Shklovskii, Phys. Status Solidi B **76**, 475 (1976); J. Phys. C **8**, L49 (1975).
[81] W. L. McMillan, Phys. Rev. B **24**, 2739 (1981).
[82] H.-L. Lee, J. P. Carini, D. V. Baxter, and G. Gruner, Phys. Rev. Lett. **80**, 4261 (1998); H.-L. Lee, J. P. Carini, D. V. Baxter, W. Henderson, and G. Gruner, Science **287**, 633 (2000).
[83] S. Bogdanovich, M. P. Sarachik, and R. N. Bhatt, Phys. Rev. Lett. **82**, 137 (1999); M. A. Paalanen, T. F. Rosenbaum, G. A. Thomas, and R. N. Bhatt, *ibid.* **51**, 1896 (1983).
[84] M. Pollak, Solid-State Electron. **28**, 143 (1985); A. Pérez-Garrido, M. Ortuño, E. Cuevas, J. Ruiz, and M. Pollak, Phys. Rev. B **55**, R8630 (1997).
[85] M. Dressel (private communication); M. Hering, M. Scheffler, M. Dressel, and H. Von Lohneysen, Physica B **359**, 1469 (2005).
[86] W. Hofstetter, Adv. Solid State Phys. **45**, 109 (2005).
[87] K. G. Singh and D. S. Rokhsar, Phys. Rev. B **49**, 9013 (1994).
[88] K. Ø. Rasmussen, D. Cai, A. R. Bishop, and N. Grønbech-Jensen, Europhys. Lett. **47**, 421 (1999).
[89] D. L. Shepelyansky, Phys. Rev. Lett. **70**, 1787 (1993).
[90] R. T. Scalettar, G. G. Batrouni, and G. T. Zimanyi, Phys. Rev. Lett. **66**, 3144 (1991); M. Enjalran, F. Hebert, G. G. Batrouni, R. T. Scalettar, and S. Zhang, Phys. Rev. B **64**, 184402 (2001).
[91] P. W. Anderson, J. Phys. Chem. Solids **11**, 26 (1959); L. P. Gorkov, Sov. Phys. JETP **10**, 998 (1960).
[92] S. Maekawa and H. Fukuyama, J. Phys. Soc. Jpn. **51**, 1380 (1982).
[93] M. A. Paalanen, A. F. Hebard, and R. R. Ruel, Phys. Rev. Lett. **69**, 1604 (1992).
[94] Y. Liu, K. A. McGreer, B. Nease, D. B. Haviland, G. Martinez,

J. W. Halley, and A. M. Goldman, Phys. Rev. Lett. **67**, 2068 (1991).
[95] For a review see, A. M. Goldman and N. Marković, Phys. Today **51**, 39 (1998).
[96] N. Marković, A. M. Mack, G. Martinez-Arizala, C. Christiansen, and A. M. Goldman, Phys. Rev. Lett. **81**, 701 (1998); K. A. Parendo, K. H. Sarwa, B. Tan, A. Bhattacharya, M. Eblen-Zayas, N. E. Staley, and A. M. Goldman, Phys. Rev. Lett. **94**, 197004 (2005).
[97] G. Grimmett, *Percolation*, 2nd ed. (Springer, Berlin, 1999).
[98] H. L. Frisch and J. M. Hammersley, J. Soc. Ind. Appl. Math. **11**, 894 (1963).
[99] Y. Shapir, A. Aharony, and A. B. Harris, Phys. Rev. Lett. **49**, 486 (1982).
[100] T. Odagaki and K. C. Chang, Phys. Rev. B **30**, 1612 (1984).
[101] A. W. W. Ludwig, M. P. A. Fisher, R. Shankar, and G. Grinstein, Phys. Rev. B **50**, 7526 (1994); R. F. Kazarinov and S. Luryi, *ibid.* **25**, 7626 (1982); D. H. Lee, Z. Wang, and S. Kivelson, Phys. Rev. Lett. **70**, 4130 (1993).
[102] Y. Imry and S. Ma, Phys. Rev. Lett. **35**, 1399 (1975).
[103] D. S. Fisher, J. Frölich, and T. Spencer, J. Stat. Phys. **34**, 863 (1984); J. Z. Imbrie, Phys. Rev. Lett. **53**, 1747 (1984); J. Bricmont and A. Kupiainen, *ibid.* **59**, 1829 (1987).
[104] M. Aizenman and J. Wehr, Phys. Rev. Lett. **62**, 2503 (1989); Commun. Math. Phys. **130**, 489 (1990).
[105] B. J. Minchau and R. A. Pelcovits, Phys. Rev. B **32**, 3081 (1985).
[106] J. Wehr, A. Niederberger, L. Sanchez-Palencia, and M. Lewenstein (unpublished).
[107] D. S. Fisher and D. A. Huse, Phys. Rev. Lett. **56**, 1601 (1986); A. J. Bray and M. A. Moore, *ibid.* **58**, 57 (1987); D. S. Fisher and D. A. Huse, Phys. Rev. B **38**, 373 (1988); **38**, 386 (1988).
[108] D. Sherrington and S. Kirkpatrick, Phys. Rev. Lett. **35**, 1792 (1975).
[109] S. F. Edwards and P. W. Anderson, J. Phys. F: Met. Phys. **5**, 965 (1975).
[110] G. H. Wannier, Phys. Rev. **52**, 191 (1937).
[111] C. Kittel, *Quantum Theory of Solids* (Wiley, New York, 1987).
[112] Transitions from fermionic phases to superfluid are of second order. In the limit of asymptotically small J, we also expect transitions to be of second order but this regime needs more detailed analysis beyond the mean Gutzwiller or BCS theory. Also, some of the phases, such the small regions of density waves of Fig. 1(b) might be smeared out by quantum fluctuations.
[113] For the general case of $\tilde{n} \neq 1$ boson per site, see [52–54].
[114] C. Cohen-Tannoudji, J. Dupont-Roc, and G. Grynberg, *Atom-Photon Interactions: Basic Processes and Applications* (Wiley, New York, 1992).
[115] K. C. Chang and T. Odagaki, J. Phys. A **20**, L1027 (1987).
[116] L. J. Root, J. D. Bauer, and J. L. Skinner, Phys. Rev. B **37**, 5518 (1988).
[117] C. M. Soukoulis and G. S. Grest, Phys. Rev. B **44**, 4685 (1991).
[118] C. M. Soukoulis, Q. Li, and G. S. Grest, Phys. Rev. B **45**, 7724 (1992).
[119] D. S. Rokhsar and B. G. Kotliar, Phys. Rev. B **44**, 10328 (1991); W. Krauth, M. Caffarel, and J. P. Bouchaud, *ibid.* **45**, 3137 (1992); K. Sheshadri, H. R. Krishnamurthy, R. Pandit, and T. V. Ramakrishnan, Europhys. Lett. **22**, 257 (1993).
[120] In all the work presented below, we considered a sufficiently large $n_{\max}$ so that the numerical results are not affected by its finite value.
[121] W. H. Press, B. P. Flannery, S. A. Teukolsky, and W. T. Vetterling, *Numerical Recipes* (Cambridge University Press, Cambridge, England, 1992).
[122] Note that we do not use a standard grand canonical ensemble corresponding to $\langle H_{\mathrm{FBH}} \rangle - \mu^{\mathrm{f}} \langle \Sigma_i m_i - N_{\mathrm{f}} \rangle - \mu^{\mathrm{b}} \langle \Sigma_i n_i - N_{\mathrm{b}} \rangle$ because in the case of composites, we checked that it turns out to be very difficult to choose the chemical potentials μ^{f} and μ^{b} in order to get reasonable values of $\langle \Sigma_i m_i \rangle$ and $\langle \Sigma_i n_i \rangle$. This is because both total numbers of particles depend on both μ^{f} and μ^{b} in a nonstraightforward way. On the contrary, using Λ_{f} and Λ_{b} large enough and positive ensures that $\langle \Sigma_i m_i \rangle \simeq N_{\mathrm{f}}$ and $\langle \Sigma_i n_i \rangle \simeq N_{\mathrm{b}}$ without effort.
[123] D. Jaksch, V. Venturi, J. I. Cirac, C. J. Williams, and P. Zoller, Phys. Rev. Lett. **89**, 040402 (2002).
[124] C. Schori, T. Stöferle, H. Moritz, M. Köhl, and T. Esslinger, Phys. Rev. Lett. **93**, 240402 (2004); M. Köhl, H. Moritz, T. Stöferle, C. Schori, and T. Esslinger, J. Low Temp. Phys. **138**, 635 (2005).
[125] S. Peil, J. V. Porto, B. L. Tolra, J. M. Obrecht, B. E. King, M. Subbotin, S. L. Rolston, and W. D. Phillips, Phys. Rev. A **67**, 051603(R) (2003).
[126] In current experiments, the exact commensurate filling factor 1 appears in the central region of the lattice due to the presence of a weak confining potential [127].
[127] G. G. Batrouni, V. Rousseau, R. T. Scalettar, M. Rigol, A. Muramatsu, P. J. H. Denteneer, and M. Troyer, Phys. Rev. Lett. **89**, 117203 (2002).
[128] Although not presented in this paper, we also performed calculations in the regions corresponding to composites of types *I* and *II* (see composites diagram in Fig. 1) that demonstrate formation of the corresponding composites. For instance, for type *I* composites, $N_{\mathrm{b}}=100$ and $N_{\mathrm{f}}=40$, we found that the only nonzero probabilities were $|g^{(i)}_{n=1,m=0}|^2$ (absence of a composite) and $|g^{(i)}_{n=1,m=1}|^2$ (presence of a composite) with $|g^{(i)}_{n=1,m=0}|^2 + |g^{(i)}_{n=1,m=1}|^2 = 1$. Similarly, for type *II* composites, $N_{\mathrm{b}}=140$ and $N_{\mathrm{f}}=40$, we found that the only nonzero probabilities were $|g^{(i)}_{n=1,m=0}|^2$ (absence of composite) and $|g^{(i)}_{n=2,m=1}|^2$ (presence of composite) with $|g^{(i)}_{n=1,m=0}|^2 + |g^{(i)}_{n=2,m=1}|^2 = 1$.
[129] R. Oppermann and B. Rosenow, Phys. Rev. B **60**, 10325 (1999); R. Oppermann and D. Sherrington, *ibid.* **67**, 245111 (2003).
[130] K. Binder and A. P. Young, Rev. Mod. Phys. **58**, 801 (1986).
[131] A. Georges, O. Parcollet, and S. Sachdev, Phys. Rev. B **63**, 134406 (2001).
[132] As the standard deviation of K_{ij} is given by $K/\sqrt{N}$, it vanishes in the thermodynamic limit. This choice is necessary on the technical level to obtain a sensible limit. Physically this corresponds to the case where the impurities are very dense (each bond is a separately fluctuating impurity) and influence the system collectively, but are negligible individually.
[133] Generally, the lower critical dimension for this transition to happen at nonzero T is believed to be two (cf. references in [7]).
[134] Ph. Refrigier, E. Vincent, J. Hammann, and M. Ocio, J. Phys.

(Paris) **48**, 1533 (1987).

[135] A. C. D. van Enter and J. L. van Hemmen, J. Stat. Phys. **32**, 141 (1983); A. C. D. van Enter and J. L. van Hemmen, Phys. Rev. A **29**, 355 (1984).

[136] In an ultrametric space, the distance measure does not obey the triangle inequality, but the stronger relation $d(x,y) \leqslant \max[d(x,z),d(y,z)]$. Pictorially, the distances between any three points x, y, and z can only form an equilateral or an acute isosceles triangle.

[137] J. R. L. de Almeida and D. J. Thouless, J. Phys. A **11**, 983 (1978).

[138] M. Köhl, H. Moritz, T. Stöferle, K. Günter, and T. Esslinger, Phys. Rev. Lett. **94**, 080403 (2005).

[139] M. R. Andrews, M. O. Mewes, N. J. vanDruten, D. S. Durfee, D. M. Kurn, and W. Ketterle, Science **273**, 84 (1996); C. C. Bradley, C. A. Sackett, and R. G. Hulet, Phys. Rev. Lett. **78**, 985 (1997).

[140] R. Onofrio, C. Raman, J. M. Vogels, J. R. Abo-Shaeer, A. P. Chikkatur, and W. Ketterle, Phys. Rev. Lett. **85**, 2228 (2000).

[141] M. Greiner, O. Mandel, T. Rom, A. Altmeyer, A. Widera, T. W. Hänsch, and I. Bloch, Physica B **329**, 11 (2003).

[142] M. Ben Dahan, E. Peik, J. Reichel, Y. Castin, and C. Salomon, Phys. Rev. Lett. **76**, 4508 (1996); G. Roati, E. de Mirandes, F. Ferlaino, H. Ott, G. Modugno, and M. Inguscio, *ibid.* **92**, 230402 (2004).

[143] J. Stenger, S. Inouye, A. P. Chikkatur, D. M. Stamper-Kurn, D. E. Pritchard, and W. Ketterle, Phys. Rev. Lett. **82**, 4569 (1999); D. M. Stamper-Kurn, A. P. Chikkatur, A. Görlitz, S. Inouye, S. Gupta, D. E. Pritchard, and W. Ketterle, *ibid.* **83**, 2876 (1999).

[144] S. Richard, F. Gerbier, J. H. Thywissen, M. Hugbart, P. Bouyer, and A. Aspect, Phys. Rev. Lett. **91**, 010405 (2003); F. Gerbier, J. H. Thywissen, S. Richard, M. Hugbart, P. Bouyer, and A. Aspect, Phys. Rev. A **67**, 051602(R) (2003).

[145] G. V. Shlyapnikov, *Proceedings of the XVIII International Conference on Atomic Physics*, edited by H. R. Sadeghpour, D. E. Pritchard, and E. J. Heller (World Scientific, Singapore, 2002).

[146] P. Törmä and P. Zoller, Phys. Rev. Lett. **85**, 487 (2000); J. Kinnunen, M. Rodriguez, and P. Törmä, *ibid.* **92**, 230403 (2004); Science **305**, 1131 (2004); H.-P. Büchler, P. Zoller, and W. Zwerger, Phys. Rev. Lett. **93**, 080401 (2004).

[147] C. Chin, M. Bartenstein, A. Altmeyer, S. Riedl, S. Jochim, J. Hecker Denschlag, and R. Grimm, Science **305**, 1128 (2004).

[148] K. W. Madison, F. Chevy, W. Wohlleben, and J. Dalibard, Phys. Rev. Lett. **84**, 806 (2000).

[149] M. V. Zwierlein, J. R. Abo-Shaeer, A. Schirotzek, C. H. Schunck, and W. Ketterle, Nature (London) **435**, 1047 (2005).

[150] E. Altman, E. Demler, and M. D. Lukin, Phys. Rev. A **70**, 013603 (2004).

[151] J. Grondalski, P. M. Alsing, and I. H. Deutsch, Opt. Express **5**, 249 (1999); A. R. Kolovsky, Europhys. Lett. **68**, 330 (2004); R. Bach and K. Rzażewski, Phys. Rev. A **70**, 063622 (2004); L. Mathey, E. Altman, and A. Vishwanath, e-print cond-mat/0507108.

[152] S. Fölling, F. Gerbier, A. Widera, O. Mandel, T. Gericke, and I. Bloch, Nature (London) **434**, 481 (2005).

[153] M. Greiner, C. A. Regal, J. T. Stewart, and D. S. Jin, Phys. Rev. Lett. **94**, 110401 (2005).

[154] R. Roth and K. Burnett, J. Phys. B **37**, 3893 (2004).

[155] H.-P. Büchler and P. Zoller proposed to prepare arrays of 2D lattices with randomly distributed transverse columns of chains of auxiliary atoms that could serve as the same distribution of random scatterers in each 2D lattice.

Disorder versus the Mermin-Wagner-Hohenberg effect: From classical spin systems to ultracold atomic gases

J. Wehr,[1,2] A. Niederberger,[1] L. Sanchez-Palencia,[3] and M. Lewenstein[1,4]
[1]*ICREA and ICFO-Institut de Ciències Fotóniques, Parc Mediterrani de la Tecnologia, E-08860 Castelldefels (Barcelona), Spain*
[2]*Department of Mathematics, The University of Arizona, Tucson, Arizona 85721-0089, USA*
[3]*Laboratoire Charles Fabry de l'Institut d'Optique, CNRS and Univ. Paris-Sud, campus Polytechnique, RD 128, F-91127 Palaiseau cedex, France*
[4]*Institut für Theoretische Physik, Universität Hannover, D-30167 Hannover, Germany*
(Received 14 April 2006; revised manuscript received 27 October 2006; published 29 December 2006)

We propose a general mechanism of *random-field-induced order* (RFIO), in which long-range order is induced by a random field that breaks the continuous symmetry of the model. We particularly focus on the case of the classical ferromagnetic *XY* model on a two-dimensional lattice, in a uniaxial random field. We prove rigorously that the system has spontaneous magnetization at temperature $T=0$, and we present strong evidence that this is also the case for small $T>0$. We discuss generalizations of this mechanism to various classical and quantum systems. In addition, we propose possible realizations of the RFIO mechanism, using ultracold atoms in an optical lattice. Our results shed new light on controversies in existing literature, and open a way to realize RFIO with ultracold atomic systems.

DOI: 10.1103/PhysRevB.74.224448 PACS number(s): 75.10.Nr, 05.30.Jp, 64.60.Cn, 75.10.Jm

I. INTRODUCTION

A. Disordered ultracold quantum gases

Studies of disordered systems constitute a new, rapidly developing, branch of the physics of ultracold gases. In condensed-matter physics (CM), the role of *quenched* (i.e., independent of time) disorder cannot be overestimated: it is present in nearly all CM systems, and leads to numerous phenomena that dramatically change both qualitative and quantitave behaviors of these systems. This leads, for instance, to novel thermodynamical and quantum phases,[1,2] and to strong phenomena, such as Anderson localization.[3–6] In general, disorder can hardly be controlled in CM systems. In contrast, it has been proposed recently, that quenched disorder (or pseudodisorder) can be introduced in a controlled way in ultracold atomic systems, using optical potentials generated by speckle radiations,[7–9] impurity atoms serving as random scatterers,[10] or quasicrystalline lattices.[11] This opens fantastic possibilities to investigate the effect of disorder in controlled systems (for a review in the context of cold gases, see Ref. 12). Recently, several groups have initiated the experimental study of disorder with Bose-Einstein condensates (BEC),[13–15] and strongly correlated Bose gases.[16] In the center of interest of these works is one of the most fundamental issues of disordered systems that concerns the interplay between Anderson localization and interactions in many-body Fermi or Bose systems at low temperatures. In noninteracting atomic systems, localization is feasible experimentally,[17] but even weak interactions can drastically change the scenario. While weak repulsive interactions tend to delocalize, strong ones in confined geometries lead to Wigner-Mott-type localization.[18] Both experiments and theory indicate that in gaseous systems with large interactions, stronger localization effects occur in the excitations of a BEC,[14,19–21] rather than on the BEC wave function itself. In the limit of weak interactions, a Bose gase enters a *Lifshits glass* phase, in which several BECs in various localized single-atom orbitals from the low-energy tail of the spectrum coexist[22] (for "traces" of the Lifshits glass in the mean-field theory, see Ref. 15). Finally, note that disorder in Fermi gases, or in Femi-Bose atomic mixtures, should allow one to realize various fermionic disordered phases, such as a Fermi glass, a Mott-Wigner glass, "dirty" superconductors, etc.[12]), or even quantum spin glasses.[23]

B. Large effects by small disorder

One of the most appealing effects of disorder is that even extremely small randomness can have dramatic consequences. The paradigm example in classical physics is the Ising model for which an arbitrarily small random magnetic field destroys magnetization even at temperature $T=0$ in two-dimensions, 2D (Refs. 24 and 25), but not in $D>2$.[26] This result has been generalized to systems with continuous symmetry in random fields distributed in accordance with this symmetry.[24,25] For instance, the Heisenberg model in a SO(3) symmetrically distributed field does not magnetize up to four dimensions (4D).

In quantum physics, the paradigm example of large effects induced by small disorder is provided by the abovementioned Anderson localization, which occurs in one dimension and two dimensions in arbitrarily small random potentials.[5] In this paper, we propose an even more intriguing opposite effect, where disorder counterintuitively favors ordering: a general mechanism of *random-field-induced order* (RFIO) by which certain spin models magnetize at a higher temperature in the presence of arbitrarily small disorder than in its absence, provided that the disorder breaks the continuous symmetry of the system.

C. Main results and plan of the paper

As is well known, as a consequence of the Mermin-Wagner-Hohenberg theorem,[27] spin- or field-theoretic

systems with continuous symmetry in dimensions less or equal to 2D cannot exhibit long-range order. The mechanism that we propose here breaks the continuous symmetry, and in this sense acts against the Mermin-Wagner-Hohenberg no-go rule in 2D. In particular, we prove rigorously that the classical *XY* spin model on a 2D lattice in a uniaxial random field magnetizes spontaneously at $T=0$ in the *direction perpendicular* to the magnetic-field axis, and provide strong evidence that this is also the case at small positive temperatures. We discuss generalizations of this mechanism to classical and quantum *XY* and Heisenberg models in 2D and 3D. In 3D, the considered systems do exhibit long-range order at finite $T>0$, but in this case the critical temperature decreases with the "size" of the symmetry group: it is the largest for the Ising model (the discrete group Z_2), higher for the *XY* model [the continuous group U(1)], and the highest for the Heisenberg model [the continuous group SU(2) or SO(3)]. In this case we expect that our mechanism will lead to an increase of the critical temperature for the *XY* and Heisenberg models, and to an increase of the order-parameter value at a fixed temperature for the disordered system in comparison to the nondisordered one. Finally, we propose three possible and experimentally feasible realizations of the RFIO phenomenon using ultracold atoms in optical lattices.

The paper is organized as follows. In Sec. II, we present the results concerning the RFIO in the classical *XY* model on a 2D lattice. First, we rigorously prove that the system magnetizes in the direction perpendicular to the direction of the random magnetic field at $T=0$, and then, we present arguments that the magnetization persists in the small $T>0$ case, as well as the results of numerical classical Monte Carlo simulations. Section III is fully devoted to the discussion of the generalizations of the RFIO mechanism to several other classical and quantum spin systems. In Sec. IV, we discuss several experimentally feasible realizations of RFIO in ultracold atomic systems. Finally, we summarize our results in Sec. V.

II. RFIO IN CLASSICAL *XY* MODEL

A. System under study

Consider a classical spin system on the 2D square lattice $\mathbf{Z}^2$, in a random magnetic field $\mathbf{h}$ (see Fig. 1). The spin variable $\sigma_i=(\cos\theta_i,\sin\theta_i)$, at a site $i\in\mathbf{Z}^2$ is a unit vector in the *xy* plane. The Hamiltonian (in units of the exchange energy *J*) is given by

$$H/J=-\sum_{|i-j|=1}\sigma_i\cdot\sigma_j-\epsilon\sum_i \mathbf{h}_i\cdot\sigma_i. \tag{1}$$

Here the first term is the standard nearest-neighbor interaction of the *XY* model, and the second term represents a small random-field perturbation. The $\mathbf{h}_i$'s are assumed to be independent, identically distributed random, 2D vectors.

For $\epsilon=0$, the model has no spontaneous magnetization *m* at any positive *T*. This was first pointed out in Ref. 28, and later developed into a class of results known as the Mermin-Wagner-Hohenberg theorem[27] for various classical, as well as quantum 2D spin systems with continuous symmetry. In higher dimensions the system does magnetize at low temperatures. This follows from the spin-wave analysis,[29] and has been given a rigorous proof in Ref. 30. The impact of a random-field term on the behavior of the model was first addressed in Refs. 24 and 25, where it was argued that if the distribution of the random variables $\mathbf{h}_i$ is invariant under rotations, there is no spontaneous magnetization at any positive *T* in any dimension $D\leqslant 4$. A rigorous proof of this statement was given in Ref. 25. Both works use crucially the rotational invariance of the distribution of the random-field variables.

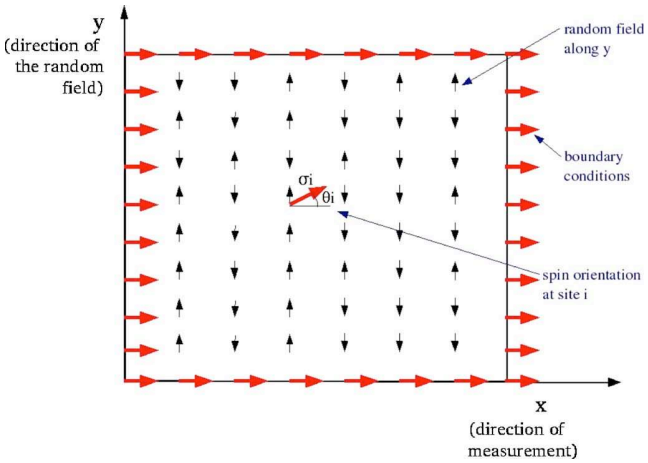

FIG. 1. (Color online) *XY* model on a 2D square lattice in a random magnetic field. The magnetic field is oriented along the *y* axis, $\mathbf{h}_i=\eta_i\mathbf{e}_y$, where η_i is a real random number. Right boundary conditions are assumed on the outer square, possibly placed at infinity (see text).

Here we consider the case where $\mathbf{h}_i$ is directed along the *y* axis: $\mathbf{h}_i=\eta_i\mathbf{e}_y$, where $\mathbf{e}_y$ is the unit vector in the *y* direction, and η_i is a random real number. Such a random field obviously breaks the continuous symmetry of the interaction and a question arises whether the model still has no spontaneous magnetization in two dimensions. This question has been given contradictory answers in Refs. 31 and 32: while Ref. 31 predicts that a small random field in the *y* direction does not change the behavior of the model, Ref. 32 argues that it leads to the presence of spontaneous magnetization *m* in the direction perpendicular to the random-field axis in low (but not arbitrarily low) temperatures. Both works use renormalization-group analysis, with Ref. 32 starting from a version of the Imry-Ma scaling argument to prove that the model magnetizes at zero temperature.

The same model was subsequently studied by Feldman,[33] using ideas similar to the argument given in the present paper. As we argue below, however, his argument contains an essential gap, which is filled in the present work. We first present a complete proof that the system indeed magnetizes at $T=0$, and argue that the ground-state magnetization is stable under inclusion of small thermal fluctuations. For this, we use a version of the Peierls contour argument,[34] eliminating first the possibility that Bloch walls or vortex configurations destroy the transition.

B. RFIO at $T=0$

Let us start by a rigorous analysis of the ground state. Consider the system in a square Λ with the "right" boundary conditions, $\sigma_i=(1,0)$, for the sites i on the outer boundary of Λ (see Fig. 1). The energy of any spin configuration decreases if we replace the x components of the spins by their absolute values and leave the y components unchanged. It follows that in the ground-state, x components of all the spins are nonnegative. As the size of the system increases, we expect the x component of the ground-state spins to decrease, since they feel less influence of the boundary conditions and the ground state value of each spin will converge. We thus obtain a well-defined infinite-volume ground state with the "right" boundary conditions at infinity.

We emphasize that the above convergence statement is nontrivial and requires a proof. Physically it is, however, quite natural. A similar statement has been rigorously proven for ground states of the random-field Ising model using Fortuin-Kasteleyn-Ginibre monotonicity techniques.[25,35]

C. Infinite volume limit

A priori this infinite-volume ground state could coincide with the ground state of the random field Ising model, in which all spins have zero x component. The following argument shows that this is *not* the case. Suppose that the spin σ_i at a given site i is aligned along the y axis, i.e., $\cos\theta_i=0$. Since the derivative of the energy function with respect to θ_i vanishes at the minimum, we obtain

$$\sum_{j:|i-j|=1} \sin(\theta_i-\theta_j)=0. \tag{2}$$

Since $\cos\theta_i=0$, this implies $\Sigma_{j:|i-j|=1}\cos\theta_j=0$. Because in the right ground state all spins lie in the (closed) right half-plane $x\geqslant 0$, all terms in the above expression are non-negative and hence have to vanish. This means that at all the nearest neighbors j of the site i, the ground-state spins are directed along the y axis as well. Repeating this argument, we conclude that the same holds for all spins of the infinite lattice, i.e., the ground state is the (unique) random-field Ising model ground state. This, however, leads to a contradiction, since assuming this, one can construct a field configuration, occurring with a positive probability, which forces the ground-state spins to have nonzero x components. To achieve this we put strong positive ($\eta_i>0$) fields on the boundary of a square and strong negative fields on the boundary of a concentric smaller square. If the fields are very weak in the area between the two boundaries, the spins will form a Bloch wall, rotating gradually from $\theta=\pi/2$ to $\theta=-\pi/2$. Since such a local field configuration occurs with a positive probability, the ground state *cannot have* zero x components everywhere, contrary to our assumption.

We would like to emphasize the logical structure of the above argument, which proceeds indirectly assuming that the ground-state spins (or, equivalently, at least one of them) have zero x components and reach a contradiction. The initial assumption is used in an essential way to argue existence of the Bloch wall interpolating between spins with y components equal to +1 and −1. It is this part of the argument that we think is missing in Ref. 33. Note that this argument applies to strong, as well as to weak random fields, so that the ground state is never, strictly speaking, field-dominated and always exhibits magnetization in the x direction. Moreover, the argument does not depend on the dimension of the system, applying, in particular, in one dimension. We argue below that in dimensions greater than one the effect still holds at small positive temperatures, the critical temperature depending on the strength of the random field (and presumably going to zero as the strength of the field increases).

D. RFIO at low positive T

To study the system at low positive T, we need to ask what are the typical low-energy excitations from the ground state. For $\epsilon=0$, continuous symmetry allows Bloch walls, i.e., configurations in which the spins rotate gradually over a large region, for instance from left to right. The total excitation energy of a Bloch wall in 2D is of order one, and it is the presence of such walls that underlies the absence of continuous symmetry breaking. However, for $\epsilon>0$, a Bloch wall carries additional energy, coming from the change of the direction of the y component of the spin, which is proportional to the area of the wall (which is of the order L^2 for a wall of linear size L in two dimensions), since the ground-state spins are adapted to the field configuration, and hence overturning them will increase the energy per site. Similarly, vortex configurations, which are important low-energy excitations in the nonrandom XY model, are no longer energetically favored in the presence of a uniaxial random field.

We are thus left, as possible excitations, with sharp domain walls, where the x component of the spin changes sign rapidly. To first approximation we consider excited configurations, in which spins take either their ground-state values, or the reflections of these values in the y axis. As in the standard Peierls argument,[34] in the presence of the right boundary conditions, such configurations can be described in terms of contours γ (domain walls), separating spins with positive and negative x components. If m_i is the value of the x component of the spin σ_i in the ground state with the right boundary conditions, the energy of a domain wall is the sum of $m_i m_j$ over the bonds (ij) crossing the boundary of the contour. Since changing the signs of the x components of the spins does not change the magnetic-field contribution to the energy, the Peierls estimate shows that the probability of such a contour is bounded above by $\exp(-2\beta\Sigma_{(ij)}m_i m_j)$, with $\beta=J/k_B T$.

We want to show that for a typical realization of the field $\mathbf{h}$, (i.e., with probability one), these probabilities are summable, i.e., their sum over all contours containing the origin in their interior is finite. It then follows that at a still lower T, this sum is small, and the Peierls argument proves that the system magnetizes (in fact, a simple additional argument shows that summability of the contour probabilities already implies the existence of spontaneous m). To show that a series of random variables is summable with probability one, it suffices to prove the summability of the series of the expected values. We present two arguments for the last statement to hold.

If the random variables m_i are bounded away from zero, i.e., $m_i > \sqrt{c}$, for some $c > 0$, the moment-generating function of the random variable $\Sigma_{(ij)} m_i m_j$ satisfies

$$\mathbf{E}\left[\exp\left(-\beta \sum_{(ij)} m_i m_j\right)\right] \leqslant \exp[-c\beta L(\gamma)], \tag{3}$$

with $L(\gamma)$ denoting the length of the contour γ. The sum of the probabilities of the contours enclosing the origin is thus bounded by $\Sigma_\gamma \exp[-c\beta L(\gamma)]$. The standard Peierls-Griffiths bound proves the desired summability.

The above argument does not apply if the distribution of the ground state m contains zero in its support. For unbounded distribution of the random field this may very well be the case, and then another argument is needed. If we assume that the terms in the sum $\Sigma_{(ij)} m_i m_j$ are independent and identically distributed, then $\mathbf{E}[\exp(-2\beta\Sigma_{(ij)} m_i m_j)] = \mathbf{E}[\exp(-2\beta m_i m_j)]^{L(\gamma)} = \exp\{L(\gamma) \log \mathbf{E}[\exp(-2\beta m_i m_j)]\}$ and we just need to observe that $\mathbf{E}[\exp(-2\beta m_i m_j)] \to 0$ as $\beta \to \infty$ (since the expression under the expectation sign goes pointwise to zero and lies between 0 and 1) to conclude that $\mathbf{E}[\exp(-2\beta\Sigma_{(ij)} m_i m_j)]$ behaves as $\exp[-g(\beta)L(\gamma)]$ for a positive function $g(\beta)$ with $g(\beta) \to \infty$ as $\beta \to \infty$. While $m_i m_j$ are not, strictly speaking, independent, it is natural to assume that their dependence is weak, i.e., their correlation decays fast with the distance of the corresponding bonds (ij). The behavior of the moment-generating function of their sum is then qualitatively the same, with a renormalized rate function $g(\beta)$, still diverging as $\beta \to \infty$. As before, this is enough to carry out the Peierls-Griffiths estimate, which implies spontaneous magnetization in the x direction. We remark that our assumption about the fast decay of correlations implies that the sums of $m_i m_j$ over subsets of $\mathbf{Z}^2$ satisfy a large deviation principle analogous to that for sums of independent random variables and the above argument can be restated using this fact.

E. Numerical Monte Carlo simulations

Based on the above discussion it is expected that the RFIO effect predicted here will lead to the appearance of magnetization m in the x direction of order 1 at low temperatures in systems much larger than the correlation length of typical excitations. For small systems, however, the effect may be obscured by finite size effects, which, due to long-range power-law decay of correlations, are particularly strong in the XY model in 2D. In particular, the 2D XY model shows finite magnetization (m) in small systems,[36] so that RFIO is expected to result in an increase of the magnetization.

We have performed numerical Monte Carlo simulations[37] for the 2D XY classical model [Hamiltonian (1), with $\epsilon = 1$]. We generate a random magnetic field $\mathbf{h}_i = \eta_i \mathbf{e}_y$ in the y direction. The η_i's are independent random real numbers, uniformly distributed in $[-\sqrt{3}\Delta h^y, \sqrt{3}\Delta h^y]$. Note that Δh^y is thus the standard deviation of the random field $\mathbf{h}_i$. Boundary conditions on the outer square correspond to $\sigma_i = (1,0)$ (see Fig. 1). The calculations were performed in 2D lattices with up to 200×200 lattice sites for various temperatures. The results are presented in Fig. 2.

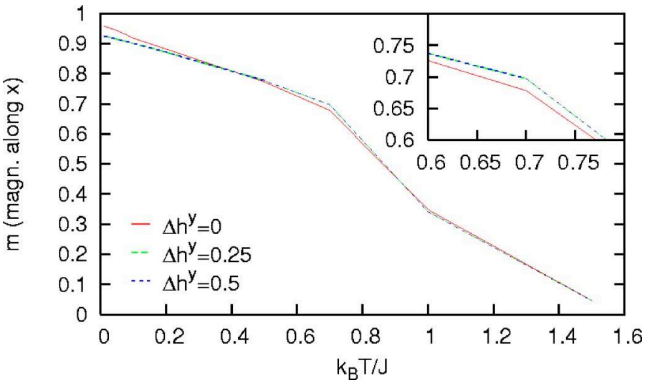

FIG. 2. (Color online) Results of the Monte Carlo simulation for the classical 2D XY model in a 200×200 lattice. The inset is a magnetification of the main figure close to $T = 0.7J/k_B$.

At very small temperature, the system magnetizes in the absence of disorder (m approaches 1 when T tends to 0) due to the finite size of the lattice.[36] In this regime, a random field in the y direction tends to induce a small local magnetization, parallel to $\mathbf{h}_i$, so that the magnetization in the x direction, m, is slightly reduced. At higher temperatures ($T \simeq 0.7J/k_B$ in Fig. 2), the magnetization is significantly smaller than one in the absence of disorder. This is due to non-negligible spin-wave excitations. In the presence of small disorder, these excitations are suppressed due to the RFIO effect discussed in this paper. We indeed find that, at $T = 0.7J/k_B$, m increases by 1.6% in presence of the uniaxial disordered magnetic field. At larger temperatures, excitations, such as Bloch walls or vortices are important and no increase of the magnetization is found when applying a small random field in the y direction.

III. RFIO IN OTHER SYSTEMS

The RFIO effect predicted above may be generalized to other spin models, in particular, those that have finite correlation length. Here we list the most spectacular generalizations:

A. Heisenberg ferromagnet (HF) in random fields of various symmetries

Here the interaction has the same form as in the XY case, but spins take values on a unit sphere. As for the XY Hamiltonian, if the random-field distribution has the same symmetry as the interaction part, i.e., if it is symmetric under rotations in three dimensions, the model has no spontaneous magnetization up to four dimensions.[24,25] If the random field is uniaxial, e.g., oriented along the z axis, the system still has a continuous symmetry (rotations in the xy plane), and thus cannot have spontaneous magnetization in this plane. It cannot magnetize in the z direction either, by the results of Ref. 25. Curiously enough, a field distribution with an intermediate symmetry may lead to symmetry breaking. Namely, arguments fully analogous to the previous ones imply that if the random field takes values in the yz plane with a distribution invariant under rotations, the system will magnetize in

the x direction. We are thus faced with the possibility that a planar-field distribution breaks the symmetry, while this is broken neither by a field with a spherically symmetric distribution nor by a uniaxial one.

B. Three-dimensional *XY* and Heisenberg models in a random field of various symmetries

We have argued that the 2D XY model with a small uniaxial random field orders at low T. Since in the absence of the random field spontaneous magnetization occurs only at $T=0$, this can be equivalently stated by saying that a small uniaxial random field raises the critical temperature T_c of the system. By analogy, one can expect that the (nonzero) T_c of the XY model in 3D becomes higher and comparable to that of the 3D Ising model, in the presence of a small uniaxial field. A simple mean-field estimate suggests that T_c might increase by a factor of 2. The analogous estimates for the Heisenberg model in 3D suggest an increase of T_c by a factor 3/2 (or 3) in a small uniaxial (or planar rotationally symmetric) field, respectively. These conjectures are the subject of a forthcoming project.

C. Antiferromagnetic systems

By flipping every second spin, the classical ferromagnetic models are equivalent to antiferromagnetic ones (on bipartite lattices). This equivalence persists in the presence of a random field with a distribution symmetric with respect to the origin. Thus the above discussion of the impact of random fields on continuous symmetry breaking in classical ferromagnetic models translates case by case to the antiferromagnetic case.

D. Quantum systems

All of the effects predicted above should, in principle, have quantum analogs. Quantum fluctuations might, however, destroy the long-range order, so each of the discussed models should be carefully reconsidered in the quantum case. Some models, such as the quantum spin $S=1/2$ Heisenberg model, for instance, have been widely studied in literature.[38] The Mermin-Wagner theorem[27] implies that the model has no spontaneous magnetization at positive temperatures in 2D. For $D>2$ spin-wave analysis[39–41] shows the existence of spontaneous magnetization (though a rigorous mathematical proof of this fact is still lacking). In general, one does not expect major differences between the behaviors of the two models at $T\neq 0$. It thus seems plausible that the presence of a random field in the quantum case is going to have effects similar to those in the classical Heisenberg model. Similarly, one can consider the quantum Heisenberg antiferromagnet (HAF) and expect phenomena analogous to the classical case, despite the fact that unlike their classical counterparts, the quantum HF and HAF systems are no longer equivalent. We expect to observe spontaneous staggered magnetization in a random uniaxial XY model, or random planar field HF. A possibility that a random field in the z direction can enhance the antiferromagnetic order in the xy plane has been pointed out in Ref. 42.

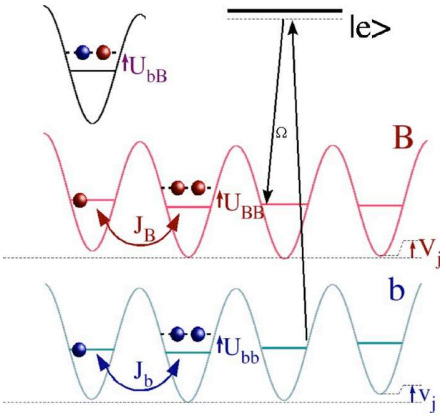

FIG. 3. (Color online) Atomic-level scheme of a two-component Bose mixture in a random optical lattice used to design spin models in random magnetic fields (see text).

IV. TOWARDS THE EXPERIMENTAL REALIZATION OF RFIO IN ULTRACOLD ATOMIC SYSTEMS

Further understanding of the phenomena described in this paper will benefit from experimental realizations and investigations of the above-mentioned models. Below, we discuss the possibilities to design quantum simulators for these quantum spin systems using ultracold atoms in optical lattices (OL).

A. Two-component lattice Bose gas

Consider a two-component Bose gas confined in an OL with on-site inhomogeneities. The two components correspond here to two internal states of the same atom. The low-T physics is captured by the Bose-Bose Hubbard model (BBH) (Ref. 43) (for a review of ultracold lattice gases see Ref. 44):

$$H_{\mathrm{BBH}} = \sum_j \left[\frac{U_b}{2}\mathbf{n}_j(\mathbf{n}_j-1) + \frac{U_B}{2}\mathbf{N}_j(\mathbf{N}_j-1) + U_{bB}\mathbf{n}_j\mathbf{N}_j \right] + \sum_j (v_j\mathbf{n}_j + V_j\mathbf{N}_j) - \sum_{\langle j,l\rangle} [(J_b\mathbf{b}_j^\dagger\mathbf{b}_l + J_B\mathbf{B}_j^\dagger\mathbf{B}_l) + \mathrm{H.c.}] - \sum_j \left(\frac{\Omega_j}{2}\mathbf{b}_j^\dagger\mathbf{B}_j + \mathrm{H.c.} \right), \quad (4)$$

where $\mathbf{b}_j$ and $\mathbf{B}_j$ are the annihilation operators for both types of bosons in the lattice site j, $\mathbf{n}_j=\mathbf{b}_j^\dagger\mathbf{b}_j$ and $\mathbf{N}_j=\mathbf{B}_j^\dagger\mathbf{B}_j$ are the corresponding number operators, and $\langle j,l\rangle$ denote a pair of adjacent sites in the OL. In Hamiltonian (4), (i) the first term describes on-site interactions, including interaction between bosons of different types, with energies U_b, U_B, and U_{bB}; (ii) the second accounts for on-site energies; (iii) the third describes quantum tunneling between adjacent sites, and (iv) the fourth transforms one boson type into the other with a probability amplitude $|\Omega|/\hbar$. The last term can be implemented with an optical two-photon Raman process if the two Bosonic "species" correspond to two internal states of the same atom (see also Fig. 3). Possibly, both on-site energies v_j, V_j, and the Raman complex amplitude Ω_j can be made site-dependent using speckle laser light.[13–15]

Consider the limit of strong repulsive interactions $(0<J_b,J_B,|\Omega_j|\ll U_b,U_B,U_{Bb})$ and a total filling factor of 1 (i.e., the total number of particles equals the number of lattice sites). Proceeding as in the case of Fermi-Bose mixtures, recently analyzed by two of the authors in Ref. 23, we derive an effective Hamiltonian, $H_{\rm eff}$, for the Bose-Bose mixture. In brief, we restrict the Hilbert space to a subspace $\mathcal{E}_0$ generated by $\{\Pi_j|n_j,N_j\rangle\}$ with $n_j+N_j=1$ at each lattice site, and we incorporate the tunneling terms via second-order perturbation theory as in Ref. 23 We then end up with

$$H_{\rm eff}=-\sum_{\langle j,l\rangle}(J_{j,l}\mathcal{B}_j^\dagger\mathcal{B}_l+\text{H.c.})+\sum_{\langle j,l\rangle}K_{j,l}\mathcal{N}_j\mathcal{N}_l+\sum_j\mathcal{V}_j\mathcal{N}_j-\sum_j\left(\frac{\Omega_j}{2}\mathcal{B}_j+\text{H.c.}\right),\tag{5}$$

where $\mathcal{B}_j=\mathbf{b}_j^\dagger\mathbf{B}_j\mathcal{P}$, $\mathcal{P}$ is the projector onto $\mathcal{E}_0$ and $\mathcal{N}_j=\mathcal{B}_j^\dagger\mathcal{B}_j$. Hamiltonian $H_{\rm eff}$ contains (i) a hopping term $J_{j,l}$, (ii) an interaction term between neighbor sites $K_{j,l}$, (iii) inhomogeneities $\mathcal{V}_j$, and (iv) a creation/annihilation term. Note that the total number of composites is not conserved except for a vanishing Ω. The coupling parameters in Hamiltonian (5) are (Ref. 45):

$$J_{j,l}=\frac{J_bJ_B}{U_{bB}}\left[\frac{1}{1-\left(\frac{\delta_{j,l}}{U_{bB}}\right)^2}+\frac{1}{1-\left(\frac{\Delta_{j,l}}{U_{bB}}\right)^2}\right],\tag{6}$$

$$K_{j,l}=-\frac{4J_b^2/U_b}{1-\left(\frac{\delta_{j,l}}{U_b}\right)^2}+\frac{2J_b^2/U_{bB}}{1-\left(\frac{\delta_{j,l}}{U_{bB}}\right)^2}-\frac{4J_B^2/U_B}{1-\left(\frac{\Delta_{j,l}}{U_B}\right)^2}+\frac{2J_B^2/U_{bB}}{1-\left(\frac{\Delta_{j,l}}{U_{bB}}\right)^2},\tag{7}$$

$$\mathcal{V}_j=V_j-v_j+\sum_{\langle j,l\rangle}\left[\frac{4J_b^2/U_b}{1-\left(\frac{\delta_{j,l}}{U_b}\right)^2}-\frac{J_b^2/U_{bB}}{1-\frac{\delta_{j,l}}{U_{bB}}}-\frac{J_B^2/U_{bB}}{1+\frac{\Delta_{j,l}}{U_{bB}}}+\frac{4J_B^2/U_B}{1-\left(\frac{\Delta_{j,l}}{U_B}\right)^2}\right],\tag{8}$$

where $\delta_{j,l}=v_j-v_l$ and $\Delta_{j,l}=V_j-V_l$. Hamiltonian $H_{\rm eff}$ describes the dynamics of *composite particles* whose annihilation operator at site j is $\mathcal{B}_j=\mathbf{b}_j^\dagger\mathbf{B}_j\mathcal{P}$. In contrast to the case of Fermi-Bose mixtures discussed in Ref. 23, where the composites are fermions, in the present case of Bose-Bose mixtures, they are *composite Schwinger bosons* made of one B boson and one b hole.

Since the commutation relations of $\mathcal{B}_j$ and $\mathcal{B}_j^\dagger$ are those of Schwinger bosons,[46] we can directly turn to the spin representation[46] by defining $\mathbf{S}_j^x+i\mathbf{S}_j^y=\mathcal{B}_j$ and $\mathbf{S}_j^z=1/2-\mathcal{N}_j$, where $\mathcal{N}_j=\mathcal{B}_j^\dagger\mathcal{B}_j$. It is important to note that since Raman processes can convert b bosons into B bosons (and conversely), $\Sigma_j\langle\mathcal{N}_j\rangle$ *is not fixed* by the total number of bosons of each species, i.e., the z component of m, $\Sigma_j\langle\mathbf{S}_j^z\rangle$ is not constrained. For small inhomogeneities $(\delta_{j,l}=v_j-v_l,\Delta_{j,l}=V_j-V_l\ll U_b,U_b,U_{bB})$, Hamiltonian $H_{\rm eff}$ is then equivalent to the anisotropic Heisenberg XXZ model[46] in a random field

$$H_{\rm eff}=-J_\perp\sum_{\langle j,l\rangle}(\mathbf{S}_j^x\mathbf{S}_l^x+\mathbf{S}_j^y\mathbf{S}_l^y)-J_z\sum_{\langle j,l\rangle}\mathbf{S}_j^z\mathbf{S}_l^z-\sum_j(h_j^x\mathbf{S}_j^x+h_j^y\mathbf{S}_j^y+h_j^z\mathbf{S}_j^z),\tag{9}$$

where

$$J_\perp=\frac{4J_bJ_B}{U_{bB}},\tag{10}$$

$$J_z=2\left(\frac{2J_b^2}{U_b}+\frac{2J_B^2}{U_B}-\frac{J_b^2+J_B^2}{U_{\rm bB}}\right),\tag{11}$$

$$h_j^x=\Omega_j^R,\quad h_j^y=-\Omega_j^I,\quad h_j^z=\mathcal{V}_j-\zeta J_z/2,\tag{12}$$

with ζ the lattice coordination number, $\mathcal{V}_j=V_j-v_j+\zeta[4J_b^2/U_b+4J_B^2/U_B-(J_b^2+J_B^2)/U_{bB}]$ and $\Omega_j=\Omega_j^R+i\Omega_j^I$. In atomic systems, all these (possibly site-dependent) terms can be controlled almost at will.[23,44,47] In particular, by employing various possible control tools one can reach the HF $(J_\perp=J_z)$ and XY $(J_z=0)$ cases.

B. Bose lattice gas embedded in a BEC

The quantum ferromagnetic XY model in a random field may be alternatively obtained using the same BBH model, but with strong state dependence of the optical dipole forces. One can imagine a situation in which one component (say b) is in the strong interaction limit, so that only one b atom at a site is possible, whereas the other (B) component is in the Bose condensed state and provides only a coherent BEC "background" for the b atoms. Mathematically speaking, this situation is described by Eq. (4), in which n_i's can be equal to 0 or 1 only, whereas B_i's can be replaced by a classical complex field (condensate wave function). In this limit the spin $S=1/2$ states can be associated with the presence or absence of a b atom in a given site. In this way, setting $v_j=0$ and $\Omega_j^I=0$, one obtains the quantum version of the XY model (1) with $J=J_b$ and a uniaxial random field in the x direction with the strength determined by Ω_j^R.

C. Two-component Fermi lattice gas

Finally, the $S=1/2$ antiferromagnetic Heisenberg model may be realized with a fermi-fermi mixture at half filling for each component. This implementation might be of special importance for future experiments with lithium atoms. As recently calculated,[48] the critical temperature for the Néel state in a 3D cubic lattice is of the order of 30 nK. It is well known that in a 3D cubic lattice the critical temperatures for the antiferromagnetic Heisenberg, the XY and the Ising models are $T_{c,XY}\simeq 1.5T_{c,Heis}$, and $T_{c,Ising}\simeq 2T_{c,Heis}$. The estimates of these critical temperatures can be, for instance, obtained applying the Curie-Weiss mean-field method to the classical models. Suppose that we put the Heisenberg antiferromagnet

in a uniaxial (respectively, planar) random field, created using the same methods as discussed above, i.e., we break the SU(2) symmetry and put the system into the universality class of *XY* (respectively, Ising) models. Mean-field estimates suggest then that we should expect the increase of the critical temperature by factor 1.5 (respectively, 2), that is, up to $\simeq$45 (respectively, 90) nK. Even if these estimates are too optimistic, and the effect is two or three times smaller, one should stress, that even an increase by, say 10 nK, is of great experimental relevance and could be decisive for the achievment of an antiferromagnetic state.

We would like to stress that similar proposals, as the three discussed above, have been formulated before,[49] but none of them treat simultaneously essential aspects for the present schemes: (i) disordered fields, but not bonds; (ii) arbitrary directions of the fields; (iii) possibility of exploring Ising, *XY*, or Heisenberg symmetries; (iv) realizing the coherent source of atoms; and (v) avoiding constraints on the magnetization along the z axis.

It is also worth commenting on what are the most important experimental challenges that have to be addressed in order to achieve RFIO. Evidently, for the proposals involving the strong interaction limit of two-component Bose or Fermi systems, the main issue is the temperature, which has to be of the order of tens of nanokelvins. Such temperatures are starting to be achievable nowadays (for a careful discussion in the context of Fermi-Bose mixtures see Ref. 50), and there exist several proposals for supplementary cooling of lattice gases, using laser (photons) or couplings to ultracold BEC (phonon cooling) that can help [for reviews see Refs. 44 and 47].

V. SUMMARY

In this paper, we have proposed a general mechanism of *random-field-induced order* (RFIO), occurring in systems with continuous symmetry, placed in a random field that breaks, or reduces this symmetry. We have presented rigorous results for the case of the 2D classical ferromagnetic *XY* model in a random uniaxial field, and proved that the system has spontaneous magnetization at temperature $T=0$. We have presented also a rather strong evidence that this is also the case for small $T>0$. Several generalizations of this mechanism to various classical and quantum systems were discussed. We have presented also detailed proposals to realize RFIO in experiments using two-component Bose lattice gases, one-component Bose lattice gases embedded in BECs, or two-component Fermi lattice gases. Our results shed light on controversies in existing literature, and open the way to realize RFIO with ultracold atoms in an optical lattice.

It is worth mentioning two further realizations of RFIO studied by us recently. RFIO occurs in a two-component trapped Bose gas at $T=0$, when the gas is condensed and the two components are coupled by Raman transition of random strength, but fixed phase. Although such a system belongs to the universality class of the (trapped, i.e., located in an inhomogenous field) *XY* model, it exhibits the RFIO effect in a much stronger manner than the *XY* model discussed in the present paper. We have found this observation important enough to devote a separate detailed paper to it.[51] Similarly, we have studied numerically RFIO in 1D for quantum *XY* and Heisenberg chains.[52] In such systems, even at $T=0$, magnetization vanishes, but amazingly enough the RFIO effect seems to work at the level of the magnetic susceptibilities. Adding a random field confined to a certain axis (respectively, plane), *increases* siginificantly the magnetic suceptibility in the perpedicular directions (respectively, direction).

ACKNOWLEDGMENTS

We thank I. Bloch, T. Roscilde, and C. Salomon for very enlightening discussions. We acknowledge the support of DFG, ESF Programme QUDEDIS, Spanish MEC Grant No. FIS2005-04627, Acciones Integradas and Consolider QOIT, EU IP SCALA, the Délégation Générale de l'Armement, the Ministère de la Recherche, the Agence Nationale de la Recherche, the European Union, and INTAS. LCFIO is a member of the Institut Francilien de Recherche sur les Atomes Froids (IFRAF).

[1] I. M. Lifshits, S. A. Gredeskul, and L. A. Pastur, *Introduction to the Theory of Disordered Systems* (Wiley, New York, 1988).

[2] E. Akkermans and G. Montambaux, *Physique Mésoscopique des Électrons et des Photons* (EDP Science, Paris, 2004); *Mesoscopic Physics of Electrons and Photons* (Cambridge University Press, Cambrigde, 2006).

[3] P. W. Anderson, Phys. Rev. **109**, 1492 (1958).

[4] N. F. Mott and W. D. Towes, Adv. Phys. **10**, 107 (1961); R. Borland, Proc. R. Soc. London, Ser. A **274**, 529 (1963); B. I. Halperin, Adv. Chem. Phys. **13**, 123 (1968).

[5] E. Abrahams, P. W. Anderson, D. C. Licciardello, and T. V. Ramakrishnan, Phys. Rev. Lett. **42**, 673 (1979).

[6] B. van Tiggelen, in *Wave Diffusion in Complex Media*, Lectures Notes at Les Houches 1998, edited by J. P. Fouque, NATO Science (Kluwer, Dordrecht, 1999).

[7] B. Damski, J. Zakrzewski, L. Santos, P. Zoller, and M. Lewenstein, Phys. Rev. Lett. **91**, 080403 (2003).

[8] R. Roth and K. Burnett, J. Opt. Soc. Am. B **5**, S50 (2003); R. Roth and K. Burnett, Phys. Rev. A **68**, 023604 (2003).

[9] G. Grynberg, P. Horak, and C. Mennerat-Robilliard, Europhys. Lett. **49**, 424 (2000); L. Guidoni, C. Triché, P. Verkerk, and G. Grynberg, Phys. Rev. Lett. **79**, 3363 (1997).

[10] U. Gavish and Y. Castin, Phys. Rev. Lett. **95**, 020401 (2005) P. Massignan and Y. Castin, Phys. Rev. A **74**, 013616 (2006).

[11] L. Sanchez-Palencia and L. Santos, Phys. Rev. A **72**, 053607 (2005).

[12] V. Ahufinger, L. Sanchez-Palencia, A. Kantian, A. Sanpera, and M. Lewenstein, Phys. Rev. A **72**, 063616 (2005).

[13] J. E. Lye, L. Fallani, M. Modugno, D. S. Wiersma, C. Fort, and M. Inguscio, Phys. Rev. Lett. **95**, 070401 (2005); C. Fort, L.

Fallani, V. Guarrera, J. E. Lye, M. Modugno, D. S. Wiersma, and M. Inguscio, *ibid.* **95**, 170410 (2005).
[14] D. Clément, A. F. Varón, M. Hugbart, J. A. Retter, P. Bouyer, L. Sanchez-Palencia, D. M. Gangardt, G. V. Shlyapnikov, and A. Aspect, Phys. Rev. Lett. **95**, 170409 (2005); D. Clément, A. F. Varón, J. A. Retter, L. Sanchez-Palencia, A. Aspect, and P. Bouyer, New J. Phys. **8**, 165 (2006).
[15] T. Schulte, S. Drenkelforth, J. Kruse, W. Ertmer, J. Arlt, K. Sacha, J. Zakrzewski, and M. Lewenstein, Phys. Rev. Lett. **95**, 170411 (2005); T. Schulte, S. Drenkelforth, J. Kruse, R. Tiemeyer, K. Sacha, J. Zakrzewski, M. Lewenstein, W. Ertmer, and J. J. Arlt, New J. Phys. **8**, 290 (2006).
[16] L. Fallani, J. E. Lye, V. Guarrera, C. Fort, and M. Inguscio, cond-mat/0603655 (unpublished).
[17] R. C. Kuhn, C. Miniatura, D. Delande, O. Sigwarth, and C. A. Müller, Phys. Rev. Lett. **95**, 250403 (2005).
[18] M. P. A. Fisher, P. B. Weichman, G. Grinstein, and D. S. Fisher, Phys. Rev. B **40**, 546 (1989); R. T. Scalettar, G. G. Batrouni, and G. T. Zimanyi, Phys. Rev. Lett. **66**, 3144 (1991).
[19] N. Bilas and N. Pavloff, Eur. Phys. J. D **40**, 387 (2006).
[20] T. Paul, P. Leboeuf, N. Pavloff, K. Richter, and P. Schlagheck, Phys. Rev. A **72**, 063621 (2005).
[21] L. Sanchez-Palencia, Phys. Rev. A **74**, 053625 (2006).
[22] P. Lugan, D. Clément, P. Bouyer, A. Aspect, M. Lewenstein, and L. Sanchez-Palencia, cond-mat/0610389 (unpublished).
[23] A. Sanpera, A. Kantian, L. Sanchez-Palencia, J. Zakrzewski, and M. Lewenstein, Phys. Rev. Lett. **93**, 040401 (2004).
[24] Y. Imry and S. Ma, Phys. Rev. Lett. **35**, 1399 (1975).
[25] M. Aizenman and J. Wehr, Phys. Rev. Lett. **62**, 2503 (1989); Commun. Math. Phys. **130**, 489 (1990).
[26] J. Z. Imbrie, Phys. Rev. Lett. **53**, 1747 (1984); J. Bricmont and A. Kupiainen, *ibid.* **59**, 1829 (1987).
[27] D. Mermin and H. Wagner, Phys. Rev. Lett. **17**, 1133 (1966); P. C. Hohenberg, Phys. Rev. **158**, 383 (1967).
[28] C. Herring and C. Kittel, Phys. Rev. **81**, 869 (1951).
[29] J. Zinn-Justin, *Quantum Field Theory and Critical Phenomena* (Oxford Science Publication, Oxford, 1989).
[30] J. Fröhlich, B. Simon, and T. Spencer, Commun. Math. Phys. **50**, 79 (1976); for more general proofs, see T. Bałaban, *ibid.* **167**, 103 (1995); **182**, 675 (1996).
[31] V. S. Dotsenko and M. V. Feigelman, J. Phys. C **14**, L823 (1981); Zh. Eksp. Teor. Fiz. **83**, 345 (1982) [Sov. Phys. JETP **56**, 189 (1982)].
[32] B. J. Minchau and R. A. Pelcovits, Phys. Rev. B **32**, 3081 (1985).
[33] D. E. Feldman, J. Phys. A **31**, L177 (1998).
[34] R. Peierls, Proc. Cambridge Philos. Soc. **32**, 477 (1936); R. B. Griffiths, Phys. Rev. **136**, A437 (1964).
[35] C. M. Fortuin, J. Ginibre, and P. W. Kasteleyn, Commun. Math. Phys. **22**, 89 (1971).
[36] S. T. Bramwell and P. C. W. Holdsworth, Phys. Rev. B **49**, 8811 (1994).
[37] Routines from the ALPS project (http://alps.comp-phys.org/) have been used to perform our classical Monte Carlo calculations. For details, see F. Alet *et al.*, J. Phys. Soc. Jpn. **74**, 30 (2005); M. Troyer, B. Ammon, and E. Heeb, Lect. Notes Comput. Sci. **1505**, 191 (1998).
[38] See for instance, G. Misguich and C. Lhuillier, in *Frustrated Spin Systems*, edited by H. T. Diep (World-Scientific, Singapore, 2004); C. Lhuillier, cond-mat/0502464 (unpublished) and references therein.
[39] F. Bloch, Z. Phys. **61**, 206 (1930).
[40] F. Dyson, Phys. Rev. **102**, 1217 (1956); **102**, 1230 (1956).
[41] N. W. Ashcroft and N. D. Mermin, *Solid State Physics* (Saunders College Publishing, New York, 1976).
[42] C. Huscroft and R. T. Scalettar, Phys. Rev. B **55**, 1185 (1997).
[43] D. Jaksch, C. Bruder, J. I. Cirac, C. W. Gardiner, and P. Zoller, Phys. Rev. Lett. **81**, 3108 (1998).
[44] M. Lewenstein, A. Sanpera, V. Ahufinger, B. Damski, A. Sen(De), and U. Sen, cond-mat/0606771, Adv. Phys. (to be published).
[45] The coupling parameters are the same as calculated in Refs. 12 and 23 except for the third term in Eq. (7), which correspondence to a virtual state with two B bosnos in the same lattice site—forbidden for fermions.
[46] A. Auerbach, *Interacting Electrons and Quantum Magnetism* (Springer-Verlag, Berlin, 1994).
[47] D. Jaksch and P. Zoller, Ann. Phys. **52**, 315 (2005).
[48] F. Werner, O. Parcollet, A. Georges, and S. R. Hassan, Phys. Rev. Lett. **95**, 056401 (2005).
[49] L.-M. Duan, E. Demler, and M. D. Lukin, Phys. Rev. Lett. **91**, 090402 (2003); A. B. Kuklov and B. V. Svistunov, *ibid.* **90**, 100401 (2003); J. J. García-Ripoll, M. A. Martin-Delgado, and J. I. Cirac, *ibid.* **93**, 250405 (2004); D. Porras and J. I. Cirac, *ibid.* **92**, 207901 (2004); A. Micheli, G. K. Brennen, and P. Zoller, Nat. Phys. **2**, 341 (2006).
[50] H. Fehrmann, M. A. Baranov, B. Damski, M. Lewenstein, and L. Santos, Opt. Commun. **243**, 23 (2004).
[51] K. Sacha *et al.* (unpublished).
[52] J. Dziarmaga *et al.* (unpublished).

Disorder-Induced Order in Two-Component Bose-Einstein Condensates

A. Niederberger,[1] T. Schulte,[1,2] J. Wehr,[1,3] M. Lewenstein,[1,4] L. Sanchez-Palencia,[5] and K. Sacha[1,6]

[1]*ICFO-Institut de Ciències Fotòniques, Parc Mediterrani de la Tecnologia, E-08860 Castelldefels (Barcelona), Spain*
[2]*Institut für Quantenoptik, Leibniz Universität Hannover, D-30167 Hannover, Germany*
[3]*Department of Mathematics, The University of Arizona, Tucson, Arizona 85721-0089, USA*
[4]*ICREA-Instituciò Catalana de Ricerca i Estudis Avançats, E-08010 Barcelona, Spain*
[5]*Laboratoire Charles Fabry de l'Institut d'Optique, CNRS and Univ. Paris-Sud, Campus Polytechnique, RD 128, F-91127 Palaiseau cedex, France*
[6]*Marian Smoluchowski Institute of Physics and Mark Kac Complex Systems Research Centre, Jagiellonian University, Reymonta 4, PL-30059 Kraków, Poland*

(Received 11 July 2007; published 24 January 2008)

We propose and analyze a general mechanism of *disorder-induced order* in two-component Bose-Einstein condensates, analogous to corresponding effects established for XY spin models. We show that a random Raman coupling induces a relative phase of $\pi/2$ between the two BECs and that the effect is robust. We demonstrate it in one, two, and three dimensions at $T = 0$ and present evidence that it persists at small $T > 0$. Applications to phase control in ultracold spinor condensates are discussed.

DOI: 10.1103/PhysRevLett.100.030403 PACS numbers: 05.30.Jp, 03.75.Hh, 03.75.Mn, 64.60.Cn

Degenerate quantum gases offer unprecedented control tools [1], opening fascinating possibilities, e.g., investigations of quantum disordered systems [2]. Current experimental [3–5] and theoretical [5–8] works are mainly devoted to studies of the interplay between disorder and nonlinearity in Bose-Einstein condensates (BEC) in a quest for traces of Anderson localization. In the regime of strong correlations, evidence for the Bose glass phase has been reported [9], and even more exotic quantum phases have been proposed [2,10].

Weak disorder can have strong effects also in classical systems. For instance, a general mechanism of *random-field-induced order* (RFIO) has been proposed recently [11,12]. It is responsible for ordering in graphene quantum Hall ferromagnets [13], ^{3}He-A in aerogel and amorphous ferromagnets [14], as well as for inducing superfluidity in hardcore bosonic systems [15]. This effect is best understood in classical ferromagnetic XY models in the presence of uniaxial random magnetic fields. For the 2D square lattice, the Hamiltonian reads

$$H = -\sum_{|i-j|=1} \boldsymbol{\sigma}_i \cdot \boldsymbol{\sigma}_j - \sum_i \mathbf{h}_i \cdot \boldsymbol{\sigma}_i, \qquad (1)$$

where the spins are unit 2D vectors in the XY plane: $\boldsymbol{\sigma}_i = (\cos\theta_i, \sin\theta_i)$ at site $i \in \mathbf{Z}^2$. When $\mathbf{h} \equiv 0$ the system does not magnetize as a consequence of the Mermin-Wagner-Hohenberg (MWH) theorem [16]. In contrast, a weak uniaxial random field $\mathbf{h}_i$ breaks the continuous $U(1)$ symmetry. Then, the MWH theorem does not apply and the system spontaneously magnetizes with a nonzero component of the magnetization perpendicular to the random field. This has been proven at zero temperature and strong arguments have been given that the effect persists at small temperatures [11]. Hamiltonian (1) can be realized with ultracold atoms in optical lattices, but the effect is rather weak [11].

In this Letter, we propose an analogue of the RFIO effect using two BECs trapped in harmonic potentials and coupled via a real-valued random Raman field. We show that the mean-field Hamiltonian of the two-component BEC is analogous to the XY spin Hamiltonian (1), with the Raman coupling playing the same role as the magnetic field in Eq. (1), and the relative phase between the BECs corresponding to the spin angle θ_i. Then, the RFIO effect shows up in the form of a relative phase between the BECs fixed at a value of $\pm\pi/2$. The finite-size two-component BEC system is continuous and formally equivalent to the discrete spin system (1) on an infinite lattice. We find that even in low dimensions, the RFIO effect is much more pronounced and robust in coupled trapped BECs than it is in uniform lattice spin models. Note that trapped (finite-size) BECs at sufficiently small T show true long range order also in one and two dimensions as phase fluctuations take place on a scale larger than the size of the systems [17]. We demonstrate the effect in one, two, and three dimensions at $T = 0$ and present strong evidence that it persists for small $T > 0$.

Interestingly, the RFIO effect is quite general. For instance, consider the two-spin lattice Hamiltonian:

$$H = -\sum_{|i-j|=1} (\boldsymbol{\sigma}_i \cdot \boldsymbol{\sigma}_j + \boldsymbol{\tau}_i \cdot \boldsymbol{\tau}_j) - \sum_i \Omega_i \boldsymbol{\sigma}_i \cdot \boldsymbol{\tau}_i, \qquad (2)$$

where Ω_i are independent real-valued random couplings with (identical) symmetric distributions. In this system, it can be proven rigorously that there is no first order phase transition with the order parameter $\boldsymbol{\sigma}_i \cdot \boldsymbol{\tau}_i$ in dimensions $d \leq 4$ [18]. More precisely, in every infinite-dimensional Gibbs state (phase), the disorder average of the thermal mean $\langle \boldsymbol{\sigma}_i \cdot \boldsymbol{\tau}_i \rangle$ takes the same value. By symmetry, this

value has to be zero, implying that the average cosine of the angle between $\boldsymbol{\sigma}_i$ and $\boldsymbol{\tau}_i$ is zero. At $T = 0$, these results also apply [18] and are consistent, by analogy, with the relative phase $\pi/2$ of two randomly coupled BECs, discussed below.

We consider a trapped two-component Bose gas with repulsive interactions and assume that the two components consist of the same atomic species in two different internal states, coupled via a position-dependent (random, quasirandom, or just oscillating) real-valued Raman field $\Omega(\mathbf{r})$ of mean zero ($\int \Omega d\mathbf{r} = 0$). The typical amplitude and spatial variation scale of $\Omega(\mathbf{r})$ are denoted by Ω_R and λ_R. At sufficiently small T, the trapped gases form BECs which can be represented by the classical fields $\psi_{1,2}(\mathbf{r})$ in the mean-field approximation. The energy functional of the system then reads

$$E = \int d\mathbf{r}[(\hbar^2/2m)|\nabla\psi_1|^2 + V(\mathbf{r})|\psi_1|^2 + (g_1/2)|\psi_1|^4 + (\hbar^2/2m)|\nabla\psi_2|^2 + V(\mathbf{r})|\psi_2|^2 + (g_2/2)|\psi_2|^4 + g_{12}|\psi_1|^2|\psi_2|^2 + (\hbar\Omega(\mathbf{r})/2)(\psi_1^*\psi_2 + \psi_2^*\psi_1)], \quad (3)$$

where $V(\mathbf{r})$ is the confining potential, and $g_i = 4\pi\hbar^2 a_i/m$ and $g_{12} = 4\pi\hbar^2 a_{12}/m$ are the intra- and interstate coupling constants, with a_i and a_{12} the scattering lengths and m the atomic mass. The last term in Eq. (3) represents the Raman coupling which can change the internal state of the atoms.

The ground state of the coupled two-component BEC system is obtained by minimizing E as a function of the fields ψ_1 and ψ_2 under the constraint of a fixed total number of atoms $N = \int d\mathbf{r}(|\psi_1|^2 + |\psi_2|^2)$. This leads to a set of two coupled Gross-Pitaevskii equations (GPE):

$$\mu\psi_i = [-\hbar^2\nabla^2/2m + V + g_i|\psi_i|^2 + g_{12}|\psi_{\bar{i}}|^2]\psi_i + (\hbar\Omega/2)\psi_{\bar{i}}, \quad (4)$$

with μ the chemical potential and $\bar{i} = 2(1)$ for $i = 1(2)$.

At equilibrium, for $\Omega_R = 0$ and $g_1, g_2 > g_{12}$, the BECs are miscible [19]. Their phases θ_i are uniform, arbitrary and independent. Now, a weak Raman coupling ($\hbar|\Omega_R| \ll \mu$) does not noticeably affect the densities. However, arbitrarily small $\Omega(\mathbf{r})$ breaks the continuous $U(1)$ symmetry with respect to the relative phase of the BECs and, following the results of Refs. [11,12,18], the relative phase can be expected to be fixed. To make this clearer, we neglect the changes of the densities when the weak Raman coupling is turned on and analyze the phases. For simplicity we suppose $g_1 = g_2$ and $\rho(\mathbf{r}) = \rho_1(\mathbf{r}) = \rho_2(\mathbf{r})$. The substitution $\psi_i = e^{i\theta_i(\mathbf{r})}\sqrt{\rho(\mathbf{r})}$ in the energy functional (3) leads to $E = E_0 + \Delta E$ where E_0 is the energy for $\Omega_R = 0$ and

$$\Delta E = \int d\mathbf{r}\rho(\mathbf{r})\left[\frac{\hbar^2}{4m}(\nabla\theta)^2 + \hbar\Omega(\mathbf{r})\cos\theta\right] + \int d\mathbf{r}\rho(\mathbf{r})\frac{\hbar^2}{4m}(\nabla\Theta)^2, \quad (5)$$

where $\Theta = \theta_1 + \theta_2$ and $\theta = \theta_1 - \theta_2$. Minimizing ΔE implies $\Theta = \text{const}$; hence, the second line in Eq. (5) vanishes and the only remaining dynamical variable in the model is the relative phase θ between the BECs. Note that if $\rho_1 \neq \rho_2$ the variables Θ and θ are coupled and one cannot consider them independent (the $\rho_1 \neq \rho_2$ case is analyzed in the sequel). Equation (5) is equivalent to the classical field description of the spin model (1) in the continuous limit, where the relative phase $\theta(\mathbf{r})$ represents the spin angle and the Raman coupling $\Omega(\mathbf{r})$ plays the role of the magnetic field. Thus, we expect RFIO [11] to show up in the form $\cos\theta \simeq 0$ for weak random $\Omega(\mathbf{r})$.

Let us examine Eq. (5) in more detail. It represents a competition between the kinetic term which is minimal for uniform θ and the potential term which is minimal when the sign of $\cos\theta$ is opposite to that of $\Omega(\mathbf{r})$. For $\hbar\Omega_R \gg \hbar^2/2m\lambda_R^2$, the potential term dominates and θ will vary strongly on a length scale of the order of λ_R. In contrast, if $\hbar\Omega_R \ll \hbar^2/2m\lambda_R^2$ the kinetic term is important and forbids large modulations of θ on scales of λ_R. The Euler-Lagrange equation of the functional (5) is

$$\nabla[\rho(\mathbf{r})\nabla\theta] + \frac{2m}{\hbar}\rho(\mathbf{r})\Omega(\mathbf{r})\sin\theta = 0. \quad (6)$$

For the homogeneous case ($\rho = \text{const}$) and for slowly varying densities (neglecting the term $\nabla\rho$), assuming small variations of the relative phase, $\theta(\mathbf{r}) = \theta_0 + \delta\theta(\mathbf{r})$ with $|\delta\theta| \ll \pi$, the solution of Eq. (6) reads

$$\delta\hat{\theta}(\mathbf{k}) \simeq (2m/\hbar)[\hat{\Omega}(\mathbf{k})/|\mathbf{k}|^2]\sin\theta_0 \quad (7)$$

in Fourier space. Inserting Eq. (7) into Eq. (5), we find

$$\Delta E \simeq -m\rho\int d\mathbf{k}(|\hat{\Omega}(\mathbf{k})|^2/|\mathbf{k}|^2)\sin^2\theta_0. \quad (8)$$

The energy is thus minimal for $\theta_0 = \pm\pi/2$, i.e., $\cos\theta_0 = 0$. This indicates RFIO in the two-component BEC system owing to the breaking of the continuous $U(1)$ symmetry of the coupled GPEs. For a random Raman coupling, even if the resulting fluctuations of θ are not small, the average phase is locked at $\theta_0 = \pm\pi/2$. Note that if $\theta(\mathbf{r})$ is a solution of Eq. (6), so is $-\theta(\mathbf{r})$. This follows from the fact that for any solution (ψ_1, ψ_2) of the GPEs (4), (ψ_1^*, ψ_2^*) is also a solution with the same chemical potential. The sign of θ_0 thus depends on the realization of the BECs and is determined by spontaneous breaking of the $\theta \leftrightarrow -\theta$ symmetry.

Let us turn to numerics starting with $g_1 = g_2$. For homogeneous ($\rho = \text{const}$) gases, we solve Eq. (6). Figure 1 shows an example for a 1D two-component BEC, where $\Omega(x)$ is a quasirandom function chosen as a sum of two sine functions with incommensurate spatial periods. The *dynamical* system (6) is not integrable. It turns out that the solution we are interested in corresponds to a hyperbolic periodic *orbit* surrounded by a considerable chaotic sea. Figure 1 confirms that $\theta(x)$ oscillates around $\theta_0 \simeq \pm\pi/2$. The oscillations of $\theta(x)$ are weak and follow

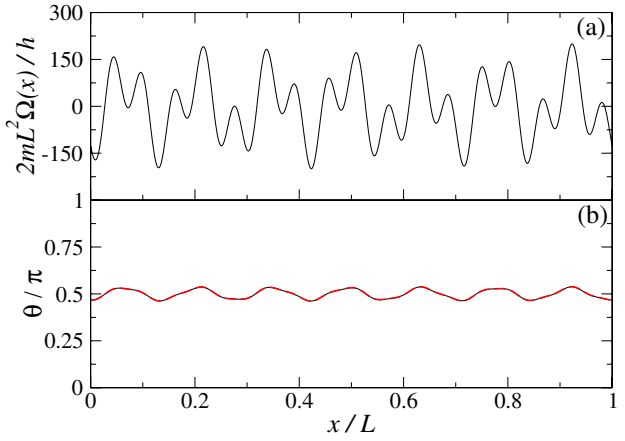

FIG. 1 (color online). RFIO effect in a 1D two-component BEC trapped in a box of length L and in a quasirandom Raman field. Panel (a) Raman coupling function $\Omega(x) = -100(\hbar/2mL^2)\{\sin(x/\lambda_R + 0.31) + \sin[x/(2.44\lambda_R) + 1.88]\}$ with $\lambda_R = 0.009\,39L$. Panel (b) Relative phase $\theta(x) = \theta_1(x) - \theta_2(x)$ obtained by solving Eq. (6) numerically (solid black line) and comparison with Eq. (7) (dashed red line—nearly identical to the solid black line).

the prediction (7), which in one dimension, after inverse Fourier transform, corresponds to the double integral of $\Omega(x)$.

For trapped gases and for $g_1 \neq g_2$ we directly solve the coupled GPEs (4). Figure 2 shows the results for a 1D two-component BEC in the Thomas-Fermi regime confined in a harmonic trap with a random $\Omega(x)$. A typical realization is shown in Fig. 2(a). For each realization of $\Omega(x)$, the resulting relative phase θ can change significantly but only on a scale much larger than λ_R because $\hbar\Omega_R \ll \hbar^2/2m\lambda_R^2$, as shown in Fig. 2(b). However, averaging over many realizations of the random Raman coupling and keeping only those with $\int \theta(x)dx > 0$ (resp. <0), we obtain $\langle\theta(x)\rangle \approx \pi/2$ $(-\pi/2)$, with the standard deviation about 0.3π as shown in Fig. 2(c).

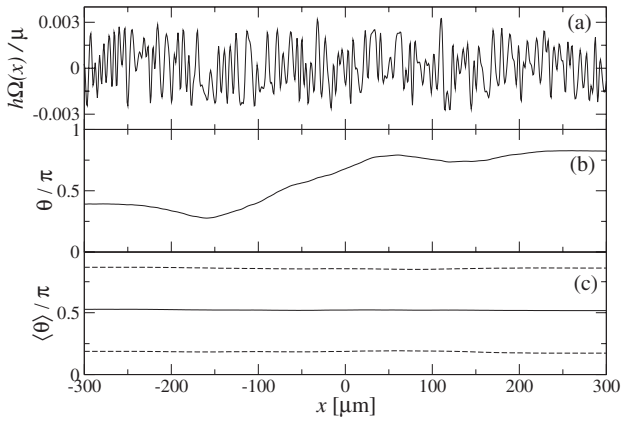

FIG. 2. RFIO effect in very elongated (effectively 1D) trapped BECs. The data correspond to ^{87}Rb atoms in two different internal states in an anisotropic harmonic trap with frequencies $\omega_x = 2\pi \times 10$ Hz and $\omega_\perp = 2\pi \times 1.8$ kHz. The total number of atoms is $N = 10^4$ and the scattering lengths are $a_1 = 5.77$ nm, $a_2 = 6.13$ nm and $a_{12} = 5.53$ nm. Panel (a) Single realization of the random Raman coupling $\hbar\Omega/\mu$ for $\lambda_R = 10^{-2}L_{TF}$ and $\hbar\Omega_R \simeq 3 \times 10^{-3}\mu$. Panel (b) Relative phase θ corresponding to $\Omega(x)$ shown in panel (a). Panel (c) θ averaged over many realizations of $\Omega(x)$ (solid line) and the averaged value $\pm$ standard deviation (dashed lines). In panel (c) the solutions with $\int \theta dx > 0$ only are collected (the other class of solutions with $\theta \to -\theta$ is not included).

The dynamical stability of the solutions of the GPEs (4) found in the 1D trapped geometry can be tested by means of the Bogoliubov–de Gennes (BdG) theory which allows also to estimate the quantum depletion of the BECs [20]. The BdG analysis shows that the solutions of the GPEs (4) are indeed stable and that the BdG spectrum is not significantly affected by the Raman coupling. It implies that turning on the Raman field does not change the thermodynamical properties of the system, and the RFIO effect should persist for sufficiently low $T > 0$. Note that the GPEs (4) possess also a solution with both components real. However, this solution is dynamically unstable. In fact, there is a BdG mode associated with an imaginary eigenvalue and the corresponding BECs phases (under a small perturbation) will evolve exponentially in time. In addition, the BdG analysis shows that the quantum depletion is about 1% and can therefore be neglected.

Calculations in two and three dimensions—whose detailed results will be published soon—show essentially the same disorder-induced ordering effect in all dimensions. For example, Fig. 3 shows the result for two coupled 3D BECs in a spherically symmetric harmonic trap. Here, the Raman coupling is a sum of quasirandom functions similar to that used for Fig. 1 in each spatial direction and with $\hbar\Omega_R \simeq 10^{-2}\mu$. The density modulations are found to be negligible. However, even for this low value

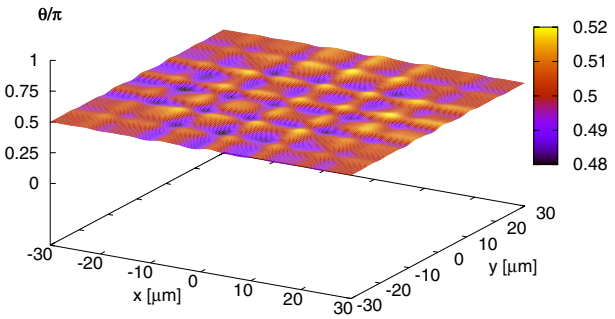

FIG. 3 (color online). RFIO effect in a 3D two-component BEC trapped in a spherically symmetric harmonic trap with frequency $\omega = 2\pi \times 30$ Hz. The total number of atoms is $N = 10^5$, the scattering lengths are as in Fig. 2 and we use a quasirandom Raman coupling $\Omega(x, y, z) \propto \sum_{u\in\{x,y,z\}}[\sin(u/\lambda_R) + \sin(u/(1.71\lambda_R))]$ with $\lambda_R = 4.68\,\mu$m$/2\pi$ and $\hbar\Omega_R \simeq 5 \times 10^{-3}\mu$. Shown is the relative phase θ in the plane $z = 0$ μm in units of π.

of the Raman coupling, Fig. 3 shows that the relative phase is fixed around $\theta_0 = \pi/2$ with small fluctuations. Other calculations confirm that the sign of θ_0 is random but with $|\theta_0| = \pi/2$ for all realizations of $\Omega(\mathbf{r})$ and that the weaker the Raman coupling, the smaller the modulations of $\theta(\mathbf{r})$ around θ_0. This shows once again the enormous robustness of RFIO in two-component BECs.

In summary, we have shown that RFIO occurs in a system of two BECs coupled via a real-valued random Raman field. It has been demonstrated in one, two, and three dimensions for homogeneous or trapped BECs. The signature of RFIO is a fixed relative phase between the BECs around $\theta_0 = \pm\pi/2$. For quasirandom Raman coupling, the fluctuations can be very small (0.05π for the parameters used in Fig. 1). For completely random Raman coupling the fluctuations can be larger (about 0.3π for the parameters used in Fig. 2). Interestingly, the two-component BEC system is continuous and RFIO is stronger and more robust than in lattice spin Hamiltonians of realistic sizes [11]. RFIO can thus be obtained in current experiments with two-component BECs [21,22] and observed using matterwave interferometry techniques [22].

Apart from its fundamental importance, RFIO can have applications for engineering and manipulations of quantum states by providing a simple and robust method to control phases in ultracold gases. We find particularly interesting applications of phase control in spinor BECs and, more generally, in ultracold spinor gases [1]. For example, in a ferromagnetic spinor BEC with $F = 1$ as in ^{87}Rb, the wave function is $\xi \propto [e^{-i\phi}\cos^2(\theta/2), \sqrt{2}\sin(\theta/2) \times \cos(\theta/2), e^{+i\phi}\cos^2(\theta/2)]$, the components correspond to $m_F = 1\ 0, -1$ and the direction of magnetization is $\vec{n} = (\sin\theta\cos\phi, \sin\theta\sin\phi, \cos\theta)$. Applying two real-valued random Raman couplings between $m_F = 0$ and $m_F = \pm 1$, fixes $\phi = 0$ or π;, i.e., the magnetization will be in the XZ plane. By applying two random real-valued Raman couplings between $m_F = 0$ and $m_F = 1$ and between $m_F = -1$ and $m_F = 1$, we force the magnetization to be along $\pm Z$. Similar effects occur in antiferromagnetic spinor BECs with $F = 1$, as ^{14}Na. Using Raman transitions with arbitrary phases, employing more couplings, and higher spins F offers a variety of control tools in ultracold spinor gases.

We acknowledge support of EU IP Program "SCALA", ESF PESC Program "QUDEDIS", Spanish MEC grants (No. FIS 2005-04627, Conslider Ingenio 2010 "QOIT"), and French DGA, IFRAF, MENRT, and ANR. J. W. was partially supported by NSF Grant No. DMS 0623941. K. S. acknowledges Polish Government scientific funds (2005-2008) as a research project and M. Curie ToK project COCOS (No. MTKD-CT-2004-517186).

[1] M. Lewenstein *et al.*, Adv. Phys. **56**, 243 (2007).
[2] V. Ahufinger *et al.*, Phys. Rev. A **72**, 063616 (2005).
[3] J. E. Lye *et al.*, Phys. Rev. Lett. **95**, 070401 (2005); C. Fort *et al.*, *ibid.* **95**, 170410 (2005).
[4] D. Clément *et al.*, Phys. Rev. Lett. **95**, 170409 (2005); D. Clément *et al.*, New J. Phys. **8**, 165 (2006).
[5] T. Schulte *et al.*, Phys. Rev. Lett. **95**, 170411 (2005); T. Schulte *et al.*, New J. Phys. **8**, 230 (2006).
[6] L. Sanchez-Palencia, Phys. Rev. A **74**, 053625 (2006); P. Lugan *et al.*, Phys. Rev. Lett. **98**, 170403 (2007).
[7] L. Sanchez-Palencia *et al.*, Phys. Rev. Lett. **98**, 210401 (2007); T. Paul *et al.*, *ibid.* **98**, 210602 (2007).
[8] N. Bilas and N. Pavloff, Eur. Phys. J. D **40**, 387 (2006); P. Lugan *et al.*, Phys. Rev. Lett. **99**, 180402 (2007).
[9] L. Fallani *et al.*, Phys. Rev. Lett. **98**, 130404 (2007).
[10] A. De Martino *et al.*, Phys. Rev. Lett. **94**, 060402 (2005); T. Roscilde and J. I. Cirac, *ibid.* **98**, 190402 (2007).
[11] J. Wehr, A. Niederberger, L. Sanchez-Palencia, and M. Lewenstein, Phys. Rev. B **74**, 224448 (2006).
[12] A. Aharony, Phys. Rev. B **18**, 3328 (1978); B. J. Minchau and R. A. Pelcovits, Phys. Rev. B **32**, 3081 (1985); D. E. Feldman, J. Phys. A **31**, L177 (1998).
[13] D. A. Abanin, P. A. Lee, and L. S. Levitov, Phys. Rev. Lett. **98**, 156801 (2007).
[14] I. A. Fomin, J. Low Temp. Phys. **138**, 97 (2005); JETP Lett. **85**, 434 (2007); G. E. Volovik, *ibid.* **81**, 647 (2005).
[15] J.-W. Lee, S. Chandrasekharan, and H. U. Baranger, arXiv:cond-mat/0611109.
[16] D. Mermin and H. Wagner, Phys. Rev. Lett. **17**, 1133 (1966); P. C. Hohenberg, Phys. Rev. **158**, 383 (1967).
[17] D. S. Petrov, D. M. Gangardt, and G. V. Shlyapnikov, J. Phys. IV France **116**, 5 (2004).
[18] M. Aizenman and J. Wehr, Phys. Rev. Lett. **62**, 2503 (1989); Commun. Math. Phys. **130**, 489 (1990).
[19] T.-L. Ho and V. B. Shenoy, Phys. Rev. Lett. **77**, 3276 (1996).
[20] See, for example, L. P. Pitaevskii and S. Stringari, *Bose-Einstein Condensation* (Oxford University, New York, 2003).
[21] M. R. Matthews *et al.*, Phys. Rev. Lett. **81**, 243 (1998); D. S. Hall *et al.*, Phys. Rev. Lett. **81**, 1539 (1998).
[22] D. S. Hall *et al.*, Phys. Rev. Lett. **81**, 1543 (1998).

CONCLUSIONS AND PERSPECTIVES

In brief – *The field of disordered quantum gases is just emerging. Recent success in observing Anderson localization open unprecedented paths to pursue many outstanding challenges in the more general field of disordered systems. Direct extensions include studies of metal-insulator transitions in dimensions higher than one, and of the effect of weak interactions on localization, for which many questions are debated. For stronger interactions, single-particle localization is usually destroyed, but new concepts such as many-body Anderson localization and Bose glasses provide original paradigms, which renew our understanding of these issues. Experiments on ultracold atoms with controlled disorder and controlled interactions can also be extended to other systems where disorder plays important roles. For instance, combining spin-exchange implementation and disorder opens the route towards random field-induced order and spin glasses.*

The impressive progress realized in the field of ultracold quantum gases during the past decades now opens a new frontier, *i.e.* the realization of quantum simulators to address unsolved questions in complex systems, where exact analytic calculations or systematic numerical simulations cannot be performed. This line of research is developing rapidly, and several landmark results have been reported, which bridge the gap between ultracold atoms and condensed-matter physics, a major field where quantum simulators would be very useful. So far, true simulators have hardly been realized and the field is rather at the stage of validating advanced experiments as possible simulators [see for instance (Trotsky *et al.*, 2010)].

Research on disordered quantum gases belongs to this more general trend, and is just emerging. The realization that disorder can be introduced in ultracold atomic systems in a controlled way paved the way to investigations of fundamental phenomena relevant to the whole field of disordered systems (Damski *et al.*, 2003; Roth and Burnett, 2003) and has triggered intensive theoretical and experimental research in a quest for the 'holy grail', *i.e.* Anderson localization of matter-waves (Clément *et al.*, 2006; Fallani *et al.*, 2008; Aspect and Inguscio, 2009; Sanchez-Palencia and Lewenstein, 2010). In 2008, the groups of Alain Aspect at Institut d'Optique and of Massimo Inguscio at LENS succeeded in observing direct evidence of Anderson localization of non-interacting particles in one-dimensional systems (Billy *et al.*, 2008; Roati *et al.*, 2008). Let us stress that the key ingredients of this success have been i) accurate control of the disorder, ii) negligible inter-atomic interactions, iii) strong isolation from the environment, iv) direct imaging of density profiles and last but not least v) joint theoretical and experimental efforts. Most probably, combination of all these features will also be the key of future breakthrough works in the field of

quantum gases, in particular in the context of disordered gases.

In this manuscript, we have reported our recent contributions to the field, performed first in Hannover (2003-2004) and then at Institut d'Optique (2004-2009). These concern single-particle localization in speckle potentials and quasi-periodic lattices (Chap. 2), the interplay of weak repulsive interactions and localization is Bose gases (Chap. 3), as well as effects of disorder in Bose-Bose and Fermi-Bose mixtures and the possibility of simulating spin-like systems with ultracold atoms (Chap. 4). Rather than commenting these results[7], let us elaborate on possible future directions. The latter are personal views of the author, who does not claim they would be exhaustive. On the other hand, they definitely owe much to many fascinating and illuminating discussions with my estimated colleagues at Institut d'Optique, in particular Alain Aspect and Philippe Bouyer, as well as with my invaluable collaborator, Maciej Lewenstein.

At a time when the field of disordered quantum gases reaches a certain maturity, two main research lines may be foreseen. The first line, which is widely considered in the community, consists in extending the experiments of Institut d'Optique and LENS towards two- and three-dimensional systems, and/or including atom-atom interactions. The second line consists in proposing new routes and new challenges. In this respect, simulators for strongly-correlated and spin systems are very promising. Hence, next outstanding challenges for disordered quantum gases are:

- Anderson localization of non-interacting quantum particles in dimensions one, two and three;
- The role of inter-particle interactions on localization;
- Strongly-correlated disordered systems (and the associated Bose or Fermi glasses);
- Spin systems with random exchange coupling terms (and the associated spin glasses).

All correspond to basic, open questions on disordered systems, which ultracold atoms could help answer. Besides new experiments, they call for advanced theoretical work on disordered quantum gases. In the following, we elaborate on some possible routes, which in our view are the most promising.

Anderson localization of ultracold atoms - Ultracold atomic gases have allowed the first direct observation of Anderson localization of a matter-wave, thus realizing a situation very close to the problem considered by Anderson in 1958 (Aspect and Inguscio, 2009). This constitutes a landmark step towards realizing quantum simulators for disordered systems in more complicated and challenging situations (Sanchez-Palencia and Lewenstein, 2010). However, as pointed out in the introduction, although ultracold atoms are very well controlled systems, they do not only simply reproduce exactly standard toy-models of condensed-matter physics, but introduce new ingredients, and thus new questions. This should not be considered a drawback of ultracold atomic systems, but conversely an opportunity. It indeed opens new horizons to further deepen our knowledge of Anderson localization in various directions. An example directly relevant to Anderson localization of matterwaves (Billy *et al.*, 2008), is that speckle potentials form an original class of disorder, where effective mobility edges exist in one dimension [see Sec. 2.3.3 and (Sanchez-Palencia *et al.*, 2007; Gurevich and Kenneth, 2009; Lugan *et al.*, 2009)]. Let us discuss two other interesting examples.

The first example concerns the behavior of localization versus the system parameters, which can be studied quantitatively with ultracold atoms. Anderson localization is sparked by elemen-

[7] Details can be found in the previous pages or in the summaries at the beginning of each chapter.

tary scattering processes of a probe particle from the asperities of the disordered potential. Localization is thus expected to be stronger when scattering is stronger, *i.e.* usually when the energy of the particle is lower. This leads to the intuitive result that the localization length increases when the energy of the probe particle decreases. In contrast to classical particles however, scattering of quantum particles need not be monotonous as a function of the particle energy, and classic examples are known from undergraduate courses of quantum mechanics. In principle, there is thus no reason that localization would always decrease with the particle energy. Together with Marie Piraud, we have recently shown that in certain one-dimensional speckle potentials, the localization length can indeed decrease when the energy increases in some region of the spectrum. In order to access this counter-intuitive situation, one has to design the autocorrelation function of the speckle potential in a proper way, which is possible with speckle potentials (Piraud, 2009). The solution we have proposed can be very easily designed in current experiments. The non-trivial question is however, how to observe this phenomena, which is not possible with expanding schemes such as that used by Billy *et al.* (2008).

The second example is the effect of harmonic trapping on localization. This question is relevant to ultracold gases produced at equilibrium in disordered potentials since they are almost always confined in harmonic traps (Fallani *et al.*, 2007; Roati *et al.*, 2008; White *et al.*, 2008; Pasienski *et al.*, 2010; Deissler *et al.*, 2010). Let us consider again usual disordered potentials for which the localization increases with the particle energy E. In infinite space, the typical size of states, $\Delta r(E)$ –which can be measured as the participation length[8] or the rms size for instance– thus increases from very low values to infinity when E increases. In a finite flat box of linear length L, $\Delta r(E)$ is bounded above to a value of the order of L, since all states are ultimately confined by the box edges. Hence, in a harmonic trap, one would expect that finite-size effects also limit the value of $\Delta r(E)$, however with an energy-dependent bound $l(E) \propto \sqrt{E}$, that is the extension of the eigenstate of energy E in a non-disordered harmonic trap. In fact, we have shown, together with Luca Pezzé, that harmonic trapping leads to a much more subtle situation. We found that at intermediate energies, localized and extended states coexist. This result was completely unexpected because, in homogeneous disorder (even in a finite box), localized and extended states do not coexist in the same energy region. The argument is that, should they coexist, an arbitrary small change of the disordered potential would hybridize them, thus forming two new extended states (Mott, 1990). Hence, when averaging over the disorder, coexistence is highly improbable[9]. The interesting point is that the argument does not hold in a disordered trap because inhomogeneous trapping allows for slight spatial segregation, which suppresses hybridization (Pezzé *et al.*, 2011).

Anderson localization in 2D and 3D speckle potentials - So far, experimental investigation of localization with ultracold atoms restricted to one-dimensional systems (Clément *et al.*, 2005; Fort *et al.*, 2005; Billy *et al.*, 2008; Roati *et al.*, 2008). Dimension $d = 1$ is a special case because non-interacting particles are localized for arbitrary energy (E) and strength of disorder. Moreover, exact analytical methods to calculate the localization length are known (Lifshits *et al.*,

[8] In the presence of the harmonic trap, which we consider here, the long-distance exponential tails of localized states are suppressed due to the trap. The localization length is thus not an adequate quantity to measure localization. Here, we refer to the participation length, which measures the typical size of a state, irrespective to the behavior of the tails (see Sec. 3.4.1 for instance).

[9] In other words, in a localized (resp. extended) regime, the ensemble of extended (resp. localized) states is of zero measure.

1988). Higher dimensions are much more demanding, and neither analytic methods nor even basic knowledge of one-dimensional Anderson localization can be easily extended to two and three dimensions. Higher dimensions actually show richer behavior, with the possibility of diffusive and localization regimes, as well as critical behaviors, which are not fully understood (see Sec. 2.1).

An interesting consequence is the existence of a localization-delocalization transition (the Anderson transition) in three dimensions. In continuous space, while the mobility edge $E_{\rm mob}$, which separates localized (for $E < E_{\rm mob}$) and extended (for $E > E_{\rm mob}$) states can be estimated from phenomenological arguments (Ioffe and Regel, 1960; Mott, 1967), a formidable task for the theory of disordered systems is to determine its precise value. Even more challenging is the design of a theory able to reproduce the critical exponents ν and s of the Anderson transition, such that the localization length diverges as $L_{\rm loc} \propto (E_{\rm mob} - E)^{-\nu}$ and the diffusion coefficient vanishes as $D_* \propto (E - E_{\rm mob})^s$. The value of $\nu = s \simeq 1.57$ in the three-dimensional case is now precise known from numerical calculations performed in the Anderson model (MacKinnon and Kramer, 1983; Schreiber and Grussbach, 1996; Slevin *et al.*, 2001) and is believed to be universal. The challenge to experiments on ultracold atoms is to provide useful insights in the critical region, able to suggest a key theoretical step ahead.

In two dimensions, scattering processes are strong enough that diffusive trajectories always loop back to their origin and interference of paths propagated in opposite ways are important. Hence, Anderson localization occurs for any energy in two dimensional systems, as in one dimension. Major interest in two-dimensional systems is that the scaling theory of localization (Abrahams *et al.*, 1979) predicts that $d = 2$ is the marginal dimension for the Anderson transition (*i.e.* there is a transition if and only if $d > 2$). It is thus expected that inter-particle interactions strongly affect Anderson localization in two-dimensional systems (Kravchenko *et al.*, 1994; Kravchenko *et al.*, 1995; Abrahams *et al.*, 2001). Precise characterization of localization lengths for non-interacting particles in two dimensions is thus crucial with a view towards studying later the effects of interactions. Experimentalists at Institut d'Optique have recently made the first step in that direction (Robert-de-Saint-Vincent *et al.*, 2010).

Spectacular success in observing one-dimensional Anderson localization (Billy *et al.*, 2008; Roati *et al.*, 2008) and the possibility of measuring precisely localization lengths as a function of the particle energy are thus of great promise to shed new light on these challenging issues in two and three dimensions.

Interplay of weak interactions and disorder in quantum gases at equilibrium - Ultracold atoms also allows us to study the effect of disorder in systems at equilibrium, rather than in transport schemes. This offers a complementary approach to localization phenomena, a route chosen in the experiments at LENS (Roati *et al.*, 2008), Hannover (Schulte *et al.*, 2005) and Urbana Champain (White *et al.*, 2009; Pasienski *et al.*, 2010). It is particularly promising as regards studies of the effects of interactions on localization (Giamarchi and Schulz, 1988; Fisher *et al.*, 1989). In previous studies (Lugan *et al.*, 2007a; Falco *et al.*, 2009), the properties of disordered Bose gases with weak repulsive interactions have been discussed and we have been able to work out a generic quantum-state diagram (see Sec. 3.4). This diagram has been qualitatively confirmed in recent experiments at LENS (Deissler *et al.*, 2010). In the condensate regime, the effect of disorder is very weak and well understood (Sanchez-Palencia, 2006). Conversely, the most interesting regimes (Anderson-Lifshits and fragmented condensate) where disorder plays a strong role are much more elusive and their full characterization remains an important challenge in the field of

disordered systems. Hence, several questions remain to be clarified:

- Physical arguments strongly support description of the Anderson-Lifshits regime as a Fock state of single-particle states with no phase coherence (Lugan *et al.*, 2007a; Aleiner *et al.*, 2010), but it has never been clearly demonstrated. Together with Tung-Lam Dao, we have developed a numerical technique, which extends the usual Gross-Pitaevskii approach to include such Fock states. Preliminary results do support the above conjecture.
- Full characterization of the fragmented condensate regime remains challenging. This issue is important because the fragmented condensate regime is the weak-interaction counterpart of the Bose glass phase, which is one of the most elusive key features of disordered, (strongly-)interacting Bose gases (Giamarchi and Schulz, 1988; Fisher *et al.*, 1989; Scalettar *et al.*, 1991; Krauth *et al.*, 1991). Here, an important challenge is to identify relevant observables to unambiguously characterize and discriminate all predicted states (*e.g.* density profiles, excitation spectra or correlation functions).
- So far, attractive interactions have not been much considered. This question is however relevant to ^{7}Li condensates, as used at Rice University for instance (Chen *et al.*, 2008), and/or more generally in experiments with controlled interactions (Roati *et al.*, 2007; Pollack *et al.*, 2009). In this case, one can expect a rich physical behavior, for instance, strong collapse and proliferation of very many metastable states, as it has been found in a different context, namely in trapped, attractive Bose gases (Cederbaum *et al.*, 2008).
- Finally, extension of these results to two- and three-dimensional geometries is deserved.

Dynamics of Anderson localization in the presence of interactions - Let us come back to dynamical schemes. In the experiment at Institut d'Optique (Billy *et al.*, 2008), the initial interactions determine the momentum distribution of the expanding condensate but do not significantly affect localization itself, because after expansion the density is low enough that interactions are negligible (Sanchez-Palencia *et al.*, 2007; 2008). However, in experiments with higher atomic densities or interactions, they may significantly modify the scenario. The question to know how interactions come into the picture proves puzzling.

The effect of repulsive interactions on Anderson localization has been extensively studied but, strikingly, even the most recent theoretical works (Paul *et al.*, 2007; Kopidakis *et al.*, 2008; Pikovsky and Shepelyansky, 2008; Palpacelli and Succi, 2008) lead to different conclusions. For instance, Pikovsky and Shepelyansky (2008) and Palpacelli and Succi (2008) study the effect of repulsive interactions on Anderson localization in one-dimensional, expanding condensates and conclude that interactions destroy localization above a certain threshold. In contrast, Kopidakis *et al.* (2008) show that Anderson localization persists even in the presence of significant interactions. Finally, Paul *et al.* (2007) show that weak repulsive interactions enhance localization in transmission experiments[10], while stronger interactions destroy it and induce strong temporal fluctuations of the condensate wavefunction. The interplay of interactions and disorder in dynamical schemes is thus a major issue with no obvious answer. It may not be universal and significantly depend on the considered scheme (*e.g.* expansion or transmission). Full understanding of this physics would require the development of a unified framework to address all situations, using possibly both analytical and numerical approaches.

[10]Transmission schemes differ from expansion schemes: Here one studies the transmission coefficient of a flow of quantum particles through a disordered region of finite length. Even though expansion and transmission schemes are equivalent for non-interacting particles, it is not clear that interactions preserve the equivalence.

Strongly-correlated, disordered quantum gases - Strongly-correlated systems play a central role in many aspects of condensed-matter physics. In this respect, the Hubbard Hamiltonian [see Eq. (1.3) on page 23] is a paradigmatic toy-model. In general, metal-insulator transitions are driven by a complex interplay of tunneling (*i.e.* kinetic energy), interactions and disorder (*e.g.* random on-site energy, associated to weak local modifications of the lattice potential). The most fundamental two phenomena underlying metal-insulator transitions are the Mott transition –which is driven by the competition between tunneling and interactions in non-disordered systems– and the Anderson transition –which is driven by the competition between tunneling and disorder in non-interacting systems (see Sec. 2.1.1). Both are quite well known and have been observed with ultracold atoms: Bose Mott insulators by Greiner *et al.* (2002); Fermi Mott insulators by Jördens *et al.* (2008) and Schneider *et al.* (2008); Anderson localization by Billy *et al.* (2008) and Roati *et al.* (2008). However, understanding their interplay is a much more challenging task.

In strongly-correlated lattice systems, glassy phases –the Bose (Fisher *et al.*, 1989; Scalettar *et al.*, 1991; Krauth *et al.*, 1991) and Fermi (Freedman and Hertz, 1977; Imry, 1995; von Oppen and Wettig, 1995; Jacquod and Shepelyansky, 1997) glasses– have been predicted, but full description of the phase diagram is very difficult. One should thus rely on approximate methods (*e.g.* Gutzwiller ansatz) or heavy numerical approaches (*e.g.* quantum Monte-Carlo simulations or Density-Matrix Renormalization Group). Identifying powerful, unbiased, and physically insightful techniques turns out to be a hard task in this field. For instance, even recently, there have been debates about the exact phase diagram of strongly-correlated disordered bosons. Using a stochastic meanfield method, it was predicted that a direct transition between the superfluid and Mott insulator phases may exist for certain parameters (Bissbort and Hofstetter, 2009), in contradiction to previous estimates (Buonsante *et al.*, 2007). The debate was finally closed by Pollet *et al.* (2009) who showed using extensive quantum Monte Carlo simulations that a Bose glass phase always separates the Mott insulator and superfluid phases. In addition, even the microscopic nature of Bose and Fermi glasses is still under debate.

Pioneering experiments to realize quantum simulators able to address these questions for bosons have already started (Fallani *et al.*, 2007; White *et al.*, 2009; Pasienski *et al.*, 2010). In this respect, further theoretical investigations are called for, and one can for instance point out the following directions:

- Early experiments suffered from the lack of a 'smoking-gun' signature of the Bose glass phase, so that identifying one is an important challenge. A possible signature is that Bose glasses are 'gapless, compressible insulators' (Giamarchi and Schulz, 1988; Fisher *et al.*, 1989), which can be probed via time-dependent modulations of the trap (Delande and Zakrzewski, 2009). In order to fully characterize Bose glasses compared to other gapless insulators –*e.g.* those that appear in weakly-interacting Bose gases (Lugan *et al.*, 2007a; Falco *et al.*, 2009)– other techniques should be developed to directly probe microscopic quantities. Promising routes include Bragg-like spectroscopy (Clément, 2009a; 2009b), and stimulated-Raman (ARPES-like) spectroscopy (Dao *et al.*, 2007; Stewart, 2008). Another interesting route, which has been hardly considered so far, is to study finite-temperature effects.
- Ultracold atomic systems may show novel features, beyond standard toy-models. Questions that have been hardly considered in the context of condensed-matter physics so far include long-range correlations of the disorder (for instance those of speckle potentials), and correlations between on-site disorder and perturbations of the tunneling rate [which can be important as pointed out by White *et al.* (2009)]. Systematic studies of the phase diagrams

for speckle potentials and/or bichromatic lattices are thus deserved.

– With a view towards studying systems of direct relevance to electronic materials, strongly-correlated Fermi gases is a formidable challenge, which is impressively progressing. Investigating the effect of disorder in these systems would open a new frontier, which has not been addressed experimentally so far. The issue is even more difficult than it is for bosons. On one hand, Quantum Monte-Carlo techniques cannot be used owing to the difficulty to include Fermi anti-symmetrization (the famous 'sign problem'). On the other hand, Fermi systems show even richer behavior due to competition with spin-exchange coupling, which can be responsible for antiferromagnetic ordering for instance (Byczuk *et al.*, 2009).

Spin-like disordered systems: A new frontier to disordered ultracold atoms - Most investigations of disordered systems with ultracold atoms focused on Anderson localization and its most relevant extension, *i.e.* interplay of disorder and interactions. In contrast, other important effects of disorder have been less considered so far. Let us just mention one: spin systems in the presence of disorder. From the point of view of condensed-matter physics, the class of systems to be considered is drastically different from the ones considered above: Instead of studying the behavior of quantum particles in disordered potentials (for instance in disordered Hubbard-like model), we now wonder how disorder in spin-exchange couplings affects the magnetization of an assembly of spins (for instance in disordered Ising/Heisenberg-like models). From the point of view of atomic physics however, it is strongly connected to previous studies as the same ultracold atomic systems can serve to simulate spin systems (Duan *et al.*, 2003; Imambekov *et al.*, 2003; Altman *et al.*, 2003; Jaksch and Zoller, 2005).

Disordered spins in ultracold atomic systems have been considered in theoretical works under the impulsion of Maciej Lewenstein, demonstrating abilities to simulate Random-Field Induced Order (Wehr *et al.*, 2006; Niederberger *et al.*, 2008; 2009) and spin glasses (Sanpera *et al.*, 2004; Ahufinger *et al.*, 2005). As discussed in Chap. 4, many questions are still open regarding both issues, not only from a basic point of view but also to propose relevant directions (experimental and theoretical ones) in the context of ultracold atoms. In particular, the problem of spin glasses is one of the most challenging and debated issue in the field of disordered spin systems. Spin glasses are the paradigm of disordered spin systems, just like Anderson localization is for quantum particles in disordered potentials. Determining the nature of spin order in spin glasses is an outstanding challenge, and competing theories exist (Binder and Young, 1986; Mézard *et al.*, 1987). On one hand, the *droplet picture* (Fisher and Huse, 1986; Bray and Moore, 1987; Fisher and Huse, 1988) relies on exchange coupling terms limited to nearest neighbors and presumed scaling of characteristic energies. It is supported by numerics and believed to be relevant for spin glasses with short-range coupling. On the other hand, the *ultrametric picture* (Parisi, 1980; Mézard *et al.*, 1987) assumes complex topology of graphs connecting an infinite number of Gibbs states. It has been demonstrated for models with a distribution of exchange coupling terms independent of the distance between the spins. It is believed to be valid for spin glasses with long-range coupling but its very applicability to systems with finite-range coupling is however still unproven. Combining spin-exchange implementation (Anderlini *et al.*, 2007; Trotsky *et al.*, 2008) and controlled disorder (Clément *et al.*, 2006; Fallani, 2008) in ultracold atomic systems offers fantastic routes to investigate spin glasses with the original methods, tools and approaches of atomic physics. We stop here without elaborating or speculating too much on this fascinating subject, as it is probably a next chapter of the field of disordered quantum gases to be written.

Reprints of papers associated with the chapter

1. SANCHEZ-PALENCIA L. and LEWENSTEIN M., *Disordered quantum gases under control*, Nature Phys. **6**, 87 (2010); ▷ ***page 211***.

2. SANCHEZ-PALENCIA L., *Joint forces against disorder*, Nature Phys. **6**, 328 (2010); ▷ ***page 221***.

3. PEZZE L. and SANCHEZ-PALENCIA L., *Localized and extended states in a disordered trap*, Phys. Rev. Lett. **106**, 040601 (2011); ▷ ***page 223***.

nature physics

PROGRESS ARTICLE

PUBLISHED ONLINE: 1 FEBRUARY 2010 | DOI: 10.1038/NPHYS1507

Disordered quantum gases under control

Laurent Sanchez-Palencia[1]* and Maciej Lewenstein[2]*

When attempting to understand the role of disorder in condensed-matter physics, we face considerable experimental and theoretical difficulties, and many questions are still open. Two of the most challenging ones—debated for decades—concern the effect of disorder on superconductivity and quantum magnetism. We review recent progress in the field of ultracold atomic gases, which should pave the way towards the realization of versatile quantum simulators, which help solve these questions. In addition, ultracold gases offer original practical and conceptual approaches, which open new perspectives to the field of disordered systems.

Phase coherence and interference effects underlie many basic phenomena in mesoscopic physics, for instance electronic conduction[1], magnetism[2], superfluidity and superconductivity[3], as well as the propagation of light and sound waves in inhomogeneous media[4]. Both also play central parts in high-precision devices such as interferometers, accelerometers and gyroscopes. An important issue concerns the effects of disorder, that is, of small random impurities, which cannot be completely avoided in real-life systems. *A priori*, we may expect that weak disorder slightly affects most physical systems and that averaging over the disorder smoothens possible effects. We may also expect that in quantum systems the spatial spread of wavefunctions leads to even weaker effects, through some kind of self-averaging. These naive ideas, however, turn out to be wrong. Disorder often leads to subtle situations in which strong effects survive averaging over the disorder[4], in particular in the quantum world. One of the most celebrated examples is Anderson localization[5] (AL). It is now understood that AL results from interference of the many paths associated with coherent multiple scattering from random impurities, yielding wavefunctions with exponentially decaying tails and absence of diffusion[6]. This strongly contrasts with the Drude–Boltzmann theory of classical transport, which predicts that incoherent scattering induces diffusion[1].

AL was first introduced for non-interacting quantum particles to explain the absence of electronic conduction in certain dirty solids[5], but remained difficult to observe for matter waves. It was realized later that AL is actually ubiquitous in wave physics, paving the way for the first observations of AL, reported in classical waves: light in diffusive media[7,8] and photonic crystals[9,10], microwaves[11] and sound waves[12]. In condensed-matter physics, AL is now considered a fundamental phenomenon underlying certain metal–insulator transitions. Considering non-interacting particles in purely disordered potentials is however oversimplistic, as a complete theory of disordered solids should incorporate the Coulomb interaction, the underlying crystal structure, the interaction with phonons, and magnetic effects. Unfortunately, understanding the physics of even the simplest models including all ingredients poses severe difficulties, and many issues are still unsolved or even controversial. The most challenging ones concern the interplay of disorder with interparticle interactions, and spin-exchange couplings.

Maybe somewhat unexpectedly, new approaches to these issues come from atomic physics. The field of ultracold atoms has been developing rapidly in the past decades, making it possible to produce, probe and manipulate Bose[13,14] and Fermi[15,16] gases with unprecedented versatility, tunability and measurement possibilities (Box 1). Control over these systems is now such that ultracold atoms can realize quantum simulators[17,18], that is, platforms to investigate various fundamental models[19–21]. Landmark results have already been reported, including the observation of Mott insulators[22–24], Tonks–Girardeau[25,26] and Berezinskii–Kosterlitz–Thouless[27] physics and spin-like exchange[28,29]. Investigation of Bose–Einstein condensates (BECs) in disordered potentials[30,31] has also emerged in a quest for direct signatures of AL of matter waves. Joint theoretical[32–34] and experimental efforts[35–40] made this possible, and two groups succeeded recently in observing one-dimensional AL (refs 41, 42).

Prima facie, the observation of AL might mean the end of a quest. It is, however, just a beginning, as the two experiments of refs 41, 42 provide the route to tackling many outstanding challenges in the field of disordered systems. Direct extensions include studies of metal–insulator transitions in dimensions greater than one, and of the effect of weak interactions on localization—areas where many aspects are debated. For stronger interactions, single-particle localization is usually destroyed, but new concepts such as many-body Anderson localization[43–45] and Bose glass[46,47] provide original paradigms that advance our understanding of these issues. Experiments on ultracold atoms with controlled disorder and controlled interactions can also be extended to other systems where disorder plays important parts. For instance, combining spin-exchange implementation[28,29] and disorder[30,31] opens the route towards random field-induced order[48–50] and spin glasses[51–54]. These few examples illustrate the promises of the emerging field of quantum gases in controlled disorder. Here, we review theoretical and experimental progress in the field and discuss perspectives that are now within our grasp.

The nature of Anderson localization

Localization, as introduced by Anderson in 1958, is strictly speaking a single-particle effect[5]. There are several ways to introduce AL. As it is a universal phenomenon, they are all almost equivalent. Consider a free particle of mass m and energy E, in a d-dimensional quenched disordered potential $V(\mathbf{r})$. Its wavefunction $\psi(\mathbf{r})$ is governed by the Schrödinger equation

$$E\psi(\mathbf{r}) = -\frac{\hbar^2\nabla^2}{2m}\psi(\mathbf{r}) + V(\mathbf{r})\psi(\mathbf{r}) \qquad (1)$$

[1]Laboratoire Charles Fabry de l'Institut d'Optique, CNRS and Univ. Paris-Sud, Campus Polytechnique, RD 128, F-91127 Palaiseau cedex, France, [2]ICREA—Institució Catalana de Recerca i Estudis Avançats and ICFO—Institut de Ciències Fotòniques, Parc Mediterrani de la Tecnologia, E-08860 Castelldefels, Barcelona. *e-mail: lsp@institutoptique.fr; maciej.lewenstein@icfo.es.

Box 1 | Ultracold quantum gases.

Creating and manipulating ultracold gases. Ultracold quantum gases are dilute atomic systems that are cooled to temperatures of the order of a few tens of nano-Kelvins and confined in immaterial traps using combinations of magnetic and optic fields[14,16]. Owing to strong dilution, the prominent interparticle interactions are two-body interactions, whereas many-body interactions can often be ignored. At ultralow temperatures, *s*-wave scattering dominates and the interaction is accurately described by a contact pseudopotential[13,15]. In the general case of mixtures of atoms in different species (or different internal states), the physics is thus governed by the Hamiltonian

$$\hat{H} = \sum_{\sigma}\int \mathrm{d}\mathbf{r}\ \hat{\Psi}^{\dagger}_{\sigma}(\mathbf{r})\left[-\frac{\hbar^2\nabla^2}{2m_{\sigma}}+V_{\sigma}(\mathbf{r})\right]\hat{\Psi}_{\sigma}(\mathbf{r}) + \sum_{\sigma,\sigma'}\frac{g_{\sigma,\sigma'}}{2}\int \mathrm{d}\mathbf{r}\ \hat{\Psi}^{\dagger}_{\sigma}(\mathbf{r})\,\hat{\Psi}^{\dagger}_{\sigma'}(\mathbf{r})\,\hat{\Psi}_{\sigma'}(\mathbf{r})\,\hat{\Psi}_{\sigma}(\mathbf{r}) \qquad (2)$$

where $\hat{\Psi}_{\sigma}$ and m_{σ} are the field operator and the mass of an atom of species σ, respectively. The first integral in equation (2) represents the single-particle Hamiltonian, where the potential $V_{\sigma}(\mathbf{r})$ is controlled by the configuration of the magnetic and/or optic fields (Fig. B1a). In most cases, it is nearly a harmonic trap[14,16] ($V_{\sigma}(x,y,z)=\sum_{\zeta\in\{x,y,z\}} m_{\sigma}\omega^2_{\sigma,\zeta}\zeta^2/2$, where $\omega_{\sigma,\zeta}$ is the trap frequency in the ζ direction for an atom of species σ), the anisotropy of which can be adjusted in experiments. For instance, making it strongly anisotropic offers the possibility to produce one-[104,105] or two-[27] dimensional gases. Another possibility is to create a guide for the atoms using a strongly focused laser beam[106]. The second integral in equation (2) represents the interaction operator, where $g_{\sigma,\sigma'}$ is the coupling constant for interacting atoms of same or different species ($g_{\sigma,\sigma'}>0$ and $g_{\sigma,\sigma'}<0$ correspond to repulsive and attractive interactions, respectively). The value and the sign of $g_{\sigma,\sigma'}$ can be controlled in quantum gases using Feshbach resonances[21].

Optical lattices. Considering different limits of the Hamiltonian in equation (1) enables us to design various models initially introduced in the context of condensed-matter physics, but here in a controlled way. One important example is that of optical lattices, which are produced from the interference pattern of several laser beams[20,21]. The matter–light interaction creates a periodic potential whose geometry and amplitude are determined by the laser configuration and intensity. Both can be controlled in experiments. For instance, using pairs of counterpropagating laser beams (Fig. B1b), the lattice potential reads $V^{\mathrm{latt}}_{\sigma}(x,y,z)=V^{0}_{\sigma}\sum_{\zeta\in\{x,y,z\}}\cos(2k_{\mathrm{L}}\zeta)$, where V^{0}_{σ} is the lattice depth and k_{L} the laser wavevector. In deep lattices, the atoms are trapped at the periodically arranged minima of the lattice potential (so-called lattice sites). They can jump from site to site through quantum tunnelling (with a rate J), and two atoms interact only in the same site (with an energy U). This physics is governed by the Hubbard Hamiltonian, that is, the discrete version of Hamiltonian (1):

$$\hat{H} = -\sum_{\sigma,\langle j,l\rangle} J_{\sigma}\left(\hat{a}^{\dagger}_{\sigma,j}\hat{a}_{\sigma,l}+\mathrm{h.c.}\right)+\sum_{\sigma,j}V_{\sigma,j}\,\hat{a}^{\dagger}_{\sigma,j}\hat{a}_{\sigma,j} + \frac{1}{2}\sum_{\sigma,\sigma',j}U_{\sigma,\sigma'}\,\hat{a}^{\dagger}_{\sigma,j}\hat{a}^{\dagger}_{\sigma',j}\hat{a}_{\sigma',j}\hat{a}_{\sigma,j} \qquad (3)$$

where the sum over $\langle j,l\rangle$ covers all pairs of neighbour sites, and $\hat{a}_{\sigma,j}$ is the annihilation operator of an atom of species σ in site j. Hence, ultracold atoms (bosons or fermions) in optical lattices mimic the Hubbard model, which is widely considered in condensed-matter physics, for instance to capture the essential physics of electrons in solids. However, in contrast to condensed-matter systems, Hamiltonian (2) can be shown to be exact in the limit of deep lattices, low temperature and low interactions[19]. The parameters J_{σ}, $V_{\sigma,j}$ and $U_{\sigma,\sigma',j}$ in equation (3) can be calculated *ab initio* from the potential $V_{\sigma}(\mathbf{r})\rightarrow V_{\sigma}(\mathbf{r})+V^{\mathrm{latt}}_{\sigma}(\mathbf{r})$ and the coupling constant $g_{\sigma,\sigma'}$ in equation (2), and are thus controllable in experiments.

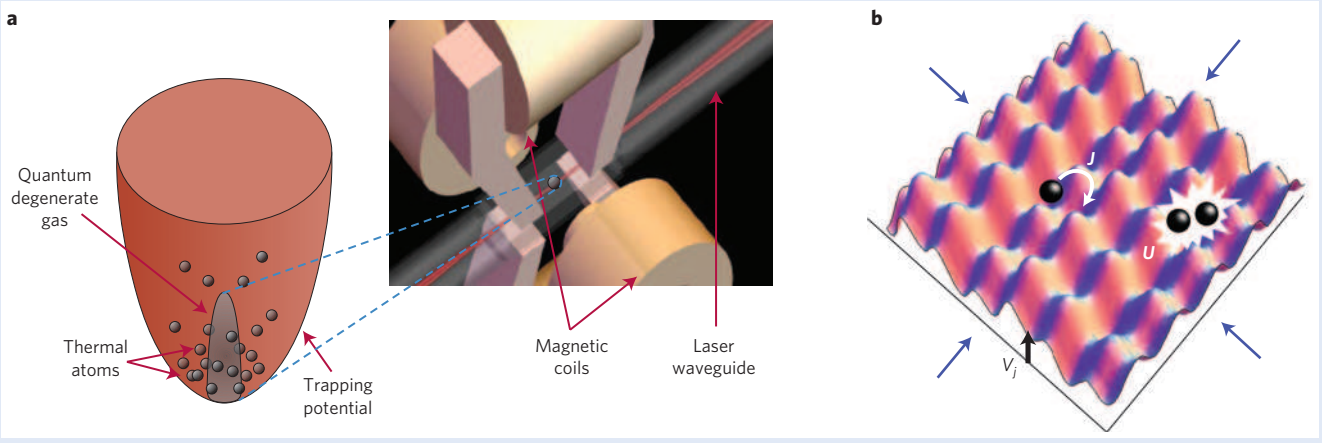

Figure B1 | Confining ultracold atoms in magnetic and optical traps. a, Harmonic trapping and laser waveguide (coutesy of V. Josse and P. Bouyer). Magnetic coils create a nearly harmonic trapping potential, at the bottom of which a degenerate quantum gas, surrounded by a cloud of thermal atoms, is formed. A focused laser beam, which creates an almost one-dimensional waveguide, is also represented. **b**, Optical lattice. The interference pattern of pairs of counterpropagating laser beams forms a periodic potential (represented here in two dimensions). The atoms are trapped in the lattice sites, but they can tunnel from site to site with a tunnelling rate J and interact when placed in the same site with an energy U.

In free space, $\psi(\mathbf{r})$ is an extended plane wave, but it can be shown rigorously[55,56] that, in the presence of disorder, any solution with arbitrary E is exponentially localized in one dimension, that is, $\ln(|\psi(z)|)\sim|z|/L_{\mathrm{loc}}$, with localization length $L_{\mathrm{loc}}(E)\propto l_{\mathrm{B}}$ (where l_{B} is the transport (Boltzmann) mean-free path). Even though L_{loc} often increases with E, it is striking that interference effects of multiply scattered waves are strong enough to profoundly affect $\psi(z)$ even for very high energies. In two dimensions, the situation is similar[57], but interference effects are weaker, and $L_{\mathrm{loc}}\propto l_{\mathrm{B}}\exp(\pi k l_{\mathrm{B}}/2)$, where $k=\sqrt{2mE}/\hbar$ is the particle wavevector

Box 2 | Creating controlled disordered potentials

In atomic gases, disorder can be created in a controlled way. For instance, the so-called speckle potentials are formed as follows[107]. A coherent laser beam is diffracted through a ground-glass plate and focused by a converging lens (Fig. B2a). The ground-glass plate transmits the laser light without altering the intensity, but imprints a random phase profile on the emerging light. Then, the complex electric field $E(\mathbf{r})$ on the focal plane results from the coherent superposition of many independent waves with equally distributed random phases, and is thus a Gaussian random process. In such a light field, atoms with a resonance slightly detuned with respect to the laser light experience a disordered potential $V(\mathbf{r})$, which, up to a shift introduced to ensure that the statistical average $\langle V\rangle$ of $V(\mathbf{r})$ vanishes, is proportional to the light intensity, $V(\mathbf{r}) \propto \pm(|E(\mathbf{r})|^2 - \langle|E|^2\rangle)$, an example of which is shown in Fig. B2b. Hence, the laws of optics enable us to precisely determine all statistical properties of speckle potentials. First, although the electric field $E(\mathbf{r})$ is a complex Gaussian random process, the disordered potential $V(\mathbf{r})$ is not Gaussian itself, and its single-point probability distribution is a truncated, exponential decaying function, $P(V(\mathbf{r})) = \mathrm{e}^{-1}|V_\mathrm{R}|^{-1}\exp(-V(\mathbf{r})/V_\mathrm{R})\Theta(V(\mathbf{r})/V_\mathrm{R}+1)$, where $\sqrt{\langle V^2\rangle} = |V_\mathrm{R}|$ is the disorder amplitude and Θ is the Heaviside function. Both the modulus and sign of V_R can be controlled experimentally[30]: the modulus is proportional to the incident laser intensity whereas the sign is determined by the detuning of the laser relative to the atomic resonance (V_R is positive for 'blue-detuned' laser light[30,36,39,41], and negative for 'red-detuned' laser light[35,37,40]). Second, the two-point correlation function of the disordered potential, $C_2(\mathbf{r}) = \langle V(\mathbf{r})V(0)\rangle$, is determined by the overall shape of the ground-glass plate but not by the details of its asperities[107]. It is thus also controllable experimentally[30]. There is however a fundamental constraint: as speckle potentials result from interference between light waves of wavelength λ_L coming from a finite-size aperture of angular width 2α (Fig. B2a), they do not contain Fourier components beyond a value $2k_\mathrm{C}$, where $k_\mathrm{C} = (2\pi/\lambda_\mathrm{L})\sin(\alpha)$. In other words, $C_2(2\mathbf{k}) = 0$ for $|\mathbf{k}| > k_\mathrm{C}$.

Speckle potentials can be used directly to investigate the transport of matter waves in disordered potentials[35–38]. They can also be superimposed on deep optical lattices[83]. In the latter case, the physics is described by Box 1 Hamiltonian (3) with $V_{\sigma,j}$ a random variable whose statistical properties are determined by those of the speckle potential. In particular, $V_{\sigma,j}$ is non-symmetric and correlated from site to site. Yet another possibility to create disorder in deep optical lattices is to superimpose a shallow optical lattice with an incommensurate period[38,42,82]. In this case, $V_{\sigma,j} = \Delta\cos(2\pi\beta j + \phi)$, where Δ and ϕ are determined by the amplitude and the phase of the second lattice and $\beta = k_2/k_1$ is the (generally irrational) ratio of the wavevectors of the two lattices. Although the quantity $V_{\sigma,j}$ is deterministic, it mimics disorder in finite-size systems[32,33,84,85]. In contrast to speckle potentials, these bichromatic lattices form a pseudorandom potential, which is bounded ($|V_{\sigma,j}| \lesssim \Delta$) and symmetrically distributed.

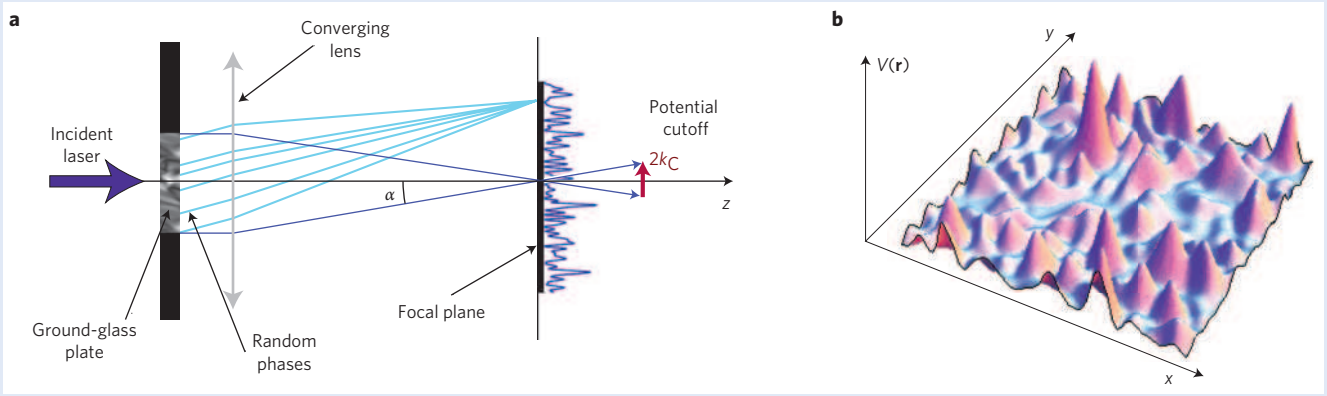

Figure B2 | Optical speckle potentials. a, Optical configuration. **b**, Two-dimensional representation of a speckle potential.

in free space. Hence L_loc explodes exponentially for $k > 1/l_\mathrm{B}$, inducing a crossover from extended to localized states in finite-size systems. The situation is dramatically different in three dimensions, where a proper phase transition (the Anderson transition) occurs at the so-called mobility edge k_mob: although low-energy states with $k < k_\mathrm{mob}$ are exponentially localized, those with $k > k_\mathrm{mob}$ are extended. The exact features of the mobility edge are unknown, but approximately captured by the Ioffe–Regel criterion[58,59], which basically states that localization requires that the phase accumulated between two successive deflecting scattering processes is less than 2π. In other words, the de Broglie wavelength must exceed the memory of the initial particle direction, thus yielding $k_\mathrm{mob} \sim 1/l_\mathrm{B}$.

Anderson localization of matter waves

Observing AL of matter waves requires meeting several challenging conditions. First, we must use weak enough disorder that interference effects at the origin of AL dominate over classical trapping in potential minima. Second, we must eliminate all perturbations such as time-dependent fluctuations of the medium, or interparticle interactions. Finally, we must demonstrate exponential localization, not only suppression of transport, as this can also arise from classical trapping. Although these conditions are very demanding in condensed-matter physics, they can be accurately fulfilled with ultracold atoms, using (1) controlled disorder, (2) negligible interactions, (3) strong isolation from the environment and (4) direct imaging of atomic density profiles. This way, direct signatures of AL of non-interacting matter waves were reported in refs 41, 42. As we shall see, these two experiments are complementary rather than similar, because they significantly differ as regards both observation scheme and class of disorder.

In ref. 41, a weakly interacting BEC is created in a trap, which is abruptly switched off at time $t = 0$. Then, the condensate expands in a guide and in the presence of disorder (Fig. 1a), created with optical speckle (Box 2). This physics is captured by the Gross–Pitaevskii equation

$$i\hbar\frac{\partial\psi}{\partial t} = -\frac{\hbar^2\nabla^2}{2m}\psi + V(\mathbf{r})\psi + g|\psi|^2\psi \qquad (4)$$

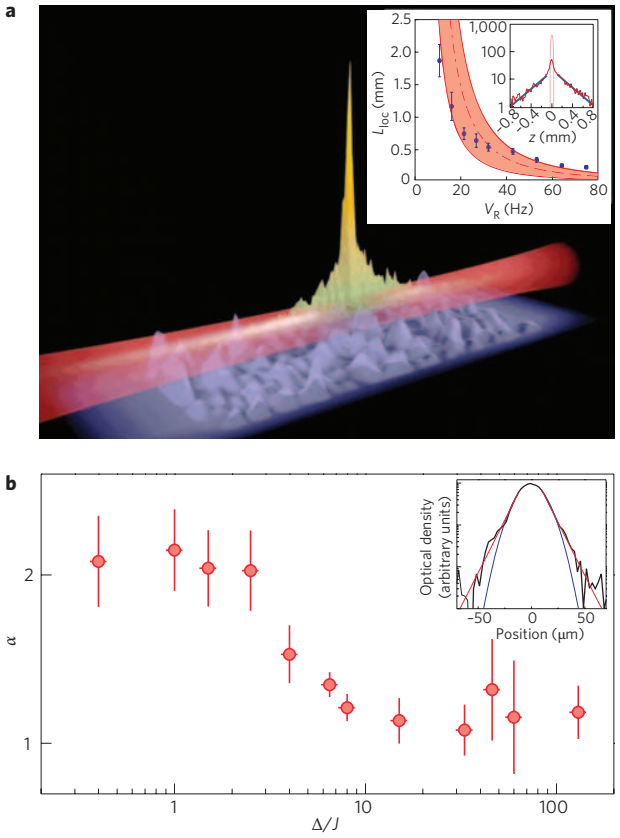

Figure 1 | Experimental observation of Anderson localization of matter waves with Bose–Einstein condensates. a, Experiment of Institut d'Optique (courtesy of V. Josse and P. Bouyer): an interacting BEC expands in a tight one-dimensional guide (in red) in the presence of a speckle potential (in blue). The expansion stops in less than 500 ms and the density profile of the condensate is directly imaged (shown in orange–green; from the data of ref. 41). The column density, plotted in semilogarithmic scale in the inset, shows a clear exponential decay characteristic of Anderson localization. The localization length L_{loc}, extracted by fitting an exponential $\exp(-2|z|/L_{loc})$ to the experimental profiles, shows a good agreement with theoretical calculations[34]. **b**, Experiment of LENS (adapted from ref. 42 with permission of the authors): a non-interacting BEC is created in a combination of a harmonic trap and a one-dimensional bichromatic lattice. The plot shows the exponent α of a fit of a function $\exp(-|(x-x_0)/l|^{\alpha})$ to the tails of the condensate at equilibrium in the combined potential, versus the ratio of the disorder strength (Δ) to the site-to-site tunnelling rate (J). The onset of localization corresponds to the crossover to $\alpha \to 1$ for $\Delta/J > 9$. The inset shows a plot of the density profile of the condensate together with the fit for $\Delta/J = 15$. Error bars in **a** inset and **b** correspond to 95% confidence intervals for the fitted values (±2 s.e.m.).

which corresponds to Hamiltonian (2) in the mean-field regime. The dynamics of the BEC can be understood in a two-stage scheme[34]. In the first stage, it is dominated by interactions and the BEC expands, creating a coherent wavefunction with a stationary momentum distribution, $D(k) \propto 1-(k\xi)^2$, where $\xi = \hbar/\sqrt{4m\mu}$ is the initial healing length, which measures the initial interaction strength[13], and μ is the initial chemical potential of the BEC. In the second stage, once the expansion has strongly lowered the atomic density $|\psi(z)|^2$, the interaction term vanishes and we are left with a superposition of (almost) non-interacting waves ψ_k; the population of each is $D(k)$. Then each ψ_k eventually localizes by interacting with the disordered potential, so that $\ln(|\psi_k(z)|) \sim |z|/L_{loc}(k)$, and the total BEC density reduces to[34] $n_{BEC}(z) \simeq \int \mathrm{d}k\, D(k)\langle|\psi_k(z)|^2\rangle$. Direct imaging of the localized matter wave reveals exponentially decaying tails[41], with a localization length equal to that of a non-interacting particle with momentum $k = 1/\xi$ (inset of Fig. 1a). Hence, this experiment corresponds to a 'transport scheme', which probes AL of non-interacting particles with a wavevector controlled by the initial interaction, through the healing length ξ.

In contrast, the experiment of ref. 42 uses a 'static scheme'. The interactions are switched off already in the trap using Feshbach resonances, so that the gas is created in a superposition of a few (typically one to three) low-energy, single-particle eigenstates. They are subsequently imaged *in situ*, revealing exponentially decaying tails (inset of Fig. 1b). It is worth noting that ref. 42 uses a one-dimensional quasiperiodic, incommensurate lattice (Box 2), thus realizing the celebrated Aubry–André model[60,61]

$$\hat{H} = -\sum_{\langle j,l\rangle} J\left(\hat{a}_j^{\dagger}\hat{a}_l + \text{h.c.}\right) + \sum_j \Delta\cos(2\pi\beta j + \phi)\hat{a}_j^{\dagger}\hat{a}_j \qquad (5)$$

that is, Box 1 equation (3) with $U = 0$, $V_j = \Delta\cos(2\pi\beta j + \phi)$, and β an irrational number. Different from the case of truly disordered potentials, there is a metal–insulator transition (mobility edge) in one dimension, which is theoretically expected at $\Delta/J = 2$ and experimentally observed as a crossover from Gaussian ($\alpha \simeq 2$) to exponential ($\alpha \simeq 1$) tails (Fig. 1b).

These works open new horizons to further deepen our knowledge of AL in various directions. In one dimension, although all states are localized, subtle effects arise in correlated disorder, for instance in speckle potentials[34]. To lowest order in the disorder amplitude, $V_R = \sqrt{\langle V(z)^2\rangle}$, the Lyapunov exponent, $\gamma(k) = 1/L_{loc}(k)$, can be calculated analytically[62], and we find $\gamma(k) \propto \langle V(2k)V(-2k)\rangle/k^2$, reflecting in particular the role of coherent second-order back-scattering, $+k \to -k \to +k$, in the localization process. As the power spectrum of speckle potentials has a cut-off k_C, such that $C_2(2k) = \langle V(2k)V(-2k)\rangle = 0$ for $k > k_C$ (Box 2), we find an abrupt change (effective mobility edge) in the k-dependence of γ for weak disorder[63,64]: although $\gamma(k) \sim V_R^2$ for $k < k_C$, higher-order scattering processes dominate for $k > k_C$ and $\gamma(k) \sim V_R^4$.

In dimensions higher than one, the self-consistent theory of localization[65] enables us to calculate L_{loc} and shows a mobility edge in three dimensions. It is however known that it is not fully exact owing to uncontrolled approximations, which in particular ignore large fluctuations near the Anderson transition. Therefore, a major challenge for disordered, ultracold atoms is to extend the works of refs 41, 42 to two[66,67] and three[68] dimensions. Observing the three-dimensional mobility edge would be a landmark result, which might stimulate further theoretical developments and drive new approaches by providing precise measurements of the mobility edge k_{mob}. Even more important would be the determination of the critical exponent ν, such that $L_{loc} \sim (E_{mob} - E)^{-\nu}$ for $E \lesssim E_{mob}$, which is debated[68].

Interactions versus Anderson localization

Another outstanding challenge is to understand how interactions affect localization, a question that has proved puzzling ever since AL was introduced[69]. It might be believed that even weak interactions destroy localization. Different approaches however provide apparently contradicting answers in different transport schemes. For instance, recent numerical calculations[70] suggest that, for expanding BECs, repulsive interactions destroy AL beyond a given threshold. Conversely, other results[71] predict that localization should persist even in the presence of interactions. Finally, in transmission experiments (which amount to releasing a monokinetic wavepacket to a disordered region and measuring transmission), perturbative calculations and numerical results indicate that repulsive interactions decrease the localization length before completely destroying localization[72]. As a nonlinear term is naturally present in BECs

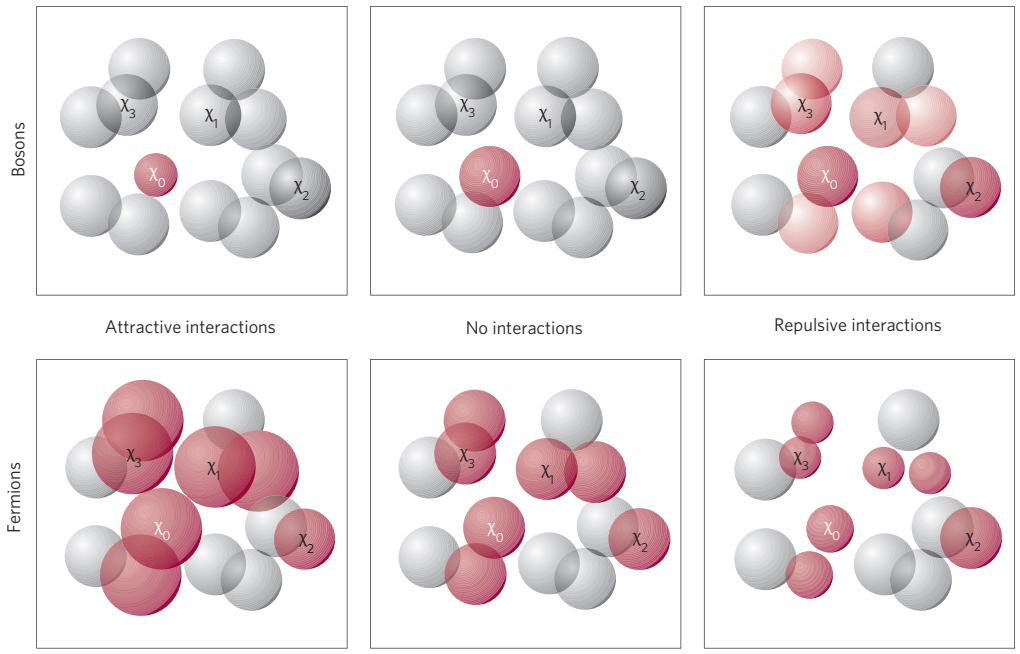

Figure 2 | Effect of interactions in disordered Bose and Fermi gases. The gas is described using the single-particle (non-interacting) states $|\chi_\nu\rangle$. In the presence of disorder, these states, which are localized and distributed in a given volume, are represented by the spheres (in red when they are populated). Bose gas: for non-interacting bosons (top, central panel), only the ground state, $|\chi_0\rangle$, is populated. Then, attractive interactions (top, left panel) tend to contract this state, thus favouring localization. Conversely, repulsive interactions (top, right panel) work against localization by populating more and more $|\chi_\nu\rangle$ states. Fermi gas: in the absence of interactions, a gas of N fermions populates the N lowest-energy $|\chi_\nu\rangle$ states (bottom, central panel). Then, each state tends to extend under the action of attractive interactions as for maximizing the overlap between different populated $|\chi_\nu\rangle$ states (bottom, left panel). Conversely, for repulsive interactions, they tend to minimize their mutual overlap, thus favouring localization (bottom, right panel).

(see the last term of equation (4)), and can be controlled through Feshbach resonances[42], transport experiments with interacting condensates are particularly promising to address this question.

A different approach to the interplay of interactions and localization consists in considering a Bose gas at equilibrium in a d-dimensional box of volume Ω in the presence of interactions and disorder (Fig. 2). For vanishing interactions and zero temperature, all bosons populate the single-particle ground state, $|\chi_0\rangle$. Very weak attractive interactions are expected to favour localization by contracting the Bose gas, but also induce instabilities for moderate interactions, pretty much like the case for trapped BECs (ref. 13). Conversely, weak to moderate repulsive interactions do not much affect stability, but work against localization, by populating an increasing number of single-particle states, $|\chi_\nu\rangle$. Weak interactions populate significantly only the lowest-energy states. As they are strongly bound in rare, low-energy modulations of the potential, their mutual overlap is small. The gas then forms a Fock state, $|\Psi\rangle \propto \prod_\nu (b_\nu^\dagger)^{N_\nu}|0\rangle$, where $b_\nu^\dagger$ is the creation operator in state $|\chi_\nu\rangle$. The population N_ν of each is determined by the competition between single-particle energy ϵ_ν and interaction within each state $|\chi_\nu\rangle$. This results in the characteristic equation of state[73], $Ng = \int^\mu \mathrm{d}\epsilon\, D_\Omega(\epsilon)(\mu-\epsilon)P(\epsilon)$, where $D_\Omega(\epsilon)$ is the density of states and $P_\nu = 1/\int \mathrm{d}\mathbf{r}|\chi_\nu(\mathbf{r})|^4$ is the participation volume of $|\chi_\nu\rangle$. This state is an insulator with finite compressibility, $\kappa = \partial N/\partial\mu$, and can thus be referred to as a Bose glass[46,47]. It attains particularly interesting features in disordered potentials bounded below (that is, when $V(\mathbf{r}) \gtrsim V_{\min}$ everywhere), for which Lifshitz has shown[74] that the relevant single-particle states are determined by large-scale modulations of the potential. As they are exponentially far apart, the density of states is exponentially small, $D_\Omega(\epsilon) \sim \exp[-c(\epsilon - V_{\min})^{-d/2}]$. As we can see, the equation of state is determined by both the density of states $D_\Omega(\epsilon)$ and the localization through $P(\epsilon)$ in the Lifshitz tail, which leads us to name this state the Lifshitz–Anderson glass[73]. In the opposite limit of strong interactions, there are very many populated states $|\chi_\nu\rangle$, which thus overlap, and the above description breaks down. In turn, the gas forms an extended, connected (quasi-) BEC of density $n(\mathbf{r}) = [\mu - V(\mathbf{r})]/g$, which is well described in the mean-field approach[75]. This state is a superfluid. Finally, the intermediate region interpolates between the Lifshitz–Anderson glass and the BEC regime. Then, the Bose gas separates into fragments, forming a compressible insulator (Bose glass). The characteristic features of the fragments can then be estimated in the mean-field framework[76].

The description above is consistent with the idea that even weak interactions destroy single-particle localization. However, in interacting systems the relevant states are not the single-particle eigenstates, but of collective nature; for interacting BECs, they are Bogolyubov quasiparticles[13]. We then find that, although the ground state is extended, the Bogolyubov quasiparticles are localized[44,45,77]. Their localization properties however differ from those of Schrödinger particles, owing to a strong screening of disorder[45]. In one dimension, the Lyapunov exponent of a Bogolyubov quasiparticle reads $\Gamma(k) = [S(k)]^2\gamma(k)$, where $\gamma(k)$ is the single-particle Lyapunov exponent and $S(k) = 2(k\xi)^2/(1+2(k\xi)^2)$ is the screening function. We thus find that in the phonon regime ($k \ll 1/\xi$) the screening is strong and $\Gamma(k) \ll \gamma(k)$. Conversely, in the free-particle regime ($k \gg 1/\xi$) the screening vanishes and $\Gamma(k) \simeq \gamma(k)$. Hence, surprisingly, localization can survive in the presence of strong mean-field interactions. This poses new challenges to ultracold atoms. Not only should many-body AL be directly observable, but also possible consequences on quantum coherence might be seen, in sound-wave propagation or thermalization processes.

Fermi systems and 'dirty' superconductors

Consider now a Fermi gas, and focus again on the ground-state properties (Fig. 2). In the absence of interactions, the gas of N fermions populates the N lowest single-particle states. For

low density, short-range interactions do not play a significant part, as the populated states are spatially separated. However, for large enough density, they do overlap. Then, for repulsive interactions, each populated state tends to contract to minimize its overlap with other populated states, thus favouring localization. Conversely, for attractive interactions, the populated states tend to extend to maximize their overlap, thus favouring delocalization. Hence, strikingly, interactions have opposite consequences for fermions and bosons.

Perhaps even more fascinating is the possibility to study 'dirty' Fermi liquids. Experiments with two-component Fermi gases (such as ^{6}Li or ^{40}K), with interactions controlled by Feshbach resonances, have already significantly advanced our understanding of the so-called BEC–BCS crossover[15,16]. On the attractive side of the resonance and for weak interactions, the Fermi superfluid is well described by the Bardeen–Cooper–Schrieffer (BCS) theory and formation of spatially extended Cooper pairs consisting of two fermions of opposite spins and momenta. On the repulsive side, pairs of fermions form bosonic molecules, which undergo Bose–Einstein condensation. Although disorder should not significantly affect pairing, BCS superfluidity and BEC superfluidity are expected to react differently to disorder[78,79]. The famous Anderson theorem[80] indicates that disorder should not affect very much the BCS superfluid owing to the long-range and overlapping nature of the Cooper pairs. Conversely, disorder should seriously affect the molecular BEC, enhancing phase fluctuations.

Strongly correlated lattice gases

Strong interactions are also very important in various disordered systems, such as superfluids in porous media or 'dirty' superconductors. Metal–insulator transitions attain a particularly interesting, but not fully understood, character in lattice systems. In this respect, the Bose–Hubbard model,

$$\hat{H} = -\sum_{\langle j,l\rangle} J(\hat{a}_j^\dagger \hat{a}_l + \text{h.c.}) + \sum_j V_j \hat{a}_j^\dagger \hat{a}_j + \frac{1}{2}\sum_j U \hat{a}_j^\dagger \hat{a}_j^\dagger \hat{a}_j \hat{a}_j \qquad (6)$$

is central in condensed-matter physics[47], for it forms a tractable model, which captures the elementary physics of strongly interacting systems. Hamiltonian (6) describes bosons, in a lattice with inhomogeneous on-site energies V_j, which can tunnel between neighbour sites with rate J, and interact when placed in the same site with interaction energy U. Interestingly, this model contains the most fundamental two phenomena underlying metal–insulator transitions. They correspond to the Anderson transition[5,6] in the absence of interactions ($U = 0$) as discussed above, and to the Mott transition[81] in the absence of disorder ($V = 0$). In systems dominated by repulsive interactions, density fluctuations, which are energetically costly, are suppressed, and a Mott insulator (MI) state, $|\Psi_{\text{MI}}\rangle \propto \prod_j (\hat{a}_j^\dagger)^n |0\rangle$, is formed. Then, the number of bosons per site, $n = [\mu/U + 1]$ is determined, and phase coherence between the lattice sites vanishes. MIs are insulating, incompressible and gapped, as the first excitation corresponds to transferring one atom from a given site to another, which costs the finite energy U. At the other extreme, when tunnelling dominates, the bosons form a superfluid state, $|\Psi_{\text{SF}}\rangle \propto (\sum_j \hat{a}_j^\dagger)^N |0\rangle$, with normal density fluctuations and perfect coherence between the lattice sites. This state is gapless and compressible.

In the presence of disorder, a glassy phase is formed, which interpolates between Lifshitz–Anderson glass for weak interactions and Bose glass for strong interactions[47]. The latter can be represented as $|\Psi_{\text{BG}}\rangle \propto \prod_j (\hat{a}_j^\dagger)^{n_j} |0\rangle$ with $n_j = [(\mu - V_j)/U + 1]$. This phase is thus insulating but compressible and gapless because the ground state is quasidegenerate, as in many other glassy systems[47]. With the possibility of realizing experimentally systems exactly described by Hubbard models (Box 1), ultracold atoms in optical lattices also offer here unprecedented opportunities to investigate this physics in detail, and to directly observe the Bose glass, which has not been possible in any system so far. Two experimental groups have made the first steps in this direction[82,83]. The authors of ref. 82 applied a bichromatic, incommensurate lattice to one-dimensional Mott insulators. With increasing disorder, a broadening of Mott resonances was observed, suggesting a vanishing of the gap and transition to an insulating state with a flat density of excitations. Intensive theoretical studies have been devoted to understanding these results, using quantum Monte Carlo[84] and density-matrix renormalization-group[85] techniques. The results of ref. 84 suggest that, in the conditions of ref. 82, we should expect a complex phase diagram with competing regions of gapped, incompressible band-insulator and compressible Bose-glass phases. Clearly, new and more precise detection schemes are needed to characterize this kind of physics, such as direct measurements of compressibility[86] or condensate fraction in superfluid, or coexisting superfluid and MI phases. The latter has been approached experimentally in ref. 83, where disorder-induced suppression of the condensate fraction in a lattice with superimposed speckle was observed.

We can also investigate the corresponding Fermi counterparts with ultracold atoms. These systems are particularly interesting as they would mimic superconductors, even better than bosons. In this respect, an outstanding challenge is definitely to understand high-critical-temperature (high-T_{C}) superconductors, and possibly important effects of disorder in these systems. Consider the two-component ($\sigma \in \{\uparrow, \downarrow\}$) Fermi–Hubbard Hamiltonian

$$\hat{H} = -\sum_{\sigma,\langle j,l\rangle} J_\sigma (\hat{a}_{\sigma,j}^\dagger \hat{a}_{\sigma,l} + \text{h.c.}) + \sum_{\sigma,j} V_{\sigma,j} \hat{a}_{\sigma,j}^\dagger \hat{a}_{\sigma,j} + \sum_j U \hat{a}_{\uparrow,j}^\dagger \hat{a}_{\downarrow,j}^\dagger \hat{a}_{\downarrow,j} \hat{a}_{\uparrow,j} \qquad (7)$$

For weak interactions, we have a Fermi liquid similar to that discussed above. For strong interactions and low temperature, $T \lesssim U/k_{\text{B}}$, where k_{B} is the Boltzmann constant, the Fermi gas enters an MI state, pretty much like that for bosons, but with a single ($n = 1$) fermion per site (either $\uparrow$ or $\downarrow$). Evidence of vanishing double occupancy and incompressibility have been reported recently in gaseous Fermi MIs (refs 23, 24). Then, in the presence of disorder ($V_j \neq 0$ in Hamiltonian (7)), various phases could be searched for, such as Fermi glasses. At even lower temperatures, spin exchange starts to have a role, and a transition from paramagnetic to antiferromagnetic insulator phases is predicted for the Néel temperature $T_{\text{N}} \sim 4J^2/k_{\text{B}}U$ in non-disordered systems[87]. Interestingly, the interplay of interactions and disorder might lead to the appearance of new 'metallic' phases between the Fermi glass and the MI. Hence, dynamical mean-field theory[88] at half-filling predicts that disorder tends to stabilize paramagnetic and antiferromagnetic metallic phases for weak interactions. For strong interactions, however, only the paramagnetic Anderson–Mott insulator (for strong disorder) and antiferromagnetic insulator (for weak disorder) phases survive.

Simulating disordered spin systems

In condensed-matter physics, other important paradigm models where disorder induces subtle effects are lattice spin systems, described by the Hamiltonian

$$\hat{H} = -\sum_{\langle j,l\rangle} \left(J_{j,l}^x \hat{S}_j^x \cdot \hat{S}_l^x + J_{j,l}^y \hat{S}_j^y \cdot \hat{S}_l^y + J_{j,l}^z \hat{S}_j^z \cdot \hat{S}_l^z \right) - \sum_j \mathbf{h}_j \cdot \hat{\mathbf{S}}_j \qquad (8)$$

where $\hat{\mathbf{S}}_j$ is the spin operator at the lattice site j, with either random spin exchange, $J_{j,l}$, or random magnetic field, $\mathbf{h}_j$. Ultracold gases can also simulate this class of systems, although not as straightforwardly

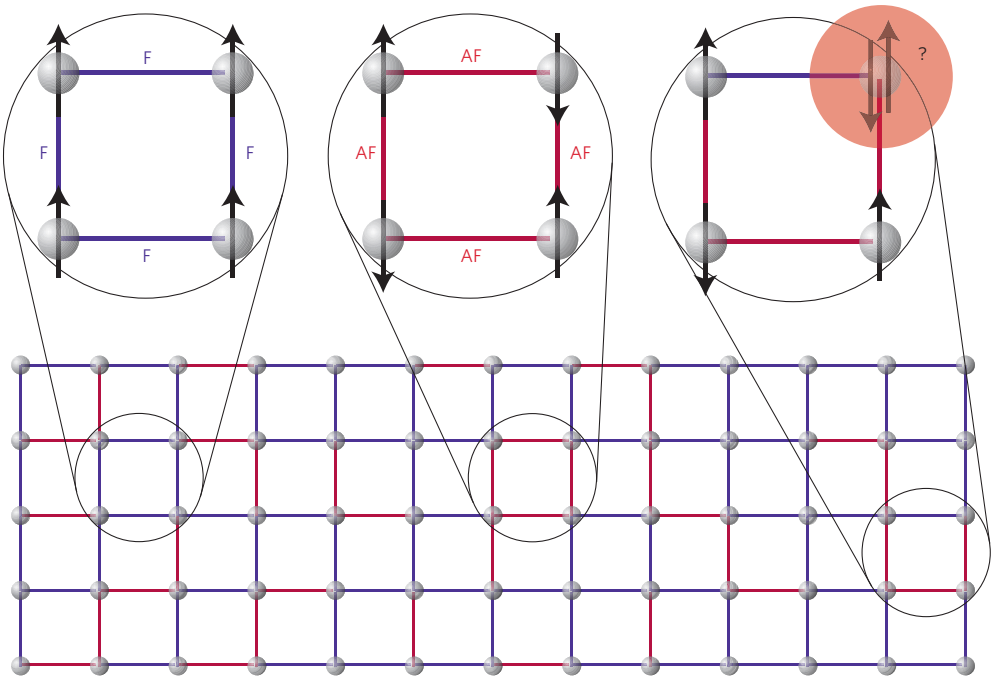

Figure 3 | The spin-glass problem. An assembly of spins located at the nodes of a cubic lattice interacts according to Hamiltonian (8), where only the exchange term $J_{j,l}$ is randomly distributed, and can be either ferromagnetic (F; blue bonds) or antiferromagnetic (AF; red bonds). The ground state of the system corresponds to the spin configuration that minimizes the total energy. The inherent complexity of spin glasses results from frustration, which appears when the topography of ferromagnetic and antiferromagnetic bonds makes it impossible to fulfil the local constraints all together. In some plaquettes of four sites, local minimization is easy, for instance when all bonds are ferromagnetic (left disc) or antiferromagnetic (central disc). In some others, it leads to frustration, for instance for odd numbers of ferromagnetic and antiferromagnetic bonds (right disc). In the latter case, at least one spin is frustrated, that is its spin orientation is not determined. Hence, frustration is at the origin of a manifold of metastable states, which corresponds to configurations with similar energies.

as for Hubbard models. Consider a two-component (Bose–Bose or Fermi–Bose) ultracold gas in an optical lattice, as described by Hamiltonian (3). In the strongly correlated (Mott-like) regime, the couplings between the particles can be understood as exchange-mediated interactions between composite (bosonic or fermionic) particles[89,90]. We can then frequently map Hamiltonian (3) onto Hamiltonian (8), with spins encoded in the internal (spin or pseudospin) states of the composite particles. The couplings $J_{j,l}$ and $\mathbf{h}_j$ in the resulting effective spin Hamiltonian can be calculated analytically, but have a rather complicated dependence on the parameters of Hamiltonian (3). In the presence of disorder, these parameters are random[49,54] and we can reach various limiting cases corresponding to Fermi glass, quantum spin glass and quantum percolation[53].

Particularly promising is the possibility of simulating spin glasses[53] (Fig. 3), for which only the exchange term, $J_{j,l}$, is randomly distributed. Finding the phase diagram of (even classical) spin glasses is an outstanding challenge in condensed-matter physics. The nature of spin glasses is still debated and there exist competing theories: the Parisi replica symmetry breaking[51] and the Nelson–Huse droplet model[52]. Ultracold atoms might contribute to the resolution of this issue, not only on the classical level but also on the quantum level, because they offer original ways of carrying out quenched averages. Importantly, with a view towards testing the replica theory, overlap between two spin configurations between two (or more) replicas can be measured directly by preparing a pair of two-dimensional lattices with the same realization of disorder[91]. Quenched averages for systems with binary disorder can also be simulated by replacing the classical disorder variables by quantum 1/2-spins, and preparing them in a superposition state[92].

Another fascinating possibility is to simulate various random field-induced order (RFIO) phenomena in systems with continuous symmetry, such as BECs or XY-spin models with $U(1)$ symmetry, or Heisenberg models with $SU(2)$ symmetry[49,50]. A prototype model[93] is the two-dimensional XY version of Hamiltonian (8) with fixed exchange $J_{j,l}$ but random field $\mathbf{h}_j$. In the absence of disorder, symmetry leads to strong fluctuations, which suppress long-range order, according to the Mermin–Wagner–Hohenberg theorem. Disorder distributed in a symmetric way suppresses ordering even more. However, disorder that breaks symmetry might actually favour ordering. This model can be implemented within Bose–Bose mixtures[49,50], where random uniaxial $\mathbf{h}_j$ can be implemented using two internal states of the same atom, coupled through a random Raman field, $\hbar\Omega(\mathbf{r})\,\Psi_1(\mathbf{r})^\dagger\,\Psi_2(\mathbf{r}) + \text{h.c.}$ To break the continuous symmetry, we use a Raman coupling with constant phase, but random strength. In lattice systems, RFIO shows up but is limited by finite-size effects, even in very large systems[49]. In this respect, ultracold atoms offer an alternative and fruitful route. Indeed, RFIO turns out to be particularly efficient in two- (or multi-) component BECs in the mean-field regime, where the energy functional reads $\Delta E \simeq \mathrm{d}\mathbf{r}\, n[(\hbar^2/4m)(\nabla\theta)^2 + \hbar\Omega(\mathbf{r})\cos(\theta)]$, with $n(\mathbf{r})$ the atomic density and $\theta(\mathbf{r}) = \theta_1(\mathbf{r}) - \theta_2(\mathbf{r})$ the phase difference between the two BECs. This is the continuous counterpart of the two-dimensional XY lattice model. Then, RFIO manifests itself as a fixed $\theta(\mathbf{r}) = \pm\pi/2$, and thus enables us to control the relative phase between the components[50]. This is a striking example where ultracold atoms can be used to not only simulate classic models, but also offer new and fruitful viewpoints on fundamental issues.

Further directions

The limited size of the present review has not enabled us to discuss all interesting directions that can be tackled with ultracold atomic systems. Two-component (Bose–Bose or Bose–Fermi)

mixtures offer an alternative method to create disorder in optical lattices, namely, by quenching one component in random sites, to form a background of randomly distributed impurities[92,94]. Theoretical analysis using the Gutzwiller method confirms the appearance of incompressible MI and partially compressible Bose-glass phases[95]. The idea of freezing the motion of the second species to form random impurities (that is, classical disorder) can be generalized to freezing of any quantum state[96]. In this case, the system does not involve any classical disorder, but nevertheless localization occurs, owing to quantum fluctuations in the frozen state of the second species.

We can even relax the freezing condition and consider, say, two bosonic species, one of which tunnels much more slowly than the other, forming quasistatic disorder. In a large region of parameters (for repulsive interspecies interactions), the ground state corresponds to full phase segregation. In practice, it is marked by a large number of metastable states in which microscopic phase separation occurs, reminiscent of emulsions in immiscible fluids[97]. Such quantum emulsions are predicted to have very similar properties to the Bose-glass phase, that is, compressibility and absence of superfluidity. Such quasistatic or even time-dependent disorder effects have been suggested to underlie the rather large shift of the SF–MI transition in Bose–Fermi[98,99] and Bose–Bose[100] mixtures. This issue was rather controversial, and the most recent works suggest that, although the fermions tend to localize the bosons for attractive boson–fermion interactions, higher Bloch bands have a significant role[101–103].

References

1. Ashcroft, N. W. & Mermin, N. D. *Solid State Physics* (Saunders, 1976).
2. Auerbach, A. *Interacting Electrons and Quantum Magnetism* (Springer, 1994).
3. Lifshitz, E. M. & Pitaevskii, L. P. *Landau and Lifshitz Course of Theoretical Physics: Statistical Physics, Part 2* (Pergamon, 1980).
4. Akkermans, E. & Montambaux, G. *Mesoscopic Physics of Electrons and Photons* (Cambridge Univ. Press, 2006).
5. Anderson, P. W. Absence of diffusion in certain random lattices. *Phys. Rev.* **109,** 1492–1505 (1958).
6. Lee, P. A. & Ramakrishnan, T. V. Disordered electronic systems. *Rev. Mod. Phys.* **57,** 287–337 (1985).
7. Wiersma, D. S., Bartolini, P., Lagendijk, A. & Righini, R. Localization of light in a disordered medium. *Nature* **390,** 671–673 (1997).
8. Störzer, M., Gross, P., Aegerter, C. M. & Maret, G. Observation of the critical regime near Anderson localization of light. *Phys. Rev. Lett.* **96,** 063904 (2006).
9. Schwartz, T., Bartal, G., Fishman, S. & Segev, M. Transport and Anderson localization in disordered two-dimensional photonic lattices. *Nature* **446,** 52–55 (2007).
10. Lahini, Y. *et al.* Anderson localization and nonlinearity in one-dimensional disordered photonic lattices. *Phys. Rev. Lett.* **100,** 013906 (2008).
11. Chabanov, A. A., Stoytchev, M. & Genack, A. Z. Statistical signatures of photon localization. *Nature* **404,** 850–853 (2000).
12. Hu, H., Strybulevych, A., Skipetrov, S. E., van Tiggelen, B. A. & Page, J. H. Localization of ultrasound in a three-dimensional elastic network. *Nature Phys.* **4,** 945–948 (2008).
13. Dalfovo, F., Giorgini, S., Pitaevskii, L. P. & Stringari, S. Theory of Bose–Einstein condensation in trapped gases. *Rev. Mod. Phys.* **71,** 463–512 (1999).
14. Ketterle, W., Durfee, D. S. & Stamper-Kurn, D. M. in *Proc. of the International School of Physics 'Enrico Fermi', Course CXL* (eds Inguscio, M., Stringari, S. & Wieman, C. E.) (IOP Press, 1999); preprint at <http://arxiv.org/abs/cond-mat/9904034>.
15. Giorgini, S., Pitaevskii, L. P. & Stringari, S. Theory of ultracold atomic Fermi gases. *Rev. Mod. Phys.* **80,** 1215–1274 (2008).
16. Ketterle, W. & Zwierlein, M. W. in *Proc. of the International School of Physics 'Enrico Fermi', Course CLXIV* (eds Inguscio, M., Ketterle, W. & Salomon, C.) (IOS Press, 2008); preprint at <http://arxiv.org/abs/0801.2500>.
17. Feynman, R. P. Simulating physics with computers. *Int. J. Theor. Phys.* **21,** 467–488 (1982).
18. Cirac, J. I. & Zoller, P. New frontiers in quantum information with atoms and ions. *Phys. Today* **57,** 38–44 (2004).
19. Jaksch, D., Bruder, C., Cirac, J. I., Gardiner, C. W. & Zoller, P. Cold bosonic atoms in optical lattices. *Phys. Rev. Lett.* **81,** 3108–3111 (1998).
20. Lewenstein, M. *et al.* Ultracold atomic gases in optical lattices: Mimicking condensed-matter physics and beyond. *Adv. Phys.* **56,** 243–379 (2007).
21. Bloch, I., Dalibard, J. & Zwerger, W. Many-body physics with ultracold atoms. *Rev. Mod. Phys.* **80,** 885–964 (2008).
22. Greiner, M., Mandel, O., Esslinger, T., Hänsch, T. W. & Bloch, I. Quantum phase transition from a superfluid to a Mott insulator in a gas of ultracold atoms. *Nature* **415,** 39–44 (2002).
23. Jördens, R., Strohmaier, N., Günter, K., Moritz, H. & Esslinger, T. A Mott insulator of fermionic atoms in an optical lattice. *Nature* **455,** 204–207 (2008).
24. Schneider, U. *et al.* Metallic and insulating phases of repulsively interacting fermions in a 3D optical lattice. *Science* **322,** 1520–1525 (2008).
25. Paredes, B. *et al.* Tonks–Girardeau gas of ultracold atoms in an optical lattice. *Nature* **429,** 277–281 (2004).
26. Kinoshita, T., Wenger, T. & Weiss, D. S. Observation of a one-dimensional Tonks–Girardeau gas. *Science* **305,** 1125–1128 (2004).
27. Hadzibabic, Z., Krüger, P., Cheneau, M., Battelier, B. & Dalibard, J. Berezinskii–Kosterlitz–Thouless crossover in a trapped atomic gas. *Nature* **441,** 1118–1121 (2006).
28. Anderlini, M. *et al.* Controlled exchange interaction between pairs of neutral atoms in an optical lattice. *Nature* **448,** 452–456 (2007).
29. Trotzky, S. *et al.* Time-resolved observation and control of superexchange interactions with ultracold atoms in optical lattices. *Science* **319,** 295–299 (2008).
30. Clément, D. *et al.* Experimental study of the transport of coherent interacting matter-waves in a 1D random potential induced by laser speckle. *New J. Phys.* **8,** 165 (2006).
31. Fallani, L., Fort, C. & Inguscio, M. Bose–Einstein condensates in disordered potentials. *Adv. At. Mol. Opt. Phys.* **56,** 119–160 (2008).
32. Damski, B., Zakrzewski, J., Santos, L., Zoller, P. & Lewenstein, M. Atomic Bose and Anderson glasses in optical lattices. *Phys. Rev. Lett.* **91,** 080403 (2003).
33. Roth, T. & Burnett, K. Ultracold bosonic atoms in disordered optical superlattices. *J. Opt. B: Quant. Semiclass. Opt.* **5,** S50–S54 (2003).
34. Sanchez-Palencia, L. *et al.* Anderson localization of expanding Bose–Einstein condensates in random potentials. *Phys. Rev. Lett.* **98,** 210401 (2007).
35. Lye, J. E. *et al.* Bose–Einstein condensate in a random potential. *Phys. Rev. Lett.* **95,** 070401 (2005).
36. Clément, D. *et al.* Suppression of transport of an interacting elongated Bose–Einstein condensate in a random potential. *Phys. Rev. Lett.* **95,** 170409 (2005).
37. Fort, C. *et al.* Effect of optical disorder and single defects on the expansion of a Bose–Einstein condensate in a one-dimensional waveguide. *Phys. Rev. Lett.* **95,** 170410 (2005).
38. Schulte, T. *et al.* Routes towards Anderson-like localization of Bose–Einstein condensates in disordered optical lattices. *Phys. Rev. Lett.* **95,** 170411 (2005).
39. Clément, D., Bouyer, P., Aspect, A. & Sanchez-Palencia, L. Density modulations in an elongated Bose–Einstein condensate released from a disordered potential. *Phys. Rev. A* **77,** 033631 (2008).
40. Chen, Y. P. *et al.* Phase coherence and superfluid–insulator transition in a disordered Bose–Einstein condensate. *Phys. Rev. A* **77,** 033632 (2008).
41. Billy, J. *et al.* Direct observation of Anderson localization of matter-waves in a controlled disorder. *Nature* **453,** 891–894 (2008).
42. Roati, G. *et al.* Anderson localization of a non-interacting Bose–Einstein condensate. *Nature* **453,** 895–898 (2008).
43. Basko, D. M., Aleiner, I. L. & Altshuler, B. L. On the problem of many-body localization. *Ann. Phys.* **321,** 1126–1205 (2006).
44. Bilas, N. & Pavloff, N. Anderson localization of elementary excitations in a one dimensional Bose–Einstein condensate. *Eur. Phys. J. D* **40,** 387–397 (2006).
45. Lugan, P., Clément, D., Bouyer, P., Aspect, A. & Sanchez-Palencia, L. Anderson localization of Bogolyubov quasiparticles in interacting Bose–Einstein condensates. *Phys. Rev. Lett.* **99,** 180402 (2007).
46. Giamarchi, T. & Schulz, H. J. Anderson localization and interactions in one-dimensional metals. *Phys. Rev. B* **37,** 325–340 (1988).
47. Fisher, M. P. A., Weichman, P. B., Grinstein, G. & Fisher, D. S. Boson localization and the superfluid–insulator transition. *Phys. Rev. B* **40,** 546–570 (1989).
48. Minchau, B. J. & Pelcovits, R. A. Two-dimensional *XY* model in a random uniaxial field. *Phys. Rev. B* **32,** 3081–3087 (1985).
49. Wehr, J., Niederberger, A., Sanchez-Palencia, L. & Lewenstein, M. Disorder versus the Mermin–Wagner–Hohenberg effect: From classical spin systems to ultracold atomic gases. *Phys. Rev. B* **74,** 224448 (2006).
50. Niederberger, A. *et al.* Disorder-induced order in two-component Bose–Einstein condensates. *Phys. Rev. Lett.* **100,** 030403 (2008).
51. Mezard, M., Parisi, G. & Virasoro, M. *Spin Glass Theory and Beyond* (World Scientific, 1987).
52. Newman, C. M. & Stein, D. L. Ordering and broken symmetry in short-ranged spin glasses. *J. Phys. Condens. Mater* **15,** R1319–R1364 (2003).
53. Sanpera, A., Kantian, A., Sanchez-Palencia, L., Zakrewski, J. & Lewenstein, M. Atomic Fermi–Bose mixtures in inhomogeneous and random optical lattices: From Fermi glass to quantum spin glass and quantum percolation. *Phys. Rev. Lett.* **93,** 040401 (2004).

54. Ahufinger, V., Sanchez-Palencia, L., Kantian, A., Sanpera, A. & Lewenstein, M. Disordered ultracold atomic gases in optical lattices: A case study of Fermi–Bose mixtures. *Phys. Rev. A* **72,** 063616 (2005).
55. Mott, N. F. & Twose, W. D. The theory of impurity conduction. *Adv. Phys.* **10,** 107–163 (1961).
56. Borland, R. E. The nature of the electronic states in disordered one-dimensional systems. *Proc. R. Soc. A* **274,** 529–545 (1963).
57. Abrahams, E., Anderson, P. W., Licciardello, D. C. & Ramakrishnan, T. V. Scaling theory of localization: absence of quantum diffusion in two dimensions. *Phys. Rev. Lett.* **42,** 673–676 (1979).
58. Ioffe, A. F. & Regel, A. R. Non-crystalline, amorphous and liquid electronic semiconductors. *Prog. Semicond.* **4,** 237–291 (1960).
59. Mott, N. F. Electrons in disordered structures. *Adv. Phys.* **16,** 49–144 (1967).
60. Harper, P. G. Single band motion of conduction electrons in a uniform magnetic field. *Proc. Phys. Soc. A* **68,** 874–878 (1955).
61. Aubry, S. & André, G. Analyticity breaking and Anderson localization in incommensurate lattices. *Ann. Israel Phys. Soc.* **3,** 133–140 (1980).
62. Lifshits, I. M., Gredeskul, S. A. & Pastur, L. A. *Introduction to the Theory of Disordered Systems* (Wiley, 1988).
63. Lugan, P. *et al.* One-dimensional Anderson localization in certain correlated random potentials. *Phys. Rev. A* **80,** 023605 (2009).
64. Gurevich, E. & Kenneth, O. Lyapunov exponent for the laser speckle potential: A weak disorder expansion. *Phys. Rev. A* **79,** 063617 (2009).
65. Vollhardt, D. & Wölfle, P. Anderson localization in $d \leq 2$ dimensions: A self-consistent diagrammatic theory. *Phys. Rev. Lett.* **45,** 842–845 (1980).
66. Kuhn, R. C., Miniatura, C., Delande, D., Sigwarth, O. & Müller, C. A. Localization of matter waves in two-dimensional disordered optical potentials. *Phys. Rev. Lett* **95,** 250403 (2005).
67. Shapiro, B. Expansion of a Bose–Einstein condensate in the presence of disorder. *Phys. Rev. Lett.* **99,** 060602 (2007).
68. Skipetrov, S. E., Minguzzi, A., van Tiggelen, B. A. & Shapiro, B. Anderson localization of a Bose–Einstein condensate in a 3D random potential. *Phys. Rev. Lett.* **100,** 165301 (2008).
69. Anderson, P. W. in *Nobel Lectures, Physics 1971–1980* (ed. Lundqvist, S.) (World Scientific, 1992).
70. Pikovsky, A. S. & Shepelyansky, D. L. Destruction of Anderson localization by a weak nonlinearity. *Phys. Rev. Lett.* **100,** 094101 (2008).
71. Kopidakis, G., Komineas, S., Flach, S. & Aubry, S. Absence of wave packet diffusion in disordered nonlinear systems. *Phys. Rev. Lett.* **100,** 084103 (2008).
72. Paul, T., Schlagheck, P., Leboeuf, P. & Pavloff, N. Superfluidity versus Anderson localization in a dilute Bose gas. *Phys. Rev. Lett.* **98,** 210602 (2007).
73. Lugan, P. *et al.* Ultracold Bose gases in 1D random potentials: From Lifshits glasses to Bose–Einstein condensates. *Phys. Rev. Lett.* **98,** 170403 (2007).
74. Lifshitz, I. M. The energy spectrum of disordered systems. *Adv. Phys.* **13,** 483–536 (1964).
75. Sanchez-Palencia, L. Smoothing effect and delocalization of interacting Bose–Einstein condensates in random potentials. *Phys. Rev. A* **74,** 053625 (2006).
76. Falco, G. M., Nattermann, T. V. & Pokrovsky, L. Localized states and interaction-induced delocalization in Bose gases with quenched disorder. *Europhys. Lett.* **85,** 30002 (2009).
77. Gurarie, V., Refael, G. & Chalker, J. T. Excitations of the one-dimensional Bose–Einstein condensates in a random potential. *Phys. Rev. Lett.* **101,** 170407 (2008).
78. Orso, G. BCS–BEC crossover in a random external potential. *Phys. Rev. Lett.* **99,** 250402 (2007).
79. Han, L. & Sa de Melo, C. A. R. Disorder effects during the evolution from BCS to BEC superfluidity. Preprint at <http://arxiv.org/abs/0904.4197> (2009).
80. Anderson, P. W. Theory of dirty superconductors. *J. Phys. Chem. Solids* **11,** 26–30 (1959).
81. Mott, N. F. Metal–insulator transition. *Rev. Mod. Phys.* **40,** 677–683 (1968).
82. Fallani, L., Lye, J. E., Guarrera, V., Fort, C. & Inguscio, M. Ultracold atoms in a disordered crystal of light: Towards a Bose glass. *Phys. Rev. Lett.* **98,** 130404 (2007).
83. White, M. *et al.* Strongly interacting bosons in a disordered optical lattice. *Phys. Rev. Lett.* **102,** 055301 (2009).
84. Roscilde, T. Bosons in one-dimensional incommensurate superlattices. *Phys. Rev. A* **77,** 063605 (2008).
85. Roux, G. *et al.* Quasiperiodic Bose–Hubbard model and localization in one-dimensional cold atomic gases. *Phys. Rev. A* **78,** 023628 (2008).
86. Delande, D. & Zakrzewski, J. Compression as a tool to detect Bose glass in cold atoms experiments. *Phys. Rev. Lett.* **102,** 085301 (2009).
87. Georges, A. in *Proc. of the International School of Physics 'Enrico Fermi', Course CLXIV* (eds Inguscio, M., Ketterle, W. & Salomon, C.) (IOS Press, 2008); preprint at <http://arxiv.org/abs/cond-mat/0702122>.
88. Byczuk, K., Hofstetter, W. & Vollhardt, D. Competition between Anderson localization and antiferromagnetism in correlated lattice fermion systems with disorder. *Phys. Rev. Lett.* **102,** 146403 (2009).
89. Kuklov, A. B. & Svistunov, B. V. Counterflow superfluidity of two-species ultracold atoms in a commensurate optical lattice. *Phys. Rev. Lett.* **90,** 100401 (2003).
90. Duan, L.-M., Demler, E. & Lukin, M. D. Controlling spin exchange interactions of ultracold atoms in optical lattices. *Phys. Rev. Lett.* **91,** 090402 (2003).
91. Morrison, S. *et al.* Physical replicas and the Bose glass in cold atomic gases. *New J. Phys.* **10,** 073032 (2008).
92. Paredes, B., Verstraete, F. & Cirac, J. I. Exploiting quantum parallelism to simulate quantum random many-body systems. *Phys. Rev. Lett.* **95,** 140501 (2005).
93. Abanin, D. A., Lee, P. A. & Levitov, L. S. Randomness-induced *XY* ordering in a graphene quantum Hall ferromagnet. *Phys. Rev. Lett.* **98,** 156801 (2007).
94. Gavish, U. & Castin, Y. Matter-wave localization in disordered cold atom lattices. *Phys. Rev. Lett.* **95,** 020401 (2005).
95. Buonsante, P., Penna, V., Vezzani, A. & Blakie, P. B. Mean-field phase diagram of cold lattice bosons in disordered potentials. *Phys. Rev. A* **76,** 011602 (2007).
96. Horstmann, B., Cirac, J. I. & Roscilde, T. Dynamics of localization phenomena for hard-core bosons in optical lattices. *Phys. Rev. A* **76,** 043625 (2007).
97. Roscilde, T. & Cirac, J. I. Quantum emulsion: A glassy phase of bosonic mixtures in optical lattices. *Phys. Rev. Lett.* **98,** 190402 (2007).
98. Ospelkaus, S. *et al.* Localization of bosonic atoms by fermionic impurities in a three-dimensional optical lattice. *Phys. Rev. Lett.* **96,** 180403 (2006).
99. Günter, K., Stöferle, T., Moritz, M., Köhl, M. & Esslinger, T. Bose–Fermi mixtures in a three-dimensional optical lattice. *Phys. Rev. Lett.* **96,** 180402 (2006).
100. Catani, V., De Sarlo, L., Barontini, G., Minardi, F. & Inguscio, M. Degenerate Bose–Bose mixture in a three-dimensional optical lattice. *Phys. Rev. A* **77,** 011603(R) (2008).
101. Lühmann, D.-S., Bongs, K., Sengstock, K. & Pfannkuche, D. Self-trapping of bosons and fermions in optical lattices. *Phys. Rev. Lett.* **101,** 050402 (2008).
102. Best, T. *et al.* Role of interactions in ^{87}Rb–^{40}K Bose–Fermi mixtures in a 3D optical lattice. *Phys. Rev. Lett.* **102,** 030408 (2009).
103. Lutchyn, R. M., Tewari, S. & Das Sarma, S. Loss of superfluidity by fermions in the boson Hubbard model on an optical lattice. *Phys. Rev. A* **79,** 011606(R) (2009).
104. Dettmer, S. *et al.* Observation of phase fluctuations in elongated Bose–Einstein condensates. *Phys. Rev. Lett.* **87,** 160406 (2001).
105. Richard, S. *et al.* Momentum spectroscopy of 1D phase fluctuations in Bose–Einstein condensates. *Phys. Rev. Lett.* **91,** 010405 (2003).
106. Guerin, W. *et al.* Guided quasicontinuous atom laser. *Phys. Rev. Lett.* **97,** 200402 (2006).
107. Goodman, J. W. *Speckle Phenomena in Optics: Theory and Applications* (Roberts, 2007).

Acknowledgements

This research was supported by the French Centre National de la Recherche Scientifique (CNRS), Agence Nationale de la Recherche (ANR), Triangle de la Physique and Institut Francilien de Recherche sur les Atomes Froids (IFRAF), the German Alexander von Humboldt foundation, the Spanish MEC grants FIS 2005-04627 and Conslider Ingenio 2010 'QOIT', the European Union IP Programme SCALA and the European Science Foundation–MEC Euroquam Project FerMix.

Additional information

The authors declare no competing financial interests. Reprints and permissions information is available online at http://npg.nature.com/reprintsandpermissions. Correspondence and requests for materials should be addressed to L.S.P. or M.L.

QUANTUM GASES

Joint forces against disorder

An experiment with ultracold gases reveals how weakly interacting atoms cooperate to protect long-range coherence against disorder-induced localization, and should offer insight into long-standing questions on the complex interplay of interactions and disorder in quantum systems.

Laurent Sanchez-Palencia

Imagine a troop of soldiers trying to clear a path through a dense jungle. They have to decide between acting independently to explore a larger area but lacking mutual help, or cooperating to coordinate their action but taking more time to explore the territory. A similar problem exists for quantum particles in dirty materials, although in a slightly different way: do disorder and interactions cooperate or compete to determine whether a material behaves like a metal or like an insulator? Writing in *Nature Physics*, Benjamin Deissler and colleagues[1] report that weak repulsive interactions act against disorder to restore metallic-like behaviour in ultracold Bose gases.

Disorder plays an important role in many condensed-matter systems and strongly influences a variety of phenomena, including electronic conductivity or superfluidity in liquid helium. Philip Anderson showed more than fifty years ago that disorder alone can lead to metal–insulator transitions through spatial localization of quantum particles[2]. In most materials however, Anderson localization is hardly separable from other mechanisms that induce metal–insulator transitions, such as band filling in crystal structure (leading to band insulators) or particle–particle interactions (leading to Mott insulators). Hence, many parameters determine the metallic or insulating nature of materials, and drawing a clear and comprehensive picture is obfuscated by the interplay of all these effects in most condensed-matter systems.

Ultracold atoms avoid these drawbacks because they are versatile and controllable systems. Several research groups are at present making an effort to use them as playgrounds to simulate theoretical models in real experiments. The field of disordered systems is one where ultracold atoms are promising in terms of addressing open questions[3].

A first step in this endeavour was to demonstrate Anderson localization of quantum particles. This was successfully achieved two years ago in two complementary experiments[4,5]: using a gas of ultracold atoms in a controlled disordered potential created by laser light, exponential decay of the atomic density profile was observed. This was the first direct evidence of Anderson localization of matter waves. Those experiments were performed in a regime of negligible interactions between the atoms. Deissler and colleagues[1] now go an important step further and introduce controlled interparticle interactions.

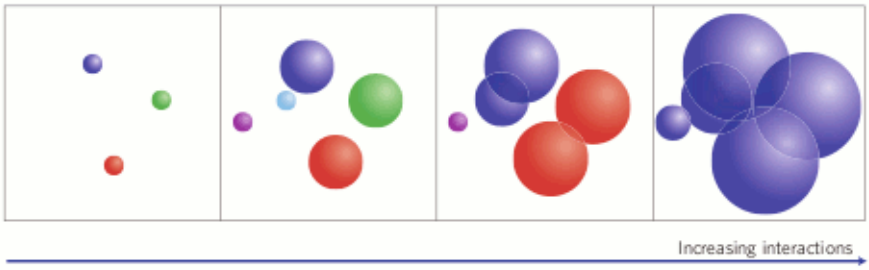

Figure 1 | The effect of weak repulsive interactions in a disordered Bose gas. For very weak interactions (far left), the bosons populate a couple of independent islands with random phases (represented by different colours). When interactions increase, more islands are populated and inflate. When two islands overlap, they rapidly form a locally coherent patch. For sufficiently large interactions, a single patch is formed with long-range coherence.

In their experiment, Deissler *et al.* first create a periodic potential using two, strong, counter-propagating laser beams. Bosonic ^{39}K atoms are then trapped in a perfectly periodic one-dimensional array of wells (the nodes of the corresponding standing wave); quantum tunnelling allows them to jump from one well to another. Disorder is subsequently introduced using a second, independent and much weaker standing wave with an incommensurate spatial period. This mimics disorder in the form of random-like shifts of the depth of the wells. Such a model is known to exhibit a metal–insulator transition[6]. For a small degree of disorder, the quantum states are extended over the full system, as in a metal. Conversely, when the disorder strength passes a critical value, the states become exponentially localized, leading to the absence of long-range coherence, as in an insulator. Control of the tunnelling rate and disorder strength in the same experimental setting as used by Deissler *et al.* demonstrated such a localization–delocalization scenario[5].

But how do interactions affect the localization–delocalization transition? To address this question, Deissler *et al.*[1] exploited another form of control available for ultracold atoms: so-called Feshbach resonance techniques, where a magnetic field modifies the two-body internal structure and thus the interaction strength. For a given amount of disorder and interactions, the Bose gas is produced close to its ground state. The momentum distribution is then precisely measured by releasing the atoms from the disordered lattice and cancelling the interactions. Fourier analysis of the data provides information on localization properties, spatial correlations and phase coherence. Repeating the experiment for a variety of parameters, Deissler *et al.* confirm the main features of a delocalization crossover induced by weak repulsive interactions[7,8]: for very weak interactions, the bosons populate low-energy states and form independent, strongly localized islands with no phase coherence. When interactions are increased, more islands are populated. When many islands are

populated, they overlap and start to form locally coherent patches (Fig. 1). For even stronger interactions, these patches inflate so as to minimize the interaction energy and finally condense into a single patch with long-range coherence.

This experiment constitutes an important step forward in the understanding of disordered systems with ultracold atoms, showing that weakly interacting bosons do cooperate to counteract localization in disordered systems, thus turning an insulator-like material into a metal-like material. The next step would be to study strongly interacting Bose gases, for which theory predicts that interactions should conversely cooperate with disorder to enhance localization. In strongly correlated Bose lattices the formation of an intriguing Bose glass phase has been predicted[9], the nature of which is still debated. Recent experiments with ultracold atoms in this regime suggest that the gap is suppressed[10] and the condensed fraction destroyed[11]. Further efforts are needed, however, to measure key features such as compressibility and suppression of the superfluid fraction (a related but more elusive quantity than the condensed fraction).

So far, disordered quantum gases have focused on bosons, which are relevant to ^{4}He in porous media. With a view to studying systems of direct relevance to metal–insulator transitions in electronic systems, a future challenge will be to study the fermion counterparts of this physics. ❐

Laurent Sanchez-Palencia is in the Laboratoire Charles Fabry de l'Institut d'Optique, CNRS and Univ. Paris-Sud, F-91127, Palaiseau, France.
e-mail: lsp@institutoptique.fr

References

1. Deissler, B. *et al. Nature Phys.* **6,** 354–358 (2010).
2. Anderson, P. W. *Phys. Rev.* **109,** 1492–1505 (1958).
3. Sanchez-Palencia, L. & Lewenstein, M. *Nature Phys.* **6,** 87–95 (2010).
4. Billy, J. *et al. Nature* **453,** 891–894 (2008).
5. Roati, G. *et al. Nature* **453,** 895–898 (2008).
6. Aubry, S. & André, G. *Ann. Israel Phys. Soc.* **3,** 133–140 (1980).
7. Lee, D. K. K. & Gunn, J. M. F. *J. Phys. Condens. Matter* **2,** 7753–7768 (1990).
8. Lugan, P. *et al. Phys. Rev. Lett.* **98,** 170403 (2007).
9. Fisher, M. P. A., Weichman, P. B., Grinstein, G. & Fisher, D. S. *Phys. Rev. B* **40,** 546–570 (1989).
10. Fallani, L., Lye, J. E., Guarrera, V., Fort, C. & Inguscio, M. *Phys. Rev. Lett.* **98,** 130404 (2007).
11. White, M. *et al. Phys. Rev. Lett.* **102,** 055301 (2009).

Localized and Extended States in a Disordered Trap

Luca Pezzé and Laurent Sanchez-Palencia

Laboratoire Charles Fabry de l'Institut d'Optique, CNRS and Univ. Paris-Sud, Campus Polytechnique, RD 128, F-91127 Palaiseau cedex, France

(Received 20 June 2010; revised manuscript received 8 December 2010; published 25 January 2011)

We study Anderson localization in a disordered potential combined with an inhomogeneous trap. We show that the spectrum displays both localized and extended states, which coexist at intermediate energies. In the region of coexistence, we find that the extended states result from confinement by the trap and are weakly affected by the disorder. Conversely, the localized states correspond to eigenstates of the disordered potential, which are only affected by the trap via an inhomogeneous energy shift. These results are relevant to disordered quantum gases and we propose a realistic scheme to observe the coexistence of localized and extended states in these systems.

DOI: 10.1103/PhysRevLett.106.040601 PACS numbers: 05.60.Gg, 03.75.Ss, 67.85.−d, 72.15.Rn

Disorder underlies many fields in physics, such as electronics, superfluid helium and optics [1–3]. It poses challenging questions, regarding quantum transport [4] and the interplay of disorder and interactions [5]. In this respect, ultracold gases offer exceptionally well controlled simulators for condensed-matter physics [6] and are particularly promising for disordered systems [7]. They recently allowed for the direct observation of one-dimensional (1D) Anderson localization of matter waves [8–11]. It should be noticed, however, that ultracold gases do not only mimic standard models of condensed-matter physics, but also raise new issues which require special analysis in its own right. For instance, they are most often confined in spatial traps, which has significant consequences. On the one hand, retrieving information about bulk properties requires specific algorithms [12]. On the other hand, trapping induces novel effects, such as the existence of Bose-Einstein condensates in low dimensions [13], and suppression of quantum tunneling in periodic lattices [14].

Consider Anderson localization [15]. In *homogeneous* disorder, linear waves can localize owing to coherent multiple scattering, with properties depending on the system dimension and the disorder strength [1]. A paradigm of Anderson localization is that localized and extended states generally do not coexist in energy. This relies on Mott's *reductio ad absurdum* [1]: Should there exist a localized state and an extended state with infinitely close energies for a given configuration of disorder, an infinitesimal change of the configuration would hybridize them, forming two extended states. Hence, for a given energy, almost all states should be either localized or extended. Exceptions only appear for specific models of disorder with strong local symmetries [16]. Then, a question arises: Can *inhomogeneous* trapping modify this picture so that localized and extended states coexist in energy?

In this Letter, we study localization in a disordered potential combined with an inhomogeneous trap. The central result of this work is the coexistence, at intermediate energies, of two classes of eigenstates. The first class corresponds to states which spread over the full (energy-dependent) classically allowed region of the bare trap, and which we thus call "extended." The second class corresponds to states of width much smaller than the trap size, which are localized by the disorder, and which we thus call "localized." We give numerical evidence of the coexistence of extended and localized states for different kinds of traps. We show that while the extended states are confined by the trap and weakly affected by the disorder, the localized states correspond to eigenstates of the disordered potential, which are only affected by the trap via an inhomogeneous energy shift. Finally, we propose an experimentally feasible scheme using energy-selective time-of-flight techniques to observe this coexistence with ultracold Fermi gases.

Let us consider a d-dimensional gas of noninteracting particles of mass m, confined into a spatial trap $V_T(\boldsymbol{r})$ and subjected to a homogeneous disordered potential $V(\boldsymbol{r})$ of zero average, amplitude V_R and correlation length σ_R. Hereafter, we use "red-detuned" speckle potentials ($V_R < 0$), which are relevant to quantum gases [7,17]. For the trap, we take $V_T(\boldsymbol{r}) = (\hbar^2/2ma^2)|\boldsymbol{r}/a|^\alpha$, being a the trap length scale. For instance, $\alpha = \infty$ and $a = L/2$ for a homogeneous box of length L, while $\alpha = 2$ and $a = \sqrt{\hbar/m\omega}$ for a harmonic trap of angular frequency ω. We numerically compute the eigenstates $|\psi_n\rangle$ and eigenenergies E_n of the Hamiltonian

$$\hat{H} = -\hbar^2\boldsymbol{\nabla}^2/2m + V(\boldsymbol{r}) + V_T(\boldsymbol{r}). \tag{1}$$

The eigenstates are characterized by their center of mass, $\boldsymbol{r}_n \equiv \langle\psi_n|\hat{\boldsymbol{r}}|\psi_n\rangle$, and spatial extension (rms size), $\Delta r_n \equiv (\langle\psi_n|\hat{\boldsymbol{r}}^2|\psi_n\rangle - \boldsymbol{r}_n^2)^{1/2}$. The quantity Δr_n quantifies localization: the smaller, the more localized.

Numerical results for the 1D ($d = 1$) case are reported in Fig. 1. In infinite, homogeneous disorder ($\alpha = \infty, L = \infty$), all states $|\psi_n\rangle$ are localized, uniformly distributed in space, and, for most models of disorder, their extension Δz_n increases with the energy [18]. As Figs. 1(a) and 1(f)

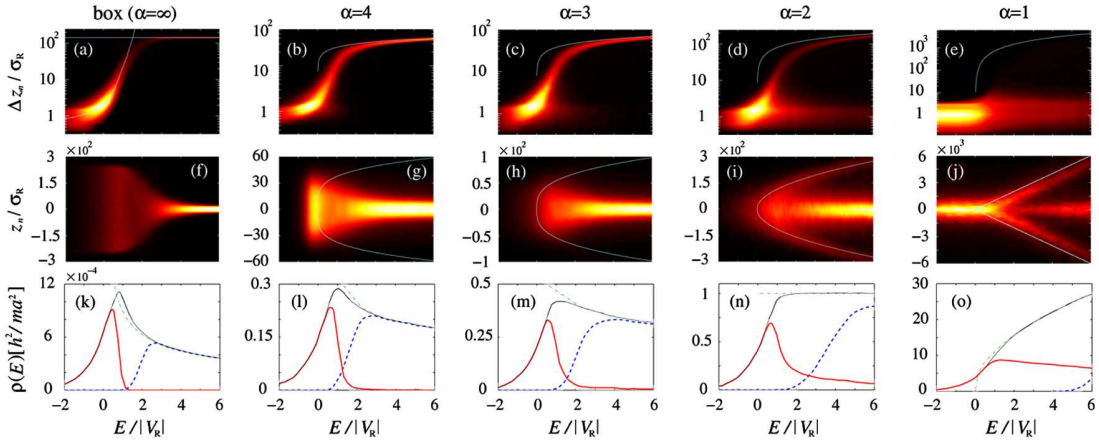

FIG. 1 (color online). Extension (a)–(e), center of mass (f)–(j) and density of states (DOS) (k)–(o) of the eigenstates versus energy in various kinds of 1D disordered traps. The plots result from accumulation of numerical data over 5000 realizations of a red-detuned speckle potential with $m\sigma_R^2|V_R|/\hbar^2 = 0.256$. The first column refers to a flat box of length $L = 500\sigma_R$. The curved line in (a) corresponds to an infinite system [28] and the horizontal line is $\Delta z^0 = L/2\sqrt{3}$. The other columns refer to inhomogeneous traps with $a = 12.5\sigma_R$ and various trap powers α. The solid lines correspond to the nondisordered case, i.e., Δz^0 in panels (b)–(e) and $\pm z_{\rm cl}(E)$ in panels (g)–(j). The last row shows the full DOS $\rho(E)$ (solid black line), as well as the DOS restricted to localized ($\rho_<$, solid red line) and extended ($\rho_>$, dashed blue line) states [19]. The dot-dashed green lines are the nondisordered limits.

show, using a finite flat box ($L < \infty$) only induces a trivial finite-size effect: For low-enough energy E, we find $\Delta z_n \ll L$ and the states are not significantly affected by the finite size of the box. For larger energies, however, boundary effects come into the picture. The states are centered close to the box center and their extension saturates to the value obtained for a plane wave ($\Delta z^0 = L/2\sqrt{3}$). A central outcome of these results is that the curve giving Δz_n versus E displays a single branch. In particular, there is no energy window where localized and extended states coexist. This holds independently of the finite box size and is in agreement with Mott's argument [1].

For inhomogeneous traps ($\alpha < \infty$), we find a completely different behavior. The curves giving Δz_n and z_n versus E now display two clearly separated branches [see Figs. 1(b)–1(e) and 1(g)–1(j)]. For low energy, the states are strongly localized and, for $E > 0$, they are roughly uniformly distributed in a region bounded by the (energy-dependent) classical turning points, $z_{\rm cl}(E)$, defined as the solutions of $V_T(z_{\rm cl}) = E$. For higher energy, the extension of the states corresponding to the upper branch in Figs. 1(b)–1(e) grows and eventually saturates to that of the eigenstates of the nondisordered trap, $\Delta z^0(E)$. The centers of mass of these states approach the trap center and form the horizontal branch in Figs. 1(g)–1(j). This branch corresponds to extended states. It is easily interpreted in terms of finite-size effects, similarly as for a finite flat box. The lower branch in Figs. 1(b)–1(e) is more surprising. It identifies strongly localized states of relatively large energy. It has no equivalent in the flat box and cannot be interpreted as a finite-size effect. The corresponding states are located close to the classical turning points $z_{\rm cl}(E)$ and form the outer branches in Figs. 1(g)–1(j). As Fig. 1 shows, this holds for all inhomogeneous traps. When the trap power α increases, the branch of extended states gets denser at the expense of that of localized states, and completely vanishes for $\alpha = \infty$ (homogeneous box).

The coexistence of localized and extended states in the same energy window for disordered traps is confirmed on more quantitative grounds in the last row of Fig. 1. It shows the full density of states (solid black line), as well as the density of localized ($\rho_<$, solid red line) and extended ($\rho_>$, dashed blue line) states [19]. The different nature of the localized and extended states is even more striking when one studies the wave functions. Let us focus for instance on the harmonic trap ($\alpha = 2$) and on a narrow slice of the spectrum around $E \sim 4|V_R|$, where $\rho_</\rho \simeq 14\%$ of the states are localized [20]. Figure 2(a) shows the spatial density $|\psi_n(z)|^2$ of all states found for a *single realization* of the disorder. We can clearly distinguish localized (thick red lines) and extended (thin blue lines) states, which shows that they coexist in the same energy window for each realization of the disorder. The localized states are very narrow and present no nodes (e.g., states A and E) or a few nodes (e.g., states C and H). They may be identified as bound states of the local deep wells of the disordered potential, similarly as the lowest-energy states creating the Lifshits tail in bare disorder [18]. To confirm this, let us decompose the eigenstates $|\psi_n\rangle$ of the disordered trap onto the basis of the eigenstates $|\chi_p\rangle$ of the bare disordered potential [i.e., Hamiltonian (1) with $V_T \equiv 0$], associated to the eigenenergies ϵ_p. For a localized state $|\psi_n\rangle$, we find $|\langle\chi_p|\psi_n\rangle|^2 \sim 1$ for a single state $|\chi_p\rangle$ such that $\epsilon'_p \simeq E_n$, where $\epsilon'_p = \epsilon_p + \langle\chi_p|V_T(z)|\chi_p\rangle$ is the eigenenergy of $|\chi_p\rangle$ shifted by the trapping potential [see Fig. 2(b)]. Conversely, the same decomposition for an extended state shows a broad distribution of amplitude much smaller than unity. A localized state $|\psi_n\rangle$ of the disordered trap thus

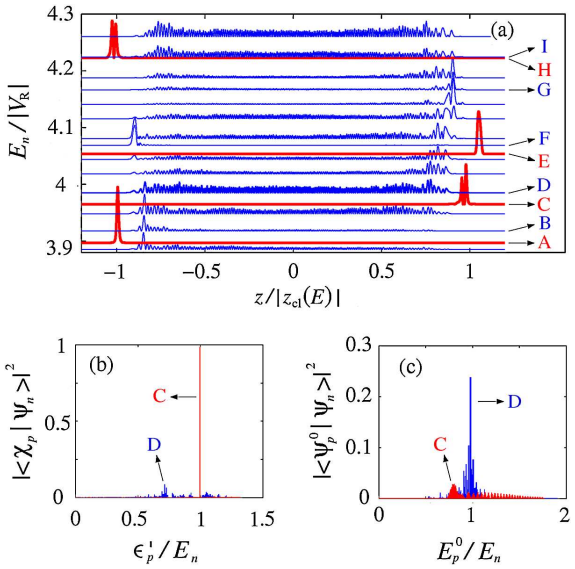

FIG. 2 (color online). Eigenstates for a single realization of a 1D disordered harmonic trap. (a) Non-normalized spatial densities, $|\psi_n(z)|^2$, vertically displaced to their eigenenergy E_n. Thick red lines correspond to localized states, and thin blue lines to extended states [19]. Note that extended and localized states may occupy almost-degenerate energy levels (e.g., H and I). The states C and D are projected: (b) over the eigenstates of the bare disordered potential, $|\chi_p\rangle$, and (c) over those of the bare harmonic trap, $|\psi_p^0\rangle$. The parameters are as in Fig. 1.

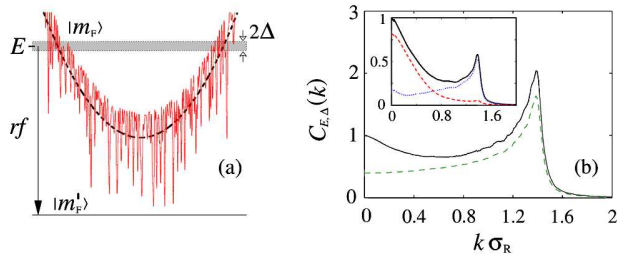

FIG. 3 (color online). Scheme to observe the coexistence of localized and extended states in disordered traps (solid red line). (a) Atoms occupying the eigenstates of energy $E \pm \Delta$ (shaded region) are transferred to a different internal state via rf coupling. The corresponding momentum distribution is then measured by TOF. (b) Correlation function $\mathcal{C}_{E,\Delta}(k)$ (black solid line) and momentum distribution $\overline{\mathcal{D}_{E,\Delta}(k)}$ (dashed green line, arbitrary units), for $\Delta = 2\hbar\omega$. Inset: $\mathcal{C}_{E,\Delta}(k)$ of all states (solid black line), and separating localized (dashed red line) and extended (dotted blue line) states [19], for $\Delta = 0.01\hbar\omega$. Here $E = 4|V_R|$ and the other parameters are as in Fig. 1.

corresponds to a strongly localized state $|\chi_p\rangle$ in the bare disorder, which is affected by the trap by just the energy shift $\langle\chi_p|V_T(z)|\chi_p\rangle$. We generally find that $|\epsilon_p| \ll \langle\chi_p|V_T(z)|\chi_p\rangle \simeq \langle\psi_n|V_T(z)|\psi_n\rangle$, and, due to the reduced spatial extension of $|\psi_n\rangle$, we get $E_n \simeq V_T(z_n)$ [21]. This explains that the localized states are located close to the classical turning points, as observed in Figs. 1 and 2(a).

Let us now decompose the states $|\psi_n\rangle$ of the disordered trap onto the basis of the eigenstates $|\psi_p^0\rangle$ of the bare trap [i.e., Hamiltonian (1) with $V = 0$], associated to the eigenenergy E_p^0. For a localized state, the distribution is broad. Conversely, for an extended state, the distribution is sharp and peaks at $E_p^0 \simeq E_n$ to a value equal to a fraction of unity [see Fig. 2(c)]. An extended state may thus be seen as reminiscent of an eigenstate of the bare trap, which is weakly affected by the disorder. Still, the main peak in Fig. 2(c) is smaller than unity. Only for significantly higher energy, the state $|\psi_n\rangle$ results from weak perturbation of $|\psi_n^0\rangle$, and $|\langle\psi_p^0|\psi_n\rangle|^2$ displays a main peak of the order of unity as predicted by standard perturbation theory.

Our results can now be easily interpreted. In bare disorder, the typical size Δz of the localized states increases faster than the classically allowed region $z_{cl} \propto E^{1/\alpha}$ provided by the trap. For low energy, $\Delta z \ll z_{cl}$ so that the states are strongly localized by the disorder and weakly affected by the trap. For higher energy, however, the disorder would localize the states on a scale exceeding z_{cl}. The states are then bounded by the trap and the effect of disorder becomes small. This forms the branch of extended states in both the disordered box and traps. In addition, some strongly localized states with very low energy in the bare disorder and located around point z_n are shifted by the trap to approximately the energy $V_T(z_n)$. This forms the branch of localized states only in disordered traps ($\alpha < \infty$) since, in the box, a state cannot be placed at intermediate energy due to the infinitely sharp edges. Quantitatively, since the localized states in the bare disorder are uniformly distributed in space, the density of localized states can be estimated to roughly scale as $\rho_< \propto (1/\alpha) \times E^{1/\alpha - 1}$, which is consistent with the disappearance of the branch of localized states when α grows and with its vanishing for $\alpha = \infty$ (see Fig. 1). Still, it is striking that localized and extended states can coexist in the same energy window. The disordered potential combined with a *smooth* trap permits localized states to sit slightly outside the classically allowed region occupied by extended states [see Fig. 2(a)]. Then, the Mott argument does not apply here because the spatial segregation can be strong enough to suppress hybridization for an infinitesimal change of the disorder configuration.

Let us now discuss a possible scheme to observe the coexistence of localized and extended states in a disordered trap. Consider an ideal gas of ultracold fermions prepared in a given internal state, at temperature T and chemical potential μ. A class of energies $|E_n - E| \lesssim \Delta$ [see Fig. 3(a)] deep in the Fermi sea (i.e., with $\mu - E \ll k_B T$) can be selected by applying a spin-changing radio-frequency (rf) field of frequency $\nu = E/h$ and duration $\tau \sim h/\Delta$ (with h the Planck constant) [14,22,23]. The rf field transfers the corresponding atoms to an internal state insensitive to the disordered trap. The transferred atoms expand freely, which provides their momentum distribution:

$$\mathcal{D}_{E,\Delta}(k) \simeq \sum_{|E_n - E| \lesssim \Delta} |\hat{\psi}_n(k)|^2, \qquad (2)$$

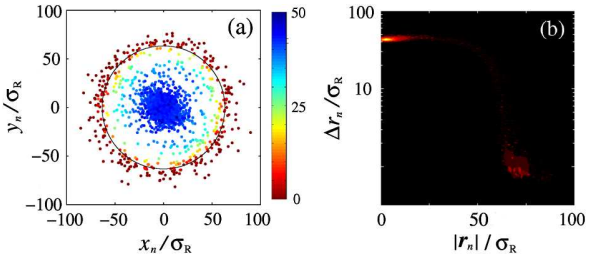

FIG. 4 (color online). Coexistence of localized and extended states in a 2D disordered harmonic trap for $E/|V_R| = 4 \pm 0.0003$. The figure results from accumulation of data from 2×10^4 realizations of the disorder, with $m\sigma_R^2|V_R|/\hbar^2 = 0.8$ and $\omega = 0.05|V_R|/\hbar$. (a) Centers of mass $\boldsymbol{r}_n$ of the eigenstates and corresponding values of $\Delta r_n/\sigma_R$ in color scale. The solid black line is the line of classical turning points, $r_{\rm cl}(E) = \sqrt{2E/m\omega^2} \simeq 63.2\sigma_R$. (b) Extension Δr_n versus distance from the trap center $|\boldsymbol{r}_n|$.

where $\hat{\psi}_n(k)$ is the Fourier transform of $\psi_n(z)$ [time-of-flight (TOF) technique]. In the coexistence region, $\mathcal{D}_{E,\Delta}(k)$ has two significantly different contributions: For localized states, $|\hat{\psi}_n(k)|^2$ is centered around $k \simeq 0$ with tails of width $\Delta k_n \sim \Delta z_n^{-1}$. Conversely, for extended states, $|\hat{\psi}_n(k)|^2$ is peaked at $k \simeq \sqrt{2mE}/\hbar$ with long tails towards small momenta. We however found that averaging over realizations of the disorder blurs the central peak associated to the localized states in $\overline{\mathcal{D}_{E,\Delta}(k)}$. In turn, the quantity $\mathcal{C}_{E,\Delta}(k) \equiv \overline{\mathcal{D}_{E,\Delta}(k) \times \mathcal{D}_{E,\Delta}(0)}/\overline{\mathcal{D}_{E,\Delta}(0)}^2$ displays two distinct peaks for a rf pulse of realistic durations [see Fig. 3(b)]. The central one is more pronounced for narrower pulses. Selecting either the localized states or the extended states [19] confirms that the central peak corresponds to the localized states and the side peak to the extended states [see Inset of Fig. 3(b)].

Finally, we have performed similar calculations as above in a 2D harmonic trap. Figure 4(a) shows the centers of mass $\boldsymbol{r}_n$ of the eigenstates with $E_n \simeq 4|V_R|$, the color scale giving Δr_n. Figure 4(b) shows a density plot of Δr_n versus $|\boldsymbol{r}_n|$ for the same data. Again, the eigenstates clearly separate into two classes: Some states are extended (large Δr_n) and centered nearby the trap center (small $|\boldsymbol{r}_n|$). The other states are strongly localized (small Δr_n) and located nearby the line of classical turning points ($|\boldsymbol{r}_n| \simeq r_{\rm cl}(E) = \sqrt{2E/m\omega^2}$). Hence, the two classes of states can coexist at intermediate energies also in 2D disordered traps.

In conclusion, we have shown that, in a disordered inhomogeneous trap, localized and extended states can coexist in a given energy window. The localized states correspond to eigenstates of the disordered potential which are only affected by the trap via an inhomogeneous energy shift. Conversely, the extended states spread over the classically allowed region of the trap and are weakly affected by the disorder. This effect is directly relevant to present-day experiments with disordered quantum gases, which are most often created in harmonic traps [11,24–27]. We have proposed a realistic scheme to observe it in these systems. In the future, it would be interesting to extend our results to higher dimensions and to other kinds of inhomogeneous disordered systems.

We thank T. Giamarchi and B. van Tiggelen for discussions and ANR (Contract No. ANR-08-blan-0016-01), Triangle de la Physique, LUMAT and IFRAF for support.

[1] N. F. Mott, *Metal-Insulator Transitions* (*Taylor and Francis*, London, 1990).
[2] J. D. Reppy, J. Low Temp. Phys. **87**, 205 (1992).
[3] E. Akkermans and G. Montambaux, *Mesoscopic Physics of Electrons and Photons* (Cambridge University Press, New York, 2006).
[4] A. Lagendijk *et al.*, Phys. Today **62**, No. 8, 24 (2009); A. Aspect and M. Inguscio, Phys. Today **62**, No. 8, 30 (2009).
[5] T. Giamarchi and H. J. Schulz, Phys. Rev. B **37**, 325 (1988); M. P. A. Fisher *et al.*, Phys. Rev. B **40**, 546 (1989).
[6] M. Lewenstein *et al.*, Adv. Phys. **56**, 243 (2007); I. Bloch *et al.*, Rev. Mod. Phys. **80**, 885 (2008).
[7] L. Sanchez-Palencia and M. Lewenstein, Nature Phys. **6**, 87 (2010); L. Fallani, C. Fort, and M. Inguscio, Adv. At. Mol. Opt. Phys. **56**, 119 (2008).
[8] B. Damski *et al.*, Phys. Rev. Lett. **91**, 080403 (2003).
[9] L. Sanchez-Palencia *et al.*, Phys. Rev. Lett. **98**, 210401 (2007); New J. Phys. **10**, 045019 (2008).
[10] J. Billy *et al.*, Nature (London) **453**, 891 (2008).
[11] G. Roati *et al.*, Nature (London) **453**, 895 (2008).
[12] T.-L. Ho and Q. Zhou, Nature Phys. **6**, 131 (2010).
[13] D. S. Petrov *et al.*, J. Phys. IV (France) **116**, 5 (2004).
[14] L. Pezzé *et al.*, Phys. Rev. Lett. **93**, 120401 (2004); L. Viverit *et al.*, Phys. Rev. Lett. **93**, 110401 (2004); H. Ott *et al.*, Phys. Rev. Lett. **93**, 120407 (2004);
[15] P. W. Anderson, Phys. Rev. **109**, 1492 (1958).
[16] S. Kirkpatrick and T. P. Eggarter, Phys. Rev. B **6**, 3598 (1972); Y. Shapir, A. Aharony, and A. B. Harris, Phys. Rev. Lett. **49**, 486 (1982); O. N. Dorokhov, Solid State Commun. **51**, 381 (1984).
[17] We obtained the same qualitative behavior as reported in the Letter using other models of disorder, such as ''blue-detuned'' speckle potentials and Gaussian impurities.
[18] I. M. Lifshits *et al.*, *Introduction to the Theory of Disordered Systems* (Wiley, New York, 1988).
[19] We use the condition $\Delta z < 10\sigma_R$ to identify localized states, and $\Delta z > (3/4)\Delta z^0(E)$ for extended states.
[20] We obtained qualitatively-similar results for different energies and different traps.
[21] For instance, we find $E_n \simeq 3.97|V_R|$, $\epsilon_p \simeq 0.24|V_R|$ and $\langle\chi_p|V_T|\chi_p\rangle \simeq 3.71|V_R|$ for state C in Fig. 2.
[22] M. Greiner *et al.*, Nature (London) **426**, 537 (2003).
[23] W. Guerin *et al.*, Phys. Rev. Lett. **97**, 200402 (2006).
[24] D. Clément *et al.*, Phys. Rev. A **77**, 033631 (2008).
[25] Y. P. Chen *et al.*, Phys. Rev. A **77**, 033632 (2008).
[26] L. Pezzé *et al.*, Europhys. Lett. **88**, 30 009 (2009).
[27] B. Deissler *et al.*, Nature Phys. **6**, 354 (2010).
[28] Here, we use a box of length $3000\sigma_R$ much larger than Δz for all states considered.

REFERENCES

ABANIN D.A., LEE P.A., and LEVITOV L.S., *Randomness-induced XY ordering in a graphene quantum Hall ferromagnet*, Phys. Rev. Lett. **98**, 156801 (2007).

ABRAHAMS E., ANDERSON P.W., LICCIARDELLO D.C., and RAMAKRISHNAN T.V., *Scaling theory of localization: Absence of quantum diffusion in two dimensions*, Phys. Rev. Lett. **42**, 673 (1979).

ABRAHAMS E., KRAVCHENKO S.V., and SARACHIK M.P., *Metallic behavior and related phenomena in two dimensions*, Rev. Mod. Phys. **73**, 251 (2001).

AEGERTER C.M., STÖRZER M., and MARET G., *Experimental determination of critical exponents in Anderson localization of light*, Europhys. Lett. **75**, 562 (2006).

AHARONY A., *Spin-flop multicritical points in systems with random fields and in spin glasses*, Phys. Rev. B **18**, 3328 (1978).

AHUFINGER V., SANCHEZ-PALENCIA L., KANTIAN A., SANPERA A., and LEWENSTEIN M., *Disordered ultracold atomic gases in optical lattices: A case study of Fermi-Bose mixtures*, Phys. Rev. A **72**, 063616 (2005).

AIZENMAN M. and WEHR J., *Rounding of first-order phase transitions in systems with quenched disorder*, Phys. Rev. Lett. **62**, 2503 (1989).

AIZENMAN M. and WEHR J., *Rounding effects of quenched randomness on first-order phase transitions*, Comm. Math. Phys. **130**, 489 (1990).

AKKERMANS E., GHOSH S., and MUSSLIMANI Z.H., *Numerical study of one-dimensional and interacting Bose-Einstein condensates in a random potential*, J. Phys. B: At. Mol. Opt. Phys. **41**, 045302 (2008).

AKKERMANS E. and MONTAMBAUX G., *Mesoscopic Physics of Electrons and Photons* (Cambridge Univ. Press, UK, 2006).

ALBERT A. and LEBOEUF P., *Localization by bichromatic potentials versus Anderson localization*, Phys. Rev. A **81**, 013614 (2010).

ALBERT A., PAUL T., PAVLOFF N., and LEBOEUF P., *Dipole oscillations of a Bose-Einstein*

condensate in the presence of defects and disorder, Phys. Rev. Lett. **100**, 250405 (2008).

ALEINER I., ALTSHULER B., and GERSHENSON M., *Interaction effects and phase relaxation in disordered systems*, Waves in Random Media **9**, 201 (1999).

ALEINER I., ALTSHULER B., and SHLYAPNIKOV G.V., *Finite temperature phase transition for disordered weakly interacting bosons in one dimension*, Nature Phys. **6**, 900 (2010).

ALET F., DAYAL P., GRZESIK A., HONECKER A., KÖRNER M., LÄUCHLI A., MANMANA S.R., MCCULLOCH I.P., MICHEL F., NOACK R.M., SCHMID G., SCHOLLWÖCK U., STÖCKLI F., TODO S., TREBST S., TROYER M., WERNER P., and WESSEL S., *The ALPS project: Open source software for strongly correlated systems*, J. Phys. Soc. Jpn. **74**, 30 (2005).

ALTMAN E., DEMLER E., and LUKIN M.D., *Probing many-body states of ultracold atoms via noise correlations*, Phys. Rev. A **70**, 013603 (2004).

ALTMAN E., HOFSTETTER W., DEMLER E., and LUKIN M.D., *Phase diagram of two-component bosons on an optical lattice*, New J. Phys. **5**, 113 (2003).

ALTSHULER B., ARONOV A.G., and LEE P.A., *Interaction effects in disordered Fermi systems in two dimensions*, Phys. Rev. Lett. **44**, 1288 (1980).

ANDERLINI M., LEE P.J., BROWN B., SEBBY-STRABLEY J., PHILLIPS W.D., and PORTO J.V., *Controlled exchange interaction between pairs of neutral atoms in an optical lattice*, Nature **448**, 452 (2007).

ANDERSEN J.O., AL KHAWAJA U., and STOOF H.T.C., *Phase fluctuations in atomic Bose gases*, Phys. Rev. Lett. **88**, 070407 (2002).

ANDERSON B.P. and KASEVICH M.A., *Macroscopic quantum interference from atomic tunnel arrays*, Science **282**, 1686 (1998).

ANDERSON M.H., ENSHER J.R., MATTHEWS M.R., WIEMAN C.E., and CORNELL E.A., *Observation of Bose-Einstein condensation in a dilute atomic vapor*, Science **269**, 198 (1995).

ANDERSON P.W., *Absence of diffusion in certain random lattices*, Phys. Rev. **109**, 1492 (1958).

ANDERSON P.W., *Theory of dirty superconductors*, J. Phys. Chem. Solids **11**, 26 (1959).

ANDERSON P.W., *Local moments and localized states*, Nobel lecture (1977).

ANDERSON P.W., *The question of classical localization: A theory of white paint ?*, Phil. Mag. B **52**, 505 (1985).

ANDERSON P.W. and LEE P.A, *The Thouless conjecture for a one-dimensional chain*, Suppl. Prog. Theor. Phys. **69**, 212 (1980).

ANDERSON P.W., THOULESS D.J., ABRAHAMS E., and FISHER D.S., *New method for a scaling theory of localization*, Phys. Rev. B **22**, 3519 (1980).

ANKER T., ALBIEZ M., GATI V., HUNSMANN S., EIERMANN B., TROMBETTONI A., and OBERTHALER M.K., *Nonlinear self-trapping of matter waves in periodic potentials*, Phys. Rev. Lett. **94**, 020403 (2005).

ASHCROFT N.W. and MERMIN N.D., *Solid State Physics* (Saunders College Publishing, New York, 1976).

ASPECT A., ARIMONDO E., KAISER R., VANSTEENKISTE N., and COHEN-TANNOUDJI C., *Laser cooling below the one-photon recoil energy by velocity-selective coherent population trapping*, Phys. Rev. Lett. **61**, 826 (1988).

ASPECT A., ARIMONDO E., KAISER R., VANSTEENKISTE N., and COHEN-TANNOUDJI C., *Laser cooling below the one-photon recoil energy by velocity-selective coherent population trapping: Theoretical analysis*, J. Opt. Soc. Am. B **6**, 2112 (1989).

ASPECT A. and INGUSCIO M., *Anderson localization of ultracold atoms*, Phys. Today **62**, 30 (2009).

AUBRY S. and ANDRÉ G. *Analyticity breaking and Anderson localization in incommensurate lattices*, Ann. Israel Phys. Soc. **3**, 133 (1980).

AUERBACH A., *Interacting Electrons and Quantum Magnetism* (Springer, New York, 1994).

BALABAN T., *A low temperature expansion for classical N-vector models I: A renormalization group flow*, Comm. Math. Phys. **167**, 103 (1995).

BALABAN T., *A low temperature expansion for classical N-vector models II: Renormalization group equations*, Com. Math. Phys. **182**, 675 (1996).

BALATSKY A.V., VEKHTER I., and ZHU J.-X., *Impurity-induced states in conventional and unconventional superconductors*, Rev. Mod. Phys. **78**, 373 (2006).

BARDEEN J., COOPER L., and SCHRIEFFER J., *Theory of superconductivity*, Phys. Rev. **108**, 1175 (1957).

BASDEVANT J.L. and DALIBARD J., *Quantum Mechanics* (Springer, Berlin, 2002).

BASKO D.M., ALEINER I.L., and ALTSHULER B.L., *On the problem of many-body localization*, Ann. Phys. **321**, 1126 (2006).

BEN DAHAN M., PEIK E., REICHEL J., CASTIN Y., and SALOMON C., *Bloch oscillations of atoms in an optical potential*, Phys. Rev. Lett. **76**, 4508 (1996).

BENENTI G., WAINTAL X., and PICHARD J.-L., *New quantum phase between the Fermi glass and the Wigner crystal in two dimensions*, Phys. Rev. Lett. **83**, 1826 (1999).

BEREZINSKII V.L., *Kinetics of a quantum particle in a one-dimensional random potential*, Sov. Phys. JETP **38**, 620 (1974).

BERG-SØRENSEN K., CASTIN Y., MØLMER K., and DALIBARD J., *Cooling and tunnelling of atoms in a 2D laser field*, Europhys. Lett. **22**, 663 (1993).

BILAS N. and PAVLOFF N., *Anderson localization of elementary excitations in a one dimensional Bose-Einstein condensate*, Eur. Phys. J. D **40**, 387 (2006).

BILLY J., Ph-D thesis, Université Paris-sud, Orsay, France (2010); available online under <http://tel.archives-ouvertes.fr/tel-00492482/en/>.

BILLY J., JOSSE V., ZUO Z., BERNARD A., HAMBRECHT B., LUGAN P., CLÉMENT D., SANCHEZ-PALENCIA L., BOUYER P., and ASPECT A., *Direct observation of Anderson localization of matter-waves in a controlled disorder*, Nature **453**, 891 (2008).

BINDER K. and YOUNG A.P., *Spin glasses: Experimental facts, theoretical concepts, and open questions*, Rev. Mod. Phys. **58**, 801 (1986).

BINDI L., STEINHARDT P.J., YAO N., and LU P.J., *Natural quasicrystals*, Science **324**, 1306 (2009).

BISSBORT U. and HOFSTETTER W., *Stochastic mean-field theory for the disordered Bose-Hubbard model*, Europhys. Lett. **86**, 50007 (2009).

BLOCH I., *Ultracold quantum gases in optical lattices*, Nature Phys. **1**, 23 (2005).

BLOCH I., DALIBARD J., and ZWERGER W., *Many-body physics with ultracold atoms*, Rev. Mod. Phys. **80**, 885 (2008).

BLOCH I., HÄNSCH T.W., and Esslinger T., *Atom laser with a cw output coupler*, Phys. Rev. Lett. **82**, 3008 (1999).

BOGOLYUBOV N.N., *Theory of superfluidity*, J. Phys. (USSR) **11**, 23 (1947).

BOGOLYUBOV N.N., *New method in the theory of superconductivity*, Sov. Phys. JETP **7**, 41 (1958).

BOIRON D., MENNERAT-ROBILLIARD C., FOURNIER J.-M., GUIDONI L., SALOMON C., and GRYNBERG G., *Trapping and cooling cesium atoms in a speckle field*, Eur. Phys. J. D **7**, 373 (1999).

BORLAND R.E., *The Nature of the electronic states in disordered one-dimensional systems*, Proc. Roy. Soc. A **274**, 529 (1963).

BOURDEL T., KHAYKOVICH L., CUBIZOLLES J., ZHANG J., CHEVY F., TEICHMANN M., TARRUELL L., KOKKELMANS S.J.J.M.F., and SALOMON C., *Experimental study of the BEC-BCS crossover region in lithium 6*, Phys. Rev. Lett. **93**, 050401 (2004).

BOUYER P., BILLY J., JOSSE V., ZUO Z., BERNARD A., HAMBRECHT B., LUGAN P., CLÉMENT D., SANCHEZ-PALENCIA L., AND ASPECT A., *Anderson localization of matter-waves*, Proceedings of the International Conference on Atomic Physics (ICAP2008), Storrs, USA, july 2008.

BRADLEY C.C., SACKETT C.A., and HULET R.G., *Bose-Einstein condensation of lithium: Observation of limited condensate number*, Phys. Rev. Lett. **78**, 985 (1997).

BRAMWELL S.T. and HOLDSWORTH P.C.W., *Magnetization: A characteristic of the Kosterlitz-Thouless-Berezinskii transition*, Phys. Rev. B **49**, 8811 (1994).

BRAY A.J. and MOORE M.A., *Chaotic nature of the spin-glass phase*, Phys. Rev. Lett. **58**, 57 (1987).

BUONSANTE P., PENNA V., VEZZANI A., and BLAKIE P.B., *Mean-field phase diagram of cold lattice bosons in disordered potentials*, Phys. Rev. A **76**, 011602(R) (2007).

BYCZUK K., HOFSTETTER W., and VOLLHARDT D., *Competition between Anderson localization and antiferromagnetism in correlated lattice fermion systems with disorder*, Phys. Rev. Lett. **102**, 146403 (2009).

CARMONA R., *Exponential localization in one dimensional disordered systems*, Duke Math. J. **49**, 191 (1982).

CASTIN Y., *Bose-Einstein condensates in atomic gases: Simple theoretical results*, in *Coherent atomic matter waves*, edited by KAISER R., WESTBROOK C., and DAVID F., Lecture Notes of Les Houches Summer School, p. 1 (EDP Sciences and Springer-Verlag, 2001).

CASTIN Y., BERG-SØRENSEN K., DALIBARD J., and MØLMER K., *Two-dimensional Sisyphus cooling*, Phys. Rev. A **50**, 5092 (1994).

CASTIN Y., DALIBARD J., and COHEN-TANNOUDJI C., *The limits of Sisyphus cooling*, in *Light-induced kinetic effects on atoms, ions and molecules*, edited by MOI L., GOZZINI S., GABBANINI C., ARIMONDO E., and STRUMIA F., ETS Editrice, Pisa (1991).

CASTIN Y. and DUM R., *Bose-Einstein condensates in time dependent traps*, Phys. Rev. Lett. **77**, 5315 (1996).

CASTIN Y. and MØLMER K., *Monte Carlo wave-function analysis of 3D optical molasses*, Phys. Rev. Lett. **74**, 3772 (1995).

CEDERBAUM L.S., STRELTSOV A.I., and ALON O.E., *Fragmented metastable states exist in an attractive Bose-Einstein condensate for atom numbers well above the critical number of the Gross-Pitaevskii theory*, Phys. Rev. Lett. **100**, 040402 (2008).

CHABANOV A.A., STOYTCHEV M., and GENACK A.Z., *Statistical signatures of photon localization*, Nature **404**, 850 (2000).

CHABÉ J., LEMARIÉ G., GRÉMAUD B., DELANDE D., SZRIFTGISER P., and GARREAU J.C., *Experimental observation of the Anderson metal-insulator transition with atomic matter waves*, Phys. Rev. Lett. **101**, 255702 (2008).

CHALKER J.T. and SHAPIRO B., *Caustic formation in expanding condensates of cold atoms*, Phys. Rev. A **80**, 013603 (2009).

CHEN Y.P., HITCHCOCK J., DRIES D., JUNKER M., WELFORD C., and HULET R.G., *Phase coherence and superfluid-insulator transition in a disordered Bose-Einstein condensate*, Phys. Rev. A **77**, 033632 (2008).

CHU S., *Nobel lecture: The manipulation of neutral particles*, Rev. Mod. Phys. **70**, 685 (1998).

CIRAC J.I. and ZOLLER P., *New frontiers in quantum information with atoms and ions*, Phys. Today **57**, 38 (2004).

CLAIRON A., SALOMON C., GUELATTI S., and PHILLIPS W.D., *Ramsey resonance in Zacharias fountain*, Europhys. Lett. **16**, 165 (1991).

CLÉMENT D., *Propriétés statiques et dynamiques d'un condensat de Bose-Einstein dans un potentiel aléatoire*, Ph-D thesis, Université Pierre et Marie Curie, Paris, France (2007); available online under <http://tel.archives-ouvertes.fr/tel-00262463/en/.>; Ann. Phys. (France) **33**, 1

(2008).

CLÉMENT D., BOUYER P., ASPECT A., and SANCHEZ-PALENCIA L., *Density modulations in an elongated Bose-Einstein condensate released from a disordered potential*, Phys. Rev. A **77**, 033631 (2008).

CLÉMENT D., FABBRI N., FALLANI L., FORT C., and INGUSCIO M., *Exploring correlated 1D Bose gases across from the superfluid to the Mott insulator state by inelastic light scattering*, Phys. Rev. Lett. **102**, 155301 (2009a)

CLÉMENT D., FABBRI N., FALLANI L., FORT C., and INGUSCIO M., *Multi-band spectroscopy of inhomogeneous Mott-insulator states of ultracold bosons*, New. J. Phys. **11**, 103030 (2009b).

CLÉMENT D., VARON A.F., RETTER J.A., BOUYER P., SANCHEZ-PALENCIA L., GANGARDT D.M., SHLYAPNIKOV G.V., and ASPECT A., *Suppression of transport of an interacting elongated Bose-Einstein condensate in a random potential*, Phys. Rev. Lett. **95**, 170409 (2005).

CLÉMENT D., VARON A.F., RETTER J.A., SANCHEZ-PALENCIA L., ASPECT A., and BOUYER P., *Experimental study of the transport of coherent interacting matter-waves in a 1D random potential induced by laser speckle*, New J. Phys. **8**, 165 (2006).

COHEN-TANNOUDJI C., in *Fundamental systems in quantum optics*, edited by DALIBARD J, RAIMOND J.M., and ZINN-JUSTIN J., Les Houches session LIII, p. 1 (North Holland, Amsterdam, 1992).

COHEN-TANNOUDJI C., *Nobel lecture: Manipulating atoms with photons*, Rev. Mod. Phys. **70**, 707 (1998).

CORNELL E.A. and WIEMAN C.E., *Nobel lecture: Bose-Einstein condensation in a dilute gas, the first 70 years and some recent experiments*, Rev. Mod. Phys. **74**, 875 (2002).

CORNISH S.L., CLAUSSEN N.R., ROBERTS J.L., CORNELL E.A., and WIEMAN C.E., *Stable ^{85}Rb Bose-Einstein condensates with widely tunable interactions*, Phys. Rev Lett. **85**, 1795 (2000).

CROWELL P.A., VAN KEULS F.W., and REPPY J.D., *Superfluid-insulator transition in ^{4}He films adsorbed in Vycor glass*, Phys. Rev. Lett. **75**, 1106 (1995).

CROWELL P.A., VAN KEULS F.W., and REPPY J.D., *Onset of superfluidity in ^{4}He films adsorbed on disordered substrates*, Phys. Rev. B **55**, 12620 (1997).

DALFOVO F., GIORGINI S., PITAEVSKII L.P., and STRINGARI S., *Theory of Bose-Einstein condensation in trapped gases*. Rev. Mod. Phys. **71**, 463 (1999).

DALIBARD J., *Helsinki workshop on laser manipulation of atoms* (unpublished, 1987).

DALIBARD J. and COHEN-TANNOUDJI C., *Laser cooling below the Doppler limit by polarization gradients: Simple theoretical models*, J. Opt. Soc. Am. B **6**, 2023 (1989).

DAMSKI B., ZAKRZEWSKI J., SANTOS L., ZOLLER P., and LEWENSTEIN M., *Atomic Bose and Anderson glasses in optical lattices*, Phys. Rev. Lett. **91**, 080403 (2003).

DAO T.-L., GEORGES A., DALIBARD J., SALOMON C., and CARUSOTTO I., *Measuring the one-particle excitations of ultracold fermionic atoms by stimulated Raman spectroscopy*, Phys. Rev. Lett. **98**, 240402 (2007).

DAVIS K.B., MEWES M.O., ANDREWS M.R., VAN DRUTEN N.J., DURFEE D.S., KURN D.M., and KETTERLE W., *Bose-Einstein condensation in a gas of sodium atoms*, Phys. Rev. Lett. **75**, 3969 (1995).

DE BOER J.H. and VERWEY E.J.W., *Semi-conductors with partially and with completely filled 3d-lattice bands*, Proc. Phys. Soc. (London) **49**, 59 (1937).

DE GENNES P.-G., *Superconductivity of Metals and Alloys* (Benjamin, New York, 1966).

DEISSLER B., ZACCANTI M., ROATI G., D'ERRICO C., FATTORI M., MODUGNO M., MODUGNO G., and INGUSCIO M., *Delocalization of a disordered bosonic system by repulsive interactions*, Nature Phys. **6**, 354 (2010).

DELANDE D. and ZAKRZEWSKI J., *Compression as a tool to detect Bose glass in cold atoms experiments*, Phys. Rev. Lett. **102**, 085301 (2009).

DEMARCO B. and JIN D.S., *Onset of Fermi degeneracy in a trapped atomic gas*, Science **285**, 1703 (1999).

DETTMER S., HELLWEG D., RYYTTY P., ARLT J.J., ERTMER W., SENGSTOCK K., PETROV D.S., SHLYAPNIKOV G.V., KREUTZMANN H., SANTOS L., and LEWENSTEIN M., *Observation of phase fluctuations in elongated Bose-Einstein condensates*, Phys. Rev. Lett. **87**, 160406 (2001).

DOTSENKO D.S., FEIGEL'MAN M.V., and IOFFE L.B., *Spin Glasses and Related Phenomena* (Harwood, Glassgow,, U.K., 1990).

DRENKELFORTH S., KLEINE BÜNING G., WILL J., SCHULTE T., MURRAY N., ERTMER W., SANTOS L., and ARLT J.J., *Damped Bloch oscillations of Bose-Einstein condensates in disordered potential gradients*, New J. Phys. **10**, 045027 (2008).

DUAN L.-M., DEMLER E., and LUKIN M.D., *Controlling spin exchange interactions of ultracold atoms in optical lattices*, Phys. Rev. Lett. **91**, 090402 (2003).

EDWARDS E.E., BEELER M., TAO HONG, and ROLSTON S.L., *Adiabaticity and localization in one-dimensional incommensurate lattices*, Phys. Rev. Lett. **101**, 260402 (2008).

EDWARDS J.T. and THOULESS D.J., *Numerical studies of localization in disordered systems*, J. Phys. C: Solid State Phys. **5**, 807 (1972).

EFETOV K.B., *Supersymmetry and theory of disordered metals*, Adv. Phys. **32**, 53 (1983).

EINSTEIN A., *Quantentheorie des einatomigen idealen gases / Quantum theory of ideal monoatomic gases*, Sitz. Ber. Preuss. Akad. Wiss. (Berlin) **22**, 261 (1924).

FALCO G.M., NATTERMANN T.V., and POKROVSKY L., *Localized states and interaction-induced delocalization in Bose gases with quenched disorder*, Europhys. Lett. **85**, 30002 (2009).

FALLANI L., FORT C., and INGUSCIO M., *Bose-Einstein condensates in disordered potentials*, Adv. At. Mol. Opt. Phys. **56**, 119 (Academic Press, 2008).

FALLANI L., LYE J.E., GUARRERA V., FORT C., and INGUSCIO M., *Ultracold atoms in a disordered crystal of light: Towards a Bose glass*, Phys. Rev. Lett. **98**, 130404 (2007).

FELDMAN D.E., *Exact zero-temperature critical behaviour of the ferromagnet in the uniaxial random field*, J. Phys. A **31**, L177 (1998).

FERLAINO F., KNOOP S., BERNINGER M., HARM W., D'INCAO J.P., NÄGERL H.-C., and GRIMM R., *Evidence for universal four-body states tied to an Efimov trimer*, Phys. Rev. Lett. **102**, 140401 (2009).

FETTER A.L., *Rotating trapped Bose-Einstein condensates*, Rev. Mod. Phys. **81**, 647 (2009).

FETTER A.L. and WALECKA J.D., *Quantum Theory of Many-Particle Systems* (Dover, New York, 2002).

FEYNMAN R.P., *Simulating physics with computers*, Int. J. Th. Phys. **21**, 467 (1982).

FIGOTIN A., GERMINET F., KLEIN A., and MÜLLER P., *Persistence of Anderson localization in Schrödinger operators with decaying random potentials*, Ark. Mat. **45**, 15 (2007).

FISCHER K.H. and HETZ J.A., *Spin Glasses* (Cambridge University, Cambridge, U.K., 1991).

FISHER D.S. and HUSE D.A., *Ordered phase of short-range Ising spin-glasses*, Phys. Rev. Lett. **56**, 1601 (1986).

FISHER D.S. and HUSE D.A., *Nonequilibrium dynamics of spin glasses*, Phys. Rev. B **38**, 373 (1988).

FISHER M.P.A., WEICHMAN P.B., GRINSTEIN G., and FISHER D.S., *Boson localization and the superfluid-insulator transition*, Phys. Rev. B **40**, 546 (1989).

FÖLLING S., GERBIER F., WIDERA A., MANDEL O., GERICKE T., and BLOCH I., *Spatial quantum noise interferometry in expanding ultracold atom clouds*, Nature **434**, 481 (2005).

FOMIN I.A., *Superfluid phases of ^{3}He in aerogel*, J. Low Temp. Phys. **138**, 97 (2005).

FOMIN I.A., *Kapitza pendulum effect in an amorphous magnet with a weak disorder*, JETP Lett. **85**, 434 (2007).

FONTANESI L., WOUTERS M., and SAVONA V., *Superfluid to Bose-glass transition in a 1D weakly interacting Bose gas*, Phys. Rev. Lett. **103**, 030403 (2009).

FONTANESI L., WOUTERS M., and SAVONA V., *private communication* (2010).

FORT C., FALLANI L., GUARRERA V., LYE J.E., MODUGNO M., WIERSMA D.S., and INGUSCIO M., *Effect of optical disorder and single defects on the expansion of a Bose-Einstein condensate in a one-dimensional waveguide*, Phys. Rev. Lett. **95**, 170410 (2005).

FREEDMAN R. and HERTZ J.A., *Theory of a Fermi glass*, Phys. Rev. B **15**, 2384 (1977).

FRIED D.G., KILLIAN T.C., WILLMANN L., LANDHUIS D., MOSS S.C., KLEPPNER D.,

and GREYTAK T.J., *Bose-Einstein condensation of atomic hydrogen*, Phys. Rev. Lett. **81**, 3811 (1998).

FRÖHLICH J., SIMON B., and SPENCER T., *Infrared bounds, phase transitions and continuous symmetry breaking*, Comm. Math. Phys. **50**, 79 (1976).

GAMBETI-CÉSARE E., WEINMANN D., JALABERT R.A., and BRUNE P., *Disorder-induced enhancement of the persistent current for strongly interacting electrons in one-dimensional rings*, Europhys. Lett. **60**, 120 (2002).

GARG A., RANDERIA M., and TRIVEDI N., *Strong correlations make high-temperature superconductors robust against disorder*, Nature Phys. **4**, 762 (2008).

GATZKE M., BIRKL G., JESSEN P.S., KASTBERG A., ROLSTON S.L., and PHILLIPS W.D., *Temperature and localization of atoms in three-dimensional optical lattices*, Phys. Rev. A **55**, R3987 (1997).

GAVISH U. and CASTIN Y., *Matter-wave localization in disordered cold atom lattices*, Phys. Rev. Lett. **95**, 020401 (2005).

GEORGES A., *Condensed matter physics with light and atoms: Strongly correlated cold fermions in optical lattices*, Proceedings of the International School of Physics 'Enrico Fermi', Course CLXIV, edited by INGUSCIO M., KETTERLE W. and SALOMON C. (IOS Press, Amsterdam, 2008); Preprint at <http://arxiv.org/abs/cond-mat/0702122>.

GEORGES A., PARCOLLET O., and SACHDEV S., *Quantum fluctuations of a nearly critical Heisenberg spin glass*, Phys. Rev. B **63**, 134406 (2001).

GERTSENSHTEIN M.E. and VASIL'EV V.B., *Waveguides with random inhomogeneities and Brownian motion in the Lobachevsky plane*, Theor. Prob. Appl. **4**, 391 (1959).

GERZ C., HODAPP T.W., JESSEN P., JONES K.M., PHILLIPS W.D., WESTBROOK C.I., and MØLMER K., *The temperature of optical molasses for two different atomic angular momenta*, Europhys. Lett. **21**, 661 (1993).

GHOSAL A., RANDERIA M., and TRIVEDI N., *Spatial inhomogeneities in disordered d-wave superconductors*, Phys. Rev. B **63**, 020505(R) (2000).

GIAMARCHI T., *Quantum Physics in One Dimension* (Carendon press, Oxford, 2004).

GIAMARCHI T. and SCHULZ H.J., *Localization and interactions in one-dimensional quantum fluids*, Europhys. Lett. **3**, 1287 (1987).

GIAMARCHI T. and SCHULZ H.J., *Anderson localization and interactions in one-dimensional metals*, Phys. Rev. B **37**, 325 (1988).

GIORGINI S., PITAEVSKII L.P., and STRINGARI S., *Theory of ultracold atomic Fermi gases*, Rev. Mod. Phys. **80**, 1215 (2008).

GIRARDEAU M., *Relationship between systems of impenetrable bosons and fermions in one dimension*, J. Math. Phys. **1**, 516 (1960).

GOMMERS R., LEBEDEV V., BROWN M., and RENZONI F., *Gating ratchet for cold atoms*,

Phys. Rev. Lett. **100**, 040603 (2008).

GOODMAN J.W., *Speckle Phenomena in Optics: Theory and Applications* (Roberts & co. publisher, Englewood, USA, 2007).

GORDON J.P. and ASHKIN A., *Motion of atoms in a radiation trap*, Phys. Rev. A **21**, 1606 (1980).

GRAHAM R., SCHLAUTMANN M., and ZOLLER P., *Dynamical localization of atomic-beam deflection by a modulated standing light wave*, Phys. Rev. A **45**, R19 (1992).

GREINER M., BLOCH I., MANDEL O., HÄNSCH T.W., and ESSLINGER T., *Exploring phase coherence in a 2D lattice of Bose-Einstein condensates*, Phys. Rev. Lett. **87**, 160405 (2001).

GREINER M., MANDEL O., ESSLINGER T., HÄNSCH T.W., and BLOCH I., *Quantum phase transition from a superfluid to a Mott insulator in a gas of ultracold atoms*, Nature **415**, 39 (2002).

GREINER M., REGAL C.A., and JIN D.S., *Emergence of a molecular Bose-Einstein condensate from a fermi gas*, Nature **426**, 537 (2003).

GRIESMAIER A., WERNER J., HENSLER S., STUHLER J., and PFAU T., *Bose-Einstein condensation of chromium*, Phys. Rev. Lett. **94**, 160401 (2005).

GRISON D., LOUNIS B., SALOMON C., COURTOIS J.-Y., and GRYNBERG G., *Raman spectroscopy of cesium atoms in a laser trap*, Europhys. Lett. **15**, 149 (1991).

GRYNBERG G., HORAK P., and MENNERAT-ROBILLIARD C., *Spatial diffusion of atoms cooled in a speckle field*, Europhys. Lett. **49**, 424 (2000a).

GRYNBERG G., LOUNIS B., VERKERK P., COURTOIS J.-Y., and SALOMON C., *Quantized motion of cold cesium atoms in two- and three-dimensional optical potentials*, Phys. Rev. Lett. **70**, 2249 (1993).

GRYNBERG G. and ROBILLIARD C., *Cold atoms in dissipative optical lattices*, Phys. Rep. **355**, 335 (2001).

GRYNBERG G., TRICHÉ C., GUIDONI L., and VISSER P.M., *Mechanical bistability of atoms cooled in an optical lattice*, Europhys. Lett. **51**, 506 (2000b).

GUERIN W., RIOU J.-F., GAEBLER J.P., JOSSE V., BOUYER P., and ASPECT A., *Guided quasicontinuous atom laser*, Phys. Rev. Lett. **97**, 200402 (2006).

GUÉRY-ODELIN D., SÖDING J., DESBIOLLES P., and DALIBARD J., *Is Bose-Einstein condensation of atomic Cesium possible ?*, Europhys. Lett. **44**, 25 (1998).

GUIDONI L., DÉPRET B., DI STEFANO A., and VERKERK, P., *Atomic diffusion in an optical quasicrystal with five-fold symmetry*, Phys. Rev. A **60**, R4233 (1999).

GUIDONI L., TRICHÉ C., VERKERK P., and GRYNBERG G., *Quasiperiodic optical lattices*, Phys. Rev. Lett. **79**, 3363 (1997).

GURARIE V., REFAEL G., and CHALKER J.T., *Excitations of one-dimensional Bose-Einstein condensates in a random potential*, Phys. Rev. Lett. **101**, 170407 (2008).

GUREVICH E. and KENNETH O., *Lyapunov exponent for the laser speckle potential: A weak disorder expansion*, Phys. Rev. A **79**, 063617 (2009).

GUSTAVSON T.L., BOUYER P., and KASEVICH M.A., *Precision rotation measurement with an atom interferometer gyroscope*, Phys. Rev. Lett. **78**, 2046 (1997).

GUSTAVSON T.L., LANDRAGIN A., and KASEVICH M.A., *Rotation sensing with a dual atom interferometer Sagnac gyroscope*, Class. Quant. Grav. **17**, 1 (2000).

HADZIBABIC Z., KRÜGER P, CHENEAU M., BATTELIER B., and DALIBARD J., *Berezinskii-Kosterlitz-Thouless crossover in a trapped atomic gas*, Nature **441**, 1118 (2006).

HÄNSCH T.W. and SCHAWLOW A.L., *Cooling of gases by laser radiation*, Opt. Comm. **13**, 68 (1975).

HAGLEY E.W., DENG L., KOZUMA M., WEN J., HELMERSON K., ROLSTON S.L., and PHILLIPS W.D., *A well-collimated quasi-continuous atom laser*, Science **283**, 1706 (1999).

HARPER P.G., *Single band motion of conduction electrons in a uniform magnetic field*, Proc. Phys. Soc. A **68**, 874 (1955).

HARTUNG M., WELLENS T., MÜLLER C.A., RICHTER K., and SCHLAGHECK P., *Coherent backscattering of Bose-Einstein condensates in two-dimensional disorder potentials*, Phys. Rev. Lett. **101**, 020603 (2008).

HEMMERICH A. and HÄNSCH T.W., *Two-dimesional atomic crystal bound by light*, Phys. Rev. Lett. **70**, 410 (1993).

HEMMERICH A., ZIMMERMANN C., and HÄNSCH T.W., *Sub-kHz Rayleigh resonance in a cubic atomic crystal*, Europhys. Lett. **22**, 89 (1993).

HEMMERICH A., ZIMMERMANN C., and HÄNSCH T.W., *Multiphoton transitions in a spin-polarized 3D optical lattice*, Phys. Rev. Lett. **72**, 625 (1994).

HERTZ J.A., FLEISHMAN L., and ANDERSON P.W., *Marginal fluctuations in a Bose glass*, Phys. Rev. Lett. **43**, 942 (1979).

HO T.-L. and SHENOY V.B., *Binary mixtures of Bose condensates of alkali atoms*, Phys. Rev. Lett. **77**, 3276 (1996).

HODAPP T.W., GERZ C., FURTLEHNER C., WESTBROOK C.I., PHILIPPS W.D., and DALIBARD J., *Three-dimensional spatial diffusion in optical molasses*, Appl. Phys. B **60**, 135 (1995).

HOHENBERG P.C., *Existence of long-range order in one and two dimensions*, Phys. Rev. **158**, 383 (1967).

HORAK P., COURTOIS J.-Y., and GRYNBERG G., *Atom cooling and trapping by disorder*, Phys. Rev. A **58**, 3953 (1998).

HU H., STRYBULEVYCH A., SKIPETROV S.E., VAN TIGGELEN B.A., and PAGE J.H., *Localization of ultrasound in a three-dimensional elastic network*, Nature Phys. **4**, 945 (2008).

HUBBARD J., *Electron correlations in narrow energy bands*, Proc. Roy. Soc. A **276**, 238 (1963).

IMAMBEKOV A., LUKIN M.D., and DEMLER E., *Spin-exchange interactions of spin-one bosons in optical lattices: Singlet, nematic and dimerized phases*, Phys. Rev. A **68**, 063602 (2003).

IMRY Y., *Coherent propagation of two interacting particles in a random potential*, Europhys. Lett. **30**, 405 (1995).

IMRY Y. and MA S., *Random-field instability of the ordered state of continuous symmetry*, Phys. Rev. Lett. **35**, 1399 (1975).

INOUYE S., ANDREWS M.R., STENGER J., MIESNER H.-J., STAMPER-KURN D.M., and KETTERLE W., *Observation of Feshbach resonances in a Bose-Einstein condensate*, Nature **392**, 151 (1998).

IOFFE A.F. and REGEL A.R., *Non-crystalline, amorphous and liquid electronic semiconductors*, Prog. Semicond. 4, 237 (1960).

ISHII K., *Localization of eigenstates and transport phenomena in the one-dimensional disordered system*, Prog. Theor. Phys. Suppl. **53**, 77 (1973).

JACOUD P. and SHEPELYANSKY D.L., *Two interacting quasiparticles above the Fermi sea*, Phys. Rev. Lett. **78**, 4986 (1997).

JAKSCH D., BRUDER C., CIRAC J.I., GARDINER C.W., and ZOLLER P., *Cold bosonic atoms in optical lattices*, Phys. Rev. Lett. **81**, 3108 (1998).

JAKSCH D. and ZOLLER P., *The cold atom Hubbard toolbox*, Ann. Phys. **315**, 52 (2005).

JERSBLAD J., ELLMANN H., SANCHEZ-PALENCIA L., and KASTBERG A., *Anisotropic velocity distributions in 3D dissipative optical lattices*, Eur. Phys. J. D **22**, 333 (2003).

JESSEN P.S. and DEUTSCH I.H., *Optical lattices*, Adv. At. Mol. Opt. Phys. **37**, 95 (1996).

JESSEN P.S., GERZ C., LETT P.D., PHILLIPS W.D., and WESTBROOK C.I., *Observation of quantized motion of Rb atoms in an optical field*, Phys. Rev. Lett. **69**, 49 (1992).

JOCHIM S., BARTENSTEIN M., ALTMEYER A., HENDL G., RIEDL S., CHIN C., HECKER-DENSCHLAG J., and GRIMM R., *Bose-Einstein condensation of molecules*, Science **302**, 2101 (2003).

JOHN S., *Electromagnetic absorption in a disordered medium near a photon mobility edge*, Phys. Rev. Lett. **53**, 2169 (1984).

JÖRDENS R., STROHMAIER N., GÜNTERK., MORITZ H., and ESSLINGER T., *A Mott insulator of fermionic atoms in an optical lattice*, Nature **455**, 204 (2008).

KAGAN YU., SURKOV E.L., and SHLYAPNIKOV G.V., *Evolution of a Bose-condensed gas under variations of the confining potential*, Phys. Rev. A **54** R1753 (1996).

KASEVICH M. and CHU S., *Laser cooling below a photon recoil with three-level atoms*, Phys. Rev. Lett. **69**, 1741 (1992a).

KASEVICH M. and CHU S., *Measurement of the gravitational acceleration of an atom with a light-pulse atom interferometer*, Appl. Phys. B **54**, 321 (1992b).

KASEVICH M., RIIS E., CHU S., and DE VOE R., *RF spectroscopy in an atomic fountain*, Phys. Rev. Lett. **63**, 612 (1989).

KETTERLE W., *Nobel lecture: When atoms behave as waves: Bose-Einstein condensation and the atom laser*, Rev. Mod. Phys. **74**, 1131 (2002).

KETTERLE W., DURFEE D.S., and STAMPER-KURN D.M., *Making, probing and understanding Bose-Einstein condensates*, Proceedings of the International School of Physics 'Enrico Fermi', Course CXL, edited by INGUSCIO M., STRINGARI S. and WIEMAN C.E. (IOP Press, Amsterdam, 1999); Preprint at <http://arxiv.org/abs/cond-mat/9904034>.

KETTERLE W. and VAN DRUTEN N.J., *Comprehensive review paper on evaporative cooling*, Adv. At. Mol. Opt. Phys. **37**, 181 (1996); edited by BEDERSON B. and WALTHER H.

KETTERLE W. and ZWIERLEIN M.W., *Making, probing and understanding ultracold Fermi gases*, Proceedings of the International School of Physics 'Enrico Fermi', Course CLXIV, edited by INGUSCIO M., KETTERLE W., and SALOMON C. (IOS Press, Amsterdam, 2008); Preprint at <http://arxiv.org/abs/0801.2500>.

KINOSHITA T., WENGER T., and WEISS D.S., *Observation of a one-dimensional Tonks-Girardeau gas*, Science **305**, 1125 (2004).

KÖHL M., MORITZ H., STÖFERLE T., GÜNTER K., and ESSLINGER T., *Fermionic atoms in a three dimensional optical lattice: Observing Fermi surfaces, dynamics, and interactions*, Phys. Rev. Lett. **94**, 080403 (2005).

KOPIDAKIS G., KOMINEAS S., FLACH S., and AUBRY S., *Absence of wave packet diffusion in disordered nonlinear systems*, Phys. Rev. Lett. **100**, 084103 (2008).

KRAEMER T., MARK M., WALDBURGER P., DANZL J.G., CHIN C., ENGESER B., LANGE A.D., PILCH K., JAAKKOLA A., NÄGERL H.-C., and GRIMM R., *Evidence for Efimov quantum states in an ultracold gas of caesium atoms*, Nature **440**, 315 (2006).

KRAFT S., VOGT F., APPEL O., RIEHLE F., and STERR U., *Bose-Einstein condensation of alkaline earth atoms:* ^{40}Ca, Phys. Rev. Lett. **103**, 130401 (2009).

KRAUTH W., CAFFAREL M., and BOUCHAUD J., *Gutzwiller wave function for a model of strongly interacting bosons*, Phys. Rev. B **45**, 3137 (1992).

KRAUTH W., TRIVEDI N., and CEPERLEY D., *Superfluid-insulator transition in disordered boson systems*, Phys. Rev. Lett. **67**, 2307 (1991).

KRAVCHENKO S.V., KRAVCHENKO G.V., FURNEAUX J.E., PUDALOV V.M., and D'IORIO M., *Possible metal-insulator transition at* $B = 0$ *in two dimensions*, Phys. Rev. B **50**, 8039 (1994).

KRAVCHENKO S.V., MASON W.E., BOWKER G.E., FURNEAUX J.E., PUDALOV V.M., and M. D'IORIO, *Scaling of an anomalous metal-insulator transition in a two-dimensional system in silicon at* $B = 0$, Phys. Rev. B **51**, 7038 (1995).

KROHA J., KROPP T., and WÖLFE P., *Self-consistent theory of Anderson localization for the tight-binding model with site-diagonal disorder*, Phys Rev. B **41**, 888 (1990).

KUHN R.C., MINIATURA C., DELANDE D., SIGWARTH O., and MÜLLER C.A., *Localization of matter waves in two-dimensional disordered optical potentials* Phys. Rev. Lett. **95**, 250403 (2005).

KUHN R.C., MINIATURA C., DELANDE D., SIGWARTH O., and MÜLLER C.A., *Coherent matter wave transport in speckle potentials*, New J. Phys. **9**, 161 (2007).

KUKLOV A.B. and SVISTUNOV B.V., *Counterflow superfluidity of two-species ultracold atoms in a commensurate optical lattice*, Phys. Rev. Lett. **90**, 100401 (2003).

LABEYRIE G., DE TOMASI F., BERNARD J.-C., MÜLLER C.A., MINIATURA C., and KAISER R., *Coherent backscattering of light by cold atoms*, Phys. Rev. Lett. **83**, 5266 (1999).

LABEYRIE G., MÜLLER C.A., WIERSMA D.S., MINIATURA C., AND KAISER R., *Observation of coherent backscattering of light by cold atoms*, J. Opt. B: Quantum Semiclass. Opt **2**, 672 (2000).

LAGENDIJK A., VAN TIGGELEN B., and WIERSMA D.S., *Fifty years of Anderson localization*, Phys. Today **62**, 24 (2009).

LAHAYE T., MENOTTI C., SANTOS L., LEWENSTEIN M., and PFAU T., *The physics of dipolar bosonic quantum gases*, Rep. Prog. Phys. **72**, 126401 (2009).

LAHINI Y., AVIDAN A., POZZI F., SOREL M., MORANDOTTI R., CHRISTODOULIDES D.N., and SILBERBERG Y., *Anderson localization and nonlinearity in one-dimensional disordered photonic lattices*, Phys. Rev. Lett. **100**, 013906 (2008).

LANGER J.S. and NEAL T., *Breakdown of the concentration expansion for the impurity resistivity of metals*, Phys. Rev. Lett. **16**, 984 (1966).

LEE D.K.K. and GUNN J.M.F., *Bosons in a random potential - condensation and screening in a dense limit*, J. Phys.: Condens. Matter **2**, 7753 (1990).

LEE J.-W., CHANDRASEKHARAN S., and BARANGER H.U., *Disorder-induced superfluidity in hardcore bosons in two dimensions*, Preprint at <http://arxiv.org/abs/cond-mat/0611109> (2006).

LEE P.A. and RAMAKRISHNAN T.V., *Disordered electronic systems*, Rev. Mod. Phys. **57**, 287 (1985).

LESCHKE H., MÜLLER P., and WARZEL S., *A survey of rigorous results on random Schrödinger operators for amorphous solids*, Markov Processes and Related Fields **9**, 729 (2003).

LESCHKE H., MÜLLER P., and WARZEL S., in *Interacting Stochastic Systems*, edited by DEUSCHEL J.-D. and GREVEN A., p. 119 (Springer, Berlin, 2005).

LEVINE D. and STEINHARDT P.J, *Quasicrystals: A new class of ordered structures*, Phys. Rev. Lett. **53**, 2477 (1984).

LEVINSEN J., TIECKE T.G., WALRAVEN J.T.M., and PETROV D.S., *Atom-dimer scattering and long-lived trimers in fermionic mixtures*, Phys. Rev. Lett. **103**, 153202 (2009).

LEWENSTEIN M., SANPERA A., AHUFINGER V., DAMSKI B., SEN A.(DE), and SEN U.,

Ultracold atomic gases in optical lattices: Mimicking condensed-matter physics and beyond, Adv. Phys. **56**, 243 (2007).

LEWENSTEIN M., SANTOS L., BARANOV M.A., and FEHRMANN H., *Atomic Bose-Fermi mixtures in an optical lattice*, Phys. Rev. Lett. **92**, 050401 (2004).

LIFSHITS I.M., GREDESKUL S.A., and PASTUR L.A., *Introduction to the Theory of Disordered Systems* (Wiley, New York, 1988).

LIFSHITZ I.M., *The energy spectrum of disordered systems*, Adv. Phys. **13**, 483 (1964).

LLOYD S., *Universal quantum simulators*, Science **273**, 1073 (1996).

LONDON F., *The lambda.-phenomenon of liquid helium and the Bose-Einstein degeneracy*, Nature **141**, 643 (1938).

LUGAN P., *Ultra-cold Bose gases in random potentials: Collective excitations and localization effects*, Ph-D thesis, Ecole Polytechnique, Palaiseau, France (2010); available online under <http://tel.archives-ouvertes.fr/tel-00468888/en/>.

LUGAN P., ASPECT A., SANCHEZ-PALENCIA L., DELANDE D., GRÉMAUD B., MÜLLER C.A., and MINIATURA C., *One-dimensional Anderson localization in certain correlated random potentials*, Phys. Rev. A **80**, 023605 (2009).

LUGAN P., CLÉMENT D., BOUYER P., ASPECT A., LEWENSTEIN M., and SANCHEZ-PALENCIA L., *Ultracold Bose gases in 1D disorder: From Lifshits glass to Bose-Einstein condensate*, Phys. Rev. Lett. **98**, 170403 (2007a).

LUGAN P., CLÉMENT D., BOUYER P., ASPECT A., and SANCHEZ-PALENCIA L., *Anderson localization of Bogolyubov quasiparticles in interacting Bose-Einstein condensates*, Phys. Rev. Lett. **99**, 180402 (2007b).

LUGAN P. and SANCHEZ-PALENCIA L., *Localization of Bogoliubov quasiparticles in interacting Bose gases with correlated disorder*, Phys. Rev. A **84**, 013612 (2011).

LYE J.E., FALLANI L., FORT C., GUARRERA V., MODUGNO M., WIERSMA D.S., and INGUSCIO M., *Effect of interactions on the localization of a Bose-Einstein condensate in a quasi-periodic lattice*, Phys. Rev. A **75**, 061603(R) (2007).

LYE J.E., FALLANI L., MODUGNO M., WIERSMA D.S., FORT C., and INGUSCIO M., *Bose-Einstein condensate in a random potential*, Phys. Rev. Lett. **95**, 070401 (2005).

MACKINNON A. and KRAMER B., *The scaling theory of electrons in disordered solids: Additional numerical results*, Z. Phys. B **53**, 1 (1983).

MARKSTEINER S., ELLINGER K., and ZOLLER P., *Anomalous diffusion and Lévy walks in optical lattices*, Phys. Rev. A **53**, 3409 (1996).

MARTE P., DUM R., TAÏEB R., LETT P.D., and ZOLLER P., *Quantum wave function simulation of the resonance fluorescence spectrum from one-dimensional optical molasses*, Phys. Rev. Lett. **71**, 1335 (1993).

MARTINEZ DE ESCOBAR Y.N., MICKELSON P.G., YAN M., DESALVO B.J., NAGEL S.B.,

and KILLIAN T.C., *Bose-Einstein Condensation of* ^{84}*Sr*, Phys. Rev. Lett. **103**, 200402 (2009).

MCGUIRK J.M., FOSTER G.T., FIXLER J.B., SNADDEN M.J., and KASEVICH M.A., *Sensitive absolute-gravity gradiometry using atom interferometry*, Phys. Rev. A **65**, 033608 (2002).

MENNERAT-ROBILLIARD C., LUCAS D., GUIBAL S., TABOSA J., JURCZAK C., COURTOIS J.-Y., and GRYNBERG G., *Ratchet for cold rubidium atoms: The asymmetric optical lattice*, Phys. Rev. Lett. **82**, 851 (1999).

MERMIN N.D. and WAGNER H., *Absence of ferromagnetism or antiferromagnetism in one- or two-dimensional isotropic Heisenberg models*, Phys. Rev. Lett. **17**, 1133 (1966).

MEWES M.-O., ANDREWS M.R, KURN D.M., DURFEE D.S., TOWNSEND C.G., and KETTERLE W., *Output coupler for Bose-Einstein condensed atoms*, Phys. Rev. Lett. **78**, 582 (1997).

MÉZARD M., PARISI G., and VIRASORO M.A., *Spin Glass Theory and Beyond* (World Scientific, Singapour, 1987).

MICHELI A., BRENNEN G.K., and ZOLLER P., *A toolbox for lattice spin models with polar molecules*, Nature Phys. **2**, 341 (2006).

MINCHAU B.J. and PELCOVITS R.A., *Two-dimensional XY model in a random uniaxial field*, Phys. Rev. B **32**, 3081 (1985).

MODUGNO G., FERRARI G., ROATI G., BRECHA R.J., SIMONI A., and INGUSCIO M., *Bose-Einstein condensation of potassium atoms by sympathetic cooling*, Science **294**, 1320 (2001).

MODUGNO G., ROATI G., RIBOLI F., FERLAINO F., BRECHA R.J., and INGUSCIO M., *Collapse of a degenerate Fermi gas*, Science **297**, 2240 (2002).

MOLCHANOV S.A., *The structure of eigenfunctions of one-dimensional unordered structures*, Math. USSR Izv. **12**, 69 (1978).

MOORE F.L., ROBINSON J.C., BHARUCHA C., WILLIAMS P.E., and RAIZEN M., *Observation of dynamical localization in atomic momentum transfer: A new testing ground for quantum chaos*, Phys. Rev. Lett. **73**, 2974 (1994).

MORA C. and CASTIN Y., *Extension of Bogoliubov theory to quasicondensates*, Phys. Rev. A **67**, 053615 (2003).

MOTT N.F., *The basis of the electron theory of metals, with special reference to the transition metals*, Proc. Phys. Soc. (London), Series A **62**, 416 (1949).

MOTT N.F., *Electrons in disordered structures*, Adv. Phys. **16**, 49 (1967).

MOTT N.F., *Metal-insulator transition*, Rev. Mod. Phys. **40**, 677 (1968).

MOTT N.F., *Metal-Insulator Transitions* (Taylor and Francis, London, 1990).

MOTT N.F. and PEIERLS R., *Discussion of the paper by de Boer and Verwey* (1937), Proc. Phys. Soc. (London) **49**, 72 (1937).

MOTT N.F. and TWOSE W.D., *The theory of impurity conduction*, Adv. Phys. **10**, 107 (1961).

NACHUMI B., KEREN A., KOJIMA K., LARKIN M., LUKE G.M., MERRIN J., TCHERNYSHÖV O., UEMURA Y.J., ICHIKAWA N., GOTO M., and UCHIDA S., *Muon spin relaxation studies of Zn-substitution effects in high-T_c cuprate superconductors*, Phys. Rev. Lett. **77**, 5421 (1996).

NEWMAN C.M. and STEIN D.L., *Ordering and broken symmetry in short-ranged spin glasses*, J. Phys.-Condens. Mat. **15**, R1319 (2003).

NIEDERBERGER A., SCHULTE T., WEHR J., LEWENSTEIN M., SANCHEZ-PALENCIA L., and SACHA K., *Disorder-induced order in two-component Bose-Einstein condensates*, Phys. Rev. Lett. **100**, 030403 (2008).

NIEDERBERGER A., WEHR J., LEWENSTEIN M., and SACHA K., *Disorder-induced phase control in superfluid Fermi-Bose mixtures*, Europhys. Lett. **86**, 26004 (2009).

OLSHANII M., *Atomic scattering in the presence of an external confinement and a gas of impenetrable bosons*, Phys. Rev. Lett. **81**, 938 (1998).

PAALANEN M.A., ROSENBAUM T.F., THOMAS G.A., and BHATT R.N., *Critical scaling of the conductance in a disordered insulator*, Phys. Rev. Lett. **51**, 1896 (1983).

PALPACELLI S. and SUCCI S. *Quantum lattice Boltzmann simulation of expanding Bose-Einstein condensates in random potentials*, Phys. Rev. E **77**, 066708 (2008).

PAREDES B., VERSTRAETE F., and CIRAC J.I., *Exploiting quantum parallelism to simulate quantum random many-body systems*, Phys. Rev. Lett. **95**, 140501 (2005).

PAREDES B., WIDERA A., MURG V., MANDEL O., FÖLLING S., CIRAC J.I., SHLYAPNIKOV G.V., HÄNSCH T.W., and BLOCH I., *Tonks-Girardeau gas of ultracold atoms in an optical lattice*, Nature **429**, 277 (2004).

PARISI G., *Mean field theory for spin glasses*, Phys. Rep. **67**, 25 (1980).

PASIENSKI M., MCKAY D., WHITE M., and DEMARCO B., *A disordered insulator in an optical lattice*, Nature Phys. **6**, 677 (2010).

PAUL T., SCHLAGHECK P., LEBOEUF P., and PAVLOFF N., *Superfluidity versus Anderson localization in a dilute Bose gas*, Phys. Rev. Lett. **98**, 210602 (2007).

PEIK E., BEN DAHAN M., BOUCHOULE I., CASTIN Y., and SALOMON C., *Bloch oscillations of atoms, adiabatic rapid passage, and monokinetic atomic beams*, Phys. Rev. A **55**, 2989 (1997).

PEREIRA DOS SANTOS F., LÉONARD J., WANG J., BARRELET C.J., PERALES F., RASEL E., UNNIKRISHNAN C.S., LEDUC M., and COHEN-TANNOUDJI C., *Bose-Einstein condensation of metastable helium*, Phys. Rev. Lett. **86**, 3459 (2001).

PETERS A., CHUNG K.Y., and CHU S., *Measurement of the gravitational acceleration by dropping atoms*, Nature **400**, 849 (1999).

PETERS A., CHUNG K.Y., and CHU S., *High-precision gravity measurements using atom interferometry*, Metrologia **38**, 25 (2001).

PETROV D.S., *Three-boson problem near a narrow Feshbach resonance*, Phys. Rev. Lett. **93**, 143201 (2004).

PETROV D.S., GANGARDT D.M., and SHLYAPNIKOV G.V., *Low-dimensional trapped gases*, J. Phys. IV France **116**, 3 (2004).

PETROV D.S., HOLZMANN M., and SHLYAPNIKOV G.V., *Bose-Einstein condensation in quasi-2D trapped gases*, Phys. Rev. Lett. **84**, 2551 (2000a).

PETROV D.S., SHLYAPNIKOV G.V., and WALRAVEN J.T.M., *Regimes of quantum degeneracy in trapped 1D gases*, Phys. Rev. Lett. **85**, 3745 (2000b).

PETROV D.S., SHLYAPNIKOV G.V., and WALRAVEN J.T.M., *Phase-fluctuating 3D Bose-Einstein condensates in elongated traps*, Phys. Rev. Lett. **87**, 050404 (2001).

PEZZÉ L., HAMBRECHT B., and SANCHEZ-PALENCIA L., *Dipole oscillations of a Fermi gas in a disordered trap: Damping and localization*, Europhys. Lett. **88**, 30009 (2009).

PEZZÉ L. and SANCHEZ-PALENCIA L., *Localized and extended states in a disordered trap*, Phys. Rev. Lett. **106**, 040601 (2011).

PHILLIPS W.D., *Nobel lecture: Laser cooling and trapping of neutral atoms*, Rev. Mod. Phys. **70**, 721 (1998).

PIKOVSKY A.S. and SHEPELYANSKY D.L., *Destruction of Anderson localization by a weak nonlinearity*, Phys. Rev. Lett. **100**, 094101 (2008).

PIRAUD M., *Localisation d'Anderson dans un potentiel de speckle exotique*, work of Master 2 (unpublished) (2009).

PIRAUD M., LUGAN P., BOUYER P., ASPECT A., and SANCHEZ-PALENCIA L. *Localization of a matter wave packet in a disordered potential* , Phys. Rev. A **83**, 031603(R) (2011).

PITAEVSKII L.P. and STRINGARI S., *Bose-Einstein Condensation* (Oxford University press, 2003).

POLLACK S.E., DRIES D., JUNKER M., CHEN Y.P., CORCOVILOS T.A., and HULET R.G., *Extreme tunability of interactions in a ^{7}Li Bose-Einstein condensate*, Phys. Rev. Lett. **102**, 090402 (2009).

POLLET L., PROKOF'EV N.V., SVISTUNOV B.V., and TROYER M., *Absence of a direct superfluid to Mott insulator transition in disordered Bose systems*, Phys. Rev. Lett. **103**, 140402 (2009).

POPOV V.N., *On the theory of the superfluidity of two- and one-dimensional bose systems*, Theor. Math. Phys. (Engl. Transl.) **11**, 565 (1972).

RAAB E., PRENTISS M., CABLE A., CHU S., and PRITCHARD D., *Trapping of neutral sodium atoms with radiation pressure*, Phys. Rev. Lett. **59**, 2631 (1987).

RAITHEL G., BIRKL G., KASTBERG A., PHILLIPS W.D., and ROLSTON S.L., *Cooling and localization dynamics in optical lattices*, Phys. Rev. Lett. **78**, 630 (1997).

REICHEL J., BARDOU F., BEN DAHAN M., PEIK E., RAND S., SALOMON C., and COHEN-

TANNOUDJI C., *Raman cooling of cesium below 3nK: New approach inspired by Lévy flight statistics*, Phys. Rev. Lett. **75**, 4575 (1995).

REPPY J., ^{4}*He as a dilute bose gas*, Physica B+C **126**, 335 (1984).

RICHARD S., GERBIER F., THYWISSEN J.H., HUGBART M., BOUYER P., and ASPECT A., *Momentum spectroscopy of 1D phase fluctuations in Bose-Einstein condensates*, Phys. Rev. Lett. **91**, 010405 (2003).

RIEHLE F., KISTERS TH., WITTE A., HELMCKE J., and BORDÉ C.J., *Optical Ramsey spectroscopy in a rotating frame: Sagnac effect in a matter-wave interferometer*, Phys. Rev. Lett. **67**, 177 (1991).

ROATI G., D'ERRICO C., FALLANI L., FATTORI M., FORT C., ZACCANTI M., MODUGNO G., MODUGNO M., and INGUSCIO M., *Anderson localization of a non-interacting Bose-Einstein condensate*, Nature **453**, 895 (2008).

ROATI G., ZACCANTI M., D'ERRICO C., CATANI J., MODUGNO M., SIMONI A., INGUSCIO M., and MODUGNO G., ^{39}*K Bose-Einstein condensate with tunable interactions*, Phys. Rev. Lett. **99**, 010403 (2007).

ROBERT A., SIRJEAN O., BROWAEYS A., POUPARD J., NOWAK S., BOIRON D., WESTBROOK C.I., and ASPECT A., *A Bose-Einstein condensate of metastable atoms*, Science **292**, 461 (2001).

ROBERT-DE-SAINT-VINCENT M., BRANTUT J.-P., ALLARD B., PLISSON T., PEZZÉ L., SANCHEZ-PALENCIA L., ASPECT A., BOURDEL T., and BOUYER P., *Anisotropic 2D diffusive expansion of ultra-cold atoms in a disordered potential*, Phys. Rev. Lett., **104**, 220602 (2010).

ROKHSAR D.S. and KOTLIAR B.G., *Gutzwiller projection for bosons*, Phys. Rev. B **44**, 10328 (1991).

ROM T., BEST TH., VAN OOSTEN D., SCHNEIDER U., FÖLLING S., PAREDES B., and BLOCH I., *Free fermion antibunching in a degenerate atomic Fermi gas released from an optical lattice*, Nature **444**, 733 (2006).

ROSENBAUM T.F., MILLIGAN R.F., PAALANEN M.A., THOMAS G.A., BHATT R.N., and LIN W., *Metal-insulator transition in a doped semiconductor*, Phys. Rev. B 27, **7509** (1983).

ROTH R. and BURNETT K., *Ultracold bosonic atoms in disordered optical superlattices*, J. Opt. B: Quantum Semiclass. Opt. **5**, S50 (2003).

SACHDEV S., *Quantum Phase Transitions* (Cambridge Univ. Press, Oxford, 1999).

SALOMON C., DALIBARD J., PHILLIPS W.D., CLAIRON A., and GUELLATI S., *Laser cooling of cesium atoms below 3 microKelvins*, Europhys. Lett. **12**, 683 (1990).

SANCHEZ-PALENCIA L., *Etude théorique de la dynamique non linéaire d'atomes froids dans un réseau optique dissipatif: Transport spontané et transport stimulé*, Ph-D thesis, Ecole Polytechnique, Palaiseau, France (2003); available online under <http://tel.archives-ouvertes.fr/tel-00003425>.

SANCHEZ-PALENCIA L., *Directed transport of Brownian particles in a double symmetric potential*, Phys. Rev. E **70**, 011102 (2004).

SANCHEZ-PALENCIA L., *Smoothing effect and delocalization of interacting Bose-Einstein condensates in random potentials*, Phys. Rev. A **74**, 053625 (2006).

SANCHEZ-PALENCIA L., *Joint forces against disorder*, Nature Phys. **6**, 328 (2010).

SANCHEZ-PALENCIA L., CARMINATI F.-R., SCHIAVONI M., RENZONI F., and GRYNBERG G., *Brillouin propagation modes in optical lattices: Interpretation in terms of nonconventional stochastic resonance*, Phys. Rev. Lett. **88**, 133903 (2002).

SANCHEZ-PALENCIA L., CLÉMENT D., LUGAN P., BOUYER P., and ASPECT A., *Disorder-induced trapping versus Anderson localization in Bose-Einstein condensates expanding in disordered potentials*, New J. Phys. **10**, 045019 (2008).

SANCHEZ-PALENCIA L., CLÉMENT D., LUGAN P., BOUYER P., SHLYAPNIKOV G.V., and ASPECT A., *Anderson localization of expanding Bose-Einstein condensates in random potentials*, Phys. Rev. Lett. **98**, 210401 (2007).

SANCHEZ-PALENCIA L. and GRYNBERG G., *Synchronization of Hamiltonian motion and dissipative effects in optical lattices: Evidence for a stochastic resonance*, Phys. Rev. A **68**, 023404 (2003).

SANCHEZ-PALENCIA L., HORAK P., and GRYNBERG G., *Spatial diffusion in a periodic optical lattice: Revisiting the Sisyphus effect*, Eur. Phys. J. D **18**, 353 (2002).

SANCHEZ-PALENCIA L. and LEWENSTEIN M., *Disordered quantum gases under control*, Nature Phys. **6**, 87 (2010).

SANCHEZ-PALENCIA L. and SANTOS L., *Bose-Einstein condensates in optical quasicrystal lattices*, Phys. Rev. A **72**, 053607 (2005).

SANPERA A., KANTIAN A., SANCHEZ-PALENCIA L., ZAKREWSKI J., and LEWENSTEIN M., *Atomic Fermi-Bose mixtures in inhomogeneous and random optical lattices: From Fermi glass to quantun spin glass and quantum percolation*, Phys. Rev. Lett. **93**, 040401 (2004).

SAUBAMÉA B., HIJMANS T.W., KULIN S., RASEL E., PEIK E., LEDUC M., and COHEN-TANNOUDJI C., *Direct measurement of the spatial correlation function of ultracold atoms*, Phys. Rev. Lett. **79**, 3146 (1997).

SCALETTAR R.T., BATROUNI G.G., and ZIMANYI G.T., *Localization in interacting, disordered, Bose systems*, Phys. Rev. Lett. **66**, 3144 (1991).

SCHEFFOLD F., LENKE R., TWEER R., and MARET G., *Localization or classical diffusion of light ?* Nature **398**, 206 (1999).

SCHIAVONI M., CARMINATI F.-R., SANCHEZ-PALENCIA L., RENZONI F., and GRYNBERG G., *Stochastic resonance in periodic potentials: Realization in a dissipative optical lattice*, Europhys. Lett. **59**, 493 (2002).

SCHIAVONI M., SANCHEZ-PALENCIA L., RENZONI F., and GRYNBERG G., *Phase-control of directed diffusion in a symmetric optical lattice*, Phys. Rev. Lett. **90**, 094101 (2003).

SCHMITTECKERT P., JALABERT R.A., WEINMANN D., and PICHARD J.-L., *From the Fermi glass towards the Mott insulator in one dimension: Delocalization and strongly enhanced persistent currents*, Phys. Rev. Lett. **81**, 2308 (1998).

SCHNEIDER U., HACKERMULLER L., WILL S., BEST T., BLOCH I., COSTI T.A., HELMES R.W., RASCH D., and ROSCH A., *Metallic and insulating phases of repulsively interacting fermions in a 3D optical lattice*, Science **322**, 1520 (2008).

SCHRECK F., KHAYKOVICH L., CORWIN K., FERRARI G., BOURDEL T., CUBIZOLLES J., and SALOMON C., *Quasipure Bose-Einstein condensate immersed in a Fermi sea*, Phys. Rev. Lett. **87**, 080403 (2001).

SCHREIBER M. and GRUSSBACH H., *Dimensionality dependence of the metal-insulator transition in the Anderson model of localization*, Phys. Rev. Lett. **76**, 1687 (1996).

SCHULTE T., DRENKELFORTH S., KRUSE J., ERTMER W., ARLT J., SACHA K., ZAKRZEWSKI J., and LEWENSTEIN M., *Routes towards Anderson-like localization of Bose-Einstein condensates in disordered optical lattices*, Phys. Rev. Lett. **95**, 170411 (2005).

SCHULTE T., DRENKELFORTH S., KRUSE J., TIEMEYER R., SACHA K., ZAKRZEWSKI J., LEWENSTEIN M., ERTMER W., and ARLT J. *Analysis of localization phenomena in weakly interacting disordered lattice gases*, New J. Phys. **8**, 230 (2006).

SCHWARTZ M., *Off-diagonal long-range behavior of interacting Bose systems*, Phys. Rev. B **15**, 1399 (1977).

SCHWARTZ T., BARTAL G., FISHMAN S., and SEGEV M., *Transport and Anderson localization in disordered two-dimensional photonic lattices*, Nature **446**, 52 (2007).

SESKO D., WALKER T., MONROE C., GALLAGHER A., and WIEMAN C., *Collisional losses from a light-force atom trap*, Phys. Rev. Lett. **63**, 961 (1989).

SHAPIRO B., *Expansion of a Bose-Einstein condensate in the presence of disorder*, Phys. Rev. Lett. **99**, 060602 (2007).

SHECHTMAN D., BLECH I., GRATIAS D., and CAHN J.W., *Metallic phase with long-range orientational order and no translational symmetry*, Phys. Rev. Lett. **53**, 1951 (1984).

SHERRINGTON D. and KIRKPATRICK S., *Solvable model of a spin-glass*, Phys. Rev. Lett. **35**, 1792 (1975).

SHESHADRI K., KRISHNAMURTHY H.R., PANDIT R., and RAMAKRISHNAN T.V., *Superfluid and insulating phases in an interacting-boson model: Mean-field theory and the RPA* , Europhys. Lett. **22**, 257 (1993).

SINGHA DEO P., *Thouless conductance formula in one dimension and its relevance to persistent-current experiments*, Phys. Rev. B 55, 13795 (1997).

SJÖLUND P., PETRA S., DION C., JONSELL S., NYLÉN M., SANCHEZ-PALENCIA L., and KASTBERG A., *Demonstration of a controllable three-dimensional Brownian motor in symmetric potentials*, Phys. Rev. Lett. **96**, 190602 (2006).

SKIPETROV S.E., MINGUZZI A., VAN TIGGELEN B.A., and SHAPIRO B., *Anderson local-*

ization of a Bose-Einstein condensate in a 3D random potential, Phys. Rev. Lett. **100**, 165301 (2008).

SLEVIN K., MARKOS P., and OHTSUKI T., *Reconciling conductance fluctuations and the scaling theory of localization*, Phys. Rev. Lett. **86**, 3594 (2001).

SNADDEN M.J., MCGUIRK J.M., BOUYER P., HARITOS K.G., and KASEVICH M.A., *Measurement of the Earth's gravity gradient with an atom interferometer-based gravity gradiometer*, Phys. Rev. Lett. **81**, 971 (1998).

SOKOLOFF J.B., *Unusual band structure, wave functions and electrical conductance in crystals with incommensurate periodic potentials*, Phys. Rep. **126**, 189 (1985).

SORTAIS Y., BIZE S., and ABGRALL M., *Cold atom clocks*, Physica Scripta 2001, 50 (2001).

SOUILLARD B., *Waves and electrons in inhomogeneous media*, in *Chance and Matter*, edited by SOULETIE J., VANNIMENUS J., and STORA R., Les Houches session XLVI, p. 305 (Elsevier, New York, 1987).

STAMPER-KURN D.M., CHIKKATUR A.P., GÖRLITZ A., INOUYE S., GUPTA S., PRITCHARD D.E., and KETTERLE W., *Excitation of phonons in a Bose-Einstein condensate by light scattering*, Phys. Rev. Lett. **83**, 2876 (1999).

STEINHAUER J., KATZ N., OZERI R., DAVIDSON N., TOZZO C., and DALFOVO F., *Bragg spectroscopy of the multibranch Bogoliubov spectrum of elongated Bose-Einstein condensates*, Phys. Rev. Lett. **90**, 060404 (2003).

STELLMER S., MENG KHOON TEY, BO HUANG, GRIMM R., and SCHRECK F., *Bose-Einstein Condensation of Strontium*, Phys. Rev. Lett. **103**, 200401 (2009).

STEWART J.T., GAEBLER J.P., and JIN D.S., *Using photoemission spectroscopy to probe a strongly interacting Fermi gas*, Nature **454**, 744 (2008).

STÖRZER M., GROSS P., AEGERTER C.M., and MARET G., *Observation of the critical regime near anderson localization of light*, Phys. Rev. Lett. **96**, 063904 (2006).

TAÏEB R., MARTE P., DUM R., and ZOLLER P., *Spectrum of resonance fluorescence and cooling dynamics in quantized one-dimensional molasses: Effects of laser configuration*, Phys. Rev. A **47**, 4986 (1993).

TAKASU Y., MAKI K., KOMORI K., TAKANO T., HONDA K., KUMAKURA M., TABUZAKI T., and TAKAHASHI Y., *Spin-singlet Bose-Einstein condensation of two-electron atoms*, Phys. Rev. Lett. **91**, 040404 (2003).

TESSIERI L., *Delocalization phenomena in one-dimensional models with long-range correlated disorder: A perturbative approach*, J. Phys. A **35**, 9585 (2002).

THOULESS D.J., *Electrons in disordered systems and the theory of localization*, Phys. Rep. **13**, 93 (1974).

TONKS L., *The complete equation of state of one, two and three-dimensional gases of hard elastic spheres*, Phys. Rev. **50**, 955 (1936).

TROMBETTONI A. and SMERZI A., *Discrete solitons and breathers with dilute Bose-Einstein condensates*, Phys. Rev. Lett. **86**, 2353 (2001).

TROTZKY S., CHEINET P., FÖLING S., FELD M., SCHNORRBERGER U., REY A.M., POLKOVNIKOV A., DEMLER E., LUKIN M.D., and BLOCH I., *Time-resolved observation and control of superexchange interactions with ultracold atoms in optical lattices*, Science **319**, 295 (2008).

TROTZKY S., POLLET L., GERBIER F., SCHNORRBERGER U., BLOCH I., PROKOF'EV N.V., SVISTUNOV B., and TROYER M., *Suppression of the critical temperature for superfluidity near the Mott transition*, Nature Phys. **6**, 996 (2010).

TROYER M., AMMON B., and HEEB E., *Parallel object oriented Monte-Carlo simulations*, Lect. Notes Comput. Sci. **1505**, 191 (1998).

TRUSCOTT A., STRECKER K., MCALEXANDER W., PARTRIDGE G., and HULET R.G., *Observation of Fermi pressure in a gas of trapped atoms*, Science **291**, 2570 (2001).

UNGAR P.J., WEISS D.S., RIIS E., and CHU S., *Optical molasses and multilevel atoms: Theory*, J. Opt. Soc. of Am. B **6**, 2058 (1989).

VAN TIGGELEN B., in *Diffuse Waves in Complex Media*, edited by FOUQUE J.P., p. 1 (Kluwer, Dordrecht, 1999).

VERKERK P., LOUNIS B., SALOMON C., COHEN-TANNOUDJI C., COURTOIS J.-Y., and GRYNBERG G., *Dynamics and spatial order of cold cesium atoms in a periodic optical potential*, Phys. Rev. Lett. **68**, 3861 (1992).

VERKERK P., MEACHER D.R., COATES A.B., COURTOIS J.-Y., GUIBAL S., SALOMON C., and GRYNBERG G., *Designing optical lattices: An investigation with cesium atoms*, Europhys. Lett. **26**, 171 (1994).

VOLLHARDT D. and WÖLFLE P., *Anderson localization in $d \lesssim 2$ dimensions: A self-consistent diagrammatic theory*, Phys. Rev. Lett. **45**, 842 (1980a).

VOLLHARDT D. and WÖLFLE P., *Diagrammatic, self-consistent treatment of the Anderson localization problem in $d \leq 2$ dimensions*, Phys. Rev. B **22**, 4666 (1980b).

VOLLHARDT D. and WÖLFLE P., *Scaling equations from a self-consistent theory of Anderson localization*, Phys. Rev. Lett. **48**, 699 (1982).

VOLLHARDT D. and WÖLFLE P., in *Electronic phase transitions*, edited by HANKE W. and KOPAEV Y.V. (Elsevier Science, Amsterdam, 1992), Chap. 1.

VOLOVIK G.E., *No robust phases in aerogel: ^{3}He-A with orientational disorder in the Ginzburg-Landau model*, JETP Lett. **81**, 647 (2005).

VON OPPEN F. and WETTIG T., *Interaction-induced delocalization of quasiparticle pairs in the Anderson insulator*, Europhys. Lett. **32**, 741 (1995).

WAINTAL X., BENENTI G., and PICHARD J.-L., *Delocalized Coulomb phase in two dimensions*, Europhys. Lett. **49**, 466 (2000).

WEAVER R., *Anderson localization of ultrasound*, Wave Motion **12**, 129 (1990).

WEBER V., HERBIG J., MARK M., NÄGERL H.-C., and GRIMM R., *Bose-Einstein condensation of cesium*, Science **299**, 232 (2003).

WEHR J., NIEDERBERGER A., SANCHEZ-PALENCIA L., and LEWENSTEIN M., *Disorder versus the Mermin-Wagner-Hohenberg effect: From classical spin systems to ultracold atomic gases*, Phys. Rev. B **74**, 224448 (2006).

WEICHMAN P., *Large rare patches of order in disordered boson systems*, Physics **2**, 81 (2009).

WEISSMAN M.B., *What is a spin glass ? A glimpse via mesoscopic noise*, Rev. Mod. Phys. **65**, 829 (1993).

WERNER F., PARCOLLET O, GEORGES A., and HASSAN S.R., *Interaction-induced adiabatic cooling and antiferromagnetism of cold fermions in optical lattices*, Phys. Rev. Lett. **95**, 056401 (2005).

WESTBROOK C.I., WATTS R.N., TANNER C.E., ROLSTON S.L., PHILLIPS W.D., and LETT P.D., *Localization of atoms in a three-dimensional standing wave*, Phys. Rev. Lett. **65**, 33 (1990).

WHITE M., PASIENSKI M., MCKAY D., ZHOU S., CEPERLEY D., and DEMARCO B., *Strongly interacting bosons in a disordered optical lattice*, Phys. Rev. Lett. **102**, 055301 (2009).

WIERSMA D.S., BARTOLINI P., LAGENDIJK A., and RIGHINI, R., *Localization of light in a disordered medium*, Nature **390**, 671 (1997).

WINELAND D. and DEHMELT H., *Proposed 1014 Dν < ν laser fluorescence spectroscopy on Tl+ mono-ion oscillator III (side band cooling)*, Bull. Am. Phys. Soc. **20**, 637 (1975).

ZAKRZEWSKI J. and DELANDE D., *Breakdown of adiabaticity when loading ultracold atoms in optical lattices*, Phys. Rev. A **80**, 013602 (2009).

ZINN-JUSTIN J., *Quantum Field Theory and Critical Phenomena* (Oxford Science Publication, Oxford, 1989).

ZWIERLEIN M.W., ABO-SHAEER J.R., SCHIROTZEK A., SCHUNCK C.H., and KETTERLE W., *Vortices and superfluidity in a strongly interacting Fermi gas*, Nature **435** , 1047 (2005).

ZWIERLEIN M.W., STAN C.A., SCHUNCK C.H., RAUPACH S.M.F., GUPTA S., HADZIBABIC Z., and KETTERLE W., *Observation of Bose-Einstein condensation of molecules*, Phys. Rev. Lett. **91**, 250401 (2003).

APPENDICES

▷ Curriculum vitae and list of publications

▷ Teaching

Laurent Sanchez-Palencia

CNRS researcher at Institut d'Optique
Head of the "Quantum Matter Theory" team
Laboratoire Charles Fabry, Institut d'Optique, CNRS, Univ Paris Sud,
2 avenue Augustin Fresnel, F-91127 Palaiseau, France
phone: (33) 1 64 53 33 47 - e-mail: lsp@institutoptique.fr
http://www.atomoptic.fr/∼lsp
http://www.atomoptic.fr/∼theory

Born on 19 December 1975 - living in free union, two children - French citizen

▷ Researcher ID (ISI-publications/citations): http://www.researcherid.com/rid/C-5586-2012
▷ name to use in *Web of Science* "sanchez-palencia, l"
▷ name to use in *Essential Science Indicators* "sanchezpalencia l"

MAIN ACTIVITIES

since 2008: **CNRS researcher** (CR1, Permanent researcher), Laboratoire Charles Fabry, Institut d'Optique (Palaiseau, France)

since 2006: **Leader of the "Quantum Matter Theory" team** at Laboratoire Charles Fabry, Institut d'Optique, (Palaiseau, France)

2004-2008: CNRS researcher (CR2, Permanent researcher), Laboratoire Charles Fabry, Institut d'Optique (Palaiseau, France), Atom Optics group

2003-2004: Post-doctoral researcher at Institut für Theoretische Physik, group of M. Lewenstein (University of Hannover, Germany): *Quantum gases in disordered optical lattices*

2000-2003: Ph-D student at Laboratoire Kastler-Brossel (Ecole Normale Supérieure, Paris, France), group of G. Grynberg: *Theoretical study of the atom dynamics in dissipative optical lattices*

2000: MSc training course (6 months) at Laboratoire Kastler-Brossel (Ecole Normale Supérieure, Paris, France): *Spatial diffusion in a dissipative optical lattice* (advisor: G. Grynberg)

1999: Research training course (3 months) at the Center for Ultrafast Optical Science (University of Michigan, Ann Arbor, Michigan, USA): *Object reconstruction using terahertz single-cycle laser pulses* (advisor: T. Norris)

GRANTS AND AWARDS

2011-2015: ERC Starting grant 2010 (European Research Council)

2010: ANR Young Researcher grant (Agence Nationale de la Recherche; declined)

2004: Prize of Ecole Polytechnique for an outstanding Ph-D thesis in physics

2003: Marie Curie individual fellowship from the European Union Commission (declined)

2003-2004: Postdoctoral fellowship from the von Humboldt fundation (Germany)

2000-2003: Research grant Allocataire-Moniteur (AMX) from the French Ministery of Research

TEACHING ACTIVITIES

since 2010: **Course of Statistical Physics** (M1; with J.-J. Greffet; ∼50 students/year) at Institut d'Optique (Palaiseau)

since 2008: **Course of Statistical Quantum Physics** (M2; with A. Browaeys; ∼24 students/year) at Institut d'Optique (Palaiseau)

2007-2012: **Exercice courses in Quantum Physics** (M1: with A. Sinatra; ∼45 students/year) at Ecole Normale Supérieure de Cachan and Université Pierre et Marie Curie (Paris)

2006-2010: **Lectures in Atomic Physics** at Ecole Normale Supérieure de Cachan (préparation à l'agrégation de physique)

2004: **Series of lectures in strongly correlated quantum gases** at the University of Hannover

2000-2003: **Tutor and demonstrator for first year physics** at the Université Pierre et Marie Curie (Paris)
1999-2000: **Small physics classes** at Lycée Saint-Louis
1997-1998: **Small mathematics classes** at Lycée Saint-Louis

ORGANIZATION OF SCIENTIFIC MEETINGS

2011: Summer school *Disordered Systems: From Condensed-Matter Physics to Ultracold Atomic Gases* (Cargèse, France; with T. Giamarchi and G. Roati)
2011: Workshop *Quantum Simulators with Ultracold Atoms* (Palaiseau, France)
2004: International conference *Disordered Quantum gases* (Hannover, Germany; with M. Lewenstein)

EDUCATION

2010-2011: **Habilitation à Diriger des Recherches**, *Disordered, ultracold quantum gases: Theoretical studies and experimental perspectives* (Université Paris-sud, France); Committee: A. Aspect, J. Dalibard (pres.), T. Giamarchi, M. Inguscio, M. Lewenstein, P. Zoller
2000-2003: **Ph-D degree of Ecole Polytechnique** defended in *Quantum Physics* at Laboratoire Kastler-Brossel (Ecole Normale Supérieure, Paris, France). Advisor: G. Grynberg; Committee: A. Aspect, J. Dalibard, R. Kaiser, A. Kastberg, P. Pillet (pres.), J.-Y. Courtois; *mention très honorable avec les félicitations écrites du jury (highest)*
1999-2000: **Master of Science** (M2, former DEA) in *Quantum Physics* headed by J. Dalibard (Ecole Normale Supérieure, Paris, France), *mention bien*
1996-1999: **Ecole Polytechnique** multidisciplinary scientific education (Palaiseau, France)
1993-1996: **Lycée Saint-Louis** (Paris, France): University-level preparation for the competitive entrance exams to French engineering and scientific schools.

ACTIVITIES AS A SCIENTIFIC EXPERT

- **Member of the Governing Committee of the RTRA-"Triangle de la Physique"** (2011-)
- **Member of Direction Board of Laboratoire Charles Fabry**
- **Expert** for
  the French Agence Nationale de la Recherche ("projets blancs"),
  the Austrian Science Fund (FWF),
  the Australian Marsden Fund Council,
  the ECOS-Sud of the French Foreign Ministry
- **Member of the Ph-D committees** of
  N. Cherroret (Grenoble, 2009)
  A. Niederberger (Barcelona, Spain, 2010)
- **Referee for several international journals** (Nature Physics, Physical Review Letters, Physical Review A, Physical Review B, Europhysics Letters, European Physical Journal D, New Journal of Physics, Journal of Low Temperature Physics)
- **Member of selection committees** for permanent positions at Université Pierre et Marie Curie (since 2007) and Institut d'Optique (2009)

ADVISING TASKS

Post-doc researchers
since 2009: Tung-Lam Dao (Vietnamese)
since 2007: Luca Pezzé (Italian)

Ph-D students

since Sep 2009:	Marie Piraud
2005-2009:	Pierre Lugan (co-advised with P. Bouyer)

Master students

Jan-Aug 2011:	Samuel Lellouch (Master 2 of *Quantum Physics*)
Apr-Jul 2010:	Thomas Koffel (Master 1, ENS-Cachan)
Jan-Aug 2009:	Marie Piraud (Master 2 of *Quantum Physics*)
2007-2009:	Ben Hambrecht (co-advised with A. Aspect)
Mar-June 2006:	Mehdi Ayouz (Master 2 of *Condensed-matter Physics*)

LIST OF PUBLICATIONS OF LAURENT SANCHEZ-PALENCIA

▷ Researcher ID (ISI-publications/citations): http://www.researcherid.com/rid/C-5586-2012

▷ name to use in *Web of Science* "sanchez-palencia, l"
▷ name to use in *Essential Science Indicators* "sanchezpalencia l"

Publications in refereed journals

[1] A.B. Ruffin, J. Decker, L. Sanchez-Palencia, L. Le Hors, J.F. Whitaker, T.B. Norris and J.V. Rudd, *Time Reversal and object reconstruction with single-cycle pulses*, Optics Letters **26**, 681-683 (2001)

[2] F.-R. Carminati, M. Schiavoni, L. Sanchez-Palencia, F. Renzoni and G. Grynberg, *Temperature and spatial diffusion of atoms cooled in a 3d lin⊥lin bright optical lattice*, European Physical Journal D **17**, 249-254 (2001)

[3] L. Sanchez-Palencia, P. Horak and G. Grynberg, *Spatial diffusion in a periodic optical lattice: revisiting the Sisyphus effect*, European Physical Journal D **18**, 353-364 (2002)

[4] L. Sanchez-Palencia, F.-R. Carminati, M. Schiavoni, F. Renzoni and G. Grynberg, *Brillouin propagation modes in optical lattices: interpretation in terms of nonconventional stochastic resonance*, Physical Review Letters **88**, 133903 (2002)

[5] A.B. Ruffin, J. Van Rudd, J. Decker, L. Sanchez-Palencia, L. Le Hors, J.F. Whitaker and T.B. Norris, *Time-reversal therahertz imaging*, IEEE Journal of Quantum Electronics **38**, 1110-1119 (2002)

[6] M. Schiavoni, F.-R. Carminati, L. Sanchez-Palencia, F. Renzoni and G. Grynberg, *Stochastic resonance in periodic potentials: realization in a dissipative optical lattice*, Europhysics Letters **59**, 493-499 (2002)

[7] M. Schiavoni, L. Sanchez-Palencia, F.-R. Carminati, F. Renzoni and G. Grynberg, *Dark propagation modes in optical lattices*, Physical Review A **66**, 053821 (2002)

[8] F.-R. Carminati, L. Sanchez-Palencia, M. Schiavoni, F. Renzoni and G. Grynberg, *Rayleigh scattering and atomic dynamics in dissipative optical lattices*, Physical Review Letters **90**, 043901 (2003)

[9] J. Jersblad, H. Ellmann, L. Sanchez-Palencia and A. Kastberg, *Anisotropic velocity distributions in 3D dissipative optical lattices*, European Physical Journal D **22**, 333-339 (2003)

[10] M. Schiavoni, L. Sanchez-Palencia, F. Renzoni and G. Grynberg, *Phase-control of directed diffusion in a symmetric optical lattice*, Physical Review Letters **90**, 094101 (2003)

[11] L. Sanchez-Palencia, M. Schiavoni, F.-R. Carminati, F. Renzoni and G. Grynberg, *Damping rates of the atomic velocity in Sisyphus cooling*, Journal of the Optical Society of America B **20**, 925-930 (2003)

[12] L. Sanchez-Palencia and G. Grynberg, *Synchronization of Hamiltonian motion and dissipative effects in optical lattices: evidence for a stochastic resonance*, Physical Review A **68**, 023404 (2003)

[13] J. Jersblad, H. Ellmann, K. Stochkel, A. Kastberg, L. Sanchez-Palencia and R. Kaiser, *Non-gaussian velocity distributions in optical lattices*, Physical Review A **69**, 013410 (2004)

[14] A. Sanpera, A. Kantian, L. Sanchez-Palencia, J. Zakrzewski and M. Lewenstein, *Atomic Fermi-Bose mixtures in inhomogeneous and random optical lattices: from Fermi glass to quantun spin glass and quantum percolation*, Physical Review Letters **93**, 040401 (2004)

[15] L. Sanchez-Palencia, *Directed transport of Brownian particles in a double symmetric potential*, Physical Review E **70**, 011102 (2004)

[16] L. Sanchez-Palencia and L. Santos, *Bose-Einstein condensates in optical quasicrystal lattices*, Physical Review A **72**, 053607 (2005)

[17] D. Clément, A.F. Varon, M. Hugbart, J.A. Retter, P. Bouyer, L. Sanchez-Palencia, D.M. Gangardt, G.V. Shlyapnikov and A. Aspect, *Suppression of transport of an interacting elongated Bose-Einstein condensate in a random potential*, Physical Review Letters **95**, 170409 (2005)

[18] V. Ahufinger, L. Sanchez-Palencia, A. Kantian, A. Sanpera and M. Lewenstein, *Disordered ultracold atomic gases in optical lattices: a case study of Fermi-Bose mixtures*, Physical Review A **72**, 063616 (2005)

[19] P. Sjölund, S. Petra, C. Dion, S. Jonsell, M. Nylén, L. Sanchez-Palencia and A. Kastberg, *Demonstration of a controllable three-dimensional Brownian motor in symmetric potentials*, Physical Review Letters **96**, 190602 (2006)

[20] T. Schulte, S. Drenkelforth, J. Kruse, W. Ertmer, J. Arlt, A. Kantian, L. Sanchez-Palencia, L. Santos, A. Sanpera, K. Sacha, P. Zoller, M. Lewenstein and J. Zakrzewski, *Cold atom gases in optical lattices with disorder*, Acta Physica Polonica A **109**, 89 (2006)

[21] L. Sanchez-Palencia, V. Ahufinger, A. Kantian, J. Zakrzewski, A. Sanpera and M. Lewenstein, *Strongly correlated Fermi-Bose mixtures in random optical lattices*, Journal of Physics B: Atomic Molecular and Optical Physics **39**, S121-S134 (2006)

[22] D. Clément, A.F. Varon, J.A. Retter, L. Sanchez-Palencia, A. Aspect and P. Bouyer, *Experimental study of the transport of coherent interacting matter-waves in a 1D random potential induced by laser speckle*, New Journal of Physics **8**, 165 (2006)

[23] D. Clément, A.F. Varon, M. Hugbart, J. Retter, P. Bouyer, L. Sanchez-Palencia, D.M. Gangardt, G.V. Shlyapnikov and A. Aspect, *Inhibition du transport d'un condensat de Bose-Einstein dans un potentiel aléatoire 1D*, Journal de Physique IV (France) **135**, 145 (2006)

[24] J. Wehr, A. Niederberger, L. Sanchez-Palencia and M. Lewenstein, *Disorder versus the Mermin-Wagner-Hohenberg effect: from classical spin systems to ultracold atomic gases*, Physical Review B **74**, 224448 (2006)

[25] L. Sanchez-Palencia, *Smoothing effect and delocalization of interacting Bose-Einstein condensates in random potentials*, Physical Review A **74**, 053625 (2006)

[26] P. Lugan, D. Clément, P. Bouyer, A. Aspect, M. Lewenstein and L. Sanchez-Palencia, *Ultracold Bose gases in 1D disorder: from Lifshits glass to Bose-Einstein condensate*, Physical Review Letters **98**, 170403 (2007)

[27] L. Sanchez-Palencia, D. Clément, P. Lugan, P. Bouyer, G.V. Shlyapnikov and A. Aspect, *Anderson localization of expanding Bose-Einstein condensates in random potentials*, Physical Review Letters **98**, 210401 (2007)

[28] P. Lugan, D. Clément, P. Bouyer, A. Aspect and L. Sanchez-Palencia, *Anderson localization of Bogolyubov quasiparticles in interacting Bose-Einstein condensates*, Physical Review Letters **99**, 180402 (2007)

[29] A. Niederberger, T. Schulte, J. Wehr, M. Lewenstein, L. Sanchez-Palencia and K. Sacha, *Disorder-induced order in two-component Bose-Einstein condensates*, Physical Review Letters **100**, 030403 (2008)

[30] D. Clément, P. Bouyer, A. Aspect and L. Sanchez-Palencia, *Density modulations in an elongated Bose-Einstein condensate released from a disordered potential*, Physical Review A **77**, 033631 (2008)

[31] C. Dion, P. Sjölund, S. Petra, S. Jonsell, M. Nylén, L. Sanchez-Palencia and A. Kastberg, *Controllable 3D atomic Brownian motor in an optical lattice*, European Physical Journal Special Topics **159**, 11 (2008)

[32] L. Sanchez-Palencia, D. Clément, P. Lugan, P. Bouyer, and A. Aspect, *Disorder-induced trapping versus Anderson localization in Bose-Einstein condensates expanding in disordered potentials*, New Journal of Physics **10**, 045019 (2008)

[33] J. Billy, V. Josse, Z. Zuo, A. Bernard, B. Hambrecht, P. Lugan, D. Clément, L. Sanchez-Palencia, P. Bouyer and A. Aspect, *Direct observation of Anderson localization of matter-waves in a controlled disorder*, Nature (London) **453**, 891 (2008)

[34] L. Pezzé, B. Hambrecht and L. Sanchez-Palencia, *Dipole oscillations of a Fermi gas in a disordered trap: Damping and localization*, Europhysics Letters **88**, 30009 (2009)

[35] P. Lugan, A. Aspect, L. Sanchez-Palencia, D. Delande, B. Grémaud, C.A. Müller and C. Miniatura, *One-dimensional Anderson localization in certain correlated random potentials*, Physical Review A **80**, 023605 (2009)

[36] L. Sanchez-Palencia and M. Lewenstein, *Disordered quantum gases under control*, Nature Physics **6**, 87-95 (2010)

[37] M. Robert-de-Saint-Vincent, J.-P. Brantut, B. Allard, T. Plisson, L. Pezzé, L. Sanchez-Palencia, A. Aspect, T. Bourdel and P. Bouyer, *Anisotropic 2D diffusive expansion of ultra-cold atoms in a disordered potential*, Physical Review Letters **104**, 220602 (2010)

[38] L. Sanchez-Palencia, *Joint forces against disorder*, Nature Physics **6**, 328-329 (2010)

[39] L. Pezzé and L. Sanchez-Palencia, *Localized and extended states in a disordered trap*, Physical Review Letters **106**, 040601 (2011)

[40] M. Piraud, P. Lugan, P. Bouyer, A. Aspect and L. Sanchez-Palencia, *Localization of a matter wave packet in a disordered potential*, Physical Review A **83**, 031603(R) (2011)

Publications in broad audience journals

[1] D. Delande, J.-C. Garreau, L. Sanchez-Palencia and B. van Tiggelen, *La localisation forte d'Anderson*, Images de la Physique **13**, 70 (2009)

[2] A. Aspect, P. Bouyer, V. Josse and L. Sanchez-Palencia, *Localisation d'Anderson d'atomes ultrafroids dans des potentiels optiques: Vers des simulateurs quantiques*, Images de la Physique **13**, 87 (2009)

Conferences and Invitations

[1] A.B. Ruffin, L. Sanchez-Palencia, L. Le Hors, J. Van Rudd, J.F. Whitaker and T.B. Norris, *Time Reversal and object reconstruction using single-cycle terahertz pulses*, OSA annual meeting and exhibit 2000, OSA (Providence, Rhode Island, USA, oct. 2000)
with proceeding

[2] A.B. Ruffin, J.F. Whitaker, T.B. Norris, J. Decker, L. Sanchez-Palencia, L. Le Hors and J. Van Rudd, *Time reversal and object reconstruction*, 13th annual meeting LEOS 2000, IEEE (Rio Grande, Puerto Rico, nov. 2000)
with proceeding

[3] L. Sanchez-Palencia and G. Grynberg, *Cooling and diffusion of atoms in optical lattices* (oral), Quantum Structures (Munich, Germany, nov. 2000)

[4] A.B. Ruffin, J. Decker, L. Sanchez-Palencia, L. Le Hors, J.F. Whitaker, J. Van Rudd and T.B. Norris, *Terahertz imaging via time reversal using single-cycle pulses*, OSA Ultrafast Electronics and Optoelectronics (Lake Tahoe, Nevada, USA, jan. 2001)
with proceeding

[5] A.B. Ruffin, J. Decker, L. Sanchez-Palencia, L. Le Hors, J.F. Whitaker, T.B. Norris and J. Van Rudd, *Time reversed image synthesis of dielectric objects*, CLEO 2001, OSA (Baltimore, Maryland, USA, may 2001)
with proceeding

[6] M. Schiavoni, F.-R. Carminati, L. Sanchez-Palencia, F. Renzoni and G. Grynberg, *Propagation modes and stochastic resonance in a lattice of cold atoms*, 5e Rencontre du Non Linéaire (Institut Henri Poincaré, Paris, France, mar. 2002)
with proceeding

[7] L. Sanchez-Palencia, F.-R. Carminati, M. Schiavoni, F. Renzoni and G. Grynberg, *Observing stochastic resonance in dissipative optical lattices* **(invited)**, Cooling2002 (Visby, Sweden, june 2002)
with proceeding

[8] L. Sanchez-Palencia, M. Schiavoni, F. Renzoni and G. Grynberg, *Directed diffusion of cold atoms in a symmetric optical lattice* (oral), 6e Rencontre du Non Linéaire (Institut Henri Poincaré, Paris, France, mar. 2003)
with proceeding

[9] L. Sanchez-Palencia, M. Schiavoni, F. Renzoni and G. Grynberg, *Directed diffusion in optical lattices* (poster), EuroSummer school on Quantum Gases in Low Dimensions (Les Houches, France, apr. 2003)

[10] L. Sanchez-Palencia, M. Schiavoni, F. Renzoni and G. Grynberg, *Directed diffusion in a 1D symmetric optical lattice* (oral), European Quantum Electronics conference CLEO/EQEC-2003 (Munich, Germany, june 2003)

[11] L. Sanchez-Palencia, A. Kantian, J. Zakrewski, A. Sanpera and M. Lewenstein, *Fermi glass, quantun spin glass and quantum percolation phases of Fermi-Bose mixtures in inhomogeneous optical lattices* (poster), Quantum limited atom optics (Hannover, Germany, mar. 2004)

[12] L. Sanchez-Palencia, A. Kantian, J. Zakrewski, A. Sanpera and M. Lewenstein, *Fermi-Bose mixtures in inhomogeneous optical lattices* (poster), Frontiers in quantum gases (Santa Barbara, United States, may 2004)

[13] L. Sanchez-Palencia and L. Santos, *Bose-Einstein condensate in a quasiperiodic optical lattice: A quantum gas at the edge between order and disorder* (poster), Mesoscopic Phenomena in Ultracold Matter: From Single Atoms to Coherent Ensembles (Dresden, Germany, oct. 2004)

[14] P. Sjölund, S. Petra, L. Sanchez-Palencia, M. Nylén, C. Dion, S. Jonsell and A. Kastberg, *Realization of a 3D Brownian motor in a double symmetric potential* (poster), International conference on Laser Spectroscopy (Cairngorms National Park, Scotland, United Kingdom, june 2005)

[15] J. Retter, A.F. Varon, D. Clément, M. Hugbart, L. Sanchez-Palencia, P. Bouyer, A. Aspect, D.M. Gangardt and G.V. Shlyapnikov, *Inhibition of transport of a Bose-Einstein condensate in a random potential*, Conference on Optics and Laser Spectroscopy (ICOLS2005) (Scotland, UK, june 2005)
with proceeding : Laser Spectroscopy: Proceedings of the XVII International Conference, World Scientific, Singapore , 248 (2005)

[16] L. Sanchez-Palencia and L. Santos, *Bose-Einstein condensate in a optical quasicrystals* (poster), School on quantum phase transitions and non-equilibrium phenomena in cold atomic gases (Trieste, Italy, july 2005)

[17] D. Clément, A.F. Varon, M. Hugbart, J. Retter, P. Bouyer, L. Sanchez-Palencia, D.M. Gangardt, G.V. Shlyapnikov and A. Aspect, *Suppression of transport of an interacting elongated Bose-Einstein condensate in a random potential* (poster), School on quantum phase transitions and non-equilibrium phenomena in cold atomic gases (Trieste, Italy, july 2005)

[18] V. Ahufinger, L. Sanchez-Palencia, A. Kantian, B. Damski, A. Sanpera and M. Lewenstein, *Atomic Fermi-Bose mixtures in inhomogeneous and random optical lattices* (poster), School on quantum phase transitions and non-equilibrium phenomena in cold atomic gases (Trieste, Italy, july 2005)

[19] D. Clément, A.F. Varon, M. Hugbart, J. Retter, P. Bouyer, L. Sanchez-Palencia, D.M. Gangardt, G.V. Shlyapnikov and A. Aspect, *Inhibition du transport d'un condensat de Bose-Einstein dans un potentiel aléatoire 1D*, 9ème Colloque sur les Lasers et l'Optique Quantique (Dijon, France, sept. 2005)
with proceeding

[20] L. Sanchez-Palencia, V. Ahufinger, A. Kantian, J. Zakrewski, A. Sanpera and M. Lewenstein, *Strongly correlated Fermi-Bose mixtures in random optical lattices* **(invited)**, 3rd workshop on Theory of quantum gases and quantum coherence (Cortona, Italy, oct. 2005)

[21] L. Sanchez-Palencia, D.M. Gangardt, P. Bouyer, G.V. Shlyapnikov and A. Aspect, *Interacting Bose-Einstein condensates in random potentials* (poster), workshop of the Institut Francilien de Recherche sur les Atomes Froids (IFRAF) (Paris, France, may 2006)

[22] L. Sanchez-Palencia, *Quantum phase diagram of an interacting ultracold Bose gas in a 1D random potential* **(invited)**, Disorder in cold atoms (Barcelona, Spain, jan. 2007)

[23] D. Clément, P. Lugan, L. Sanchez-Palencia, P. Bouyer, G.V. Shlyapnikov and A. Aspect, *Localization of interacting Bose-Einstein condensates in 1D random potentials* (poster), Disorder in cold atoms (Barcelona, Spain, jan. 2007)

[24] P. Lugan, D. Clément, P. Bouyer, A. Aspect, M. Lewenstein and L. Sanchez-Palencia, *Quantum states of ultracold, interacting Bose gases in 1D random potentials* (poster), Disorder in cold atoms (Barcelona, Spain, jan. 2007)

[25] A. Niederberger, J. Wehr, A. Cojuhovschi, K. Sacha, L. Sanchez-Palencia and M. Lewenstein, *Random-field-induced order in systems with continuous symmetry* (poster), Disorder in cold atoms (Barcelona, Spain, jan. 2007)

[26] L. Sanchez-Palencia, D. Clément, P. Lugan, P. Bouyer, G.V. Shlyapnikov and A. Aspect, *Localization of interacting Bose-Einstein condensates expanding in a 1D random potential created by laser speckle* **(invited)**, APS March meeting (Denver, USA, mar. 2007)

[27] L. Sanchez-Palencia, *Localization in disordered, interacting ultracold Bose gases* **(invited)**, Workshop on quantum gases (Paris, France, june 2007)

[28] P. Lugan, D. Clément, P. Bouyer, M. Lewenstein, A. Aspect and L. Sanchez-Palencia, *Quantum states of interacting Bose gases in 1D random potentials* (poster), Recent progress in studies of quantum gases: theory and experiments (Paris, France, june 2007)

[29] P. Lugan, D. Clément, P. Bouyer, A. Aspect and L. Sanchez-Palencia, *Anderson localization of the Bogolyubov modes of interacting Bose-Einstein condensates in correlated random potentials* (poster), Recent progress in studies of quantum gases: theory and experiments (Paris, France, june 2007)

[30] L. Sanchez-Palencia, *Localization of Bose-Einstein condensates in disordered potentials* **(invited)**, General conference of the French Physical Society (Grenoble, France, july 2007)

[31] L. Sanchez-Palencia, *Strong localization in interacting Bose gases: meanfield and beyond* **(invited)**, Workshop on Bose-Einstein Condensates and Coherent Backscattering (Thurnau, Germany, sept. 2007)

[32] L. Sanchez-Palencia, *Ultracold Bose gases in 1D optical disorder* **(invited)**, Joint conference on Control of Quantum Correlations in Tailored Matter (Reisensburg, Germany, oct. 2007)

[33] L. Sanchez-Palencia, *Anderson localization in interacting Bose gases* **(invited)**, 38th Winter workshop on the Physics of Quantum Electronics (Snowbird, USA, jan. 2008)

[34] L. Sanchez-Palencia and V. Josse, *Direct observation of Anderson localization of matter-waves in a controlled disorder* **(invited)**, workshop of the Institut Francilien de Recherche sur les Atomes Froids (IFRAF) (Paris, France, may 2008)

[35] L. Sanchez-Palencia, *Towards many-body Anderson localization: the case of Bogolyubov quasi-particles* **(invited)**, Symposium on disorder in cold atomic quantum gases (Ecole Polytechnique, Palaiseau, France, june 2008)

[36] L. Sanchez-Palencia, *Anderson localization with ultracold atoms* **(invited)**, EGC Workshop (Gif-sur-Yvette, France, july 2008)

[37] P. Bouyer, J. Billy, V. Josse, Z. Zuo, A. Bernard, B. Hambrecht, P. Lugan, D. Clément, L. Sanchez-Palencia and A. Aspect, *Anderson localization of matter-waves*, International conference on atomic physics (ICAP2008) (Storrs, USA, july 2008)
with proceeding

[38] L. Sanchez-Palencia, J. Billy, V. Josse, Z. Zuo, A. Bernard, B. Hambrecht, P. Lugan, D. Clément, P. Bouyer and A. Aspect, *Direct observation of Anderson localization in atomic Bose-Einstein condensates* **(invited)**, 22nd General conference of the Condensed Matter Division of the European Physical Society (Roma, Italy, aug. 2008)

[39] L. Sanchez-Palencia, *Anderson localization in interacting Bose-Einstein condensates* **(invited)**, Strong correlations in multiflavor ultracold quantum gases (Munich, Germany, oct. 2008)

[40] L. Sanchez-Palencia, *Towards many-body Anderson localization in interacting Bose-Einstein condensates* **(invited)**, Workshop on Anderson localization in nonlinear and many-body systems (Dresden, Germany, mar. 2009)

[41] L. Sanchez-Palencia, J. Billy, V. Josse, Z. Zuo, A. Bernard, B. Hambrecht, P. Lugan, D. Clément, P. Bouyer and A. Aspect, *Investigating Anderson localization with gaseous Bose-Einstein condensates* **(invited)**, DPG March meeting (Dresden, Germany, mar. 2009)

[42] L. Sanchez-Palencia, *Anderson localization of atomic matter-waves in optical speckle potentials* **(invited)**, 40th Annual Meeting of the Division of Atomic, Molecular, and Optical Physics (DAMOP 2009) (Charlottesville, Virginia, USA, may 2009)

[43] A. Aspect, J. Billy, V. Josse, Z. Zuo, A. Bernard, P. Cheinet, P. Lugan, D. Clément, L. Sanchez-Palencia and P. Bouyer, *Anderson localization of matter-waves in a controlled disorder: a quantum simulator ?*, Conference on Optics and Laser Spectroscopy (ICOLS2009) (Kusshаro, Japan, june 2009)
with proceeding

[44] L. Sanchez-Palencia, *Anderson localization of matterwaves in optical speckle* **(invited)**, Conference on Lasers and Electro-Optics and European Quantum Electronics Conference (CLEO-EQEC 2009) (Munich, Germany, june 2009)

[45] A. Aspect and L. Sanchez-Palencia, *Anderson localization of ultracold atoms in 1D optical speckles: surprises in a simple problem* **(invited)**, BEC2009 - Frontiers in Quantum Gases (San Feliu, Spain, sept. 2009)

[46] L. Sanchez-Palencia, *From single-particle to many-body Anderson localization in interacting Bose gases* **(invited)**, New Perspectives in Quantum Statistics and Correlations (Heidelberg, Germany, mar. 2010)

[47] L. Sanchez-Palencia, *Localized and extended states in a disordered trap* **(invited)**, Plenary Conference of the GdR Physique Quantique Mésoscopique (Aussois, France, sept. 2010)

[48] L. Sanchez-Palencia, *Coexistence of localized and extended states in a disordered trap* (poster), Frontiers of Ultracold Atoms and Molecules (Santa Barbara, USA, oct. 2010)

[49] L. Sanchez-Palencia, *Disordered quantum under control* **(invited)**, Workshop on Theory of Condensed Matter in Ile-de-France (Paris, France, nov. 2010)

[50] L. Sanchez-Palencia, *Ultracold atoms in disordered potentials* **(invited)**, New Trends in Quantum Information and Quantum Optics (Sant Benet (Barcelona), Spain, dec. 2010)

Seminars

[1] L. Sanchez-Palencia and T.B. Norris, *Object reconstruction using terahertz laser pulses*, Laboratory seminar of the Center for Ultrafast Optical Science (Ann Arbor, Michigan, USA, june 1999)

[2] L. Sanchez-Palencia, *Doppler and Sisyphus cooling, introduction to optical lattices*, talk given for the tutors' formation at the Université Pierre et Marie Curie (Paris VI) (Paris, France, may 2001)

[3] L. Sanchez-Palencia and G. Grynberg, *Spatial diffusion in a periodic optical lattice: Sisyphus effect from jumping to oscillating regime*, group seminar of the Ultracold Atoms Group of the Laboratoire Kastler-Brossel (Paris, France, june 2001)

[4] L. Sanchez-Palencia and G. Grynberg, *Transport in dissipative optical lattices: from Brillouin propagation modes to stochastic resonance* **(invited)**, group seminar of the Laser Cooling and Trapping Group at Stockholm University (Stockholm, Sweden, mar. 2002)

[5] L. Sanchez-Palencia, *The benefits of noise in microscopic physics: application to dissipative optical lattices*, Ph-D students seminar of the Laboratoire Kastler-Brossel (Paris, France, mar. 2002)

[6] L. Sanchez-Palencia, *Stochastic resonance, a new paradigm for noisy physical systems*, talk given for the Ph-D students formation at the Ecole Polytechnique (Palaiseau, France, may 2002)

[7] L. Sanchez-Palencia, *Nonlinear dynamics of cold atoms in dissipative optical lattices* **(invited)**, seminar of the laboratoire de Physique des Lasers, Atomes et Molécules (Lille, France, nov. 2003)

[8] L. Sanchez-Palencia, *The role of dissipation in optical lattices : atomic transport and related phenomena (talk given in the memory of Professor Gilbert Grynberg)* **(invited)**, SFB 407 Kolloquium (Hannover, Germany, nov. 2003)

[9] L. Sanchez-Palencia, *Ultracold quantum gases in ordered and disordered optical lattices, part I: quasiperiodic lattices*, group seminar of the atom optics group, Institut d'Optique, University Paris-Sud (Orsay, France, jan. 2005)

[10] L. Sanchez-Palencia, *Ultracold quantum gases in ordered and disordered optical lattices, part II: Fermi-Bose mixtures in disordered optical lattices*, group seminar of the atom optics group, Institut d'Optique, University Paris-Sud (Orsay, France, feb. 2005)

[11] L. Sanchez-Palencia, *Bose-Einstein condensates: a few challenges related to recent experiments*, Alain Bouyssy colloquium, University Paris-Sud (Orsay, France, feb. 2005)

[12] L. Sanchez-Palencia, *Ultracold quantum gases in periodic and disordered optical lattices* **(invited)**, general seminar of the Institut Non Linéaire de Nice (Nice, France, apr. 2005)

[13] L. Sanchez-Palencia, *Disordered quantum systems: a new challenge for ultracold atomic gases* **(invited)**, general seminar of the physics department of the University of Umea (Umea, Sweden, mar. 2006)

[14] L. Sanchez-Palencia, *Recipes to observe Anderson localization in the expansion of an interacting Bose-Einstein condensate* **(invited)**, seminar of the Laboratoire the Physique Théorique et Modèles Statistiques (Orsay, France, sept. 2006)

[15] L. Sanchez-Palencia, *Ultracold gases as laboratories for mesoscopic physics: the example of disordered quantum systems* **(invited)**, seminar of the theoretical physics group at the University of Bayreuth (Bayreuth, Germany, may 2007)

[16] L. Sanchez-Palencia, *Ultracold quantum gases in disordered potentials*, seminar of the Institut Francilien de Recherche sur les Atomes Froids (Palaiseau, France, nov. 2007)

[17] L. Sanchez-Palencia, *Ultracold Bose gases in controlled disorder : from single-particle to many-body Anderson localization* **(invited)**, symposium on vortex lattices and quantum Hall effect (Palaiseau, France, nov. 2008)

[18] L. Sanchez-Palencia, *Ultracold Bose gases in controlled disorder : from single-particle to many-body Anderson localization* **(invited)**, colloquim of the Institute for Condensed Matter Theory (Karlsruhe, Germany, dec. 2008)

[19] L. Sanchez-Palencia, *Anderson localization in ultracold atomic gases* **(invited)**, Seminar of theoretical physics at Ecole Normale Supérieure de Lyon (Lyon, France, feb. 2009)

[20] L. Sanchez-Palencia, *Coherent matter-waves in disordered potentials* **(invited)**, Seminar of the Applied Mathematics Center at Ecole Polytechnique (Palaiseau, France, mar. 2009)

[21] L. Sanchez-Palencia, *Anderson localization of matterwaves in speckle potentials* **(invited)**, Seminar of Laboratoire de Physique et Modélisation des Milieux Condensés (Grenoble, France, sept. 2009)

[22] L. Sanchez-Palencia, *Coexistence of localized and extended states in a disordered trap*, Seminar of the Atom Optics group of Institut d'Optique (Palaiseau, France, june 2010)

[23] L. Sanchez-Palencia, *Anderson localization of ultracold atoms in speckle potentials: New aspects of a old problem* **(invited)**, Seminar of condensed-matter theory network of Plateau de Saclay (Orsay, France, sept. 2010)

Teaching

This appendix aims at providing a brief outlook of my teaching activity. In the past years, I have been involved in several courses of advanced Quantum Mechanics and related subjects, in direct connection to my research field, *i.e.* Ultracold Atoms. I created a course of *Statistical Quantum Physics* (Master 2) at Institut d'Optique, and, together with Antoine Browaeys, a series of lectures on *Atomic and Molecular Physics* at Ecole Normale Supérieure de Cachan (Préparation à l'Agrégation de Physique, level Master 2). I also joined the course of *Statistical Physics and Evolution of Quantum Systems* of Alice Sinatra, where I lead exercise classes. Hereafter is a summary of these activities.

1. Statistical Quantum Physics

Lectures at Institut d'Optique (Master M2)

This course introduces the basics of statistical quantum physics. After presenting briefly the principles of statistical physics, we define the statistical entropy and the Gibbs ensembles and remind essentials of classical statistical physics. We then show how particle indiscernability in quantum physics deeply modifies statistical distributions. For non-interacting particles, we will calculate the populations of the various quantum states, from which many thermodynamic quantities can be obtained, for bosons and fermions.

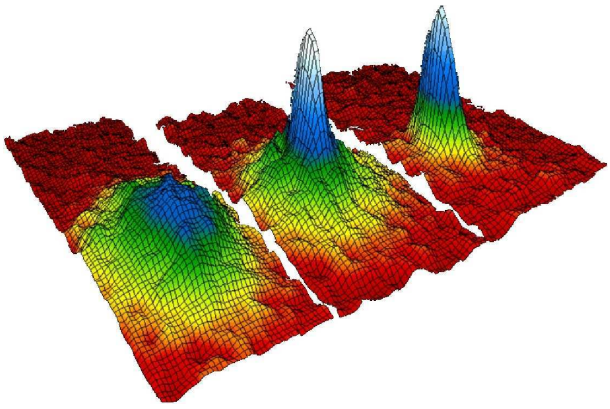

In particular, we detail Bose-Einstein condensation and Fermi degeneracy. Both play major roles in condensed-matter physics and atomic physics. Weakly interacting bosonic systems will be treated within the framework of the meanfield approach, which accounts for most properties of gaseous Bose-Einstein condensates.

The field of ultracold quantum gases is currently one of the most active frontier research domain in physics, with three recent Nobel prizes in physics (1997, 2001 and 2005) awarded for outstanding advances. It happens to be an original and a well-suited framework to apply the concepts and methods of quantum statistical physics. For instance, ultracold atoms have allowed the first direct observations of Bose-Einstein condensates in 1995 and of ideal Fermi gases in 1999. We introduce the field of ultracold atoms, describing the most advanced cooling and trapping techniques as well as some of the most recent results. This provides wonderful

illustrations of the concepts introduced during the course, showing the power of statistical physics to simply understand the fascinating physics of ultracold quantum gases.

Outlook

1. What is statistical physics ?
2. Statistical entropy and the Gibbs ensembles
3. Identical particles in classical and quantum physics
4. Boltzmann distribution and ideal, classical gases
5. Introduction to the physics of ultracold atoms
6. The Bose-Einstein statistics and Bose-Einstein condensates
7. Meanfield theory for weakly interacting particles
8. The Fermi-Dirac statistics and degenerate Fermi gases

2. Atomic and Molecular Physics

Lectures at Ecole Normale Supérieure de Cachan (Préparation à l'Agrégation de Physique ; with A. Browaeys and T. Bourdel)

The objective of this series of lectures is to provide advanced complements of quantum and atomic physics. Basic concepts, such as wave-particle duality, indiscernability, entanglement are reviewed, with illustrations inspired by the most modern experiments in atomic, molecular and optical physics. Fundamentals of atomic and molecular physics are presented as an illustration of the basic concepts, approaches and approximation methods in quantum physics. We thus introduce quantization, angular momenta and their addition, perturbative approaches, magnetic effects and spin exchange coupling.

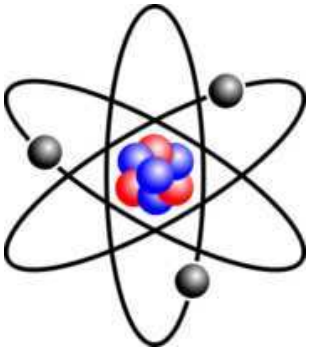

Outlook

1. Wave-particle duality (AB and TB)
2. Identical particles (AB and TB)
3. Quantum entanglement (AB and TB)
4. Ante-quantum atomic models (LSP)
5. Main structure of the hydrogen atom (LSP)
6. Relativistic corrections in atoms: Fine and hyperfine structures (LSP)
7. Many-electron atoms (LSP)
8. Atoms in external fields (LSP)
9. Elements of molecular physics and cohesion of solids (LSP)
10. The tunnel effect (AB and TB)
11. Optical cavities (AB and TB)
12. Atomic clocks (AB and TB)

3. Statistical Physics and Evolution of Quantum Systems

Exercise courses at Ecole Normale Supérieure de Cachan and Université Pierre et Marie Curie (lectures by A. Sinatra)

This course introduces Statistical Quantum Physics, assuming basic knowledge of Statistical Classical Physics. The formalism is presented in details and illustrated with examples in condensed-matter physics, ultracold atomic gases and gases of photons. Bose-Einstein condensation and non-interacting Fermi gases are discussed in connection to the most recent experimental works.
The course also provides complements of quantum physics with special emphasis on time-dependent perturbation theory and on the theory of scattering.

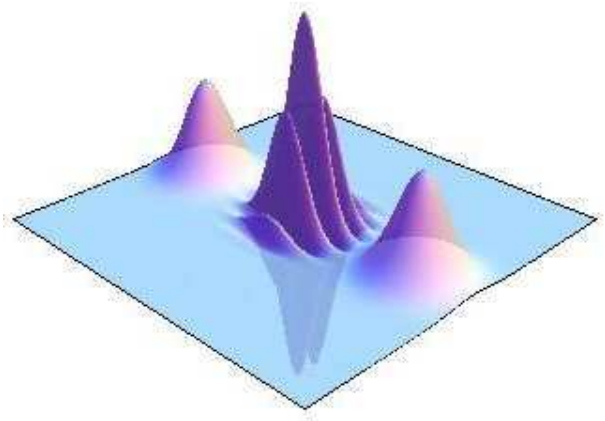

Outlook

1. Statistical quantum physics
   - 1.1 Statistical operator and Wigner distribution
   - 1.2 Statistical entropy and Gibbs ensembles
   - 1.3 Quantum statistics for bosons and fermions; Classical limit
   - 1.4 Degenerate quantum gases (occupation numbers and fluctuations)
   - 1.5 Bose-Einstein condensation and the Gross-Pitaevskii equation
   - 1.6 Non-interacting Fermi gases
   - 1.7 Applications (Condensed-matter, ultracold atoms, photons)

2. Evolution of quantum systems
   - 2.1 Time-dependent perturbation theory
   - 2.2 The Fermi golden rule
   - 2.3 Examples of oscillating perturbations
   - 2.4 The Wigner-Eckart theorem; Angular momenta; Clebsch-Gordan coefficients
   - 2.5 Elements of scattering theory

Résumé

Le désordre joue un rôle fondamental dans de nombreux domaines de la physique, tels que la matière condensée, l'optique, l'acoustique ou la physique atomique. Il est responsable de nombre d'effets surprenants, tels que la localisation d'Anderson, certaines transitions métal-isolant et d'intriguantes phases vitreuses. La complexité inhérente aux systèmes désordonnés soulève des défis considérables à la pleine compréhension de ces phénomènes. Au cours des dernières années, le désordre s'est imposé comme un axe de recherche majeur dans le domaine des gaz quantiques ultrafroids. Ces derniers offrent de fascinantes perspectives pour mieux comprendre les effets du désordre dans les systèmes quantiques, grâce non seulement à un contrôle sans précédent de leurs paramètres mais aussi à leurs propriétés originales.

Cette thèse d'Habilitation présente nos contributions récentes à la théorie des gaz quantiques désordonnés selon trois axes directeurs:

- La localisation d'Anderson dans les gaz quantiques désordonnés;
- Le désordre dans les gaz de Bose en interaction;
- La simulation de modèles de Hubbard étendus et de modèles de spin avec des atomes ultrafroids.

D'une part, nous proposons et analysons des expériences visant à réaliser des simulateurs quantiques afin d'étudier des questions ouvertes, d'importance fondamentale pour le domaine des systèmes désordonnés. A cet égard, nous montrons que les gaz quantiques offrent des perspectives prometteuses. D'autre part, nous réalisons des travaux amont qui mettent notamment en avant les propriétés originales des gaz quantiques. Ces derniers permettent ainsi de jeter un regard nouveau sur des problèmes d'intérêt général dans le domaine des systèmes désordonnés.

Abstract

Disorder plays a fundamental role in many fields of physics such as condensed-matter physics, optics, acoustics, or atomic physics. It is responsible for a number of surprizing effects, such as Anderson localization, metal-insulator transitions and intriguing glass phases. The inherent complexity of disordered systems poses outstanding challenges to the full understanding of these phenomena. In the last years, disorder has emerged as a major line of research in the field of ultracold quantum gases. The latter offer fascinating perspectives to better understand the effects of disorder in quantum systems, thanks not only to an unprecedented control of parameters, but also to their original properties.

This Habilitation thesis reviews our recent contributions to the theory of disordered quantum gases along three main lines:

- Anderson localization in disordered quantum gases;
- Disorder in interacting Bose gases;
- Simulating extended Hubbard and spin models with ultracold gases.

On the one hand, we propose and analyze experiments aiming at realizing quantum simulators to address open questions of fundamental importance for the field of disordered systems. In this respect, we show that quantum gases offer promising perspectives. On the other hand, we lead prospective works, which in particular show that quantum gases have original properties. They hence shed new light on issues of broad interest in the field of disordered systems.